Linda Makovicka Osvaldova
Frank Markert
Samuel L. Zelinka *Editors*

Wood & Fire Safety

Proceedings of the 9th International Conference on Wood & Fire Safety 2020

Springer

Wood & Fire Safety

Linda Makovicka Osvaldova ·
Frank Markert · Samuel L. Zelinka
Editors

Wood & Fire Safety

Proceedings of the 9th International Conference on Wood & Fire Safety 2020

Springer

9th International Scientific Conference
wood & fire safety 2020
May 3-6, 2020 | The Hotel Patria | Strbske Pleso | Slovakia

Editors
Linda Makovicka Osvaldova
Department of Fire Engineering
Faculty of Security Engineering
University of Zilina
Zilina, Slovakia

Frank Markert
Department of Civil Engineering
Technical University of Denmark
Lyngby, Denmark

Samuel L. Zelinka
USDA Forest Service
Forest Products Laboratory
Madison, WI, USA

ISBN 978-3-030-41234-0 ISBN 978-3-030-41235-7 (eBook)
https://doi.org/10.1007/978-3-030-41235-7

This Springer imprint is published by the registered company Springer Nature Switzerland AG
The registered company address is: Gewerbestrasse 11, 6330 Cham, Switzerland

Foreword

Dear Wood & Fire Safety 2020 participants.

It is an honour for us to welcome you to Slovakia at the Hotel Patria in Strbske Pleso for the 9th International Scientific Conference Wood & Fire Safety 2020 (WFS 2020).

The traditional meeting of experts in the field of fire protection who prefer wood and wood-based materials, is held at regular four-year intervals since its origin in the year 1988.

All the conferences have been held at this traditional venue - the hotel Patria in Strbske Pleso, Slovakia. Since that first event up until the last one in the year 2016, the Conference has hosted more than 750 participants, of which 224 were internationals.

The regular conference participants are not only delegates from the European countries but from non - European countries as well, mostly from Canada, U.S., New Zealand, Australia, Japan, and in recent years, also from China.

The aim of the WFS 2020 conference is to gather at one place new knowledge of this multidisciplinary field, namely the combustion of solid materials, modelling, measuring, testing of flammability, structure and properties of wood and their changes at high temperatures, the study of stages of the wood burning process, flame-retardant treatment of wood and wood-based materials, fire safety in wooden buildings, fire-fighting in wooden buildings, forest fires, fire-fighting in a historical building, and others.

This year WFS2020 has attracted about 65 papers from all over the world including Australia, Canada, China, India, Japan, New Zealand, UK, U.S., Russia and Europe.

The proceeding has been subdivided into the following sections:

- Structure and properties of wood and its changes at high temperatures
- Wood burning retardation and wood-based materials
- Fire modelling, fire testing, fire certification, fire investigation, fire dynamic, fire behaviour modelling, smoke control and combustion toxicity
- Fire safety in wooden buildings

– Forest fires
– Others topics that focus on wood & fire safety

The chairman of WFS2020 would like to thank the reviewers and authors for their contribution of the papers and posters and all participants for their effort, trust and team-work during, as well as in the preparation phase of the conference.

The chairman of WFS2020 also expresses sincere acknowledgement and appraisal to the conference' sponsors, partners and media partners whose support and contributions were remarkable and without whom this conference would not be possible.

Last, but not least our enormous gratitude and recognition goes to the main organizers and co-organizers, whose dedication and enthusiasm made the WFS 2020 edition an unforgettable experience.

Strbske Pleso, Slovakia
May 2020

Linda Makovicka Osvaldova
Chairman Wood & Fire Safety 2020

Preface

The Wood & Fire Safety 2020 proceedings present the latest results of scientific research in the field of combustion of wood and wood-based materials. Since this research topic involves so many aspects and disciplines, for a more detailed analysis of the issue we have divided it into six separate sections: Structure and properties of wood and its changes at high temperatures; Wood burning retardation and wood-based materials; Fire modelling, fire testing, fire certification, fire investigation, fire dynamic, fire behaviour modelling, smoke control and combustion toxicity; Fire safety in wooden buildings; Forest fires; Others topics that focus on wood & fire safety.

The Wood & Fire Safety 2020 proceedings encompasses the latest results of research papers in 65 scientific articles presented at the conference in the form of a lecture and 22 abstracts presented at the conference by a poster presentation. 242 authors from 32 countries participated in these researches. The papers (articles) have been a subject to a peer review process.

Strbske Pleso, Slovakia
May 2020

Linda Makovicka Osvaldova
Chairman Wood & Fire Safety 2020

Organization

Chairman of Wood & Fire Safety 2020

Linda Makovicka Osvaldova	University of Zilina, Slovakia

Programme Chairs

Anthony Abu	University of Canterbury, New Zealand
Zakiah Ahmad	Universiti Teknologi Mara, Malaysia
Ladislav Andrisek	Fire Research Institute, Ministry of Interior of the Slovak Republic, Slovakia
Noureddine Benichou	National Research Council, Canada
Daniel Brandon	RISE, Sweden
Emilio Chuvieco	University of Alcala, Spain
Steve Craft	CHM Fire Consultants, Canada
Christian Dagenais	FPInnovations, Canada
Dhionis Dhima	CSTB, France
Bogdan Dlugogorski	Murdoch University, Australia
Andrew Dunn	Timber Development Association, Australia
Massimo Fragiacomo	University of L'Aquila, Italy
Milan Gaff	Czech University of Life Sciences, Czech Republic
Wojciech Grzeskowiak	Poznan University of Life Sciences, Poland
Lidia Gurau	Transilvania University of Brasov, Romania
Yuji Hasemi	Waseda University, Japan
Jaroslav Holusa	Czech University of Life Sciences, Czech Republic
Agnes Iringova	University of Zilina, Slovakia
Alar Just	Tallinn University of Technology, Estonia
Danica Kacikova	Technical University in Zvolen, Slovakia
Koji Kagiya	Building Research Institute, Japan

Jaroslav Kapusniak	Regional Headquarters of Fire and Rescue Services, Zilina, Slovakia
Michael Klippel	ETH Zurich, Switzerland
Yuriy Klyuchka	National University of Civil Defence, Ukraine
Venkatesh Kodur	Michigan State University, USA
Mirjana Laban	University of Novi Sad, Serbia
Antonin Lokaj	VSB - Technical University of Ostrava, Czech Republic
Andrea Majlingova	Technical University in Zvolen, Slovakia
Frank Markert	Technical University Denmark, Denmark
Iveta Markova	University of Zilina, Slovakia
Jozef Martinka	Slovak University of Technology in Bratislava, Slovakia
Birgitte Messerschmidt	NFPA, USA
Andrzej Mizerski	Main School of Fire Service, Poland
Robert Nemeth	University of Sopron, Hungary
Jiri Pokorny	VSB - Technical University of Ostrava, Czech Republic
Peter Rademacher	Eberswalde University, Germany
Agoston Restas	National University of Public Service, Hungary
Gervais Sawyer	International Wood Products Journal, UK
Joachim Schmid	ETH Zurich, Switzerland
Javier R. Sotomayor Castellanos	Michoacan University, Mexico
Jozef Svetlik	University of Zilina, Slovakia
Luigi Todaro	University of Basilicata, Italy
Matsagar Vasant	Indian Institute of Technology (IIT) Delhi, India
Pavlin Vitchev	University of Forestry, Bulgaria
Felix Wiesner	University of Edinburgh, UK
Qiang Xu	Nanjing University of Science and Technology, China

Steering Committee

Jaroslav Flachbart	University of Zilina, Slovakia
Michaela Horvathova	University of Zilina, Slovakia
Juraj Jancik	University of Zilina, Slovakia

Conference Organizers

Conference Co-organizers

Partners

Sponsors

Media

Contents

Structure and Properties of Wood and Its Changes at High Temperatures

Small Scale Test to Measure the Strength of Adhesives at Elevated Temperatures for Use in Evaluating Adhesives for Cross Laminated Timber (CLT)

Samuel L. Zelinka[1(✉)], Byrne Miyamoto[2], Nathan J. Bechle[1], and Douglas Rammer[1]

[1] USDA Forest Service Forest Products Laboratory, Madison, WI 53715, USA
samuel.l.zelinka@USDA.gov
[2] Oregon State University, Corvallis, OR 97331, USA

Abstract. Cross laminated timber (CLT) is becoming widely available in North America. The product standard for North American CLT, PRG-320, has strict requirements on adhesive performance under fire scenarios. To become an adhesive certified under PRG-320, a full sized CLT compartment must be built and tested without a second flashover occurring caused by delamination. Currently, only three adhesive formulations are PRG-320 certified. This large scale test is expensive to run and only yields "pass-fail" results. In this paper we present small-scale adhesive tests performed at the Forest Products Laboratory. The tests examine a single lap shear joint. The samples are tested at elevated temperatures in a universal testing machine with an environmental chamber built around the grips. The strains are measured using digital image correlation. Tests were conducted in two different manners. In the first test, thermal equilibrium was achieved and the sample was loaded to failure. In the second test, a constant load was applied and a thermal ramp was applied until failure occurs and the temperature at failure was recorded. Importantly, the tests were compared against control samples of solid wood (no adhesive) so that adhesive strength could be normalized to that of solid wood. It is hoped that this small-scale test can aid in the understanding of CLT adhesive performance and be used to screen adhesives prior to investment in large scale adhesive qualification tests.

Keywords: Mass timber · Adhesives · Elevated temperatures · Strength · Polyurethane · Creep

1 Introduction

Mass timber buildings are being adopted worldwide with the increased use of cross laminated timber (CLT) [1]. CLT is a massive engineered wood panel made from alternating layers of dimension lumber that can be easily erected as wall or floor assemblies [2]. As with any combustible construction material, the fire performance of CLT needs to be tested and validated for use in construction.

L. Makovicka Osvaldova et al. (Eds.): WFS 2020, *Wood & Fire Safety*, pp. 3–8, 2020.
https://doi.org/10.1007/978-3-030-41235-7_1

PRG 320 is the product standard for CLT in North America [3]. As part of the PRG 320 standard, CLT must pass fire tests that measure the adhesive performance under a fire scenario. In early fire tests on CLT compartments funded by the Fire Protection Research Foundation (FPRF), fire regrowth, also called a second flashover, occurred [4]. The fire regrowth occurred when a ply from a CLT panel delaminated before the char front had reached the bondline and the compartment temperatures were still high. The freshly exposed timber introduced more fuel to the fire resutling in the fire regrowth.

PRG 320 compliant CLT must pass a large-scale test designed to closely mimic the fire exposure from the FPRF tests where delamination and fire regrowth occurred. In the PRG 320 test a 2.8 m by 5.8 m by 2.4 m compartment is constructed with a fully exposed CLT ceiling loaded to 25% of the allowable design stress of the panel. Instead of a specified fuel load from furniture, a temperature profile in the compartment is specified and the fuel flow must be calibrated to meet this profile. The heat release rate of the burner used in previous testing is shown in Fig. 1. To become certified, the panel must sustain the load for the entire 240 min test and no fire regrowth can be observed after 150 min with temperatures at the ceiling of the compartment remaining below 510 °C.

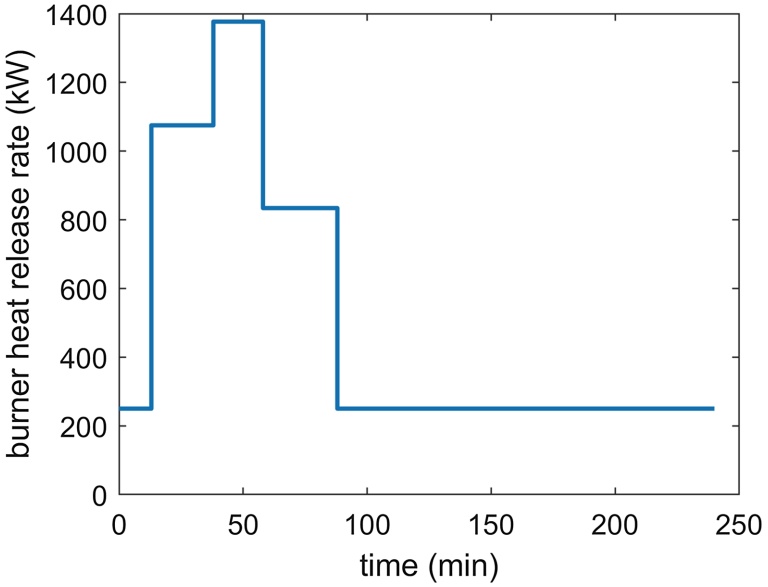

Fig. 1. Heat release profile for the burner used in the PRG 320 test [3]. To pass, the CLT must not cause any temperature increases in the compartment after 150 min.

While the PRG 320 test is the current standard for entrance to the marketplace, it is an expensive test and cannot be used for screening different adhesives nor understanding how different chemical changes to adhesives affect their fire performance in

CLT. In both the PRG 320 test and the FPRF tests, the temperature at the bondlines increased time and the rate of this increase can be closely approximated by a secant line drawn through the minimum measurable temperature and the peak temperature or temperature at failure. Therefore, it should be possible to scale down the physics of the test to a single bondline.

Small, scaled-down tests would be invaluable in the development and screening of new adhesives. Previous work has examined quasi-static testing at elevated temperatures [5, 6]. While the quasi-static test was useful in understanding the reduction in strength as a function of temperature, the loading conditions are not directly applicable to the PRG 320 standard. This paper discusses a scaled-down test designed to match the bondline temperature profile and loads of the PRG-320 test.

2 Development of Creep Test

The creep tests were designed to be representative of the physics of previous large scale compartment fire tests where delamination was observed; namely the FPRF tests and PRG 320. The temperature ramp rates were prescribed to match the bondline temperature profiles reported in the tests. Furthermore, the loads were scaled to match the shear stress at the bondline for the sample geometry used in previous quasistatic testing to that used in the PRG 320 and FPRF tests.

2.1 Sample Materials and Geometry

The specimens consisted of a single stepped-lap shear joint and were constructed from Douglas fir. The half-lap was created with the use of a router and samples were glued within 3 h of machining per the manufacturers' procedure. The sample had a bonded area of 565 mm^2; full sample details are described elsewhere [5, 6].

2.2 Temperature Profile

The bondline temperature profiles from the PRG 320 tests are shown in Fig. 2 for a melamine formaldehyde (MF) adhesive and two different polyurethane (PUR formulations). For the adhesives that passed the test, (MF and PUR2, both shown in blue) the first bondline remained below the char temperature of wood for the entire test. However, for the adhesive that delaminated (PUR1), the first bondline failed during the first part of the test when a high amount of fuel was being added to the fire. In this test, it was the second bondline that failed and caused fire regrowth. In all three tests, the temperature at the critical bondline exhibited a nearly linear increase in temperature with respect to time. The slope of the temperature increase at the bondline varied from 3.0 °C min^{-1} for the MF adhesive at the first bondline to 5.2 °C min^{-1} for the second bondline of the PUR1 adhesive. The slope of the temperature rise at the first bondline of the PUR2 adhesive was 4.0 °C min^{-1}.

Figure 2 compares the bondline temperatures from the FPRF test with the exposed ceiling and PRG 320 test. Both tests used panels made at the same manufacturing plant with the same adhesive. The temperature rise at the first bondline is nearly identical

between the two tests. However, the second bondline heated at a slower rate in the FPRF test than in the PRG 320 test. In the FPRF test, the bondline temperature increased by 2.0 °C min^{-1}. Interestingly, the bondline failed at a lower temperature (232 °C) than in the PRG 320 test (>270 °C).

In summary, in previous compartment fire testing, the temperature has been found to increase linearly with time at the bondline. The rate of the linear increase has varied from 2 to 5 °C min^{-1}.

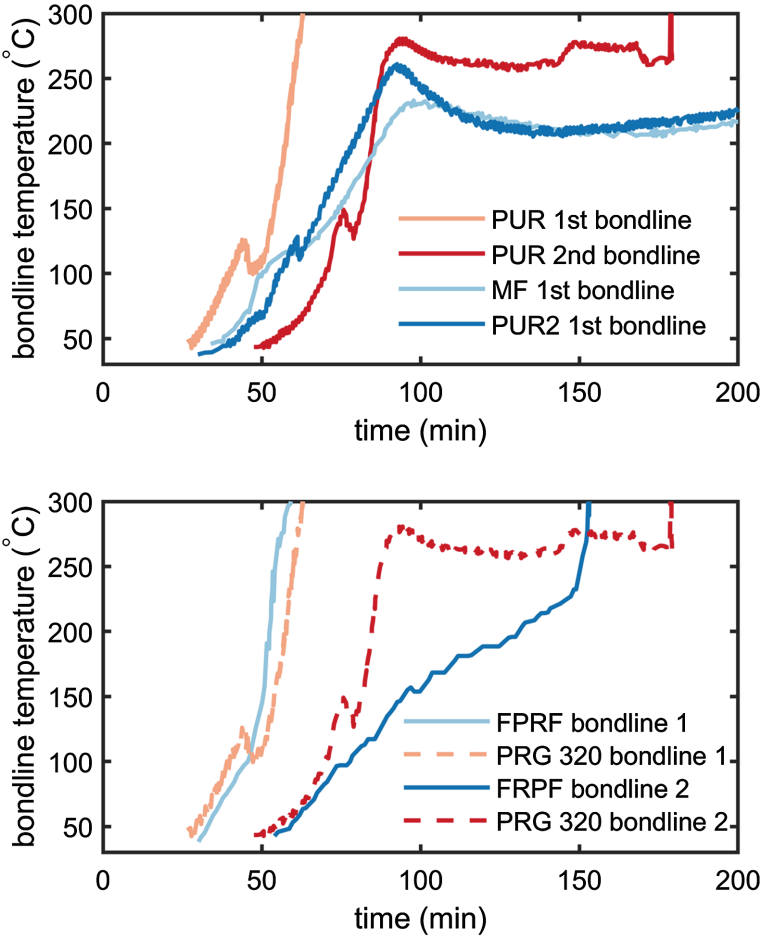

Fig. 2. Top: Bondline temperature profiles from the PRG 320 test for a melamine formaldehyde (MF) adhesive along with two polyurethane (PUR) adhesives. Bottom: Comparison of bondline temperature profiles in the FPRF and PRG 320 tests for a polyurethane adhesive labeled PUR1 in the top graph. Data replotted from [4] and [7].

2.3 Load Profile

Similar to the temperature profiles, the creep tests were conducted such that the shear stress at the bondline for the specimen would match the state of shear stress at a bondline for a panel in bending per the FPRF or PRG 320 procedures. The values were estimated as the shear stress due to bending at the first (outermost) bondline in the tensile region using classical beam theory.

For the FPRF tests, a deadload was applied at two points along the panel length, creating the equivalent of four-point bending about the major axis of the panel. The corresponding shear stress at the first bondline for a 5-ply panel was estimated to be 12 kPa. The PRG 320 test specifies a loading of 25% of the effective allowable design stress. For a V1 grade 5-ply CLT, this results in a shear stress at the first bondline of 53 kPa. The shear stress at the bondline for the specimen is assumed to be uniformly distributed over the bond area of 565 mm^2.

3 Planned Testing

Six adhesives will be tested: two formulations of PUR, two formulations of emulsion polymer isocyanate (EPI), one formulation of MF and one formulation of phenol resorcinol formaldehyde (PRF). All adhesives will be tested in a quasi-static method at room temperature and at 260 °C. These quasi-static tests will be used to benchmark adhesive performance and be used to investigate potential differences between the adhesive performance under various loading conditions.

Creep tests will also be performed. Two different temperature ramp rates will be examined, a slow temperature ramp of 2 °C min^{-1} ramp based upon the FRPF test and a 4 °C min^{-1} ramp based upon the observed temperature increases in the PRG 320 tests. In these tests the temperature ramp will be controlled based upon a thermocouple embedded to the mid-depth of the sample outside of the gauge length and therefore the temperature ramp should correspond with the bondline temperature. Based upon the observed failures in the PRG 320 and FPRF tests, it appears that the 2 °C min^{-1} test will be more challenging.

The applied load on the tests will also be examined as an experimental variable with tests being performed to match the stresses in both the FPRF and PRG 320 tests.

In total, four different tests will be performed on each of the six adhesive formulations:

- Quasi-static testing at room temperature
- Quasi-static testing at 260 °C
- Creep testing at 2 °C min^{-1} and a bondline stress of 12 kPa
- Creep testing at 4 °C min^{-1} and a bondline stress of 53 kPa

For adhesive formulations that do not exhibit failure in the creep tests will the low bondline stresses associated with the PRG-320 loading, additional creep testing may be performed at higher loads. While it is assumed that these adhesives have a high probability of passing the PRG-320 test, the goal of these additional tests is to better understand the failure mechanisms of these adhesives.

4 Discussion and Concluding Remarks

Currently, large-scale qualification tests are needed before adhesives can enter the marketplace which can be cumbersome, time consuming, and expensive with little data gathered beyond a pass/fail criterion. To this end, this project is examining how small-scale tests can be used to better understand adhesive performance at elevated temperatures and screen adhesives to avoid costly, large-scale testing.

In previous large-scale compartment fire testing, the temperature rise at the bondlines in CLT has been linear, with a rates between 2 to 5 °C min^{-1}. The planned tests will examine the behavior of single stepped-lap shear joints under the same temperature ramp as those seen in the large-scale tests. The small-scale testing will aid in the development of new adhesive formulations and improve the understanding of the fire performance of CLT.

References

1. Green M, Karsh J (2012) TALL WOOD - the case for tall wood buildings. Report prepared for the Canadian wood council on behalf of the wood enterprise coalition and forest innovation investment, Vancouver, BC
2. Mohammad M, Gagnon S, Douglas BK, Podesto L (2012) Introduction to cross laminated timber. Wood Des Focus 22:3–12
3. Anon (2018) ANSI/APA PRG 320: standard for performance rated cross-laminated timber. APA - The Engineered Wood Association, Tacoma
4. Su J, Lafrance P-S, Hoehler M, Bundy M (2018) Fire safety challenges of tall wood buildings – phase 2: task 2 & 3 cross laminated timber compartment fire tests, fire protection research foundation, Quincy, MA
5. Zelinka SL, Pei S, Bechle N, Sullivan K, Ottum N, Rammer DR, Hasburgh LE (2018) Performance of wood adhesives for cross laminated timber under elevated temperature. Paper MAT-O1-04. In: World conference of timber engineering, Seoul, Republic of Korea
6. Zelinka SL, Sullivan K, Pei S, Ottum N, Bechle N, Rammer DR, Hasburgh LE (under consideration for publication) Small scale tests on the performance of adhesives used in cross laminated timber (CLT) at elevated temperatures. Int J Adhes Adhes
7. Janssens M (2017) Development of a fire performance assessment methodology for qualifying cross-laminated timber adhesives. SwRI Project No. 01.23086.01.001a, Southwest Research Institute, San Antonio, TX

Experimental Study of the Combustion of a Single Biomass Particle

Pahola Acevedo, Angel Martinez, Corine Lacour, and Alexis Coppalle(✉)

Normandie Univ, INSA Rouen, UNIROUEN, CNRS, CORIA, 76000 Rouen, France
coppalle@coria.fr

Abstract. Biomass valorization for energy production is considered as one of the best ways to overcome the petroleum's depletion, move forward in the environmental protection concerns, but also to provide the energetic request. The combustion of biomass is an efficient valorization pathway but it still requires fundamental knowledge. To go deeper, some authors use simulation analysis combined with experimental results where a good agreement is appreciated. In the same sense, the present study explores experimentally the combustion of a single biomass particle as woody pellets and wood. An experimental free-ventilated system is built with a cone calorimeter as radiative heat source in order to heat the particles. A weighing scale is used to measure mass degradation during combustion process, and a type-k thermocouple allows measuring the temperature evolution in the center of the particle. As a result, curves of temporal evolution of mass degradation and central temperature are acquired for each kind of particle. This allows to observe the three main phases of combustion process (particle drying, volatiles combustion, and char's combustion), besides a superposition of homogeneous and heterogeneous combustions phases. Considering that the elemental composition of woody pellet and wood particles are close, similar combustion phases are identified with different time steps.

Keywords: Biomass · Combustion · Wood

1 Introduction

Biomass is all organic matter of plant, animal, bacterial or fungal origin and includes a wide range of materials, such as seaweed, products from animals, from food and paper industries, sewage sludges but also forest, agricultural (grasses, barks, crops), which are suitable for use in the production of heat and power [1]. The combustion of biomass is an efficient valorization pathway, in particular with small pieces of woody biomass, but it still requires fundamental knowledge. Indeed, physical mechanisms involved in the combustion process of solid materials are not still fully understood. As far as biomass combustion is involved, it is of particular importance to understand the material degradation process to achieve an objective of pollutant emission resulting from heating appliances based on combustion process. In a recent study [2], powder of small

L. Makovicka Osvaldova et al. (Eds.): WFS 2020, *Wood & Fire Safety*, pp. 9–15, 2020.
https://doi.org/10.1007/978-3-030-41235-7_2

particles has been injected in a flame in order to study the gas temperature and oxygen concentration on single particle ignition. Pyrolysis of centimeter-scale woody biomass particles has been studied by Corbeta [3], and Di Blasi [4] made, in a furnace, the analysis of the pyrolytic behavior of particles with a dimension of about 1 cm, and of several wood varieties. To go deeper, some authors use simulation analysis combined with experimental results [5].

In the present study, we propose an experimental setup which allows the degradation of a single pellet or a small piece of wood under a constant controlled heat flux, in order to better understand the phenomena experienced by the material until the end of combustion. Although the materials constituting the pellets and the small pieces of wood are close, it is interesting to compare the behavior of these two types of fuel because their thermal properties are rather different, due to their fabrication process. Curves of temporal evolution of mass degradation and central temperature will be shown for particles of different sizes of pellet or wood. This allows to highlight the three main phases of combustion process (particle drying, volatiles combustion, and char's combustion). First the experimental set-up is described, then the influence of particle sizes is shown for the pellet case, and finally the results obtained with pellet and wood particles with the same size are presented and analyzed.

2 Experimental Set-up

The processes undergone by the biomass sample until it becomes ash are analyzed with a cone calorimeter. The cone is generally used to test the fire reaction of materials [6]. In the present study, the cone plays the role of a radiative source. It consists of electrical resistors regulated to reach a temperature setpoint. A constant radiated heat flow of 63.7 kWm^{-2} is fixed here to reach the ignition of volatiles. The sample temperature is measured by means of a type K thermocouple with a 0.5 mm weld and is inserted along the central axis. The sample is carried by the thermocouple which is connected to a scale (Mettler Toledo XS2002S – accuracy ±0.01 g) for the mass degradation measurement. Temperature and mass are acquired each second. In order to synchronize mass and temperature time evolutions with visible phenomena (ignition and extinction of the flame), a voice recording tool is used and triggered with the data recording. It should be noted that heat transfer by convection and radiation plays a role in the pellet heating, but under our conditions, we have ensured that radiative transfer is dominant (convective flux estimated to 1 $kW.m^{-2}$).

Samples consist in cylindrical pellets and wood pieces (oak) of 6 mm diameter. Samples of 15, 20, 25- and 30-mm length are tested for both materials. Ultimate (elemental) analysis[1] and moisture contents[2] of the biomass samples have been performed and results are presented in Table 1.

[1] Refuse-Derived Fuel (RDF) standards norm ware used.

[2] E-871standard norm was used.

3 Results

First of all, the behavior of the pellets of different lengths will be presented. For each length, three tests have been carried out, and the repeatability of the experimental setup is ensured. Then, average results for each length are compared to look at the influence of the size. Finally, pellet and wood results are compared and analyzed.

Table 1. Ultimate (elemental) analysis, moisture contents and density of wood and woody pellets

Elements	Pellets contents	Wood pieces contents
C	46.68%	47.39%
H	5.71%	5.82%
O	44.61%	42%
Moisture content	7.2%	8.37%
Density (kg/m^3)	1397.56	850.16

3.1 Pellets of 15 mm Length Under 63.7 kW.m^{-2} Flux

The Fig. 1 shows, for three pellets of 15 mm size, the mass loss m/m$_0$, m$_0$ being the initial mass value, and the pellet center temperature (Tp) as functions of time. The three trends are similar, so the analysis is focused on test-1 (m/mo-1, Tp-1).

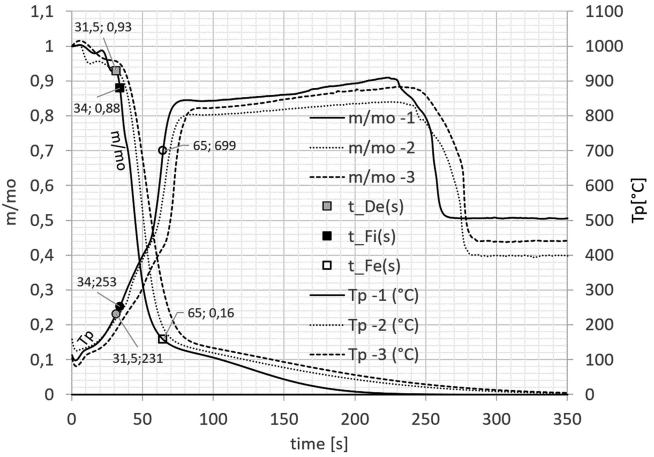

Fig. 1. Pellets of 15 mm size, temperature and mass loss for three tests. Raw measured values. The marks correspond to important phenomena observed during test-1: t_De is the end of the drying process, t_Fi the flame ignition on the pellet, t_Fe the flame extinction.

Concerning the heating of the pellet, several changes in the slope of the temperature curve are noticed. A first trend is observed from 10 s till 34 s, timing corresponding to the

ignition of volatiles (t_Fi). The flame observed after this time probably increases the temperature level reached at the center of the pellet by conduction. A second linear trend is maintained till 60 s, where the temperature reaches 450 °C, the char combustion temperature [7]. After 60 s, the temperature slope is again enhanced probably due to the heat released by the char oxidation [7] but also due to the char thermal diffusivity which may be different to the virgin material diffusivity. During this period of time (60 s to 80 s), volatiles emissions and char combustion occurs simultaneously and at t_Fe = 65 s the flame is extinguished. After 80 s, only the char heterogeneous oxidation occurs for a temperature close or slightly greater to 800 °C. The slow temperature increase during this period can be explained by an oxidation process occurring throughout the sample, leading to a heat release nearly constant in time. Finally, the temperature decreases after 250 s and the sample is reduced to ashes. The final temperature is around 450 °C corresponding roughly to the gas temperature at the center of the cone.

The ratio of instantaneous measured mass over the initial mass (m/m_o) is also plotted against time in Fig. 1. A first mass loss is observed at 31 s, reaching 7% and corresponding to the drying of the pellet (see moisture content in Table 1). Shortly after the ignition of volatiles (t_Fi = 34 s), the mass loss is enhanced. After t_Fe = 65 s, the mass degradation slows down due to the beginning of the char combustion as the last volatiles matters are still burning. After 65 s, all volatiles are burned and surrounding oxidant is able to reach the central part of the pellet. The mass of volatile matter is estimated from the mass degradation curve, from the end of the drying process to the flame extinction, and reaches 78% in test-1.

As previously noted, the curve shapes of the three tests are similar, but some delays between them are noticeable. This is mainly due to the initial time taken to introduce the pellet on the thermocouple, which is difficult to control. So, the curves have been shifted in time in order to make their time of flame extinction coincide. The results are reported on Fig. 2, where the three graphs are well superposed. All observations

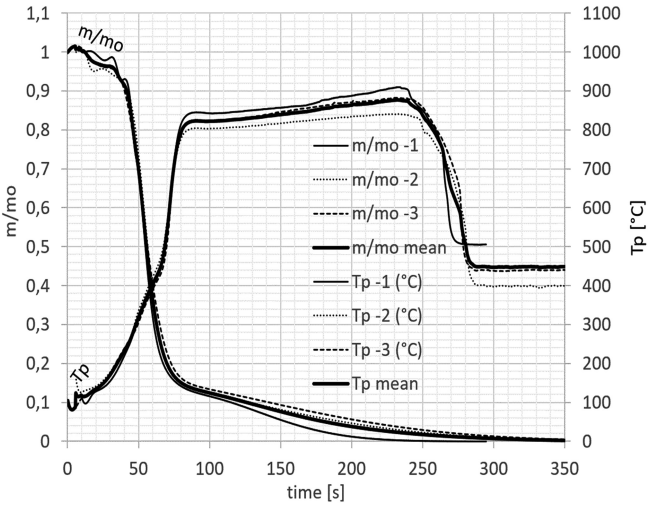

Fig. 2. Pellets of 15 mm size, temperature and mass loss for three tests. Time shifted values.

previously detailed for test-1 can be done for the two other tests, with the important processes occurring at the same times. For the remaining of the study, the time shift is applied for similar test conditions and thus temperature and mass evolutions with time are averaged.

3.2 Influence of Pellet Size Under 63.7 kW.m^{-2} Flux

Figure 3 shows the results obtained for pellets with four different lengths, 15–20–25–30 mm. For each size, the results are the average values of three tests as explained previously. Small differences are observed for the mass loss and the temperature. The length of the pellet has thus a weak influence on the heat transfer through the pellets. That means that the edge effects are non-significant and the heat and mass transfers can be assumed to be mainly occurring in the radial direction. These experiments allow to assume that for the chosen pellets, the times for drying, flame ignition and extinction do not depend on their sizes. These mean times are 32 s, 39 s and 74 s respectively for the time for drying, flame ignition and flame extinction, as indicated by the gray vertical lines on Fig. 3.

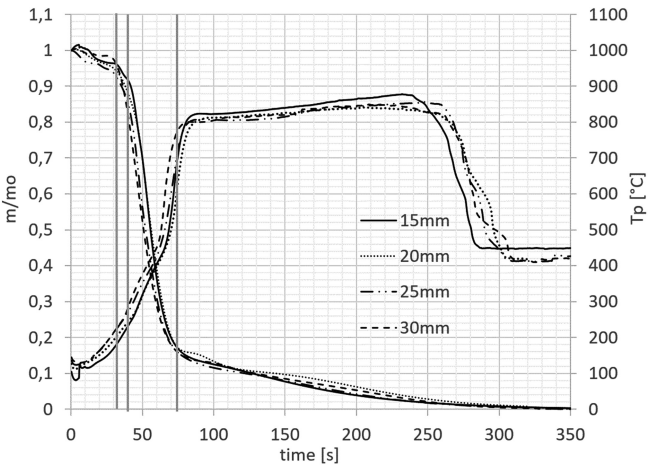

Fig. 3. Mass loss and temperature for four different pellet lengths. The dotted lines mark the drying, ignition and extinction mean times

3.3 Comparison of Pellets and Wood Pieces Under 63.7 kW.m^{-2} Flux

Small pieces of wood, with the same sizes as for the pellets, have been also degraded under the same heat flux. Their mass loss (m/m_o) and temperature are shown on Fig. 4, and compared to the pellet values. For wood and pellets, the reported results correspond to an average made on several tests with pieces of different size (15–20–25–30 mm) as previously explained for the pellets.

The temporal sequences observed for the pellets are also observed during the degradation of a sample of wood.

- A short period of drying.
- A slow heating and slow mass loss: conduction through the radial dimension.
- A flame ignition, faster heating and mass loss: presence of the flame, early release of volatiles.
- A faster heating: driven by the char thermal diffusivity, and the heat release of the char oxidation, the volatile emission and mass degradation slow down and the heterogeneous combustion of char begin to occur.
- A flame extinction, end of the emission of volatile matters.
- A temperature plateau during the heterogeneous combustion of char with a slower reaction kinetic compared to the previous volatile release, associated to the production of ashes.

All these phases occur earlier for wood samples; however, their variations and intensities are very similar to pellet ones. Considering that the elemental composition of woody pellet and wood particles are close (see Table 1), this is mainly explained by the lower density of the wood. For the same sample volume, the wood mass is lower and the durations of the main phases (drying, mass loss, and char oxidation) are shorter. The only particularity that can be noticed is that the time gap between the end of drying and the time of ignition is slightly longer for wood than for pellet. This time delay could be explained by different heat absorption and volatiles diffusivity, depending on the material structure (porosity, roughness, intern tubular cavity length and diameter, etc.). However, these small-scale parameters were not under the scope of the present study and have not been measured.

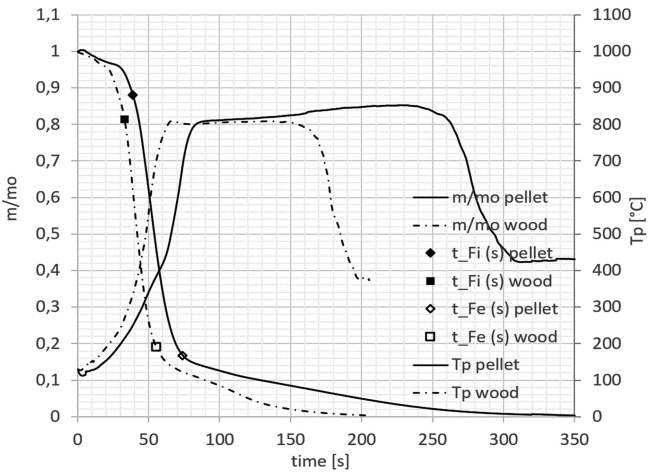

Fig. 4. Mass loss and temperature for wood and pellet samples.

4 Conclusion

The development of a new test bench has allowed the observation of the degradation of a small sample of biomass (pellet or wood) under flaming conditions. The mass loss and temperature at the center highlight the main phases of the thermal degradation of the samples, drying, ignition, extinction and char oxidation. The degradations of pellet and wood samples are very similar, the only difference is that the processes for wood are faster, mainly due to its lower density. The data will be helpful to perform further analyses, by simulating the combustion of biomass samples, in order to reproduce the obtained results and also to simulate the combustion in a biomass furnace.

Acknowledgments. The authors thank the MESCYT (Dom. Rep.) which has supported this work in the frame of the Caliope program.

References

1. U.S. Energy Information Administration (EIA) (s.d.) Consulté 22 novembre 2019, à l'adresse. https://www.eia.gov/energyexplained/biomass/
2. Simoes G et al (2017) Effect of gas temperature and oxygen concentration on single particle ignition behavior of biomass fuels. Proc Combust Inst 36(2):2235–2242
3. Corbetta AF et al (2014) Pyrolysis of centimeter-scale woody biomass particles: kinetic modeling and experimental validation. Energy Fuels 28:3884–3898
4. Di Blasi C, Branca C, Santoro A, Hernandez EG (2001) Pyrolytic behavior and products of some wood varieties. Comb Flame 124:165–177
5. Haseli Y, Van Oijen JA, De Goey LPH (2011) A detailed one-dimensional model of combustion of a woody biomass particle. Biores Technol 102(20):9772–9782
6. Hurley MJ, Gottuk DT, Hall JR Jr, Harada K, Kuligowski ED, Puchovsky M, Torero JL, Watts JM Jr, Wieczorek CJ (eds) (2015) SFPE handbook of fire protection engineering, 5th edn. Springer, New York
7. Anca-Couce A, Zobel N, Berger A, Behrendt F (2012) Smouldering of pine wood: Kinetics and reaction heats. Comb Flame 159:1708–1719

Study of Selected Fire Characteristics of Beech Wood Depending on Particle Size

Richard Kuracina(✉), Zuzana Szabová, and Karol Balog

Slovak University of Technology in Bratislava, Trnava, Slovakia
{richard.kuracina, zuzana.szabova, karol.balog}@stuba.sk

Abstract. Wood and its processing are associated with significant fire hazards. In the past, there were many significant fires of wood clouds that caused property damage and human lives. The study of flammable wood clouds fire characteristics is the basis for fire and explosion protection. The article deals with the study of the influence of particle size on the ignition temperature of settled and swirled beech wood dust. Measurement of fire characteristics was performed according to EN ISO/IEC 80079-20-2 in GG oven and heated surface. The sample was dust from beech wood with different particle sizes. By measuring, it has been found that with decreasing particle size, the flammability of the samples improves and the minimum ignition temperature (MIT) also decreases.

Keywords: Fire safety · Fire characteristics · Beech wood · Particle size

1 Introduction

The mechanical processing of wood (sawing, planning, milling, and grinding) creates a large quantity of dust, which pose a risk of fire or explosion [1]. Dust created by wood working is flammable and can form an explosive mixture with air [2]. Many authors [3–6] discuss the influences of wood properties on the flammability and external conditions affecting the thermal degradation of wood and wood dust.

Dusts form explosive atmospheres if cloud concentrations are within the explosive range. When dusts are not removed from suspension by appropriate ventilation, they settle in layers or accumulations at a rate depending on properties such as particle size. A dust layer is not an explosive atmosphere itself, but it is a potential explosive atmosphere since it may form explosive mixtures with air [7].

Besides, dusts may present hazard even if dust layers are not likely to form a dust cloud, but also ignite due to self-heating or exposure to hot surfaces or thermal flux and cause a fire hazard or overheating of equipment. One of the most common ignition sources in all kind of industrial facilities are hot surfaces. The capability of a heated surface to cause ignition depends on the type of the particle substance. This capability becomes greater with increasing temperature and increasing surface area [7, 8].

In order to quantify this risk and to establish safe working conditions, the minimum ignition temperature of dust layer (MIT) is used. MIT is the lowest temperature at which a layer of dust of specific thickness ignites on a heated surface and it is

L. Makovicka Osvaldova et al. (Eds.): WFS 2020, *Wood & Fire Safety*, pp. 16–21, 2020.
https://doi.org/10.1007/978-3-030-41235-7_3

determined according to EN ISO/IEC 80079-20-2 [9]. This standard establishes conditions to determine the MIT of a layer of 5 mm thickness.

2 Materials and Methods

To determine minimum ignition temperatures of dust layers and clouds a research method was applied, in conformity to the standard STN EN ISO/IEC 80079-20-2 [9].

The MIT at which the layer of dust (of specified thickness) located on a heated furnace plate undergo thermal decomposition and/or ignite was determined. The heated surface consists of a circular metal plate and provide a working area of 200 mm in diameter and 20 mm in thickness. The plate is heated electrically an its temperature is controlled by thermocouple [9–11].

The dust layer was formed without compression of the layer. Dust was tested in a layer of 5.0 mm depth. The temperature was measured within the layer at the height of 2 mm from the surface of the plate, at the centre of the dust layer. Temperature was measured at 1 s intervals over the test period. Ignition was confirmed if:

1. visible glowing or flaming was observed, or
2. a temperature of 450 °C was measured in the dust layer, or
3. a temperature rise of 250 K above the temperature of the heated plate was measured in the dust layer.

Godbert-Greenwald (G-G) furnace was used to measure the MIT of dust cloud. G-G furnace is a vertical pipe furnace where the silica tube placed inside the furnace is set up in a vertical position, and its lower end is open to the atmosphere. This pipe is heated to the desired temperature with the use of a device that controls furnace temperature. Below the pipe is a stainless-steel mirror which allows visual monitoring of the furnace interior [10].

Finally, the flammability of sample was determined by modified Hartmann´s tube. The test equipment consists of a vertical tube closed at the bottom with a dispersion cup. As an ignition source an electric igniter EMP-SO-U4 was used.

Beech wood dust with a moisture content of 5.7 wt% was used as a sample. The sample was sieved to 0–56 μm, 56–71 μm, 71–90 μm, 90–150 μm, and 150–200 μm fractions. Sample was sieved 60 min on a Retch AS 200 with an amplitude of 0.5 mm.

3 Results and Discussion

In a first step, the flammability of a beech dust sample in a modified Hartmann tube was determined. The test result was positive at a fraction of 0–56 μm and at a dust concentration of 500 $g.m^{-3}$. Pictures from the test record (recorded at 1000 fps) is shown in Fig. 1.

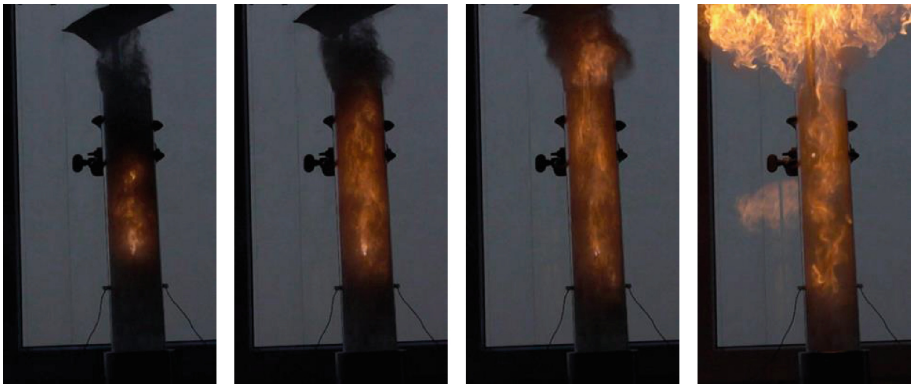

A - Ignition of the dust cloud from the igniter EMP-SO-U4

B - Burning of dust cloud inside the tube

C - Flame out of the tube

D - Burning the dust cloud outside the tube

Fig. 1. Record of flame propagation of beech wood dust (500 g.m^{-3}) during flammability test in modified Hartmann tube

The beech dust sample was then tested for MIT of settled and whirled dust at fractions of 0–56 µm, 56–71 µm, 71–90 µm, 90–150 µm, and 150–200 µm.

The minimum ignition temperature (MIT) of settled dust was measured according to standard EN ISO/IEC 80079-20-2 and the result is the temperature at which a positive test result was obtained within 10 min from the start. Temperature records for fractions 0–56 µm, 56–71 µm and 150–200 µm are shown in Figs. 2, 3 and 4.

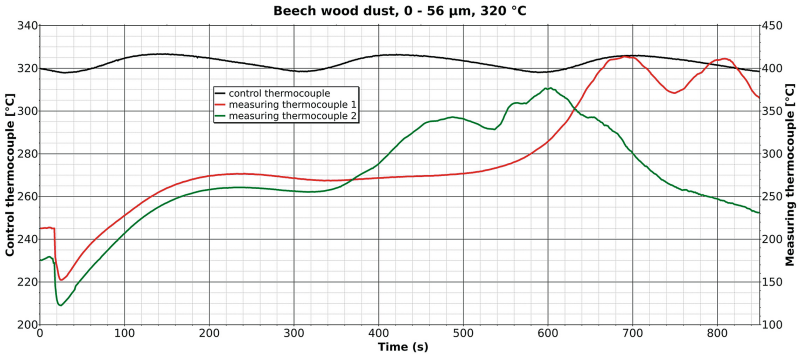

Fig. 2. MIT measuring records of 5 mm beech wood dust layer at 320 °C, fraction 0–56 µm

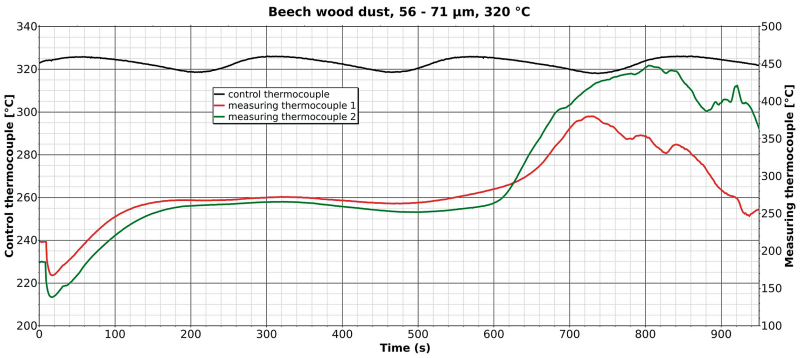

Fig. 3. MIT measuring records of 5 mm beech wood dust layer at 320 °C, fraction 56–71 µm

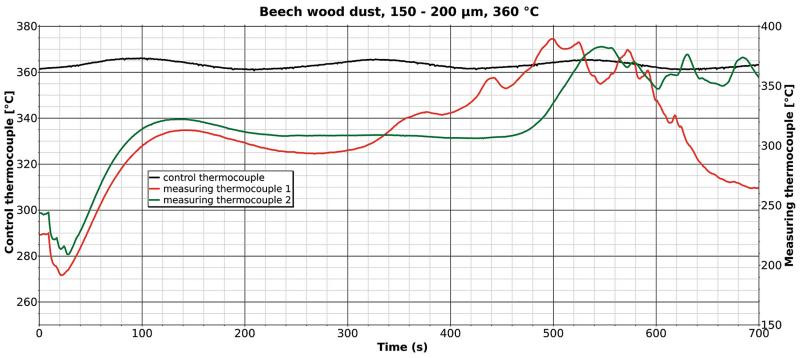

Fig. 4. MIT measuring records of 5 mm beech wood dust layer at 360 °C, fraction 150–200 µm

MIT of whirling dust was measured according to standard. The test results in a temperature at which the dust cloud in the tube ignites. The sample weight was 0.1 g and the tests were carried out at an air pressure of 30 and 50 kPa. At dispersing dust pressure of 30 kPa, higher MIT values were achieved. Therefore, only MIT values at 50 kPa are listed in Table 1. The results for all MIT measurements are shown in Table 1 and Fig. 5.

Table 1. Minimal ignition temperature (MIT) of beech wood dust with positive result

Fraction	MIT of dispersed dust (sample weight 0.1 g; 50 kPa air pressure)	MIT of settled dust (layer height 5 mm)
0–56 µm	365 °C	320 °C (340 s)
56–71 µm	370 °C	320 °C (600 s)
71–90 µm	370 °C	340 °C (100 s)
90–150 µm	380 °C	340 °C (400 s)
150–200 µm	390 °C	360 °C (330 s)

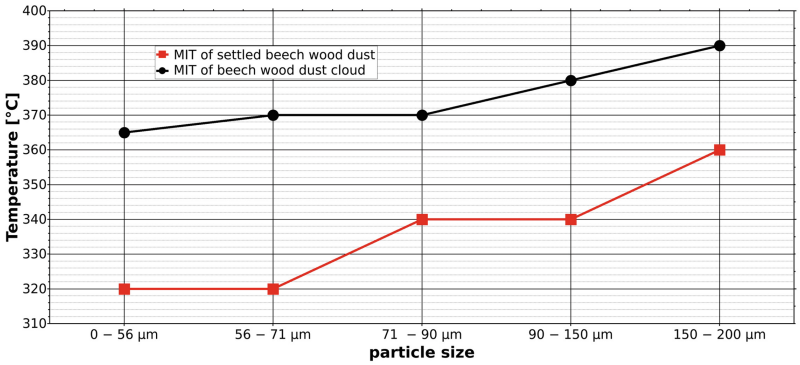

Fig. 5. MIT of beech wood dust in dependence of particle size (fraction)

A test in a modified Hartmann tube determined that the beech dust sample is flammable and explosive. The determination of the lower explosion limit (LEL) and other explosion parameters (p_{max}, dp/dt_{max}) is possible in the equipment in accordance with standard EN 14034.

The MIT of settled beech dust increases with increasing particle size of the fraction. The lowest temperature of 320 °C was reached for the fraction with particle size 0–56 and 56–71 µm, the highest temperature 360 °C was reached for the fraction with particle size 150–200 µm. MIT of dispersed dust also increases with increasing particle size of the fraction. The lowest temperature of 365 °C was reached for the fraction with a particle size of 0–56 µm, the highest value of 390 °C was reached for the fraction with a particle size of 150–200 µm.

A test in a modified Hartmann tube determined that the beech dust sample was flammable and explosive. The determination of the lower explosion limit and other explosion parameters is possible in the equipment in accordance with STN EN 14034.

4 Conclusion

A study of MIT beech wood dust found that MIT is dependent on the particle size of the sample. In both cases, MIT increases with increasing particle size of beech wood dust. The lowest MIT value of the whirling dust was reached at the 0–56 µm fraction. The lowest MIT of deposited dust was achieved with fractions 0–56 µm and 56–71 µm. The highest MIT values of settled and whirled beech dust were determined at a fraction of 150–200 µm.

Further study of beech wood dust will be focused on the determination of the explosion characteristics depending on the size of the fraction in the chamber KV 150-M2.

Acknowledgement. This work was supported by the Slovak Research and Development Agency under the contract No. APVV-16-0223 and by Institutional project 1611 DUSTCONTROL.

References

1. Marková I, Mračková E, Očkajová A, Ladomerský J (2016) Granulometry of selected wood dust species of dust from orbital sanders. Wood Res 61(6):983–992
2. Očkajová A, Marková I (2016) Particular size analysis of selected wood dust species particles generated in the wood working environment. ACTA Universitatis Matthiae BELII Ser Environ Manag 18(2):24–31
3. Zachar M, Mitterová I, Xu Q, Majlingová A, Cong J, Galla Š (2012) Determination of fire and burning properties of spruce wood. Drvna Industrija 63(3):217–223. https://doi.org/10.5552/drind.2012.1141
4. Osvaldova Makovicka L, Osvald A, Kačíková D (2014) Char layer of various tree parts from selected coniferous wood. Adv Mater Res 1001:276–281. https://doi.org/10.4028/www.scientific.net/AMR.1001.276
5. Marková I, Ladomerský J, Hroncová E, Mračková E (2018) Thermal parameters of beech wood dust. BioResources 13(2):3098–3109. https://doi.org/10.15376/biores.13.2.3098-3109
6. Marková I, Hroncová E, Tomaškin J, Tureková I (2018) Thermal analysis of granulometry selected wood dust particles. BioResources 13(4):8041–8060
7. Fernandez-Anez N, Garcia-Torrent J (2019) Influence of particle size and density on the hot surface ignition of solid fuel layers. Fire Technol 55(1):175–191
8. EN 1127-1 (2011) Explosive atmospheres. Explosion prevention and protection. Basic concepts and methodology
9. EN ISO/IEC 80079-20-2 (2016) Explosive Atmospheres - Part 20-2: Material Characteristics - Combustible dusts tests methods
10. Polka M, Salamonowicz Z, Wolinski M, Kukfisz B (2012) Experimental analysis of minimal ignition temperatures of a dust layer and clouds on a heated surface of selected flammable dusts. Proc Eng 45:414–423
11. Slabá I, Tureková I (2012) Smouldering and Flaming Combustion of Dust Layer on Hot Surface. Scientific Monographs, Dresden 88 p ISBN 978-3-9808314-5-1

Characterization of Wood Chemical Changes Caused by Pyrolysis During Flaming Combustion Using X-Ray Photoelectron Spectroscopy

Laura E. Hasburgh[1(✉)], Donald S. Stone[2], Samuel L. Zelinka[1], and Nayomi Z. Plaza[1]

[1] US Forest Products Laboratory, 1 Gifford Pinchot Drive, Madison, WI 53726, USA
laura.e.hasburgh@usda.gov
[2] Materials Science and Engineering, University of Wisconsin, 1509 University Ave, Madison, WI 53706, USA

Abstract. As heat is applied to wood, thermal degradation, called pyrolysis, occurs. A majority of what is known about the pyrolysis of wood has been obtained using either extracted component polymers or wood pyrolyzed in an inert atmosphere. However, the physical and chemical reactions that occur during pyrolysis of wood are affected by the interaction of the polymers in whole wood as well as the oxygen present in the atmosphere. X-ray photoelectron spectroscopy (XPS) is a surface measurement technique that yields information on both the chemical composition of the sample and the chemical bonds among the elements and compounds that comprise it. Here, XPS was used as a tool to examine the number and type of carbon bonds in Douglas fir exposed to flaming combustion.

Keywords: XPS · Wood · Chemical composition · Pyrolysis

1 Introduction

When exposed to high temperatures, wood thermally degrades as a series of complex chemical and physical transformations. This thermal degradation is known to adversely affect structural properties of wood [1]. Yet, current knowledge of the chemical and physical changes that occur in wood during pyrolysis remains limited, particularly the knowledge related to the wood products for structural applications. Some concerns have been raised that the current understanding might not be conservative enough when calculating the structural load capacity post-fire [2]. A more thorough understanding of thermal degradation of wood is critical in maximizing wood's potential applications while maintaining a high degree of safety [3].

L. Makovicka Osvaldova et al. (Eds.): WFS 2020, *Wood & Fire Safety*, pp. 22–27, 2020.
https://doi.org/10.1007/978-3-030-41235-7_4

1.1 Chemical Changes in Wood Due to Pyrolysis

The polymeric components of wood are irreversibly altered as wood is exposed to high temperatures. The majority of what is known about thermal degradation of wood has been obtained using thermogravimetric analysis (TGA) on isolated polymeric components [4]. Dehydration takes place at temperatures between 105 °C and 200 °C [4]. Above 200 °C, the breakdown of the major polymeric components of wood begins. Hemicelluloses are the most thermally sensitive and begin to breakdown between 200 and 260 °C [4]. Cellulose thermally decomposes between 240 and 350 °C, and lignin thermally decomposes between 280 and 500 °C. There is a great deal to learn from the previous body of work based on TGA. However, thermal degradation of the isolated wood components is different from what occurs within bulk wood because, in wood, the entwined nature of the component polymers combined with the hierarchical structural of wood can alter the resulting effect of pyrolysis. Additionally, many of the kinetic parameters obtained by traditional TGA were conducted in non-oxidizing atmospheres and likely have limited applicability in terms of pyrolysis models used to describe structural wood fires (Fig. 1).

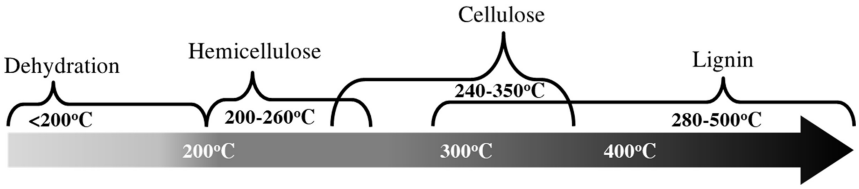

Fig. 1. Thermal stages of wood pyrolysis from TGA analysis. Redrawn from [4, 5].

The current knowledge of wood pyrolysis is mostly based on isolated wood polymers and is insufficient for understanding the formation of char in bulk wood material. In this work we present in-situ measurements of the elemental composition present in the pyrolysis zone and char layer of wood exposed to fire in atmospheric conditions.

1.2 X-Ray Photoelectron Spectroscopy (XPS)

XPS is a surface-sensitive quantitative spectroscopic technique that measures the elemental composition, chemical state and electronic state of the elements that exist within a material. XPS works by irradiating a sample material with soft x-rays, which can penetrate the surface to a depth of 10 nm. Then, when the x-rays reach the sample's surface, photoelectrons are ejected from the sample and their kinetic energies (KE) are measured by an analyzer. The binding energy of the electrons is deduced from the KE and source photon energy. The resulting energies depend upon the element, the orbital from which the electron was ejected, and the chemical state of the element.

XPS has been used to study the surface chemistry of black cherry, red oak and pine wood surfaces [6], wood surfaces post heat-treatment in inert environments [7] and on

isolated wood polymers [8]. Based on binding energy and the types of bonds found in wood constituents, there is an agreement on the number and type of bonds to use for deconvolution of the C1s peak [7]. Since the peaks for the chemical states that exist within the C1s spectrum are close together, it is necessary to deconvolute to identify individual contributions. The deconvoluted peaks were used to qualitatively evaluate the elemental changes in the charred wood (Table 1).

Table 1. Chemical bond types present in wood and the component polymer attributions.

Bond	Binding type	Binding energy (eV)
C-C or C=C	Aliphatic carbon bonding from carbon contamination or Aromatic Carbon (abundant in lignin)	285.0
C-O	From alcohols and ether functional groups (abundant in cellulose)	286.4
O-C-O	From ketones	287.6
COOH	From carboxylic acid due to oxidation of an aldehyde group	289.2
π-π*	From aromatic carbons in lignin (shake up)	291.5

2 Methods and Materials

2.1 Charred Wood

The wood specimen was obtained from one board of Douglas fir (*Pseudotsuga menziesii*) lumber with final dimensions of 100 mm × 100 mm × 21 mm. To measure the thermal wave through the Douglas fir specimen, we inserted 30-gauge, Type K thermocouples into the specimens through horizontal holes drilled at heights of 4 mm, 8 mm, 12 mm, and 16 mm below the top surface (Fig. 2a). Additional thermocouples were placed between the back of the sample and the retainer frame (i.e., at 21 mm) and on the specimen's top surface. The temperatures between thermocouples were calculated using a non-linear spline fit.

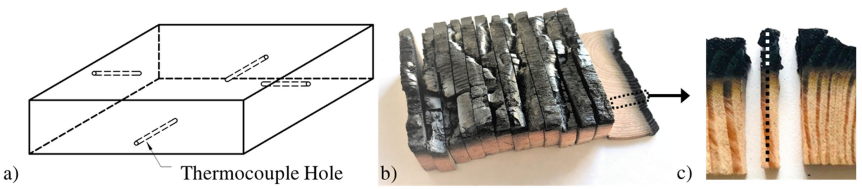

Fig. 2. (a) Schematic of wood specimen with holes for thermocouples, (b) charred wood specimen sliced into 4 mm sections and (c) sliver of charred wood with latewood for XPS analysis. The dotted line represents the line scan.

The radial face of the specimen was exposed to a constant heat flux of 50 kW/m^2 using a cone calorimeter (FTT iCone Mini, East Grinstead, West Sussex, UK) without piloted ignition. Prior to exposure in the cone calorimeter, the specimens were conditioned in an oven at 105 °C for 24 h to drive off any moisture. The test was terminated by removing the specimen and extinguishing the fire with water when the temperature of the thermocouple at 21 mm reached 100 °C.

The charred wood specimen was then cut along the transverse plane into 4 mm sections (Fig. 2b). To avoid edge effects caused by the cone calorimeter holder, a 4 mm slice from the center of the specimen was chosen and a latewood growth ring was selected for XPS line scans.

2.2 XPS Line Scan

For our experiments, the x-ray source was an aluminum Kα micro-focused monochromator housed in a Thermo K-Alpha X-Ray Photoelectron Spectrometer. With this equipment, a line scan was carried out with a total of 72 spots, each with a spot size of 30 μm. Each initial scan had an analyzer pass energy of 200 eV to obtain the survey spectra between zero and 1230 eV. Higher resolution scans were obtained with an analyzer pass energy 50 eV to increase the spectral resolution. For the C1s scans, the binding energy range surveyed was 179–298 eV. To avoid the effects of surface impurities, the surface was etched for 20 s with an Argon ion beam before the XPS measurement. The line scan was set up on a small wood sliver (Fig. 2c), measuring approximately 16 mm × 1.3 mm × 1.8 mm. The line scan started at the unexposed/uncharred edge of the specimen and ended at the exposed/charred edge.

3 Results

The XPS survey spectra at two spots in the line scan are depicted in Fig. 3. The C1s (around 285 eV) and the O1s (around 532 eV) photoelectron peaks were clearly resolved. While Auger electrons are resolved above 1200 eV, photoelectron peaks from other atoms were minor, showing the wood consists mainly of carbon and oxygen. The intensity of the C1s and O1s peaks decreased with an increase in exposure temperatures as the readings moved towards the exposed edge of the wood.

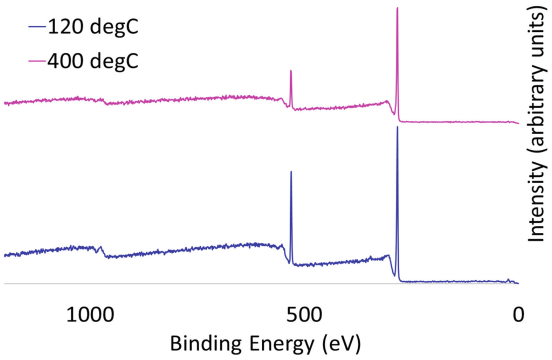

Fig. 3. XPS survey spectra at two spots within the wood sliver.

The C1s spectra was chosen to investigate the chemical structure of the charred wood due to the difficulty of O1s peak extraction that results from complex shift behavior [9]. To determine the type of chemical bonds present and their contribution to the total spectra, the C1s high resolution spectra was deconvoluted using an automated peak fitting routine [10] with a Pseudo-Voigt function [11] with a Shirley background correction [12]. Figures 4a and b shows the deconvoluted C1s spectra at the same spots as the survey spectra in Fig. 3. As shown in Fig. 4, the extracted peaks within the C1s spectra are changing with exposure temperatures. The intensity of all peaks decreases with an increasing temperature. Further analysis to quantify these changes are underway.

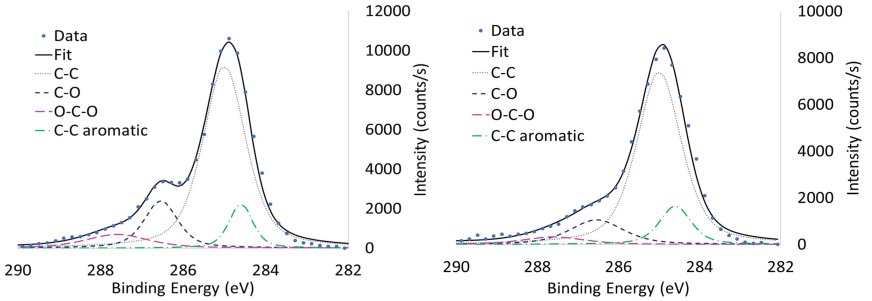

Fig. 4. Deconvoluted XPS high resolution C1s peaks at (a) 120 °C (b) 400 °C.

To take into consideration potential changes in the electrical resistivity from the unmodified wood to the charred regions, we used an internal reference that set the C-C peak at 285 eV for all spots within the line scan. The amount the peaks were shifted with respect to 285 eV is known as the charge compensation. The charge compensation changes from the uncharred wood through to the charred region (Fig. 5). This represents a reduction in electrical resistivity as the wood polymers thermally degrade and carbon is left behind [7].

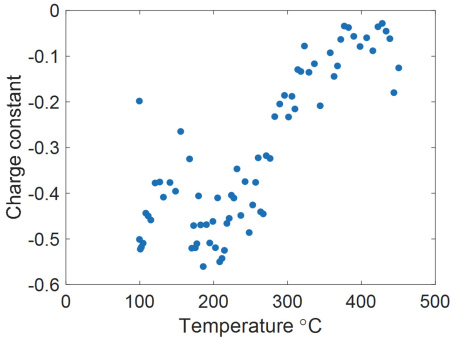

Fig. 5. Change in charge compensation through the charred wood slice from the unexposed edge at 100 °C to the charred edge at 450 °C.

4 Concluding Remarks

Current knowledge regarding the chemical and physical changes that occur in wood during pyrolysis is limited. This project utilizes XPS to examine the type of carbon bonds in Douglas fir exposed to flaming combustion in an effort to better understand the thermal degredation of the polymers in bulk wood.

Here, a change in the amount of material being irradiated is deducible from the survey spectra in addition to a noticeable change in electrical resistivity. Further data analysis of the deconvoluted C1s peak is required to quantify the relationship between the chemical structure of the wood polymers and the exposure temperatures in bulk wood.

Acknowledgements. The authors gratefully acknowledge use of facilities and instrumentation supported by NSF through the University of Wisconsin Materials Research Science and Engineering Center (DMR-1720415).

References

1. White RH (2016) Analytical methods for determining fire resistance of timber members. In: SFPE handbook of fire protection engineering. Springer, pp 1979–2011
2. Schmid J, Just A, Klippel M, Fragiacomo M (2015) The reduced cross-section method for evaluation of the fire resistance of timber members: discussion and determination of the zero-strength layer. Fire Technol 51:1285–1309
3. Zelinka SL, Hasburgh LE, Bourne KJ, Tucholski DR, Ouellette JP, Kochkin V, Hudson E, Ross RJ, Martinson KL, Lebow ST (2018) Compartment fire testing of a two-story mass timber building. Energy Technol 5:1179–1185
4. Hill CA (2007) Thermal modification of wood. In: Hill CA (ed) Wood modification: chemical, thermal and other processes. Wiley, West Sussex, UK, pp 99–126
5. Shafizadeh F, Chin PP (1977) Thermal deterioration of wood. Wood Technol: Chem Aspects 43:57–81
6. Nzokou P, Pascal Kamdem D (2005) X-ray photoelectron spectroscopy study of red oak-(Quercus rubra), black cherry-(Prunus serotina) and red pine-(Pinus resinosa) extracted wood surfaces. Surf Interf Anal 37:689–694
7. Inari GN, Petrissans M, Lambert J, Ehrhardt J, Gérardin P (2006) XPS characterization of wood chemical composition after heat-treatment. Surf Interf Anal 38:1336–1342
8. Bañuls-Ciscar J, Abel M-L, Watts JF (2016) Characterisation of cellulose and hardwood organosolv lignin reference materials by XPS. Surf Sci Spectra 23:1–8
9. Hua X, Kaliaguine S, Kokta B, Adnot A (1993) Surface analysis of explosion pulps by ESCA Part 2. Oxygen (1s) and sulfur (2p) spectra. Wood Sci Technol 28:449–459
10. Plaza N (2019) Automated Peak Fitting Routine for XPS Data from Wood (Version from March 2019). http://doi.org/10.2019/xps.wood
11. Newville M, Stensitzki T, Allen DB, Rawlik M, Ingargiola A, Nelson A (2016) LMFIT: Non-linear least-square minimization and curve-fitting for Python. Astrophysics Source Code Library
12. Herrera-Gomez A (2011) The peak-Shirley background. Internal Report. Centro de Investigación y de Estudios Avanzados del Instituto Politécnico Nacional (CINVESTAV-IPN)

Initiation Parameters of Wood Based Materials

Peter Rantuch(✉), Jozef Martinka, and Igor Wachter

Faculty of Materials Science and Technology in Trnava, Slovak University of Technology in Bratislava, 917 24 Trnava, Slovakia
peter.rantuch@stuba.sk

Abstract. Worldwide, wood-based materials are massively exploited in many industries. As a renewable material with significantly lower environmental impact compared with conventional materials is very likely that their production will grow in the future. This paper deals with the determination of parameters characterizing the initiation of not only solid wood as the original raw material but also of other composites produced from it. Specifically, the parameters are: critical heat flux, thermal response parameter, initiation temperature and apparent thermal inertia. These parameters are calculated based on the dependencies between external heat flux and time to initiation suggested in the literature. During the measurement, samples of selected materials were dried to zero humidity and subsequently exposed to thermal radiation of varying intensities using a cone emitter. The results of these measurements were evaluated by graphs. Calculated values of initiation parameters are listed in a summary table and can be used for further calculations in the area of personal and property fire protection.

Keywords: Wood · Critical heat flux · Thermal response parameter · Initiation temperature · Apparent thermal inertia

1 Introduction

Initiation parameters can be defined as material properties which determine its behavior in the initial burning phase. This paper focuses on the following parameters: critical heat flux, thermal response parameter, thermal inertia and initiation temperature.

The critical heat flux (q_{cr}) is the heat flux between the lowest incident heat flux at which ignition occurred and the highest incident heat flux where ignition did not occur. It can be used to evaluate the possibility of ignition [1].

The thermal response parameter (TRP) can be considered as an indicator of the ignition resistance of a material [1]. The higher the TRP value, the longer it takes for the material to heat up, ignite, and initiate a fire [2].

Thermal inertia (I) is an effective fire property of importance in both ignition and flame spread problems [3]. Since it is temperature dependent, the thermal inertia at ignition is not that obtained at ambient conditions. Instead the thermal inertia at ignition is an apparent value and it will be shown that this apparent thermal inertia can be obtained from ignition data [4]. The surface temperature of materials with low thermal inertia rises quickly when heated [5].

L. Makovicka Osvaldova et al. (Eds.): WFS 2020, *Wood & Fire Safety*, pp. 28–34, 2020.
https://doi.org/10.1007/978-3-030-41235-7_5

2 Material and Methods

Babrauskas states that for particle board the minimum thickness required to insure that the specimen is thermally thick can be represented by [6]:

$$L = \frac{0{,}6\rho}{q_i}, \tag{1}$$

where L is minimum thickness required to insure, ρ is density and q_i is incident heat flux.

As Spearpoint and Quintiere point out, the time to initiation for thermally thick materials is dependent on thermal conductivity (k), density, specific heat (c) a initiation temperature (T_{ig}), ambient temperature (T_∞) and incident heat flux [4]:

$$t_{ig} = \frac{\pi}{4} k\rho c \left(\frac{T_{ig} - T_\infty}{q_i} \right)^2 \tag{2}$$

Based on the graphical representation of the dependence of $t_{ig}^{1/2}$ and q_i it is possible to determine the theoretical critical heat flux $q_{i,cr}$. Some authors consider this value to be a critical heat flux [7–9], but others recommend adjusting it using certain correlations [4, 10].

The equations used to calculate the initiation parameters are shown in Table 1.

Table 1. Equations used to calculate initiation parameters

Parameter	Equation		Source
Critical heat flux	$q_{cr} = \frac{q_{i,cr}}{0{,}76}$	(3)	[4]
Thermal response parameter	$TRP = \sqrt{k\rho c}\left(T_{ig} - T_\infty\right)$	(4)	[1, 11]
Thermal inertia	$I = k\rho c$	(5)	[4, 12–14]
Initiation temperature	$T_{ig} = \sqrt{4}\left(\frac{q_{cr}}{\varepsilon\sigma} + T_\infty^4\right)$	(6)	Stefan-Boltzmann law

Initial parameters were determined for 6 materials: oriented strand board (OSB), plywood with pine veneer on the surface referred to below as pine plywood, birch plywood, pine piedroit, spruce board and thermopine. Prior to measurement the samples were all adjusted to 100 mm × 100 mm and stored in an oven at 100 °C for 48 h. The density characterization of the dried samples is in Fig. 1. All the samples can be considered as thermally thick materials (Table 2).

Table 2. Equations used to calculate initiation parameters

Thickness [mm]	OSB	Pine plywood	Birch plywood	Pine piedroit	Spruce board	Thermopine
Minimum required to thermally thick material	13.5	15.5	16.5	12.2	12.1	11.8
Declared by producer	25.0	18.0	18.0	18.0	18.0	19.0
Owen dry samples	24.0	18.2	17.5	16.9	17.1	19.0

Measurements were performed on the cone calorimeter. The time to initiation was monitored at heat fluxes of 25 kW.m $^{-2}$, 30 kW.m^{-2}, 35 kW.m^{-2} and 40 kW.m^{-2}. At each heat flux, 3 samples were used, except pine piedroit, where 5 samples were used because of the low homogeneity. During the measurement, the ambient temperature was between 28 °C and 29 °C, the air humidity was from 72% to 75%.

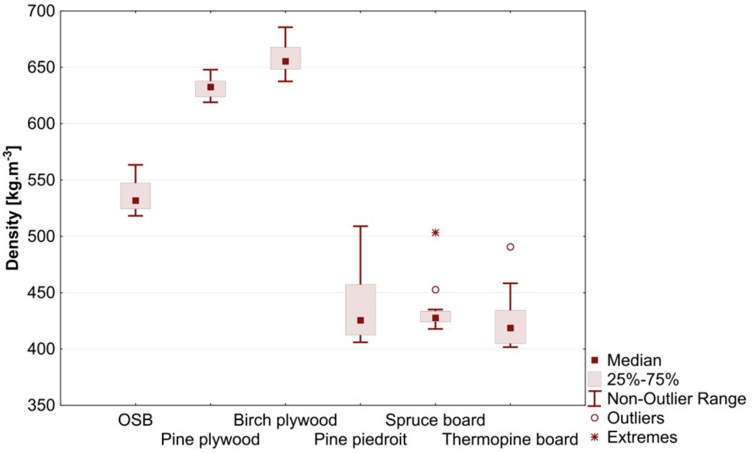

Fig. 1. Box graph of sample densities

3 Results

Time dependence of sample initiation from external heat fluxes was constructed from the measured data (Fig. 2). From the equations of their trend lines, the initiation parameters for the individual measured wood based materials, which are listed in Table 3, were calculated. It also contains the respective determination coefficients.

When calculating the initiation temperature, it is necessary to know the emissivity of the measured material. For this purpose, a value of 0.9 corresponding to the emissivity of spruce [15] and close to the emissivity of OSB [16] was used.

Dependencies for almost all materials achieved a high degree of correlation. The exception is pine piedroit, in which case there was a significant problem with the homogeneity of the sample during the measurement. By visual observation, difference in resin content was obvious. Drying at 100 °C resulted in the resin flowing out of the wood to the wood surface. This fact then influenced the whole measurement when the time to initiate the flame burning of samples with a large surface area covered with resins was significantly lower. The dependence thus shows a downward trend, but the coefficient of determination is significantly lower.

Several authors were involved in the calculation of initiation parameters. Critical heat flux for ignition has been calculated to be between 10 kW.m^{-2} and 13 kW.m^{-2} for a range of wood products [17]. Spearpoint and Quintiere report values for the critical flow of different tree species for longitudinal section from 10.8 kW.m^{-2} do 16 kW.m^{-2}, for theoretical ignition temperature 304 °C–384 °C and theoretical apparent thermal inertia between 0.22 kJ^2.m^{-4}.K^{-2}.s^{-1}–1.1 kJ^2.m^{-4}.K^{-2}.s^{-1} [4]. In Moghtaderi et al. the critical heat flux of the various species was set at 10.3 kW.m^{-2}–14 kW.m^{-2} and apparent thermal inertia from 0.071 kJ^2.m^{-4}.K^{-2}.s^{-1} to 0.478 kJ^2.m^{-4}.K^{-2}.s^{-1} [18]. Relatively high critical heat flux values are reported by Xu et al. Among the five trees the lowest value of critical heat flux was determined for shorea (16 kW.m^{-2}) and the highest for merbau (40 kW.m^{-2}). The initiation temperatures are then from 456 °C to 643 °C and thermal response parameter between 152 kW.s^{0,5}.m^{-2}–275 kW.s^{0,5}.m^{-2}. However, these results may be the result of measurements at significantly higher heat fluxes (25 kW.m^{-2}–75 kW.m^{-2}) [1]. For plywood, Batiot et al. calculated critical heat flux 12 kW.m^{-2} and 14 kW.m^{-2} and thermal response parameter 156 kW.s^{0,5}.m^{-2} and 181 kW.s^{0,5}.m^{-2} [19] and by Fateh et al. critical heat flux 10.5 kW.m^{-2} and 11 kW.m^{-2} and thermal response parameter 124 kW.s^{0,5}.m^{-2} a 136 kW.s^{0,5}.m^{-2} [20].

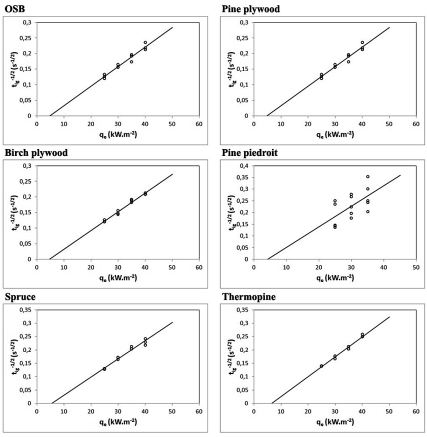

Fig. 2. The inverse of the square root of time to initiate samples by the external heat flux

The calculated critical heat fluxes range from 6 kW.m^{-2} to 9.7 kW.m^{-2}. These values are slightly lower than those measured by the authors mentioned, but in some cases, albeit less frequently, similar or lower values occur [21, 22]. Slight differences from the results of other authors may be due to the properties of materials such as those reported by White and Dietenberger [17], or the use of different initiation sources with different energies or environmental conditions [23]. Other parameters fall within the scope of the literature. The exception is pine piederoite, whose low homogeneity has been transferred to the calculations and its initiation parameters differ considerably by the results of other authors and other measured materials.

Table 3. Coefficients of determination and initiation parameters of measured materials

Material	R^2 [−]	q_{cr} [kW.m^{-2}]	TRP [kW.s^{0,5}.m^{-2}]	T_{ig} [°C]	I [kJ^2.m^{-4}.K^{-2}.s^{-1}]
OSB	0.9544	6.4	141	331	0.1929
Pine plywood	0.9401	9.3	134	387	0.1260
Birch plywood	0.9779	6.0	148	324	0.2236
Pine piedroit	0.5463	9.7	88	394	0.0517
Spruce	0.9647	7.3	130	350	0.1469
Thermopine	0.9861	8.7	118	376	0.1037

4 Conclusion

The following conclusions can be drawn from the measured data for the initiation parameters of the measured wood-based materials:

1. The critical heat flux reaches from 6.4 kW.m^{-2} to 9.3 kW.m^{-2}.
2. The thermal response parameter has been determined to 118 kW.s^{0,5}.m^{-2}–148 kW.s^{0,5}.m^{-2}.
3. The initiation temperature relative to the critical heat flux for wood based materials is 355 °C ± 32 °C, but to determine it more precisely, it is necessary to determine the emissivity of wood samples depending on the surface temperature of the wood.
4. Apparent thermal inertia was calculated to be from 0.1037 kJ^2.m^{-4}.K^{-2}.s^{-1} to 0.2236 kJ^2.m^{-4}.K^{-2}.s^{-1}.
5. The low homogeneity of resin content of the pine samples does not allow for an unambiguous determination of the initiation parameters and the calculated values should only be considered as indicative.

Acknowledgments. This work was supported by the Slovak Research and Development Agency under the contract No. APVV-16-0223.

References

1. Xu Q, Chen L, Harries KA, Zhang F, Liu Q, Feng J (2015) Combustion and charring properties of five common constructional wood species from cone calorimeter tests. Constr Build Mater 96:416–427
2. Dao DQ, Luche J, Richard F, Rogaume T, Bourhy-Weber C, Ruban S (2013) Determination of characteristic parameters for the thermal decomposition of epoxy resin/carbon fibre composites in cone calorimeter. Int J Hydrogen Energ 38:8167–8178
3. DiNenno PJ (2008) SFPE handbook of fire protection engineering. SFPE, Gaithersburg
4. Spearpoint MJ, Quintiere JG (2001) Predicting the piloted ignition of wood in the cone calorimeter using an integral model—effect of species, grain orientation and heat flux. Fire Saf J 36(4):391–415
5. Karlsson B, Quintiere J (1999) Enclosure fire dynamics. CRC Press, Boca Raton
6. Babrauskas V, Parker WJ (1987) Ignitability measurements with the cone calorimeter. Fire Mater 11:31–43
7. Fangrat J, Hasemi Y, Yoshida M, Hirata T (1996) Surface temperature at ignition of wooden based slabs. Fire Saf J. 27:249–259
8. Goff LJ (1993) Investigation of polymeric materials using the cone calorimeter. Polym Eng Sci 33:497–500
9. An W, Jiang L, Sun J, Liew KM (2015) Correlation analysis of sample thickness, heat flux, and cone calorimetry test data of polystyrene foam. J Therm Anal Calorim 119:229–238
10. Delichatsios MA (2000) Ignition times for thermally thick and intermediate conditions in flat and cylindrical geometries. Fire Saf Sci 6:233–244
11. Tewarson A, Ogden SD (1992) Fire behavior of polymethylmethacrylate. Combust Flame 89:237–259
12. Delichatsios MA, Panagiotou TH, Kiley F (1991) The use of time to ignition data for characterizing the thermal inertia and the minimum (critical) heat flux for ignition or pyrolysis. Combust Flame 84:323–332
13. Harada T (2001) Time to ignition, heat release rate and fire endurance time of wood in cone calorimeter test. Fire Mater 25:161–167
14. Patel P, Hull TR, Stec AA, Lyon RE (2011) Influence of physical properties on polymer flammability in the cone calorimeter. Polym Adv Technol 22:1100–1107
15. Kraniotis D, Nore K, Brückner C, Nyrud AQ (2016) Thermography measurements and latent heat documentation of Norwegian spruce (picea abies) exposed to dynamic indoor climate. J. Wood Sci 62:203–209
16. Rantuch P, Kačíková D, Martinka J, Balog K (2015) The influence of heat flux density on the thermal decomposition of osb. Acta Facultatis Xylologiae Zvolen res Publica Slovaca 57:125–134
17. White RH, Dietenberger MA (2001) Wood products: thermal degradation and fire. In: Encyclopedia of materials: science and technology, pp 9712–9716
18. Moghtaderi B, Novozhilov V, Fletcher DF, Kent JH (1997) A new correlation for bench-scale piloted ignition data of wood. Fire Saf J 29:41–59
19. Batiot B, Fateh T, Rogaume T, Luche J, Richard F (2013) Experimental investigation of thermal degradation for three kinds of wood. In: Fire and Materials 2013
20. Fateh T, Rogaume T, Luche J, Richard F, Jabouille F (2014) Characterization of the thermal decomposition of two kinds of plywood with a cone calorimeter–FTIR apparatus. J Anal Appl Pyrol 107:87–100

21. Tsai K-C (2009) Orientation effect on cone calorimeter test results to assess fire hazard of materials. J Hazard Mater 172:763–772
22. Boonmee N, Quintiere JG (2002) Glowing and flaming autoignition of wood. Proc Combust. Inst 29:289–296
23. Wu W, Yang L, Gong J, Qie J, Wang Y, He Y (2011) Experimental study of the effect of spark power on piloted ignition of wood at different altitudes. J Fire Sci 29:465–475

Odor and FT-IR Analysis of Chemical Species from Wood Materials in Pre-combustion Condition

Kyoko Kamiya(✉) and Osami Sugawa

Suwa University of Science, 5000-1 Toyohira, Chino-shi,
Nagano Prefecture, Japan
{kamiya, sugawa}@rs.sus.ac.jp

Abstract. Not only are signals about smoke and temperature rise, given by fire, but there is also a burnt smell characteristic of fire. Focusing on the odor quality changing, it was applied to fire detection in the early stages. In order to clarify the relationship between changes in odor quality and temperature during oxidation pyrolysis and pyrolysis, the generated odor gas is collected in a sampling bag attached to the exhaust port of the TG-DTA/FT-IR system. FT-IR was used to measure pyrolysis and combustion gases to determine chemical species based on temperature rise rate. The overall odor of the molecules generated by pyrolysis and oxidative pyrolysis in the collected gas every 300 s was then measured using electronic noses. The representation test sample was Japanese cedar. For TG-DTA, the oxygen concentration was set to 0–20% and the temperature rise rate was set to 2–20 K/min. The FT-IR results for the aldehyde group showed a lower temperature at which the absorption peaked than that by the CO. As a result of comparison between odor changes and chemical species during fire combustion, the similarity index of aldehyde groups to the odor at the time of initial fire increased by oxidative pyrolysis. From these facts, in wood and related material it was found that detection of substances based on aldehyde groups among odors generated during pyrolysis and/or combustion can be used as a possibility of fire detection for wooden materials.

Keywords: FT-IR · Odor · Wooden materials · Electronic nose · Fire detection

1 Introduction

Fire detectors are ready for sensing a fire in an early stage and alerting residents, so as to start initially them to take action of escape, evacuation and/or firefighting. In Japan, the installation of fire detectors is obligatory for fire prevention properties, such as residential houses, constructions and buildings of having a certain area, shops, and important cultural assets. Sensors detect a fire automatically based on the temperature-rise, smoke, and flame-flicker that a fire gives. Smoke, heat, and flame sensors are widely used in fire detectors, and it has been found that CO sensors are effective at detecting fire [1]. Multi-criteria fire detectors in which CO, temperature, and smoke sensors are combined are currently being studied [2–4]. Fires emit odor in addition to heat, smoke, and toxic gases such as CO [5]. The odor could be considered as one of

L. Makovicka Osvaldova et al. (Eds.): WFS 2020, *Wood & Fire Safety*, pp. 35–40, 2020.
https://doi.org/10.1007/978-3-030-41235-7_6

important physical quantities as a fire sign. It was focused on this change in quality of odor and intended to apply for fire detection in its early stage [6–8]. In this report, chemical species of gases generated during thermal decomposition and combustion were measured by FT-IR. And the quality of odor was measured by the electronic nose.

2 Experiment

A thermal analyzer, TG-DTA (Thermogravimetry–differential thermal analysis), was used for heating samples to simulate the beginning and early stage of fires, with the condition of constant temperature rising rate. TG-DTA is a method of thermal analysis in which the mass of a sample is measured over time as the temperature changes. This measurement provides information about physical phenomena, such as phase transitions, absorption, adsorption and desorption [9]. The exhaust port of TG-DTA (TG8120, Rigaku Corp.) and the gas cell of FT-IR (Fourier Transform Infrared Spectroscopy: FT-IR 4000, JASCO Corp.) were connected (TG-DTA/FT-IR simultaneous measurement method). The gas emissions from TG-DTA system was drawn continuously through a heated sample line to the Gas Cell of the FT-IR. The sampling line and the Gas Cell were heated and kept at about 140 °C [10]. The measurement conditions of the TG-DTA were set as follows: sample weight approximately 5 mg, aluminum pan, reference material Alumina, atmosphere of oxygen concentration 0–20%, gas flow rate of 300 ml/min, rate of temperature increase at 2–20 K/min, and attained temperature of 550 °C. The cell volume was 0.5 L and the optical path of 2.7 m. The cell was fitted with NaCl windows. The nominal resolution was 8 cm^{-1}. The measurement conditions of the FT-IR were set as follows: measurement range of 1000–4000 cm^{-1}, sampling interval of 30 s, total measurement time was about 0.5–5 h.

Japanese Cedar was used as one of the test samples. This sample was crushed to fine pieces by a Wonder Blender (WB-1, Osaka Chemical Co., Ltd.), and the crushed ones of its size of smaller than 200 meshes were employed in the test. In order to minimize the influence of water, the samples were dried at least 15 days in a desiccator containing silica gel at room temperature until there was no weight change.

The gas generated during the oxidative thermal decomposition in a TG-DTA system was collected by an odor bag attached to the exhaust port of the system. The odor bag was replaced every 5 min of the gas at each time. In order to collect the odor gas released from the sample before thermal decomposition, atmospheric gas was allowed to flow while the sample was in the place, and the gas was collected immediately after the start of measurement. The gas collected between 0 to 5 min was regarded as the unit sample for those of every 5 min. The collected gas was diluted by a factor of 5 to 20 with pure N_2 (G1), depending on the odor quality, and measured using the electronic noses (FF-2A, Shimadzu Corp.).

The electronic nose is a device that distinguishes between odor components based on the output balance of sensors, and unlike devices such as gas chromatography mass spectrometry and FT-IR, which does not detect the type of chemical substance. The electronic nose system imitates the way people distinguish odors. Similarity indices indicate to what extent the sensor response value patterns resemble the standard gasses. The similarity indices were defined based on the angle (θ) between the vector for the

standard gas and the odor vector for the sample gas on a 10-dimensional space created from 10 sensors. The similarity index was 100% (i.e., the sample gas was the same as the standard gas) at $\theta = 0°$ and similarity is assumed as 0% if the is equal or greater than 15° [11]. The inner product angle $\theta = 15°$ means that the similarity is 0.966. The standard gases were selected aldehyde series (Butyraldehyde) and CO gas.

3 Results and Discussion

Figure 1 shows FT-IR spectra of the Japanese cedar, measurement condition was an atmosphere of oxygen concentration 20%, the rate of temperature increase at 2 K/min. Changes among the spectra of all samples were observed at wavenumbers of 1120.44 cm^{-1}, 1182.15 cm^{-1}, 1725.98 cm^{-1}, 1787.96 cm^{-1}, 2817.49 cm^{-1}, 2177.24 cm^{-1}, and 2362.37 cm^{-1}. Regardless of wooden kinds, such as coniferous trees, hardwood trees, bamboo, etc., it changed in all wooden materials as well. The functional groups at these wavenumbers are those of secondary alcohol (1120.44 cm^{-1}), tertiary alcohol (1182.15 cm^{-1}), ester (1725.98 cm^{-1}), alkene (1787.96 cm^{-1}), aldehyde group (2817.49 cm^{-1}), CO (2177.24 cm^{-1}), and CO_2 (2362.37 cm^{-1}). Thus, we focused attention on these chemical species. Figure 2 shows relations between transmittance and temperature at these wavenumbers.

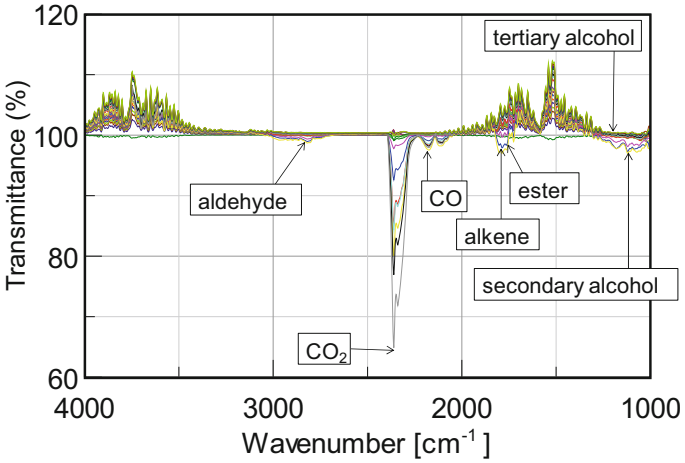

Fig. 1. FT-IR spectra of Japanese cedar (rate of temp.: 2 K/min).

Figure 2 shows (a) the TG-DTA, (b) the transmittance and temperature of the chemical species (FT-IR), and (c) the odor measurement results for the Japanese cedar. From the TG-DTA measurement results, a weight reduction due to evaporation of water in the samples was observed at temperatures up to approximately 100 °C. Then, a weight reduction due to the oxidative thermal decomposition was observed at around 230 °C and above. At approximately 320 °C, the first stage exothermic peak was observed,

which was assigned to be due to the combustion of cellulose and hemi-cellulose contained in wooden materials. The second exothermic peak due to combustion of lignin was observed at approximately 450 °C. From the FT-IR measurement results shown in (b), at approximately 250 °C and above, aldehyde group, alcohols group, ester group, alkene group, CO, and CO_2 were detected. From the odor measurement results shown in (c), at approximately 230 °C and above the similarity index for aldehyde group rose, in contrast the similarity index for CO roses at higher than 280 °C.

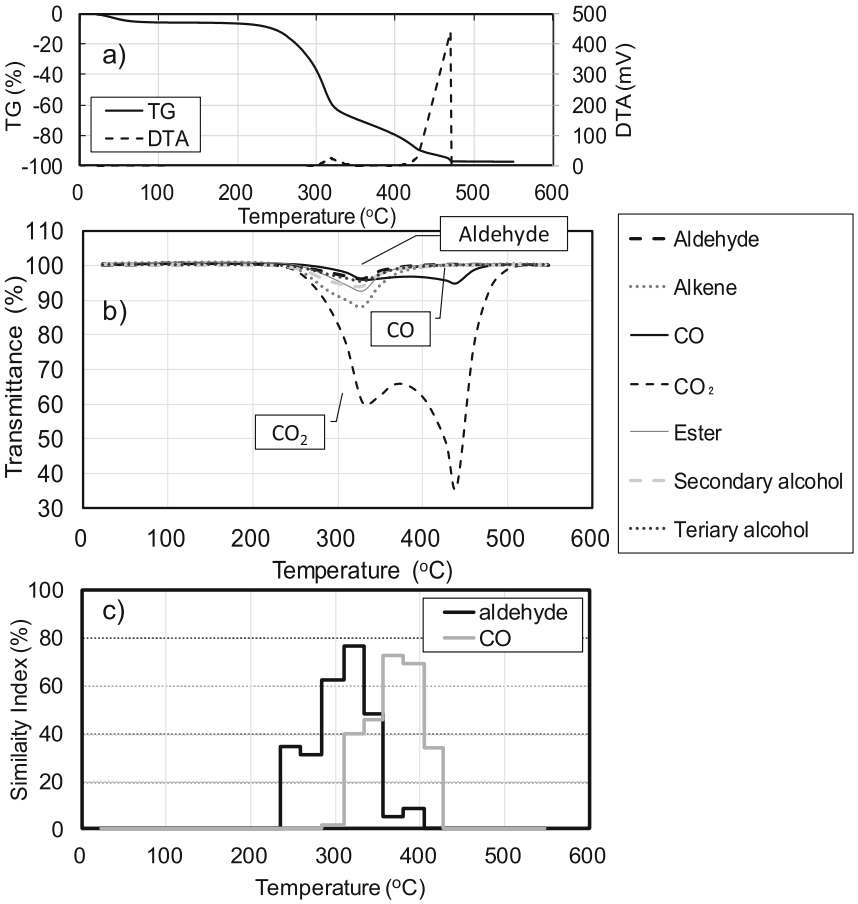

Fig. 2. Measurement results of (a) TG-DTA, (b) FT-IR, (c) Odor with O_2 concentration of 20% and temperature rise rate of 5 K/min

Figure 3 shows temperature ranges in which the aldehyde group and CO species of the Japanese cedar were detected. Aldehyde group and CO began being detected in this order from approximately 200 °C. In all experiments, aldehyde group was detected at a lower temperature than CO. As the heating rate increased, both the aldehyde group and

CO detection temperatures were increased. Through comparison with the TG-DTA measurement results shown in Fig. 2(a), it was assigned found that aldehyde group was generated in the early stage of the oxidative thermal decomposition, in which the weight began decreasing at approximately 200 °C. In this experiment the CO detection temperature was about 250 °C, nearly 50 °C higher than the aldehyde group. We found from these results that the early stage of the oxidative thermal decomposition of the wooden materials can be detected by detecting aldehyde group.

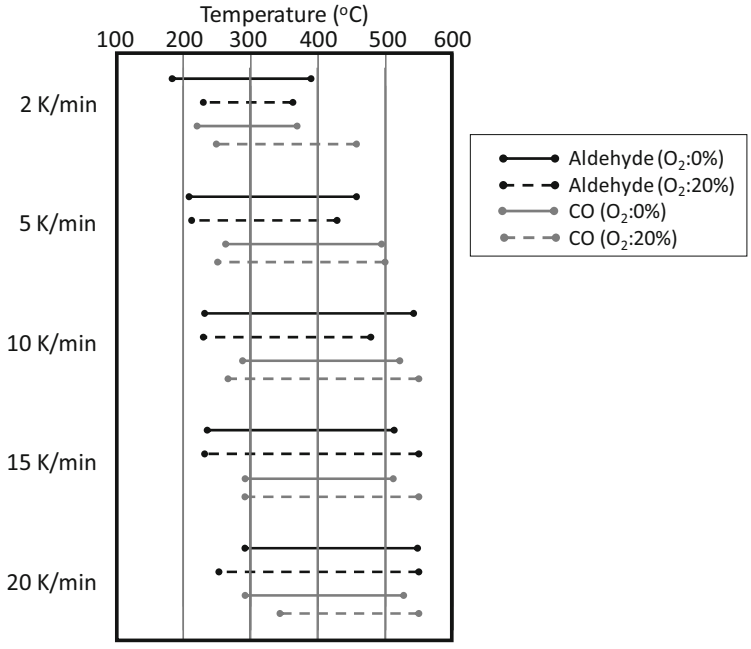

Fig. 3. Temperature ranges of the samples in each of which a substance containing an aldehyde group and CO was detected by the FT-IR.

During fire, not only wood and related material burn, but also synthetic polymers and hydrocarbon-based flammable liquids are involved in the combustion. The previous study [3] have shown that the combustion of the synthetic polymers increases the similarity index for aldehydes. However, the hydrocarbon-based flammable liquids and polystyrene do not generate aldehyde-based substances. The measurements by the electronic noses have clarified that combustion of kerosene increases the similarity index for hydrocarbons. Thus, types of burning materials can be identified by selecting several the standard gases in advance.

4 Conclusion

It is found from the TG-DTA/FT-IR simultaneous measurement results of the wooden materials that a substance containing secondary alcohol, tertiary alcohol, and an aldehyde group was generated in the early stage of the oxidative thermal decomposition (from 200 °C to 300 °C). CO and CO_2 were generated from at around 250 °C by the decomposition ended. As the sample temperature rising rate increased, the detection temperature of aldehyde groups and CO were shifted to higher. However, in all the experimental cases, aldehyde groups were generated at a lower temperature than CO. Founding from these results that strongly suggest the development of the technique of fire detection by odor, the fire can be detected in its early stage by focusing more attention on substances containing an aldehyde group than on CO and CO_2.

Acknowledgements. This study was supported partly by the Grant-in-Aid for Scientific Research (Basic Research B, No. 15H02982) FY2015-2017. The authors sincerely thank to Mr. Shou Kobayashi and Mr. Tatsuya Akahane, in Sugawa and Kamiya Lab., University of Science for their sincere contributions in conducting the tests.

References

1. Jackson MA, Robins I (1994) Gas sensing for fire detection: measurements of CO, CO_2, H_2, O_2, and smoke density in european standard fire tests. Fire Saf J. 22:181–205
2. Ryder NL (2017) Multicriteria detection: leveraging building control and comfort sensors for fire state determination. In: Proceedings of the 16th international conference on automatic fire detection I, pp 349–355
3. Mensch B, Cleary T (2017) A comparison of carbon monoxide gas sensing to particle smoke detection in residential fire scenarios. In: Proceedings of the 16th international conference on automatic fire detection I, pp 363–370
4. Arndt G, Suchy S, Vialkowitsch D (2017) Multi-criteria/multi-sensor early fire detection in the engine compartment of road vehicles: evaluation process of gas sensors. In: Proceedings of the 16th international conference on automatic fire detection II, pp 47–54
5. Kohla D, Eberheim A, Schieberle P (2005) Detection mechanisms of smoke compounds on homogenous semiconductor sensor films. Thin Solid Films 290:1–6
6. Sugawa O, Kamiya K, Oka Y (2014) Evaluation on odor intensity and quality from plastic and wood materials in pre-combustion condition. In: 15th international conference on automatic fire detection, vol 15, pp 21–28
7. Kamiya K, Sugawa O, Imamura T, Oka Y (2013) Experimental study on odor intensity and quality from wood materials in oxidative pyrolysis. Bull Japan Assoc Fire Sci Eng 63(2):25–35 (in Japanese)
8. Kamiya K, Sugawa O, Kanai H, Imamura T, Oka Y (2011) Evaluation on odor intensity and quality from wood in pre-combustion condition. In: Proceedings of Asia Pacific symposium on safety, pp 344–347
9. Tanaka, S Iida Y (1999) Instrumental Analysis, Shikabo, pp 332–338 (in Japanese)
10. ISO 19702 (2006) Toxicity testing of fire effluents – Guidance for analysis of gases and vapors in fire effluent using FTIR gas analysis
11. Kita J, Aoyama Y, Kinoshita M, Nakano H, Akamaru H (2000) Technical digest of the 17th sensor symposium, pp 301–305

Effect of Thermal Load on the Heat Release Rate of the Selected Types of Wooden Floorings

Linda Makovicka Osvaldova(✉) and Michaela Horvathova

Faculty of Safety Engineering, Department of Fire Engineering, University of Zilina, Zilina, Slovakia
linda.makovicka@fbi.uniza.sk

Abstract. The main topic of the article is the effect of thermal load on the heat release rate of the selected types of wooden floors. The article describes three types of fruit trees used for making floor - cherry, apple and plum tree. To obtain necessary information, cone calorimeter, which is described in the article in detail, was used for the experiment. The main quantity observed was the heat release rate (HRR - Heat Release Rate) depending on time. Six samples having the size of 100 × 100 × 10 mm were used for the experiment. Three types of wood samples were subjected to thermal load of 40 kW/m^2 and the other three to the load of 60 kW/m^2. Practical part focuses on the summary of individual measurement in the cone calorimeter. The description of all three types of wood is shown in tables showing the resulting values. In addition, a graphic representation of the dependence of HRR and time is included as well. On the basis of this, a comparison is carried out. Our goal was to find out the differences between the two levels of thermal load and, at the same time, to compare the wooden floors according to their flammability level based on HRR.

Keywords: Heat Release Rate · Cone calorimeter · Fruit wood · Fruit wood burning · Wooden floors

1 Introduction

Wooden floors are very popular due to their natural look, nice smell and thermal properties. Such floors are beautiful and also pleasant to the touch. Moreover, wood is much warmer compared with a laminate floor. Thermal insulation properties of wood floor are much better, too. The advantage of natural wood in the form floor is its easy repair. After any reconstruction, the floor looks as good as new. Floors have a wide range of use, e.g. as floor covering for the interior of houses, cottages or it is suitable for the exterior e.g. as garden houses, terraces or around pools. We can choose from a variety of dimensions and materials.

Economic aspect is often taken into consideration - some types of floorings are very expensive and therefore people often opt for an imitation. Robust structure of wood makes the floor resistant to rot, fungi and insects, without using any harmful chemicals. These floors are also, to a large extent, fire-resistant. Another natural property of wood - the ability to catch fire and burn - can sometimes be a problem.

L. Makovicka Osvaldova et al. (Eds.): WFS 2020, *Wood & Fire Safety*, pp. 41–49, 2020.
https://doi.org/10.1007/978-3-030-41235-7_7

The article presents some examples of tree species which are used for making floorings and we want to point out different behaviors of the selected types of fruit tree species under various thermal loads. We evaluated the results of the tests using cone calorimeter and assessed fruit wood from the point of view of fire protection.

1.1 Cone Calorimeter and Its Use

Cone calorimeter is a device which can determine heat release rate (HRR - Heat Release Rate) using model materials on the basis of oxygen consumption and the measurement of carbon monoxide and carbon dioxide concentration under thermal load during small-scale tests. This device monitors the heat, weight loss and time to ignition in the process of burning. Its name is derived from its cone-shaped heating element, which is the source of radiant heat. Fire technical characteristics can be determined using cone calorimeter as well.

The measurement using cone calorimeter is carried out according to the technical standards ISO 5660-1-2002. Fire tests. Reaction to fire performance. 1. Part: Heat release rate of construction products (cone calorimeter method). This test method is used to compare or to find a certain behavior pattern of the material, since HRR generally has an impact on the course of fire. HRR is thermal energy produced per unit of time from a material in the course of burning under the given test conditions. HRR is one of the basic characteristics of fire, which should be taken into account when estimating fire hazard, since it has an important influence on the development of fire in a building. The standard specifies a method of determining HRR of smooth materials exposed to controlled values of radiant heat using an additional ignitor or without it. HRR is determined by measuring the oxygen consumption derived from concentration of oxygen and mass flow of combustion products. Time to ignition measurement is a part of the test method (steady flame burning).

2 Selection and Description of Samples

At the beginning of the article, we stressed out that the selection of a particular type of flooring is influenced by the interior itself, the stress it will be exposed to and our own preferences. In general, beech and oak floorings may seem dull to one because, out of all tree species, they are the most frequently used ones. Oak is, thanks to its properties, resistant to moisture and light. We selected non-standard types of tree species, which are less frequently used for floorings, however, thanks to their color, structure, characteristics, they are as practical as the other ones. We selected three types of fruit trees - apple, plum and cherry. The given type of tree species reflects the key features of the floor. Hardness, strength and color of the flooring depend on the type of the material used. We will have a closer look at these types of tree species.

2.1 Hardness

The harder wood is, the more expensive it gets. Deciduous tree species have hard wood and coniferous ones have soft wood. Apple, plum, cherry has the hardness degree (level) No. IV.

2.2 Flooring and Fruit Tree Species

Fruit trees floorings, perhaps with the exception of cherry tree, are not too popular, which is a pity. The wood is highly contrastive and of interesting color. Perhaps the most obvious differences in color are in the case of apple wood. It is therefore not suitable for larger floors. Apple wood is hard (hardness IV), thanks to its contrast it is used in places where its creates an optical dominant feature. Cherry wood is very firm (hardness (IV). Floors made out of cherry wood can be used in almost every single room of the house, its color is more vivid. Plum wood is similar to cherry wood in color, but its prevailing color is reddish over yellow. In addition, the wood and its tree rings have softer graining. Floors from plum wood are very hard (hardness IV) and they are usually used for rather small areas of smaller rooms, where they form an optical dominant feature of the space. Typical color is indicated by the given tree species. In the following figures (Fig. 1), we can see various color shades depending on the wood and its different structure.

Fig. 1. Types of floors (1) cherry tree (2) apple tree (3) plum tree

2.3 Samples

For measurements in cone calorimeter, three types of trees were used (apple, cherry, plum). Their dimensions were 100 × 100 × 10 mm. The samples were cut lengthwise. The samples were tested for two different heat loads - 40 kW/m^2 and 60 kW/m^2. This means that two measurements were carried out for each sample. 6 samples were tested altogether. The differences between the heat loads are specified in the experimental part of the article. All data from calorimeter were processed, tabled, plotted into a graph and evaluated. Each test was in accordance with the conditions defined in ISO 5660-1.

3 Experiment

The practical part focused on summary of individual measurement in the cone calorimeter. The description of all three types of wood is depicted as follows: tables of test results (apple, plum, cherry) under the heat load of 40 kW/m^2 and 60 kW/m^2, graphic representation of HRR vs time dependance.

A brief overview of the measured values is created using tables and graphs. Thanks to the obtained data, we can carry out a high-quality evaluation of the samples, allowing us to draw some conclusions. The table of the resulting parameters of the test includes all necessary data. In the table, we can compare data, times, peaks and total resulting parameters of the tests under the heat load of 40 kW/m^2 and 60 kW/m^2, that allow us to compare and find out the differences in values. The graphic section presents the measured values of HRR under different heat loads. The graphic section also describes the curves, the deviations between the samples, which occurred upon changing the head load.

3.1 Comparison of Results - Apple Tree Under the Heat Load of 40 kW/m^2 and 60 kW/m^2

The measured values for apple tree under the heat load of 40 kW/m^2 and 60 kW/m^2 are shown in Fig. 2 and Table 1. Table 1 shows the basic values of the measurement.

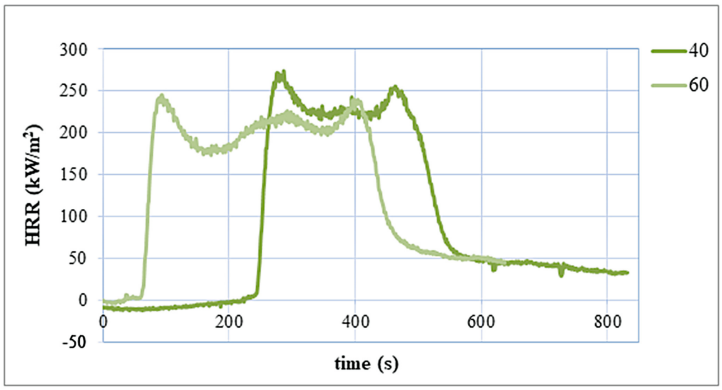

Fig. 2. The HRR curves for apple tree under the heat load of 40 and 60 kW/m^2

The curves are, at first sight, approximately the same. The curve under the heat load of 60 kW/m^2 is on the x-axis shifted a little bit more leftwards. This means that the sample of 60 kW/m^2 ignited 188 s sooner than the sample under the heat load of 40 kW/m^2. Both curves indicate that the heat from cone calorimeter is first absorbed by the samples, which results in negative HRR values on the y-axis. If we follow the curves away from negative values to positive HRR values, this means that the heat release from the sample grows slowly as a result of gases and vapors being released. If the right flammable concentration is created, ignition of the sample occurs which can also be seen on the curve, at 60 kW/m^2 ignition occurred in 62th second and at 40 kW/m^2 the sample ignited a little later - in 250th second. After ignition, flame burning occurs what is reflected in the graph by a sharp growth in HRR values.

HRR is reflected by the sharpness or perpendicularity of the curves. Rapid growth in values ends with the first peak, which is the maximum HRR value. The sample under the thermal load of 60 kW/m^2 reached the value of 246,598 kW/m^2 in 93 s. The sample of

Table 1. The resulting parameters for apple tree - 40 kW/m^2 and 60 kW/m^2

Data on the sample	Parameter	unit	40 kW/m^2		60 kW/m^2	
	Thickness	Mm	10		10	
	Initial weight	g	70.344		69.368	
Time of the test	Ignition time	s	250		62	
	Flame burning time	s	531		509	
	End of test	s	864		670	
	70% weight loss	s	459		346	
Peak values	parameter	unit	value	In time	value	In time
	HRR	kW/m^2	274.875	286	246.598	93
	Combustion heat	MJ/kg	80.137	277	72.391	101
	Weight loss rate	g/s	0.855	226	0.794	67
The results of the test	parameter	unit	value		value	
	Total HRR	MJ/m^2	62.07		81.377	
	Maximum HRR	kW.m^2	274.875		246.598	
	Average combustion heat	MJ.kg^{-1}	13.462		13.464	
	Average weight release rate	g/m^2	4610.880		6043.902	
	Average specific weight loss rate	g/(m^2.s)	16.409		13.521	

40 kW/m^2 - its value was a little bit higher - 274,875 kW/m^2. After reaching the peak HRR, burning persists in a moderate way, with a short decline and then slowly decreases what can be attributed to a gradual burn-away of certain layers of wood. The curve achieves its second peak for 60 kW/m^2 in 346 s and 40 kW/m^2 sample in 459 s.

By the end of second peak, most of the material of the sample has burned away - around 70%. Homogeneous combustion at higher thermal load was by 22 s shorter than with lower thermal load. After the peak, the curve suggests a gradual decrease, which smoothly changes into heterogeneous burning, in which the HRR goes down until the end of test. The end of test was for the 60 kW/m^2 sample reached 194 s sooner than for the sample with a lower thermal load.

3.2 Comparison of Results - Plum Under the Thermal Load of 40 kW/m^2 and 60 kW/m^2

After testing the apple tree samples, plum samples followed. The resulting values are shown in Fig. 3 and Table 2.

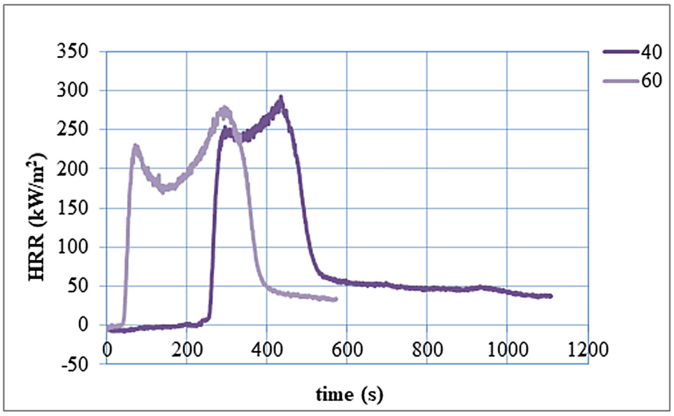

Fig. 3. HRR curves for plum wood samples under the load of 40 and 60 kW/m^2

Table 2. The resulting parameters of tests - plum under 40 kW/m^2 and 60 kW/m^2

Data on the sample	Parameter	unit	40 kW/m^2		60 kW/m^2	
	Thickness	Mm	10		10	
	Initial weight	g	65.095		64.668	
Time of the test	Ignition time	s	262		44	
	Flame burning time	S	513		475	
	End of test	s	1140		605	
	70% weight loss	S	439		314	
Peak values	parameter	unit	value	In time	value	In time
	HRR	kW/m^2	293.017	434	279.499	293
	Combustion heat	MJ/kg	86.662	424	83.862	280
	Weight loss rate	g/s	0.855	271	0.855	76
The results of the test	parameter	unit	value		value	
	Total HRR	MJ/m^2	57.370		71.838	
	Maximum HRR	kW.m^2	293.017		279.499	
	Average combustion heat	MJ.kg^{-1}	14.759		13.553	
	Average weight release rate	g/m^2	3887.032		5300.495	
	Average specific weight loss rate	g/(m^2.s)	15.486		12.298	

The chart shows that the curves are not as similar as it might seem at first glance. The sample at a higher thermal load and its representation in a chart is shifted leftwards along the horizontal axis. The beginning of the preparation stage before the ignition, when gases and vapors are being released from the sample, is much shorter for the higher thermal load compared to the lower thermal load. The sample at 60 kW/m^2 ignites in 44-s in comparison with the sample at 40 kW/m^2, which ignited much later - in 262th s. The arc, which represents the change into flame burning, is much smoother at the higher thermal load than at the lower thermal load. This phenomenon may be caused by an uneven surface of the sample. Upon ignition, there is a rapid increase in HRR. The curves have two peaks, where the first peak is much lower than the second one. This means that the maximum HRR values are achieved during the second peak. For the 60 kW/m^2 it is 279,499 kW/m^2 in 293th s and for 40 kW/m^2 it is 293,017 kW/m^2 in 434 s. The difference between the maximum values of higher and lower thermal load is 13,518 kW/m^2. The peaks are joined by a fine arc, in the first curve the arc is more rounded than in the other one. It is caused by a difference in the wood structure. The first curve is slightly wider than the second one. This can be explained by the length of flame burning. For the 60 kW/m^2 sample, flame burning occurs after 475 s and for 40 kW/m^2 after 513 s. By gradually reducing the heat release values, the curve changes from homogeneous burning into a heterogeneous one. By this time, more than 70% of the material has burned away. Length of combustion of the first curve ends in 605 s and the second curve ends in 1140 s.

3.3 Results - Cherry Wood Under the Thermal Load of 40 kW/m^2 and 60 kW/m^2

Next sample was cherry wood. The summary of the data is shown in Fig. 4 and the relevant data are shown in Table 3.

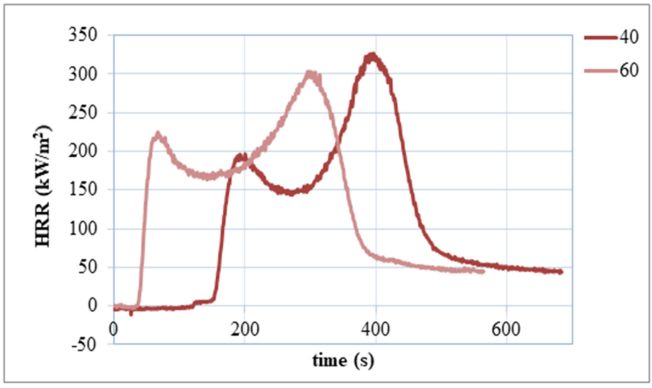

Fig. 4. HRR curves for cherry wood under the thermal load of 40 and 60 kW/m^2

Table 3. The resulting parameters of the test - cherry wood at 40 kW/m^2 and 60 kW/m^2

Data on the sample	Parameter	unit	40 kW/m^2		60 kW/m^2	
	Thickness	Mm	10		10	
	Initial weight	g	60.822		62.165	
Time of the test	Ignition time	s	150		42	
	Flame burning time	s	660		387	
	End of test	s	716		597	
	70% weight loss	s	394		312	
Peak values	parameter	unit	value	In time	value	In time
	HRR	kW/m^2	327.576	396	303.976	296
	Combustion heat	MJ/kg	60.583	194	67.106	64
	Weight loss rate	g/s	0.763	370	0.855	155
The results of the test	parameter	unit	value		value	
	Total HRR	MJ/m^2	72.935		68.658	
	Maximum HRR	kW.m^2	327.576		303.976	
	Average combustion heat	MJ.kg^{-1}	15.460		13.561	
	Average weight release rate	g/m^2	4717.581		5062.779	
	Average specific weight loss rate	g/(m^2.s)	9.250		14.675	

As soon as we look at curves, we can notice their similarity in shape. However, the preparatory phase for the curve at higher thermal load is only 42 s, while it is 150 s for the curve with the lower thermal load. After igniting the samples, rapid linear increase in HRR occurs and the first peak is reached. After reaching the first peak, HRR is slowly decreasing up to a point of a change. After that, the curve changes and again reaches a maximum peak. Second peak means the maximum HRR. During the load of 60 kW/m^2 it is 303,976 kW/m^2 in 296th second, for 40 kW/m^2, it is 327,576 kW/m^2 in 396th s. If we take a look at the second peak, we can say that the growth curve is the same as the downward curve. The sample with the higher peak, longer duration of the test is observed, which is affected in particular, by the thermal load the sample is exposed to. It means that the greater the heat load is, the sooner the wood burns away.

4 Conclusion

Based on the results, we can conclude that the HRR curve for all the three untreated samples of wood is approximately the same. If we comment on the shape of the curve briefly, each one begins with heat, which is transmitted by a thermal radiator and absorbed by a sample. The ignition and rapid combustion occur and reach its peak and then gradually decrease transforming into heterogeneous burning until it ceases to burn completely.

An assessment of the results at 40 kW/m^2, untreated samples of - apple, plum and cherry wood. If we compare the three types of wood samples, cherry wood ignited first - 150 s after being exposed to the thermal radiator of a cone calorimeter. The longest flame burning was recorded for cherry wood - 660 s. At the same time, cherry wood had the shortest testing time - 716 s. The value of 327,576 kW/m^2, belonging to cherry wood as well, was the highest HRR out of the three wood samples.

An assessment of the results at 60 kW/m^2, untreated samples of apple, plum and cherry wood. The fastest ignition time occurred in cherry wood - in 42 s. Its flame burning was the shortest - only 387 s - and the test ended after 597 s. Compared to the other samples, the HRR was the highest - 303,976 kW/m^2.

The shape of the curve is influenced by the thermal load. The structure of the tree species and the quantity of gases and vapors released during combustion played an important role as well. Getting to know the essential thermo-physical properties may be a prerequisite to eliminate the risk of fire. The order of the tree species from the point of view of their flammability can be done based on the test results. Cherry sample reacted in the most sensitive way to the heat load of 40 kW/m^2, followed by plum and the apple tree sample comes last. The order of the samples under the load of 60 kW/m^2 is then as follows: cherry, apple, plum wood samples.

References

1. Sonnier R, Otazaghine B, Ferry L, Lopez-Cuesta JM (2013) Study of the combustion effiency of polymers using a pyrolysis-combustion flow calorimeter. Combust Flame 160:2182–2193
2. ISO 5660-1:2015 (2015) Reaction-to-fire tests — heat release, smoke production and mass loss rate — Part 1: heat release rate (cone calorimeter method) and smoke production rate (dynamic measurement). International Standards Organisation
3. Gao M, Xu Y (2016) Flame retardancy of wood treated with GUP by cone calorimetry. In: 3rd international conference on mechatronics and information technology
4. Gerad J, Guibal D, Paradis S, Cerre JC (2017) Tropical timber atlas: technological characteristics and uses, 1st edn. Editions Quæ, Paris, pp 600–602
5. ASTM E1354-17 (2017) Standard test method for heat and visible smoke release rates for materials and products using an oxygen consumption calorimeter. ASTM International
6. Cone calorimeter. http://polymer.sav.sk/old/index.php
7. Babrauskas V (2016) The cone calorimeter. In: Hurley MJ et al (eds) SFPE handbook of fire protection engineering. Springer, New York, pp 952–980

Toxic Gas Emissions from Plywood Fires

Bintu Grema Mustafa[1,2(✉)], Miss H. Mat Kiah[1], Gordon E. Andrews[1(✉)], Herodotos N. Phylaktou[1], and Hu Li[1]

[1] School of Chemical and Process Engineering, University of Leeds, Leeds, UK
{pm08bgm, G.E.Andrews}@leeds.ac.uk
[2] Chemical Engineering, University of Maiduguri, Maiduguri, Nigeria

Abstract. Toxic emissions from four construction plywoods were investigated using a freely ventilated cone calorimeter with raw predilution hot gas sampling. Each plywood sample was exposed to the conical heater of the cone calorimeter radiating at 35 kw/m^2. Rich mixtures occurred in some of the tests, these rich mixtures produced high concentrations of toxic gases. The 4 samples had different peak heat release rate HRR, but similar steady state HRR. The elemental analysis of the four samples showed that they had different nitrogen content, indicating different glues were used. Plywood B had the highest N content of 6.43%, which resulted in the highest HCN concentration. The most important toxic species were CO, HCN, acrolein, formaldehyde and benzene on both an LC_{50} and $COSHH_{15\ min}$ basis.

Keywords: Toxicity · Wood fires · FTIR

1 Introduction

Wood products are extensively used in building construction, furniture and interior furnishing. Commonly used construction wood products include: plywood, MDF, Oriented strand board (OSB) and chipboard. However, despite these products being in common usage little information has been published on their toxic hazards in fires. This work is concerned with plywoods and uses four commercially available types, where the thickness and number of wood layers differ. These processed wood products generally use glues as a binder and these contain organically bound nitrogen which can give rise to HCN in the fire products and so the burning of these potentially pose a greater health hazard in fires than for unprocessed wood. The authors have shown [1–3] for pure construction pine wood crib fires in a confined 1.6 m^3 enclosure that the main toxic gases were CO, acrolein, formaldehyde and benzene. In most of these pine wood compartment fires HCN was not significant, apart from during the early stages of one fire where HCN had a significant contribution to the toxicity [3]. It will be shown in this work that for all four plywoods that HCN and NO_2 emissions were very significant additional toxic gases to those for pure pine wood.

The majority of deaths and injuries from exposure to fire smoke are as a result of inhalation of toxic effluents [4]. Wood as the most dominant fire load accounts for approximately 65% of CO emissions [5]. Survivors of fires often describe toxic gases as acidic and/or irritant gases, and these slow the movement of people eventually

L. Makovicka Osvaldova et al. (Eds.): WFS 2020, *Wood & Fire Safety*, pp. 50–57, 2020.
https://doi.org/10.1007/978-3-030-41235-7_8

leading to their death [6–9] through the impairment of escape. There is currently no legislation that requires toxic gas measurements from fires for any material used in buildings. Only light obscuration by smoke in standard fire tests is required to be measured for building materials. The main toxic products in most fires were shown by Purser [6] to be CO, HCN and irritant or acidic gases. The concentration of each depends on the type of fuel and on the thermal decomposition products of the materials when heated in a fire, which also depends on the fire temperature and ventilation.

The most common method of assessing the toxicity of fire products is the LC_{50} 30 min exposure concentration which aim at predicting the concentrations at which 50% of the people will die in the fire if exposed to the gas concentration for 30 min [7]. COSHH [10] is the European statutory law on occupational exposure limits equivalent to the US short term (10 min) exposure limits AEGL2. The $COSHH_{15\ min}$ toxic gas concentration represents a safe condition for 15 min for escape not to be impaired. The USA Acute Exposure Guideline Levels [7] AEGL 2 10 min exposure are equivalent to the $COSHH_{15\ min}$ levels for disabling and impairment of escape. This work used the $COSHH_{15\ min}$ and the LC_{50} to assess the toxicity of gases emitted from plywood fires based on impairment of escape and lethality.

2 Materials and Methods

Four types of construction plywood were investigated as shown in Table 1: plywood A (PWA), plywood B (PWB), Dark plywood (DPW) and Light Plywood (LPW).

Table 1. Fuel characteristics

Parameter	PWA	PWB	LPW	DPW
Proximate Analysis (wt%) (daf)				
Volatile Matter	79.47	80.81	82.64	84.23
Fixed Carbon	20.53	19.19	17.36	15.77
Ultimate Analysis (wt%) (daf)				
Carbon	52.00	47.39	50.03	45.88
Hydrogen	6.56	6.22	6.66	5.94
Nitrogen	0.38	6.43	3.51	1.74
Sulphur	0.00	0.00	0.00	0.00
Oxygen	41.06	39.97	39.80	46.45
Stoichiometric A/F by carbon balance	5.35	4.83	5.35	4.50
Gross Calorific value (MJ/kg)	18.80	18.30	18.40	18.60
Moisture (as received) (%)	6.68	6.91	5.02	4.58
Ash (as received) (%)	3.42	1.68	3.30	3.27

The standard cone calorimeter (ISO 5660) was modified for raw fire smoke toxicity measurements by adding a cone heater exit chimney and gas sampler [9]. The oxygen analysis from the chimney was used to determine the primary HRR. The 100 mm

square wood samples had a thickness of 20 mm (PWA), 18 mm (PWB), 11 mm (DPW) and 11 mm (LPW). Each plywood sample was exposed to 35 kw/m^2 radiant heat with free ventilation. The ignition delay for the four samples was 54 s (Plywood A), 53 s (Plywood B), 73 s (Dark Plywood) and 49 s (Light Plywood). The fire continued until flaming combustion ceased and there was only char burning. It will be shown that this transition from flaming combustion to char smouldering combustion was associated with a change in the release of toxic gases. A modified N-gas model for toxicity assessment was used for the total toxicity of the gases produced by the fires. This was obtained by taking the ratio n of the concentration of the species measured by the FTIR and dividing by either the LC_{50} values or the $COSHH_{15\ min}$ values. These ratios were added to give the total toxic gas N.

3 Results and Discussion

3.1 Mass Loss, Equivalence Ratio and Heat Release Rates (HRR)

The mass loss rate, shown in Fig. 1a, at steady state for all the samples was about 0.06 g/s, with a much slower burn rate during the char burning phase. The equivalence ratios (from carbon balance) in Fig. 1b showed that rich mixtures occurred in some of the tests, indicating that some features of confinement occurred even though the fire was freely ventilated. Most of the samples had rich mixtures in the initial stage of the combustion except for Plywood B which was only rich in the second burning phase. These rich mixtures produced high concentrations of toxic gases. The four samples had different peak HRR, but similar steady state HRR as shown in Fig. 2. The primary HRR in Fig. 2a was significantly lower than the mass loss HRR in Fig. 2b, indicating significant post cone fire combustion. This is why the cone calorimeter diluted sample cannot be used for toxic gas assessment.

3.2 Toxic Gas Concentration

The most important toxic gas emissions are shown in Fig. 3. All plywood samples had an almost zero concentration of CO during the steady state burning phase. The highest concentration of each of the toxic gases released occurred during the early rich combustion, indicating that entrainment of air into the fire gases was not sufficient to

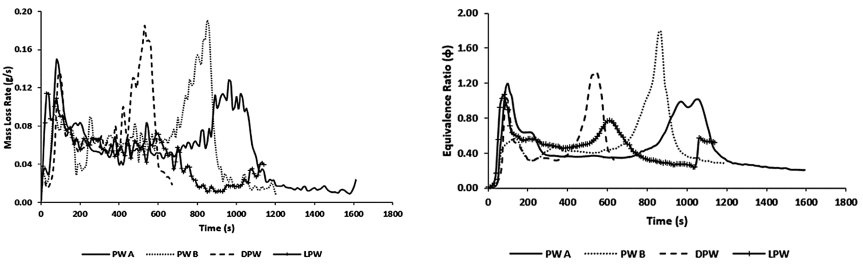

Fig. 1. Mass loss rate (a) and equivalence ratio (b)

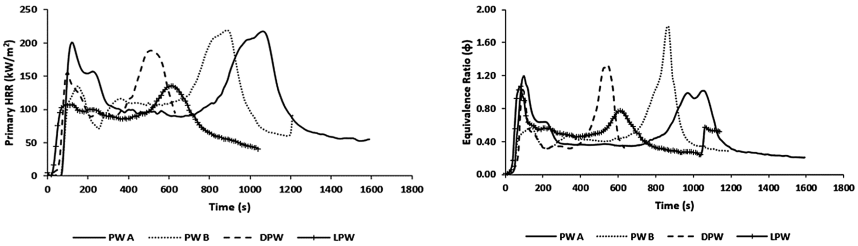

Fig. 2. Primary HRR (a) and HRR based on mass loss rate (b)

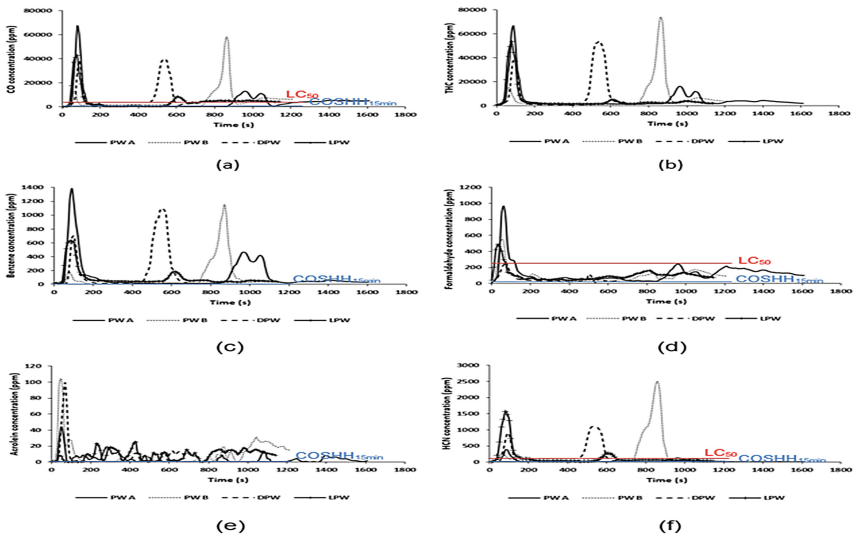

Fig. 3. Toxic gas concentrations; CO (a), total hydrocarbon (b), benzene (c), formaldehyde (d), acrolein (e) and hydrogen cyanide (f)

produce overall lean mixtures, even though the experiments were freely ventilated. The highest concentration of benzene was released by plywood A, followed by the dark plywood, plywood B and the light plywood. There were significant differences in the concentration of the toxic gases (CO, Benzene, Formaldehyde, Acrolein, HCN), both in terms of the magnitude and the time the peak concentrations occurred. The toxicity was higher for richer fires, and the toxicity peaked at maximum HRR. Plywood B had the highest Nitrogen content of 6.43%, which resulted in the highest HCN concentration by a factor of 2–4. All toxic gas concentration levels were considerably higher than the LC_{50} limit except for acrolein and benzene, but all the toxic gas emissions were above the $COSHH_{15\ min}$, with each plywood with different concentrations.

3.3 Total Fire Toxicity N on an LC_{50} and $COSHH_{15\ min}$ Basis

The most important toxic species were CO, HCN, acrolein, formaldehyde and benzene on an LC_{50} and $COSHH_{15\ min}$ basis. Figure 4 shows that the peak **N** for LC_{50} toxic assessment were all >20 and were different for each plywood, both in terms of the magnitude and the time when the peak N occurred. The peak **N** on a $COSHH_{15\ min}$ basis was >900. This means that the toxic gases need to be diluted with fresh air by a factor of about 900–1500 before escape is not impaired and it has to be diluted by a factor of >20 before it doesn't kill anybody in 30 min. The two methods of deriving **N** show that the dependence of **N** on time were similar for all plywoods.

The major contribution to the total toxicity is shown on an LC_{50} and $COSHH_{15\ min}$ basis in Figs. 5 and 6 for the 4 plywood fires. For PWA the toxicity was dominated by CO, followed by formaldehyde, HCN and acrolein on an LC_{50} basis and formaldehyde, acrolein, benzene, CO and HCN on a $COSHH_{15\ min}$ basis. HCN was the third most important toxic gas, but its contribution never exceeded 10% on an LC_{50} basis.

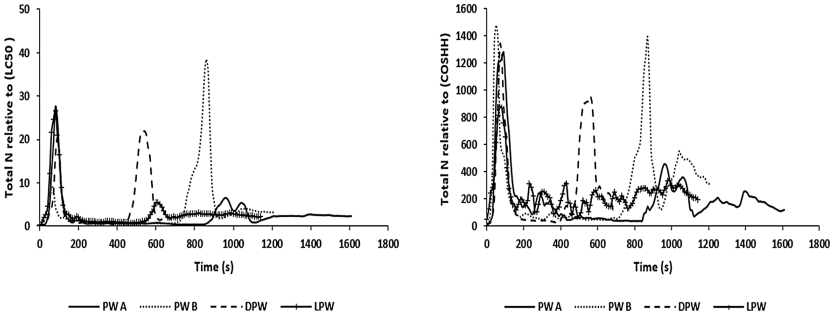

Fig. 4. Total toxicity N relative LC_{50} (a) and relative to $COSHH_{15\ min}$ (b)

For the PWB the toxicity was dominated by CO, HCN, formaldehyde and acrolein on an LC_{50} basis, but formaldehyde was more significant on a $COSHH_{15\ min}$ basis, followed by acrolein, HCN, benzene and CO. For the DPW the toxicity was dominated by CO, HCN, formaldehyde on an LC_{50} basis, with <10% contribution of acrolein. However, on a $COSHH_{15\ min}$ basis, formaldehyde dominated the toxicity, followed by acrolein, benzene, CO and HCN. The LPW fire was also dominated by CO, HCN, formaldehyde on an LC_{50} basis, with <10% contribution of acrolein. However, acrolein was the most important toxic gas on $COSHH_{15\ min}$ basis followed by formaldehyde, benzene, CO and HCN. The results showed that benzene was also a significant contribution to the toxicity in these plywood fires. The differences between LC_{50} and $COSHH_{15\ min}$ toxic assessments in these fires show that the relative importance of the four toxic gases for death are different from that of impairment of escape. For these plywood fires CO dominates in relation to death and for impairment of escape the other three gases are more important and each plywood had different toxic gases dominating. These toxic emissions were similar to those for pine wood crib compartment fires [1–3] with the added significance of HCN emissions from the glues used in plywood construction.

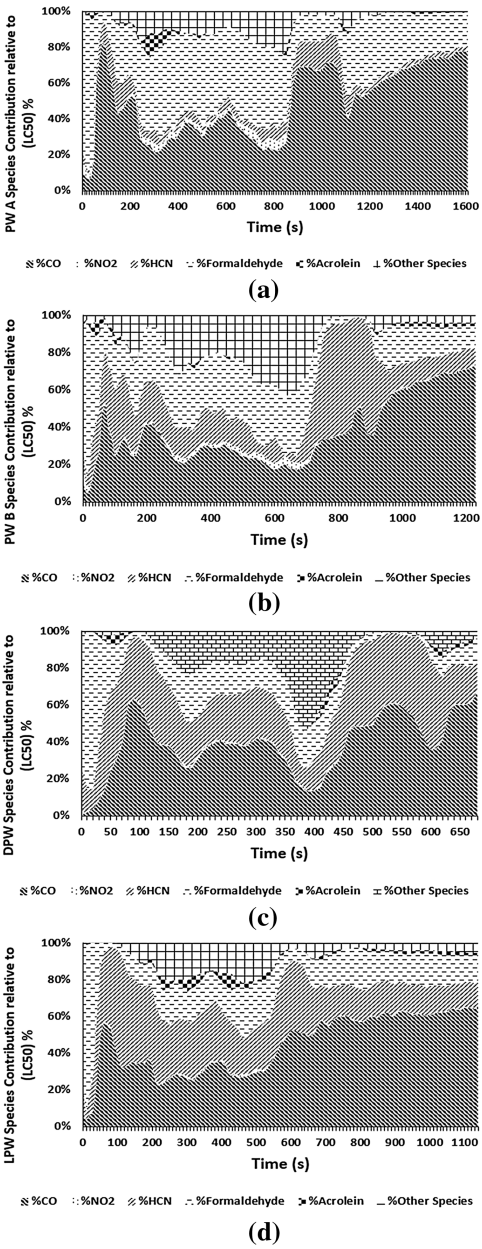

Fig. 5. N-gas species contribution relative to LC_{50}: PWA (a) PWB (b) DPW (c) and LPW (d)

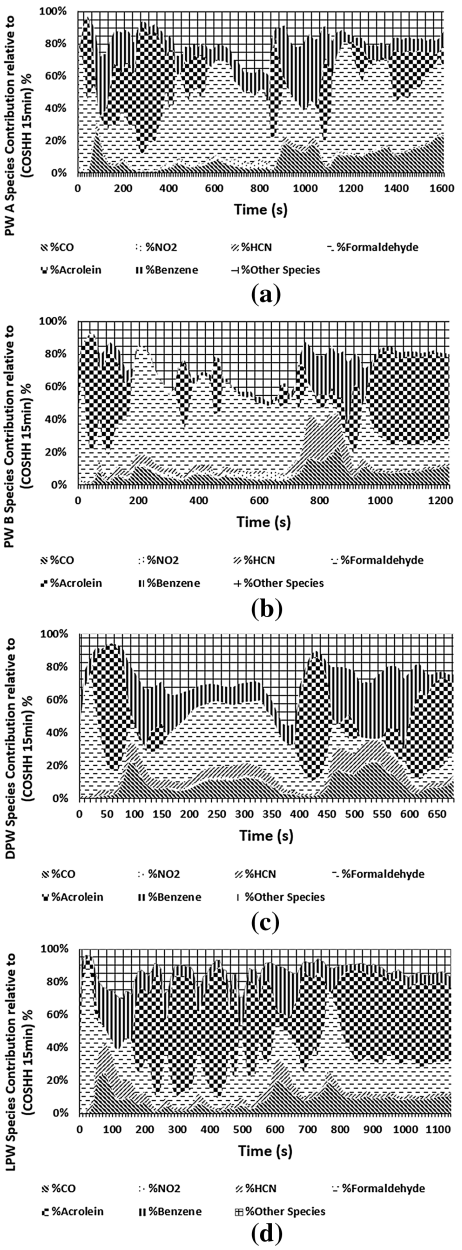

Fig. 6. N-gas species contribution relative to $COSHH_{15\ min}$: PWA (a) PWB (b) DPW (c) and LPW (d)

4 Conclusions

1. High concentrations of toxic gases that would impair escape were produced in the initial stage of the fire, where escape is occurring in a fire.
2. The 4 plywoods had different compositions indicating that the manufacturing processes were different and hence released different concentrations of the toxic gases. Toxic gas regulation for plywoods should be introduced to control this.
3. The modified standard cone calorimeter is a good technique to use for the realistic determination of toxic gases when used with a heated FTIR.

Acknowledgements. The Petroleum Technology Development Fund, Nigeria and the University of Maiduguri are thanked for sponsoring the PhD of Bintu G. Mustafa. Thanks to Garry Fitzgibbon of Galliford Try for providing some of the test materials.

References

1. Andrews GE, Daham B, Mmolawa MD, Boulter S, Mitchell J, Burrel G, Ledger J, Gunamusa W, Boreham RA, Phylaktou HN (2006) FTIR investigations of toxic gases in air starved enclosed fires. In: Gottuk DT, Lattimer BY (eds) 8th international symposium on fire safety science. International Association for Fire Safety Science, Beijing
2. Aljumaiah O, Andrews GE, Phylaktou HN, Mustafa BG, Al-Qattan H, Shah V (2011) Air starved compartment wood crib fire heat release and toxic gas yields. In: Fire safety science - proceedings of the tenth international symposium. International Association for Fire Safety Science, pp 1263–1276
3. Mustafa BG, Andrews GE, Phylaktou HN, Al-Shammri A, Shah V (2015) Impact of wood fire load on toxic emissions in ventilation controlled compartment fires. In: IFireSS - international fire safety symposium, Coimbra, Portugal
4. Wilkins E, Murray F (1980) Toxicity of emissions from combustion and pyrolysis of wood. Wood Sci Technol 14:281–288
5. Persson B, Simonson M (1998) Fire emissions into the atmosphere. Fire Technol 34:266–279
6. Purser DA (2002) Toxic assessment of combustion products. In: Dinenno PJ (ed) SFPE handbook of fire protection engineering. National Fire Protection Association, p 2-83-82-171
7. Purser DA (2010) 3 - hazards from smoke and irritants. In: Fire toxicity. Woodhead Publishing, pp 51–117
8. Purser DA (2000) Toxic product yields and hazard assessment for fully enclosed design fires. Polym Int 49:1232–1255
9. Hartzell GE (2001) Engineering analysis of hazards to life safety in fires: the fire effluent toxicity component. Saf Sci 38:147–155
10. EH40/2005: EH40/2005 workplace exposure limits (2005)

Ignition of Wood Dust of African Padauk (Pterocarpus Soyauxii)

Miroslava Vandličková and Iveta Marková(✉)

Faculty of Security Engineering, University of Žilina, Univerzitná 8215/1, 010 26 Žilina, Slovakia
iveta.markova@fbi.uniza.com

Abstract. The article deals with wood dust of African Padauk (*Pterocarpus soyauxii*). The wood dust was prepared by Makita 9556CR 1400 W and the K36 sandpaper for various fractions (<63; 63; 71; 100; 200; 315; 500 μm) of the wood dust. The aim of the article is granulometric analysis of the wood dust of African Padauk (*Pterocarpus soyauxii*), to identify its morphological structure and to assess the effect of particle size of airborne dust on minimum ignition temperatures. The most frequent dust particle size was represented by 100 μm fraction (42.14 ± 1.049%). The minimum ignition temperature of airborne dust was 370 °C the 71 μm fraction.

Keywords: African padauk · Granulometric analysis · Morphology · Ignition

1 Introduction

African Padauk (*Pterocarpus soyauxii)* is a very popular decorative wood in the interior and exterior. The use of padauk is increasing, so its processing also increases. The article deals with wood dust of African Padauk (*Pterocarpus soyauxii*).

For its beautiful and unusual tinge and patterns, African Padauk (*Pterocarpus soyauxii*) is used in the production of floor coverings, furniture and interior decorations [1, 2]. It has a very unique reddish orange coloration, and the wood is sometimes referred to by the name of Vermillion. Unfortunately, this dramatic color darkens, becoming reddish brown in color. Padauk is moderately heavy, strong, and stiff, with exceptional stability. It's popular hardwood among hobbyist woodworkers because of its unique color [3].

Tropical wood species are more homogeneous (not such a significant difference between summer and spring wood) than European tree species. [4–6] evaluates tropical tree species as the wood types with a great resistance against biological agents and mechanical wear. They have good dimensional stability and nice aesthetics. The wood is commonly used for the outer structures, cladding, veneer, garden furniture or special plywood. First-class furniture and cabinet wood, Padauk also makes fine turnings, carvings [7], and musical instruments [8, 9]. Since it has high resistance to abrasion, great strength, and it doesn't readily decay, it adapts well to cutting board stock [3]. African Padauk (*Pterocarpus soyauxii*) is mainly used in the (exterior or interior) carpentry, in particular in more humid environments [9].

L. Makovicka Osvaldova et al. (Eds.): WFS 2020, *Wood & Fire Safety*, pp. 58–65, 2020.
https://doi.org/10.1007/978-3-030-41235-7_9

In generally, wood dust is by-product of wood processing [10–16]. Wood dust plays a negative role in fire risk assessment [17, 18] or an explosion [19–22]. In addition, it is an undesirable factor having a negative effect on human body [23, 24].

Ignition temperature is the key parameter evaluating the risk of airborne dust initiation. It is monitored in a standardized test apparatus (ceramic tube furnace), in line with EN 50281-2-1:2002 [25], where the airborne wood dust sample is exposed to radiation heat with the given ambient temperature [26].

The aim is presenting the granulometric analysis of wood dust of padauk, monitoring its microscopic structure and monitoring the temperature of ignition of airborne dust African Padauk (*Pterocarpus soyauxii*).

2 Samples

The African Padauk (*Pterocarpus soyauxii*) in the shape of a board (131 × 50 × 20 mm) have been dried with the moisture level of approx. 8÷10%. They were made in a woodworking shop owned by private company manufacturing interior elements based in Žilina (Fig. 1).

Fig. 1. Padauk samples used in the experiment. 1 – as board, 2 – as dust

The samples were prepared by an expert on grinding to make the process as realistic as possible considering certain important factors - the pressure against the surface of the fragment, the grinding speed as well as the direction of the sanding (scissors cut). The samples sanded, using Makita 9556CR 1400 W disc sander and K36 sandpaper, in order to get homogeneous dust particles. The dust has been collected into the hopper and poured into a hermetically sealed glass container in order to prevent the dust from absorbing any moisture.

3 Methodology

The shape and the size of wood dust particles have been determined by microscopic analysis using Nikon Eclipse Ni with Nikon DS-Fi2 camera (Fig. 2a). Wood dust structure was observed under the stereomicroscope Nikon SMZ 1270 (Fig. 2b). Microscopic analyses of wood dusts were made for the 100 μm fraction.

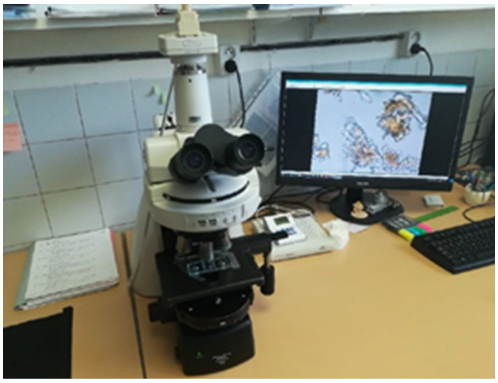

(a)

(b)

Fig. 2. Microscopic analysis equipment for wood dust. Legend: (a) Nikon Eclipse Ni Microscope with Nikon DS-Fi2 Camera, (b) Nikon SMZ 1270 Stereomicroscope.

The experiments were carried out in a test device measuring minimum ignition temperatures of airborne dusts using automatic weighing machines HL 100, ZU, EINHELL air compressor and ALMEMO device measuring the temperature inside the experimental device. The procedure was carried out in line with STN EN 50281-2-1 [25].

4 Results and Discussion

The granulometric analysis showed different percentages of fractions. The percentages, starting from the 500 μm fraction (Table 1), are presented below. Bigger fractions occurred only minimally - at 1%. The same outcome is presented for the domestic tree species [11, 16].

Table 1. Evaluation of % fractions

Fractions [μm]	African Padauk *(Pterocarpus soyauxii)*	
	% of shares	Ignition temperature (°C)
500	1,55 ± 0.115	390
315	6,29 ± 0.621	390
200	28,37 ± 0.547	390
100	42,14 ± 1.049	380
71	10,97 ± 1.453	370
63	4,92 ± 0.312	370
<63	5,81 ± 0.399	370

The results determining the ignition temperature of airborne dust (Table 1) show a decrease in values depending on the fraction size which was getting smaller. The results of the thermogravimetric analysis [27] show initial temperature changes in the Padauk sample at the temperature above 350 °C.

The explosion of airborne wood dust and its risk assessment on the basis of ignition temperature is generally applied and accepted. However, it is necessary to take into account other factors that may have a significant effect on ignition temperature [28].

Tureková [31] investigated the airborne dusts of oak, beech, spruce and mixtures taken from woodworking operations. After sieving she used dust samples <71 μm to investigate the ignition temperature of airborne dust.

Sample of airborne beech dust had the highest ignition temperature 390 °C. On the contrary, the lowest value of the minimum ignition temperature of the airborne dust, 360° C, was a sample of mixed wood dust. The minimum ignition temperature of the spruce and oak dust sample was 380 °C (Table 2). The initiation temperature of the padauk dust fraction <71 μm (370 °C) is comparable to the ignition temperatures of domestic wood dusts.

Table 2. Minimum ignition temperature of airborne dusts (frakcie <71 μm) in °C

Dust samples	ISO 871:1999 (Induction period) [31]	Tureková [32]	Martinka, Rantuch [33] (p = 5 kPa)	Kasalová and Balog [34]
Oak	250 (9:57)	380	440	410 to 550
Spruce	240 (9:33)	380		
Beech	240 (9:03)	390		
Mixture	250 (9:59)	360		

4.1 Microscopic Analysis

The particles of African Padauk (Fig. 3) have the size of <100 μm. The scans show the fibers of the dust particles maintaining their anatomical structure [29, 30].

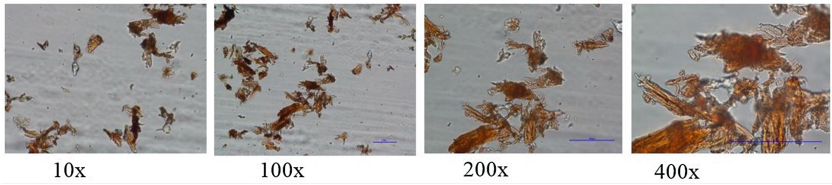

Fig. 3. Light microscopy images of Padauk dust fibers with 10×, 100×, 200× and 400× zoom.

4.2 Shape Analysis

Padauk dust samples preserve their anatomical structure. The size analysis of the particles has been performed for the fractions of 500, 315, 200 and 100 µm (Fig. 4). When zoomed in, they appear different and have their own specific shapes.

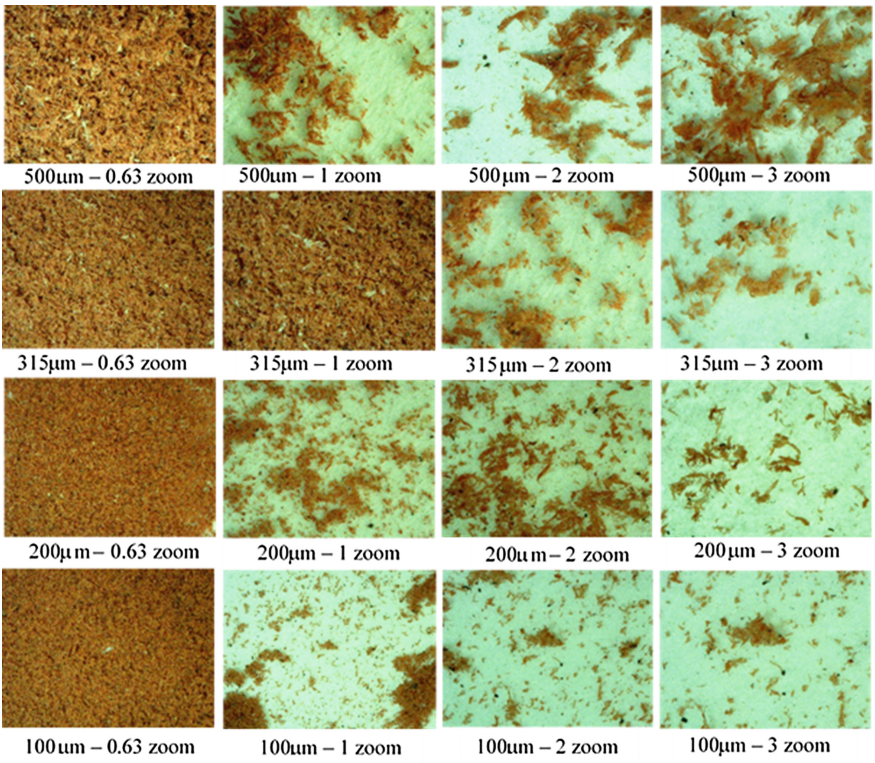

Fig. 4. Dust particles (100, 200, 315 and 500 µm) of African Padauk (*Pterocarpus soyauxii*) and their shape

5 Conclusion

On the basic experimental results, we can present following conclusions:

- The shape of the particles and its wood morphology was preserved. Microscopy confirmed that the anatomical structure of the wood dust particles remained unchanged as well.
- The ignition temperature of the airborne dust determined under experimental conditions starts at 390 °C (fraction 500 μm) and as the particles change their size, it is reduced to 370 °C (fraction 71 μm).
- Sieve analysis shows the percentages of the given fractions. The most common particle size was the 100 μm fraction (42.14 ± 1.049%). The percentage of particles <100 μm was 63,84%.

References

1. CARO DREVA (2019) Domáce drevo alebo exotika? Dostupné z: https://carodreva.sk/drevo-v-kocke/domace-drevo-alebo-exotika. Accessed 13 June 2019
2. Van Gemerden B, Shu GN, Olff H (2003) Recovery of conservation values in Central African rain forest after logging and shifting cultivation. Biodivers Conserv 12:1553. https://doi.org/10.1023/A:1023603813163
3. Fan MZ, Ndikontar MK, Zhou XM, Ngamveng JN (2012) Cement-bonded composites made from tropical woods: compatibility of wood and cement. Constr Build Mater 36:135–140
4. Jankowska A (2018) Assessment of sorptive properties of selected tropical wood species. Drvna Ind 69(1):35–42. https://doi.org/10.5552/drind.2018.1733
5. Vigué J (2006) Dřevo od A do Z. 1. vydanie. Čestlice: Rebo Productions CZ, spol. s r. o. ISBN: 80-734-531-1
6. Reinprecht L, Kmeťová L, Iždinský J (2012) Fungal decay and bending properties of beech plywood overlaid with tropical veneers. J Trop For Sci 24(4):490–497
7. Tchinda JBS, Petrissans A, Molina S, Ndikontar MK, Mounguengui S, Dumarcay S, Gerardin P (2014) Study of the feasibility of a natural dye on cellulosic textile supports by red padouk (Pterocarpus soyauxii) and yellow movingui (Distemonanthus benthamianus) extracts. Ind Crops Prod 60:291–297. https://doi.org/10.1016/j.indcrop.2014.06.029
8. Brémaud I, Nadine A, Minato K, Gril J, Thibaut B (2011) Effect of extractives on vibrational properties of African Padauk (Pterocarpus soyauxii Taub.) August 2011. Wood Sci Technol 45(3):461–472. https://doi.org/10.1007/s00226-010-0337-3
9. Straze A, Mitkovski B, Tippner J, Cufar K, Gorisek Z (2015) Structural and acoustic properties of African padouk (Pterocarpus soyauxii) wood for xylophones. Eur J Wood Wood Prod 73(2):235–243
10. Bernard O, Rostand MP, Evelyne T, Michel G (2018) Experimental investigation of mixed mode fracture of tropical wood material. In: Sedmak A, Radakovic Z, Rakin M (eds) Book series: procedia structural integrity, vol 13, pp 347–352. https://doi.org/10.1016/j.prostr.2018.12.058
11. Marková I, Mračková E, Očkajová A, Ladomerský J (2016) Granulomerty of selectes wood dust species of duat from orbital sanders. Wood Res 61(6):983–992
12. Dzurenda L, Orlowski KA, Grzeskiewicz M (2010) Effect of thermal modification of oak wood on sawdust granularity. Drvna Ind 61(2):89–94

13. Dzurenda L, Orlowski KA (2011) The effect of thermal modification of ash wood on granularity and homogeneity of sawdust in the sawing process on a sash gang saw prw 15-M in view of its technological usefulness. Drewno 54(186):27–37
14. Eckhoff RK (2003) Dust explosions in the process industries. Gulf Professional Publishing, Boston, 719 s. ISBN 978-0750676021
15. Očkajová A, Kučerka M, Krišťák Ľ, Igaz R (2018) Granulometric analysis of sanding dust from selected wood species. BioResources 13(4):7481–7495
16. Mračková E, Krišťák Ľ, Kučera M, Gaff M, Gajtanská M (2016) Creation of wood dust during wood processing: size analysis, dust separation, and occupational health. BioResources 11(1):209–222
17. Rohr AC, Campleman SL, Long CM, PetersonN MK, Weatherstone S, Quick W, Lewis A (2015) Potential occupational exposures and health risks associated with biomass-based power generation. Int J Environ Res Public Health 12(7):8542–8605. https://doi.org/10.3390/ijerph120708542
18. Kovshov S, Nikulin A, Kovshov V, Mračková E (2015) Application of equipment for aerological researching of characteristics of wood dust. Acta Fac Xylol Zvolen 57(1):111–118
19. Amyotte P (2013) An introduction to dust explosions: understanding the myths and realities of dust explosions for a safer workplace. In: An introduction to dust explosions: understanding the myths and realities of dust explosions for a safer workplace. Elsevier Inc. http://www.scopus.com/inward/record.url?eid=2-s2.0-84899749632-&partnerID=tZOtx3y1
20. Amyotte PR, Eckhoff RK (2010) Dust explosion causation, prevention and mitigation: an overview. J Chem Health Saf 17(1):15–28. https://doi.org/10.1016/j.jchas.2009.05.002
21. Žigo J, Rantuch P, Balog K (2014) Experimental analysis of minimum ignition temperature of dust cloud obtained from thermally modified spruce wood. Adv Mater Res 919-921, 2057–2060. http://doi.org/10.4028/www.scientific.net-/AMR.919-921.2057
22. Krentowski J (2015) Disaster of an industrial hall caused by an explosion of wood dust and fire. Eng Failure Anal 56:403–411. https://doi.org/10.1016/j.engfailanal.2014.12.015
23. Marková I, Ladomerský J, Hroncová E, Mračková E (2018) Thermal parameters of beech wood dust. BioResources 13(2):3098–3109
24. Top Y, Adanur H, Öz M (2016) Comparison of practices related to occupational health and safety in microscale wood-product enterprises. Saf Sci 82:374–381. https://doi.org/10.1016/j.ssci.2015.10.014
25. EN 50281-2-1 (2002) Electrical apparatus for use in the presence of combustible dust. Part 2-1: test methods. Methods for determining the minimum ignition temperatures of dust. European Committee for Standardization, Brussels, Belgium
26. Marková I, Hroncová E, Tomaškin J, Tureková E (2018) Thermal ananlysis of granulometry selected wood dust. BioResources 13(4):8041–8060
27. Misse SE, Brillard A, Brilhac J-F, Obonou M, Ayina LM, Schönnenbeck C, Caillat S (2018) Thermogravimetric analyses and kinetic modeling of three Cameroonian biomass. J Ther Anal Calorimetry 132(3):1979–1994. https://doi.org/10.1007/s10973-018-7108-z
28. Mračková E, Milanko V (2016) Characteristics of wood particulates as a function of safety parameters. CRC Press, Balkema, pp 487–490
29. IAWA list of microscopic features for hardwood identification with an Appendix on non-anatomical information IAWA Committee (1989) IAWA Bulletin n. s. vol 10, no 3, pp 219–332. www.iawa-website.org/uploads/soft/Abstracts/IAWA%20list%20of%20microscopic%20features%20for%20hardwood%20identification.pdf

30. Wang Y, Su M, Sun H, Ren H (2018) Comparative studies on microstructures and chemical compositions of cell walls of two solid wood floorings. J Wood Sci. https://doi.org/10.1007/s10086-018-1743-7
31. Tureková I (2008) Riziká priemyselných drevných prachov. In: Rusko M (ed) Zborník z XII. Konferencie so zahraničnou účasťou, 5–6 December 2008, Bratislava. Strix et VeV. Prvé vydanie, Žilina, pp 167–175. ISBN 978-80-89281-34-3
32. STN ISO 871 (1999) Plastics. Determination of ignition temperature using a hot-air furnace
33. Martinka J, Rantuch P (2013) Posúdenie vplyvu veľkosti častíc dubového dreva na teplotu vznietennia rozvíreného prachu. Acta Fac Tech XVIII 2013(2):75–82
34. Kasalová I, Balog K (2010) Minimum ignition temperatures of wood dust clouds determi - ned by planed experiment. In: Fire engineering, Zvolen, 5th–6th October 2010. Bratia Sabovci, Zvolen, pp 119–126. ISBN 978-80-89241-38-8

Experimental Study on Odor from Combustible Wood Materials in Their Pre-fire Situation in House

Osami Sugawa(✉) and Kyoko Kamiya

Suwa University of Science, 5000-1 Toyohira, Chino-shi, Nagano Prefecture, Japan
{sugawa, kamiya}@rs.sus.ac.jp

Abstract. Various burning odors are signs of early fire and are perceived as fire by residents. Electronic noses were used to determine the odor qualitative changes during pyrolysis and oxidative pyrolysis of various combustible materials to clarify the possibility of fire detection using odor. The odor generated during combustion depends on the type of flammable substance in the house, so wood and plastic materials were targeted for flammable materials.

The precursors of odor during the beginning of pyrolysis and oxidative pyrolysis of house materials and also odor gas during the active period of those were defined as the standard odor gases, respectively. Using these odor gases as respective reference gases, it was used for proper selection and detection of odor fire gas generated during a model fire. These standard odor gases were then used as the fire test reference gas for the two-story model house fire test. Three types of model fire sources, a fast-growing fire, a plastic trash bin fire with wastepaper, and a wood crib fire with towels, were used as model fire sources. Comparison of the output from the fire detector already available with the measured odor change showed that the odor change was detected simultaneously with or immediately after the normal fire detector with a rapidly spreading fire. This situation was obtained because the fire sensor and odor sensor were in the same fire room. The change in odor on the second floor showed a sign of fire about 30 s before the fire was detected by the smoke and temperature rise type detector. When residual odors were present in the room, by making this odor level the reference level, it was possible to prevent false detection of fires by the odor sensor system.

Keywords: Fire detection · Electronic nose(s) · Room fire · Wood crib

1 Introduction

Fire detectors are installed in buildings and residential houses to detect fires quickly and give warning signs to residents to help extinguish and/or escape the fire. In Japan, it was obliged to install a fire detector in a house in 2004. Due to the widespread use of detectors and many other measures, the number of deaths due to fire has decreased each year. There were 27% fewer deaths caused by fire in 2016 than in 2005 [1]. This proved that fire detectors help save lives with other counter- measures. Smoke, heat,

L. Makovicka Osvaldova et al. (Eds.): WFS 2020, *Wood & Fire Safety*, pp. 66–71, 2020.
https://doi.org/10.1007/978-3-030-41235-7_10

and flame sensors are widely used in fire detectors, and it has been found that CO sensor is also effective at detecting fire [2]. And based on these research findings, the multi-criteria fire detectors of which combination of CO, temperature, and smoke sensors are currently being studied [3–5]. Fires emit odor in addition to heat, smoke, and toxic gases such as CO and HCN [6, 7]. Odor is often the first and early sign of a fire to be noticed by the people in buildings or residential houses. The size of the molecules that make up odor is approximately 10^{-10} m, while smoke particles are 10^{-8} to 10^{-7} m. Therefore, odor molecules are diffused by thermal air currents from a fire quicker and widely than smoke particles, and it may be possible to detect a fire more quickly using odor than using a smoke detector. It has been performed that many tests using the odor identification sensors to detect odor changes during the oxidative pyrolysis of wood, plastic, and mixture of these ones [8, 9]. It was found that oxidative pyrolysis caused drastic odor changes and increased odor strength [10, 11]. Mixtures of chemicals including various thermally decomposed materials are responsible for the odors produced, so determining the concentrations of the specific substances was not helpful. Here, odors related to fire(s) are therefore selected experimentally and then used as reference odors to allow a fire to be detected based on the odor changes. The results obtained using the electronic nose system in reduced-size fire experiments were compared with the results obtained using other usual fire detection systems.

2 Experimental

2.1 Odor Analysis and Standard Gases

An electronic nose (FF-2A, Shimadzu Corp.) with ten oxide semiconductor sensors (to imitate receptor proteins in a human nose) was used. The data obtained were subjected to multiple classification analysis to characterize the sensor signal patterns. The electronic nose detected the overall odor molecule balance rather than individual chemicals (which would be the case using analytical methods such as gas chromatography mass spectrometry). The electronic noses were exposed to the standard gases and produced indices that were used to determine the angle of vector products between vector of the standard gas odor components and vector of the sample gas odor. A calibration curve was produced for each index using the sensor responses at different standard gas concentrations [12]. Studies were performed to develop similarity indices to represent odor quality. The methods used to analyze the indices are described below. The similarity indices indicated the vector which the sensor response patterns represented the nine standard gas odor types. Calculations were performed using the angle θ of the vector product between the standard gas vector and sample gas vector in the 10-dimensional space created from the responses of the 10 sensors. The similarity index was 100% (i.e., the sample gas vector was the same as the standard one) at $\theta = 0°$, and 0% for $\theta > 15°$ with the acceptable angle of θ ($\leq 5°$). The inner product angle $\theta = 5°$ means that the similarity is 0.996. Each odor gases from wood and plastic materials were collected from the exhaust port of a TG-DTA system during their oxidative pyrolysis. The collected odor gases were measured with 9 electronic noses of the FF-2A system. The gases emitted when the maximum sensor output was found and in the

step before the maximum pyrolysis were used as standard gases. The odor gases obtained from the full-scale room fire experiments, were compared with the odor gases generated from Cedar, LDPE, HDPE, and PS which has adopted as the standard (reference) gases [13].

2.2 Reduced-Sized Experiment in Part of a Two-Story House

The experiment was performed in a mock-up of three rooms at 75% of the actual size as is illustrated in Fig. 1. There was a 0.36 m^2 square opening, representing a staircase hole, in the center of the floor of the upper-floor room. The rooms were constructed to allow smoke and gases generated in the fire room (on the ground floor) to pass under the upper wall of hanging partition and spread into the adjoining room and through the square opening in the center of that room to the upper floor. No furniture or other items were placed in the rooms.

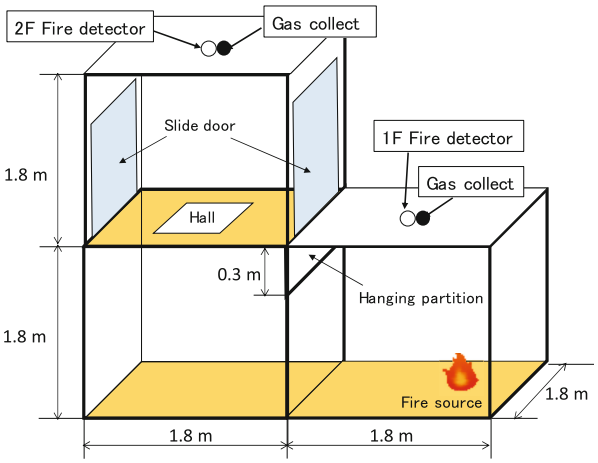

Fig. 1. Layout of the rooms used in the experiment using part of a two-story building.

Temperature measurements were made at 28 points, including at the point where a fire source (combustible materials) was placed, in front of the upper wall in the room where the fire was started, and along the vertical axis of the center of the rooms on each floor. The combustion gases were directly sent to the gas analyzer and measured the concentrations of O_2, CO_2, and CO gas. The gas collection points were set at eight points, including directly above the fire source, in the center of the room where the fire was started, in front of the upper wall which was a part of upper partition wall of the fire room to the next room and on the surface of upper-floor ceiling. Odor gas samples were also collected and sent into respective small bags for 30 s and the odor gas bags at each sampling point were changed every 30 s during the experiment. Two types of fire detectors; A photoelectric spot sensor (Type 2) and a differential temperature sensor (Type 2), were installed to the ceiling at the center of the fire room and in the upper room, and the response time for each sensor was compared with the time taken for an

odor change to be detected. Each odor gas sample was diluted by a factor of 5–50 with pure N_2 and then analyzed using the electronic noses of FF-2A. Gas emitted during oxidative pyrolysis was adopted as the reference gas. Odor from an experiment lingered within each room during subsequent experiments. The odor gas from the previous experiment was used as the base-odor for each experiment to remove the effects of the odor contamination due to previous experiments. Tests were performed using three types of combustible material to identify odors emitted by different combustible materials. In the first experiment, three cotton (100%) towels were placed on top of an electric heater. In the second experiment, three polyethylene bags each containing 5–10 sheets of A4 paper were placed in a plastic garbage box and ignited using an electric heater. In the third experiment, a small alcohol candle was used as an ignitor and was set under a wood crib pile (5 × 5 × 200 mm, 28 steps).

3 Results and Discussion

In the third test, using a wood crib pile as the fire source, the smoke generated about 15 s after ignition and flames were observed at about 30 s. The smoke and heat detectors mounted under the ceiling in ground floor operated after 62 and 75 s,

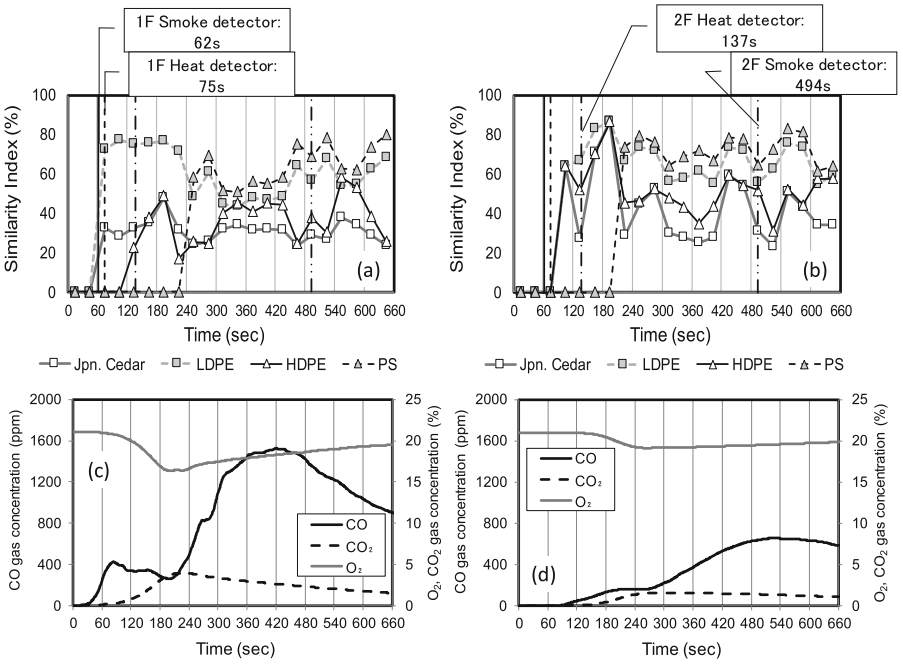

Fig. 2. Odor and gas concentration measurement results when wood crib was used as the fire source. (a) Odor results for the center of the ground-floor room in which the fire was started, (b) Odor results for the center of the upper-floor room, (c) gas concentration results for the center of the ground-floor room, (d) gas concentration results for the center of the upper-floor room.

respectively. The smoke and heat detectors installed in the upper room operated after 494 and 137 s, respectively. The fire transitioned to the flaming combustion stage immediately after the candle caught fire, and this caused heat and smoke generated from wood combustion which was observed at the early stage. The odor and combustion gas concentrations are shown in Fig. 2.

The odor before the experiment was performed the first time (i.e., with no smoke odor present) was used as the base-odor, and the similarity indices for all of the standard gases increased relative to the indices before ignition. Odor changes were only found in the test using a wood crib to start the fire because the odor from the previous experiment was used as the base-odor. It can be seen from Fig. 2(a) and (b) that the odor on the ground floor and upper room changed from 60–90 s. This was around the same time that heat and smoke detectors in the ground room reacted, respectively. In the upper room, odor change was detected 30 s before the smoke and temperature detectors reacted. The polystyrene odor similarity index appeared later than the ones given by similarity indices of Cedar, low-density polyethylene (LDPE), and high-density polyethylene (HDPE). Wood and polyethylene emit components containing aldehyde groups during oxidative pyrolysis, but polystyrene doesn't. Emissions of large amounts of materials containing aldehyde groups during the oxidative pyrolysis of the wooden materials could therefore explain the high similarity indexes for Cedar and polyethylene. From the result of gas concentration in the ground room, CO gas concentration increased to 400 ppm over 30 to 60 s. After about 200 s, CO gas concentration rose again, it was approximately 1600 ppm in 420 s. Also, it was estimated that acrolein occurred at this time. On the upper room, CO gas concentration increased after 100 s of the same time as the odor change. This value of CO concentration was the largest compared to the value obtained in using towels (the first experiment) and the bin box (the second experiment) as the fire source.

From these results, it was found that the change in odor was observed at a time earlier than that of the usual fire detectors, and at the same time as the increase in CO gas concentration. The CO gas concentration increased as the combustion time increased, but the odor similarity index did not change significantly. The odor similarity indexes were values indicating the quality of the odor, indicating that the odor quality did not change.

4 Conclusions

Appropriate reference gases need to be selected to allow the fire detectors based on odor changes to recognize the various kinds of fires. Odor gases created during the oxidative pyrolysis of wood and synthetic polymers and/or mixtures of these were therefore used as standard gases. These standard gases were used in model fire experiments in which heat was generated rapidly by an accelerated fuel in the initial stage of a model fire and in the model fire experiments involving smoldering combustion. The output results obtained using already available fire detector systems and the odor change detecting by electronic nose system were compared, and then it was found that the odor-change was detected at almost the same time or later than the other fire detectors reacted in the case of the fire was spreading rapidly or the sensors were close to the fire source. However,

odor changes were detected more quickly than the other fire detectors reacted when the fire was smoldering and had only small flames. Various odors (such as those produced during normal combustion activities) will be emitted in a room, but the results of this study indicate that misdetection of fire by the odor sensor system can be prevented by using odorous gases from the room as the base-odor.

Acknowledgements. This study was partly supported through a grant-in-aid for scientific research (Basic Research B, grant No. 15H02982) for the financial years 2015–2017. The authors sincerely thank to Mr. Satoshi Echigoya of Sugawa Laboratory, Suwa University of Science for his sincere contribution in conducting the tests.

References

1. Japanese Fire and Disaster Management Agency (2018) Overview of the 2017 white paper on the fire service, no 2018, pp 68–71 (in Japanese)
2. Jackson MA, Robins I (1994) Gas sensing for fire detection: measurements of CO, CO_2, H_2, O_2, and smoke density in european standard fire tests. Fire Saf J 22:181–205
3. Ryder NL (2017) Multicriteria detection: leveraging building control and comfort sensors for fire state determination. In: Proceedings of 16th international conference on automation and fire detection, vol I, pp 349–355
4. Mensch A, Cleary T (2017) A comparison of carbon monoxide gas sensing to particle smoke detection in residential fire scenarios. In: Proceedings of 16th international conference on automation and fire detection, vol I, pp 363–370
5. Arndt G, Suchy S, Vialkowitsch D (2017) Multi-criteria/multi-sensor early fire detection in the engine compartment of road vehicles: evaluation process of gas sensors. In: Proceedings of 16th international conference on automation and fire detection, vol II, pp 47–54
6. Kohla D, Eberheim A, Schieberle P (2005) Detection mechanisms of smoke compounds on homogenous semiconductor sensor films. Thin Solid Films 290:1–6
7. Morikawa T, Yanai E, Watanabe T, Okada T, Sato Y (1991) Toxicity of atmosphere in second floor room due to inflow of fire effluent gases rising from first floor. Bull Jpn Assoc Fire Sci Eng 40(2):37–44
8. Sugawa O, Kamiya K, Oka Y (2017) Evaluation on odor intensity and quality from plastic and wood materials in pre-combustion condition. In: Proceedings of 16th international conference on automation and fire detection, vol II, pp 21–28
9. Kamiya K, Sugawa O, Imamura T, Oka Y (2013) Experimental study of odor intensity and quality for wood materials undergoing oxidative pyrolysis. Bull Jpn Assoc Fire Sci Eng 63:25–35 (in Japanese)
10. Kamiya K, Sugawa O, Kanai H, Imamura T, Oka Y (2011) Evaluation on odor intensity and quality from wood in pre-combustion condition. In: Proceedings of Asia Pacific Symposium Saftey, pp 344–347
11. Sugawa O, Kamiya K (2017) Experimental study on FT-IR analysis of chemical species from wooden materials in pre-combustion condition. In: Proceedings of 16th international conference on automation and fire detection, vol I, pp 371–378
12. Kita J, Aoyama Y, Kinoshita M, Nakano H, Akamaru H (2000) Technical digest of the 17th sensor symposium, pp 301–305
13. Kamiya K, Sugawa O, Watanabe N (2019) Using odors to detect fire in a study with rooms reduced to 75% size. In: Proceedings of 9th international seminar fire and explosion hazards, pp 1210–1220

The Impact of Radiant Heat on the Flexural Strength and Impact Strength in Spruce Wood Bending

Anton Osvald[1(✉)] and Jaroslava Štefková[2]

[1] Zvolen, Slovakia
anton.osvald@hotmail.com
[2] The Institute of Foreign Languages, Technical University in Zvolen, Zvolen, Slovakia
stefkova@tuzvo.sk

Abstract. Thermal degradation influences the wood in a complex way; i.e. it causes the alteration of its properties (weight, volume, shape, and color), as well as the changes of mechanical properties. The main aim of this work is to compare the changes of selected mechanical properties in dependence on the detected weight loss and compare the size of the radiation source. The aim of the research was to examine the changes of strength in bending and impact strength in bending of spruce wood under the influence of radiant heat of S1 source with 1000 W and S2 source of 2000 W outputs. The position of the sample towards the heat source was also observed, in particular, in 50 mm, 100 mm and 150 mm distance. The mass loss measured as the difference of weights before and after the test expressed in per cents was an additional evaluation criterion. The results confirm that the radiant heat, as well as the distance, have an influence on the measured parameters.

Keywords: Spruce wood · Thermal loading · Flexural strength · Impact strength

1 Introduction

The experiment consisted of the choice of material, proposing the laboratory testing method and laboratory testing instrument, the selection of the evaluation criteria and the complete procedure of the evaluation [1].

1.1 Spruce Wood

Norway Spruce (*Picea abies* (L) Karst.) is the second most common species in Slovakia, while economically most significant. It is up to 50 m high, cone-like coniferous tree, branches in whorls. At present, the representation of Norway Spruce in Slovak forests is 24.92%. The spruce wood is yellowish to brownish color, glossy, no heartwood coloring, and pale. It withstands loading well. The boundaries of annual rings are clear, narrow, summer wood verges gradually to wide spring wood. The wood is light, soft, flexible, fissile, easy to stain and not easy to impregnate [2, 4, 6, 7].

L. Makovicka Osvaldova et al. (Eds.): WFS 2020, *Wood & Fire Safety*, pp. 72–79, 2020.
https://doi.org/10.1007/978-3-030-41235-7_11

Spruce timber can be classified as medium durable wood species. Considering the contact of the wood and soil, there is a threat of damaging wood by all kinds of rot, it is classified as little durable wood species. Spruce wood is, bearing in mind its physical and mechanical properties and importance for the processing industry, markedly important raw material. The spruce wood is most commonly and importantly utilized as building timber, namely, in above-grade construction. It is also used for production of roof constructions of utility as well as special-purpose buildings. It is a proven material for production of windows, exterior and interior doors, balconies, and staircases. Spruce wood is a component in panels of frame construction systems in timber buildings.

In testing fire and technical properties, it is mostly considered as a basic reference standard.

1.2 Laboratory Set up and Experiment Procedure

Laboratory set up construction consisted of the frame in which one of two radiant heat sources, either with one tube of 1000 W output or two tubes of 1000 W (overall output of the source 2000 W), was placed. A sliding (adjustable) holder of a test sample able to hold the sample in 50, 100, 150 mm was also the part of the frame.

The heat source was heated to maximal output and then a sample was placed into the holder in the defined position. The dimensions of the sample were 350 × 200 × 20 mm. The moisture content of the samples was 10 ± 1% [9]. The samples were also sorted out before the experiment based on the density; since the density influences fire and technical properties as well as mechanical properties of the spruce wood. The experiment density value of the samples was 385 ± 10 kg/m^3. The test specimens were sorted out from a big number of samples into 5 sets, 6 test specimens each. In total, there were 5 samples tested on the additional test criterion of mass loss.

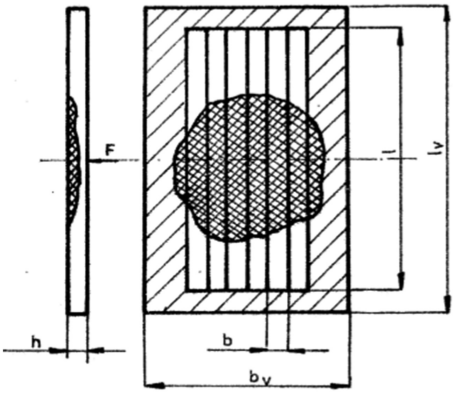

Fig. 1. The sampling scheme and the method of cutting out the test specimen. Where l_v-sample length, l-test specimen length, b_v-sample width, b-test specimen width, h-thickness of the test specimen.

The samples were used to cut out 30 specimens in the dimensions of 20 × 20 × 300 mm, 15 test specimens were tested on flexural strength and 15 test specimens on impact strength. There are stated average values gained in the measurement. The test specimen scheme is illustrated in Fig. 1. The samples were thermally exposed for 2, 5, 10, 15 and 20 min at every defined distance and under every heat source.

1.3 Evaluation Criteria

The mass loss was an additional evaluation criterion. It was proposed additional because if there was recorded no mass loss at bigger distance and shorter time of exposure, the samples were excluded from further cutting out and assessment as there was recorded no influence of thermal loading. The mass loss was calculated according to Eq. (1):

$$\Delta m = \frac{m_1 - m_2}{m_1}(\%) \tag{1}$$

Where:
Δm – mass loss (%),
m_1 – mass of the sample prior to the experiment (g),
m_2 – mass of the sample after the experiment (g).

Modulus of rupture (MOR) was one of the most important evaluation criteria [5, 7]. The essence of the test is investigating maximal loading before the test sample breaks. The loading force is applied in the point of the greatest damaging of the test specimen but on the reverse side from the exposure. The MOR in bending was calculated according to the Eq. (2):

$$\sigma_{oh} = \frac{3.F.l_0}{2.b.h^2}(MPa) \tag{2}$$

Where:
σ_{oh} – modulus of rupture (MPa),
F – loading force (N),
b – test specimen's width (mm),
h – test specimen's height (mm),
l_0 – span distance between the supports (mm) (240 mm).

Impact strength in bending is based on finding the toughness of the samples in a section bending under dynamic loading. The testing device is an impact pendulum. The energy used to break the test specimen is measured with 0.01 J precision. It is calculated according to Eq. (3):

$$A = \frac{W}{b.h}(J/cm^2) \tag{3}$$

Where:
A – impact strength in bending (J/cm^2),
W – impact energy (J),
b – test specimen's width (cm),
h – test specimen's height (cm).

2 Results and Discussion

During the experiment, measured values are evaluated in two separate steps. In the first step (see Fig. 2, 3 and 4), the investigation focuses on the influence of the heat source on the sample. The second step (see Fig. 5, 6 and 7) deals with the influence of the heat source at the 50 mm distance.

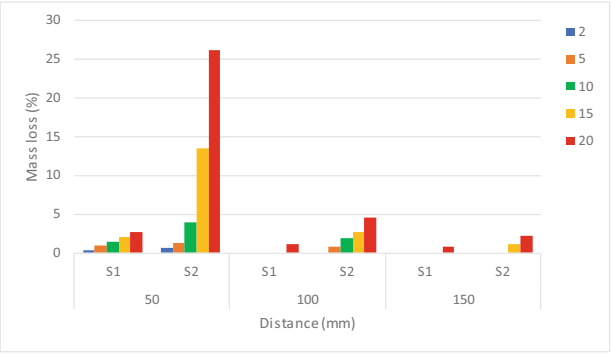

Fig. 2. The mass loss values depending on the time of radiant heat exposure (2, 5, 10, 15, 20 min), its power (S1, S2) and distance from the sample.

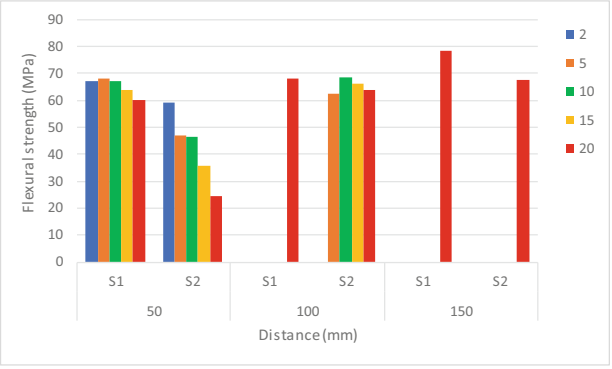

Fig. 3. The modulus of rupture depending on the time of radiant heat exposure (2, 5, 10, 15, 20 min), its power (S1, S2) and the distance from the sample.

The choice of the additional evaluation criterion proved to be appropriate, as the mass loss was not recorded at shorter times of loading and a bigger distance from the source. As Fig. 2 shows, at 50 mm distance and S1 source, the mass loss values grew in a linear way which was also confirmed by the second step of the experiment. Regarding S2 source, the changes in the mass loss values are jump-like and considerably more distinct.

The influence of the radiant heat source demonstrated itself in flexural strength and impact strength too. The decrease in the flexural strength (see Fig. 3) as well as in the impact strength in bending (see Fig. 4) is visible for the heat source S1 and clearly visible for the heat source S2.

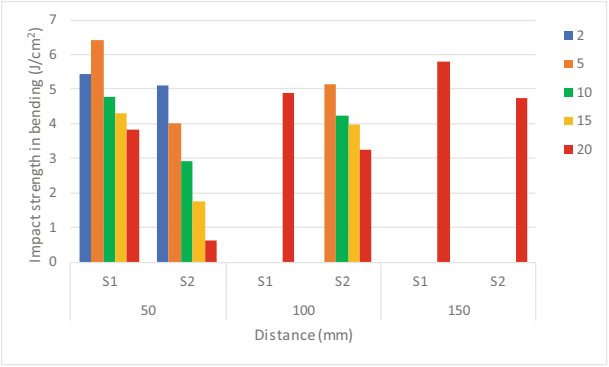

Fig. 4. The modulus of rupture depending on the time of radiant heat exposure (2, 5, 10, 15, 20 min), its power (S1, S2) and the distance from the sample.

The influence of the radiant heat source S1 did not occur at a distance of 100 mm. The mass loss occurred only for the time of 20 min; the shorter exposure of this heat source did not influence the spruce wood. Double-output heat source (S2) impact was displayed in all measured times; the mass loss values increased with the increasing time. There was observed only a slight decrease in the strength in bending. Several authors [3, 4, 6–8] found out that the appropriate heating for an appropriate time can increase flexural strength. Under this particular impact loading, the influence of radiant heat source S2 showed a decrease of impact strength in bending in time.

The distance of 150 mm seems to be "safe" for both sources of radiant heat. The mass loss was recorded at longer times of heat exposure and did not have a significant influence on the examined mechanical properties. All measured values are presented in figures; Fig. 2 shows the values of mass loss depending on the time of radiant heat exposure, its power, and the distance from the sample. Figure 3 shows the values of modulus of rupture depending on time of radiant heat exposure, its power and distance from the sample. Figure 4 shows the values of impact strength in bending depending on the time of radiant heat source exposure, power of the source, and distance from the sample.

The second separate evaluation included the comparison of radiant heat source S1, S2 (1000 W and 2000 W) at the shortest distance of 50 mm. At this distance, all measured values (for both sources) can make a statement. Their development and brief statistical evaluation are shown in Figs. 5, 6 and 7. Figure 5 shows the development of mass loss values depending on time and heat source output. Figure 6 shows the development of the modulus of rupture depending on time and output of the heat source. Figure 7 shows the development of the impact strength in bending depending on time and output of the heat source.

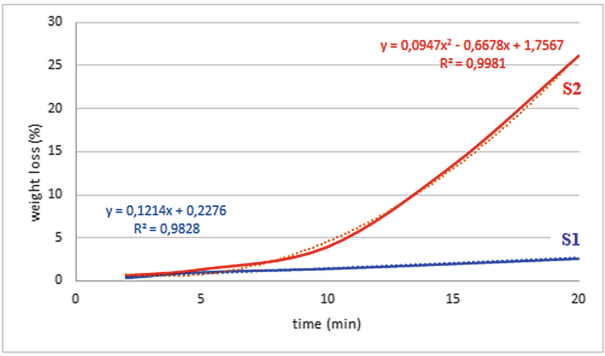

Fig. 5. The development of the mass loss values depending on the **time** and the output of the heat source.

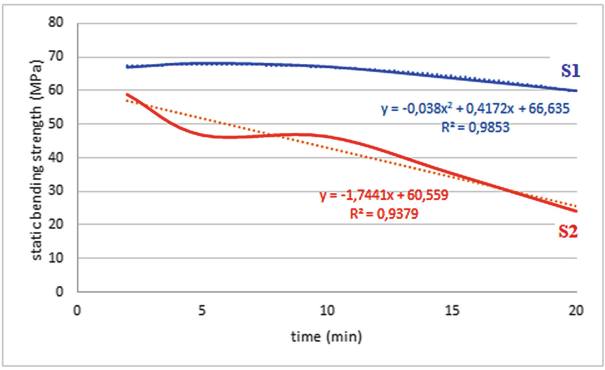

Fig. 6. The development of the modulus of rupture depending on the time and output of the heat source.

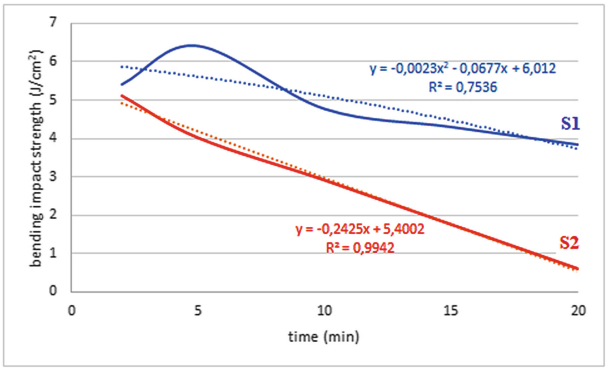

Fig. 7. The development of the impact strength in bending depending on time and the output of the heat source.

Based on the parameters' developments, an interesting finding can be stated. While the mass loss is of a linear characteristic for the source S1, the strength properties are of polynomic quadratic characteristic for the development in time. For the source S2 with a double output, it has exactly the opposite characteristic. The measured developments of the values have a linear characteristic of the decrease in observed values.

3 Conclusions

It is possible to conclude that observed values can form a statement regarding the burning and ignition of wood, in our case, particularly, spruce wood. The change in mechanical properties seems to be important information on wood behavior. Therefore, it is recommended to conduct the experiment with other wood species, various retardation treatments. The recommendation also includes tropical wood species and the thermally treated wood. The evaluation criterion shall cover also measuring the char layer depth [8].

References

1. Harada T (1996) Effects of density on charring and mass loss rate in wood specimens. In: 3rd international scientific conference on wood & fire safety. Technical University Zvolen, Zvolen, pp 149–156
2. Chovanec D, Osvald A (1992) Spruce wood structure changes caused by flame and radiant source. Technical University Zvolen (1992)
3. Irvine GM (1984) The glass transitions of lignin and hemicellulose and their measurement by diffferential thermal analysis. Tappi J 67:118–121
4. Kitahara RN, Matsumoto T (1974) Temperature dependence of dynamic mechanical loss of wood. Wood Res Soc
5. Krakovsky A, Kral S (2004) Changes of mechanical properties of primary spruce wood under mechanical and thermal loading. Scientific studies 5/2004/B, Technical University Zvolen

6. Kudela J (1992) Study of temperature influence on wood properties. In: Wood burning 1992. Technical University Zvolen, Zvolen, pp 201–222
7. Osvald A, Vercimak P (1984) Change in the yield strength of spruce wood due to heat sources. Drevo
8. White RH, Nordheim EV (1992) Charring rate of wood for ASTM E 119 exposure. Fire Technology 28:5–30
9. White RH, Schaffer EL (1981) Transient moisture gradient in fire-exposed wood slab. Wood Fiber 13(1):17–38

Wood Burning Retardation and Wood-Based Materials

Fire Retardancy and Leaching Resistance of Pine Wood Impregnated with Melamine Formaldehyde Resin *in-Situ* with Guanyl-Urea Phosphate/Boric Acid

Chia-feng Lin[1], Olov Karlsson[1], George I. Mantanis[2], Dennis Jones[1], and Dick Sandberg[1(✉)]

[1] Wood Science and Engineering, Luleå University of Technology, Luleå, Sweden
{chia-feng.lin,dick.sandberg}@ltu.se
[2] Lab of Wood Science and Technology, University of Thessaly, Karditsa, Greece

Abstract. This work aimed at finding ways to improve the leaching resistance of Scots pine (*Pinus sylvestris* L.) wood impregnated with water soluble fire retardant (FR). Sapwood specimens of Scots pine (10 × 10 × 50 mm) were impregnated with aqueous solution of guanyl-urea phosphate (GUP)/boric acid (BA). Limiting oxygen index (LOI) revealed that treatment could improve the fire performance. At the same time, thermogravimetric analysis (TGA) illustrated increased thermal stability after the treatment. However, since the FR itself was not fixed within the wood cell wall, it was extracted during water leaching (EN 84), and the wood lost its fire retarding property. The resistance to leaching of FR from the treated wood can be primarily improved while maintaining high fire retarding performance and thermal stability of treated wood by mixing melamine-formaldehyde (MF) resin with GUP/BA before impregnation to the wood. To mix GUP/BA to MF solution, due to the acidic nature of GUP/BA, the condensation/polymerisation reaction would be accelerated in an undesired way even if the solution was adjusted to non-acidic by NaOH. The resulting solution would not penetrate deeply into the wood structure, whilst it would be difficult to re-use the FR solution. In order to avoid the reaction proceeding in an undesired way, introducing 0.5 wt% of pentaerythritol to the GUP/BA/MF solution can decrease the reaction rate. Additionally, it improved the weight percentage gain (WPG) and fire retarding performance, without significantly influencing the leaching resistance and thermal stability. Overall, it is suggested that such a treatment could be a suitable methodology for producing exterior-use fire-retardant pine wood.

Keywords: Fixation · Fire retardant · *in-situ* polymerization

L. Makovicka Osvaldova et al. (Eds.): WFS 2020, *Wood & Fire Safety*, pp. 83–89, 2020.
https://doi.org/10.1007/978-3-030-41235-7_12

1 Introduction

Fire-retardant treated (FRT) wood can be produced by impregnation under high pressure with an aqueous solution containing guanyl-urea phosphate (GUP) and boric acid (BA) [1]. However, neither GUP nor BA bond strongly to the wood polymers and normally leach out during weathering; thus, such FRT wood is limited for interior-use if no further protection is applied. One simple method that can reduce the loss of water-soluble fire retardants (FRs) during weathering is through surface treatment, such as painting. However, a recent study revealed that this type of FRT wood is not suitable for long-term exterior use, due to the FR migrating to the surface because of water movement within the wood, so reducing fire retarding property [2]. However, if the FRs can be fixed within the wood such as by *in-situ* polymerisation, fire-retarding property is likely to be preserved during weathering. It has been found that melamine formaldehyde (MF) resin modified wood provided better dimensional stability [3], thermal stability [4], and to some extent, improved fire performance [5], but there have only been limited studies to date.

Therefore, this study aimed to reduce the leachability of FRs by treating the wood with MF resin/GUP/BA solution. The hydrophobic property of the cured MF resin is possible to microencapsulate FRs [6], so preventing leaching of FRs out of wood. Nevertheless, the acidity of FRs may inhibit blending into the alkaline MF resin solution. The acidity of FRs would accelerate the polymerisation of MF resin, which could cause processing problems in the way that the solution cannot penetrate deeply into the wood during impregnation as well as being difficult to recycle. Consequently, another aim of the study was to mitigate the undesired polymerisation.

Pentaerythritol acts as a charring reagent (carbonisation agent) and, together with a nitrogen phosphate salt, can be microencapsulated by MF resin [9] and enhance compatibility in other polymers [6]. Additionally, pentaerythritol with melamine phosphate [7] or ammonium polyphosphate [8] can enhance fire retardant performance better than nitrogen phosphate salt itself.

To study the treated samples' water leaching resistance, the European standard EN 84 for accelerated ageing was selected. The standard was originally developed in connection to studies on the durability of preservative-treated timber. The wood becomes more or less filled with water, with new water cycled 10 times within 14 days, allowing the chemicals to be in contact with pure water, facilitating diffusion. The fire performance, thermal property and chemical functionalities of the samples before and after water leaching (EN 84) were examined by limiting oxygen index (LOI), TGA and FTIR, respectively. LOI is the minimum concentration of oxygen (expressed as a percentage) that will support combustion of a polymer, e.g. wood. It is typically measured by passing a mixture of oxygen and nitrogen over a burning sample until a critical level is reached, which corresponds to LOI value. A higher LOI value indicates enhanced fire retarding performance.

2 Experimental Section

Materials. Guanyl-urea phosphate (GUP) was obtained from Fisher Scientific Sweden. Pentaerythritol, 98+ % was bought from Thermo Fisher Scientific, USA. ACS-grade boric acid (BA) and analysis-grade sodium hydroxide (NaOH) pellets were purchased from Merck, Germany. Melamine formaldehyde (MF) resin powder Prefere 4866 was provided by Dynea AS, Norway. The MF resin powder was dissolved entirely in deionized (DI) water before use. All chemicals were used as received without further purification.

Impregnation. Scots pine (*Pinus sylvestris* L.) sapwood samples measuring 10 mm × 10 mm × 150 mm (TxRxL) with a density of approx. 450 kg m^{-3} were oven dried at 103 °C for 48 h, then conditioned at 20 °C/65% relative humidity (RH),until the final moisture content (MC) was around 11%.

Preparation of the FR solution was made by dissolving GUP/BA (weight ratio 7:3) in deionised water, before mixing it with the MF resin solution. The mixed solutions' pH was then adjusted by 10 M NaOH to pH of 7.0 to prevent the immediate condensation. The naming of the FR solutions is shown in Table 1.

Table 1. The naming of the solution for impregnation.

Solution	10% GUP/BA	10% GUP/BA + 30% MF resin	10%GUP/BA + 30%MF resin + 0.5% Pentaerythritol
Naming	7G3B	10-30MF	10-30MF-0.5P

Fully immersed samples (10 replicates) were impregnated using a full-cell vacuum-pressure procedure (30 min. of reduced pressure at 20 mbar followed by 15 bar pressure for 1 h).The resulting samples were then heated at 40 °C for 1 day followed by heating at 120 °C for 1 day before measuring the dried mass. These were conditioned at 20 °C/65% RH in a conditioning chamber for 1 week before further analysis.

Accelerating Ageing EN 84. Leaching tests were performed on 5 replicates according to standard EN 84 (1997), i.e. immersing the samples in a container with 5 times more volume of deionized water and replacing the water 10 times during the 14-day leaching period. The samples were then oven-dried at 103 °C to dried mass.

Limiting Oxygen Index (LOI). Fire tests were carried out on 5 replicates, using the limiting oxygen index (LOI) according to ISO 4589-2:2006. LOI on samples before and after EN84 water leaching was performed on conditioned specimens.

Fourier Transform Infrared Spectroscopy (FT-IR). PerkinElmer FT-IR spectrometer Frontier equipped with UATR Diamond/ZnSe ATR (Single Reflection) over the wavenumber range of 4000–650 cm^{-1} with 4 scans at a resolution of 4 cm^{-1} was utilised to analyse the chemical functionalities of the samples. Each sample was ground and sieved through a 0.25 mm mesh before analysis.

Thermal Gravimetric Analysis (TGA). PerkinElmer TGA 4000 was utilised for the thermal gravimetric analysis (TGA) of the specimens. Each specimen was firstly ground and sieved through a 0.25 mm mesh. A total of 15 ± 2 mg sample of each specimen was loaded into an alumina crucible. The sample was then heated at a rate of 10 °C min^{-1} from 30 to 800 °C with N_2 flow rate of 20 ml min^{-1}. Three replicates were performed for each specimen, with curves smoothed using a 10-Point-Adjacent-Averaging algorithm.

3 Results and Discussion

Figure 1 shows the measurement of weight percentage gain (WPG), WPG loss and LOI of the specimens. GUP/BA treated wood (7G3B in Fig. 1c) could achieve excellent fire retardant performance, though its poor bonding with wood led to its loss after water leaching. LOI was found to be similar to untreated wood, and the WPG implied that GUP/BA was almost all lost. As a comparison, MF resin/GUP/BA treated wood (10-30MF in Fig. 1) had lower WPG loss and better LOI after water leaching than without resin. From the results, it is suggested that MF resin might encapsulate FRs and improve the resistance to leaching.

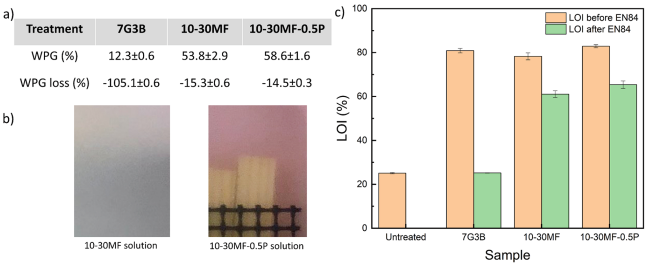

Fig. 1. (a) WPG and WPG loss of GUP/BA (*7G3B*), GUP/BA/MF resin (*10-30MF*) and GUP/BA/MF resin/Pentaerythritol (*10-30MF-0.5P*) treated samples, (b) images of 10-30MF (*Left*) and 10-30MF-0.5P (*Right*) solution. Both images were made after impregnation, (c) LOI of untreated sample, 7G3B, 10-30MF and 10-30MF-0.5P.

A difficulty of preparing MF resin/GUP/BA solution was that the resin polymerisation resin was accelerated due to the acidity of GUP/BA solution. The undesired reaction would cause problems, limiting penetration into the wood and hindering subsequent recycling of the used solution. To alleviate the undesired reaction, pentaerythritol (10-30MF-0.5P) was mixed with the other chemicals before impregnation. Figure 1b shows that by adding 0.5 wt% of pentaerythritol to the mixture, transparency after impregnation was dramatically improved. By adding pentaerythritol, the weight percent gain (WPG) was increased from 53.8 wt% to 58.6 wt%, and LOI was slightly increased both before and after water leaching (Fig. 1c).

The thermal stability of samples was performed by thermogravimetry (TGA), with first derivative of thermogravimetry (DTG) curves shown in Fig. 2. TGA measured the mass loss as the temperature increased while DTG curve displays distinct different thermal degradation steps. All samples had approx. 4% mass loss from 30 °C to around 110 °C, assumed to be related to loss of physical bonded water. FR treatment influenced the thermal property of the wood, with the main decomposition peak of 7G3B shifting to a lower temperature compared to the untreated sample. This was due to GUP/BA accelerating the thermal degradation and formation of char at the lower temperature. Furthermore, inorganic phosphate and boron element from GUP/BA could provide a protective layer at higher temperatures, as demonstrated with the mass loss at up 800 °C [10].

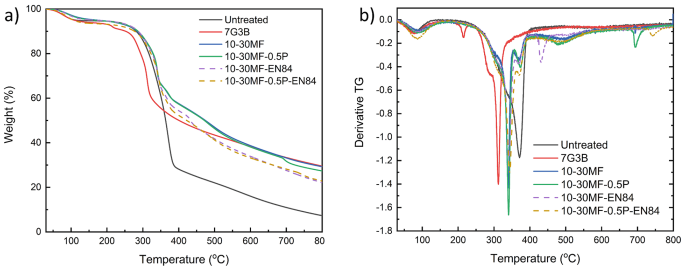

Fig. 2. (a) TGA curve of untreated wood, 7G3B, 10-30MF and 10-30MF-0.5P, (b) Derivative TG curves of the Fig. 2a.

Introducing MF resin and pentaerythritol to the FR treatment also changed the thermal property of the wood. Two degradation peaks around 210 °C and 290 °C could be attributed to the decomposition of GUP [10], but these were not observed when the resin was introduced (10-30MF and 10-30MF-0.5P). The main thermal decomposition peaks of 10-30MF and 10-30MF-0.5P were noted at around 340 °C (between those for 7G3B and the untreated wood). Additionally, a new degradation peak located at approx. 370 °C could be assigned to the degradation of the MF resin polymeric network [11]. Both 7G3B and 10-30MF had almost the same mass residues at 800 °C, while10-30MF-0.5P had slightly lower mass residue at 800 °C due to an extra thermal degradation step occurring around 690 °C.

TGA was also used to investigate the impact of water leaching on the thermal property of the samples. TGA result of 7G3B after water leaching was not included since the LOI result was almost the same as the untreated sample. The main decomposition peaks of 10-30MF and 10-30MF-0.5P after EN 84 to before EN 84 were all located at the same temperature, around 340 °C, though peak intensities decreased after water leaching. Simultaneously, the peak at around 370 °C related to MF resin degradation was slightly enhanced by the water leaching. The results indicated that the relative percentage of MF resin increased whilst that of other material decreased upon water leaching of samples. More materials such as FR and/or wood than MF resin might be removed during water leaching.

FTIR analysis was undertaken to identify the chemical functionalities of the samples. Figure 3a shows the FTIR spectra of untreated wood, 7G3B, 10-30MF and 10-30MF-0.5P respectively. The peak located at 1698 cm^{-1} corresponding to GUP [12] was noted in the spectra of 7G3B, while with MF resin treatment (10-30MF and 10-30MF-0.5P) the peak was not clearly revealed. A wavenumber of 810 cm^{-1} corresponding to triazine ring bending vibration of MF resin [13] was noted in the spectra of 10-30MF and 10-30MF-0.5P, whilst 10-30MF-0.5P showed a slightly different spectrum compared to 10-30MF. Some difference related to the presence of sharper peaks at 3000–2900 cm^{-1} (possibly due to sp^3 C-H stretching vibrations) and two small new peaks at 1393 cm^{-1} (due to methylene C-H bending vibrations) and 1035 cm^{-1} (due to C-O stretching vibrations) were observed in samples with pentaerythritol. The results implied that either (a) pentaerythritol reacted with other compounds to form new bonds, or (b) extractives such as fatty acids migrated to the surface of samples [14]. Figure 3b compared the FTIR spectra of before and after water leaching according to EN 84, showing little variation, implying the water leaching has small impact on the resin treated wood's chemical functionalities.

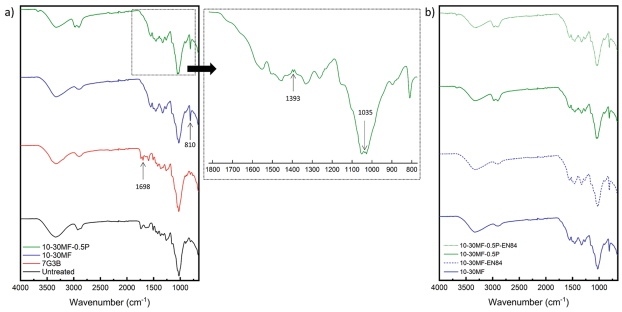

Fig. 3. FTIR spectrum of (a) untreated wood, 7G3B, 10-30MF and 10-30MF-0.5P, (b) comparing before and after water leaching EN 84 of 10-30MF and 10-30MF-0.5P.

4 Conclusion

A novel method for improving leaching resistance of the water-soluble fire retardant chemicals was demonstrated in this study. From analysis by LOI, TGA and FTIR results, it is suggested that the cured MF resin help retain the chemicals within the wood and provide good fire retardant performance, even after water leaching according to EN 84. Furthermore, the addition of low concentration of pentaerythritol could improve the impregnating liquid stability, WPG of treated wood and its fire retarding performance, whilst having a negligible influence on the thermal stability of the product.

Acknowledgements. Financial support from the Swedish Innovation Agency (Vinnova), project: "Swedish wood - Innovation potential for the bio-based society", DP2: Needed processing of Swedish wood, 2017-02697, is greatly acknowledged.

References

1. Oberley WJ (1988) Non-resinous, uncured fire retardant and products produced therewith
2. Kawarasaki M, Hiradate R et al (2018) Fire retardancy of fire-retardant-impregnated wood after natural weathering I. Mokuzai Gakkaishi 64:105–114
3. Inoue M, Ogata S et al (1993) Dimensional stability, mechanical properties, and color changes of a low molecular weight melamine-formaldehyde resin impregnated wood. Mokuzai Gakkaishi 39:181–189
4. Deka M, Saikia C, Baruah K (2002) Studies on thermal degradation and termite resistant properties of chemically modified wood. Bioresour Technol 84:151–157
5. Xie Y, Xu J et al (2016) Thermo-oxidative decomposition and combustion behavior of scots pine (pinus sylvestris L.) sapwood modified with phenol- and melamine-formaldehyde resins. Wood Sci Technol 50:1125–1143
6. Wang B, Sheng H et al (2015) Recent advances for microencapsulation of flame retardant. Polym Degrad Stab 113:96–109
7. Chen Y, Wang Q (2007) Reaction of melamine phosphate with pentaerythritol and its products for flame retardation of polypropylene. Polym Adv Technol 18:587–600
8. Camino G, Costa L, Trossarelli L (1984) Study of the mechanism of intumescence in fire retardant polymers: part I-thermal degradation of ammonium polyphosphate-pentaerythritol mixtures. Polym Degrad Stab 6:243–252
9. Sun L, Qu Y, Li S (2012) Co-microencapsulate of ammonium polyphosphate and pentaerythritol and kinetics of its thermal degradation. Polym Degrad Stab 97:404–409
10. Wang Q, Li J, Winandy J (2004) Chemical mechanism of fire retardance of boric acid on wood. Wood Sci Technol 38:375–389
11. Anderson IH, Cawley M, Steedman W (1971) Melamine - formaldehyde resins II.-thermal degradation of model compounds and resins. Br Polym J 3:86–92
12. Wang Q, Li J, Li S (2006) Fire-retardant mechanism of fire-retardant FRW by FTIR. Front For China 1:438–444
13. Merline DJ, Vukusic S, Abdala AA (2013) Melamine formaldehyde: curing studies and reaction mechanism. Polym J 45:413–419
14. Fengel D (1989) Wegener G (1989) Wood: Chemistry, Ultrastructure, Reactions. Verlag Kessel, Remagen

Application of a Bio-Based Coating for Wood as a Construction Material: Fire Retardancy and Impact on Performance Characteristics

Stephanie Rensink[1(✉)], Michael F. Sailer[1], Roy J. H. Bulthuis[2], and Mieke A. R. Oostra[3]

[1] Chair Sustainable Building Technology & Material, Saxion University of Applied Sciences, M.H. Tromplaan 28, P.O. Box 70.000, 7500 KB Enschede, The Netherlands
{s.rensink, m.f.sailer}@saxion.nl
[2] Chair Nanobio, Saxion University of Applied Sciences, M.H. Tromplaan 28, P.O. Box 70.000, 7500 KB Enschede, The Netherlands
r.j.h.bulthuis@saxion.nl
[3] Centre of Expertise Smart Sustainable Cities, Utrecht University of Applied Sciences, Padualaan 99, P.O. Box 182, 3584 CH Utrecht, The Netherlands
mieke.oostra@hu.nl

Abstract. The use of living micro-organisms as a protection method on surfaces of wooden building components becomes more common. Since wood is one of the relevant building materials to be used in a circular economy, fire safety and environmental issues are relevant aspects. Up to now, there is little experience in their potential contribution to fire-retardancy. This research aimed to get more information of a wood treatment with a so-called biofinish in combination with an ammonium phosphate based fire retardant. This biofinish system is comprised of a linseed oil impregnation and a protective and decorative coating based on the yeast-like fungus *Aureobasidium* [1]. Initial tests of wood treated with this biofinish and an ammonium phosphate based fire retardant showed positive effects on the fire growth rate index (FIGRA) and the heat release rate (HRR) in an European fire classification as well as in thermogravimetric analysis (TGA) assessments [2]. This is remarkable since linseed-oil is part of the coating formulation and used by the fungus as a nutrient. The behavior of samples treated with an ammonium phosphate based fire retardant and the biofinish was further studied in an one-year exposure test. This test revealed the potential esthetical stability of such a coating. The study resulted in crack formation and leaching of samples treated with ammonium phosphate and biofinish and stood in contrast with the behavior of wood samples treated with biofinish without an ammonium phosphate treatment.

Keywords: Fire retardant · Biofinish · *Aureobasidium* spp. · Outdoor performance

L. Makovicka Osvaldova et al. (Eds.): WFS 2020, *Wood & Fire Safety*, pp. 90–96, 2020.
https://doi.org/10.1007/978-3-030-41235-7_13

1 Introduction

Sustainability and functionality become more and more relevant in the development of new products. A sustainable economy, which is based on the use of renewable resources in a sustainable way and minimizing the negative impact on the environment is the core of the circular economy action plan of the Commission of the European Parliament [3, 4]. Wood is an important renewable construction material and contributing to such developments. However, like all natural substances, wood is subject to degradation. Degradation of wood can be caused by different factors e.g. ultraviolet (UV) radiation and wood-decaying fungi [5]. Also, fire is a potential risk due to the poor inherent flammability resistance of timber [6]. In addition, sometimes some of these factors interact, causing increased degradation.

The use of fire retardants and building safety are often at odds. Although usually technically necessary, the use of fire retardants is often disadvantageous due to related environmental pollution and since it may cause a barrier to reuse [7]. Mainly persistent bio accumulative and toxic substances such as PBT and persistent organic pollutants (POP) are considered as concerning [8, 9]. Timber is frequently impregnated with fire retardants but it's also treated in different ways to improve fixation and reduce leaching of fire retardant substances from building components. This fixation property is still subject to be enhanced. Although there is a lot of information available related to flammability, the effects of phosphate and nitrogen containing fire retardants on the wood quality and stability during application and the growth of microorganisms on wood surfaces are not well assessed [10].

Recently, it was discovered that a surface treatment of wood based on linseed oil and a microbial coating (biofinish) using the black pigmented fungus *Aureobasidium pullulans* is an environmentally friendly concept to protect wood against degradation [1]. Results showed that this biofinish contributed positively to fire retardance in combination with ammonium phosphate [2, 11]. It showed positive effects on the fire growth rate index (FIGRA) and the heat release rate (HRR) as well as in thermogravimetric analysis (TGA) assessments [2, 11]. The lack of in-service experience using the combination of an ammonium phosphate based fire retardant and the microbial coating required outdoor exposure to achieve information about potential properties and risks during application. The initial effects of the treatment on the timber surface and wood behavior is described in this study.

2 Material and Methods

The most well-known method for treating wood with a fire retardant is with an impregnation using vacuum/pressure. The agent penetrates deeper into the wood structure compared to dipping or surface treatments e.g. vacuum coating or brushing. In this study samples of 195 × 145 × 17 mm^3 Scots Pine (*Pinus sylvestris*) with a micro-riffled surface and 14% moisture content were treated in a three-step procedure including a fire retardant impregnation, raw linseed oil treatment and a biofinish application. The wood samples were impregnated with an ammonium phosphate based fire retardant from Fire Resistant with a concentration of 180 g/L fire retardant in water.

The impregnation was carried out in an impregnation vessel (Scholz) (Fig. 1) using a vacuum period of 15 min at 8×10^3 Pa followed by a 15 min pressure of 8×10^5 Pa. Following the fire retardant treatment, the wood samples were exposed to the ambient air of the indoor production area for a week. Afterwards, the wood samples were impregnated with 2 layers raw linseed oil obtained from Scaldis-Ruien without vacuum or pressure applied by a brush. Finally, after a drying period of a week at the ambient air of the indoor production area, the samples were coated on all sides with two layers of Xyhlo biofinish obtained from Xylotrade. 3 of the treated samples were exposed outdoors for 12 months, the other samples remained indoors. After exposure, the sample weights were determined after climatizing to equilibrium moisture content (EMC) at 23 °C and 65% RH for 1 week and after 18 h incubation at 103 °C. The samples were visually assessed using a stereo microscope of Leica Wild M32 with a KL 1500 LCD light source. Microscopic images were made using the DineEye C-mount Camera.

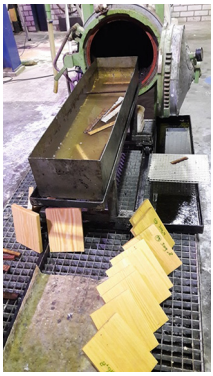

Fig. 1. Impregnation of wooden samples using a Scholtz impregnation vessel.

3 Results and Discussion

Recently, it has been shown that good fire retardation of wood could be achieved in the combination of ammonium phosphates and a microbial coating resulting in a fire resistance class B [2]. The $FIGRA_{0.2MJ}$ results of three initially tested SBI-tests were on average 118 W/s and for $FIGRA_{0.4MJ}$ 94 W/s, which meets the requirements for fire class B [2]. The compatibility of microorganisms and ammonium phosphate seems to allow long-term exposure although some fading appeared compared to untreated samples.

Assessment of the EMC revealed a moisture content at 23 °C and 65% RH of indoor exposed samples at 9.3% and outdoor exposed samples at 10.3% which is lower than the expected EMC of untreated Scots pine wood at around 11,5% [12]. Although the measured results showed a lower EMC, it's in accordance with results found by

Stevens et al. who assessed chemically reactive phosphorus acids [13]. Other authors expect that ammonium phosphate has the potential to increase the moisture content of wood in humid conditions with the potential effect of increased fungal growth and potential decay promotion [10]. If the lower moisture content can be attributed to a reaction with hydroxyl-groups of the wood or other wood interaction probably in combination with hydrophobating effects of the linseed oil treatment has to be assessed.

Using the vacuum pressure impregnation process, an average uptake of 40.9 g ammonium phosphate per sample was achieved. After an outdoor exposure of 12 months, a reduction of 23.4 g of the added compounds was noticed. This would mean that a considerable loss of 57% during outdoor exposure occurred. The loss could mainly be attributed to fire retardant components since no degradation of the wood and substantial loss of the microbial coating was observed. Similar leaching results were achieved in a previous study on wooden samples tested in vitro in a watery environment [2]. In the study was shown that the use of a special biofinish treatment with an extra linseed oil containing top-coating reduced leaching of ammonium phosphate in a watery environment [2]. Leaching of the ammonium phosphate is a well-known phenomenon and was mentioned in several publications [10, 14]. Ellis and Rowell showed leaching of phosphorous compounds in laboratory tests close to 50%, an amount which would fit to the value of 57% loss that was found after 12 months outdoor exposure. This could be taken as an indication that the biofinish and linseed oil applied did not significantly contribute to the reduction of leaching which could be interpreted in such a way that at least most of the ammonium phosphate did not react with wood components. To what extend fire resistance remains has to be tested later on.

The results show a serious impact of ammonium phosphate treatments on the timber. During outdoor exposure of Scots pine samples deformation and formation of (severe) cracks were observed at samples treated with ammonium phosphate (Fig. 2A–D). In samples treated with biofinish (without ammonium phosphate) no cracks were observed (Fig. 2E). Also, the microscopic observations of samples with biofinish (without ammonium phosphate) didn't indicate increased crack formation (Fig. 3A). Samples treated with ammonium phosphate without a biofinish and without outside exposure didn't indicate formation of cracks (Fig. 3E). In contrast, samples treated with ammonium phosphate and biofinish show possibly phosphate salts particles (Fig. 3B) and crack formation with cracks of widths of 0.061 mm, 0.493 mm (Fig. 3C) and 0.383 mm (Fig. 3D). These results could be interpreted in such a way that the addition of an ammonium phosphate based fire retardant to biofinish treated Scots pine wood can stimulate crack formation when exposed outside. A significant problem of some phosphorus-based fire retardants (e.g. monoammonium phosphate, MAP) seems to be the in-service reductions in strength of treated wood products. This reduction in strength occurs when wood members are exposed to elevated temperatures [15]. Winandy explains this with initial pH of wood and the buffering capacity of the fire retardant, which could damage the wood integrity [16]. This could probably also explain the extend crack forming of the treated timber.

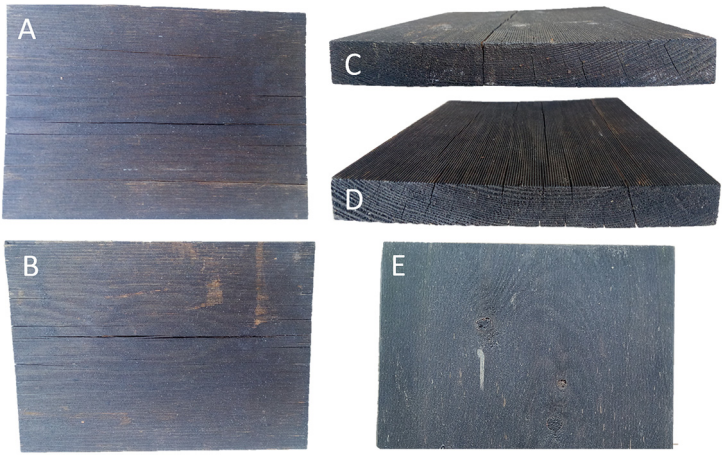

Fig. 2. After 12 months outdoor exposure of wood samples treated with an ammonium phosphate based fire retardant and biofinish (A–D) and biofinish (E). Cracking and deformation is seen in samples treated with phosphate based fire retardant at the sample surface (A, B) and head site (C, D) Samples treated with biofinish after outdoor exposure didn't show cracking (E).

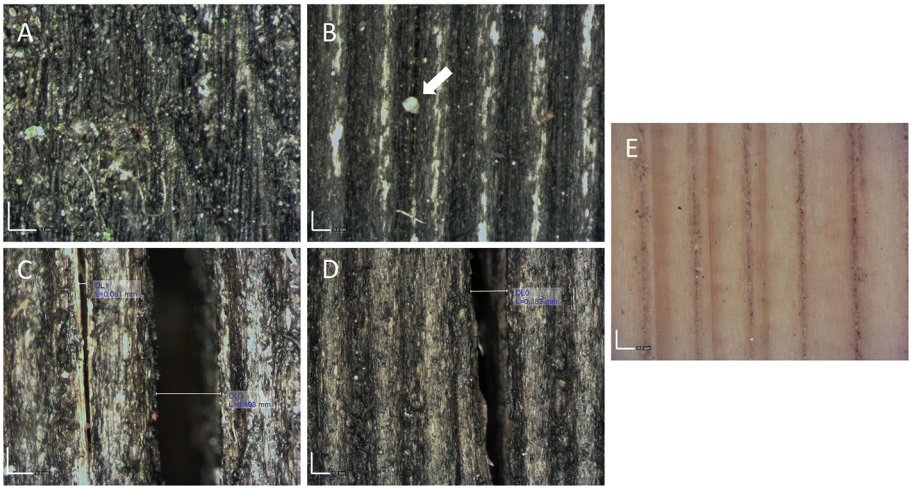

Fig. 3. Stereo microscopic images of sample surfaces after outdoor exposure of *Pinus sylvestris* treated with biofinish (A), biofinish and fire retardant (B, C, D) and *P. sylvestris* treated with fire retardant (E). Measurements of crack widths (DL0 and DL1) are shown in mm. White arrow possibly indicate a phosphate particle. Scale bar image A is 0.1 mm, B-E is 0.2 mm.

4 Conclusion

The use of a microbial coating in combination with an ammonium phosphate based fire retardant improves the resistance against fire resulting in class B. During outdoor exposure however the effect of the ammonium phosphate seems to be dominating above the positive properties of the microbial coating, resulting in crack forming and leaching. However, with the use of a special biofinish treatment provided with an extra linseed oil top-coating, leaching of ammonium phosphate in a watery environment could be reduced.

References

1. Sailer MF, van Nieuwenhuijzen EJ, Knol W (2010) Forming of a functional biofilm on wood surfaces. Ecol Eng 36(2):163–167
2. Rensink S, van Nieuwenhuijzen EJ, Sailer MF (2018) Effects of wood protecting biofinish and linseed oil on fire behaviour and leachability of the fire retardant. In: Proceedings IRG annual meeting. IRG/WP 18-30728, 16 p
3. Bourguignon D (2016) EPRS, European parliament briefing January 2016, closing the loop, new circular economy package. Members Research Service. EN PE573.899
4. European Commission (2011) Communication from the Commission to the European Parliament, the Council, the European Economic and Social Committee and the Committee of the Regions. Roadmap to a Resource Efficient Europe. European Commission, Brussels, Belgium. COM 2011 571
5. Gobakken LR, Høibø OA, Solheim H (2010) Mould growth on paints with different surface structures when applied on wooden claddings exposed outdoors. Int Biodeterior Biodegradation 64(5):339–345
6. Hapuarachchi TD (2010) Development and characterisation of flame retardant nanoparticulate bio-based polymer composites. Ph.D. thesis, Queen Mary University of London
7. Muñoz I et al (2009) Chemical evaluation of contaminants in wastewater effluents and the environmental risk of reusing effluents in agriculture. TrAC Trends Anal Chem 28(6):676–694
8. Regulation (EU) 2019/1021 (2019) European Parliament and the Council of the European Union Regulation (EU) 2019/1021 on persistent organic pollutants. Official Journal of the European Union
9. Regulation (EC) No 1907/2006, Registration, Evaluation, Authorisation and Restriction of Chemicals (REACH) (2006) Establishing a European Chemicals Agency, amending Directive 1999/45/EC and repealing Council Regulation (EEC) No 793/93 and Commission Regulation (EC) No 1488/94 as well as Council Directive 76/769/EEC and Commission Directives 91/155/EEC, 93/67/EEC, 93/105/EC and 2000/21/EC
10. Lowden LA, Hull TR (2013) Flammability behaviour of wood and a review of the methods for its reduction. Fire Science Rev 2(1):4
11. Rensink S, Klein Rot EAM, Sailer MF (2017) Thermal stability of a wood protective biofinish and the influence of flame retardants on Aureobasidium cells. In: Proceedings IRG annual meeting. IRG/WP 17-30716, 15 p
12. Wangaard FF (1979) The hygroscopic nature of wood. Colorado State Univ Fort Collins
13. Stevens R et al (2006) The structure–activity relationship of fire retardant phosphorus compounds in wood. Polym Degrad Stab 91(4):832–841

14. Ellis W, Rowell R (1989) Flame-retardant treatment of wood with a diisocyanate and an oligomer phosphonate. Wood Fiber Sci 21(4):367–375
15. LeVan S, Collet M (1989) Choosing and applying fire-retardant-treated plywood and lumber for roof designs. General Technical report FPL-GTR-62. Madison, vol 62. WI: US Department of Agriculture, Forest Service, Forest Products Laboratory, 11 p
16. Winandy JE (1995) Effects of fire retardant treatments after 18 months of exposure at 150 F (66 C), vol 264. US Dept. of Agriculture, Forest Service, Forest Products Laboratory

Fire Retardant Treatment of Wood – State of the Art and Future Perspectives

Philipp Sauerbier(✉), Aaron Kilian Mayer, Lukas Emmerich, and Holger Militz

Wood Biology and Wood Products, Faculty of Forest Sciences, University of Goettingen, Buesgenweg 4, 37077 Goettingen, Germany
psauerb@gwdg.de

Abstract. Outdoor and indoor exposed wooden structures are prone to the hazard of fire. Thisr is often inevitable and hardly avoidable by factors such as the design. However, wood is widely used as a structural element in buildings, it is present all-over public places and the main source for indoor furniture. Thus, and due to recent incidents, the demand for an effective and leaching-resistant fire protection is rising. In addition, fire protection technologies are desired, which survive mechanical processing. Considering the latter, protective surface coatings show a high fire protection, while on opposite they are very sensitive to mechanical damages. Therefore, various approaches based on a full impregnation of timber with fire retardants have been studied. In the past aluminum, boron, halogens (e.g. bromine) and more recently phosphorus and nitrogen, were shown to be effective fire retardants in wood. Nowadays, most conventional fire retardant systems are halogen-free, while boron is still used. However, boron shows a low resistance to leaching and is classified as a SVHC candidate, which brings up health and environmental issues. The same is true for formaldehyde. Concerning environmental issues, nitrogen and phosphorus were found to be promising alternatives and highly effective fire retardants. Leaching in service was slightly reduced compared to boron but a decrease in strength properties was detected after treatment of wood with those compounds. In general, an increased hygroscopicity of wood was found after any of the listed treatments, together with a leaching of the flame-retardant chemical which was still too high to guarantee a long-term fire protection in wood exposed outside. The overall aim of this study is to (1) give an overview about the past developments and most established fire retardant chemicals and (2) review recent findings and developments in terms of permanent fire retardant treatments of wood.

Keywords: Chemical wood modification · Fire retardant · Impregnation · Review

1 Introduction

Wood as a construction material is closely linked to human history. Recently, it's experiencing a renaissance due to its sustainable and regenerative properties. Following this trend, larger and higher construction projects made of wood are being built worldwide in e.g. Vienna (AUT), Vancouver (CAN) or Brumunddal (NOR).

L. Makovicka Osvaldova et al. (Eds.): WFS 2020, *Wood & Fire Safety*, pp. 97–102, 2020.
https://doi.org/10.1007/978-3-030-41235-7_14

The use of wood allows the construction of energy efficient buildings in a relatively short time. Wood is characterized as a construction product by a high strength to weight ratio, low heat conductivity and easy machinability. It also binds carbon and thus contributes to reducing the CO_2 content of the atmosphere. However, the many positive features also face some disadvantages. In addition to the low dimensional stability and low resistance to wood-degrading fungi, the use of wood is limited primarily by its flammability. This creates specific risks for use as a construction material in terms of: (1) flammability and fire formation, (2) fire propagation in the form of smoke and fire, and (3) change in load bearing capacity due to combustion [1]. Additionally, an exclusively constructive solution of the fire protection on the dimensioning of components is not always possible or in case of capsuling wood with e.g. gypsum boards not aesthetically desired.

The development of fire-retardant chemicals for wood is thus a necessity as there is a demand for this sustainable building material. However, challenges arise since a fire retardant wood modification should be permanent, not worsening its durability or mechanical properties, non-toxic and should not contribute to smoke generation [2]. A sustainable, no risk to health and leaching resistant treatment of wood is therefore of economic and social interest.

2 Wood Composition and Thermal Decomposition

Wood is a three-dimensionally structured and porous material with hydroscopic and anisotropic properties caused by its chemical and anatomical composition. The three main polymeric components are cellulose, hemicellulose and lignin - this composition is supplemented by a small proportion of extractives. The cellulose is composed of β1-4 linked glucose units which build up the cell wall. These cellulose fibrils are embedded in a matrix of hemicelluloses, a heterogeneous group of polysaccharides, and polyaromatic lignin. Regarding the anatomy, wood reveals a complex cellular structure with significant differences between species, e.g. coniferous and deciduous wood. A detailed description of the anatomy and composition of wood can be found e.g. in [3].

Even though the chemical and anatomical composition of wood is highly complex, processes during the exposure to fire are well understood on a practical level and are predictable [4]. On a microscopic and chemical level, the thermal decomposition into volatile gases, levoglucosan (tar) and char is described as a superposition of wood's main component decomposition. The decomposition is described well in literature; even though the exact temperatures differ slightly and is dependent on the wood species, the general pyrolysis follows the same path [5, 6]: Temperatures above 100 °C lead to dehydration and generate noncombustible gases like CO_2, formic acid or acetic acid. Beginning at about T > 200–225 °C significant pyrolysis takes place, beginning with hemicellulosic components. From this temperature on, combustible gases are formed and flaming combustion might occur after an initial pilot flame. With temperatures reaching >300 °C the significant depolymerization of cellulose takes place and high amounts of volatile and combustable gases are formed. Due to its heavily cross-linked structure the relatively stable lignin decomposes last at temperatures of about 370–400 °C.

Throughout the decomposition the emitted (volatile) gases contain more hydrogen and oxygen than the original polymeric chains of wood. This leads to carbon enriched residues – this char is stable against thermal decomposition (<3000 °C). However, due to smouldering the char can undergo further degradation by being oxidized to CO_2, CO and H_2O.

3 Fire Retardant - Modes of Action

The in the following described modes of action can, in most cases, not be seen exclusively, since most retardants will combine several of them, to be as effective as possible.

To reduce the effective concentration of oxygen and combustible material, a fire retardant might set free an **inert gas that dilutes** the previously combustible gas mix. A gas released might on the other hand be very reactive and able to **quench the reactions happening in the gaseous phase**. This leads to an incomplete combustion and therefore less heat to sustain the fire. In some cases, this gas is released by an **endothermic degradation of the retardant**, thus lowering the temperature and the amount of combustible products. A **ceramification by adding larger quantities of inorganic non-combustible material** does also increase the fire resistance. The naturally occurring char layer also works as a fire retardant since it is limiting heat transfer and oxygen diffusion to the area of decomposition and combustibles into the flame zone. Therefore, chemicals that **increase the char formation by dehydration** are also able to increase the fire retardancy [7, 8].

4 Important Fire Retardant Chemicals

Boron-based fire retardants have been used for decades as fire retardant and preservation chemical. Most common are Borax and boric acid compounds, possibly in combination with various other nitrogen, phosphor or inorganic salt retardants. The mode of action is based on forming a protective layer that lowers heat, oxygen and combustible gas transfer [9]. Additionally, the release of water of crystallization will dilute the gaseous phase. However, boric acid and other boron-based retardants may very well be harmful to our reproduction system. Therefore, it has been added to the list of Substances of Very High Concern (SVHC) [10]. Since this is a first step to further regulatory limitations of the usage of such a chemical, recent research, especially in Europe, did focus on finding suitable alternatives. Nevertheless in other parts of the world, the research continues and looks into leaching prevention by using e.g. phenylboronic acid [9] or utilizing tannin-boron chemicals [11].

Halogenic fire retardants capture free radicals, which will reduce the heat and propagation of the flame. Even though all halogens quench radicals well, only chlorine and bromine based compounds decompose, and set free the active halogen component, at a temperature range that is suitable for fire retardants. However, brominated once have become the most popular due to a higher trapping efficiency [12]. Brominated retardants are widely used commercially for polymeric systems, nonetheless authorities

are monitoring these chemicals continuously as some of them have proven to be harmful and accumulate in the body and environment. For wood treated with brominated fire retardants there is only limited recent data available [13, 14]. A bromination of wood is also possible, leaching resistant, since it is a chemical modification, and showed promising results regarding fire retardancy [15].

It is expected that **nitrogen-based fire retardants** decompose and release an incombustible that dilutes the otherwise flammable gas that is necessary to sustain a flame, while also lowering the temperature due to its endothermic decomposition [16]. The potential of nitrogen-based fire retardant is mostly used in combination with **phosphorus chemicals** (in particular phosphorus acid and its salts), which are efficient catalysts for cellulose dehydration. Therefore, they accelerate the charring and by this provide a protective layer to the wood. Additionally the decomposition of phosphoric acid is endothermic. The efficacy of the phosphor compound is proportional to its acidity [17]. However one has to bear in mind, that higher acidity may also significantly reduce the mechanical stability [18]. Inorganic ammonium phosphates have not only been used since over a century, but also extensively researched [16, 19]. Organic phosphorus chemicals based on e.g. guanidine, guanylurea or melamine also proved to be effective fire retardants [16, 18].

Various **hydroxides and carbonates** (e.g. magnesium or aluminium) have been investigated in the past [20]. The endothermic decomposition of this material class does not only cool the wood and therefore slows down the combustion process, but also releases CO_2 or water to dilute the flammable gases. Additionally, the remaining oxides residues build a protective layer. Due to their low efficiency, a high load would be necessary which limits the use settings, even though they are low cost. In combination with silanes the leaching of potassium carbonate could be reduced [21].

Silicates provide fire retardancy effects by filling the lumens with incombustible material and in some cases being intumescent and therefore forming a protective layer in case of elevated temperatures [22, 23]. Utilizing nanoscale alkaline silicates, a good fire retardant performance and sufficient impregnation loads were achieved [24].

5 Outlook and Conclusion

Recent developments and commercial availability lead to the assumption that the synergetic combination of nitrogen and phosphorus based fire retardants may be the most suitable way to pursue.

However, new technologies enable promising research either regarding the modification process or the chemicals itself. Atmospheric plasma treatments may offer new ways of plasma impregnation [25]. Nano technology has the potential to enable this field even more. Not only because of the small size of the particles but also due to the high volume to surface ratio of the particles, for example with inorganic nano rods [26]. Another interesting approach are in situ reactions inside the wood to prevent leaching of the fire retardant chemicals. Finally, following the natural approach wood as a material offers, bio-based flame retardants can be a viable option in the future. Fire retardant alternatives may be based on e.g. DNA, proteins, saccharides or phytic acid [27].

References

1. Odeen K (1985) Fire resistance of wood structures. Fire Technol 21:34–40. https://doi.org/10.1007/BF01095562
2. Cisek T, Piechocki J (1985) Influence of fire retardants on smoke generation from wood and wood derived materials. Fire Technol 21:122–133. https://doi.org/10.1007/BF01040154
3. Rowell RM (ed) (2013) Handbook of wood chemistry and wood composites. CRC Press, Boca Raton
4. Barber D, Gerard R (2015) Summary of the fire protection foundation report - fire safety challenges of tall wood buildings. Fire Sci Rev 4. https://doi.org/10.1186/s40038-015-0009-3
5. Buschow KHJ (ed) (2001) Encyclopedia of materials: science and technology. Elsevier, Amsterdam
6. Lowden L, Hull T (2013) Flammability behaviour of wood and a review of the methods for its reduction. Fire Sci Rev 2:4. https://doi.org/10.1186/2193-0414-2-4
7. Green J (1996) Mechanisms for flame retardancy and smoke suppression-a review. J Fire Sci 14:426–442. https://doi.org/10.1177/073490419601400602
8. Browne F (1958) Theories of the combustion of wood and its control a survey of the literature. Report #2136, Forest Products Laboratory, Madison (Wi)
9. Deveci I, Baysal E, Toker H, Yuksel M, Turkoglu T, Peker H (2017) Thermal characteristics of oriental beech wood treated with some leaching resistant bor ates. Wood Res 62:12
10. Boric acid - Registry of SVHC intentions until outcome – ECHA. https://echa.europa.eu/de/registry-of-svhc-intentions/-/dislist/details/0b0236e180e4b39c
11. Tondi G, Haurie L, Wieland S, Petutschnigg A, Lacasta A, Monton J (2014) Comparison of disodium octaborate tetrahydrate-based and tannin-boron-based formulations as fire retardant for wood structures: dot and tannin-boron as fire retardant. Fire Mater 38:381–390. https://doi.org/10.1002/fam.2186
12. Alaee M (2003) An overview of commercially used brominated flame retardants, their applications, their use patterns in different countries/regions and possible modes of release. Environ Int 29:683–689. https://doi.org/10.1016/S0160-4120(03)00121-1
13. Marney DCO, Russell LJ, Mann R (2008) Fire performance of wood (*Pinus radiata*) treated with fire retardants and a wood preservative. Fire Mater 32:357–370. https://doi.org/10.1002/fam.973
14. Hirata T, Kawamoto S, Nishimoto T (1991) Thermogravimetry of wood treated with water-insoluble retardants and a proposal for development of fire-retardant wood materials. Fire Mater 15:27–36. https://doi.org/10.1002/fam.810150106
15. Lewin M (1997) Flame retarding of wood by chemical modification with bromate-bromide solutions. J Fire Sci 15:29–51. https://doi.org/10.1177/073490419701500103
16. Horacek H, Grabner R (1996) Advantages of flame retardants based on nitrogen compounds. Polym Degrad Stab 54:205–215. https://doi.org/10.1016/S0141-3910(96)00045-6
17. Stevens R, van Es DS, Bezemer R, Kranenbarg A (2006) The structure–activity relationship of fire retardant phosphorus compounds in wood. Polym Degrad Stab 91:832–841. https://doi.org/10.1016/j.polymdegradstab.2005.06.014
18. LeVan SL, Winandy JE (1990) Effects of fire retardant treatments on wood strength: a review. Wood Fiber Sci 22:20
19. Truax TR, Harrison CA, Baechler RH (1956) Experiments in fireproofing wood, fifth progress report. Forest Products Laboratory, US Department of Agriculture
20. Hull TR, Witkowski A, Hollingbery L (2011) Fire retardant action of mineral fillers. Polym Degrad Stab 96:1462–1469. https://doi.org/10.1016/j.polymdegradstab.2011.05.006

21. Mazela B, Broda M, Perdoch W Fire resistance of wood treated with potassium carbonate and silanes. 8
22. Mai C, Militz H (2004) Modification of wood with silicon compounds inorganic silicon compounds and sol-gel systems: a review. Wood Sci Technol 37:339–348. https://doi.org/10.1007/s00226-003-0205-5
23. Bulewicz EM, Pelc A, Kozlowski R, Miciukiewicz A (1985) Intumescent silicate-based materials: mechanism of swelling in contact with fire. Fire Mater 9:171–175. https://doi.org/10.1002/fam.810090405
24. Giudice CA, Pereyra AM (2009) Silica nanoparticles in high silica/alkali molar ratio solutions as fire-retardant impregnants for woods. Fire Mater. n/a-n/a (2009). https://doi.org/10.1002/fam.1018
25. Pabeliña KG, Lumban CO, Ramos HJ (2012) Plasma impregnation of wood with fire retardants. Nucl Instrum Methods Phys Res Sect B: Beam Interact Mater Atoms 272:365–369. https://doi.org/10.1016/j.nimb.2011.01.102
26. Sun QF, Lu Y, Zhang HM, Yang DJ, Xu JS, Li J, Liu YX, Shi JT (2012) Flame retardancy of wood coated by ZnO nanorod arrays via a hydrothermal method. Mater Res Innov 16:326–331. https://doi.org/10.1179/1433075X11Y.0000000066
27. Costes L, Laoutid F, Brohez S, Dubois P (2017) Bio-based flame retardants: when nature meets fire protection. Mater Sci Eng: R: Rep 117:1–25. https://doi.org/10.1016/j.mser.2017.04.001

Fire Behavior of Bamboo, *Guadua angustifolia*

Laia Haurie(✉), Alina Avellaneda, and Joaquin Monton

Barcelona School of Building Construction,
Universitat Politecnica de Catalunya, BarcelonaTech (UPC),
Av. Doctor Marañon, 44, 08028 Barcelona, Spain
laia.haurie@upc.edu

Abstract. Bamboo is a promising building material because it is a renewable resource and it grows extremely fast. Bamboo has been widely used in the traditional architecture of some countries, but now the development of different bamboo products can expand its applications. As in the case of timber products, one of the main concerns about bamboo is the fire behavior. Therefore, in this work we have studied the fire behavior of the *Guadua angustifolia* depending on various parameters. We have evaluated the effect of moisture and also the influence of the microstructure on the flammability of bamboo. The results show a clear influence of the level of moisture on the fire behavior and some differences depending on the microstructure of bamboo. The internal part, which is rich in vascular cells and parenchyma tissue, has less ability to form a charred residue than the external layer rich in silicon.

Another part of this work consisted on evaluating the performance of different flame retardants added into bamboo trough impregnation. We have used different combinations of flame retardants, based on boron and phosphorous salts. We have found promising results that could allow the improvement of the fire reaction classification of some bamboo products.

Keywords: Bamboo · Fire reaction · Flame retardant · Impregnation

1 Introduction

Bamboo is the common name that woody grasses that belong to the *Bambusoideae* subfamily receive. The *Bambusoideae* are divided into three tribes, the *Olyreae* that contains herbaceous species, and the *Arundinarieae* and *Bambuseae* tribes that are formed by woody species. On all continents, with the exception of Europe and Antarctica, there are endemic bamboo species [1]. Bamboo is a material with excellent mechanical performance widely used in the vernacular architecture of many Asian, African and Latin American countries [2, 3]. The rapid growth of bamboo, whose cultivation can yield from 5–6 years, and the adaption of its cultivation to a wide variety of climates make bamboo an excellent candidate to consider in sustainable architecture [4]. The development of gluing techniques opens the door to bamboo products, both structural and cladding [5, 6].

One of the aspects to take into account when designing with bamboo is its fire behavior. This work aims to deepen the knowledge of the fire behavior of the *Guadua angustifolia* species taking into account variables such as the humidity of the piece or

L. Makovicka Osvaldova et al. (Eds.): WFS 2020, *Wood & Fire Safety*, pp. 103–108, 2020.
https://doi.org/10.1007/978-3-030-41235-7_15

the influence of the microstructure of the bamboo cane. In order to evaluate the best strategy to improve the fire reaction of bamboo, the behavior of pieces impregnated with a flame retardant based on boron and another based on phosphorous has been characterized [7, 8]. On one hand, it has been selected a boron salt, sodium octaborate tetrahydrate, of greater solubility than boric acid and borax, usually used in the treatment of bamboo [9]; and on the other hand, a commercial flame retardant based on ammonium polyphosphate.

2 Materials and Methodology

The *Guadua angustifolia* used for the tests was supplied by Bamboo Import Europe. Pieces of different dimensions and sections were cut (Fig. 1), depending on the type of test. A set of pieces was conditioned in a climatic chamber for a minimum of 24 h, at a temperature of 23 °C and with a relative humidity of 50%. Equilibrium moisture content of bamboo samples after conditioning in the climatic chamber was around 8% for all the cases. The other set was allowed to dry in the oven at 50 °C until the time of testing.

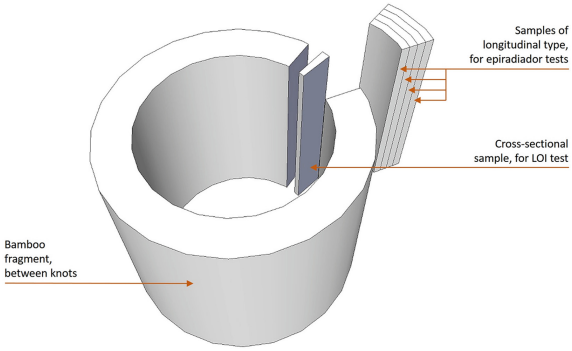

Fig. 1. Diagram with the types of bamboo samples used.

Of this second set, a third part of the pieces were impregnated in an autoclave with a solution of sodium borate ($Na_2B_8O_{13}{\cdot}4H_2O$ tetrahydrated sodium octaborate (DOT), Solubor®), dissolved in distilled water and with a concentration of 20%, achieving a 5% absorption. Another third part of the pieces was also impregnated in an autoclave but this time with the phosphate flame retardant.

The tests carried out are detailed below:

- Pyrolysis microcalorimeter (PCFC): The objective of the test is to analyze the heat release rate of bamboo samples based on the cutting section (exterior, center and interior of the piece) and the humidity of the samples. One sample of each of these cases was tested. For this, a Fire Testing Tecnology microcalorimeter was used, which consists of a pyrolysis chamber, where the samples are heated to 750 °C, at 1 °C/s in a nitrogen atmosphere. The gases released ascend to a combustion chamber that contains oxygen and, depending on the oxygen consumption, the heat release rate is determined.

- Epiradiador: The aim of the test is to evaluate the capacity of self-extinguishing of the material, subjected to a radiator configured according to the standard UNE 23725-90 [10] and with a nominal power of 500 W. The bamboo samples are deposited in a metal grid on the sample holder, which is previously placed at a distance of 3 cm under the radiator.

The test lasts 5 min, and from it the time that elapses until the first ignition occurs, the total number of ignitions and the average value of the duration of the ignitions produced during that period of time are obtained. Triplicates were performed for each type of sample.

- Limit oxygen index (LOI): The objective of the test is to determine the minimum oxygen concentration, in a mixture with nitrogen, which allows the combustion of the samples and the indications of ISO UNE-EN 4589-2 are used as reference [11]. The samples are placed vertically in a controlled atmosphere of nitrogen and oxygen. The amount of specimens used for each test corresponds to the number indicated in the standard.

In addition to the fire behavior tests, observations have been made on a Jeol JSM 6510 scanning electron microscope (SEM) coupled to an X-ray dispersive energy detector (EDS) to identify the elements present.

3 Results

Figure 2 shows SEM images of the different areas of the longitudinal direction of bamboo specimens (Fig. 1). In the image corresponding to the central zone, parenchyma cells, vascular cells and tissues of metaxylem and metafloem can be observed [12]. The other two images show the outer bamboo parts: on the one hand, the upper part of the culm that shows a smooth surface and, on the other, the inner part that has a poorly structured morphology with some areas covered by white fragments such as the one seen in Fig. 2c. The elementary analysis carried out by EDS shows that these two zones (Fig. 2a and 2c) are rich in silicon, unlike the central zone (Fig. 2b) in which silicon is much less detected.

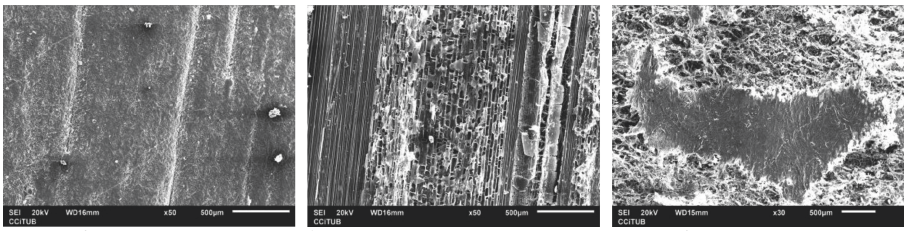

a. Exterior b. Center c. Interior

Fig. 2. SEM images of longitudinal cuts of bamboo culm.

Figure 3 shows the heat release rate as a function of temperature and Table 1 shows the main results obtained with the PCFC test: the values of the maximum heat release peak (pHRR), the temperature at which the maximum peak occurs (TpHRR) and the total heat released (THR). Although no large differences are observed between samples, there is a trend related with the moisture of the samples. As expected, the samples conditioned in the climatic chamber, which have an equilibrium humidity greater than those dried in an oven, exhibit a lower value of the total heat released, since part of the sample mass corresponds to the moisture of the sample. For the same reason, the central and internal cuts conditioned in a climatic chamber have a lower value of the heat release peak. In the case of the external cut the moisture content modifies the behavior in the microcalorimeter to a lesser extent.

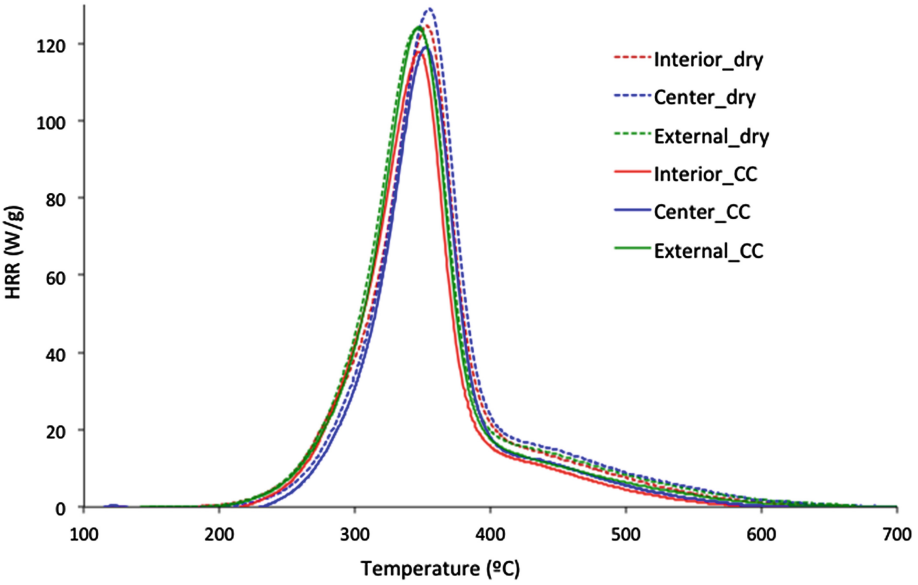

Fig. 3. Release curve of the heat rhythm versus the temperature obtained in the PCFC test.

Table 1. Results obtained with the pyrolysis microcalorimeter.

Source	**Conditioning**	pHRR (W/g)	TpHRR (°C)	THR (kJ/g)
Interior	Oven	124	352	10.3
Center	Oven	129	354	10.3
External	Oven	124	346	10.4
Interior	Climatic chamber	118	347	8.7
Center	Climatic chamber	119	352	8.6
External	Climatic chamber	124	347	9.6

Table 2 shows the results corresponding to the epiradiador tests according to the conditioning of the pieces; the position of the samples; and of the presence of flame retardant.

The LOI test performed in cross-sections for the samples untreated gives a limit oxygen percentage of 29 for the oven dried sample; and 32 for climate chamber conditioning. The samples treated with sodium octaborate tetrahydrate significantly improve the result of LOI and increase up to 47% of oxygen index needed to maintain combustion under test conditions. In case of the samples treated with the phosphate based flame retardant a significant improvement of the oxygen index occurs and it reaches values of 60%.

Table 2. Results of the epiradiador, according to the preparation and the source of the sample.

Preparation	Source	t_0 (s)	No	t_m (s)	% final mass loss
Climatic chamber, no impregnation	Interior	49	6	21	71
	Center	49	4	29	83
	Exterior	100	3	52	46
Oven, no impregnation	Interior	46	2	27	90
	Center	47	3	30	97
	Exterior	57	2	53	68
Oven, impregnation (Boron based FR)	Interior	29	5	6	54
	Center	32	5	7	61
	Exterior	65	7	22	36
Oven, impregnation (Phosporous based FR)	Interior	43	7	7	52
	Center	49	8	5	51
	Exterior	48	11	9	68

4 Conclusions

The fire behavior of several pieces of bamboo, of the species *Guadua angustifolia*, cut transversely and longitudinally, differentiating its origin (exterior, center and interior) has been evaluated. The presence of moisture in the bamboo samples makes more difficult to burn the bamboo samples, but does not significantly change the reaction to fire in bamboo. External areas that are rich in silicon have a higher resistance to combustion, but since the areas are less affected by variations in humidity, their fire behavior is also less affected by the hygroscopic conditions. The addition of 5% sodium octaborate tetrahydrate improves the fire behavior of bamboo; it reduces the duration of combustion in the case of the application of a radiation source and significantly increases the oxygen value necessary to produce combustion in the test of LOI. The use of a phosphate based fire retardant also improves de fire behavior of bamboo; it further reduces the duration of combustion under the radiator compared to samples treated with sodium octaborate tetrahydrate and it requires more oxygen to produce combustion in the test of LOI. The main mechanism of action of boron based flame retardants is the

formation of a protective glassy layer that protects the condensed phase, while the phosphorous based flame retardants tend to promote charring during combustion. According to the results obtained both mechanisms lead to a clear improve of the fire reaction of bamboo, and it seems that promotion of charring could be more effective.

Acknowledgments. This work has been funded by the BIA2017-88401-R project (AEI / FEDER, EU).

References

1. Lizarazu MA (2013) Bambúes leñosos (Poaceae: Bambusoideae: Bambuseae) del Noreste argentino y regiones limítrofes: estudios taxonómicos, morfológicos, anatómicos y biogeográficos. Facultad de Ciencias Exactas y Naturales. Universidad de Buenos Aires, Buenos Aires
2. Hidalgo Lopez O (2003) Bamboo: the gift of the gods. Bogotá, ISBN: 958334298X (2003)
3. Langlais G (2002) Maisons de bambou, Ed. Paris, Fernand Hazan. ISBN10: 2850258296
4. Jayanetti DL, Follett PR (2008) Bamboo in construction. In: Xiao Y, Inoue M, Paudel SK (eds) Modern bamboo structures. Taylor & Francis Group, London
5. Wang R, Wei SQ, Li Z, Xiao Y (2019) Performance of connection system used in lightweight glubam shear wall. Constr Build Mater 206:419–431
6. Xiao Y, Shan B, Chen G, Zhou Q, She LY (2008) Development of a new type Glulam—GluBam. In: Xiao Y, Inoue M, Paudel SK (eds) Modern bamboo structures. Taylor & Francis Group, London
7. Yu LL, Lu F, Qin DC, Ren HQ, Fei BH (2017) Combustibility of boron-containing fire retardant treated bamboo filaments. Wood Fiber Sci 49(2):125–133
8. Jin XB, Jiang ZH, Wen XW, Zhang R, Qin DC (2017) Flame retardant properties of laminated bamboo lumber treated with monoammonium phosphate (MAP) and boric acid/borax (SBX) compounds. BioResources 12(3):5071–5085
9. Yu L, Cai J, Li H, Lu F, Qin D, Fei B (2017) Effects of boric acid and/or borax treatments on the fire resistance of bamboo filament. BioResources 12(3):5296–5307
10. Asociación Española de Normalización (1990) UNE 23-725-90: Ensayos de reacción al fuego de los materiales de construcción. Ensayo de goteo aplicable a los materiales fusibles. Ensayo Complementario. AENOR, Madrid
11. Asociación Española de Normalización (2017) UNE-EN ISO 4589-2:2017: Determinación del comportamiento al fuego mediante el índice de oxígeno. Parte 2: Ensayo a temperatura ambiente. AENOR, Madrid
12. Ito R, Miyafuji H, Kasuya N (2015) Rhizome and root anatomy of moso bamboo (Phyllostachys pubescens) observed with scanning electron microscopy. J Wood Sci. 61:431–437

The Study of Various Factors Influencing the Fire Retardant Efficiency of Wood Varnish

Tatyana Eremina[1(✉)], Irina Kuznetsova[2], and Lyubov Rodionova[2]

[1] "National Research Moscow State University of Civil Engineering" (MGSU), Moscow, Russia
main@stopfire.ru
[2] International Scientific Innovative Center of Construction and Fire Safety Ltd., Saint Petersburg, Russia
{grants,gl-texnolog}@stopfire.ru

Abstract. The problem of fire safety of wooden structures is considered. The method of protection of wood materials with fire protection varnish is given. Antipyrene and its quantity were selected to ensure Group I fire protection efficiency. The properties of the acrylic binder and the possibility of its use in the formulation of fire protection varnish are considered and analyzed. Complex tests for the time of independent attenuation of the samples of Group I fire retardant efficiency and fire propagation with a brief description of the methods are carried out. Accelerated climatic and full-scale tests of the fire protection varnish samples were carried out and the service life of the coating was determined to be 10 years. Additionally, in order to confirm the declared operating conditions, the fire protection efficiency of "Intol" fire protection varnish samples was tested. Conclusions were made that the selection of the optimal ratio of components and the study of the influence of various factors on the fire retardant efficiency of the wood varnish allow increasing the fire safety of facilities.

Keywords: Fire safety · Fire protection varnish · Wooden structures

1 Introduction

In 2018, fires in Russia caused the death of 7,296 people. A major fire in Karelia in 2018 completely destroyed a wooden cathedral of the XVIII century. In this regard, at present, to protect wooden structures materials of Group I and II of fire protection efficiency are used. This is part of the system of measures to ensure the fire safety of a facility. The fire resistance of structures is characterized by the time during which they retain their bearing capacity and stability in fire conditions.

One of the methods of fire protection of wooden structures is fire protectionvarnishes based on solvents and polymer resins. These compositions are able not only to protect wooden structures from the fire, but also to preserve the original texture of the wood and its decorative properties, which is important for sites of cultural importance, the appearance of which must not be changed.

The most frequently used and effective in fire protection are acrylic and polyurethane-based fire retardants with the addition of fire retardants and functional

L. Makovicka Osvaldova et al. (Eds.): WFS 2020, *Wood & Fire Safety*, pp. 109–113, 2020.
https://doi.org/10.1007/978-3-030-41235-7_16

additives. Films formed by three-dimensional acrylic copolymers of butyl methacrylate or methylmethacrylate with methacrylic acid by evaporation of the solvent form weather-resistant, UV-resistant waterproof coatings. To reduce the flammability of wood, fire protectionvarnishes contain anti-pyrene components, which inhibit combustion and fire propagation over the surface. Various salts are used as fire retardants: ammonium phosphates and chlorides, boron salts, as well as liquid organic-based additives: chlorinated paraffins, phosphoric acid esters (tris-(2-monochloroethyl)phosphate, tricresilphosphate, triphenylphosphate) [1–3].

Fire protection organobletting varnish "Intol" for wood is a composition of organic binder and solvent with the addition of effective liquid fire retardant and modifying additives. By means of a series of experiments, the optimal ratio of components has been selected, which helps to reduce the spread of fire over the surface and improves the fire protection properties [4] of the material, with no residual stickiness of the final coating. Wooden structures treated with Intol fire retardant varnish are resistant to ignition under prolonged exposure to a fire source and belong to the non-combustible building materials [5, 6]. Also, due to its optimal composition, the varnish has good decorative and physical-chemical properties. "Intol" varnish does not hide the natural texture of the wood, which is a key factor in the fire protection of wooden structures, which for aesthetic reasons should retain their original appearance. "Intol" fire protection varnish penetrates well into the structure of the wood and forms a fireproof film on the surface. In the event of fire, the liquid fire protection decomposes under high temperatures, releasing gases that prevent oxygen from reaching the surface of the wood, thus preventing fire [7].

2 Essence of Work

The aim of the research work was to select the effective amount of liquid fire retardant tris-(2-mono-chloroethyl)-phosphate TCEP to provide the I group of fire retardant efficiency without residual stickiness of the final coating.

3 Results

Thus, the optimal amount of TCEP was selected as 5% by weight (Table 1).

Table 1. Determining the effective quantity of TCEP

TCEP content, %	3	5	7	10	12
Residual stickiness of the final coating	None	None	Moderate	Moderate	Strong
Fire protection efficiency	Attenuation within 10 s	Attenuation within 5 s	Attenuation within 5 s	Attenuation within 5 s	Attenuation within 5 s

In the course of the study the optimal ratio of solvent-binder system for the formation of defect-free coating and achievement of the required parameters for drying time and application modes was also selected. Various aromatic and aliphatic solvents and their mixtures were tested. The required coating characteristics were achieved during the testing of the acrylic binder system - o-Xylene. As a result, the time of complete drying was 4 h, with the possibility to apply manually and automatically with the formation of a uniform coating, which has an impact on the fire protection efficiency as a whole (Fig. 1).

In order to evaluate the fire retardant properties of "Intol" varnish, tests were carried out to determine the fire protection efficiency group according to NPB 251-98, GOST R 53292-2009. According to the results of the tests, the varnish provides the Group I fire retardant efficiency, with the loss of mass of the sample less than 9%.

Fig. 1. Appearance of "Intol" fireproof varnish

The fire propagation was also tested in accordance with GOST R 51032-97. According to the results of the test "Intol" fire retardant varnish belongs to RP1 group of fire propagation on the surface - nonpropagating.

Since "Intol" fire retardant varnish can be used for external works, it was tested for resistance to atmospheric conditions and their influence on the fire protection properties. Coatings are subjected to a combined effect of temperature, humidity, light, with the use of series of accelerated climatic tests simulating the conditions of the open atmosphere of moderate climate [8, 9]. Result: samples of fire retardant varnish coatings have been tested in 45 cycles, which corresponds to 10 years of service life of the coating under the conditions of the open air in compliance with the technology of use and operation [10]. After the end of climatic tests the assessment of the fire retardant efficiency of "Intol" varnish was carried out. The varnish retains its properties with a mass loss of 15% of the sample.

Further on, full-scale tests of “Intol” varnish in the open air were carried out (Fig. 2).

Fig. 2. Condition of samples with “Intol” fire retardant varnish after 10 years of exposure in the open air: 1 - on the test bench at an angle of 45°, 2 - on the wall, 3 - control.

All 3 samples after climatic tests in the open air [11] were subjected to fire protection efficiency tests. After 10 years of outdoor exposure, “Intol” varnish retained its fire protection properties. Similar tests were also carried out for different types of wood, the data are shown in Fig. 3.

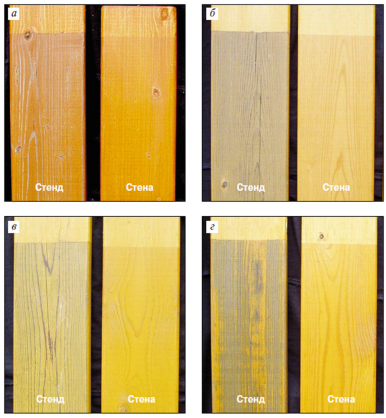

Fig. 3. Condition of samples with fire retardant varnish “Intol” after 10 years of exposure in the open air: a - cherry, b - maple, c - beech, d - ash.

In conditions of operation with increased humidity, “Intol” fire retardant varnish exhibits low water absorption [12]. The ageing of the coating, which occurs due to the processes of thermal, photochemical and oxidative destruction, and as a consequence, the loss of fire protection properties, is affected by all the components of the

composition. Accelerated climatic and full-scale tests have allowed to estimate accurately the picture of the coating aging under the conditions of the open atmosphere - the service life of the coating is not less than 10 years.

Thus, the development of fire retardant varnish for wooden structures with the use of an effective amount of liquid fire retardant and the choice of the optimal ratio of components, can be a way to solve the problem of effective fire protection of wooden structures for a long period of time. New scientific researches of influence of various factors on fire-protective efficiency of a varnish for wooden structures allow to predict and improve fire safety of facilities in general.

References

1. Overview (1982) A series of acrylates and polyvinylchlorides. Production, properties and application of suspension acrylic (co) polymers. NIITECHIM, Moscow, p 34
2. Khasanov AI, Efremov EA, Gareeva AN, Garipov RM Influence of molecular mass of acryl co-polymers on coating properties. https://cyberleninka.ru
3. Chuang C-S, Tsai K-C, Yang T-H et al (2011) Effects of adding organo-clays for acrylic-based intumescent coating on fire-retardancy of painted thin plywood. Appl Clay Sci 53:709–715
4. Polishchuk EYu, Sivenkov AB, Biryukov EP (2016) Normative requirements for fire protection of wood and expert evaluation of its quality. Fires Incidents: Prevent Eliminat 2:77–80
5. Korolchenko AYa, Trushkin DV (2005) Fire safety of building materials. Learning guide, Moscow, p 95
6. White RH, Dietenberger MA (2010) Fire Safety of wood construction. General Technical report FPL–GTR–190, 18:7–8
7. Petrova NP, Ushmarin NF, Koltsov NI (2012) Improving the fire resistance of BNK-based rubber using combinations of trichloroethyl phosphate with various flame retardants. J Kazan Technol Univ 19:94
8. GOST 9.401-91, method 2
9. Eremina TYu, Krasheninnikova MV, Dmitrieva YuN, Semenov DS (2007) Fire retardant coating quality control and fire resistance retention forecasting in service. In: Historical and modern aspects of solving the problems of combustion, extinguishing and people safety during fires: proceedings of XX international scientific and research conference dedicated to the 70th anniversary of the institute, Moscow, vol 1, pp 210–214
10. Afanasiev SV, Roshenko OS, Korotkov SV (2012) Forecasting of fire resistance of wood under atmospheric conditions. Sci Vector Tollyatti State Univ 1(19):20–22
11. GOST 6992-68
12. GOST 33352-2015

Flammability and Tribological Properties of Pine Sapwood, Reinforced with Sodium Metasilicate and Non-food Oil

Edita Garskaite[1](✉), Dalia Brazinskiene[2], Svajus Asadauskas[2], Lars Hansson[3], and Dick Sandberg[1]

[1] Wood Science and Engineering, Luleå University of Technology, Forskargatan 1, 931 87 Skellefteå, Sweden
edita.garskaite@ltu.se
[2] FTMC Tribology Laboratory, Saulėtekio 3, 10257 Vilnius, Lithuania
[3] Department of Ocean Operations and Civil Engineering, Faculty of Engineering, Norwegian University of Science and Technology, Larsgårdsvegen 2, 6025 Ålesund, Norway

Abstract. Modification of Scots pine (*Pinus sylvestris* L.) sapwood using aqueous formulations of Na_2SiO_3 via vacuum-pressure technique and subsequent treatment with cashew nut-shell liquid (CNSL) is reported. Morphology, elemental distribution within wood matrix, and structural properties of wood-composites were investigated by FE-SEM/EDS, FTIR analysis. Microstructure and density of modified wood blocks were further assessed by X-ray computed tomography. The flammability of Na_2SiO_3-CNSL-wood composites was evaluated simultaneously performing thermogravimerical (TG) and FTIR gas analysis; the results showed that maximum weight loss for the modified wood was obtained at up to 70 °C lower temperatures compared to the untreated wood, whilst substantially reducing terminal weight losses. The coefficient of friction significantly increased after the CNSL treatment compared to that of untreated wood, but addition of Na_2SiO_3 to CNSL eliminated most of the friction increase. Enhanced tribological properties along with industrial wood-impregnation method suggest that wood modification using Na_2SiO_3 in combination with CNSL has a potential for the exploration of a broader range of wood material properties in agreement with sustainable material management.

Keywords: Scots pine · Na_2SiO_3 · Computed tomography · Tribology

1 Introduction

Conventional flame-retardant processing techniques involve impregnation with flame retardants or applying fire-proof coatings to the wood surface. However, most of the treatments are not durable as treated wood often becomes moisture sensitive, discolored or corrosive. The mechanical strength of wood might also be reduced. Studies showed that wood modification with silicate compounds can improve the elasto-mechanical properties, dimensional stability, and reduce the moisture sorption of the wood material [1, 2]. Furthermore, to enhance protection of the wood various natural extracts,

L. Makovicka Osvaldova et al. (Eds.): WFS 2020, *Wood & Fire Safety*, pp. 114–119, 2020.
https://doi.org/10.1007/978-3-030-41235-7_17

turpentines and oils, including cashew nut-shell liquid (CNSL), were explored throughout the history. CNSL is a renewable and biobased raw material, composed mainly from anacardic acids, Fig. 1A.

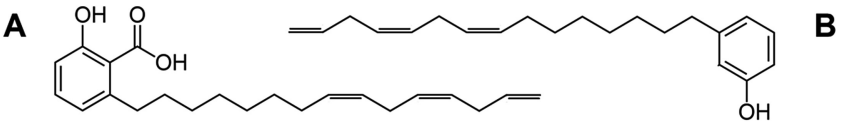

Fig. 1. Chemical structure of (A) anacardic acid, and cardanol (B), main components of CNSL.

During CNSL processing, decarboxylation of anacardic acid often takes place, resulting in cardanol, Fig. 1B. Phenolic nature of cardanols makes it possible for CNSL to function as an efficient antimicrobial and water repellent agent [3].

In this work, we study the synergy between inorganic and organic components as a potential environmentally benign wood-protective material. The modification of Scots pine sapwood using aqueous formulations of sodium silicate (Na_2SiO_3) via vacuum-pressure technique is reported. The blocks of modified wood were then treated with CNSL. Morphological, elemental distribution within wood matrix, structural properties and density of modified wood were investigated by FE-SEM/EDS, CT and FTIR spectroscopy. The flammability was studied by TG-FTIR analysis. The tribological behavior of modified wood was also investigated and the relationship between the concentration of the initial solution, drying temperature and the mechanical strength is discussed.

2 Experimental Part

2.1 Materials and Wood Modification

Two precursor solutions, denoted as 10% and 20% Na_2SiO_3, were prepared by mixing a standard sodium silicate ($Na_2O{\cdot}(SiO_2)_x{\cdot}xH_2O$ (26.1% silica, 8.1% sodium oxide), Technical, VWR Chemicals) at 10% or 20% by volume in deionized water.

Specimens of Scots pine (*Pinus sylvestris* L.) sapwood having sizes of 18 × 70 150 mm (Tangential (T) × Radial (R) × Longitudinal (L)) were cut from boards obtained from northern Sweden. Specimens were conditioned at a temperature of 20 °C, and 65% relative humidity (RH) to reach the moisture content (MC) of approximately 12%. These specimens were then submerged into the aqueous Na_2SiO_3 formulations and subsequently treated by vacuum-pressure technique using a MAVEB impregnation tube (autoclave). The specimens were kept in vacuum (−50 kPa) for 30 min and then for 1 h at pressure of 1500 kPa. Afterwards, the treated specimens were dried at room temperature for 24 h and then additionally conditioned in a climate chamber at a temperature of 20 °C and 65% RH for 5 days. Part of the Na_2SiO_3-modified wood blocks were then cut into specimens of 3 mm in thickness and submerged into CNSL oil for 1 h. Samples were dried at 100 °C, 120 °C and 130 °C (drying time: 24 h and 48 h) respectively to induce the polymerisation of oil.

2.2 Characterization

The morphological features and elemental composition of wood-Na_2SiO_3 composites were evaluated by using field emission scanning electron microscope (FE-SEM, SU70, Hitachi) equipped with the energy dispersive X-ray spectrometer (EDS). The uncoated specimens of 1.0–1.5 mm in thickness were examined (the electron beam acceleration voltage of 15 kV) to obtain the EDS spectra. Thermal behaviour of Na_2SiO_3-CNSL-modified wood was evaluated by performing thermogravimetry (TG) coupled with the Fourier transform infrared (FT-IR) spectroscopy, using a Perkin Elmer TGA 4000 instrument. The specimens were heated from 30 °C to 800 °C with a constant rate of 10 °C/min. (nitrogen was used as the purge gas). FT-IR spectrometer (Frontier FT-IR, Perkin Elmer, DTGS detector) equipped with a gas flow cell (the temperature for gas flow cell and transfer line was 275 °C, nitrogen gas flow rate was 20 mL/min.) was used in conjunction with TG analysis to record IR absorption spectra (collected every 6 s at 8 cm^{-1}, the range of 4000–500 cm^{-1}) of volatile components evolved from the sample.

2.3 X-Ray Computed Tomography (CT)

A medical CT-scanner Siemens Somatom Emotion Duo with a field of view of 500 × 500 mm^2 represented in a 512 × 512 pixel image, which gives a resolution of 0.98 mm, was used to evaluate the density of unmodified, and 10% and 20% Na_2SiO_3-modified sapwood blocks. The scanning was performed every 3 mm (total of 173 scans). Principle of CT scanning is presented elsewhere [4]. Matlab software was used to reconstruct 3D images of wood blocks.

2.4 Tribology

Tribological measurements were performed using CSM Tribometer (Anton Paar TriTec SA, Switzerland) and utilizing ball-on-plate linearly reciprocal configuration, as described in detail previously [5]. The steel ball (AISI 52100) of 6 mm OD was held stationary in order to exert loads of 5 N. The moving part was untreated, Na_2SiO_3- and Na_2SiO_3-CNSL-treated wood specimens (10 × 10 mm specimens, the amplitude of linear reciprocal motion was 2 mm, and the velocity of 2 cm/s). Calculation of friction coefficient μ was performed by built-in software dividing the lateral force, i.e. torque by the normal force, i.e. load. The results are presented as μ variation with respect to the number of friction cycles (total of 1000 cycles, 1.59 Hz).

3 Results and Discussion

3.1 Microstructure and Distribution of Inorganics in Wood Matrix

The representative cross-section FE-SEM image of the 10% Na_2SiO_3-modified wood material is presented in Fig. 2A. It was observed that after the pressure-treatment, the cell lumen was filled with a solidified inorganic material. All materials exhibited similar morphological features. The EDS analysis showed that the elements such as C, O, Na, Al (from the sample holder) and Si were detected (Fig. 2A (inset)) confirming the

diffusion of sodium silicate aqueous solution into the wood matrix. To assess the micro-distribution of Na-O-Si gel within the wood matrix the EDS elemental mapping was performed. The pseudo-colour map of three elements, where the red-green-blue (RGB) colour channels were assigned as follows: C – red, Na – green and Si – blue, further confirmed that Na and Si were distributed within entire wood matrix (Fig. 2A (red square)). The results also showed that analysed elemental atomic concentrations for each material were strongly influenced by the specific place of the specimens.

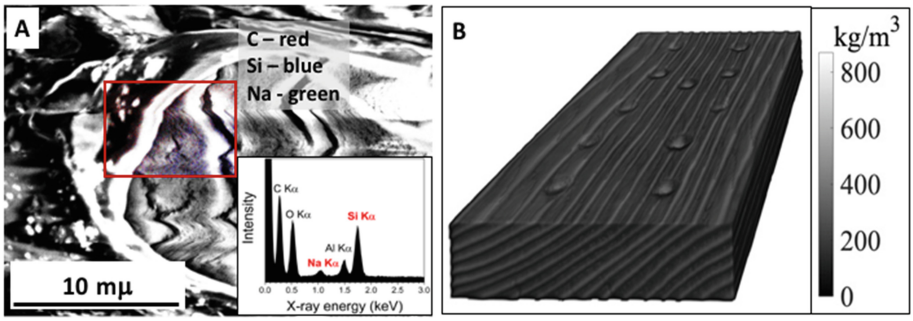

Fig. 2. (A) Cross-sectional FE-SEM image showing EDS mapping of 10% Na_2SiO_3-treated wood material (inset: EDS spectrum), and (B) X-ray computed tomography image of pine sapwood reinforced with 10% Na_2SiO_3 aqueous solution.

Reconstructed image of 10% Na_2SiO_3-modified wood block and calculated relative density is presented in Fig. 2B. CT analysis confirmed that treated wood blocks were crack-free exhibiting different density of annual rings.

3.2 Flammability of Na_2SiO_3-CNSL Modified Wood

TG curves of untreated and Na_2SiO_3-CNSL-modified wood are presented in Fig. 3. The most significant step of weight loss (63%) for untreated wood was observed in the range of 270–400 °C. At such temperature range wood components undergo rapid pyrolysis, as the hemicelluloses, celluloses and lignin components pyrolyze in the range of 200–300 °C, 280–350 °C and 280–650 °C, respectively. At higher temperature, in the range of 400–800 °C the further degradation of lignin should occur. Modified-wood exhibit different thermal behaviour compared to the Scots pine sapwood; wood components of modified-wood undergo pyrolysis at lower temperatures. The maximum weight loss was observed at 375, 345, 310 and 302 °C for untreated, CNSL-, 10% Na_2SiO_3-CNSL- and 20% Na_2SiO_3-CNSL-modified wood, respectively. The increase in residual mass of solid inorganic-carbon rich material after the burn-off confirm reinforcement of Scots pine sapwood. The FTIR absorbance spectra (Fig. 3 (inset)) of volatile components at 375 °C and 302 °C (the major weight losses during the pyrolysis) for the Scots pine sapwood and 20% Na_2SiO_3-CNSL-modified wood, respectively, show different absorbencies of volatile components. Untreated wood shows higher weight losses than CNSL-modified specimens. Weight losses are inhibited very

significantly when Na_2SiO_3 is introduced into CNSL treatment. The different thermal behaviour suggests chemical changes in wood material induced by the alkali- and CNSL-treatments.

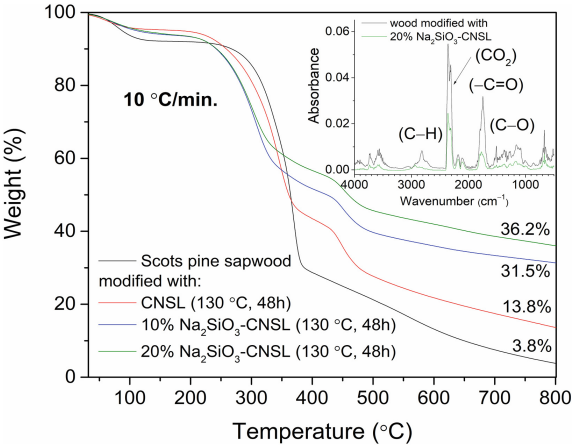

Fig. 3. TG curves of the untreated and Na_2SiO_3-CNSL-modified wood (inset: extracted FTIR absorbance spectra of volatile components at maxima weight loss during the pyrolysis of the untreated and 20% Na_2SiO_3-CNSL-modified wood).

3.3 Tribological Evaluation of Na_2SiO_3-CNSL Modified Wood

Coefficient of friction (μ) under dry friction regime between steel ball and untreated or modified wood is shown in Fig. 4 as a function of number of test cycles. For specimens without CNSL the μ is relatively stable throughout the test. Although it increased somewhat on 10% Na_2SiO_3-treated wood, on 20% Na_2SiO_3-treated blocks μ was

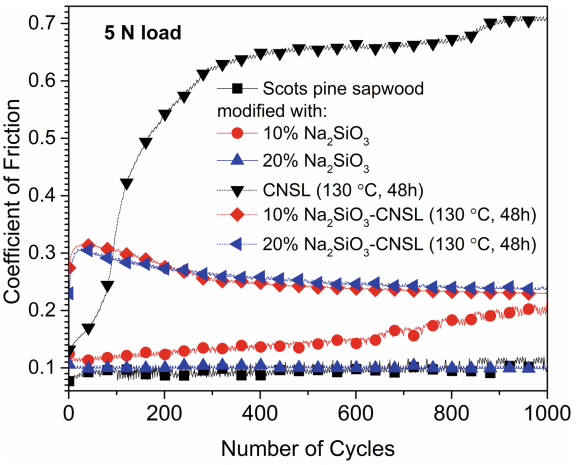

Fig. 4. Tribological curves of the untreated and Na_2SiO_3-CNSL modified sapwood.

nearly the same compared to the untreated wood. Behaviour of CNSL-treated wood was very different. The μ significantly increased in the presence of CNSL, exceeding 0.6 within 300 cycles. This could be attributed to oil polymerization or film formation on the wood surface. However, when combined with silicates, CNSL effect on friction was less significant. On 10% Na_2SiO_3-CNSL and 20% Na_2SiO_3-CNSL treated wood the μ increased to 0.3 only, which suggests good tribological properties.

4 Conclusions

Na_2SiO_3-wood composites were successfully prepared by vacuum-pressure treatment. FE-SEM/EDS analysis revealed the homogeneous distribution of the sodium and silicon within wood cell lumen and cell wall. CT analysis showed that treated wood blocks are crack-free exhibiting different density of annual rings. TG-FTIR analysis showed that Na_2SiO_3-CNSL modified wood starts to pyrolyze at up to 70 °C lower temperature compared to the untreated wood, slowing down weight loss. Friction tests showed that Na_2SiO_3-CNSL treatment retains good tribological properties of the modified wood.

Acknowledgments. The work has been partially supported by the Swedish Research Council FORMAS (grant no. 2018-01198) and IPOS (No. DP2 BFAST AP4 Brand) projects.

References

1. Donath S, Militz H, Mai C (2004) Wood modification with alkoxysilanes. Wood Sci Technol 38:555–566
2. Pfeffer A, Mai C, Militz H (2012) Weathering characteristics of wood treated with water glass, siloxane or DMDHEU. Eur J Wood Wood Prod 70:165–176
3. Adetogun AC, Adegeye AO, Omole AO (2009) Evaluation of Cashewnut Shell Liquid (CNSL) as a wood preservative using weight loss. Agric J 4:32–35
4. Hansson L, Couceiro J, Fjellner B-A (2017) Estimation of shrinkage coefficients in radial and tangential directions from CT images. Wood Mater Sci Eng 12:251–256
5. Raudoniene J, Laurikenas A, Kaba MM, Sahin G, Morkan AU, Brazinskiene D, Asadauskas S, Seidu R, Kareiva A, Garskaite E (2018) Textured WO3 and WO3:Mo films deposited from chemical solution on stainless steel. Thin Solid Films 653:179–187

Expandable Graphite Flakes as an Additive for a New Fire Retardant Coating for Wood and Cellulose Materials – Comparison Analysis

Batista Anielkis(✉), Grześkowiak Wojciech, and Mazela Bartłomiej

Institute of Wood Chemical Technology, Faculty of Wood Technology,
Poznań University of Life Sciences,
Wojska Polskiego 28, 60-637 Poznań, Poland
anielkis.batista@up.poznan.pl

Abstract. The aim of this study was to observe the effectiveness of a new intumescent fire retardant (IFR) formulation for wood and cellulose material, while maintaining its mechanical properties, as well as to affair the effectiveness of the proposed formulation towards ignitability of the referred materials using the parameters of heat release rate (HRR), mass loss (ML) time to ignition (T_i) and time to flame out (T_f). Oxygen Index (OI) was also part of measurements. Whatman filter paper (WFP) and pinewood were used for comparison analysis; three different IFR formulations where designed and exerted to assert the influence of each formulation to the parameters of HRR, ML, T_i and T_f for both materials. WFP and wood samples were coated through the dipping method. After seasoning and drying all samples were submitted to mass loss calorimeter (MLC) measurements. Histogram for each parameter was obtained for all formulations and materials. Preliminary results showed improvements of fire properties of WFP. Control sample did ignite in 9 s (in average); coated samples however, showed a remarkably prolonged T_i = 17 s (in average), representing an increase of 88.88%; Similar results were observed in terms T_f (s). However, it was observed anomalies for the HRR (KW/m^2) and MLR (g/s) parameters. An inverse profile of histogram for some IFR formulations was observed at the initial time and at the end of the experiment. The IFR formulations are clearly slowing burning performance of the materials; anomalies in the profile HRR, MLR and HC is due to irregularities within the extremities of the material structure (porosity and permeability).

Keywords: Expandable graphite · Char · Cellulose · Flammability

1 Introduction

Fire retardant formulation (FRF) based on expandable graphite (EG) is a fire reinforcement method for flammable materials taking the attention of researchers in the past few years [1]. As a carbon-layered crystal, EG consists of sheets of carbon atoms strongly bound to each other [2]. The literature indicate that EG is a good source of carbonization agent for effective design of environmentally friendly intumescent systems [3]. According to literature, the amount of flame retardant that must be added to

L. Makovicka Osvaldova et al. (Eds.): WFS 2020, *Wood & Fire Safety*, pp. 120–124, 2020.
https://doi.org/10.1007/978-3-030-41235-7_18

achieve the desired level of fire safety can range from less than 1% for highly effective flame retardants up to more than 50% for inorganic fillers [4]. In this experiment we are working with concentrations of around 30% of EG as the inorganic fillers. There are insufficient detailed reports in literature on the behavior of EG-intumescent fire retardants (IFR) systems concerning cellulosic materials. Although EG is used in a growing number of IFR systems as a blowing agent that will suppress flammable gases up to 75%, while reducing the flame spread index, its application to cellulosic material is not so popular in the cellulose industry today [5].

Mass loss calorimeter (MLC) is frequently used to explore flammability properties of different type of materials, delivering a suitable sort of technical data [6]. Recent analysis of thermal stability of lingo-cellulosic materials under controlled conditions showed the decomposition temperatures (T_d) for lignin, hemicelluloses and cellulose. This last component, with T_d = 320 °C, char 6% by mass [7, 8]. The current study focuses on flammability concerning cellulose component only.

The objective of this work was cellulose-based model material (CMM) encrusted with expandable graphite (EG). The general aim of the research was to determine its basic fire resistance properties. The scope of the research involved measurement of the following parameters: time to ignition (T_i), time to flame out (T_f), heat release rate (HRR) and mass loss (ML).

2 Methods and Materials

This preliminary experiment was conduct in the laboratory (H7) in the Institute of Wood Chemical Technology, Faculty of Wood Technology, Poznań University of Life Sciences. Samples of cellulose sheets were manufactured with the use of hydropulper and rapid-koethen devices (Fig. 1).

Fig. 1. Rapid-koethen devices

Cellulose sheets were encrusted with two types of EG (i.e. ES20 C200 and ES100 C10). EG was dispersed in a cellulose pulp at the preparation stage. ES20 C200 had higher amount of fine-grained fraction (90% < 75 μm) and thus was characterised by

lower expansion volume (20 ml/g) in comparison to ES100 C10 type. Three variants of cellulose sheets were prepared: control sheets (pure cellulose) and sheets encrusted with graphite ES200 C20 or ES100 C10. Sodra Black Cellulose fibers (700 kg/m^3), with the following dimensions of fibers: 2.05 mm length, 30,0 µm width, were used for the process of cellulose sheets manufacture. The cellulose milling time was 30 min and the drying time 40 min. The drying temperature of the final sheets was reduced to 93 °C to avoid graphite activation. The final sheets were conditioned at room temperature at 20 °C and relative humidity 60%. All the samples were subjected to MLC measurements (Fig. 2 below).

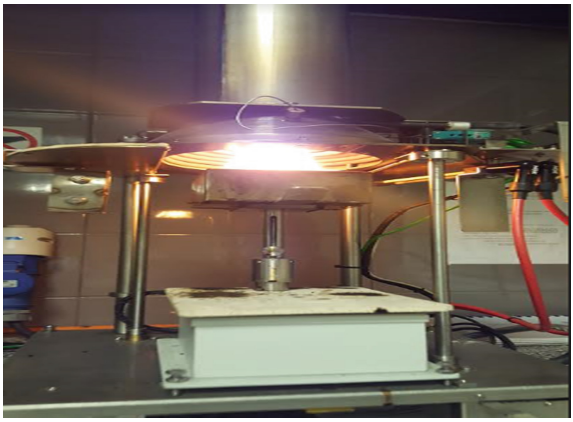

Fig. 2. MLC apparatus set at 35 kW/m^2

Heat flux at 35 kW/m^2 was estimated as suitable level for all tested samples. This work inferred conclusions on flammability properties of CMM by measuring time to ignition (T_i), time to flame out (T_f), heat release rate (HRR) and mass loss (ML).

3 Discussion

To increase time to ignition (T_i) of all cellulosic modified materials (CMM) samples in comparison to pure cellulose samples was an expectation of this experiment. However, the single most important observation was the fact that pure cellulosic material presented T_i higher than that of CMM encrusted with ES100 C10 and ES20 C200. In average, T_i for CMM encrusted with ES100 C10 and CMM encrusted with ES20 C200 was 19.0 and 21.0 s respectively, while for control samples (Pure cellulose) the estimation was on 23.3 s.

Furthermore, it was remarkable to observe that the average value of time to flame out (T_f) for CMM encrusted with ES100 C10 (Fig. 3) was 112.7 s, while pure cellulose and CMM with ES20 C200 did register an average of 87.7 s and 108.0 s, respectively. This means that despite the fact that CMM encrusted with ES100 C10 ignites 2 s

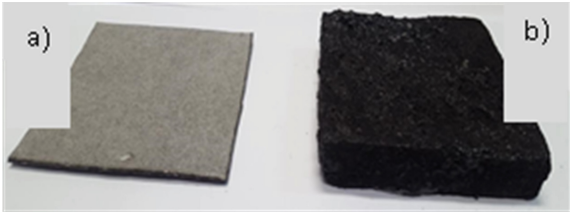

Fig. 3. CMM before (a) and after (b) MLC exposure

earlier than CMM encrusted with ES20 C200 therefore faster than all other samples, it has a sustainable burning process. Maximum heat release rate (HRR) was observed to be 229.72 KW/m^2 for pure cellulose, 91.87 KW/m^2 for CMM with ES20 C200 and 71.51 KW/m^2 for CMM with ES100 C10, as presented in the Fig. 4 below.

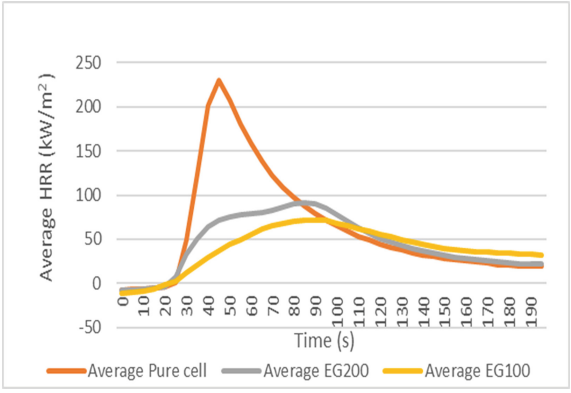

Fig. 4. Average HRR for all variants

4 Conclusion

The addition of EG was found to increase the flame resistance and effectiveness of cellulosic material. Although Ti for all CMM species were lower than for control samples, this fact actually favored the promotion of char forming. The improved physical characteristics of char is achieved by increasing the amount of the insulated layer and reducing crack formation. This aspect allowed the combustion process of CMM with ES100C10, to be 25 s longer than combustion process of pure cellulose and almost 5 s longer than that of CMM with ES20 C200. In addition, the maximum HRR for CMM with ES100C10 was 69% smaller than its compared value for pure cellulose and 22% smaller than its compared value for CMM with ES20 C200. CMM with ES100 C10 is consequently the best performing system in terms of the observed parameters.

Acknowledgement. The work was financially supported by the Ministry of Science and Higher Education as the Project No. 507.423.09. With subsidies for maintaining the research capacity.

References

1. Xie R, Qu B (2000) Synergistic effects of expandable graphite with some halogen-free flame-retardants in polyolefin blends. Polym Degrad Stab 71(3):375–380
2. Kruger HJ (2017) Characterization of expandable graphite and its flame retardant abilities in flame retardant systems for polyethylene. PhD thesis, Pretoria University
3. Feng C, Zhang Y, Lang D, Liu S, Chi Z, Xu J (2013) Flame retardant mechanism of a novel intumescent flame retardant polypropylene. Procedia Eng 52:97–104
4. Beard A, Angeler D (2010) Flame retardants: chemistry, applications, and environmental impacts. Handb Combust. https://doi.org/10.1002/9783527628148.hoc017
5. Krassowski DW, Hutchings DA, Qureshi SP (2012) Expandable graphite flake as an additive for a new flame retardant resin. GrafTech International Holdings Inc
6. Mazela B, Perdoch W, Grześkowiak W, Batista A (2018) Selection of heat flux value for wood fire retardants testing using MLC. IRG-WP doc, No. 18-40846
7. Fox DM, Lee J, Zammarano J, Katsoulis D, Eldred DV, Haverhals ML, Trulove PC, DeLong HC, Gilman JW (2012) Char-forming behavior of nanofibrillated cellulose treated with glycidyl phenyl POSS. Carbohyd Polym 88(3):847–858
8. Mazela B, Broda M (2015) Natural polymer-based flame retardants for wood and wood products. In: Proceedings of the 11th meeting of the Northern European network for wood sciences and engineering (WSE), 14–15 September 2015. Poznan University of Life Sciences, Poland, pp 146–155

Research of Effectiveness of Wood Fire Protection by Modified Epoxy Polymers

Oleksandr Hryhorenko[1(✉)], Nataliia Saienko[2], Volodymyr Lypovyi[1], and Serhii Harbuz[1]

[1] National University of Civil Defence of Ukraine, Chernyshevska Street 94, Kharkiv 61023, Ukraine
hryhorenko81@gmail.com
[2] Kharkiv National University of Construction and Architecture, Sumska Street 40, Kharkiv 61002, Ukraine
natause@ukr.net

Abstract. Providing of fire protection for wood using modified epoxy compositions today is a prospective area of research. Modification of epoxy polymers is achieved by the introduction of fire retardants, dispersed mineral fillers and additives that regulate the properties of materials. The analysis of these components effect on the flammability of epoxy polymers, their flame-retardant, technological and operational properties is an important scientific and practical task.

As research objects, compositions based on epoxy oligomer ED-20, hardened with an amine-type hardening agent, were used. To regulate the flammability and operating abilities of epoxy polymers, flame retardants, dispersed mineral fillers and additives, which differed by the nature of oxides, their quantitative ratio and by the particles shape, were used.

To determine the flammability of the researched samples, was used the oxygen index method. The effectiveness of the flame-retardant effect of the developed material as wood coatings was determined by the method of weight loss.

As a result of the research, it was established that improvement of the flame-retardant properties of epoxy polymers is associated with an increasing of their self-ignition temperature and depends from the properties of used additives. The effectiveness of the used additives of metal oxides of transient valence increases with decreasing basicity of these oxides.

As a result of the research, it was established that, according to the effectiveness of fire protection, the developed fire retardant coating corresponds to the I group of fire retardant efficiency for wood, and the weight loss of the test samples is on average 2.21%.

Keywords: Epoxy compositions · Fire retardants · Flammability · Oxygen index

In modern construction, both industrial and civil, the most common materials are reinforced concrete, metal and wood. In terms of fire danger, they have a number of shortcomings: wooden products are combustible, and reinforced concrete and metal under the influence of high temperatures lose their bearing capacity and are destroyed. In comparison with metal, wooden structures, being fire hazardous, have greater fire resistance, since they perform their functions longer being in a fire. Therefore, wood, as

L. Makovicka Osvaldova et al. (Eds.): WFS 2020, *Wood & Fire Safety*, pp. 125–128, 2020.
https://doi.org/10.1007/978-3-030-41235-7_19

a building material, is widely used in low-rise construction due to its high physical, mechanical and operational properties. However, one of the main shortcomings of wood is its combustibility.

Improving the fire safety of wood is achieved by applying impregnations based on flame retardants, plasters, claddings from non-combustible sheet or tile materials, polymeric materials.

The most effective method today is to treat wood with special flame retardants: varnishes, enamels, coatings [1], including those based on epoxy oligomers [2–4], which can slow down heating and prevent thermal decomposition of wood, ignition, burning and flame spread.

Providing of fire protection for wood using modified epoxy compositions today is a prospective area of research. Modification of epoxy polymers is achieved by the introduction of fire retardants, dispersed mineral fillers and additives that regulate the properties of materials [5, 6]. The analysis of these components effect on the flammability of epoxy polymers, their flame-retardant, technological and operational properties is an important scientific and practical task.

Compositions based on the ED-20 epoxy oligomer cured by the amine type hardener monocyanethyl diethylenetriamine (MDETA) were used as research objects. To control the flammability and operational properties of epoxy polymers, basalt scales activated at increased temperatures (ABS) and monoammonium phosphate (MAF) with a particle size of 50–63 μm were used, as well as transition metal oxides as modifying additives: vanadium oxide (V), copper oxide (II) and zinc oxide (II).

Researched compositions of epoxy resins are presented in Table 1.

Table 1. The composition of the epoxy resins.

Sample	ED-20 (mass parts)[a]	MDETA (mass parts)[a]	ABS (mass parts)[a]	MAF (mass parts)[a]	Vanadium oxide (V) (mass parts)[a]	Copper oxide (II) (mass parts)[a]	Zinc oxide (II) (mass parts)[a]
Epoxy resin	100	20	0	0	0	0	0
ERM	100	20	15	23	0	0	0
ERMV	100	20	15	23	10	0	0
ERMCu	100	20	15	23	0	10	0
ERMZn	100	20	15	23	0	0	10

[a]Regarding epoxy content

To determine the flammability of the researched samples, was used the oxygen index (OI) method according to EN ISO 4589. The effectiveness of the flame-retardant effect of the developed material as wood coatings was determined by the method according to GOST 16363. In addition, the self-ignition temperature of fire retardant coatings with various contents of modifying additives was determined according to ISO 871:2006.

The research results are presented in Table 2.

Table 2. The properties of epoxy compositions.

Sample	Oxygen index, %	Spontaneous-ignition temperature, °C	Mass loss, %[a]
Raw pine	–	–	37.8
Epoxy resin	18	465	–
ERM	27	525	7.20
ERMV	25	535	4.85
ERMCu	26	545	2.21
ERMZn	23	525	2.47

[a]Average weight loss of 10 samples of pine beams with dimensions of 150 × 60 × 30 mm, coated with the investigated compounds with a thickness of 1 mm the test results

As can be seen from the results of the research Table 1, the modification of the epoxypolymer with activated basalt scales and monoammonium phosphate (composition ERM) transforms the ER coating from the class of combustible material into self-extinguishing (OI = 27%). Spontaneous-ignition temperature of this composition is 525 °C. Testing in accordance with GOST 16363 of wood samples treated with the tested compound show that this coating provides I group of fire-retardant efficiency with an average weight loss of 7.2%.

Modification of the ERM composition with transition metal oxides increases the flammability of the coating to oxygen index values of 25, 26 and 23% for ERMV, ERMCu and ERMZn compositions, accordingly. But at the same time, the average weight loss of samples according to GOST 16363 decreases and is 4.85, 2.21 and 3.17 for compositions ERMV, ERMCu and ERMZn, accordingly.

The data in Table 1 show that, according to the efficiency of increasing the self-ignition temperature of the epoxy composition ERM, transition metal oxides can be arranged in the following sequence ZnO, V_2O_5, CuO.

As a result of the research it can be assumed that the improvement of the epoxy polymers fire-retardant properties is related with an increase in the temperature of their self-ignition and depends on the properties of the used additives. The effectiveness of the used transition metal oxides additives increases with decreasing basicity of these oxides.

Conclusions

Thus, monoammonium phosphate and activated basalt scales use in the composition of epoxy resins makes it possible to obtain a fire-retardant coating for wood with good performance and reduced combustibility. Especially The effect is enhanced especially when used together with transition metal valences. The most effective modifying additive is copper oxide (II).

As a result of researches, it was found that in terms of the effectiveness of fire protection, the developed fire-retardant coating corresponds to group I of fire-retardant efficiency for wood, and the weight loss of the tested samples is on average 2.21%.

References

1. Ryabova VI, Deriglazova NO, Chernyshev AA, Vershinin AA (2018) The fire resistance of wooden structures. J Sci New 5:367–375 Рябова ВИ, Дериглазова НО, Чернышев АА, Вершинин АА (2018) Огнестойкость деревянных конструкций. Журнал Научные вести 5:367–375
2. Belikov AS, Korzh EN, Ragimov SJ, Nesterenko SV, Grishko AN (2019) Influence of components in the composition on the protective ability of the coating. J Sci Herit 32(P.1):50–54 Беликов АС, Корж ЕН, Рагимов СЮ, Нестеренко СВ, Гришко АН (2019) Влияние компонентов в композиции на защитную способность покрытия. Журнал The Scientific Heritage 32(P.1):50–54
3. Andronov VA, Danchenko YuM, Saienko NV, Kosse AG, Plisiuk TA (2014) Evaluation of the epoxy polymer compositions effectiveness for laminated timber fire protection. J Fire Saf Iss 36:10–16 Андронов ВА, Данченко ЮМ, Саенко НВ, Коссе АГ, Плисюк ТА (2014) Оценка эффективности применения эпоксидных полимерных композиций для огнезащиты клееной древесины. Журнал Проблемы пожарной безопасности 36:10–16
4. Yakovleva RA, Nekhaiev VV, Kharchenko NA, Popov YuV, Dmytriieva NV (2003) Assessment of fire hazard and toxicity of low flammability epoxy polymers. In: 5th international scientific and technical conference on low flammability polymer materials, Volgograd, pp 77–78. Яковлева РА, Нехаев ВВ, Харченко НА, Попов ЮВ, Дмитриева НВ (2003) Оценка пожарной опасности и токсичности эпоксиполимеров пониженной горючести. В: 5-я Международная научно-техническая конференция Полимерные материалы пониженной горючести, Волгоград, с. 77–78
5. Silveira MR, Peres RS, Moritz VF, Ferreira CA (2019) Intumescent coatings based on tannins for fire protection. Mater Res 22(2)
6. Grigorenko AN (2012) Effectiveness study of fire protection wood of epoxy compositions with low smoke-generation ability. J Fire Saf Iss 31:155–159 Григоренко АН (2012) Влияние металлсодержащих добавок на механизмы снижения дымообразования эпоксиполимерных композиций: Журнал Проблемы пожарной безопасности 31:155–159

The Study of the Complex of Properties of Water-Dispersion Fire Retardant Paint for Wooden Structures

Tatyana Eremina[1(✉)], Dmitry Korolchenko[2], and Irina Kuznetsova[3]

[1] Laboratory for Testing Building Materials, Structures and fire Retardants of the Institute of Integrated Safety in Construction of the Federal State Budgetary Educational Institution of Higher Education, National Research Moscow State University of Civil Engineering (MGSU), Moscow, Russia
main@stopfire.ru

[2] Institute of Integrated Safety in Construction of the Federal State Budgetary Educational Institution of Higher Education, National Research Moscow State University of Civil Engineering (MGSU), Moscow, Russia
KorolchenkoDA@mgsu.ru

[3] International Scientific Innovative Center of Construction and Fire Safety Ltd., Saint Petersburg, Russia
grants@stopfire.ru

Abstract. The problem of ensuring fire safety of facilities with wooden structures is discussed. The method of protection of structures made of wood with fire-retardant intumescent paints and its advantages are considered. The complex of properties of fire protection paint of intumescent Therma type is considered and analyzed. The results of complex thermophysical tests of Therma paint for such parameters as expansion ratio, group of fire retardant efficiency and brief descriptions of methods are given. An important parameter in assessing the quality of fire retardant materials is singled out, namely the fire retardant efficiency over time (throughout the entire period of operation). The method of testing the Therma paint for accelerated aging is considered. The results of testing the paint for fire retardant efficiency after accelerated aging are given. In addition, to confirm the declared operating conditions, the research was conducted to study the fire retardant efficiency of the Therma paint samples after the static water resistance tests, and the test results are given. In order to obtain more complete information about the fire protection properties of the Therma paint, a complex thermal analysis was carried out, the thermoanalytical curves and their description were given. Conclusions about the necessity of constant improvement of complex research of Fire protection paints for wood structures in various fields of application are made.

Keywords: Fire retardant efficiency · Fire retardant paint · Wooden structures

1 Introduction

Today, the problem of fire safety of public and industrial facilities with structures made of wood is still relevant. A major fire in 2019 almost destroyed the Cathedral of Our Lady of Paris, the symbol of France. The use of wooden structures increases the fire

L. Makovicka Osvaldova et al. (Eds.): WFS 2020, *Wood & Fire Safety*, pp. 129–134, 2020.
https://doi.org/10.1007/978-3-030-41235-7_20

load of the building. However, the environmental purity, high decorative and aesthetic qualities and a number of technological properties determine this choice. Improvement of fire safety of wooden structures by means of developing and applying fire-retardant paints that comply with modern trends is an important task in this field.

Unprotected wood is a material with increased fire hazard. Fire-protection treatment of wooden structures allows to reduce this parameter on the average by 30%. When wooden structures are in direct contact with open fire, they are destroyed at an average speed of 0.7–1 mm per minute. Thus the temperature of the beginning of charring is reached on the average in 4 min and makes an order of 250 °C, and at temperature above 300 °C designs begin to be destroyed quickly. The rate of charring of wood depends on the size of the cross-section of the structure element, these values are inversely proportional [1–4].

The physical and chemical basis of wood combustion is that it is a composite polymeric material in which carbonization reactions with the formation of a non-volatile coke layer occur under thermal influence. It influences the dynamics of fire development and its hazardous factors (heat emission, toxic gases, smoke generation). From all the above mentioned it is possible to draw a conclusion that fire-protection treatment of wood is a mandatory procedure in the design of various types of structures. The main task of fire protection is to slow down combustion, prevent the spread of fire, localize it, and maintain the structural integrity of the building for a period of time sufficient for evacuation of people [5–8].

There are several ways of Fire protectioning wood structures, divided into two main groups - structural and chemical. Fire protection efficiency of the means used for protection of wood should be confirmed by fire tests conducted in accordance with GOST R 53292-2009. Structural fire protection is a mechanical method, which protects the wooden structure from the direct impact of fire, thus protecting the wood from possible ignition. Chemical fire protection is the use of fire-retardant paintwork or wood impregnation with chemical compounds [9].

2 Essence of the Work

The authors have developed and researched intumescent type fire retardant paint for wooden structures. Fire protection water-dispersion paint Therma for infusion type of wood-based structures is a modern and effective means of fire protection. The paint composition is a suspension of fire retardants and modifying additives, of polyvinyl acetate dispersion in an aquatic environment, without adding solvents. Thanks to its composition, the paint is quite environmentally friendly compared to the same type of organobleachable paints. The paint has an optimal set of protective and decorative properties, can be used for difficult operating conditions (high humidity, condensate, temperature differences, seismic zones) inside various types of premises.

To determine the fire retardant efficiency of the Intumescent paint Therma, complex thermophysical tests were carried out for such parameters as the expansion ratio, the group of fire retardant efficiency, adhesive-cohesive indexes of foam coke, adhesion to the substrate, as well as thermogravimetric (TG), differential thermogravimetric (DTG) and differential thermal analysis (DTA).

3 Results

The expansion ratio of the fire retardant paint Therma was determined according to GOST 12.3.047-98. To determine this parameter, all the geometric dimensions of the sample are measured and the average volume of the sample is calculated (at least three measurements are made), the sample is kept in a muffle furnace at a temperature of 600 °C for 5 min. Under the influence of high temperature the surface of the sample expands to form a foam coke layer (Table 1).

Table 1. Results of expansion rate of Therma paint

Sample №	Geometrical dimension before expansion, mm	Geometrical dimension after expansion, mm	Expansion rate (not less than 10 by OD)
1	1.20	50.4	42
2	1.20	48.0	40
3	1.10	46.2	42
4	1.25	60.0	48
5	1.00	45.0	45

The expansion ratio of the paint of the described composition according to the research data is not less than 40. After the expansion test, the adhesive-cohesive properties of foam coke were evaluated. Foam coke is an elastic cellular structure, the maximum size of cells is 4 × 1 mm, it remains on the protected surface, and for a long period of time is able to resist the destruction in the process of burnup.

The fire protection efficiency of Therma paint was assessed by the ceramic pipe method according to ND. For the tests, the paint was applied on the previously prepared wooden substrates with a consumption of at least 300 g/m^2. Wooden substrates are rectangular bars with a cross section of 30 × 60 mm and a length of 150 mm along the fibers. The tests were carried out on 10 colored samples. After all the stages of sample preparation, the samples were placed in the test facility and exposed to the fire of a gas burner for 2 min. The gas flow rate shall be constant throughout the test. The test results are shown in Table 2. According to the results, the loss of mass of the sample is of minimal importance, which means that the treatment of the wood structure with this composition can reduce its flammability in general and convert it into a non-flammable material.

According to the requirements for Group 1, the loss of mass after combustion shall not exceed 9%, for Group 2, the loss of mass shall be between 9 and 25%, and if the loss of mass exceeds 25%, the coating shall be considered combustible. According to the results of tests Therma paint provides Group 1 fire protection efficiency according to NPB 251-98, GOST R 53292-2009, the average arithmetic value of the sample mass loss is 4,71%.

An important parameter in assessing the quality of fire protection materials is the fire retardant efficiency over time, as throughout the entire period of operation, taking into account the influence of external factors, it should remain as constant as possible.

Table 2. Results of Therma paint tests for fire protection efficiency

Sample number	Sample mass, g			Sample mass loss		Average arithmetic loss of sample mass, %
	Pre-test	Before combustion	After combustion	Gramms	%	
1	237.4	246.6	233.7	12.9	5.23	4.71
2	233.7	245.7	231.9	13.8	5.62	
3	229.6	237.4	228.3	9.1	3.83	
4	231.7	241.3	229.4	11.9	4.93	
5	235.2	243.6	230.6	13.0	5.34	
6	234.6	243.1	231.3	11.8	4.85	
7	231.7	240.3	229.1	11.2	4.66	
8	229.8	237.6	231.4	6.2	2.61	
9	229.3	238.2	227.9	10.3	4.32	
10	231.7	240.1	226.5	13.6	5.66	

To assess the operational properties of Therma paint and, accordingly, fire protection efficiency over time, the method of accelerated aging according to NPB 251-98 was used. The samples were successively kept: 8 h in the drying cabinet at the temperature of (60 ± 5) °C, 16 h in the desiccator with relative humidity of 100% at normal temperature, 8 h in the drying cabinet at the temperature of (60 ± 5) °C, 16 h in normal conditions. The tests included seven cycles according to the above scheme. Then three samples subjected to artificial aging were tested for fire protection efficiency by the method described above. The following results were obtained after the artificial aging test and the fire retardant test (Table 3):

Table 3. Therma paint test results for artificial aging

Appearance of the coating after the aging test	Fire protection efficiency, mass loss, %
Preservation of integrity: no cracks, breaks, peeling	5.62

According to the test results, the reduction of the fire retardant properties of the Thermal paint after aging is less than 20% of the values defined for the control samples. This indicates that Therma paint coating has good protective properties and is resistant to aging, while maintaining the declared fire protection efficiency.

Also, to confirm the declared operating conditions, the fire retardant efficiency of Therma Paint was tested after static water resistance (water resistance) tests by the immersion method. The prepared samples had been immersed in a container with water for 72 h, during the test the changes in the appearance of the coating were constantly monitored. During the exposure of water Therma paint coating the protective layer was not destroyed, in particular, there was no cracking or peeling. After the water resistance test, the coated samples were subjected to a standard fire protection efficiency test. Test result - Therma fire protection efficiency is maintained.

In order to obtain more complete information about the fire retardant properties of Therma paint its comprehensive thermal analysis was carried out: thermogravimetric (TG), differential thermogravimetric (DTG) and differential thermal analysis (DTA) [10–12]. As a result of thermoanalytical tests, the corresponding graphical dependencies of the samples and of the identifier were obtained (Fig. 1).

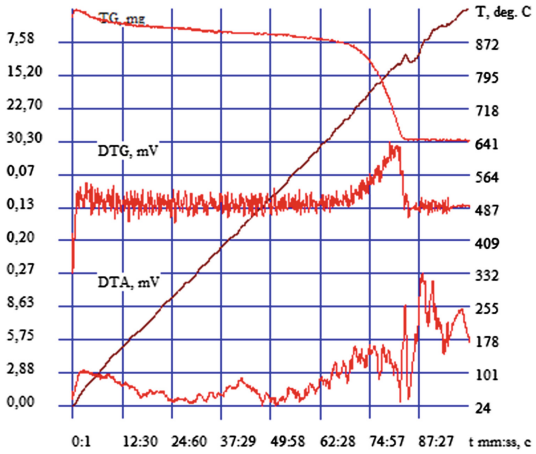

Fig. 1. Thermogravimetric curves (TG, DTG, DTA) of the Therma paint sample

Exothermal effects observed on all DTA curves at the initial stage of thermolysis of the intumescent composition are presumably related to combustion of polymer binder destruction products. Endothermic effects in the intermediate temperature range of 135–450 °C are related to the melting of ammonium polyphosphate, restructuring and dehydration of pentaeritrite, destruction of melamine and its salt forms. Carbonization is represented by the endo-effect in the temperature range of 450–570 °C. Exothermal peaks in the high-temperature region (more than 600 °C) can be due to the decomposition of methylene bridges by the radical mechanism and the subsequent formation of condensed structures. The resulting foam coke layer has good insulating properties and protects the structure for a long period of time in conditions of developing fire. The nature of the curves obtained during the thermal analysis shows that the samples studied have a thermal expansion effect inherent in fire retardant compositions.

Based on the above studies, it can be concluded that the conducted studies of the water-dispersion fire protection paint Therma are sufficient to confirm the compliance with the declared field of application.

Constant improvement of comprehensive research into the properties of fire protection paints for wooden structures allows for an in-depth assessment of fire safety of various facilities in general.

References

1. Aseeva RM, Serkov BB, Sivenkov AB (2012) Burning and fire danger of wood. Fire Explos Saf 21(1):19–32
2. Lowden LA, Hull TR (2013) Flammability behavior of wood and a review of the methods for its reduction. Fire Sci Rev 2:1–19
3. Kenzhekhan SK, Polishchyuk EYu, Sivenkov AB (2017) Problems and perspectives of complex fire protection of wooden constructions. In: Annual international scientific and research conference safety systems, no 26, pp 247–249
4. Solovyeva ME, Khafizov FSh (2014) Analysis of fire retardant coating influence on strength of wooden building constructions. Online Sci Rev Oil Gas Eng (1):490–502
5. Akhrarov BB, Saifutdinov RF, Mukhamedgaliev BA (2016) Investigation of combustion regimes for fire retardant wooden materials. Chem Chem Technol 4(55):45–48
6. Korolchenko AYa, Korolchenko DA (2004) Fire and explosion safety of materials and substances and their supressants. In: Handbook, vol 1, p 713
7. Chuang C-S, Tsai K-C, Yang T-H et al (2011) Effects of adding organo-clays for acrylic-based intumescent coating on fire-retardancy of painted thin plywood. Appl Clay Sci 53:709–715
8. Serkov BB, Aseeva RM, Sivenkov AB (2012) Physical and chemical basis of burning and fire danger of wood (part 2). Technol Technosph Saf 1(41):1
9. Sharipkhanov SD, Khasanova GSh, Sivenkov AB (2013) Effective fire protection mechanisms for reduction of wood fire danger. YUFU Report. Techn Sci 8(145):76–79
10. Bezzaponnaya OV, Golovina EV, Mansurov TKh, Akulov AYu (2017) Application of thermal analysis method for complex investigation and improvement of intumescent fire retardant compounds. Technosph Saf 2(15):3–7
11. Eremina TYu, Krasheninnikova MV, Dmitrieva YuN, Semenov DS (2007) Normative requirements for fire retardant coating quality at facility commissioning and application of thermal analysis method for coating age forecasting. Fire Explos Saf (5), 31–33
12. Eremina TYu, Gravit MV (2010) Complex estimation of reliability of intumescent fireproof covers for increase of fire resistance limits for building constructions. In: 11th International symposium on fire protection, Leipzig. VFDB (German Fire Protection Association)

Fire Modeling, Fire Testing, Fire Certification, Fire Investigation, Fire Dynamic, Fire Behaviour Modelling, Smoke Control and Combustion Toxicity

Pine Wood Crib Fires: Toxic Gas Emissions Using a 5 m^3 Compartment Fire

Bintu G. Mustafa[1,2], Rosmawati Zahari[1], Yangfu Zeng[1], Miss H. Mat Kiah[1], Gordon E. Andrews[1(✉)], and Herodotos N. Phylaktou[1]

[1] School of Chemical and Process Engineering, University of Leeds, Leeds, UK
G.E.Andrews@leeds.ac.uk
[2] Chemical Engineering, University of Maiduguri, Maiduguri, Nigeria

Abstract. Toxic emissions from pinewood crib fires were determined using heated FTIR gas analysis from a 5 m^3 compartment fire with an air opening equivalent to 5% of the compartment cross-sectional area ($V^{2/3}$) in the floor of the compartment and a vent in the ceiling layer, with the air inlet controlling the flow. A 20 mm square pine wood crib size of 400 × 400 × 260 mm was investigated. The crib was ignited using a small ethanol pool fire. The flaming fire had a peak HRR of 40 kW and average ceiling temperature of 400 °C. The fire was lean overall at the peak HRR and the fire self-extinguished through lack of air with subsequent smouldering combustion. In spite of the lean combustion in the fire, very high toxic emissions were determined with an FEC LC_{50} of >6. The peak toxicity occurred just before the fire self-extinguished and the key toxic emissions were CO and formaldehyde for deaths, while formaldehyde and acrolein were the most important for impairment of escape.

Keywords: Toxicity · Compartment fires · FTIR

1 Introduction

About 56% of fire incidents in the UK occur in buildings [1] and most deaths as are caused by the inhalation of toxic smoke. Despite this, no legislation requires toxic gas measurements from fires for any building material, apart from visible smoke production. This work investigates the toxic gas emissions in a pine wood crib ventilation controlled fire in a 5 m^3 compartment, larger than the 1.6 m^3 compartment previously used by the authors [2–4]. In compartment fires, not only does smoke reduce visibility to occupants, but it is also an irritant which causes respiratory problems, leading to slower movement of people and eventually death [5–8]. Purser [5] showed that the main toxic products in fires are CO, HCN and irritant or acidic gases. The authors have shown [2–4] for pine wood crib fires in a 1.6 m^3 enclosure that the main toxic gases were CO, acrolein, formaldehyde and benzene. The most common method of assessing the toxicity of fire products is the LC_{50} 30 min exposure concentration at which 50% of rats died in a test fire for 30 min exposure [6]. COSHH [9] is the European statutory law on occupational exposure limits equivalent to the US short term (10 min) impairment of escape limits AEGL2. The $COSHH_{15min}$ toxic gas concentration represents a safe condition for 15 min for escape not to be impaired.

L. Makovicka Osvaldova et al. (Eds.): WFS 2020, *Wood & Fire Safety*, pp. 137–143, 2020.
https://doi.org/10.1007/978-3-030-41235-7_21

2 Materials and Methods

A pine wood crib 400 × 400 × 260 mm was the fire load with 35 20 mm square sticks, as shown in Fig. 1a. The pine had a GCV of 18.9 MJ/kg, a volatile content of 79.2%, fixed carbon of 12.3%, moisture of 6.2% and ash for 2.3%. Elemental analysis was used to determine the stoichiometric A/F by mass as 5.9. The 6.22 kg crib was supported on load cells in the centre of a 5 m^3 compartment with a floor area of 4 m^2 as shown in Fig. 1b. This corresponds to a fire loading of 29.2 MJ/m^2 or 223.6 MJ/m^3. Ethanol, at 1% of the energy in pine, was used as an accelerant to ignite the fire.

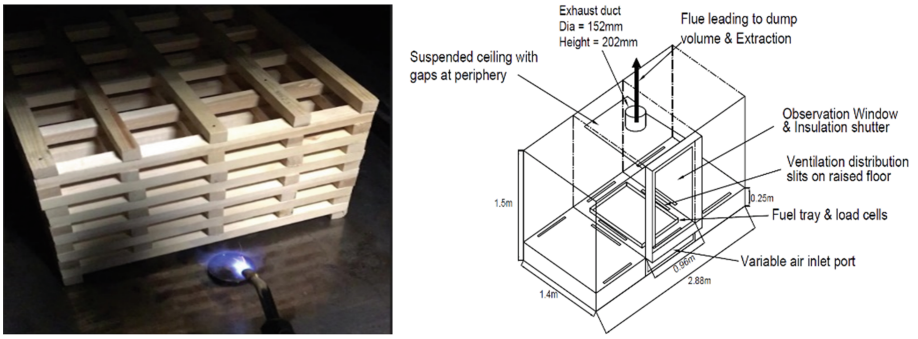

Fig. 1. Pine wood crib (a) and schematic of the 5 m^3 compartment

An air distribution plenum located below the compartment was used to provide air into the compartment by the chimney effect of the hot gases in the compartment. The air distribution plenum inlet was fully open and this was equivalent to a ventilation factor ($A_v/V^{2/3}$) of 5%. The N-gas model for toxicity assessment was used by taking the ratio n of the concentration of all the toxic species measured by the FTIR and dividing by either the LC_{50} values or the $COSHH_{15min}$ values. Their sum is the total toxic gas N.

3 Results and Discussion

3.1 Mass Loss, Equivalence Ratio, Heat Release Rates (HRR), Oxygen Concentration and Mean Ceiling Temperature

Figures 2a and b show the mass loss and the mass loss rate as a function of time. A gradual decrease in mass loss was observed after ignition at 34 s until 2000 s when flameout occurred and smouldering combustion continued. The equivalence ratio (from carbon balance) in Fig. 2c was 0.5 during the period of maximum HRR of 42 kW at 400 s with a peak ceiling temperature of 400 °C. However, the fire then began to decay to a HRR of about 25 kW with an equivalence ratio of 0.7. This was due to the large mass of 6 kg of air in the compartment at the start of the fire. The initial fire growth was as a freely ventilated fire and then the effect of the restricted ventilation occurred with

reduced HRR and richer mixtures. The fire continued to decay until flame out occurred at 7% oxygen and 170 °C. There was then a long period of smouldering combustion with a HRR of about 1 kW.

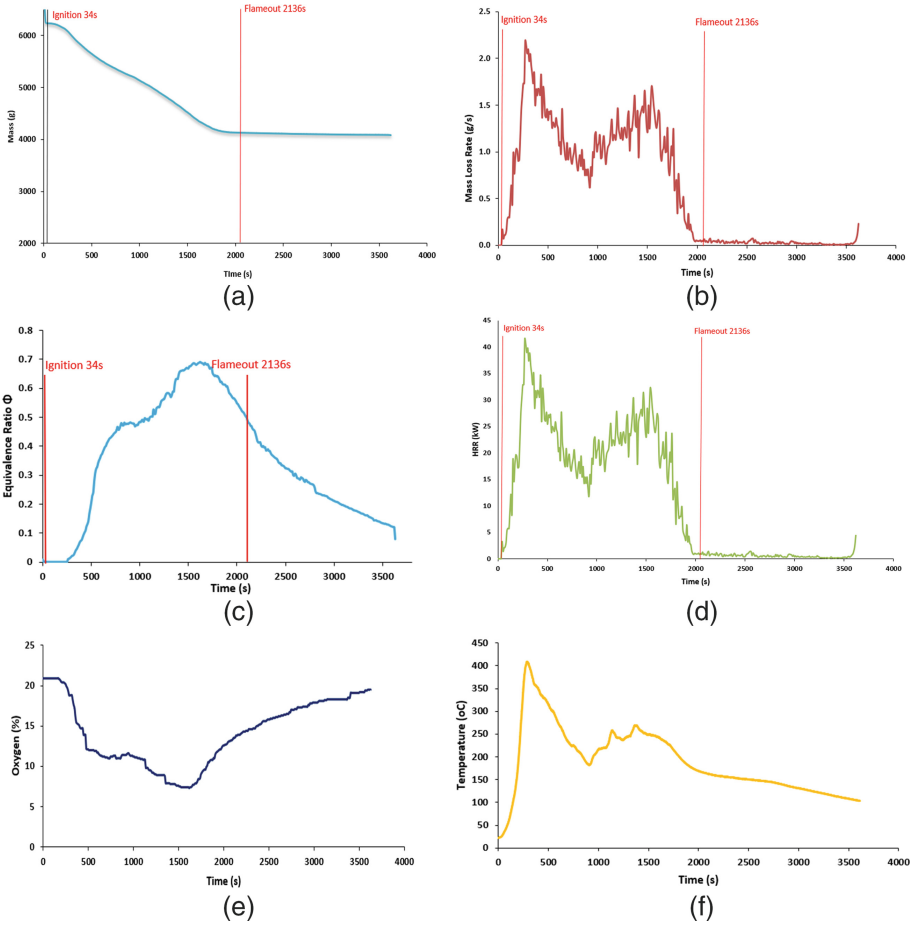

Fig. 2. Mass loss (a) mass loss rate (b) equivalence ratio (c) heat release rate (d) oxygen concentration (f) and mean ceiling temperature (g)

3.2 Toxic Gas Concentration

Figure 3 shows the most important toxic gas emissions, which had their highest concentration between 1500 s to 2000 s during the restricted ventilation phase of the fire. The transition from flaming to smouldering combustion with low oxygen concentration of <10% was associated with the release of peak levels of toxic gases. The main toxic gases were CO, Formaldehyde and Acrolein. Benzene was also found to be significant in this fire. This agrees with results obtained by the authors [2–4, 10] for a 1.6 m^3

compartment fire. CO exceeded the LC_{50} exposure limit by a factor of 3 while it exceeded the $COSHH_{15min}$ exposure limit by a factor of 40. Formaldehyde also exceeded the exposure limits on both the LC_{50} and $COSHH_{15min}$ basis. Although Acrolein did not exceed the LC_{50} exposure limit, it exceeded the $COSHH_{15min}$ limit by a factor of 5000. Even though the compartment was considered well ventilated with lean combustion, high concentrations of toxic gases were produced that will lead to the impairment of escape and eventual death.

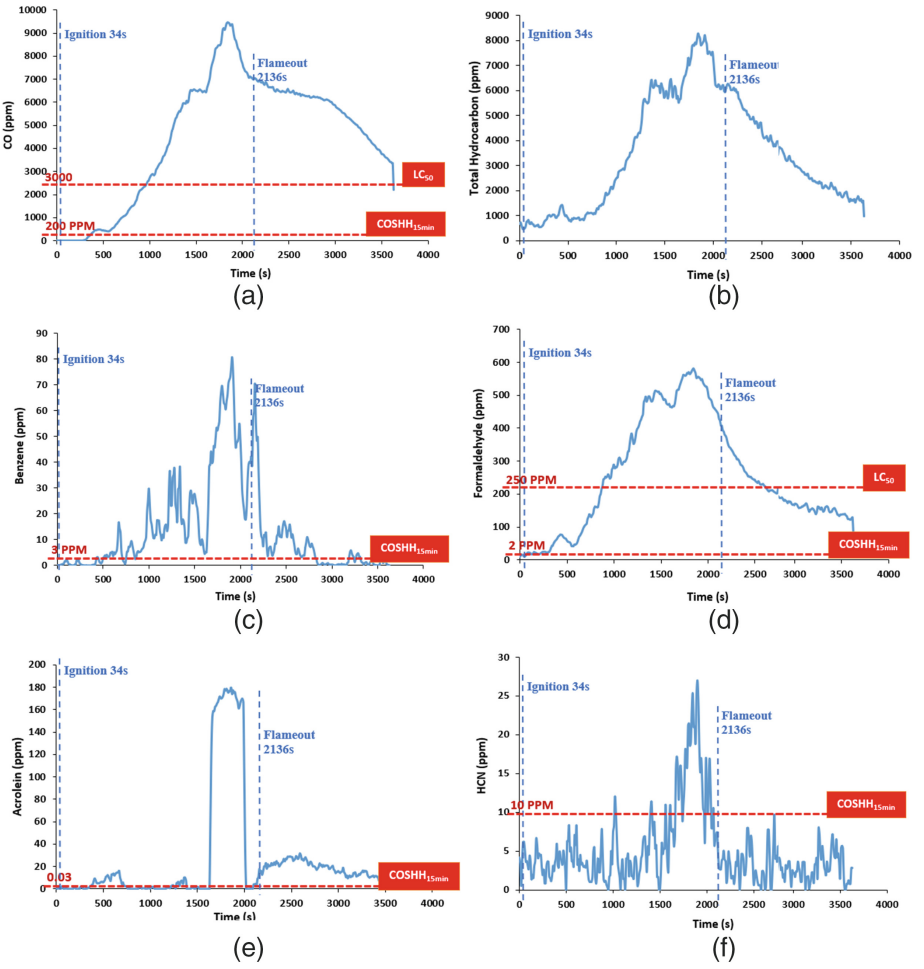

Fig. 3. Toxic gas concentrations; CO (a), total hydrocarbon (b), benzene (c), formaldehyde (d), acrolein (e) and hydrogen cyanide (f)

3.3 Total Fire Toxicity N on an LC_{50} and $COSHH_{15min}$ Basis

Figure 4 shows that the peak **N** for LC_{50} was >6 and the peak **N** on a $COSHH_{15min}$ basis was >2000, but they occurred at the same time in the transition from the flaming to smouldering combustion. The **N** values indicate that the toxic gases on escaping from the compartment would need to be diluted with air by a factor of >2000 before escape was not impaired and by a factor of >6 before deaths would not occur. Figure 5 shows that on an LC_{50} basis the toxicity was dominated by CO, formaldehyde, acrolein and HCN and on a $COSHH_{15min}$ basis formaldehyde, CO and benzene. Between 1600 s and 2000 s there was a large increase in impairment of escape $COSHH_{15min}$ total toxicity and this can be traced to the large increase in acrolein in Fig. 3e. This period, as shown in Fig. 2d, coincided with the onset of fire decay with the peak HRR reducing to flame out over this period of high acrolein emissions. There was also a reduction in fire ceiling temperature as shown in Fig. 2g.

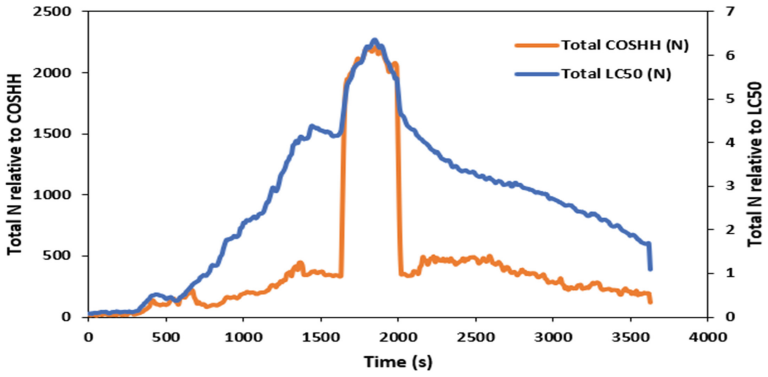

Fig. 4. Total toxicity N relative LC_{50} and relative to $COSHH_{15min}$

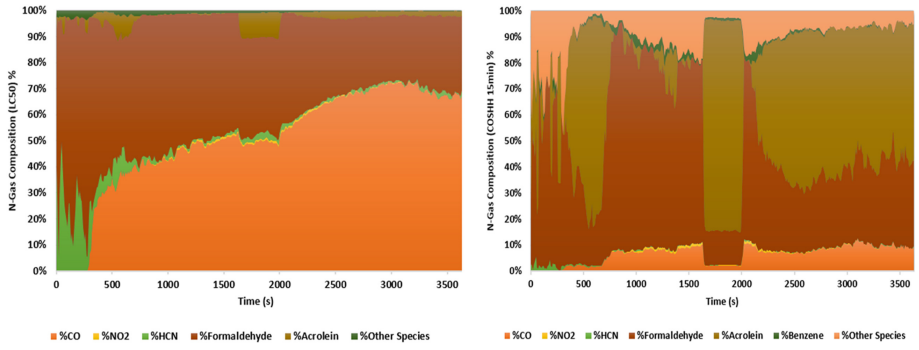

Fig. 5. N-Gas composition (LC_{50}) (a) and N-Gas composition ($COSHH_{15min}$) (b)

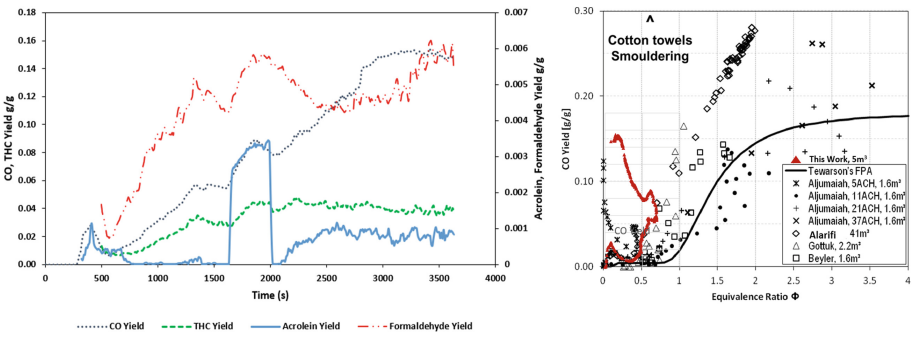

Fig. 6. Toxic gas yield as a function of time (a) and yield comparison (b)

3.4 Toxic Yields

The toxic yields of the most important gases in Fig. 6a were high during 1500–2000 s and increased during the smouldering combustion for CO and formaldehyde. CO had a peak yield of 0.15 g/g while formaldehyde had a peak yield of 0.006 g/g. Acrolein peaked at 0.003 g/g while the total unburnt hydrocarbon yield was at 0.04 g/g. The CO yield was compared in Fig. 6b with the yield from wood in smaller compartments [3, 11], 41 m^3 compartment [12] and Tewarson's correlation [13]. The present result shows good agreement with the results in the literature for equivalence ratios 0–0.7.

4 Conclusions

High concentrations of toxic gases that would impair escape were produced in lean restricted ventilation compartment wood fires. Peak toxicity occurred just before flame out.

Acknowledgments. The Petroleum Technology Development Fund, Nigeria and the University of Maiduguri are thanked for sponsoring the PhD of Bintu G. Mustafa.

References

1. Home Office (2018) Fire and rescue incident statistics: England. London
2. Andrews GE, Daham B, Mmolawa MD, Boulter S, Mitchell J, Burrel G, Ledger J, Gunamusa W, Boreham RA, Phylaktou HN (2006) FTIR investigations of toxic gases in air starved enclosed fires. In: Proceedings of the 8th international symposium on fire safety science. International Association for Fire Safety Science, Beijing
3. Aljumaiah O, Andrews GE, Phylaktou HN, Mustafa BG, Al-Qattan H, Shah V (2011) Air starved compartment wood crib fire heat release and toxic gas yields. In: Proceedings of tenth international symposium on fire safety science. International Association for Fire Safety Science, pp 1263–1276

4. Mustafa BG, Andrews GE, Phylaktou HN, Al-Shammri A, Shah V (2015) Impact of wood fire load on toxic emissions in ventilation controlled compartment fires. In: Proceedings of the IFireSS - international fire safety symposium, Coimbra, Portugal
5. Purser DA (2002) Toxic assessment of combustion products. In: Dinenno PJ (ed.) SFPE handbook of fire protection engineering, Quincy, MA, National Fire Protection Association, pp 2-83-82-171
6. Purser DA (2010) Hazards from smoke and irritants. In: Fire toxicity, chap. 3. Woodhead Publishing, pp 51–117
7. Purser DA (2000) Toxic product yields and hazard assessment for fully enclosed design fires. Polym Int 49:1232–1255
8. Hartzell GE (2001) Engineering analysis of hazards to life safety in fires: the fire effluent toxicity component. Saf Sci 38:147–155
9. EH40/2005 (2005) EH40/2005 Workplace Exposure Limits
10. Aljumaiah O, Andrews GE, Abdullahi A, Mustafa BG, Phylaktou HN (2010) Wood crib fires under high temperature low oxygen conditions. In: Proceedings of the 6th international seminar on fire and explosion hazards. Research Publishing, Leeds, p 1044
11. Gottuk DT, Roby RJ, Beyler CL (1992) A study of carbon monoxide and smoke yields from compartment fires with external burning. In: 24th symposium (international) on combustion, pp 1729–1735
12. Alarifi A, Phylaktou HN, Andrews GE, Dave J, Aljumaiah O (2017) Toxic gas emissions from a timber-pallet-stack fire in a large compartment. Springer
13. Alpert RL (2008) Ceiling jet flows. In: DiNenno PJ, et al (ed) SFPE handbook of fire protection engineering. National Fire Protection Association & Society of Fire Protection Engineers, Quincy, pp. 18–31

Comparison of Cone Calorimetry and FDS Model of Low-Density Fiberboard Pyrolysis

Juraj Jancík[1(✉)], Paulína Magdolenová[1], and Frank Markert[2]

[1] University of Žilina, Univerzitná 8215/1, 010 26 Žilina, Slovakia
{juraj.jancik, paulina.magdolenova}@fbi.uniza.sk
[2] Technical University of Denmark, Anker Engelunds Vej 1,
2800 Kongens Lyngby, Denmark
fram@byg.dtu.dk

Abstract. Combining bench scale physical experiments with numerical simulations become more and more common to enable upscaling to large scale conditions. Bench scale experiments are easier to control and to reproduce. They are less demanding in time and costs. However, it is essential to verify these simulations during their development process with real tests because incorporating all the factors that affect the burning process into numerical calculations is very challenging and doesn't necessarily have to correspond to reality. The aim of the paper is to compare time to ignition of the FDS model with a real bench-scale experiment. Low-density fibreboards, commonly used for thermal insulation of buildings, are tested. Cone calorimetry is conducted to estimate time to ignition of the fibreboard specimens, which will provide a baseline for further accuracy assessment of the FDS simulation. A simultaneous thermal analysis of wood fibres is carried out to provide input data for the model. Plausible results accuracy would enable application of the obtained outcomes in large-scale FDS enclosure fire simulation.

Keywords: Cone calorimetry · Wooden fibreboard · Fire Dynamics Simulator · Simultaneous thermal analysis

1 Introduction

Wood as a thermally thick [1] construction material is widely used in various forms in different types of buildings globally while its fire resistant properties still remain a big issue [2–5]. Wooden fibreboards are one of thermal insulation systems based on mostly renewable raw materials, very common in civil engineering these days. Different types of wooden fibreboards serve different purposes, where low-density fibreboards were chosen for this experiment as those are best known for their remarkable thermal insulation properties compared to other types.

A cone calorimetry with igniter is used to estimate time to ignition of tested specimens. Simultaneous thermal analysis (STA) [6] is conducted as well to provide input data for the numerical simulation, such as reference rate and reference temperature etc. STA integrates two measurement methods, i.a. thermogravimetric analysis (TGA) and differential scanning calorimetry (DSC).

L. Makovicka Osvaldova et al. (Eds.): WFS 2020, *Wood & Fire Safety*, pp. 144–151, 2020.
https://doi.org/10.1007/978-3-030-41235-7_22

Simultaneously to laboratory experiment, numerical simulation of cone calorimetry was carried out. Burning was modelled using the NIST Fire Dynamics Simulator (FDS) which is widely used for CFD (computational fluid dynamics) models of fire-driven fluid flow. Besides enclosure fire and evacuation simulations, FDS could be used to design smoke handling and sprinkler systems and provides a practical engineering tool for fundamental fire dynamics and combustion study [7].

2 Experiment Description

Steico Therm fibreboards [8] 6 cm thick made out of 3 layers were chosen for this experiment. Despite wood being considered an anisotropic material, fibreboards are isotropic as grain is not present and fibreboards are a relatively homogenous material. Boards were sawed to 10 × 10 × 6 cm specimens as demanded for cone calorimeter holder with square 100 cm^2 surface area exposed to heat flux from the cone. Density of the specimens was measured to 110 $kg.m^{-3}$. Example of specimens used in the experiment is shown in the following Fig. 1.

Fig. 1. Tested fibreboard sample

Four thermocouples were placed in the central area of the exposed surface. Thermocouples were imbedded approximately 3–5 mm deep in the surface to prevent them from leaping above the specimen. Several tests were conducted at different heat fluxes (15/20/25/30/35 $kW.m^{-2}$). Data collected from all thermocouples were averaged in order to reduce inaccuracies. Surface temperature is an output of this experiment that helps estimate the time of ignition. This is verified by video records of the experiments (photo in Fig. 2).

Fig. 2. Cone calorimetry experiment

The cone calorimetry burning of samples was modelled in FDS version 6.7.1. At first, a numerical TGA analysis was carried out to provide reliable material and reaction inputs for cone calorimetry scenarios. Input data for TGA analysis in FDS were based on known fibreboard material properties and conducted STA experiment. Heat release rate per unit area (*HRRPUA*) and mass loss rate per unit area (*MLRPUA*) provided the base for numerical simulation parameters, such as reference temperature, reference rate and fraction values of reactive material components. For fibreboards, cellulose ($C_6H_{10}O_5$) is assumed to be liberated from the sample surface when the surface reaches the ignition temperature as also assumed and explained in [11].

Because experimental samples were completely dried out before the test at 100 °C in the heating cabinet, no water vapour was defined for both, TGA analysis and cone calorimetry simulation, in the reaction parameters. As one of the material properties, specific heat c [kJ/(kg.K)] was necessary to be defined for the TGA analysis and the value for fibreboards was taken from [9]. With this parameter it was possible to evaluate the heat of reaction l [J/kg] based on reference temperature ΔT [K] with following mathematical formula [10]:

$$l = c.\Delta T \tag{1}$$

Part of the script for the TGA analysis in FDS with reactant and material parameters:

```
&REAC FUEL='CELLULOSE',C=6,H=10,O=5,SOOT_YIELD=0.015 /

&MATL ID                     = 'fibreboard'
      EMISSIVITY             = 0.75
      DENSITY                = 110.
      SPECIFIC_HEAT          = 2.5
      CONDUCTIVITY           = 0.039
      N_REACTIONS            = 1
      REFERENCE_TEMPERATURE  = 360
      REFERENCE_RATE         = 0.0016
        HEATING_RATE           = 10
        NU_SPEC                = 0.65
        SPEC_ID                = 'CELLULOSE'
        NU_MATL                = 0.35
        MATL_ID                = 'residue'
        HEAT_OF_REACTION       = 900 /
```

Output and comparison of the STA experiment and the numerical TGA analysis is shown in Fig. 3 as *HRRPUA* and in Fig. 4 *MLRPUA* development.

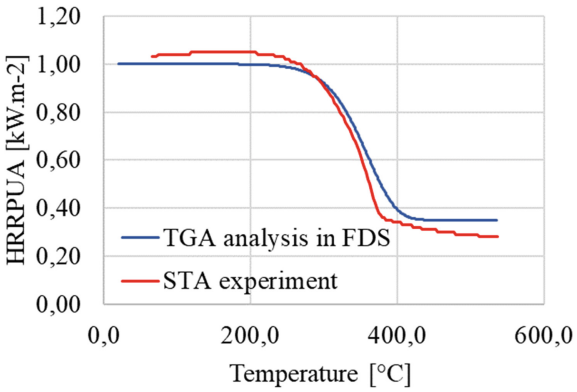

Fig. 3. STA experiment and TGA simulation *HRRPUA* output

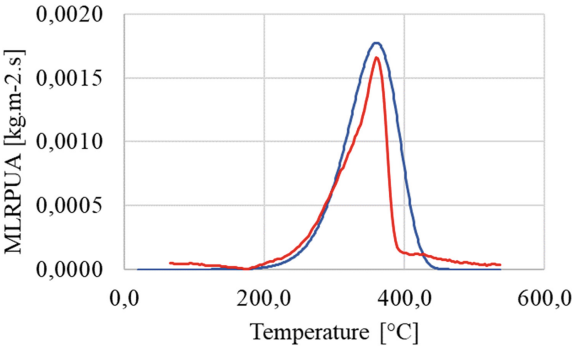

Fig. 4. STA experiment and TGA simulation *MLRPUA* output

After reaching sufficient output of TGA analysis (matching on a large scale with experiment – Figs. 3 and 4), fibreboard material properties were inserted into FDS cone calorimetry script.

Parts of FDS input script for cone calorimetry simulation:

```
&MESH IJK=3,1,4, XB=-0.15,0.15,-0.05,0.05,0,0.4 /

&REAC FUEL='CELLULOSE',C=6,H=10,O=5,SOOT_YIELD=0.015 /

&VENT XB=-0.05,0.05,-0.05,0.05,0.,0.,SURF_ID='SAMPLE'/
&VENT MB='ZMAX', SURF_ID='OPEN' /
&VENT MB='XMIN', SURF_ID='OPEN' /
&VENT MB='XMAX', SURF_ID='OPEN' /

&SURF ID             = 'SAMPLE'
      COLOR          = 'RED'
      EXTERNAL_FLUX  = 35.
      THICKNESS      = 0.060
      MATL_ID(1,1) = 'fibreboard' /

&PART ID='ignitor particle', SURF_ID='ignitor',
STATIC=.TRUE. /

&SURF ID='ignitor', TMP_FRONT=1000.,
GEOMETRY='CYLINDRICAL', LENGTH=0.002, RADIUS=0.001 /

&INIT XYZ=0.0,0.0,0.02, DX=0.0, PART_ID='ignitor parti-
cle', N_PARTICLES=1 /

&DEVC XB=-0.15,0.15,-0.05,0.05,0.,0.4, QUANTITY='HRR' /
```

All material and reaction properties, as well as sample thickness, were modelled for sample surface (SURF) which was bonded to mesh border area (VENT) of

10 × 10 cm to match the sample dimensions. The created mesh measurements are 15 × 10 × 40 cm which is divided into 5 × 5 × 5 cm numerical grid cells. The cone calorimetry heat flux is defined as external heat flux (EXTERNAL_FLUX) in the surface input data (SURF). To represent real experiment conditions, hot particle (PART, IGNI) was modelled 2 cm above the sample surface to simulate cone calorimetry ignitor.

Overall, 5 scenarios were created with the variety of external heat flux according to the carried out experiment – 15/20/25/30/35 kW.m^{-2}. To predict the ignition time of the sample, devices measuring *HRR* and *MLR* were modelled (DEVC). The start, or sharp rise, of *HRR* represents the time of ignition and this method was used also in study by NIST [11].

3 Results

Results from the experimental measurements are shown in the Fig. 5. Average values from all experiments are plotted and ignition is indicated using red dots for clearer visualisation.

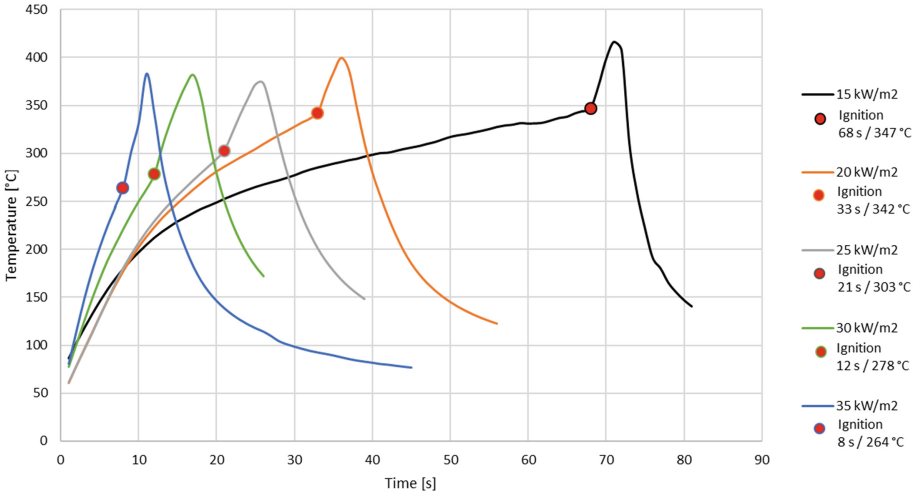

Fig. 5. Experimental measurement results

Times of ignition vary from 8 to 68 s at different heat fluxes. Both temperatures and times of ignitions appear to be in inverse proportionality with heat flux emitted from the cone calorimeter, which was expected and confirms validity of collected data. Specimens were also tested at 10 kW.m^{-2} heat flux, however this is at the edge of ignitability of wooden fibreboards, which means time to ignition acquires values of several minutes. This measurement was left out to keep the results compendious and easier to visualize.

In Fig. 6 results from modelled cone calorimetry are plotted as *HRR* values for all created scenarios. According to cone calorimetry heat flux (external flux), maximum *HRR* values are reached, meaning that the higher heat flux evokes higher values of *HRR*. As can be seen in Fig. 6, the higher the heat flux rate is, the development of *HRR* starts sooner and the rise of its curve is sharper.

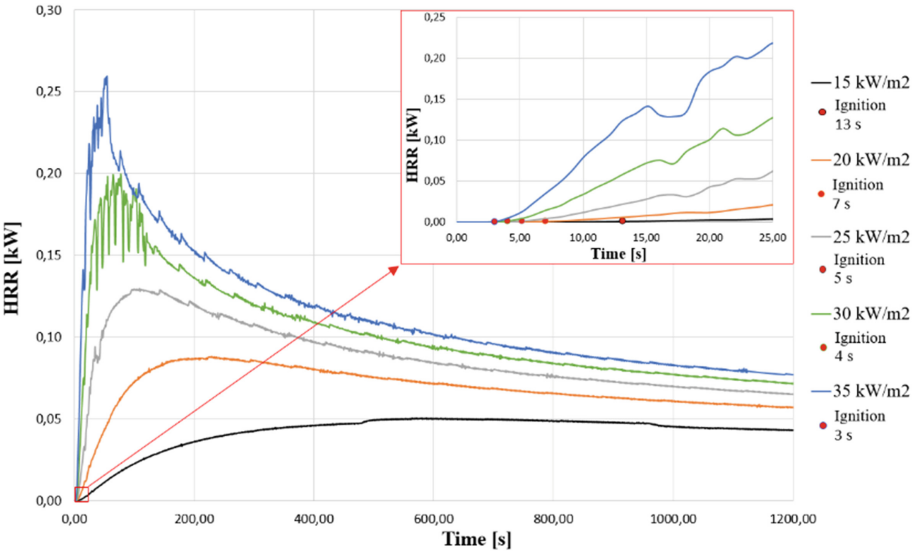

Fig. 6. Cone calorimetry FDS simulation results

Point, where the *HRR* curve starts to rise from zero value, represents the ignition time of the sample. That is why a zoomed insight is provided in Fig. 6 for a clearer description of the most important part of the simulation outputs. The zoomed part of Fig. 6 shows the beginning of the measurement displaying the first 25 s, where it is easy to determine the time of ignition points for all scenarios, which vary from 3 to 13 s.

4 Conclusions

Comparison of experiment and model results shows us quiet significant differences in these approaches. Ignition times estimated from the model acquired distinctly lower values, compared to laboratory measurements. Differences in results are inversely proportional to heat flux used, increasing in ignition time with lowering heat flux rates. Results are shown together in Table 1 for clearer display.

Table 1. Final time of ignition results from both approaches

Heat flux					
	15 kW.m^{-2}	20 kW.m^{-2}	25 kW.m^{-2}	30 kW.m^{-2}	35 kW.m^{-2}
t_{ig} EXP[s]	68	33	21	12	8
t_{ig} FDS[s]	13	7	5	4	3
Δt_{ig}[s]	**55**	**26**	**16**	**8**	**5**

According to gathered outcomes we can see that, in this case, FDS model doesn't correspond to laboratory experiment. Reaching the difference of 55 s in ignition time at 15 kW.m^{-2} heat flux only highlights unacceptability of the model as a whole. Cone calorimetry of wooden materials is therefore not reliable for FDS models.

High inaccuracies might be caused by limited possibilities in material defining of the model. Besides cellulose, which was the only one defined as fuel in the model, there are also other substances contained in wood. One of the other substances is e.g. lignin, however, FDS failed to run a simulation with lignin chemical formula defined as fuel. Cellulose has also been used as the only defined fuel in previous cone calorimetry models [12] of wooden materials.

References

1. Babrauskas V (2014) Ignition handbook. Fire Science Publishers, Issaquah
2. Gašpercová S, Osvaldová L (2015) Fire protection in various types of wooden structures. Civil Env Eng 11. https://doi.org/10.1515/cee-2015-0007
3. Osvaldová L, Gašpercová S (2015) The evaluation of flammability properties regarding testing methods. Civil Env Eng 11. https://doi.org/10.1515/cee-2015-0018
4. Osvaldová L, Osvald A (2013) Flame retardation of wood. Adv. Mater. Res. 690–693:1331–1334. https://doi.org/10.4028/www.scientific.net/AMR.690-693.1331
5. Martinka J, Mózer V, Hroncová E, Ladomerský J (2015) Influence of spruce wood form on ignition activation energy. Wood Res. 60(5):815–822 ISSN 1336-4561
6. Netzsch. https://www.netzsch-thermal-analysis.com/en/commercial-testing/methods/simulneous-thermal-analysis-sta/
7. McGrattan KB, Forney GP (2013) Fire dynamics simulator (version 6): user's guide (No. NIST SP 1019). National Institute of Standards and Technology, Gaithersburg
8. Steico. https://www.steico.com/en/products/wood-fibre-insulation/steicotherm/overview/
9. The Engineering ToolBox. https://www.engineeringtoolbox.com/specific-heat-solids-d_154.html
10. Quora. https://www.quora.com/Is-there-any-relation-between-latent-heat-and-specific-heat capacity
11. Linteris GT, Gewuerz L, McGrattan K, Forney G (2004) NISTIR 7178. Modeling solid sample burning with FDS
12. Hietaniemi J, Hostikka S, Vaari J (2004) FDS simulation of fire spread – comparison of model results with experimental data. VTT Building and Transport

Behaviour of Timber Doors in Fire Conditions

Bartłomiej Sędłak(✉), Paweł Sulik, and Daniel Izydorczyk

Zakład Badań Ogniowych, Instytut Techniki Budowlanej,
Ksawerów 21, 00-611 Warsaw, Poland
b.sedlak@itb.pl

Abstract. Wood and wood-based materials are combustible materials. This does not mean, however, that in the event of a fire, the elements made of these materials pose a threat. Separate the flammability from the spread of fire and fire resistance. Contrary to appearances, doors made of wood and wood-based composites obtain good results in the field of fire resistance and constitute an effective barrier for the spread of fire to neighbouring fire zones.

Fire doors play a key role in the fulfilment of fire safety requirement. In fire conditions, they are to form a barrier to fire, smoke and heat. Therefore, this type of elements should be appropriately fire-rated with respect to the fire integrity, fire insulation and smoke control.

This paper presents the main issues related to the fire resistance of timber doorsets. Aspects such as requirements, test methodology and way of classification for this type of elements have been discussed. Moreover, there are shown examples of test result and the conclusions regarding the behaviour of timber fire doors in standard fire scenario, based on many years of researches conducted in the Fire Research Department of Building Research Institute.

Keywords: Wood-based composites · Timber doors · Fire resistance · Fire integrity · Fire insulation

1 Introduction

Fire resistant doorsets (doors) for pedestrian or industrial traffic with frame, door leaf or leaves, rolled or folded curtain etc. are designed for installation in the openings of the building's vertical internal partitions. The building and its associated equipment shall be designed and made so that in case of fire they ensure the necessary load-bearing capacity of the structure for the time specified in national regulations, limitation of fire and smoke propagation within the building, limitation of fire propagation onto the adjacent buildings and evacuation of people, and they provide safety of the rescue teams. The aforementioned detailed requirements are not usually considered individually, therefore individual elements of buildings can play several roles during a fire. This also refers to the building elements such as doors which are usually required, in terms of design and execution, to ensure in case of fire that they shall, for a specific period of time, prevent its development from the room or a specific zone where the fire started, and that for the period of time the fire and smoke shall not propagate to other rooms or zones, to allow evacuation of people by limiting heat radiation, and to facilitate rescue team activities. Doors with proper fire resistance classification allow

L. Makovicka Osvaldova et al. (Eds.): WFS 2020, *Wood & Fire Safety*, pp. 152–158, 2020.
https://doi.org/10.1007/978-3-030-41235-7_23

meeting such requirements. Three different types of door designs can be distinguished: metal doors (usually of steel or aluminium) with metal frames [1–3], wooden doors with metal frames or wooden doors with wooden frames [4, 5]. All the above door design solutions can be made as panelled or glazed (using special fire resistant glazing [6–10]). The special group being the subject of this paper are the designs made of wood-based materials. In this context, wooden door leaf is a one in which the majority of the structure and the main components are made of wood (e.g. deciduous wood, coniferous wood, chipboard, blockboard, high-density fibreboard, plywood, medium-density fibreboard and other materials which have cellulose as the main component).

Wooden fire-resistant doors are used as closures for openings in horizontal fire separations found usually in public buildings, such as hotels, hospitals, cinemas, schools and shopping malls or high-rise buildings [11–13]. This type of buildings and structures must be built so as to make possible efficient and safe evacuation of occupants in the event of a fire. Fire-resistant doors play a key role in the fulfilment of this requirement. In addition to providing all the above mentioned functions, the materials used in the wooden door sets enable perfect adaptation to the specific character of many rooms, and make an excellent decorational element of the building interior.

2 Design of Wooden Fire Resistant Doors

Worldwide, there are many producers of wooden fire resistant doors, and thus there is a great diversity in products of this type. Although each producer uses its own individual design solutions, some common features can be found in most cases.

A solid wood fire resistant door leaf is usually constructed of a frame of a specified cross-section depending on the expected fire resistance rating (comprising two horizontal: top and bottom rails, and two vertical stiles: latch-side and hinge-side) and made of deciduous or coniferous wood. Frame members are adhesive bonded together or joined (e.g. using steel staples). The leaf filling is made of special high-density particle board sandwich panels, rock wool or special fire-resistant boards (e.g. calcium silicate boards). Individual layers of the sandwich structure have different densities and thickness depending on the expected fire resistance rating. Both the stiles and rails and the filling are faced on both sides with high-density MDF or HDF boards. All the door leaf filling elements are joined to the frame and the facing with a special adhesive. An important component of the entire door set is the door frame, consisting of jambs and the header, usually joined together with steel screws. The frame can be made of wood, wood-based materials or steel. In the case of wooden frames, it is important to apply the cross-section of a suitable size and a material of a suitable density. For steel frames, it is important to fill them with a suitable material. Most often, they are filled with plasterboard [14], gauged mortar or fire-resistant caulking foam. Wooden fire resistant doors should be fitted with special intumescent door seals [15]. The seals are placed in milled grooves or directly glued along all door leaf edges and a door frame. Under the temperature, these seals increase their volume and thus close the gaps that fire could penetrate.

3 Fire Resistance Tests and Rating

The wooden fire resistant door fire rating cannot be calculated or assessed based on comparison. The sole method allowing to obtain a realistic and clear classification of a specific element is the fire resistance testing. According to the PN-EN 13501-2 [16] standard, a door should be fire-rated based on results of test carried out in accordance with the PN-EN 1634-1 [17] standard.

The tested piece is heated in accordance with the standard temperature/time curve. This relationship is the model of a fully developed fire in a room and is presented in Fig. 1 (marked with solid red line).

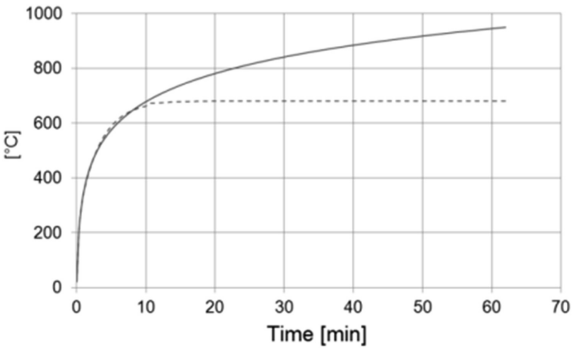

Fig. 1. Temperature-time curves, solid line – standard curve, dashed line – external fire curve, based on [18]

Fig. 2. The view of the exposed side of tested specimen prior (left side) and after (right side) the test

During the fire resistance testing of doors, the following performance efficiency criteria are verified: fire integrity, fire insulation and radiation. The detailed research methods and the ways of rating fire resistant doors are extensively described in the literature, e.g. [2, 19–21].

4 Behaviour of Wooden Fire Resistant Doors in Case of Fire

When considering the behaviour of wooden fire resistant doors in case of fire, the considerations should start with dividing such designs into two types, which show different behaviour when exposed to fire and heat. The issue is connected with the very important part of the entire door set, namely the frame, which in case of wooden door can be made either of wood or wood-based materials like the leaf itself (so-called wooden frame) or of metal (usually steel, although aluminium frames are also used). This division results from completely different (or even opposite) behaviour of both materials when exposed to fire. Under heat, wood shrinks, whereas metal expands. When exposed to fire, wooden door leaf (regardless of the frame used) will tend to warp towards the fire. Exposed surface of the leaf will try to shrink in relation to the unexposed surface, which will result in "pulling" the upper and lower edges of the leaf towards the fire. A wooden frame of a door set tends to behave similarly as the wooden leaf, however, because it is mounted to a supporting construction and is usually thicker and/or larger in diameter and consequently more rigid, when exposed to fire it cannot move as much as the leaf. If the leaf of such a door set opens towards the fire, then, as described above, the upper and lower edges of the leaf will tend to warp in the direction of fire and thus away from the edging strip, enabling flames to pass and hot gases to be discharged from the furnace, which will be supported with positive pressure inside the furnace, leading to the loss of fire integrity. If the door opens in the direction away from the fire, the upper and lower edges of the leaf tends to warp towards the fire and to the edging strip, which will improve the door set performance. Interestingly, the direction of door leaf opening should not affect the fire insulation in this case. According to the research described in [22, 23] door (leaf and frame) made entirely of wood-based materials present the best insulation performance among all types of door sets which is clearly shown in Fig. 3. Contrary to a wooden frame, metal one, when exposed to fire, starts to expand on the side exposed to fire, which results in bending of its upper and lower part away from the fire (also, away from the leaf). If a door leaf opens towards the fire, then, as stated above, the upper and lower edge of the leaf tends to bend in the direction of fire and thus from the edging strip. It makes it possible for flames to pass and for hot gases to be discharged from the furnace, supported by positive pressure in the furnace, prematurely compromising the fire integrity. This condition worsens the bending of the metal frame in the opposite direction. If the door opens away from the fire, the upper and lower edges of the leaf tend to warp towards the fire and to the edging strip, which tends to help maintaining the fire integrity of the door set.

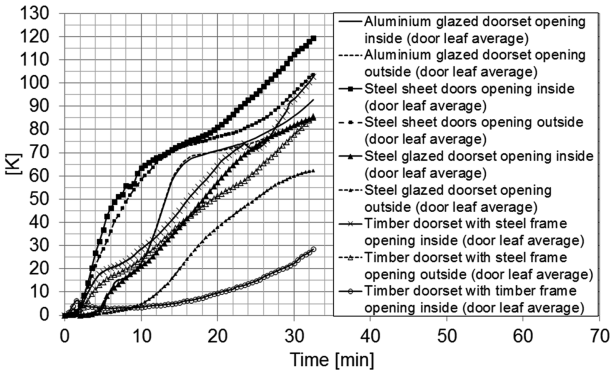

Fig. 3. Diagrams of average temperature rise on the unexposed surface of the leaf of various types of fire resistant doors (prepared based on [22, 23])

According to the curves shown in Fig. 3, the direction of door opening also affects fire insulation. It can be noted that the higher temperature was recorded in case of the door that opened into the furnace, which can be caused by the hot gases discharged from the furnace through the slots resulting from opposite bending of the frame and leaf.

The supporting construction of the door also affects its behaviour. In case of a wooden frame, a rigid supporting construction will hold the frame in place, limiting its displacement. Structural frame of flexible supporting construction is made of steel sections, therefore, such a construction will tend to bend in the opposite direction than the wooden frame. However, the majority of wooden fire resistant doors have a frame with sufficient cross-section, being rigid enough to resist the forces caused by a flexible supporting construction. Rigid supporting construction will also limit bending of a metal frame. However, a flexible supporting construction will bend together with the frame, increasing its deformation in relation to the wooden leaf.

5 Summary

Properly executed wooden fire-resistant door can create a perfect barrier for fire and hot gases. According to the foregoing analysis, in case of fire the behaviour of a wooden door is affected by the material used for making the frame of the entire set as well as the construction where it is mounted. As it can be seen in the case of wooden frame, the most worst-case scenario is when the door opens towards the fire. However, the impact of the supporting construction, in which the door is mounted, is negligible. This is clearly used in research practice and in case of this type of elements, there is no need to test them on both sides or with various supporting constructions, making them stand out among any other door sets. In case of a metal frame, it is necessary to test the door set from both sides. This results from the fact that even though the leaf opening towards the fire is the situation with the most difficult conditions for fire integrity, it is difficult to determine the worse side for fire insulation. According to Fig. 2, worse insulation of

leaf occurs for the door opened into the furnace, yet in case of the frame, higher temperatures were recorded in case of the door set opened in the opposite direction, which is presented in [22, 23]. For a wooden fire resistant door it is very important to pay attention to every single detail both at production and fixing stage [24–27], because even a slight change in the design or the method of fixing can significantly affect their fire resistance properties.

References

1. Sędłak B, Sulik P (2018) Zachowanie się drzwi stalowych w warunkach pożaru. Mater Bud 7:10–12
2. Izydorczyk D, Sędłak B, Sulik P (2017) Fire doors in tunnels emergency exits – smoke control and fire resistance tests. In: IFireSS 2017 – 2nd international fire safety symposium, Naples, Italy, 7–9 June 2017, pp 1–8
3. Wakili KG, Wullschleger L, Hugi E (2008) Thermal behaviour of a steel door frame subjected to the standard fire of ISO 834: measurements, numerical simulation and parameter study. Fire Saf J 43(5):325–333
4. Izydorczyk D, Sędłak B, Sulik P (2014) Fire resistance of timber doors - part I: test procedure and classification. Ann Warsaw Univ Life Sci SGGW For Wood Technol 86:125–128
5. Izydorczyk D, Sędłak B, Sulik P (2014) Fire resistance of timber doors - part II: technical solutions and test results. Ann Warsaw Univ Life Sci SGGW For Wood Technol 86:129–132
6. Laufs W, Luible A (2003) Introduction on use of glass in modern buildings, Rapp. N° ICOM 462
7. Zhan Y, Xia Z, Xin W, Hai-lun L (2011) Application and integrity evaluation of monolithic fire-resistant glass. Procedia Eng 11:603–607
8. Wu M, Chow WK, Ni X (2015) Characterization and thermal degradation of protective layers in high-rating fire-resistant glass. Fire Mater 39(1):26–40
9. Laskowska Z, Borowy A (2015) Szyby w elementach o określonej odporności ogniowej. Świat Szkła 20(12):10–15
10. Laskowska Z, Borowy A (2016) Szyby zespolone w elementach o określonej odporności ogniowej. Świat Szkła 21(3):15–20, 28
11. Glass RA, Rubin AI (1979) Fire safety for high-rise buildings, Gaithersburg, MD
12. Sassi S et al (2016) Fire safety engineering applied to high-rise building facades. In: MATEC web conferences, vol 46, p 04002
13. Sulik P, Sędłak B, Turkowski P, Węgrzyński W (2014) Bezpieczeństwo pożarowe budynków wysokich i wysokościowych. In: Halicka A (ed) Budownictwo na obszarach zurbanizowanych, Nauka, praktyka, perspektywy. Politechnika Lubelska, pp 105–120
14. Thomas G (2002) Thermal properties of gypsum plasterboard at high temperatures. Fire Mater 26(1):37–45
15. Camino G, Lomakin S (2001) Intumescent materials. In: Horrocks AR, Price D (eds) Fire retardant materials. Woodhead Publishing Limited, pp 318–335
16. EN 13501-2:2016 (2016) Fire classification of construction products and building elements - part 2: classification using data from fire resistance tests, excluding ventilation services
17. EN 1634-1:2014 + A1:2018 (2018) Fire resistance and smoke control tests for door and shutter assemblies, openable windows and elements of building hardware - part 1: fire resistance test for door and shutter assemblies and openable windows

18. EN 1363-2:1999 (1999) Fire resistance tests. Alternative and additional procedures
19. Izydorczyk D, Sędłak B, Papis B, Turkowski P (2017) Doors with specific fire resistance class. Procedia Eng 172:417–425
20. Borowy A (2014) Fire resistance testing of glazed building elements. In: POŽÁRNÍ OCHRANA 2014, pp 15–17
21. Kinowski J, Sędłak B, Sulik P, Izydorczyk D (2016) Fire resistance glazed constructions classification, changes in the field of application. Appl Struct Fire Eng
22. Izydorczyk D, Sędłak B, Sulik P (2017) Thermal insulation of single leaf fire doors: test results comparison in standard temperature-time fire scenario for different types of doorsets. Appl Struct Fire Eng
23. Izydorczyk D, Sędłak B, Sulik P (2016) Izolacyjność ogniowa drzwi przeciwpożarowych. Izolacje 21(1):52–63
24. Sulik P, Izydorczyk D, Sędłak B (2016) Bezinwazyjna weryfikacja poprawności wykonania i montażu drzwi przeciwpożarowych. In: Problemy techniczno-prawne utrzymania obiektów budowlanych: Ogólnopolska konferencja, Warszawa, 22–23 January 2016, pp 147–150
25. Izydorczyk D, Sędłak B, Sulik P (2014) Problematyka prawidłowego odbioru wybranych oddzieleń przeciwpożarowych. Mater Bud 11(11):62–64
26. Sulik P, Izydorczyk D, Sędłak B (2015) Elementy decydujące o awariach wybranych oddzieleń przeciwpożarowych. In: XXVII Konferencja Naukowo-Techniczna Awarie Budowlane, Szczecin, Międzyzdroje, pp 771–778
27. Sulik P, Sędłak B (2015) Prawidłowy odbiór przeszklonych drzwi przeciwpożarowych. Świat Szkła 20(2):46–49, 56

Charring of Timber with Fissures in Experimental and Numerical Simulations

Jaroslav Sandanus[1(✉)], Zuzana Kamenická[2], Peter Rantuch[3], Jozef Martinka[3], and Karol Balog[3]

[1] Faculty of Civil Engineering, Department of Steel and Timber Structures, Slovak University of Technology in Bratislava, Radlinského 11, 810 05 Bratislava, Slovakia
jaroslav.sandanus@stuba.sk
[2] Distler Engineering, Kominárska 2,4, 832 03 Bratislava, Slovakia
[3] Faculty of Materials Science and Technology in Trnava, Institute of Integrated Safety, Slovak University of Technology in Bratislava, Botanická 49, 917 08 Trnava, Slovakia

Abstract. Drying fissures occur in some timber structures what can lead to an issue for a mechanical resistance of these structures. There is no proposal to quantify the effect of various fissures and gaps on the charring of timber structural members. Therefore, this contribution deals with the numerical and experimental analysis of selected dimensions and number of fissures. The numerical analysis was conducted in a software based on FEM. There were created models with local fissures and simplified "smeared" models. The samples were tested in a cone calorimeter. There were two types of samples. The charring depth was measured from a split cross-section for the first group of samples. Temperatures were measured by means of thermocouples for the second group of samples and the charring depth was calculated based on these temperatures. The aim of this paper is to compare values of the charring rate and depth for the samples with different fissures. In terms of results, the bigger fissures or larger quantity of fissures should be considered by means of advanced design methods, or by increased value of the charring rate. However, the smaller fissures can be neglected.

Keywords: Charring · Fissures · Timber

1 Introduction

The position of the char-line is considered as the position of the 300-degree isotherm according to Eurocode 5, Part 2 [1]. This is significant to determine the residual cross-section what may change the mechanical resistance of structural members. Constant value of the design charring rate for one-dimensional charring of solid and glued laminated timber is $\beta_0 = 0.65$ mm/min according to simplified methods in the standard [1]. Constant value of the notional design charring rate of solid timber is $\beta_n = 0.8$ mm/min and of glued laminated timber is $\beta_n = 0.7$ mm/min. Therefore, the ratio for solid timber is $\beta_n/\beta_0 = 1.23$ and for glued laminated timber $\beta_n/\beta_0 = 1.08$ [2]. This difference is caused by the greater number of fissures in solid timber. There are 91.9%

L. Makovicka Osvaldova et al. (Eds.): WFS 2020, *Wood & Fire Safety*, pp. 159–165, 2020.
https://doi.org/10.1007/978-3-030-41235-7_24

of drying fissures, while 83.5% are external drying fissures in timber [3]. Fissures and gaps with a width greater than 4 mm [4] (or 2 mm according to [5]) should be taken into account, but no proposal to quantify this effect is given [6]. The author of the publication [5] analyses timber structural members with different gaps in timber, but it is relevant to develop rules for structures with fissures and gaps more in detail.

2 Experimental Simulations in a Cone Calorimeter

There were two types of samples. 30 samples had dimensions 60 × 100 × 100 mm (Fig. 1a) and 50 samples 140 × 100 × 100 mm (Fig. 1b). Samples were made of timber with strength class C24. Samples were divided into six groups. The first group of samples had the fissure 4 × 16 mm, the second group was without fissures, the third group had a fissure 4 × 32 mm, the fourth group 6 × 24 mm, the fifth group 6 × 60 mm (this fissure was not in samples 60 × 100 × 100 mm due to dimensions and this group was also without fissures) and the sixth group had three fissures 4 × 32 mm. The average density of samples 60 × 100 × 100 mm was 445.05 kg/m^3 and of samples 140 × 100 × 100 mm was 398.76 kg/m^3. The average moisture content of samples 60 × 100 × 100 mm was 7.4% and of samples 140 × 100× 100 mm was 7.61%. The average temperature of air during tests was 27 °C and relative ambient humidity was 30%. Two different measuring approaches were used for the experimental analysis. The first is measuring of the charring depth from a split cross-section as in [7]. The second is measuring of temperatures by means of thermocouples like as in [8]. According to [8], there is a ratio between charring depths in the cone calorimeter with the heat flux 50 kW/m^2 and the furnace with the standard fire exposure during 30–40 min.

Both types of samples were tested in a cone calorimeter. The heater and samples were oriented in a horizontal direction. Thermal radiation from the cone heater and action of spark igniter were applied on samples according to the standard [9].

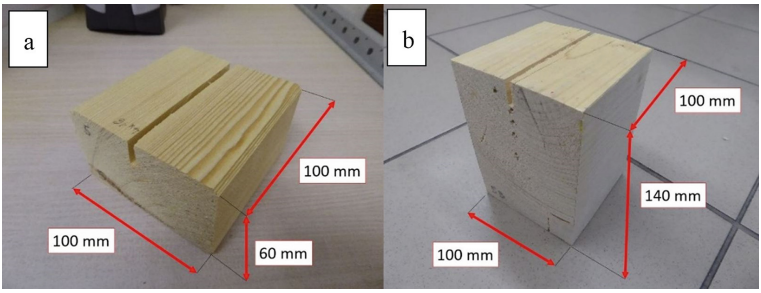

Fig. 1. Samples 60 × 100 × 100 mm (a) and samples 140 × 100 × 100 mm (b).

2.1 Samples 60 × 100 × 100 mm

Samples 60 × 100 × 100 mm were exposed to a constant heat flux 25 kW/m^2. These samples were split in a half and the charring depth was determined visually, thus allowing the calculation of the charring rate (Fig. 2a). The highest values of the charring depth and rate are for samples with three fissures 4 × 32 mm and the lowest values for samples without fissures. The mass loss of samples depending on time (Fig. 2b) was measured, as well. Results from values of the mass loss correspond to values of the charring rate.

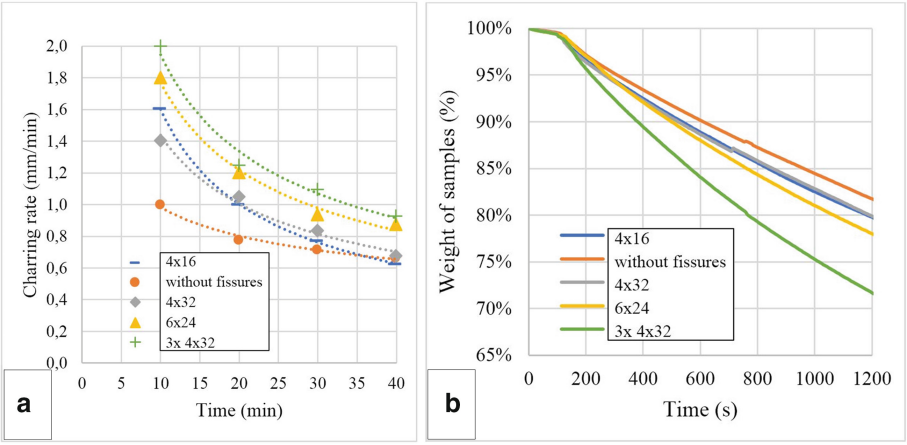

Fig. 2. The charring rate (a) and the weight of samples in time (b) of samples 60 × 100 × 100 mm.

2.2 Samples 140 × 100 × 100 mm

Samples 140 × 100 × 100 mm were exposed to a constant heat flux 50 kW/m^2 and were used with thermocouples to measure temperatures in specific points (different distances from the exposed surface). These thermocouples were used to identify the time of reaching the temperature 300 °C (the char-line) in different depths and to compare the numerical model with the experiment. Resultant values of the charring rate are in the Fig. 3a. The highest values are for samples with three fissures 4 × 32 mm and the lowest values are for samples without fissures.

A time to ignition of samples 140 × 100 × 100 mm and 60 × 100 × 100 mm was monitored. This time was bigger for samples 60 × 100 × 100 mm, because the time to ignition increases with lower heat flux [10]. The time to ignition depending on a density of samples 140 × 100 × 100 mm is in the Fig. 3b. Although this dependence is often described in publications (for example [11] or [12]), it was not clearly demonstrated due to an impact of other factors during this measuring.

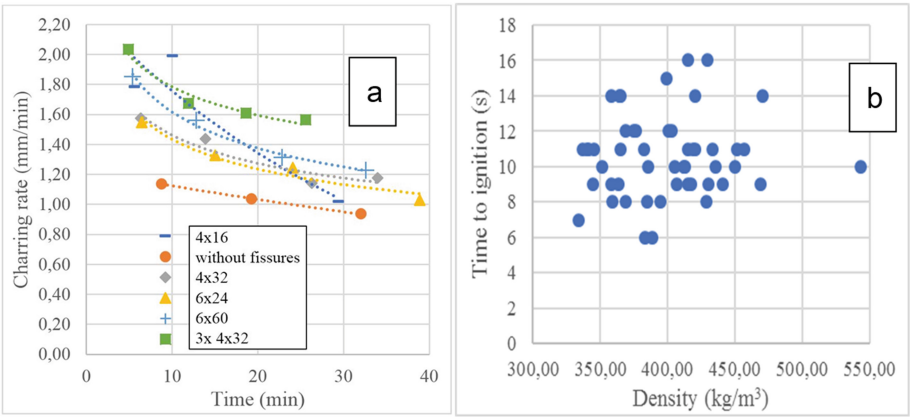

Fig. 3. The charring rate (a) and the time to ignition (b) of samples 140 × 100 × 100 mm.

3 Numerical Simulations

For the purpose of this study, the software Ansys Workbench was used. There were created several numerical models on a base of samples from the experimental analysis. Emissivity was 0.8 (according to [1]). Film coefficient was 25 W/(m^2.K). Thermal properties of timber according to [1] were modified in compliance of a regression analysis. Thermal properties of air were according to [13] and values of a thermal conductivity were multiplied by a factor from [14]. More detailed information is presented in a thesis of the author [15].

At first, the thermal load was specified according to the experiment with constant heat flux. Numerical models of local fissures were simplified to "smeared" models with thermal properties, which were averaged according to an area of timber and area of air. These models were created with different thickness of the layer with averaged properties. Then, other models were created with the standard fire curve ISO 834 as the thermal load (thermal properties were modified accordingly) to satisfy the standard requirements. These models with the curve ISO 834 and the thickness of the "smeared" layer which is equal to a half of the fissure depth were used for mutual comparison of the charring rates and the residual cross-sections for different fissures (Figs. 4 and 5).

The charring rate should increase in case of one fissure which is not very deep (<35 mm), as is derived from the Eq. (1a and 1b). The charring rate should increase in case the fissure which is deeper (≥ 35 mm) or in case there are more fissures, as can be seen in the Eq. (2a and 2b).

$$\beta' = \beta \times 2{,}0 \text{ if } t \leq 20 \text{ min}. \tag{1a}$$

$$\beta' = \beta \times 1.3 \text{ if } t > 20 \text{ min}. \tag{1b}$$

$$\beta'' = \beta \times 2{,}8 \; if \; t \leq 20 \, \text{min}. \tag{2a}$$

$$\beta'' = \beta \times 1.9 \; if \; t > 20 \, \text{min}. \tag{2b}$$

where β' = increased charring rate for smaller fissures (mm/min); β'' = increased charring rate for bigger fissures (mm/min); β = charring rate of timber without fissures (mm/min); and t = time (s).

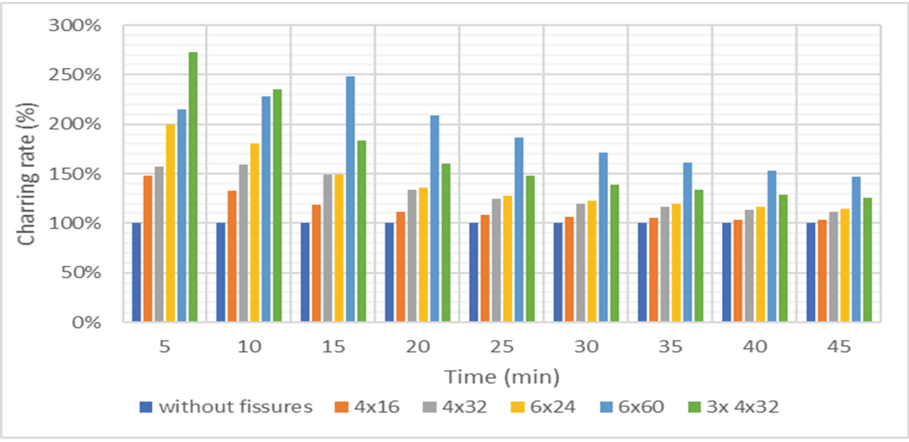

Fig. 4. Values of the charring rate from models with fissures compared to the model without fissures (β/β (model without fissures)).

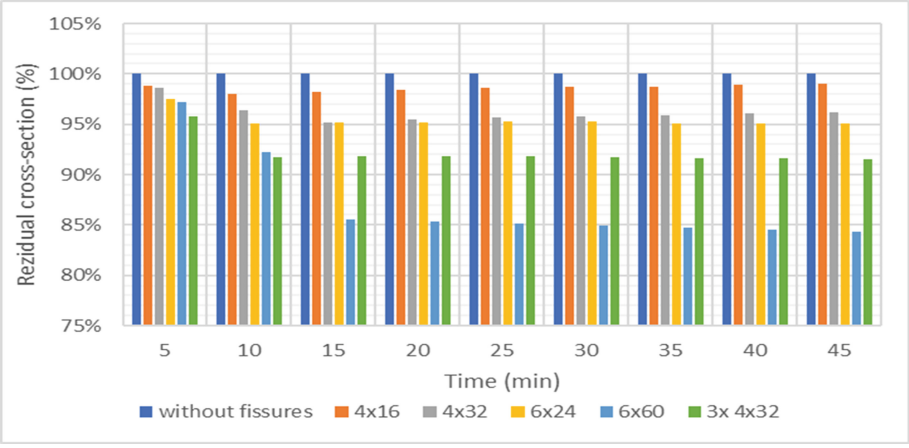

Fig. 5. Values of the residual cross-section from models with fissures compared to the model without fissures (A_{res}/A_{res} (model without fissures)).

4 Discussion and Conclusions

Fissures can increase the charring rate and decrease the residual cross-section depending on time, dimensions and number of fissures. Differences between timber structural members with and without fissures are smaller in consideration of a reduction of residual cross-sections (1 to 16%) as in consideration of a reduction of the charring rate (3 to 173%). The difference in values of the charring rate is bigger in the first minutes, then it decreases. On the contrary, the difference in values of the residual cross-section is smaller in the first minutes and then it increases.

The highest impact on the charring rate had a fissure 6 × 60 mm and three fissures 4 × 32 mm. The lowest charring rate applies for timber samples without fissures. The charring rate should increase with one fissure which is not very deep (<35 mm), as defined by the Eq. (1a) or (1b). The charring rate should increase with one fissure which is deep ($\geq$ 35 mm) or for more fissures, as stated by the Eq. (2a) or (2b).

In terms of results for the residual cross-section, the smaller fissures can be neglected, whilst the bigger ones should be taken into account by means of increased value of the charring rate (Eq. (2a) or (2b)), or by advanced calculations (e.g. FE-models). "Smeared" models are simpler in use compared to models with local fissures. They are also more appropriate for the consideration of the effect of fissures on the charring rate and the residual cross-section.

Acknowledgement. This paper has been supported by the Scientific Grant Agency of the Ministry of Education, science, research and sport of the Slovak Republic and the Slovak Academy of Sciences – grant VEGA 1/0773/18.

References

1. STN EN 1995-1-2: Eurocode 5: design of timber structures - part 1-2: general - structural fire design (2008)
2. Beilicke G et al (2009) Holz brandschutz handbuch, 3rd edn. Ernst & Sohn, Berlin
3. Mergny E et al (2016) Influence of cracks on the stiffness of timber structural elements. In: Worl conference on timber engineering, WCTE 2016, Vienna
4. Fornather J et al (2001) Versuchsbericht – Kleinbrandversuchsreihe 2 Teil 1 (KBV 2/1) – Versuche mit Rissen. Universität für Bodenkultur, Institut für konstruktiven Ingenieurbau, Vienna
5. Fornather J et al (2004) Brennbarkeit und Brandverhalten von Holz, Holzwerkstoffen und Holzkonstruktionen: Zusammenfassung und Erkenntnisse für die Bemessungspraxis; ein Forschungsprojekt des Fachverbandes der Holzindustrie Österreichs. 2. Aufl. proHolz Austria, Wien. ISBN 3902320036
6. Frangi A et al (2010) Fire safety in timber buildings: technical guideline for Europe. http://eurocodes.jrc.ec.europa.eu/doc/Fire_Timber_Ch_5-7.pdf
7. Xu Q, Chen L et al (2015) Combustion and charring properties of five common constructional wood species from cone calorimeter tests. Constr Build Mater 96:416–427. https://doi.org/10.1016/j.conbuildmat.2015.08.062

8. Tsantaridis LD, Östman BAL (1998) Charring of protected wood studs. Fire Mater https://onlinelibrary.wiley.com/doi/full/10.1002/%28SICI%291099-1018%28199803/04%2922%3A2%3C55%3A%3AAID-FAM635%3E3.0.CO%3B2-T
9. ISO 5660-1:2015 - Reaction-to-fire tests, heat release, smoke production and mass loss rate, part 1: heat release rate (cone calorimeter method) (2015)
10. Rantuch P et al (2015) The influence of heat flux density on the thermal decomposition of OSB. Acta Fac Xylologiae 57(2):125–134. https://www.researchgate.net/publication/283677358_The_influence_of_heat_flux_density_on_the_thermal_decomposition_of_OSB
11. Janssens M (1991) Piloted ignition of wood: a review. Fire Mater 15(4):151–167
12. Delichatsios MA (2000) Ignition times for thermally thick and intermediate conditions in flat and cylindrical geometries. Fire Saf Sci 6:233–244
13. Property tables and charts (SI units), [without date]. https://www.researchgate.net/file.PostFileLoader.html?id=54c8f917cf57d749248b4689&assetKey=AS%3A273740741447683%401442276287686
14. Erchinger CD (2009) Zum Verhalten von mehrschnittigen Stahl-Holz-Stabdübelverbindungen im Brandfall, Zürich, Ph.D. thesis, Institut für Baustatik und Konstruktion Eidgenössische Technische Hochschule Zürich. http://e-collection.library.ethz.ch/eserv/eth:2352/eth-2352-01.pdf
15. Kamenická Z (2018) Selected problems in determining the fire resistance of timber structural members. Ph.D. thesis. Slovak University of Technology in Bratislava, Bratislava Supervisor J. Sandanus

A Parametric Study of Numerical Modelling of Water Mist Systems in Protection of Wood Frame Buildings

Nour Elsagan(✉) and Yoon Ko

Fire Safety Unit, Construction Research Center,
National Research Council of Canada, Ottawa, Canada
Nour.Elsagan@nrc-cnrc.gc.ca

Abstract. Water mist systems are considered for the protection of timber buildings because they use significantly less water and consequently less post-suppression water damage. Water mist systems are widely used in the fire protection of electronic equipment and machinery rooms in ships and industrial buildings. However, the use of water mist systems in the protection of residential and office buildings is still limited due to the lack of data on their performance in such buildings. As such, there is a research gap that warrants the work of this paper.

In this article, numerical modelling of water mist systems in the protection of mass timber buildings was conducted using Fire Dynamics Simulators (FDS). The water mist system was modelled to suppress a fire within a compartment and an open space. Different fuel parameters were investigated; the droplet size of the mist and different finishing (exposed and gypsum-board protected walls and ceiling) of the compartment.

Keywords: Wood frame buildings · Water mist systems · Fire modelling

1 Introduction

The current 2015 National Building Code of Canada (NBC) allows the construction of wood frame buildings of up to six storeys high. The maximum permitted height is expected to increase beyond six stories in the forthcoming 2020 NBC owing to the advancements in construction products and technologies, such as Cross Laminated Timber (CLT). In addition, the International Code Council (ICC) has recently accepted the proposed changes for its 2021 International Building Code (IBC) to allow a maximum of 9 storeys of exposed mass timber construction for residential and business occupancies with sprinkler protection. The proposed changes also allow exposed mass timber for all occupancies with varying height limitations as long as sprinkler protection is provided.

Water-based suppression systems are the most commonly used fire protection systems in buildings. They are classified as sprinklers and water mist systems according to the droplet size of the injected spray. The droplet size in the sprinkler and water mist systems are around 5000 μm and less than 1000 μm; respectively.

L. Makovicka Osvaldova et al. (Eds.): WFS 2020, *Wood & Fire Safety*, pp. 166–172, 2020.
https://doi.org/10.1007/978-3-030-41235-7_25

Conventional fire sprinklers, which discharge a large volume of water, are the most commonly used systems in buildings due to their proven effectiveness in suppressing fire and preventing fire spread beyond the compartment of fire origin. However, in application to mass timber buildings, there are concerns that sprinkler systems could create post-discharge water damage and mold problems. Water mist systems are considered as an alternative to sprinkler systems in the protection of timber buildings because they use significantly less water compared to sprinkler systems. Water mist systems are widely used in the fire protection of electronic equipment and machinery rooms in ships and industrial buildings, where they have the advantage of less water used, which is accompanied by less post-suppression water damage compared to sprinklers systems. However, their use in the protection of residential and office buildings is still limited. Therefore, there is a wide research gap due to the limited data available on the performance of water mist systems in such buildings.

In this work, fire modelling of water mist systems in the protection of mass timber buildings was conducted using the Fire Dynamics Simulators (FDS) [1]. Water mist systems were modelled to suppress a fire within a compartment and an open space simulating residential fire. The fuel and dimensions of the simulation domain were based on the standard test protocols provided by UL 2167 and BS 8458. Three different parameters were investigated in this study:

1-Type of finishing materials of enclosure (exposed wood versus gypsum-board)
2-Enclosed compartment versus open space
3-Droplet size of water mist.

2 Model Description

Two domains were used for the simulations; enclosed compartment (room) and open space. The floor in both domains and the ceiling in the open space were made up of wood. In all cases, the grid size was 0.1 m (L) × 0.1 m (W) × 0.1 m (H). The dimensions of the room were 9.6 m (L) × 4.8 m (W) × 2.4 m (H). The length and width were based on the coverage area of the nozzle, as recommended by UL 2167. Two doors; 2.2 m height each; provided the ventilation in the room. One of the doors is 1.05 m wide and located at the corner opposite to the fuel, and the other one is 0.9 m wide and located at the same side of the fuel and 0.5 m from the corner. Two types of finishing were used for the walls and ceiling of the room; exposed wood and gypsum-board. The thickness of the exposed walls was 101.6 mm and the gypsum-board protected walls were simulated as 2 layers of thickness; 12.7 mm gypsum-board and 101.6 mm wood.

In all domains, a wood crib and simulated furniture were used as fuel for the fire. The crib had cross sectional area of 0.3 × 0.3 m^2 and 0.15 m thickness and placed at 0.15 m from the ground. The mass of the crib was 6.156 kg and can release a total of 107 MJ. Two polyurethane foam (PUF) sheets were used to simulate an upholstered chair. The dimensions of the sheet were 0.865 m width, 0.075 m thick and 0.775 m height. The mass of the PUF sheets was 2.5 kg and can release a total of 58.75 MJ. The PUF was ignited in the simulation using hot particles. A burner of

dimension 0.3 × 0.3 m^2 was used for igniting the wood crib. This burner simulated a heptane pool and emitted 3800 kW/m^2 for 200 s. The burner was placed on the ground in a steel pan beneath the crib. The fuel package was placed at the corner of the room in the enclosed domain and at the center of the domain in the open space.

The specifications of a commercially available water mist nozzle were applied in the simulations. These specifications are listed in Table 1.

In the simulations, wood is composed of; cellulose, hemicellulose and lignin. Each component undergoes thermal decomposition to generate volatiles and char. Then volatiles burn through a mixing controlled step to form combustion products. Char undergoes subsequent conversion to volatiles. The different kinetic rates implemented for the decomposition of wood components and char are presented in Table 2. The table also includes the rate of PUF decomposition, which is adopted from Bilbao et al. [2]. The dehydration model of gypsum-board was from Thomas [3], where a reference temperature of 110 °C and a pyrolysis range of 40 °C were used.

Table 1. Specifications of water mist nozzles and sprinklers used in the simulations

Specification	Water mist
Median particle diameter (μm)	100 or 350
RTI ($m^{1/2}s^{1/2}$)	25
Operating pressure (bar)	72
Orifice diameter (mm)	0.75
Activation temperature (°C)	68
Spray angle (°)	90

Table 2. Kinetic parameters

Material	A (1/s)	E (kJ/kmole)	References
Hemicellulose	9.83	4.27E4	[4]
Cellulose	3.02E7	1.13E5	[5]
Lignin	6.28E5	1.12E5	[5]
Char	2E4	1.2E5	[6]
Volatiles	Infinity	NA	Mixing controlled
PUF	4.6E6	97361.68	[2]

3 Results and Discussion

Simulations were conducted for 3 scenarios; exposed wood, gypsum-board protected enclosures and open space. Simulations of fire suppression using two droplet sizes of water mist were then applied for these scenarios. The following subsections discuss the results of the 9 simulations.

3.1 Fire Simulations

The heat release rate (HRR) profiles of the fire in the exposed and gypsum-board protected wood enclosures, and the open space are presented in Fig. 1. More heat was released in the exposed wood compartment than in the gypsum-board compartment due to the fire spread from the fuel package to the wooden walls and ceiling.

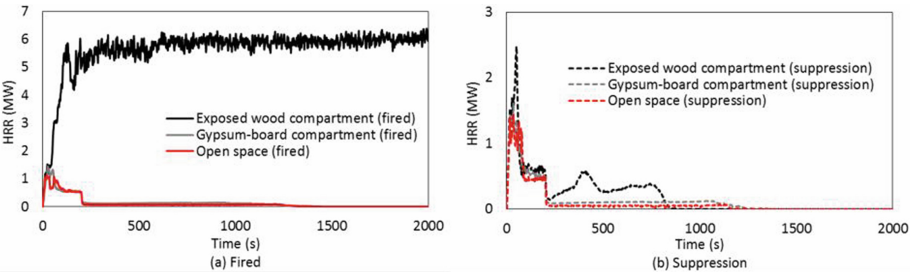

Fig. 1. HRR of (a) fire (straight lines) and (b) suppression (dashed lines) simulations in wood and gypsum-board protected enclosures, and open space

In the simulations of both compartments, the fire started by the ignition of PUF. Only the fuel (PUF foam and wood crib) ignited and released heat in the gypsum-board compartment. However, the HRR increased in the exposed wood compartment due to the presence of large amount of fuel (the wooden walls and ceiling). The onset of the fire spread to the wooden wall and ceiling occurred at about 60 s at which the HRR was approximately 1.5 MW and flashover occurred at about 200 s. Thereafter, the whole compartment was involved in the fire, and the HRR curve was plateaued at 6 MW. It is worth noting that, the HRR did not increase further due to the limitation of air within the room (ventilation-controlled fire-A HRR of 6 MW was the maximum fire size that can be achieved with given sizes of the two doors).

Interestingly, the HRR profile of the open space is similar to the gypsum board protected enclosure despite the presence of the wooden ceiling in the open space. This might be attributed to the continuous air flow into the open space which prevented the build-up of hot smoke layer. The flickering flame from the PUF fire touched the wood ceiling during the initial 200 s, which resulted in a ceiling temperature around 350 °C. However, the ceiling did not catch fire due to the short exposure time.

3.2 Suppression Simulations

Figure 1 presents the impact of water mist suppression system on HRR profiles in the simulation of exposed wood compartment, gypsum-board compartment and open space. The median diameter of the water mist droplets in these simulations was 100 μm. In all simulations, the two nozzles were activated.

The figure shows that, although the nozzles were activated, the water mist system did not affect the HRR in case of gypsum-board compartment and open space. On the other hand, water mist droplets suppressed the fire in the wood compartment at 60 s by

minimizing fire spread to the adjacent walls/ceiling, when HRR reached 2.5 MW, and completely extinguished the fire at 840 s. One of the reasons why the water mist system performs effective fire suppression (i.e. reduction in HRR compared to no-suppression scenario) in the case of wood compartment is that the effectiveness of evaporation of water mist and oxygen displacement, followed by fire suffocation, depends on relative fire size to the volume of the compartment.

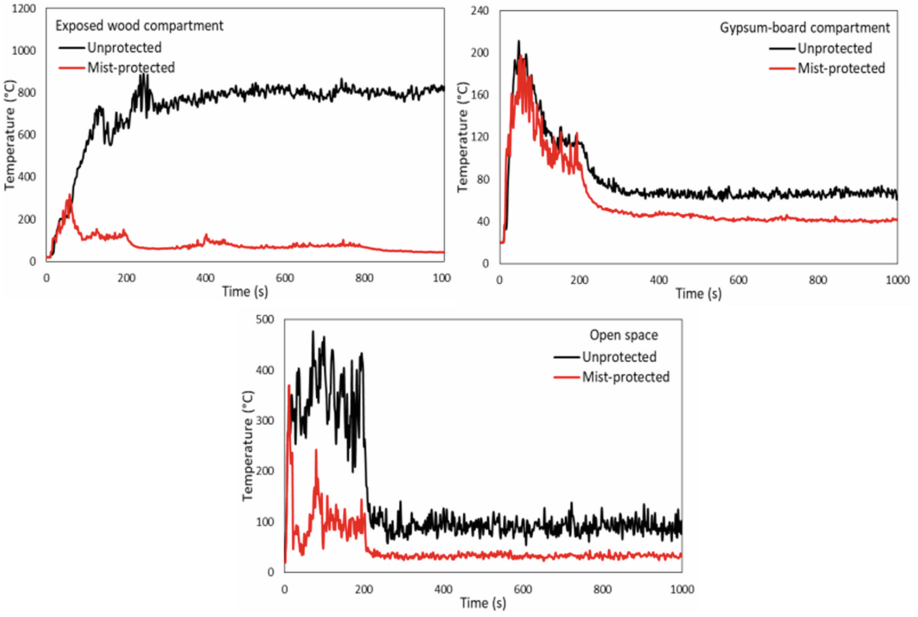

Fig. 2. Gas temperature profiles at the center of the room and 1.6 m high in protected and unprotected different compartments and open space

The temperature profiles shown in Fig. 2 demonstrate that, water mist system was capable of lowering the temperature in the room (at 1.6 m height along the center of the room), even in the open space and gypsum-board compartment. This verified that water mist system has excellent gas phase cooling effects, which control fire and limit fire spread beyond the fire origin although it may not be able to completely suppress or extinguish the fire in some circumstances. However, further testing is necessary to verify the gas phase cooling and to compare with sprinklers system.

The effectiveness of the water mist system in displacing the total oxygen in the room can be seen in Fig. 3. The figure demonstrates the oxygen mass fraction in water mist-suppression simulations in exposed wood compartment, gypsum-board compartment and open space, using 100 μm droplet median diameter. The lowest oxygen mass fraction was measured in the exposed wood compartment at the time of fire suppression by the water mist system (at about 60 s). It is also worth-noting that, the oxygen mass fraction was kept constant in case of open space, which is attributed to the continuous

inflow of air into the domain through the open boundaries. This challenged the water mist suppression system.

The effect of the water mist droplet size on fire suppression in exposed wood compartment was investigated. Two droplet sizes (100 and 350 μm median diameter) were used in simulating the fire suppression in exposed wood compartment.

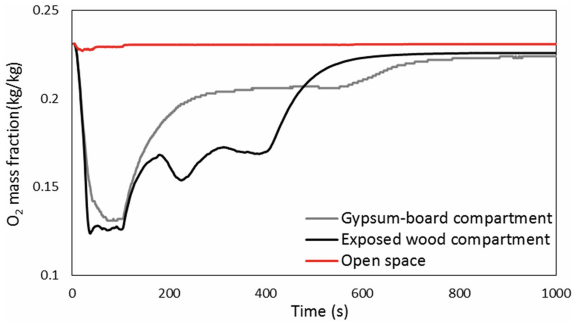

Fig. 3. Total oxygen mass fraction in mist-protected compartments and open space using 100 μm median diameter droplets

The HRR profiles are presented in Fig. 4a. The figure shows that, the smaller droplet size (100 μm) was better in lowering the HRR than the bigger droplets. This is attributed to the larger total surface area associated with the smaller droplets which increased the heat transfer from the hot smoke to the droplets. This is manifested by comparing the total heat absorbed by the droplets in Fig. 4b. The droplets of 100 μm median diameter absorbed more heat than those of 350 μm median diameter.

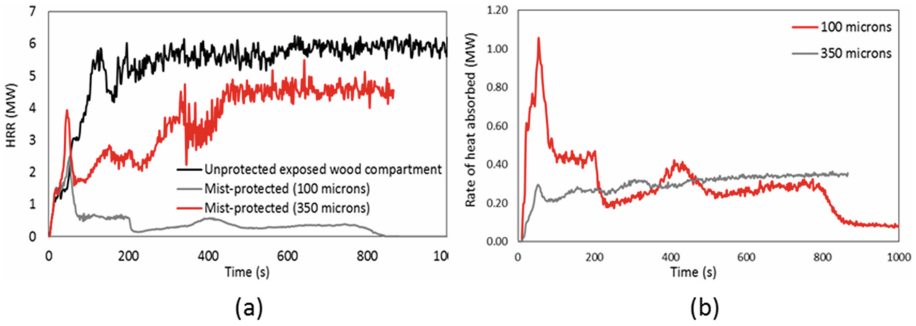

Fig. 4. (a) HRR in unprotected and mist-protected wood compartment. Two droplet median diameters are used; 100 and 350 μm. The dotted lines correspond to activation of nozzles. (b) Rate of heat absorbed by water mist droplets of different sizes

A similar trend is observed in using bigger droplet size (350 μm) in the suppression simulations in gypsum-board compartment and open space, where higher temperatures are seen within the domain compared to 100 μm droplets.

4 Conclusions

A numerical parametric study was conducted to investigate the fire suppression performance of water mist system in open space and a compartment finished with various materials including exposed timber. The simulations showed that;

- Fire was more severe in case of exposed wood compartment due to the higher fuel load, where the walls and ceiling could ignite and contribute to the compartment fire.
- Water mist system was able to control the fire in open space and gypsum-board compartment simulations, yet suppress the fire in exposed wood compartment simulation.
- The higher the heat release in the compartment fire, the more heat absorbed by the water mist droplets. This heat transfer between the hot smoke and water droplets consequently evaporated the droplets and decreased the oxygen concentration in the fire compartment, which led to fire suffocation.
- The smaller water mist droplet size improved the performance of the system as it increased the heat transfer between the smoke and the droplets.

References

1. McGrattan KB, McDermott RJ, Weinschenk CG, Forney GP (2013) Fire Dynamics Simulator, Technical Reference Guide
2. Bilbao R, Mastral JF, Ceamanos J, Aldea ME (1996) Kinetics of the thermal decomposition of polyurethane foams in nitrogen and air atmospheres. J Anal Appl Pyrolysis 37:69–82. https://doi.org/10.1016/0165-2370(96)00936-9
3. Thomas G (2002) Thermal properties of gypsum plasterboard at high temperatures. Fire Mater 26:37–45. https://doi.org/10.1002/fam.786
4. Bilbao R, Millera A, Arauzo J (1989) Kinetics of weight loss by thermal decomposition of xylan and lignin. Influence of experimental conditions. Thermochim Acta 143:137–148
5. Bilbao R, Millera A, Arauzo J (1989) Thermal decomposition of lignocellulosic materials: influence of the chemical composition. Thermochim Acta 143:149–159
6. Gomaa I, Elsagan N (2019) Effect of char burning mechanism on wood combustion. In: Proceedings of the 3rd international fire safety symposium, IFireSS 2019, Ottawa, Canada, pp 471–481

Evaluation of Structural Elements Affected by Fire

Jan Bujnak[1(✉)] and Abdelhamid Bouchair[2]

[1] University of Žilina, Univerzitná 8215/1, 010 26 Žilina, Slovakia
jan.bujnak@fstav.uniza.sk
[2] Université Clermont Auvergne, Institut Pascal,
BP 10448, Clermont-Ferrand, France

Abstract. Fire poses a serious threat to living creatures and to the environment. Presently, numerical and experimental investigations have provided calculation rules for the assessment of the carrying capacity of building components in the event of a fire. Actually, the remaining resistance of structure, depending on time exposure to fire can be evaluated using the current geometry, material and section design characteristic as well as information on fire development provided by fire-fighting crew. Beside the load bearing functions, the separation or insulation criterions could be important. The paper deals with the above mentioned passive fire measurements. Particular emphases are placed on damage assessments and suitability of structure affected by a fire, illustrated on the case study.

Keywords: Fire resistance · Remaining load capacity · Testing

1 Introduction

The earlier regulations considered usually only the *active* measures consisting of sprinklers and extinguisher locations suppressing the fire, providing partition of premises into compartments to prevent the spread of fires, setting evacuation paths and emergency ways for rescue teams. The more realistic actual approach as output of different research projects takes into account also *passive* measures evaluating the fire resistance playing an important role to ensure enough safety level of any building in case of fire. The current regulations, especially the Eurocode EN 1993-1-2 [1], take adequate account of the effect of the active firefighting measures as well as real fire characteristics.

The determination of the fire development in a building compartment requires knowledge of a large number of parameters. Nevertheless, the real fire curves for current configurations of compartment size, usual fire loads, and ordinary combustible characteristics can be obviously approximated by the single ISO-fire curve from EN 1991-1-2, [2]. Moreover, evaluation procedures can be based on analysis of members separated from the structure with the connections replaced by appropriate boundary conditions. Sometimes analysis of parts of the structure is more appropriate, directly taking into account in the assessment appropriate boundary conditions to reflect its links with other parts of the structure.

L. Makovicka Osvaldova et al. (Eds.): WFS 2020, *Wood & Fire Safety*, pp. 173–178, 2020.
https://doi.org/10.1007/978-3-030-41235-7_26

2 Building Concept and Structural Layout

2.1 Structural Arrangement of the Guesthouse Building

The eight story hotel building 80 m long and 40 m wide was built in the year of 1982, as detailed in report [3]. The cost-effective framing system consists of columns and beams interconnected to form a three-dimensional structure. While the building is theoretically complicated, it may reasonably be estimated as a series of the twenty-one plane frames 3.6 m axially spaced. Their structural members are interconnected by rigid joints, capable of resisting any lateral loads without relying on an additional bracing system for stability.

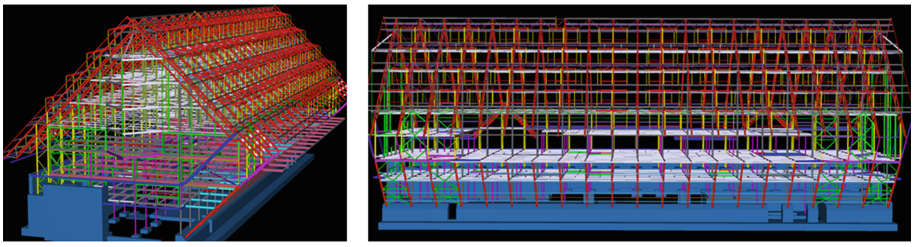

Fig. 1. Steel framework system in space calculation model

Figure 1 shows the space view of the steel structure. The longitudinal floor beams and columns are pinned connected. The stability of the entire structure in this direction is provided by bracing system in common with shear stiffness of external facade walls. Floor systems involve structural standard rolled I 200 steel beams and joists I 140 linked via shear connectors with composite slabs 120 mm thick, made using concrete with metal decking oriented perpendicularly to the composite beam span. The maximum span for steel decking was 3.1 m. Concrete encasements and sprayed-on cementitious fire-proofing material provided some fire resistance to the steel members (Fig. 2).

2.2 Fire Development and Its Consequences

A violent fire upraised in January 2016, just after midnight close to 2 a.m. in the kitchen area and department of foodstuff stockroom. Fire-fighting crews were alerted immediately. However, winter cold weather conditions made roads icy and difficult in the mountain area. Sprinkler systems and fire extinguishers were not adequate to slow the growth of the fire until firefighter had a chance to get there and to use fire hoses to put out the fire altogether. Even some sprinklers and hydrants failed due to frozen pipes, which all delayed a firefighter's job and let the fire grow. Thus, the active fire protection system did not work efficiently in the event of this fire.

Fire originated in the middle part of the ground floor, as indicated in Fig. 3. At the start, structural parts situated in the location were only moderately exposed to higher temperature. When windows in facade walls were broken, flames continued to

Fig. 2. Cross section of the building and view after fire.

propagate due to fresh air draft and the compartment temperature was increased. In half-hour later, fire spread in all upstairs floors. Consequently, large destruction of building occurred. The generation and spread of smoke to neighboring floors and within the works produced the additionally damages.

Firewalls and doors separated the building into two compartments and helped to retard the spread of fire and smoke to remaining part of hotel. This system that compartmentalize the building through the use of fire-resistance rated walls supported protection the building portion indicated by rectangle in Fig. 3. Considering damages size, it was difficult to detect fire cause. Several hypotheses were exanimated, as negligence, smoker imprudence or electric short circuit.

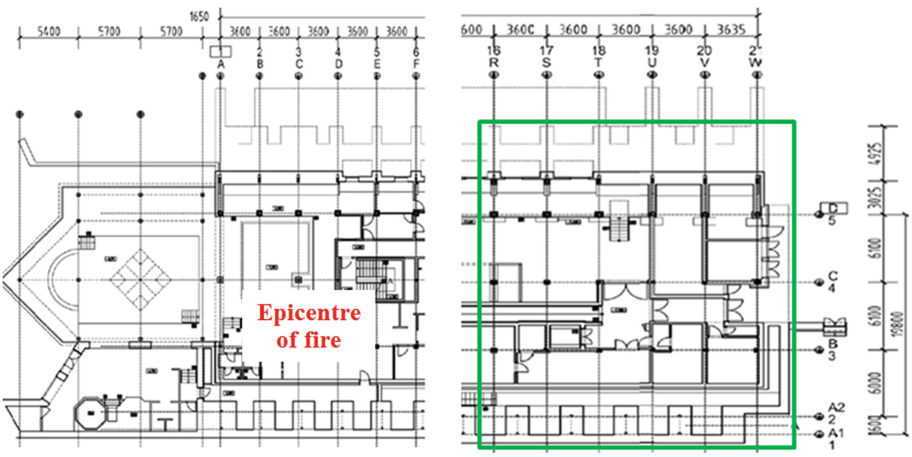

Fig. 3. Part plan view of frame location and the floor structure

3 Estimation of Load Bearing Capacity of Structure

3.1 Building Compartment Openly Exposed to Fire

Critical temperature method as the commonly accepted simplified assessment procedure was used. The applied loads to structures consisted of permanent loads, variable actions and snow. Under this fire situation, if the heated temperature is higher than the critical value, there is failure. Even simple design rule and elementary mechanical models for fire resistance assessment of structural members can be applied, since the heating behavior of the steel unprotected member was not very different from that under standard fire condition. The temperature-time standard ISO fire curve takes into account the most important physical phenomenon, which might influence the development of a fire. Thus, the evolution of the ambient gas temperature $\theta_{g,t}$ at time t within the building compartment can be given by

$$\theta_{g,t} - \theta_0 = 345 \log (8\,t + 1) \tag{1}$$

Starting from initial temperature θ° of 20 °C, the equation can provide step-by-step temperature evolution until intended time t.

Temperature variation of steel structural element $\theta_{a,t}$ exposed to a fire at time t depends on the thermal conductivity of steel λ_a and specific heat c_a. The steel is a good conductor of heat with the thermal conductivity λ_a quite high and in addition steel members are in general very slender. These factors often lead to a heating very close to uniform one if a steel member is fully engulfed in fire. The specific heat is obviously combined with density ρ_a to produce thermic capacity $c_a\,\rho_a$. The section factor defined as the ratio between the perimeter through which heat is transferred to steel A_m and the steel volume V caracterise profile form from fire exposition aspect. In case of an unprotected steel member with a constant cross-section, its section factor A_m/V is the exposed perimeter of the cross-section divided by the area of this cross-section. For heating calculation, it is necessary to consider the correction factor k_{sh}, which is a specific coefficient for the shadow effect. The increase of the temperature $\Delta\theta_{a,t}$ in an unprotected steel member during a time interval Δt may then be determined from equation [4].

$$\Delta\theta_{a,t} = k_{sh}\frac{A_m/V}{c_a\rho_a}h_{net,d}\Delta t \tag{2}$$

The net heat flux per unit area $h_{net,d}$ is composed of two parts, the first one corresponding to the radiation $h_{net,r}$ and the second one being the convection $h_{net,c}$. The step-by-step incremental application of the above relations for the main unprotected beam of rolled shape *I 200* of $A_m/V = 127{,}07\ m^{-1}$ with c_a varying as a function of temperature leads during 60 min to the temperature of 939 °C. However, when temperatures exceed approximately 400 °C, the modulus of elasticity, yield and tensile strength rate of decrease is serious. More important, when temperature above 300 °C exist, steel parts exhibit permanent deformations.

In consequence, the fire resistance of the unprotected structural elements in this building compartment openly exposed to fire were undoubtedly inadequate. The deteriorated structural parts should be rebuilt by *replacement* with the similar elements prepared in the workshop and installed in construction site.

The resistance barriers as fire wall and doors located in the plan of the sixteen frame limited temperature rise and restricted the spread of fire in this area (Fig. 3). But temperature remained enough high to continue its damaging effects on structural elements. Due to lack of appropriate information on fire situation, the above procedures were considered inaccurate. More appropriate access consisted in verification of the main material properties. For this purpose, samples from characteristic location of frame elements were isolated, as illustrated in Fig. 4.

Fig. 4. Location of some isolated samples from inclined frame trusses

The properties of steel largely result from the influence of microstructure and grain size can be strongly influenced by the heat and following cooling rate. Steel ordinarily ductile can become brittle with failure that occurs without prior plastic deformation. Notch toughness of steel affected by temperature determined by the Charpy impact, using the small rectangular simply supported beam can be an indicator of the susceptibility of brittle fracture. The bars 10.10 mm in section and 55 mm long with 2 mm deep V-notch at mid-length were fractured by a blow from the swimming pendulum (Fig. 5).

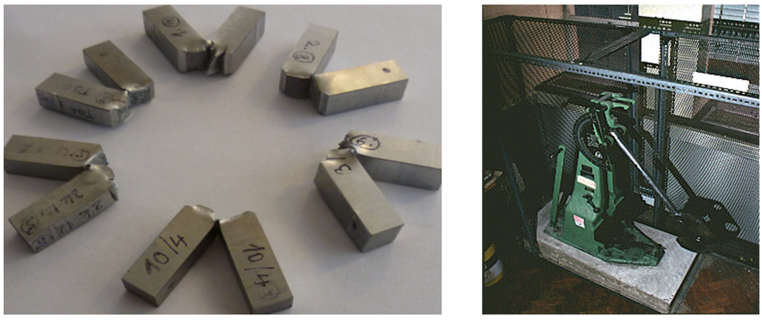

Fig. 5. Sample bars for resilience tests using the Charpy V notch impact

Thus for the steel used in ordinary structures under atmospheric temperature, the arbitrary energy absorption is habitually required, such as 34 J. The quantity of energy absorbed was calculated from the height the pendulum raised after breaking the specimens. As the resulting values were from 70 to 214 J, it can be constated that steel resilience tests proved satisfactory toughness properties in the compartment protected by fire barriers.

The tensile tests were used to control most significant material properties such as yield and ultimate tensile strength, also area of reduction. Ductility of a material was indicated by the amount of deformation that was possible until fracture. The size and shape of samples were to conform to common standard. The stress-strain diagram obtained, indicated the Young's modulus, important because deflection of structural elements could be critical for the required assessment (Fig. 6).

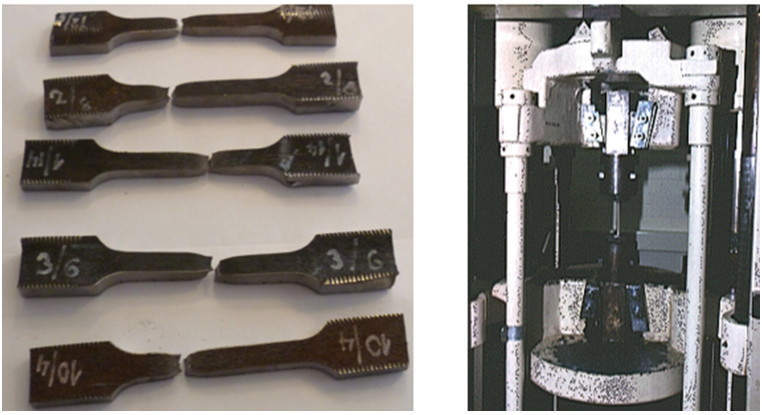

Fig. 6. Sample shapes gripped in tested machine

The experimental outputs proved that yield and ultimate strengths exceeded with large reserves requirements given in EN 1993-1-1 [5]. Thus, the structural elements located in this partially protected part of building could be *reutilised*, though exposed to the fire.

References

1. EN 1993-1-2: Eurocode 3: design of steel structures - part 1-2: general rules - structural fire CEN (2005)
2. EN 1991-1-2: Eurocode 1: actions on structures - part 1-2: general actions - actions on structures exposed to fire CEN (2009)
3. Bujnak J (2018) Evaluation report of steel structural system exposed to fire of the hotel building. Technical report, University of Zilina
4. Bujňák J (2005) Steel Structures and Bridges. (Design and Evaluation Examples). Textbook. University of Zilina
5. EN 1993-1-1: Eurocode 3: design of steel structures - part 1-1: general rules and rules for buildings. CEN (2005)

Study of the Heat and Mass Transfer in Special Furnaces During Fire Resistance Tests of Building Construction

Oleksandr Nuianzin[1(✉)], Dmytro Kryshtal[1], Oleh Zemlianskyi[1], Artem Nesterenko[1], and Taras Samchenko[2]

[1] National University of Civil Defence of Ukraine, 94 Chernyshevska Str., Kharkiv 61023, Ukraine
alexandrnuyanzin@gmail.com
[2] Ukrainian Civil Protection Research Institute, 18, Rybalska str., Kyiv 01011, Ukraine

Abstract. One of the ways to determine the fire resistance of building structures is to conduct tests in special fire furnace. The design, metrological instruments and control methods of the fuel supply system and injectors in these furnaces are not perfect. Conditions that created in this way ensure uneven temperature distribution over the heated surfaces of the tested structures in combustion furnaces.

This study shows the results of computational experiments on the fire resistance of building structures made using various configurations of combustion furnaces. Using computer software to simulate the flow of gas and liquid, a temperature gradient was calculated for the heated surfaces of the structures and the temperature distribution was calculated for every minute of the computational experiment for each firing furnace configuration.

In temperature gradients, there were from 6,000 to 7,500 cells (depending on the specific configuration) uniformly distributed over all surfaces of the structure, containing temperature data in any moment during the computational experiment. As a result of processing of these data the value of temperature dispersion value was calculated. Difference between maximum and minimum temperatures on the surface of a reinforced concrete was also determined. Based on the curves representing temperature dispersion values at the surface of each of the simulated structures of the furnace chamber for every minute of the computational experiment the configuration with the most homogeneous temperature distribution throughout the heated surfaces of building structure was defined, what allows reducing an error occurring due to temperature distribution non-homogeneity by heated surface of structures during the fire resistance test.

Keywords: Heat and mass transfer · Fire resistance · Temperature distribution

L. Makovicka Osvaldova et al. (Eds.): WFS 2020, *Wood & Fire Safety*, pp. 179–184, 2020.
https://doi.org/10.1007/978-3-030-41235-7_27

1 Formulation of the Problem

Today, to determine the limits of fire resistance of building structures in the world it is increasingly spreading calculation methods. But the test method in special fire test furnaces is also typical. It is important that such studies meet the same standard test conditions in which the furnace, laboratory or country configurations would not be conducted. However, existing methods are standardized only on temperature-time curves of furnace thermocouples. Therefore, the question arises about the uniformity of the warming of the building structure, depending on the design of the furnace.

2 Analysis of Recent Achievements and Publications

The analysis of metrological features and operation of furnaces for testing of building structures showed the imperfection of the design, metrological support and methods of control of the fuel-injector system. To improve them, a computer-based approach [1–5] is required, since real-world testing is time-consuming and very costly, also requires special conditions, large areas, and leads to environmental pollution. In addition, the test of building structures in furnaces is carried out under the conditions of a "standard" temperature regime, however, the temperature in different parts of the furnace is different [2].

In [6] was compared results of simulation with experiment to evaluate the accuracy of the model. The adequacy criteria were calculated (Student's t-test, Cochren's Q-test, Fisher's F-test). None of the criteria values exceeded critical values. Was concluded to use the program for further research in future researches.

3 Goal Setting and Its Solving

Imperfection of design, metrological support and methods of control of the fuel-injector system create conditions under which there is an uneven distribution of temperatures on the heating surface of the structure.

With the help of computer simulation we have created a number of geometric configurations of fire furnaces (changes in the location and number of burners and openings for combustion products, etc.) and showed how the design features of the installation can affect the uniformity of temperature distribution over the heating surface of the horizontal structure. This article shows the results of the application of computational gas hydrodynamics (CFD) to improve the existing design parameters of fire furnaces for testing building structures and demonstrates a method for improving the design of the installation.

Several software packages that can be used for calculation have been analyzed. Among them are Star-CD, Fluent, Sofie, FlowVision and others. The FlowVision 2.5 system is more suitable for building a mathematical model of a fire oven. First, it is based on the Navier-Stokes equation. They describe the movement of liquids and gases over a wide range of Reynolds numbers. Secondly, the system allows to build the geometry of the object in specialized CAD-programs. Thirdly, FlowVision has the

option to adjust the furnace parameters during the calculation process. Fourth, FlowVision has an advanced apparatus for visualizing the results. And also what is important the institute is licensed to use the program.

4 Presentation of the Main Research Material with Full Justification of the Obtained Result

A number of computer configurations of installations have been created to test the overlapping elements. For convenience of description, each of the models is assigned one of the letters.

Figure 1 shows the Geometric features of the configurations of installations for testing fire resistance of building structures.

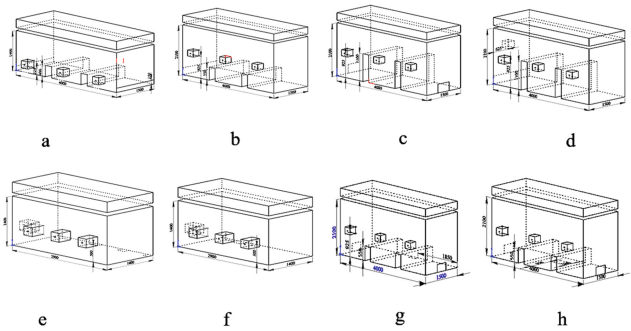

Fig. 1. Geometric features of the configurations of installations for testing fire resistance of building structures: a – configuration «A», B – configuration «b», C – configuration «C», d – configuration «D», e – configuration «E», f – configuration «F», g – configuration «G», h – configuration «H».

Figure 2 shows the temperature distribution over the surface of the structure in each of the configurations at the 60th min with the use of the color fill test (temperature gradient).

In our opinion, the main disadvantages of configuration "A" (Figs. 1a and 2a) are, in comparison with other configurations, a small volume of the furnace chamber, poor location of openings for combustion products and too high partitions inside the furnace chamber.

By changing the design of the interior space of the installation chamber (Fig. 1b), the temperature is more evenly distributed over the heating surface of the plate (Fig. 2b). However, there are places where the construction is warmed up more strongly.

In configuration "C" (Fig. 1c) a more uniform temperature distribution (Fig. 2c) was obtained compared to the configuration "A" and "B", but due to the location of openings for the removal of combustion products on the side walls - the construction above them is warmed up more.

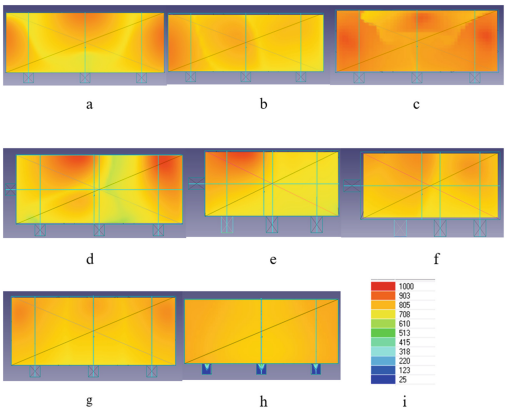

Fig. 2. Temperature gradient on the heating surface of the modeled structures: a – in configuration «A», b – in configuration «B», c – in configuration «C», d – in configuration «D», e – in configuration «E», f – in configuration «F», g – in configuration «G», h – in configuration «H», i – color matching to temperature, °C.

As it can be seen on the Fig. 2d, e and f, creation of an additional burner on the side wall did not lead to a more uniform warming compared to the "C" configuration. Therefore, the study of the configurations of burners on the sidewalls was discontinued

The following in our study of the temperature distribution were the configurations "G" (Fig. 1g) and "H" (Fig. 1h). The additional openings for diversion of combustion products between the inner partitions created conditions for a more even distribution of temperatures compared to the configurations described above (Figs. 1 and 2).

For a more visual demonstration of the simulation results Fig. 3 shows the temperature changes on the heating surface of structures using isotherms [7].

The next stage of the study was to determine the value of the temperature dispersion on the surface of each of the simulated furnace chamber structures at each minute of the computational experiment, after which a graph of its change in time was presented.

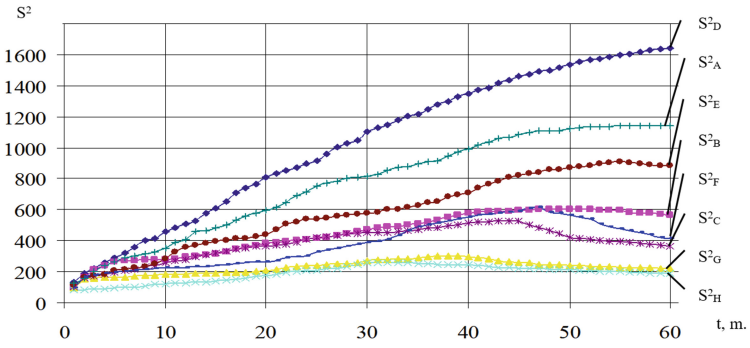

Fig. 3. Temperature dispersion over the heated surface of a reinforced concrete slab during numerical study.

By means of computational gas hydrodynamics, the pouring of temperature on the heating surface of the plate was created and the temperature distribution for each minute of tests for each configuration was obtained. Such values are from 6000 to 7500, depending on the configuration. Further, temperature variance was calculated and graphs were constructed (Fig. 3).

The obtained graphs have a certain feature: in most curves that show the numerical value of the temperature variance, there is an extreme. After the initial phase, the dispersion value increases, it gradually begins to decrease. This can be explained by considering the standard fire temperature curve [8]. A more intense change in temperature in the furnace chamber at the initial minutes of testing and a gradual decrease in the maximum and minimum limit values. Therefore, the studies were limited to the 60th min of calculation (Fig. 4).

Another feature we have highlighted is that the smaller the extremum value, the earlier it is obtained relative to the time curve.

Speaking specifically about the configurations created, the lowest values of dispersions over the entire time interval are observed in the configurations "G" and "H". The highest variance value in the configuration "H" is observed at the 33rd min of the test, in the configuration "G" at the 39th min. At the same time, the maximum dispersion value up to 60 min was not reached in configurations "D" and "E".

Having considered all the configurations created, we can say that the average time at which the extreme reaches the 45th–50th min of testing, when the allowable difference between the maximum and minimum allowable temperature in the furnace chamber decreases [8].

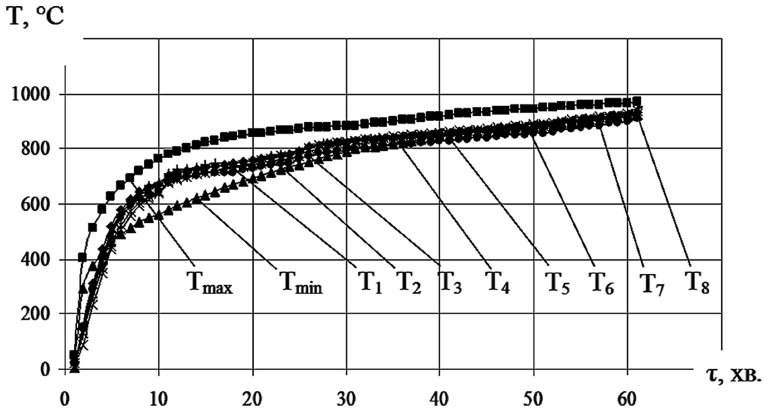

Fig. 4. Changes in the temperature in the furnace chamber of configuration "H" during the computational experiment (T_{max}, T_{min} - maximum and minimum allowable temperatures in the furnace chamber; T1–8 - temperatures at the control points of the furnace chamber.

Based on the data obtained, we can draw conclusions.

5 Conclusions

This paper presents the results of a numerical simulation of a series of computer configurations of an installation to test horizontal building structures. Based on the obtained curves of temperature variance values on the surface of each of the simulated furnace chamber structures at each minute of the computational experiment (Fig. 4) and the difference between the maximum and minimum temperature on the surface of the structures (Fig. 2), we determined the configuration (configuration "H") of the most uniform temperature distribution on the heating surface of the load-bearing wall, which allows to reduce the error due to the uneven temperature distribution on the heating surface of the structures during the tests fire.

References

1. Smith TF, Waterman MS (1981) Identification of common molecular subsequences. J Mol Biol 147:195–197
2. Novak SV, Nefedchenko LM, Abramov AA (2010) Structures and articles fire resistance testing methods. Pozhimformtechnika, Kyiv, 132 p
3. Nuianzin O, Pozdieiev S, Sidney S (2015) Mathematical modeling of the process of heat and mass transfer in chambers of fire furnaces of installations for fire resistance tests of load-bearing walls. J Fire Saf Theory Pract Coll Sci 92–98. Proceedings No. 20, ChIPB, Cherkasy
4. Nekora O, Slovynsky V, Pozdieiev S (2017) The research of bearing capacity of reinforced concrete beam with use combined experimental–computational method. In: MATEC web of conferences, vol 116, p 02024
5. Pozdieiev S, Nuianzin O, Sidnei S, Shchipets S (2017) Computational study of bearing walls fire resistance tests efficiency using different combustion furnaces configurations. In: MATEC web of conferences, vol 116, p 02027
6. Nuianzin O, Pozdieiev S, Nuianzin V (2016) Research of adequacy of mathematical model of heat-mass exchange in the furnace for fire resistance tests of bearing walls. Metall. Min. Ind. 8:66–73
7. System for simulating the movement of liquid and gas. FlowVision version 2.5.4. User's manual. TESIS, Moscow, 284 p
8. Protection from fire. Building construction. Methods of test for fire resistance. General requirements (ISO 834: 1975): DSTU B V.1.1-4-98. [Effective as of 10.28.1998]. - K.: Ukrarhbudynform, State standard of Ukraine, 21 p

Experimental and Numerical Analysis of Fire Development in Compartment Fires with Immobile Fire Load

Sven Brunkhorst(✉) and Jochen Zehfuß

Institute of Building Materials, Concrete Construction and Fire Safety (iBMB), Technische Universität Braunschweig, 38106 Braunschweig, Germany
s.brunkhorst@ibmb.tu-bs.de

Abstract. The paper reports on an experimental test series on enclosure fire dynamics for compartments with combustible surfaces and different ventilation openings. The tests were carried out in a test room according ISO 9705-1 to analyse the fire behaviour of compartment fires with unprotected or initially protected timber surfaces. The conducted compartment fire tests showed the impact of different parameters on the fire development of timber structures with exposed and initially protected surfaces, such as the influence of the ventilation conditions, the amount and positions of the exposed timber surfaces and the heat release of the fire source. Furthermore, post-combustion fire behaviour and auto-extinction (as well as the extinguishing measures) were investigated. Based on the experimental data, a numerical analysis, is presented with the CFD-Software Fire Dynamics Simulator, focussing on different approaches for considering the contribution of exposed timber. First results of the numerical analysis demonstrate two promising modelling approaches, which need further investigations.

Keywords: Compartment fire · Timber · Immobile fire load

1 Introduction

In compartment fires of timber buildings, the fire load does not only consist of the mobile fire load such as furniture and furnishings. However, exposed or initially protected timber surfaces, as the immobile fire load, can contribute to the fire and must be taken into account. A general influence of immobile fire loads on the compartment fire was analysed experimentally with different large-scale fire tests [1–4].

To investigate the various parameters that influence the fire development, a total series of 20 fire tests in a test room according ISO 9705-1 [5] were performed. The fire tests examined the influence of ventilation conditions, the amount and geometric arrangement of exposed timber surfaces and the failure of fire protection systems. In addition, there were investigations on the post-combustion behaviour, including the auto-extinction and the effectiveness of fire extinguishing measures.

The room fire tests conducted within the research project TIMpuls [6] serve to prove the approaches of the different performance-orientated and prescriptive strategies for the extended application of timber construction in Germany by experimental investigations.

L. Makovicka Osvaldova et al. (Eds.): WFS 2020, *Wood & Fire Safety*, pp. 185–190, 2020.
https://doi.org/10.1007/978-3-030-41235-7_28

2 Test Series of Compartment Fires

The test series of compartment fires took place in a test room according to ISO 9705-1 [5] at the iBMB (TU Braunschweig). The dimensions of the standardized room are shown in Fig. 1. The combustion products released during a fire test in this test room are caught above the opening with the arranged exhaust hood and derived via the exhaust pipe. The optical density (light measuring section) is measured in the exhaust pipe in addition to the volume flow rate. Due to a sampling section coupled to the exhaust pipe, the combustion gases are analysed as regards to their concentration of oxygen (O_2 gas analyser), carbon monoxide and carbon dioxide (CO/CO_2 analyser).

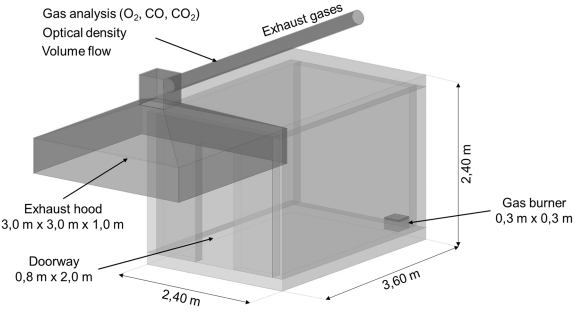

Fig. 1. Schematic illustration of the test room according to ISO 9705-1 [5]

In order to simplify the image of exposed and initially protected timber components, different panel materials were used in the test series. Solid timber panels according to [7] with a thickness of 42 mm respectively represented exposed timber surfaces. Solid wood panels in accordance to [7] with a thickness of 18 mm were always constructed with a 12.5 mm fire protection system (gypsum board type A in accordance with [8]) as initially protected timber surfaces. Depending on the objective of the individual compartment fire tests, the room walls (wall A - C, see Fig. 2) and the ceiling were differently arranged with exposed or initially protected solid wood panels.

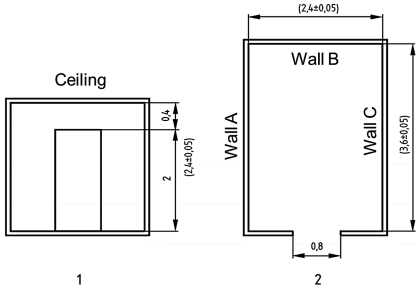

Fig. 2. Left: Front view of the test room; right: floor plan of the test room

In the room fire tests, a 300 × 300 mm^2 propane-gas-operated burner or wooden cribs with a base area of 1.0 × 1.0 m^2 were used as a fire source (supporting fire) to represent the mobile fire load. The net output of the gas burner was 100 kW during the first 10 min after ignition, according to [5], and was subsequently increased to 300 kW, whereby the duration in this output stage can vary in the individual tests. The non-nailed 50 kg wooden crib (approx. 500 kW) consisted of cross-stacked spruce bars measuring 40 × 40 mm^2. The mass to air ratio of the wooden cribs was 1:1. The ignition takes place due to three ignition pans, each containing 200 ml of methanol.

From the experimental investigations it could be determined that the arrangement of the immobile fire load results in a faster fire development time until the flashover occurs. A reduction of the ventilation opening leads to an earlier transition to a ventilation-controlled fire, which results in a lower maximum heat release rate (HRR) but a longer fire duration (Fig. 3). Accordingly, the room temperatures shows a higher maximum temperature and a longer lasting temperature exposure compared to an identical test set-up with a larger ventilation opening.

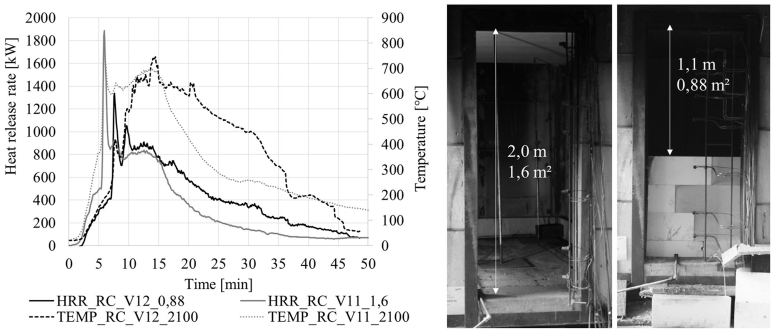

Fig. 3. Left: comparison of heat release rates and temperature development with different ventilation openings; right: different ventilation openings

The diagram in Fig. 3 shows the heat release rate determined by the oxygen consumption method and the temperature development of two experiments measured at a height of 2.1 m in the middle of the room. The experimental setups consist of one exposed timber surface on the ceiling and a supporting fire by a 50 kg wooden crib. The experimental set-ups differ only in the ventilation conditions (RC_V11: 1.6 m^2; RC_V12: 0.88 m^2), which are shown in Fig. 3 (right). Based on calculated volume flow rate a comparable flow profile over the ventilation height can be determined for both tests. These result in a different volume flow related to the ventilation area and thus a different quantity of cold and hot gases flowing in and out of the test room. For the minimum flow rates, it should be noted that this was measured in RC_V11 at a height of 220 mm and for RC_V12 at a height of 1220 mm above the floor.

A failure of the fire protection system with the ignition and sustained combustion of the protected timber surface and/or the fall-off of the protection system was not observed in these room fire tests (RC_V11 and RC_V12). Nevertheless, the initially

protected timber surfaces of RC_V12 showed local charring/discolouration after dismounting the protection system.

With increasing amount of exposed timber surfaces and depending on the heat release of the fire source, the time until the flashover occurs is shortened. The geometric arrangement of the exposed timber surfaces as ceiling or wall surfaces plays not the major role in this series of experiments in relation to the time until the flashover, but rather the heat release of the fire source showed the major influence. In addition, the quantity of flames escaping from the opening increases with increasing exposed timber surface, as the released pyrolysis gases can only oxidise with the oxygen outside the test room.

The results of the room fire tests regarding the post-combustion behaviour and the possible occurrence of auto-extinction show that auto-extinction of the immobile fire load is primarily influenced by the following boundary conditions:

- Quantity and geometric arrangement of the unprotected wood surfaces as well as
- Intensity and duration of the fire source (supporting fire).

In the test series, auto-extinction could always be observed when the mobile fire load (supporting fire) was burnout or extinguished, if only the ceiling or one wall was constructed as an exposed timber surface.

Based on the time until the flashover occurs, it is clear that the heat release of the fire source has a massive influence on the flashover time and the flame spread to the immobile fire loads. Furthermore, the area of the room and thus the distance between the fire source and the immobile fire load as well as the exposed surfaces to each other have an influence on fire development. The test results obtained show the occurrence of the flashover from the fifth to the 11th test minute of the fire test.

In individual fire tests, controlled extinguishing measures were carried out by a professional fire brigade. In this case, when using a minimum quantity of extinguishing agent, 3–4 sprays with a fog nozzle quickly extinguished the fully developed fire. The average extinguishing agent (water) requirement for extinguishing the fully developed fire was measured to be less than 10 l. Correspondingly, a controllable fire scenario and, under the given boundary conditions, a very good efficiency/effectiveness of the defensive measures carried out was shown in relation to the fire compartment of these fire tests.

3 Numerical Modelling of Combustible Surfaces

In order to investigate a wider field of influence parameters the numerical CFD-model Fire Dynamics Simulator (FDS, Version 6.7.0) [9] can be used. Initially a validation and calibration of the FDS-model has to be done. Modelling exposed timber surfaces provides a particular challenge to HRR and post-combustion behaviour. For the validation of the FDS-model, the results of the fire test series are the first base of data. The database will be completed by results of large-scale fire tests, which will be carried out in the TIMpuls project and results from the literature on well-documented timber fire tests [1–4]. First, the specific variants for modelling in FDS are presented here. According to [9], two variants for modelling the additional HRR of exposed timber

surfaces in FDS are purposeful: (a) modelling of a predefined time-dependent heat release rate based on test results where only the ceiling was exposed or (b) modelling a one-dimensional pyrolytic decomposition of timber. The pyrolysis of wood is modelled by a simple one-step solid phase reactions (wood → char).

The two modelling variants were analysed in a first run with the model of the test room shown in Fig. 4 (RC_V11). The fire source is a 50 kg wooden crib with a predefined time-dependent HRR based on the t^2-approach. In variant (a), the heat release rate of the exposed timber surface is modelled according to the measurement data from a fire test, where just the ceiling was exposed timber. In variant (b), the finite-rate reaction parameters listed in [9] were used as first approximation, whereby the kinetic parameters pre-exponential factor (A_1 = 1.89E10 s^{-1}) and the activation energy (E_1 = 1.51E5 J/mol) represent the reaction rate. In order to describe the undergoing endothermic and exothermic reactions, the values of the heat of reaction (ΔH_R = 430 kJ/kg), which is consumed to convert the reactant into reaction products, and heat of combustion (ΔH_C = 14500 kJ/kg), which is the released heat during the combustion of the reaction products, has to be defined.

As shown in Fig. 4 (temperature as well as HRR development), variant (a) shows a reasonable agreement with the experimental data. The HRR of variant (b) shows that the modelled immobile fire load is not ignited and thus no additional HRR was released. The calculated HRR underestimates the test results. Thus in the further procedure, the level of modelling as well as the reaction parameters have to be optimized.

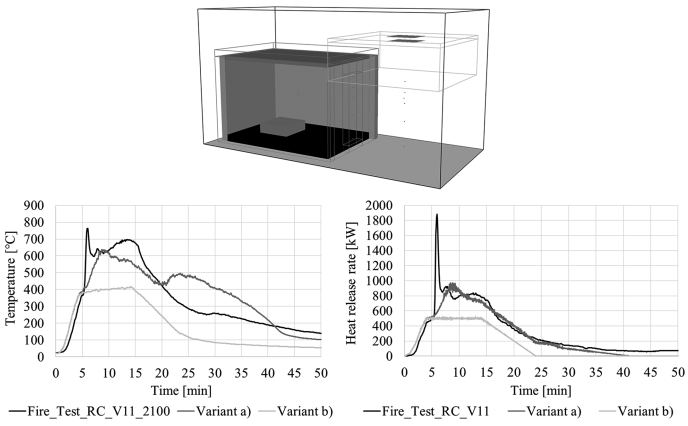

Fig. 4. Representation of the simulation model in FDS and comparison of the simulated temperature development (left) as well as heat release rates (right) of the modelling variants with the test results

4 Summary and Conclusion

In this article, the investigation of the fire development of compartments with immobile fire loads like timber structures is presented. The investigation was carried out on an experimental and numerical basis. The experimental results were gained by a series of compartment fire tests with different boundary conditions concerning fire load, ventilation conditions and fire source. Regarding the results, the essential influences on the fire behaviour including the post-combustion fire behaviour by the unprotected timber surfaces are identified.

In order to conduct a numerical parameter study with the CFD-model possible modelling variants of the immobile fire load were analysed. Two promising modelling approaches are presented and compared in a first simulation run with measurement data from one fire test. The comparison indicates the basic suitability of two variants for illustrating the fire behaviour of immobile fire load. The second modelling variant has to be analysed to gradual approximation in more detail and partly adapted. Upcoming large-scale fire tests will generate a database for an additional validation of the modelling variants on further experimental results.

Funding Reference. This joint research project is funded by the Federal Ministry of Food and Agriculture (BMEL) via the project management agency Fachagentur Nachwachsende Rohstoffe e. V. (Agency for Renewable Resources). (FNR). Co-financing of the timber industry is coordinated by the State Guild Association of Bavarian Carpenters.

References

1. Robert F, et al (2019) ÉPERNON FIRE TESTS PROGRAMME - test reports. CERiB Fire Testing Centre, France. http://www.epernon-fire-test.eu
2. Zelinka S, et al (2018) Compartment fire testing of a two-story mass timber building. General Technical report FPL–GTR–247. U.S. Department of Agriculture, Forest Service, Forest Products Laboratory
3. Su J, et al (2018) Fire safety challenges of tall wood buildings – phase 2: task 2 & 3 – cross-laminated timber compartment fire tests. National Research Council of Canada, Report number: FPRF-2018-01, Canada
4. Hadden R et al (2017) Effects of exposed cross-laminated timber on compartment fire dynamics. Fire Saf J 91:480–489
5. ISO 9705-1 (2016) Reaction to fire tests - room corner test for wall and ceiling lining products - Part 1: test method for a small room configuration, February 2016
6. Winter S, Zehfuß J, Werther N, Engel T, Brunkhorst S (2019) Brandschutztechnische Grundlagenuntersuchung für eine erweiterte Anwendung des Holzbaus. In: Proceedings of Braunschweiger Brandschutz-Tage, 25th–26th September 2019, Germany
7. EN 13353:2011-07 Solid wood panels (SWP) – requirements, German version EN 13353:2008+A1:2011
8. EN 520:2009-12 Gypsum plasterboards - definitions, requirements and test methods, German version EN 520:2004+A1:2009
9. McGrattan K, et al (2018) Fire dynamics simulator (Version 6.7.0) - user's guide. National Institute of Standards and Technology, Gaithersburg, Maryland

Behaviour of Wooden Materials Exposed to Electrical Ignition Sources

Miroslava Nejtková(✉)

Ministry of the Interior – Directorate General Fire Rescue Service Czech Republic, Population Protection Institute, Lázně Bohdaneč, Czech Republic
miroslava.nejtkova@ioolb.izscr.cz

Abstract. This paper deals with fires caused by electrical conductors placed on or near flammable materials. Our homes and accommodation facilities are equipped with many wooden or wood-based objects and many electrical conductors. This paper deals with ignition of electrical fires caused by electrical installations located in the most commonly used materials such as wood, laminate. The aim is to show how the tested materials behave when exposed to an electrical ignition source. The results of these experiments are particularly useful for fire investigators.

Keywords: Electric cabling · Fire · Ignition

1 Introduction

In recent years, wood has been increasingly used as a construction material for family homes, administrative centers and industrial buildings. However, wood and wood-based materials are used not only as construction materials, but most importantly also as part of household or office fixtures and fittings. These materials are also essential to some industrial facilities.

2 Electrical Equipment

According to the statistical information available to the FRS CR, over 20,000 fires occurred last year (2018) in the Czech Republic, of which 25% were in households. Almost 15% of all fires are caused by electrical equipment, appliances or electrical installations [1].

Electrical equipment and wiring are installed in almost all buildings and are an important potential ignition source. When assessing the risk of fire, the influence of the environment in which the electrical equipment is located (the presence of water, dust, aggressive or corrosive substances, etc.) must also be taken into account. Discharge of static or atmospheric electricity is also a potential source of fire or explosion.

One preventive measure is to perform regular checks and inspections and to maintain electrical equipment in accordance with the instructions for use [2–4].

L. Makovicka Osvaldova et al. (Eds.): WFS 2020, *Wood & Fire Safety*, pp. 191–196, 2020.
https://doi.org/10.1007/978-3-030-41235-7_29

According to statistical data, fires caused by technical failures (this includes defects of both electrical wiring and electrical appliances) and atmospheric discharge occur every year. Every year, these two reasons account for approximately 20% of all fires.

The Fire Rescue Service of the Czech Republic keeps statistics on fires and their ignition sources. Electrical ignition sources include electric sparks, electric short circuits, electric arcs, electrical transient resistance, vehicle electrics, electrostatic discharge, atmospheric discharge and electrical faults of unknown origin.

To ensure protection against the consequences of faults in electrical appliances and electrical installations, circuit breakers are installed in electric circuits. Until recently, there was no protection against the consequences of faulty electric arcs. Currently, both residual-current devices and elements protecting against arc flash hazards are available.

2.1 Faults in Electrical Installation

Faults in electrical installations can be classified into short- and long-term faults.

In the case of short-term faults, a high overload current occurs for a short period of time, while in the case of long-term defects, a low overload current occurs for a long period of time. In the latter case, accumulation of heat and degradation of inflammable materials occur. Fuses and circuit breakers protect against high overload currents. Residual-current devices [5] or arc flash detection devices [6] can be used to ensure protection against low overload currents.

During operation, electrical equipment converts some electrical power into heat, which results in heat losses. In the event of a faulty condition, the electrical equipment is capable of converting the input energy into thermal energy, which results in the accumulation of heat that cannot be dissipated into the surrounding environment. In this way, the surrounding inflammable materials can be ignited.

Hazardous conditions and generation of excessive heat can occur mainly due to:

- incorrect installation, incorrect design of electrical equipment;
- incorrect use, operation, handling or maintenance of electrical equipment;
- failure to perform inspections and tests or reviews of electrical equipment;
- unpredictable impacts of the surrounding environment;
- negligence.

During investigation of the causes of fires, faulty conditions are classified into the following categories:

- short circuits;
- increased electrical contact resistance between two conductors;
- overloading of electrical conductors and devices with overcurrent;
- overvoltage;
- electric sparks.

2.2 Short Circuits

A short circuit is a very serious fault. The term refers to a conductive low-resistance connection between two points in a circuit with different electric potentials (between two phases in an electrical system or between a phase and earth in a grounded electrical system). A perfect (minimal contact impedance) or imperfect (higher contact impedance) connection can occur at the short-circuit connection.

Most frequently, short circuits are caused by mechanical damage to wire insulation, wire insulation contamination, a contact between bare wires, faulty insulating materials or negative impacts of the environment (presence of water, aggressive substances etc.). However, a short circuit may also occur, for example, due to a faulty installation, incorrect wiring or a falling object.

The effects of a short-circuit current include thermal effects, dynamic effects, electric arc, overvoltage, induced voltage and voltage drop across the entire circuit.

Thermal effects are the biggest hazard to the equipment itself, to the electrical wiring and to inflammable substances in the surrounding environment. A short-circuit current causes an excessive rise in the temperature of all parts of the circuit. The heat generated by a short-circuit current can be calculated according to the following equation [7]:

$$Q = R \cdot I_{Ke}^2 \cdot t \quad [J, \Omega, A, s] \tag{1}$$

Q - thermal effects of short circuit [J]
R - resistance [Ω]
I - current [A]
t - short circuit duration [s]

During a short circuit, abnormal temperatures develop that cannot be dissipated to the surrounding environment, the core areas of the conductors heat up, hot metal splatters, the electric arc ignites, insulation is sublimated and, in some cases, explosive gases develop.

Another consequence is the effect of dynamic forces, which act on supports and cause the conductors to bend.

An electric arc is the consequence of a direct short circuit. The effects include radiant heat and pressure. The temperature of electric arcs ranges from 1,000 °C to 3,000 °C.

2.3 Overvoltage

An overvoltage is a voltage that exceeds the nominal value. The magnitude of the overvoltage is given by the amplitude of the voltage. Overvoltage can be classified into operational and atmospheric overvoltage. A risk of overvoltage occurs when a short circuit current is switched off with fuses.

3 Experiment to Determine Conductor Behavior Load on Wood and Wooden – Based Materials

The objective of the experiment was to verify the possibility of ignition and spreading of a fire on wood and wood-based materials used in households when the electrical installation/power cord is loaded above the design value.

For this purpose, two materials were selected for the initial/verification part of the experiment:

- a planed spruce board with a thickness of 2.5 cm
- a laminate flooring with a thickness of 0.6 cm, load class 23 (intended for floor with intensive use).

Cables of the following dimensions were used:

- 3-core with solid copper core and 1 mm^2 cross section (samples no. 1 and 2)
- 3-core with solid copper core and 1.5 mm^2 cross section (samples no. 3–6)
- 3-core with solid copper core and 2.5 mm^2 cross section (samples no. 7–10)
- 5-core with solid copper core and 4 mm^2 cross section (samples no. 11–12)

Note. For the 3- and 5-core cables, 2 or 3 conductors were loaded.

3.1 Experiment Procedure

Each cable was cut to a length of 1 m and the ends were stripped and connected to terminal blocks that were connected to an external source.

50-cm long sections of the cables were fastened to the surface of the tested material with electrical installation tape.

The first step of the test was to set the magnitude of the incoming current [A].

The current was maintained at a constant level during the experiment, while the voltage changed depending on the change in the conductor resistance (Ohm's law).

The experiment was documented using a Fluke thermal camera (thermal images and thermal video sequences), a RGB channel camera and photos. Measurement of surface temperatures by type K thermocouple was abandoned during the experiment due to the expansion of the stressed conductor and loss of contact with the conductor surface.

Planed spruce board – Sample no. 3, 5, 9, 10.

Laminate flooring – Sample no. 1, 2, 4, 6, 7, 8, 11, 12.

3.2 Assessment of the Experiment

The following occurred during the experiment:

- Short circuit on one conductor – decrease in current, increase in current after manipulation, continuation of the experiment; experiment terminated during second short circuit due to decrease in current
- Short circuit on multiple conductors – decrease in current, termination of experiment
- Rise in temperature, damage to the outer sheath of the cable, gradual stripping off of the insulation of each conductor, glowing of the conductor cores after insulation melted, no flames

– Rise in temperature, damage to the outer sheath of the cable, gradual stripping off of the insulation of each conductor, combustion of insulation with flames

The surface of the laminate flooring was not damaged during the experiment. In several cases, only the melted sheath of the cable oozed over the surface (Fig. 1 and Table 1).

Fig. 1. Sample no. 10

Table 1. Values measured out during the experiment

Sample	Surface	Current [A]	Conductor load	The highest measured temperature [°C]	Time [min:s]	Result
1	L	86	3	260	00:20	Short circuit
2	L	50	3	260	06:20	Short circuit
3	S	50	2	447	20:00	Short circuit
4	L	50	3	321	05:20	Short circuit
5	S	86	2	385[(a)]	01:58	Combustion with flames
6	L	86	3	331	01:50	Short circuit
7	L	67	2	260	19:00	Short circuit
8	L	67	3	596	15:07	Short circuit
9	S	116	2	690	03:50	Short circuit
10	S	116	3	514[(a)]	01:15	Combustion with flames
11	L	120	3	594[(a)]	06:57	Combustion with flames
12	L	120	3	672[(a)]	07:35	Combustion with flames

[(a)] Temperature before combustion with flames insulation
[(S)] Planed spruce board
[(L)] Laminate flooring

In cases of cable combustion with flames, part of the surface of the spruce board under the cables was charred.

4 Conclusion

The hypothesis that excessive overload on cables can cause fires was confirmed.

During the experiment, we encountered the problem of premature conductor short circuits, due to which the measurements were terminated.

All tests produced a large amount of toxic smoke during the tests.

In four cases, the insulation of the cable ignited and subsequently burned.

In three cases the integrity of the cord insulation was broken, exposing individual conductor cores. The bare wire was hot, but there were no flammable materials (or insulation) in its immediate vicinity, so there was no flame burning.

Due to low overload values of 2 times and 4.5 times the nominal value, the temperatures in the stressed cables were relatively low. However, if cables are installed in the immediate proximity of flammable materials (bedding, clothing, etc.), flames can spread into the surrounding area through a haphazardly placed cord even at this low overload value.

In real short circuits, when the values are 100 times the nominal value or higher, temperatures can reach 1,000–3,000 °C.

These tests of the effects of conductor load on the conductors were performed only as a pilot. Other wood-based materials will continue testing in the coming months.

References

1. Ministry of the interior – general directorate FRS Statistical yearbook 2018 Czech Republic. https://www.hzscr.cz/hasicien/article/statistical-yearbooks.aspx
2. ČSN 33 2000-4-42 ed. 2 (2012) Low-voltage electrical installations – part 4-42: safety – protection against thermal effects. Czech Office for Standards, Metrology and Testing, Prague, p 28
3. ČSN 33 2130 ed. 3 (2014) Low-voltage electrical installations – internal electric distribution lines. Czech Office for Standards, Metrology and Testing. Prague, p 4
4. ČSN 33 2000-5-52 ed. 2 (2012) Low-voltage electrical installations – part 5-52: selection and erection of electrical equipment – wiring systems. Czech Office for Standards, Metrology and Testing, Prague, p 120
5. ČSN 33 2000-5-53 ed. 2 (2016) Low-voltage electrical installations – part 5-53: selection and erection of electrical equipment – switch-gear and control-gear. Czech Office for Standards, Metrology and Testing, Prague, p 52
6. ČSN EN 62 606 (2014) General requirements for arc defect detection devices. Czech Office for Standards, Metrology and Testing, Prague
7. Yereance R, Kerkhoff T (2010) Electrical fire analysis. 3rd ed. Charles C Thomas Pub. Ltd. ISBN 978-0-398-07955-0

Feasibility Study of Correlating Mass Quantity Output and Fuel Parameter Input of Different Simulations Using Fire Dynamics Simulator

Steffen Oliver Sæle(✉)

Western Norway University of Applied Sciences,
Bjørnsonsgate 45, 5528 Haugesund, Norway
l37245@stud.hvl.no

Abstract. While fire dynamics can rarely be calculated more precisely than by use of Computational Fluid Dynamics (CFD), using such techniques in computer simulations are often highly computationally expensive. To possibly reduce computational costs in Fire Safety Design (FSD) where several simulations need to be conducted, the author has investigated the feasibility of correlating variations in mass concentration output of Fire Dynamics Simulator (FDS) to variations in fuel parameter input. In this study, such a correlation is deduced based on the relative significance of the mass source term of the FDS mass transport equation. From the results of 15 conducted simulations, the study suggests that the correlations may be applied to produce reasonable estimations of mass concentration output of a simulated scenario, based on the equivalent results of a base simulation. As such, consequences of fires as a function of fuel properties may be assessed rapidly, compared to conducting multitudes of simulations.

Keywords: Correlate input and output · Correlation factor · Output estimation · Fire Dynamics Simulator

1 Correlation Factor

For a series of fire simulations with revised input parameters, a correlation factor is, in this context, defined as the ratio of functions of input parameter values for two of these simulations. Such a factor is approximate to ratios of solutions to Fire Dynamics Simulator (FDS) computations, relevant to the functions of the factor. As such, correlating mass quantity output and fuel parameter input, requires the correlation factor-function to describe aspects paramount to transport of mass. In this study, the feasibility of such a correlation is examined, herein a correlation of measured quantities of combustion products of simulations, such as Carbon Monoxide or soot, to mass production terms of that species. If the correlation is valid, the correlation may be used to estimate the output quantity of a simulation not yet conducted, based on the results of a base simulation, and the correlation factor.

L. Makovicka Osvaldova et al. (Eds.): WFS 2020, *Wood & Fire Safety*, pp. 197–202, 2020.
https://doi.org/10.1007/978-3-030-41235-7_30

In FDS, the transport of a species, α, may be expressed by (adapted from [1]):

$$\frac{\partial}{\partial t}(\rho Z_\alpha) + \nabla \cdot (\rho Z_\alpha \boldsymbol{u}) = \nabla \cdot (\rho D_\alpha \nabla Z_\alpha) + \dot{m}'''_\alpha. \tag{1}$$

where the first and second term on the left-hand side of the equation is the accumulation rate and convective transport of mass respectively. The first term on the right-hand side is the diffusive transport. The second term is a mass source term, the volumetric mass production rate by combustion. Provided limited or no evaporation or deposition of species α, this term accounts for all mass introduced to the computational domain. It can therefore be reasoned that this term is highly influential to the measured species quantity and may therefore constitute the function applied in the correlation factor. In the following, the species mass production term will be described in terms of common fuel parameter input applied in FDS, allowing the correlation factor to be deduced.

The mass production rate of a primitive species due to combustion, $\dot{m}_\alpha$, may be expressed in terms of its yield parameter (an input to an FDS-simulation), γ_α, and the fuel loss rate, $\dot{m}_f$ (adapted from [2]):

$$\dot{m}_\alpha = \gamma_\alpha \dot{m}_f. \tag{2}$$

The fuel loss rate can be expressed in terms of the ratio of Heat Release Rate (HRR), $\dot{Q}$, to the product of the heat of combustion per unit mass of oxygen, $\Delta H_{C,ox}$, and the stoichiometric oxygen to fuel mass ratio, ψ_O (adapted from [3] and [4]):

$$\dot{m}_f = \frac{\dot{Q}}{\Delta H_{C,ox} \psi_O}. \tag{3}$$

which can be assumed a correct estimate, given that the combustion process is oxygen controlled. This allows relating the fuel mass loss rate to the stoichiometry of the combustion, as the stoichiometric oxygen to fuel mass ratio may be expressed [4]:

$$\psi_O = \frac{\nu_{O_2} W_{O_2}}{W_F}. \tag{4}$$

where W_{O_2} and W_F is the mole weight of oxygen and fuel respectively, and ν_{O_2} is the stoichiometric coefficient for oxygen. To express the latter, the default chemical reaction of FDS may be applied, and balanced (adapted from [5]):

$$\nu_{O_2,a} = x + \frac{y}{4} - \frac{z}{2} + W_F \left(\frac{\gamma_S}{W_S} \left(\frac{3X_H}{4} - 1 \right) - \frac{\gamma_{CO}}{2W_{CO}} \right). \tag{5}$$

where x, y and z are the numbers of atoms of carbon, hydrogen and oxygen in the fuel respectively. In this study, a hydrogen fraction, X_H = 0, 1 (default), is used. Mole weight data for various species may be found in the literature (see, for instance [5]).

Ratios of $\dot{m}_\alpha$, for two different sets of simulation input variables, may now be approximated to the ratios of examined mass output quantities, θ, of two simulations a and b, constituting the correlation factor as defined initially:

$$\frac{\dot{m}_{\alpha,a}}{\dot{m}_{\alpha,b}} \approx \frac{\theta_a}{\theta_b}. \tag{6}$$

Either θ_a or θ_b may now be solved for, to approximate its value, given that simulation results exist for the other. In this study, the validity of the correlation factor is assessed by examining the proximity of the ratio of the estimated quantity to the simulated quantity, to unity (given that θ_a is estimated):

$$\beta_\theta \frac{\theta_b}{\theta_a} \approx 1. \tag{7}$$

where $\beta_\theta = \frac{\dot{m}_{\alpha,a}}{\dot{m}_{\alpha,b}}$ is the correlation factor considering the quantity θ (the left side of Eq. 6). A value of Eq. 7 near unity, indicates that the correlation may be used to successfully approximate the output of simulation a, θ_a, based on the base, b, simulation output, θ_b, and the correlation factor, β_θ.

2 Simulation Series

The simulation series subjected for testing the feasibility of correlation are described in this chapter. Three simulation series are conducted, each consisting of five simulations, making a total of 15 individual simulations. In each series, one simulation is the base simulation, by which all other simulation output in the series are estimated. Differences between the base simulation and all other simulations in the series, regards fuel parameter input values. If the ratios of the estimated output, $\beta_\theta \cdot \theta_b$. to the actual simulated output, θ_a, approximates unity (Eq. 7), the correlation factor, β_θ, may be deemed suitable. Differences between individual simulation series regards HRR.

2.1 Heat Release Rates

In this study, values of HRR are predetermined, asserted through specification of HRR per unit area (HRRPUA), subsequently assigned to VENTs. The VENT releases fuel at a rate necessary to sustain the intended HRR, a method physically analogous to a burner [5]. As different values of HRR transport mass, momentum and energy differently, several HRR values are applied to validate the correlation factor. HRR values are chosen based on typical values used in Fire Safety Design (FSD). In [6], a HRR of 5000 kW is suggested for, among others, schools, hotels and apartments. This HRR is deemed suitable as a "mid value" for testing the correlation. Two additional values are used, in intervals of 2000 kW, rendering HRRs for examination: 3000, 5000 and 7000 kW. For these values, similar values of HRRPUA are used, 1038.1, 1033.1 and 1035.5 kW/m^2, and VENT areas of 2.89, 4.84 and 6.76 m^2 respectively.

2.2 Measurements of Examined Quantity and Simulation Model

A suitable output variable, θ, for examination of the feasibility of correlation, is chosen to be the soot density fraction, ρY_S. This is a variable of interest in FSD when studying visibility distance in egress routes. The form of measured output is the statistical volumetric mean values of ρY_S, of two different volumes located in different places in the simulation model.

The simulation model is illustrated in Fig. 1, with dimensions and position of volumes of measurements (both equal in size). The mean soot densities are measured in two locations to investigate differences in estimation precision due to distance from the fire source. The fire source (red VENT) is located in the tall room to the right, with its center in the center of the room, and elevated 0.5 m above floor level.

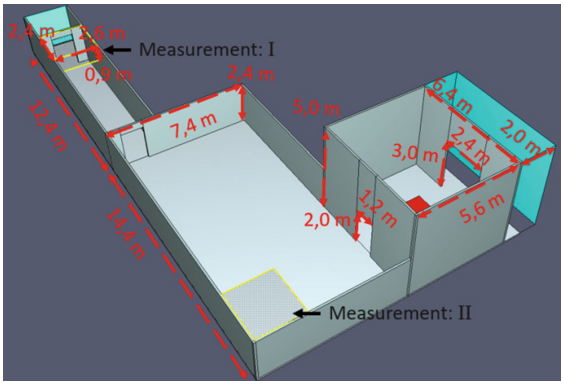

Fig. 1. Illustration of model, with dimensions and position of measurements (yellow outlines). Ceiling omitted from model for illustration purposes. Snapshot in Pyrosim ©.

The roofs, floors and walls are assigned properties consistent with 60-minute fire resistance rating (according to [7]). Walls and ceilings consist of layered mineral wool (0.15 m) and gypsum cladding (0.0125 m), and floors of concrete slabs (0.2 m).

A mesh sensitivity study found that the solution became appreciatively grid cell independent by using cubed grids of dx = 0.1 m. Differences between solutions using grid cell sizes of dx = 0.05 m where, on a time average, approximately 4%. Simulation duration was set to 600 s.

2.3 Fuel Properties

Fuel properties presented in this section are used as input to the correlation factor (in Eq. 7) and are chosen to reflect common combustibles assessed in FSD, herein wood (red oak) and polymers (polyurethane GM25). Fuel properties are altered according to a surrogate fuel method, meaning that fuel applied in simulations is meant to represent a percentile, F [%], mixture of two fuels [8]. In Table 1, the percentile distribution is referring to the volume percentile of wood, meaning the row of F [%] = 0 represents

the mixture of 0% red oak and 100% GM25, and so on. Fuel properties inserted into Eq. 7 result in correlation factor values, $\beta_{\rho Y_S}$, presented in the right column. All simulation series apply the properties of the mid-row (F [%] = 50) as the base simulation.

Table 1. Fuel properties and correlation factors. Properties collected and adapted from [9].

F [%]	Formula	$\gamma_{CO}[g/g]$	$\gamma_S[g/g]$	$\Delta H_{C,ox}[kJ/g_{ox}]$	$\beta_{\rho Y_S}$
0	$CH_{1,7}O_{0,32}N_{0,07}$	0.028	0.194	12.0	1.753
30	$CH_{1,7}O_{0,44}N_{0,05}$	0.021	0.140	12.4	1.311
50	$CH_{1,7}O_{0,52}N_{0,04}$	0.016	0.105	12.6	1
70	$CH_{1,7}O_{0,60}N_{0,02}$	0.011	0.069	12.8	0.656
100	$CH_{1,7}O_{0,72}N_{0,001}$	0.004	0.015	13.2	0.141

3 Results and Discussion

In Fig. 2, ratios of estimated soot density values, ρY_S, to actual simulated values of ρY_S is plotted against correlation factor values, $\beta_{\rho Y_S}$, used to ascertain the ratio (Eq. 7). Values are time averaged in the interval of 400–600 s. The upper and lower plot show ratios from position I and II respectively (see Fig. 1). Each line represents a simulation series using a distinct HRR, and each dot represents one time averaged ratio of estimation to simulation. As ratios of estimation to simulation are generally close to unity, the results indicate that the correlations were suitable for estimating simulation output. The maximum deviation was approximately 15% for $\beta_{\rho Y_S} = 0.141$ in position I. The average absolute discrepancy was approximately 4% from unity.

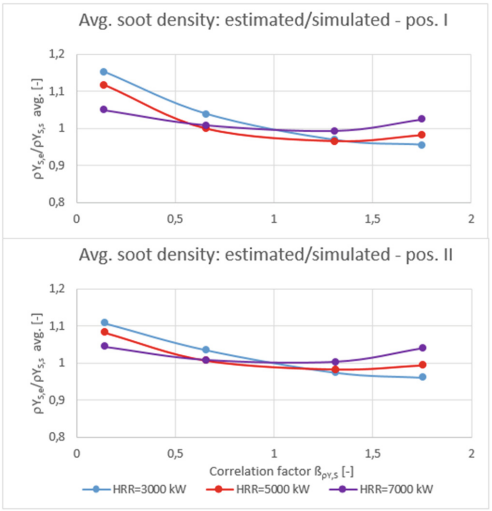

Fig. 2. Ratios of estimated to simulated values of soot densities.

The most apparent tendency is increased discrepancies for increased differences between $\beta_{\rho Y_S}$ and unity, which is indicative of increased differences between inputs of simulation a and b. This is likely due to the non-linear dependency between the mass source term and the remaining terms of the FDS mass transport equation (Eq. 1) being more pronounced for increased differences in simulation input.

Additionally, levels of overestimation and underestimation of $\rho Y_{S,a}$ increased for low and high values of $\beta_{\rho Y_S}$ respectively, when the value of HRR was reduced or when the distance between the position of measurement and fire source was increased (position I was further away than II). As such, the measured values of $\rho Y_{S,a}$ and $\rho Y_{S,b}$ were more dissimilar than predicted by $\beta_{\rho Y_S}$ when HRR was low or when the distance was increased. This suggests that particularly low or high energy and/or mass levels of the flow may also cause reduction in the performance of the correlation factors.

4 Conclusion

The findings of this study indicate that species mass quantity output of two simulations using different fuel properties may be correlated by use of ratios of species mass production rates of the two simulations. For the 15 conducted simulations examining the correlations, the maximum discrepancy was 15%, for $\beta_{\rho Y_S} = 0{,}141$. On average, the discrepancy was approximately 4%. Increased discrepancies are likely linked to differences between $\beta_{\rho Y_S}$ and unity, levels of HRR and distance between the fire source and position of measurement. Low levels of HRR and increased distance, increased the difference between $\rho Y_{S,a}$ and $\rho Y_{S,b}$ more than predicted by $\beta_{\rho Y_S}$. Any future studies should explore these tendencies further, by simulations and experiments.

References

1. NIST (2018) Fire dynamics simulator technical reference guide, vol 1: mathematical model, 6th edn. NIST NIST Special Publication 1018-1
2. Mowrer FW (2016) Enclosure smoke filling and fire-generated environmental conditions. In: 5th SFPE handbook of fire protection engineering. Springer, New York, p 1090
3. Drysdale D (2016) Thermochemistry. In: 5th SFPE handbook of fire protection engineering. Springer, New York, p 145
4. Khan MM, Tewarson A, Chaos M (2016) Combustion characteristics of materials and generation of fire products. In: 5th SFPE handbook of fire protection engineering. Springer, New York, pp 1143–1232
5. NIST (2018) Fire dynamics simulator user's guide, 6th edn. NIST Special Publication 1019
6. Boverkets författningssamling (Swedish National Board of Housing, Building and Planning) (2013) Boverkets ändring av verkets allmänna råd (2011:27) om analytisk dimensionering av byggnaders brandskydd; BFS 2013:12 BBRAD 3, Boverkets författningssamling
7. SINTEF Byggforsk (Norwegian SINTEF) (2008) 520.322 Brannmotstand for vegger. SINTEF
8. Best Practice Gruppen (Danish collaboration) (2009) CFD best practice
9. SFPE (2016) Fuel properties and combustion data. In: 5th SFPE handbook of fire protection engineering. Springer, New York, pp 3437–3475 Appendix 3

Thermography of Wood-Base Panels During Fire Tests in Laboratory and Field Conditions

Denis Kasymov[1,2(✉)], Mikhail Agafontsev[1,2], Pavel Martynov[1,2], Vladislav Perminov[1], Vladimir Reyno[2], and Egor Golubnichiy[1]

[1] Tomsk State University, Lenin Avenue, 36, 634034 Tomsk, Russia
denkasymov@gmail.com
[2] V. E. Zuev Institute of Atmospheric Optics SB RAS, 634055 Tomsk, Russia

Abstract. The paper represents the experimental study of combustion over the surface of a vertically-mounted oriented wood-based panels (plywood, chipboard and oriented strand board) under different environmental conditions. The IR thermography was used as a diagnostic method. An infrared camera JADE J530SB was used to obtain the sequences of thermograms characterizing the heat flow pattern on the surface of the sample during vertical combustion and determine the velocity of the combustion wave under laboratory and field conditions. In addition, during the field tests the change in the angle of the combustion front was estimated depending on time.

Keywords: Fire behavior of wood · Fire retardant · Infrared thermography · Timber · Combustion · Fire safety

1 Introduction

Wood finishing materials are becoming increasingly widespread in Russia. Thus, in rural and suburban areas with low-rise buildings, the use of wood finishing building materials reaches 80%.

On the one hand, new wood-composite materials and technologies that use structural elements and prefabricated modules in the construction industry have greatly increased the interest in wooden buildings. Ecological and economic attractiveness of these projects plays an important role in wooden house construction.

On the other hand, wooden building structures can contribute to the occurrence and spread of fire in a building or in a structure. Fires (especially in combination with forest fires) occurring in settlements with predominant wooden buildings cause great damage. In this regard, studying the fire behavior of wooden buildings and structures, as well as analyzing the regulatory requirements for the fire safety of buildings with wooden structures are urgent and important tasks. Combustible building materials like wood-base panels burn out their surfaces, release energy and thus combustible to fire propagation in case of fire.

Flammability and combustion propagation are key factors that determine the fire behavior of wood. The effect of different factors on the fire behavior of wood (species and kind of wood, conditions and duration of operation, humidity, fire intensity, etc.) was investigated in [1–8]. The data of these works can be used to conclude about the

L. Makovicka Osvaldova et al. (Eds.): WFS 2020, *Wood & Fire Safety*, pp. 203–209, 2020.
https://doi.org/10.1007/978-3-030-41235-7_31

fire resistance of wooden structures, but most of the methods used are classified as contact methods.

At present, up-to-date methods of infrared (IR) diagnostics are actively used to study combustion process and wildland fires [9–11]. It should be noted that information on the application of contactless methods in the fire tests of building fragments and structures is still absent in the literature. In previous experiments [12] we experimentally analyzed the effect of different fire retardants on the flammability of coniferous and broadleaf wood using the methods of IR diagnostics. Development of fire resistance and fire behavior test methods using thermography based on the data obtained for wood building structures will reduce the costs of such works and simultaneously increase the efficiency of data and resolution obtained.

This paper presents the experimental study of vertical fire spread over the surface of wood-base panels under different environmental conditions. The experiments were conducted under laboratory conditions, thereby modeling the development of combustion inside a building. In addition, a series of fire tests were conducted under field conditions, modeling the development of vertical fire spread along the facade of a building.

2 Laboratory Equipment and Experimental Procedure

Experimental equipment included an infrared camera the JADE J530SB from Cedip Infrared Systems (Cedip Infrared Systems, Croissy-Beaubourg, France). The JADE J530SB infrared camera was used with a narrow-band optical filter working in the wavelength range of 2.5–2.7 microns and recording the temperature in the range of 300–1500 °C. Accuracy was ±2% of the reading temperature (with filter). Canon LEGRIA HF R88 video camera was used to estimate the propagation of the combustion front in the visible wavelength range.

Pine needles were taken as forest fuel to model the front of a ground fire. In the experiments the humidity content of needles was 6%. The mass of forest fuel (FF) remained unchanged and was equal to 150 g to model a low- intensity surface fire. This type of fire is more common, since it occurs in areas where litter is produced from fallen leaves of trees and shrubs.

Plywood, chipboard and oriented strand board (OSB) panels was chosen as a sample of building material. The main parameters of the samples are presented in Table 1.

Table 1. Parameters of the samples of building materials used in the laboratory and field experiments.

	Laboratory experiment	Field experiment
Size, m:	0.300 × 0.300	0.61 × 1.0
Thickness, m:	0.008; 0.012; 0.018	12 mm
Density, kg/m^3:	570–590 (OSB) 705–725 (Plywood) 700–720 (Chipboard)	570–590 (OSB) 705–725 (Plywood) 700–720 (Chipboard)
Humidity content, %:	4.7	10

Before the experiments, the humidity content of the samples was measured using an AND MX-50 humidity analyzer (precision of instrument is 0.01%).

Figure 1 shows a schematic diagram of the experiment and a photo of sample under the fire exposure:

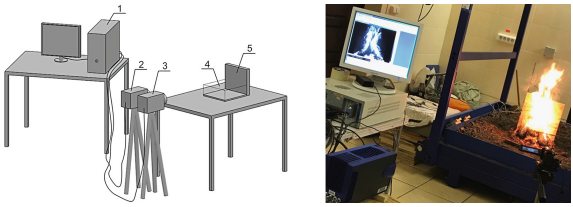

Fig. 1. Installation diagram scheme. 1 - PC, 2 - video camera Canon HF R88, 3 - JADE J530SB infrared camera, 4 - forest fuel (FF) site, 5 - wood sample.

The laboratory experiment was conducted as follows: a substrate with needles located in front of the wood building material sample mounted vertically to the substrate was ignited with a gas burner. It was resulted in the generation of the combustion front, which in turn began to affect the wood sample. The surface of the wood building material samples exposed to heat was observed using the infrared camera.

Analysis of the data obtained shows that OSB samples turned out to be susceptible to ignition with the considered experimental parameters. The thermal effect of the combustion of pine needles weighing 150 g is enough to cause a flame on the surface of the sample, followed by stable combustion. (Figure 2) presents a sequence of thermograms demonstrating the combustion over the OSB surface with a period of 120 s.

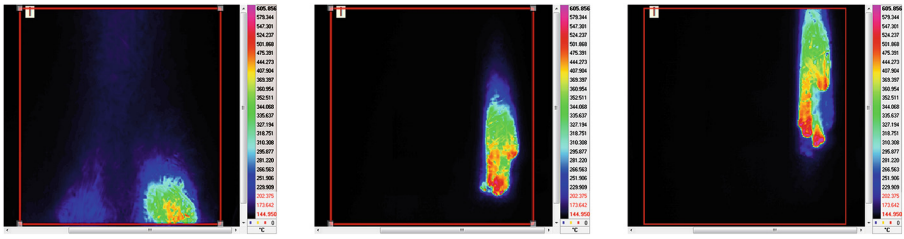

Fig. 2. Vertical propagation of the combustion front over the OSB sample. The surface of the sample in the thermogram is marked with a red rectangle.

It is note that for the selected experimental parameters, local ignition occurs in the region with the greatest amount of needles. Then the combustion wave passes vertically due to the effect of convection, and combustion on the upper part of the sample stops. For the chosen parameters of the experiment and the thermal energy released during the combustion of plant fuels in the amount of 150 g on the site (assuming 0.172–0.263 kg/m^2), the ignition of wood samples was observed for OSB and plywood panels.

Based on the obtained data and three repetitions of the experiment, the velocity of the combustion wave was 0.68 mm/s (for OSB samples) and 0.95 mm/s (for plywood) according to the data of IR diagnostics. It is of interest to conduct a similar experiment that demonstrates the development of the combustion front over the surface of a vertically-mounted sample in open space under natural weather conditions.

3 Field Tests

The experiments were conducted on the test site of V.E. Zuev Institute of Atmospheric Optics of the Siberian Branch of the Russian Academy of Science (IOA SB RAS). The air temperature and wind were measured by the weather station situated at the test site. Automated system allows one to measure a wide range of meteorological and optical atmosphere parameters as temperature (223… 323 K, ±0.2 K), relative humidity (10… 100%, ±5%), wind speed (0.5… 60 m/s, ±5%), direction (0… 360°, ±10%). Wind speed was varied over the range of 0.8–2.5 m/s, temperature was varied over the range of 301–303 K.

Figure 3 shows the sample before and during the fire test.

Fig. 3. Photographs of the wood-base panel during field fire tests.

Before the experiment, the sample fixed on wooden poles, which had previously been insulated with metal foil. The poles were driven into the soil to place the sample in the vertical position. The distance from the soil to the sample was chosen in such a way that a container with a fuel could be placed in it. After ignition of the sample and stable combustion over the surface, the propagation of the combustion wave was recorded using the infrared camera with similar settings as in laboratory experiments.

Combustion regime was observed as followed during the experiments in an open area: as a result of the thermal effect of heat flux from fuel combustion, the pyrolysis temperature was reached on the lower face of samples, then it increased with the release of combustible gases. The initiated flame increases due to the emission of combustible gases, as well as combustion area increases on the surface. Additional heat is released

during further combustion reaction, the flame height stabilizes and the material is actively burned.

(Figure 4) shows the photographs demonstrating the combustion of the OSB panel as well as the thermograms obtained using the infrared camera (120 s. step).

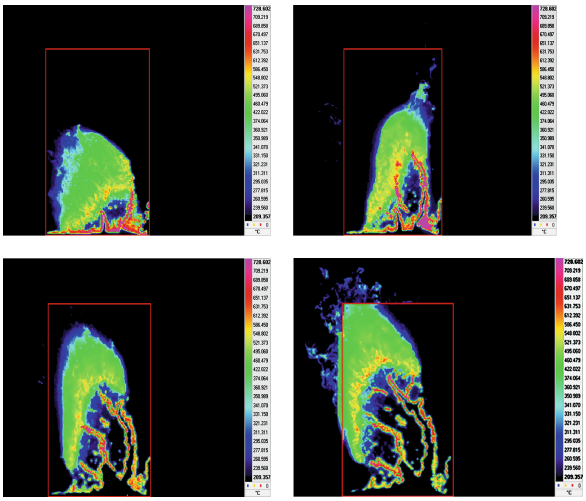

Fig. 4. Thermograms of the vertical combustion of the OSB sample.

The sequences of thermograms characterizing the heat flow pattern on the surface of the sample during vertical combustion were obtained. It is noted that the presence of changing wind in the open area leads to the fact that the combustion wave propagates nonuniformly, and the front spreads in the direction of the wind, which is shown in (Fig. 4), starting from the sixth minute. In individual cases, the speed and wind direction change drastically during the experiment. Despite the high wind with gusts of up to 15 m/s (it should be noted that such gusts were observed rarely and did not play a decisive role in the development of vertical combustion process), blowout of flame and extinguishing of the samples were not observed, the combustion process was very active. On the contrary, combustion process intensified with the presence of additional oxidants influx. The results on velocity of the combustion wave was according to the data of the infrared camera presented in Table 2. The results show good accuracy for both cases: laboratory and field conditions.

Table 2. Fire behavior parameters of the samples (* – averaging on 3 repetitions was performed).

Wood material	Vertical fire spread*, mm/s	Maximum of the surface temperature*, °C
Chipboard	0.8 ± 0.15	716 ± 25
Plywood	1.38 ± 0.33	740 ± 20
OSB	1.27 ± 0.27	765 ± 25

4 Conclusions

The vertical combustion of the sample of wood building material was experimentally studied to obtain:

1. Temperature distribution over the surface of wood-base panels;
2. The method of constructing and analyzing the temperature field on the surface of samples according to the obtained data using an infrared camera was tested;
3. The velocity of the vertical combustion front was estimated under laboratory and field conditions using infrared diagnostics. It is noted that the presence of changing wind in open areas leads to the fact that the combustion wave propagates nonuniformly, the front spreads in the direction of wind, and the front angle change is linear during the whole combustion process. Data on vertical fire spread show good accuracy for both cases: laboratory and field conditions.
4. As a result of experimental data processing, heat-stressed areas on the surface of wooden model constructions by the exposure of surface fire front were found. Available data as well as additional experiments would allow to estimate the dependence of fire hazard indexes of constructional materials of application conditions and type of fire retardant composition, geometry and design of sample, and develop laboratory method of noncontact IR diagnostics and controlling of fire hazard characteristics of constructional materials (flame front position, burnout front and flame height).

Acknowledgments. This study was supported by the Russian Science Foundation (project No. 18-79-00232).

References

1. Bartlett AI, Hadden RM, Bisby LA (2019) A review of factors affecting the burning behaviour of wood for application to tall timber construction. Fire Technol 55(1):1–49
2. Hedayati F, Yang W, Zhou A (2018) Effects of moisture content and heating condition on pyrolysis and combustion properties of structural fuels. Fire Mater 42(7):741–749
3. Hasburgh LE, Stone DS, Zelinka SL (2017) Laboratory investigation of fire transfer from exterior wood decks to buildings in the Wildland-Urban interface. Fire Technol 53(2):517–534
4. Babrauskas V (2005) Charring rate of wood as a tool for fire investigations. Fire Saf J 40:528–554
5. Mel'nikov VS, Khasanov IR, Kirillov SV, Vasil'yev VG, Vanin SA, Shcherbakov MI, Garskov RV (2015) Thermography of building elements and building structures during fire tests. Fire Saf 3:83–90 (in Russian)
6. Loboda EL, Kasymov DP, Yakimov AS (2015) Modeling of thermophysical processes in the ignition of a small wooden plank. J Eng Phys Thermophys 88(1):113–123
7. Grishin AM, Filkov AI, Loboda EL, Reyno VV, Kozlov AV, Kuznetsov VT, Kasymov DP, Andreyuk SM, Ivanov AI (2014) A field experiment on grass fire effects on wooden constructions and peat layer ignition. Int J Wildland Fire 23:445–449

8. Frangi A, Fontana M (2005) Fire performance of timber structures under natural fire conditions. Fire Saf Sci Symp 8:279–290
9. O'Brien JJ, Loudermilk EL, Hornsby B, Hudak AT, Bright BC, Dickinson MB, Hiers JK, Teske C, Ottmar RD (2016) High-resolution infrared thermography for capturing wildland fire behaviour: RxCADRE 2012. Int J Wildland Fire 25:62–75
10. Valero MM, Jimenez D, Butler B, Mata C, Rios O, Pastor E, Planas E (2018) On the use of compact thermal cameras for quantitative wildfire monitoring. In: Advances in forest fire research, pp 1077–1086
11. Meng Q, Zhu G, Yu M, Pan R (2018) The effect of thickness on plywood vertical fire spread. Procedia Eng 211:555–564
12. Kasymov DP, Agafontsev MV, Perminov VV (2018) Estimation of the influence of wood-fire retardants on fire behavior of some types of wood construction materials. J Phys Conf Ser 1105:1–7

Fire Safety in Wooden Objects

Issues and Solutions for Compartments with Exposed Structural Mass Timber Elements

David Barber[1(✉)], Robert Dixon[2], Susan Deeny[3], and Pascal Steenbakkers[4]

[1] Arup, 1120 Connecticut Avenue, Washington, DC 20036, USA
david.barber@arup.com
[2] Arup, 699 Collins Street, Docklands, VIC 3008, Australia
robert.dixon@arup.com
[3] Arup, Scotstoun House, South Queensferry, Edinburgh EH30 9SE, UK
susan.deeny@arup.com
[4] Arup, Naritaweg, 118, 1043 CA Amsterdam, The Netherlands
pascal.steenbakkers@arup.com

Abstract. High-rise mass timber buildings with CLT and glulam are being planned and constructed within the globally. As timber buildings are constructed taller, architects and building owners are requesting more timber be exposed. High-rise buildings are required to have fire resistance ratings for the structural elements that can withstand the design fire in the highly unlikely event of a fully developed fire. Addressing how exposed timber and in particular CLT, influences a fully developed fire through to fire extinguishment is a current fire safety issue. The fire heat release rate and fire duration will be increased due to the added combustible fuel available from the exposed timber, when compared to a compartment without any exposed timber, once all the fixtures and furnishings have been consumed. Existing fire test data shows that large areas of exposed timber has a significant impact on heat release rate, but limited areas of exposed timber can be accommodated within a fire safe design. To design a compartment with exposed timber requires an understanding of the susceptibility of the CLT to char fall off and the expected fire duration due to the area and location of the exposed timber.

Keywords: Mass timber · Cross laminated timber · Compartment fires · High-rise buildings · Performance-based design

1 Introduction

New mass timber technologies are available, and architects and owners are requesting high-rise timber buildings are constructed with more of the structural timber exposed. Addressing how exposed mass timber and in particular cross laminated timber (CLT), influences fire development from ignition to a fully developed fire through to decay is a current and complex fire safety issue. When a compartment has large areas of exposed timber, there is potential for fire re-growth after an initial decay, or a very long duration

L. Makovicka Osvaldova et al. (Eds.): WFS 2020, *Wood & Fire Safety*, pp. 213–218, 2020.
https://doi.org/10.1007/978-3-030-41235-7_32

fire; which can result in localized structural failure. Given that the structural fire resistance rating (FRR) is directly related to char depth, areas of exposed timber can influence the structural fire resistance. Decisions on mitigation measures need to form part of a holistic fire safety solution for a mass timber building. To date, the design of multi-story mass timber buildings has been predominantly based on timber elements being protected (encapsulated) within fire rated gypsum board products to improve the required FRR and prevent combustion of the mass timber [1–3]. Accompanying the movement for taller mass timber buildings is a desire to expose the timber structure, not protecting it with fire rated gypsum board.

2 Exposed Mass Timber in High-Rise Buildings

Exposed timber within buildings is not a new issue. Most building codes permit timber as an interior finish and in many cases, permit timber structures to be exposed for low and medium-rise buildings. The issue to be addressed is the requirement for a high-rise building to withstand full burn-out of a fully developed fire. Where there is an exposed mass timber structure and in the rare event of a fully developed fire occurring, the exposed timber impacts on the room fire dynamics (fire growth rate, fire heat release rate (HRR), fire duration and temperature) as shown through full scale testing (see Fig. 1). The fire peak HRR and fire duration will be increased due to the added combustible fuel available from the exposed timber, when compared to a compartment without any exposed timber [4].

Fig. 1. CLT compartment fire from the Fire Protection Research Foundation series of tests (undertaken by National Research Council, Canada with RISE, Sweden, at the National Institute of Standards and Technology) (image, Arup)

3 CLT Performance in Fire

CLT performance in fire has been well studied and the rate of char varies with ply thickness, number of plys and the CLT adhesive used. The initial charring behavior in the first ply is identical to that of glulam of the same density and initial moisture content. As the charring reaches the adhesive line, there are two possible events. Either the charring continues consistently through the adhesive line; or the protective char will dislodge due to lack of adhesive strength under heating, exposing the unburnt wood below, an effect called char fall off (or delamination) [5–8] (see Fig. 2).

Fig. 2. CLT panel that has been fire tested and is showing char fall off (image, Arup)

When char fall off occurs, the heat insulating function of the char is lost. The unburnt timber below the char then becomes exposed to the heat of the fire and there is a rapid localised increase in the pyrolysis, and hence charring rate. This increased burning occurs until a new char layer is formed, which then insulates the timber and the normal char rate returns. The process of char fall off in CLT has been shown to be adhesive dependent [5, 9]. Guides such as the CLT Handbook [10] provide a FRR calculation method that includes for char fall off. To improve CLT performance in fire, the North American manufacturing standard (ANSI-APA PRG-320) [11] has been updated and from 2021, all CLT panels are required to use adhesives that have a greater resistance to heat, improving fire performance and preventing char fall off.

4 Fire Testing - Impact of CLT Char Fall Off

Standard fire testing of building elements to tests such as ASTM E119 [12] provides limited information on fire performance. To better understand the influence of mass timber being exposed to long duration fires, a number of CLT compartment fire tests have been undertaken. These include tests by ETH [13], VTT [14], Carleton University [15, 16], Delft University of Technology [7], University of Edinburgh [17], SP Norway

[18], University of Queensland [19], FPRF [4], ICC [20], Tallinn University of Technology [21] and NRCC [22]. The tests have shown the additional fuel introduced by the exposed mass timber increases the compartment HRR and duration of the fire in a fully developed fire and shown the unpredictable impact of the CLT char fall off. The tests have also shown that when char fall occurs, and the uncharred timber becomes exposed, if temperatures in the compartment are sufficiently high, the increased burning rate in the freshly exposed timber can cause a second peak in HRR, after the contents have been consumed by the fire. Of concern is the unpredictability.

5 Methods to Allow Fire Decay

There are several options for mass timber structures with exposed CLT to reach fire decay, in a fully developed fire.

Adhesive Product: Small and medium scale fire testing has shown that the use of different adhesives can change the fire performance of CLT. A limited number of fire tests with exposed CLT have shown that CLT with a melamine formaldehyde (MF) adhesive, or a specifically formulated polyurethane adhesive (PUR), which do not exhibit char fall off, result in reliable fire decay in compartment fire conditions [5, 9].

Thickness of the Outer Lamella: Char fall off does not occur if the char layer does not reach the bond line. An increased thickness of the outer lamella, of up to 40 mm can prevent char fall off. However, given the variety of fuel within a compartment, variations in available fire ventilation and the inaccuracies in fire modelling, it is not practical or reliable to design with an outer thick lamella. To rely on specific initial fuel conditions and ventilation is not a realistic scenario. Hence, while this can be theoretically proven, the variability in building fires does not support this approach.

Limitation of Exposed Surface Area: The compartment fire can result in self-extinguishment if the area of exposed mass timber is limited. The amount of exposed CLT that would result in a fully developed fire decaying, even after all moveable fuel is consumed, is dependent on the timber exposed and ventilation of the compartment. The maximum allowable area of exposed CLT is complex to accurately model but can be approximated. Fire tests with 30% exposed CLT ceiling showed reliable decay [20].

Protection of CLT: A method to prevent CLT char fall off is to protect the CLT with gypsum board that remains in place and prevents charring. The CLT protection must remain in place for the growth, fully developed and decay phase of the fire. The reliability of the gypsum protection must be based on evidential fire tests with CLT.

6 Methodology for Assessing Limited Areas of Exposed Timber

The permitted area of structural mass timber that can be exposed can be assessed. There is a limit to how much timber can be exposed before the timber significantly changes the HRR and duration of the fire. Determining that limit is key to the design for

permitting a safe amount of timber to be exposed within a compartment. To accurately account for the exposed mass timber charring, the heat flux needs to be determined at the timber location, to then determine a char rate. The char depth can then be calculated based on the expected compartment HRR and the decay period of the fire can also be accounted for. This can be accomplished through relatively approximate methods using hand-calculations, or a more comprehensive approach using compartment fire modelling and computational fluid dynamics can be used.

7 Time Equivalence – Linking Char Depth and Fire Resistance

Time-equivalence is an approach developed to compare the severity of fire exposure under a real (natural) fire to a standard temperature time relationship for compliance fire testing. This enables direct comparison of an FRR for structural elements, as determined under standard fire exposure (controlled within a furnace), with the fire resistance determined through analysis or fire testing, in a natural fire. Time-equivalence is defined as the equivalent time it takes for the element to reach a maximum temperature under the natural fire, when exposed to the standard fire [23].

For a mass timber structural element, strength is a function of the size of the cross section. As timber chars in fire, the cross section reduces, which reduces the ability of the element to resist loads. For exposed mass timber, the reduced cross section of uncharred (strong) material must be sufficient to resist the design loads at the required FRR time, to achieve the required FRR. Time-equivalence for exposed timber is char related rather than temperature related (as for steel), hence the mismatch in the traditional approach to time-equivalence. For mass timber, the equivalent FRR period for a natural fire is the time at which the char depth equals the char depth resulting from exposure to the standard fire, for the required FRR period. This method ensures that the same cross section of strong un-charred timber remains to sustain loads under both heating regimes (hence equivalency, by strength).

8 Summary

High-rise buildings constructed with mass timber for the structure are being planned due to the sustainability benefits, the increased speed of construction and the potentially higher financial returns. High-rise buildings with areas of exposed timber structure will influence the fire dynamics, increasing the fire heat release rate if a fully developed fire can grow. If the area of exposed mass timber is not determined to be acceptable, then it could result in a fire that releases more energy than the structural elements have been tested to resist. CLT char fall off and gypsum board failure need to be avoided to achieve decaying fires. Calculation methods to address the impact of the increased fuel of the exposed timber on the compartment fire are being developed.

References

1. http://www.waughthistleton.com/project/murray-grove/
2. https://www.woodsolutions.com.au/Inspiration-Case-Study/forte-living
3. http://www.naturallywood.com/emerging-trends/tall-wood-buildings/ubc-brock-commons
4. Su J, LaFrance P, Hoehler M, Bundy M (2018) Fire safety challenges of tall wood buildings – phase 2: task 2 & 3 cross laminated timber compartment fire tests. Fire Protection Research Foundation, Report No. FPRF-2018-01
5. Frangi A, et al (2008) Fire behaviour of cross-laminated solid timber panels. Institute of Structural Engineering, ETH Zurich, Zurich, Switzerland
6. Klippel M (2014) Fire safety of bonded structural timber elements. ETH Zurich, Institute of Structural Engineering, thesis number 359
7. Crielaard R (2015) Self-extinguishment of cross-laminated timber, thesis, Delft University of Technology, Netherlands
8. Barber D, Crielaard R, Li X (2016) Towards fire safe design of exposed timber in tall timber buildings. In: Proceedings of the world conference of timber engineering, 22–25 August 2016, Vienna
9. Brandon D, Dagenais C (2018) Fire safety challenges of tall wood buildings – phase 2: task 5 - experimental study of delamination of cross laminated timber (CLT) in fire. Fire Protection Research Foundation, report no. FPRF-2018–05
10. Karacabeyli E, Douglas B (2013) CLT handbook, US edition FPInnovations SP529-E
11. ANSI/APA (2018) PRG-320 standard for performance-rated cross-laminated timber
12. American Society for Testing and Materials (2016) ASTM E119: standard test methods for fire tests of building construction and materials
13. Frangi A, Fontana M (2005) Fire performance of timber structures under natural fire conditions. In: Fire safety science – proceedings of the eighth international symposium, pp 279–290
14. Hakkarainen T (2002) Post-flashover fires in light and heavy timber construction compartments. J Fire Sci 20:133–175. https://doi.org/10.1177/0734904102020002074
15. McGregor C (2013) Contribution of cross laminated timber panels to room fires, thesis. Carleton University, Ottawa, Canada
16. Medina A (2014) Fire resistance of partially protected CLT rooms, thesis. Carleton University, Ottawa, Canada
17. Hadden R, Bartlett A, Hidalgo J, Santamaria S, Wiesner F, Bisby L, Deeny S, Lane B (2017) Effects of exposed engineered timber on compartment fire dynamics. In: Proceedings of the 12th international association of fire safety science symposium, Lund, 10 June to 16 2017
18. Hox K (2015) Branntest av massivtre SP fire research, report A15101 (in Norwegian, translated by Arup)
19. Emberley R, Gorska C, Bolanosa A, Lucherinia A, Solartea A, Soriguera D, Gutierrez M, Humphreys K, Hidalgoa J, Maluka C, Law A, Torero J (2017) Description of small and large-scale cross laminated timber fire tests. Fire Saf J 91:327–335
20. Zelinka S, Hasburgh L, Bourne K, Tucholski D, Ouellette J (2018) Compartment fire testing of a two-story mass timber building. General technical report FPL–GTR–247, May 2018
21. Just A, Brandon D, Nele Mäger K, Pukk R, Sjöström J, Kahl F (2018) CLT compartment fire test. In: Proceedings of world conference on timber engineering, 20–22 August 2018, Seoul
22. Su J, Leroux P, Lafrance P, Berzins R, Gratton K, Gibbs E, Weinfurter M (2018) Fire testing of rooms with exposed wood surfaces in encapsulated mass timber construction. National Research Council, Canada report no. A1-012710.1
23. Buchanan A (2001) Structural design for fire safety. Wiley, Hoboken

Australian Building Code Change - Eight-Storey Timber Buildings

Paul England[1] and Boris Iskra[2(✉)]

[1] EFT Consulting, Upwey, VIC 3158, Australia
paul.england@eftconsult.net
[2] Forest and Wood Products Australia, Melbourne, VIC 3000, Australia
boris.iskra@fwpa.com.au

Abstract. Changes introduced in the 2016 edition of the Building Code of Australia permitted residential and office buildings to be of timber-framed or massive timber construction up to 25 m in effective height as a Deemed-to-Satisfy solution for the first time; typically, eight-storeys. This approach was extended in the 2019 edition of the BCA, to all classes of buildings – including retail premises, schools, hospitals and aged-care buildings of timber-framed and massive timber construction.

Detailed fire engineering modelling and multi-scenario analyses supplemented by full-scale fire testing were undertaken as part of the BCA approval process which compared the risk-to-life achieved by fire protected timber buildings to that of similar buildings (reference cases) constructed using non-combustible forms of construction. The analysis considered factors such as the frequency of potential flashover fires, effectiveness of automatic fire sprinklers, barrier (wall, floor/ceiling) performance, enclosure heating regime, occupant behaviour and fire brigade intervention. The analysis demonstrated that structural timber building elements (wall frame, floor/ceiling, shafts) protected by specified fire-protective grade plasterboard coverings can achieve a higher level of safety than traditional non-combustible construction.

Keywords: Australia · Code · Timber · Fire · Engineering

1 Introduction

The Building Code of Australia (BCA) [1] includes two pathways to demonstrate compliance with its performance requirements; a prescriptive Deemed-to-Satisfy (DTS) pathway and a Performance pathway. The Performance pathway allows fire engineering methods to be used to demonstrate compliance of a building solution creating greater flexibility; but a more complex approval process needs to be followed. Prescriptive DTS solutions are most popular for simple low and mid-rise forms of construction where it is difficult to justify the cost and project risks associated with developing and gaining approval of complex performance solutions.

Prior to 2016, the DTS provisions required the use of non-combustible materials for the construction of structural loadbearing elements (e.g. walls, floors, columns and beams) in mid-rise buildings. These restrictions are summarised in Table 1 which is based on content from the BCA Guide to Volume One.

L. Makovicka Osvaldova et al. (Eds.): WFS 2020, *Wood & Fire Safety*, pp. 219–225, 2020.
https://doi.org/10.1007/978-3-030-41235-7_33

Table 1. Building elements required to be non-combustible, concrete or masonry in buildings of Type A and B Construction

Building element	DTS - requirement
External walls	Non-combustible
Common wall	Non-combustible
Loadbearing internal walls and shafts	Concrete or Masonry
Loadbearing fire walls	Concrete or Masonry
Non-loadbearing fire-resisting walls and shafts	Non-combustible

To remove these restrictions, a Proposal-for-Change (PFC) was prepared and submitted by Forest and Wood Products Australia, to include DTS solutions in the BCA based on the use of "fire-protected timber" construction. It was requested that these changes apply to Class 2 (apartments), Class 3 (e.g. residential parts of hotels and motels, accommodation for the aged) and Class 5 (offices). To justify these changes, a detailed fire engineering risk-based analysis was undertaken supported by full-scale fire tests. The PFC was accepted, and the necessary changes were introduced in the 2016 edition of the BCA.

Subsequently, a further PFC was submitted and accepted for the BCA 2019 which now includes DTS provisions to permit the use of fire-protected timber construction in all classes of building including retail premises, schools, hospitals and aged-care facilities up to 25 m in effective height (typically 8 storeys); the 25 m effective height limit defines the boundary between what is considered mid-rise construction and high-rise construction in Australia *Note: Effective height is the vertical distance between the floor of the lowest storey (typically the ground floor which provides direct egress to a road or open space) and the floor of the topmost habitable storey.*

As a result of these changes, for the first time in Australia, any class or combination of building classes can be constructed under the BCA DTS provisions for both traditional 'timber-frame' (lightweight) and 'massive timber' systems (e.g. laminated veneer lumber and cross-laminated timber). These solutions require the timber elements to be protected by appropriate layers of fire-protective grade coverings such as fire-protective grade plasterboard (termed *fire-protected timber*), the use of compliant automatic fire sprinkler systems, any insulation used within cavities must be non-combustible and cavity barriers must be provided unless massive timber construction is adopted.

2 The Building Code of Australia (BCA)

The BCA is an initiative of the Council of Australian Governments that incorporates all the on-site construction requirements in the one code. It is a Performance based code and the relevant performance requirements need to be satisfied by either applying the Deemed-to-Satisfy (DTS) Provisions or developing a Performance Solution (e.g. fire engineered solution). Volume One is applicable to the fire safety design of mid-rise buildings, amongst other things, and is the focus of this paper.

The BCA adopts a holistic approach to fire safety based on early work on a fire safety systems approach described by Beck [2] and developed into the Draft National Safety Systems Code [3]. This risk-based approach recognised that the optimum fire safety solution for a building can be identified by considering the interactions between fire safety sub-systems such as passive fire protection/structural design, active fire protection systems, fire brigade intervention and occupant behaviour and response etc. This is best demonstrated by examining a typical performance requirement (CP1), which had to be satisfied by the fire-protected timber mid-rise DTS solutions introduced into the BCA in the 2016 and 2019 editions, which states:

"*CP1 Structural stability during a fire*

A building must have elements which will, to the degree necessary, maintain structural stability during a fire appropriate to—

(a) *the function or use of the building; and*
(b) *the fire load; and*
(c) *the potential fire intensity; and*
(d) *the fire hazard; and*
(e) *the height of the building; and*
(f) *its proximity to other property; and*
(g) *any active fire safety systems installed in the building; and*
(h) *the size of any fire compartment; and*
(i) *fire brigade intervention; and*
(j) *other elements they support; and*
(k) *the evacuation time*."

CP1 requires the structural stability during a fire to be considered, having regard for, active fire safety systems such as automatic fire sprinklers, if provided, and fire brigade intervention, amongst other things. This enables the potential failures of passive fire protection systems to be directly considered and addressed by the provision of additional sub-systems such as automatic sprinklers to provide a more robust solution. In the case of fire-protected mid-rise timber building solutions, the risk-based fire safety systems approach, facilitated by the NCC, enabled the potential for contributions to the fire load from the timber structural elements and the risk of substitution of fire-protective coverings with non-fire-rated products to be accounted for in addition to the risk of the sprinkler system and fire brigade intervention being in-effective.

3 Fire Engineering Analyses and Risk Assessment

As part of the proposal justifying the 2016 changes, fire engineering analyses and risk assessments were undertaken for Class 2, 3 and 5 buildings which are described in England [4] with details of typical fire-protected timber construction details provided in England and Iskra [5]. A description of the fire engineering analyses and risk assessments undertaken to address the remaining building classes within the scope of Volume One of the NCC follow.

A comparative risk assessment was undertaken to demonstrate that the fire-protected timber mid-rise building solutions were equivalent to, or safer than, the DTS non-combustible construction and concrete and masonry construction for risk-based groupings categorized as high, medium and low.

3.1 Building Characteristics

A characterisation of building classes 2 to 9, and comparative risk assessments were undertaken based predominantly on the parameters for consideration extracted from the relevant performance requirements (refer Sect. 2 above).

3.2 Scenario Development

The following process was adopted to derive scenarios for further analysis and to determine the depth of analysis required

- A comparative risk analysis based on published fire data and correlations was undertaken to compare the fire risks relating to the BCA Classes of Buildings. The building classes were then grouped into high, medium and low risk classes and common key attributes identified (Fig. 1).
- The previous analyses undertaken for NCC 2016 [5], apartment, hotel/motel and office buildings were reviewed to identify to what extent the results could be applied to other building classes.
- A qualitative risk analysis was undertaken to compare the fire risk within the fire compartment of fire origin and to identify fire scenarios that are not critical to the analysis.
- Scenarios for further analysis and appropriate methods of analysis were then identified.

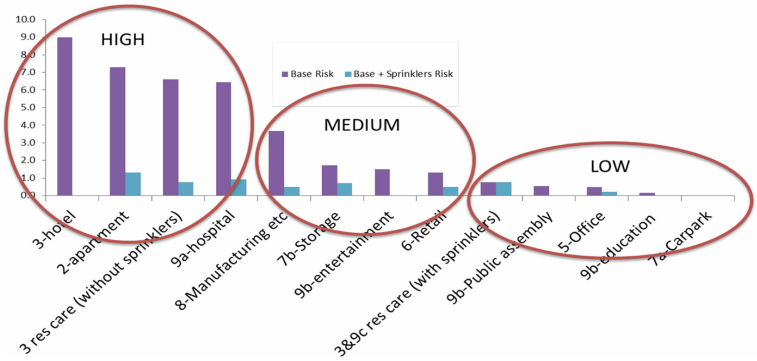

Fig. 1. Comparative fire risk assessment of building classes based on fire data. Note the BCA building class numbers modelled, and descriptions are also provided.

3.3 Medium Risk Building Multi-scenario Analysis

The risk to occupants outside the compartment of fire origin will depend on the speed of response of the occupants, amongst other things. Since apartment occupancies tend to have relatively slow evacuation times due to the occupant characteristics, limited emergency management structure and alarm system functions, a ground floor comprising retail shops with very high fire loads and with apartments on the upper floors was selected for a multi-scenario analysis to evaluate medium fire risk classes with the potential for very high fire loads.

A fast-growing potential fully developed fire was assumed to occur on the ground floor at a time when the shops are not occupied (overnight) providing the greatest potential to compromise evacuation paths from the upper levels. This configuration was expected to present the greatest societal risk to occupants on the upper floors given early identification of the fire by occupants would be unlikely, occupancy rates would be high and occupant response would be slow. Therefore, the results were considered conservative to apply to all the medium and low risk buildings.

It was also assumed that the fire isolated stairs/passageways were common to all levels even though independent exits on the ground floor would be expected to be provided in most situations. This selected configuration provided a potential path for smoke spread to higher levels and for exits from upper levels to be compromised by smoke spread representing an onerous configuration.

The results and analysis of the multi-scenario analysis provided an indication of the relative expected risk to life/individual risk for occupants in the upper apartment levels from a fire occurring in the retail area on the ground floor by comparing the total number of groups exposed to untenable conditions/100,000 fires. These results were normalised against the risk for the DTS solution showing significant reductions in risk for fire-protected timber buildings due to the provision of BCA compliant automatic fire sprinkler systems (Table 2).

Table 2. Comparative risk to apartment occupants above a retail part of the building

Building solution	Comparative risk
BCA DTS	1.00
Timber-frame	0.16
Massive timber	0.11

It was considered reasonable to apply these results to all non-residential and non-healthcare occupancies (i.e. Class 5 to 8 and 9b).

3.4 High Risk Buildings Assessment Multi-scenario Analysis

If sprinkler protection was not provided in Class 9a buildings such as hospitals and Class 9c residential aged-care buildings, these occupancies would present a high-risk. The floor plan layouts of these buildings and fire safety strategies vary from the previous analysis undertaken for apartment and hotel/motel type buildings [4] using fire

and smoke sub-compartmentation. To account for these variances, separate analyses were undertaken for these two building Classes.

For Class 9a buildings, the fire-protected timber solution requires sprinkler protection throughout the building in addition to permitting the use of fire-protected timber in lieu of non-combustible, masonry or concrete construction. The NCC 2016 DTS provisions do not mandate the use of automatic fire sprinklers if a zone pressurisation system is provided in a 9a building.

Fire data was used to compare the results within the compartment of fire origin and a large reduction in the risk-to-life would be expected due to the introduction of automatic fire sprinkler protection for the fire-protected timber building solutions; estimated to be typically in the range of 61–88%.

To evaluate the risk to occupants outside the fire compartment of fire origin, a multi-scenario analysis was undertaken based on a generic Class 9a configuration. The consolidated comparative risk results from the multi-scenario analysis indicated risk reductions between 70 and 73% for the fire-protected timber options compared to the NCC 2016 DTS building solutions. It was therefore concluded that if fire-protected timber construction requirements are applied to Class 9a buildings there is likely to be a substantial reduction in the risk-to-life from fires.

The NCC 2016 DTS Class 9c building differs from other classes described above in that sprinkler protection is mandated but combustible construction is permitted for certain internal walls and floors and lower FRLs are prescribed for some structural elements compared to other similar occupancies in recognition of the impact of sprinkler protection. Class 9c buildings did not require fire resistant or smoke proof walls to be fitted with fire protective coverings that achieve Resistance to Incipient Spread of Fire ratings, as required for fire-protected timber construction, therefore the fire-protected timber requirements enhanced the required fire resistance of some elements.

The net impact was that within the floor of origin the risk-to-life was expected to be similar for all options, based on a comparison of fire safety measures, due largely to the provision of automatic fire sprinklers in all cases with comparative risk results from the multi-scenario analysis indicated risk reductions between 3 and 13% for the fire-protected timber options compared to the corresponding NCC 2016 DTS building solutions.

4 Conclusion

This paper provides background to the fire safety analysis undertaken to achieve the 2019 Australian building code change to permit the use of fire-protected timber building elements, with an automatic fire sprinkler system, in all classes of buildings up to 25 m in effective height for both timber-framed and massive timber buildings.

Acknowledgments. The authors express their sincere appreciation to Mr Ric Sinclair (Managing Director, FWPA) and to industry stakeholders who provided their valuable time and input during the 2-year development of the NCC 2019 Proposal-for-Change.

References

1. National construction code volume one (2019) Building code of Australia – Class 2 to 9 Buildings. Australian building codes board, Canberra
2. Beck VR (1994) Fire research lecture 1993: performance-based fire safety design—Recent developments in Australia. Fire Saf J 23(2):133–158
3. Microeconomic reform (1991) Fire regulation draft national fire safety systems code, building regulation review task force. Canberra, Australia
4. England JP (2016) Fire safety design of mid-rise timber buildings – basis for the 2016 changes to the National Construction Code. In: Technical design guide 38, WoodSolutions, Melbourne
5. England JP, Iskra B (2016) Mid-rise Timber buildings – Class 2, 3 and 5 buildings. In: Technical design guide 37, WoodSolutions, Melbourne

A Case Study Comparing the Fire Risk in a Building of Non-combustible Frame and a Timber Frame Building

Bjorn Karlsson[1(✉)], Iris Gudnadottir[2], and Bodvar Tomasson[1,3]

[1] University of Iceland, Reykjavik, Iceland
bjorn@mvs.is
[2] Securitas, Reykjavik, Iceland
[3] EFLA Consulting Engineers, Reykjavik, Iceland

Abstract. In the last two decades, a considerable number of multi-storey apartment buildings have been constructed in the Nordic countries using timber as load-bearing material. Such constructions have earlier not been allowed by the authorities, mainly due to the fire risk. The Nordic countries there-fore co-operated for some years, within an organisation named Nordic Wood, with the aim of developing construction methodologies that seriously diminish the fire risk in timber-frame multi-storey buildings.

Authorities and industry found that it was necessary to develop a new fire risk assessment technique to verify that fire safety can be as high in timber-frame buildings as in other types of buildings, given that the right construction methods be used. Nordic Wood therefore initiated work that led to the development of FRIM-MAB, a Fire Risk Index Method for Multi-storey Apartment Buildings.

The method has been described in several reports and papers and was evaluated against a much more elaborate Quantitative Risk Analysis (QRA) method. Both the index method and the quantitative risk analysis were used to rank four different buildings with respect to fire risk and the ranking was identical. The method was then further tested, where 20 timber frame buildings in four Nordic countries were analysed.

This work has recently been taken further by comparing the fire risk in a building of a non-combustible frame in 6 storeys and a similar timber frame building. This paper reports on that comparison.

Keywords: Fire risk · Index method · Timber frame buildings

1 Introduction

During the last few years, the trend in a significant part of the world has been to introduce performance-based building regulations instead of the detailed regulations used earlier. The new possibilities have opened the way for new design solutions, e.g. new applications for timber-structures, and many such buildings have been constructed in the Nordic countries.

L. Makovicka Osvaldova et al. (Eds.): WFS 2020, *Wood & Fire Safety*, pp. 226–231, 2020.
https://doi.org/10.1007/978-3-030-41235-7_34

Since multi-storey timber frame buildings were earlier restricted in building regulations in the Nordic countries due to fire risk, authorities and industry found that it was necessary to develop a new fire risk assessment technique to verify that fire safety can be as high in timber-frame buildings as in other types of buildings, given that the right construction methods be used. A research and development program called Nordic Wood therefore initiated work that led to the development of FRIM-MAB, a Fire Risk Index Method for Multi-storey Apartment Buildings. The initial work was done by Magnusson et al. [1] and methodology used for developing the index method is based on principles established by a number of authors in the field.

The method, its development, its testing and its evolvement is described in a number of reports and papers [2–6] as well as by Karlsson and Tomasson [7, 8]. The method was evaluated against a much more elaborate Quantitative Risk Analysis (QRA) method. Both the index method and the quantitative risk analysis were used to rank four different buildings with respect to fire risk and the ranking was found to be identical, indicating some validity of the method.

Nordic Wood found it necessary to further test the method, where 20 timber frame buildings in four Nordic countries were analysed. This resulted in the determination of a limiting risk index value based on the minimum demands made in the building regulations for each Nordic country, thus establishing a certain benchmark for users of the index method. The repeatability of the method was also studied substantially, showing good repeadability [6].

This paper describes the above and reports on further work by Gudnadottir [9] as well as recently completed work comparing different strategies applied to a timber-frame building and a building with a concrete frame.

2 General Description of the Method

The FRIM-MAB method can be divided into 17 different parameters, P_1–P_{17}, where each parameter is given a grade. Five engineers were asked to give five grades for the same parameter, and they did this for four different buildings. The results show that the repeatability is excellent for most parameters and quite good for other parameters. The main result is that the overall repeatability is very good [6].

The Fire Risk Index Method for Multi-storey Apartment Buildings (FRIM-MAB) is based on a hierarchical system. Each "decision-making level" of the hierarchy is composed of different "attributes", i.e. components that account for an acceptably large portion of the total fire safety. The attributes of FRIM-MAB were derived using the well-established NFPA Fire Safety Concepts Tree [10]. Figure 1 shows a simplified schematic of the policy, objectives, strategies and parameters, the full definitions are given by Karlsson [2].

The 17 parameters are listed in Fig. 1. The parameters can then be divided into sub-parameters that are quantifiable, either directly or through the use of Decision Tables. Figure 2 shows a fictive example of how decision tables and sub-parameters can be used to arrive at a numerical score or grade for a given parameter. The user then works through each parameter until all parameters have been given a grade. Finally, the grades are entered into a table and multiplied by weights. A Delphi panel process was

used to determine the weight of each parameter. These weighted grades are then summed up and result in a single index value for the building in question. The lowest risk index value is 0 and the highest is 5.

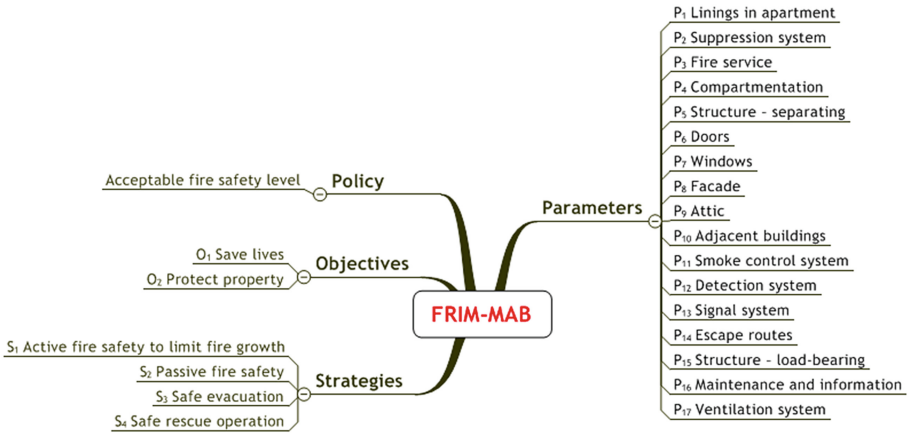

Fig. 1. Overview of the hierarchical system of FRIM-MAB.

P_2. SUPPRESSION SYSTEM
DEFINITION: Equipment and systems for suppression of fires

SUB-PARAMETER P_{2a}, Automatic sprinkler system
Type of sprinkler (N = no sprinkler, A = apartment sprinkler, O = ordinary sprinkler) and Location of sprinkler (A = in apartment, E = in escape route, B = both in apartment and escape route)

SURVEY ITEMS	DECISION RULES						
Type of sprinkler	N	A	A	A	O	O	O
Location of sprinkler	-	A	E	B	A	E	B
GRADE	N	M	L	H	M	L	H

(N = no grade, L = low grade, M = medium grade and H = high grade)

SUB-PARAMETER P_{2b}, Portable equipment

N	None
F	Extinguishing equipment on every floor
A	Extinguishing equipment in every apartment

RESULTING PARAMETER GRADE:

SUB-PARAMETERS	DECISION RULES											
Automatic sprinkler system	N	N	N	L	L	L	M	M	M	H	H	H
Portable equipment	N	F	A	N	F	A	N	F	A	N	F	A
GRADE	**0**	**1**	**1**	**2**	**2**	**2**	**3**	**3**	**4**	**4**	**5**	**5**

(Minimum grade = 0 and maximum grade = 5)

Fig. 2. A fictive example of how parameters are graded using survey items, sub-parameters and decision tables.

3 Evaluating and Testing the FRIM-MAB Method

The FRIM-MAB method has been tested and evaluated in a number of different ways. This section will describe how the method was tested against a relatively complex Quantitative Risk Analysis method and applied to 20 different multi-storey apartment buildings. These results were compared against the minimum allowable requirements made in the Nordic building regulations. Also, a repeatability test was carried out where five different engineers used the same documentation to evaluate four different buildings.

3.1 Evaluation Against a Quantitative Risk Analysis (QRA) Method

In order to get some idea of the validity of the Fire Risk Index Method, work was carried out with the aim to compare it against accepted fire design methods. A standard quantitative risk analysis (QRA) based on an event tree was used as a comparative methodology.

Four buildings were analysed, using a QRA methodology and the index method. The resulting event trees for each of these buildings are too complex to be reproduced here, but they are given by Hultquist and Karlsson [5]. When comparing results from the QRA method with the index method it was found that both methods produce the same ranking.

3.2 Testing the Method and Determining a Limiting Risk Index Value

Although the QRA and Index Method comparison gave credibility to the latter, Nordic Wood found it necessary to further test the method. Therefore, 20 timber frame buildings in four Nordic countries were analysed. Also, the building codes of the four Nordic countries were investigated in order to determine a limiting risk index value based on the minimum demands made in the building regulations for each Nordic country, thus establishing a certain benchmark for users of the index method. Results for Sweden, Norway, Finland and Denmark are given in the full report. Figure 3 shows the results when 15 Swedish multi-storey apartment buildings were analysed and the minimum demands in the Swedish Building Code were determined as being 2.75 (the maximum attainable risk index value being 5).

3.3 Repeatability of the Fire Risk Index Method

Four multi-storey apartment buildings were chosen among the 20 buildings analysed in the work by Karlsson and Christensson [1, 3]. Drawings and fire documentation of these four buildings were sent to five different fire safety engineers who analysed the buildings according to the FRIM-MAB methodology. Their results were compared with each other, in order to test the repeatability of the risk index method.

In general, it can be said that most engineering methods will have issues with repeatability. The investigation into the FRIM-MAB method shows quite good results with respect to repeatability.

4 Case Study: Comparing a Timber-Frame and Concrete Building

A case study was carried out using an existing 6 storey apartment building made mainly of concrete at Tryggvagata 18 in Reykjavik (referred to a T18), completed in 2008. A detailed study was presented by Gudnadottir [9] and this is presented very summarily here.

The study was carried out on four different design strategies as follows

- CONCRETE (no changes to the T18 building)
- TIMBER1 (timber used as load-bearing material)
- TIMBER2 (timber as load-bearing material and timber façade)
- TIMBER3 (same as TIMBER2 but sprinkler system added)

Detailed background, analysis and results are given by Gudnadottir [9], resulting in the outcome presented in Table 1.

Table 1. Resulting risk index for the four design alternatives of T18.

Design alternative	Risk index
CONCRETE	1,89
TIMBER1	1,98
TIMBER2	2,14
TIMBER3	1,83

The results show that the least fire risk is TIMBER3, a building with a timber façade and a sprinkler system. Gudnadottir [9] reports on the background of the work and recent work has been described in internal reports, soon to be published.

5 Conclusions

Due to advances in building regulations, many timber frame multi-storey apartment buildings have been constructed in the Nordic countries. However, until now, no comprehensive method to estimate fire risks in such buildings has been available to designers. This paper has:

- outlined a methodology for developing risk index methods for this purpose
- described the development and testing of such a method, FRIM-MAB
- shown how the method was evaluated against a more complex quantitative risk analysis technique
- described how it was tested on 20 different buildings in the Nordic countries, resulting in the determination of a limiting risk index value based on the minimum demands made in the building regulations for each Nordic country
- shown how five different engineers used the method to analyse four different buildings, indicating that the method has very good repeatability

- given simple examples of how the method was applied to different design problems, comparing a concrete building with timber-frame buildings with various design approaches such as a wooden façade and a sprinkler system.

References

1. Magnusson SE, Rantatalo T (1998) Risk assessment of timberframe multistorey apartment buildings – proposal for a comprehensive fire safety evaluation procedure, Report 7004, Department of Fire Safety Engineering, Lund University, Lund, Sweden
2. Karlsson B (2000) Fire risk index method for multi-storey apartment buildings report I0009025, Trätek AB, Stockholm
3. Karlsson B, Larsson D (2000) Using a delphi panel for developing a fire risk index method for multi-storey apartment buildings, Report 3114, Department of Fire Safety Engineering, Lund University, Lund, Sweden
4. Larsson D (2000) Developing the structure of a fire risk index method for multi-storey apartment buildings, Dept. of Fire Safety Eng., Lund University, Report 5062, Lund
5. Hultquist H, Karlsson B (2000) Evaluation of a fire risk index method for multi-storey apartment buildings, Report 3088, Department of Fire Safety Engineering, Lund University, Lund
6. Karlsson B, Christensson A (2002) Repeataility test of FRIM-MAB, Report P 0212052, Trätek, Stockholm
7. Karlsson B, Tomasson B (2001) A fire risk index method for multi-storey apartment buildings. In: Proceedings of the ninth international conference, interscience communications Ltd., London
8. Karlsson B, Tomasson B (2001) Repeatability tests of a fire risk index method for multi-storey apartment buildings, fire safety science. In: Proceedings of the eight international conference. International Association for Fire Safety Science, London
9. Gudnadottir I (2011) Timber as load bearing material in muldi-storey apartment buildings: a case study comparing the fire risk in a building of non-combustible fram and a timber-frame building, University of Iceland
10. NFPA (1995) NFPA 550 Guide to the fire safety concepts tree, 1995 Ed., MA, USA

Overview of North American CLT Fire Testing and Code Adoption

Samuel L. Zelinka(✉), Laura E. Hasburgh, and Keith J. Bourne

USDA Forest Service Forest Products Laboratory, Madison, WI 53715, USA
samuel.l.zelinka@USDA.gov

Abstract. Cross laminated timber (CLT) is becoming more widely available in North America. However, it has not yet achieved widespread use in construction in the United States because provisions for CLT have only recently been added to model building codes. For example, CLT was recognized for the first time in the 2015 *International Building Code* (IBC), and the 2021 IBC will allow wood buildings made of CLT and other types of mass timber to be constructed up to 18 stories high. The changes to the 2021 IBC were implemented after several years of work from an ICC Ad-Hoc committee on tall wood buildings including fire testing supervised by the US Forest Service, Forest Products Laboratory. The fire tests involved five compartment fire test scenarios on a two-story building and specifically examined occupant egress and firefighter safety in corridors near the compartments. In addition to the fire tests performed by the Forest Products Laboratory, more large-scale fire tests were performed for the revision of the PRG-320 standard; the product standard for CLT in North America. These tests examined the heat resistance of adhesives used in CLT. This paper highlights the important changes to the IBC and the PRG-320 standard as well as summarizes the tests used to validate these changes.

Keywords: Cross laminated timber (CLT) · Fire resistance · Compartment fire testing · Standardization

1 Introduction

Cross laminated timber (CLT) is a massive engineered wood composite panel made from alternating layers of dimension lumber. CLT panels can be made up to 18 m long and are delivered to the jobsite with all fenestrations precut [1]. CLT's versatility as a potential material for wall and floor systems has sparked an interest in mass timber buildings in North America [2–4]. In addition to the erection of CLT buildings, the number of North American CLT manufacturers is rapidly growing [5].

The International Building Code (IBC) dictates the maximum height and area based on construction type. To build beyond these limits with wood, including mass timber, an alternative means-and-methods approach is needed to demonstrate equivalent safety to a building allowed by the code. Typically testing is needed to demonstrate this equivalency. Recently, there have been several large, full-scale testing programs of CLT compartments conducted in North America. These tests provided data in support of mass timber projects throughout North America that justified IBC recognition of

L. Makovicka Osvaldova et al. (Eds.): WFS 2020, *Wood & Fire Safety*, pp. 232–237, 2020.
https://doi.org/10.1007/978-3-030-41235-7_35

three new mass timber construction types which allow significantly greater heights and areas than are permitted for traditional Type IV (heavy timber) construction. This paper provides an overview of these recent test series and changes to the IBC.

2 Fire Protection Research Foundation (FPRF) Tests

A large-scale test series was conducted from February to April, 2017 at the fire laboratory of the National Institute of Standards and Technology (NIST) in Gaithersburg, MD, USA. It was funded by the Fire Protection Research Foundation (FPRF) and the tests were carried out by the National Research Council of Canada (NRC). The test series was the second phase of an FPRF research program looking at CLT buildings. The goal of the test series was to better understand the contribution of CLT to compartment fire dynamics. The first phase resulted in a literature review and gap analysis of the research needs for CLT buildings [6]. Below is a summary of the test series; full details can be found in the final report [7].

2.1 Test Matrix

In total, six compartment fire tests were completed in this series. Each test compartment was 9.1 m × 4.6 m × 2.7 m and constructed from 5-ply CLT (175 mm thick) manufactured with a polyurethane adhesive that does not pass the 2018 PRG 320 fire test protocol (Sect. 4). The fuel load was 550 MJ m^{-2}. A unique aspect of the test program was that two ventilation configurations were used across the 6 tests. The two opening factors were 0.03 $m^{0.5}$ and 0.06 $m^{0.5}$. In addition to studying the effect of ventilation, the amount of protection of the CLT with gypsum wallboard was also examined. Three tests are summarized in this paper; a baseline case where all surfaces were covered with 3 layers of gypsum wallboard with an opening factor of 0.03 $m^{0.5}$ (Test 1–1), a test with one exposed wall (9.1 × 2.7 m) and an opening factor of 0.03 $m^{0.5}$ (Test 1–5), and a test with one exposed wall (9.1 × 2.7 m) and an opening factor of 0.06 $m^{0.5}$ (Test 1–3). Test 1–4 had an opening factor of 0.03 $m^{0.5}$ with a fully exposed ceiling and was used in the development of the PRG 320 standard (Sect. 4).

2.2 Results

The test matrix allows a straightforward examination of the effect of exposed CLT and ventilation factors. Figure 1 shows heat release data from tests 1–1, 1–3, and 1–5. Test 1–1 was the baseline case for the small opening factor. All CLT surfaces were protected on the walls and ceiling in this test. The fire reached flashover at 14.9 min and started to decay around 50 min until it self-extinguished between 2–3 h.

Test 1–5 had a similar opening factor to that of Test 1–1 but an exposed wall. In this test, the fire exhibited largely the same behavior during the first 50 min, except that the heat release rate was slightly higher due to the exposed wall. However, the decay period of Test 1–5 was noticeably different from that of Test 1–1. Between 50 and 75 min, the first layer of CLT delaminated; this exposed unburnt surfaces of the second

layer of CLT, which burned and increased the heat release rate. Starting at 140 min, the second layer of CLT delaminated, which resulted in an increased fuel load and thus an increase in heat release rate. This caused a second flashover in the compartment, which caused the gypsum wallboard on the ceiling to fail and continued fire growth until the test was terminated.

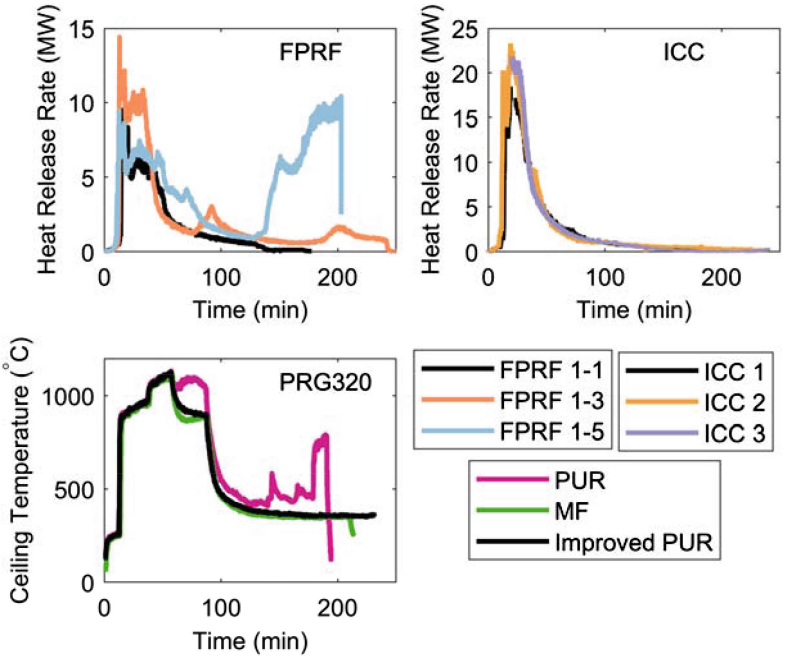

Fig. 1. Relevant test data from the three large scale test series discussed in the paper. (Data replotted from [7–9]).

Like Test 1–5, Test 1–3 had an exposed wall, but a much larger opening factor. Flashover occurred at nearly the same time. However, in Test 1–3, the fully developed fire was more intense but of a shorter duration with decay beginning to occur at 35 min. Although flaming combustion on the exposed wall had ceased by around 50 min due to the formation of a protective char layer, flaming combustion of the exposed wall was observed again at 80 min, which corresponds with the increase in heat release. This was due to the failure of the first bond line of CLT. At 180 min into the test, the second layer of CLT fell off and the third layer began to char. This second bond line failure also resulted in an increase in heat release rate, although to a lesser extent. Subsequent to both of these bond line failures, the fire self-decayed. The test was terminated at 4 h.

3 International Code Council (ICC) Tests

The International Code Council (ICC) formed an ad-hoc committee to study the safety of tall wood buildings and explore the potential adoption of tall wood buildings through the ICC code proposal process. The ad-hoc committee determined that more fire test data were needed to support potential code changes. The American Wood Council (AWC) worked with the US Forest Service, Forest Products Laboratory (FPL) to carry out the test program. The tests were conducted at the US Department of Justice Alcohol Tobacco Firearms and Explosives Fire Research Laboratory (ATF). Below is a summary of the tests; full details can be found in the final report [8].

3.1 Test Matrix

The ICC tests consisted of five fire tests conducted in a one-bedroom apartment. The test structure was two stories tall and had identical one-bedroom apartments (9 m × 9 m × 2.7 m) on each level. In addition to the apartments, there was a corridor on each floor and a stairway between the two floors, which were monitored to evaluate firefighter safety and occupant egress. The CLT was 5 layers, 175 mm thick and utilized the same polyurethane adhesive as the CLT used in the FPRF tests. The fuel load was 570 MJ m^{-2}. Compared to the FPRF tests, the ventilation factor was much bigger; 60% of one of the 9 × 2.7 m walls which is equivalent to an opening factor of 0.09 $m^{0.5}$. Tests 4 and 5 examined the effect of automatic sprinkler systems on fire suppression in CLT buildings and are not discussed further in this paper. Test 1 was a baseline where all surfaces were protected with gypsum wallboard. In Test 2, 30% of the area of the ceiling was exposed in the living room and bedroom. In Test 3, there was one, fully exposed wall in both the living room and the bedroom.

3.2 Results

Figure 1 presents the heat release rate curves collected in the ICC tests. In contrast to the FPRF tests, full burnout was achieved in all three ICC tests performed without an automatic fire sprinkler system. Furthermore, after the decay phase started, the heat release did not increase for any of the three tests. Some localized flaming and char falloff were observed late in Tests 2 and 3. However, at this time, the compartment had cooled considerably from the peak temperatures and no fire regrowth occurred.

4 Product Standard PRG 320

PRG 320 is the product standard for cross-laminated timber in North America. In the 2018 revision of the standard, a new method was developed to qualify adhesives to ensure that delamination of CLT did not occur due to adhesive failures during fire scenarios. Adhesives for use in PRG 320 compliant CLT must pass a large scale test as described in Annex B of the standard [10].

The PRG 320 large scale test method was designed to mimic the exposure to which the exposed CLT ceiling was subjected in FPRF Test 1–4, where delamination and

subsequent fire regrowth occurred. In the tests, a compartment 5.8 m × 2.7 m × 2.4 m is constructed with an exposed CLT ceiling and an opening factor of 0.03 $m^{0.5}$ to match the FPRF test.

Instead of a prescribed fuel load, the compartment temperature profile is controlled by a gas burner. In a "calibration test" where the CLT is not exposed, the fuel to the burner is measured while a specific temperature profile is maintained at the ceiling for a 240 min test. This fuel flow rate is then duplicated in tests with CLT panels. The ceiling and compartment temperatures are monitored in tests with CLT. The CLT adhesive qualifies under PRG 320 Annex B if the temperature measured within the compartment stays below 510 °C during the last 90 min of the test. As stated in PRG 320, this is intended to identify and exclude use of adhesives that permit CLT delamination resulting in fire regrowth during the decay phase of a fully developed fire.

4.1 Results

As each company is responsible for testing their own products, there is little published data on the test method. However, the American Wood Council sponsored testing on CLT made with three different adhesives and the final test report is available [9].

Three different CLT panels were tested: a CLT made from spruce-pine-fir with a polyurethane adhesive, a CLT made from Douglas fir-larch with a melamine-formaldehyde adhesive and one made from Douglas fir-larch with an "improved polyurethane adhesive". The polyurethane adhesive used on the spruce-pine-fir specimen was the same adhesive used in the FPRF and ICC tests. This specimen was tested in order to validate the test method by ensuring that the fire growth (and regrowth) behavior was similar to that observed in FPRF Test 1–4.

The ceiling temperature as a function of time are shown for three adhesives in Fig. 1. The temperature decays for the melamine-formaldehyde and improved polyurethane adhesive demonstrated that they do not exhibit delamination leading to fire regrowth under the conditions in which delamination was observed in the FPRF test. Further testing on smaller compartments has also demonstrated the effectiveness of the improved polyurethane formulation [11].

5 Conclusions

This paper summarizes several large, North American testing programs that have looked at the fire dynamics of CLT compartments and have shaped building code development in North America. Of primary importance in all testing was the performance of the adhesives during the fire.

In the FPRF tests, delamination and subsequent fire regrowth was observed in several tests, especially with the smaller opening factor. In contrast, the ICC tests used the same adhesive, however, only localized char falloff and no fire regrowth was observed. These tests highlight the importance of the opening factor in the fire safety of CLT buildings. The latest version of the PRG 320 standard contains a large-scale fire test specifically designed to screen adhesives that may delaminate and lead to fire

regrowth. The improved polyurethane adhesive showed no fire regrowth, even with the small ventilation factor.

These fire tests have been important in the code development and code adoption of CLT in the United States. The changes to the PRG 320 standard appreciably decrease the likelihood of fire regrowth caused by delamination in a potential fire in a CLT building.

References

1. Mohammad M, Gagnon S, Douglas BK, Podesto L (2012) Introduction to cross laminated timber. Wood Des Focus 22:3–12
2. Green M, Karsh J (2012) TALL WOOD- The case for tall wood buildings. Report prepared for the Canadian Wood Council on behalf of the wood enterprise coalition and forest innovation investment, Vancouver, BC
3. Iqbal A (2018) Recent developments in tall wood buildings. In: Mukhopadhyaya P (ed.) 1st international conference on new horizons in green civil engineering (NHICE-01), Uniersity of Victoria, Victoria, B.C., pp 111–116
4. Jakes JE, Arzola X, Bergman R, Ciesielski P, Hunt CG, Rahbar N, Tshabalala M, Wiedenhoeft AC, Zelinka SL (2016) Not just lumber—using wood in the sustainable future of materials, chemicals, and fuels. JOM 68:2395–2404
5. Franklin S (2019) The U.S. mass timber industry is maturing while it branches out. Archit Newsp 17:17
6. Gerard R, Barber D, Wolski A (2013) Fire safety challenges of tall wood buildings. National fire protection research foundation
7. Su J, Lafrance P-S, Hoehler M, Bundy M (2018) Fire safety challenges of tall wood buildings – phase 2: task 2 & 3 cross laminated timber compartment fire tests. Fire protection research foundation, Quincy, MA
8. Zelinka SL, Hasburgh LE, Bourne KJ, Tucholski DT, Ouellette JP (2018) Compartment fire testing of a two-story mass timber building. General technical report FPL-GTR-247, U.S. Department of Agriculture, Forest Service, Forest Products Laboratory, Madison, WI
9. Janssens M (2017) Development of a fire performance assessment methodology for qualifying cross-laminated timber adhesives. SwRI Project No.01.23086.01.001a, Southwest Research Institute, San Antonio, TX
10. Anon: ANSI/APA PRG 320: standard for performance rated cross-laminated timber. APA-The engineered wood association, Tacoma, WA
11. Su J, Leroux P, Lafrance P-S, Berzins R, Gratton K, Gibbs E, Weinfurter M (2018) Fire testing of rooms with exposed wood surfaces in encapsulated mass timber construction. National Research Council of Canada, Ottawa

From Low-Rise to High-Rise Buildings: Fire Safety of Timber Frame Facades

Anton Kraler(✉), Clemens Le Levé, Thomas Badergruber, and Michael Flach

University of Innsbruck, Technikerstraße 13, 6020 Innsbruck, Austria
{anton.kraler, clemens.le-leve, thomas.badergruber, michael.flach}@uibk.ac.at

Abstract. Timber construction and fire safety are two terms which often lead to discussions, especially if it concerns multi-storey timber buildings. The scientific investigations presented here demonstrate the extent to which the use of a timber façade provides sufficient fire safety for people and the environment. Research work on prefabricated timber frame façade systems is carried out at the Department of Timber Construction at University of Innsbruck. The investigations are performed in three steps. Step 1: Typical fire exposure of buildings, building classes, requirements of high-rise buildings (>22 m fire escape level) and the properties of the materials in question are investigated. Special attention is given to the use of sustainable and ecological materials. Step 2: Performing reaction to fire tests and fire resistance tests with various materials and constructions which are included in classification reports. For this façade system also a connector system and a specific joint design for easy mounting was developed in a PhD thesis. Step 3: This façade element is tested for its suitability for its use in high-rise buildings. In fire tests is shown that the wooden substructure in the façade does not contribute the fire during a certain time. So the ban of inflammable materials in high-rise buildings could be mitigated. The scientific results show that the use of timber in prefabricated façade elements can meet the required criteria.

Keywords: Prefabricated timber frame facade · Refurbishment with wood · Timber Construction · Fire resistance test · Residential building · High-rise building · Fire safety

1 Introduction

With fire safety of facades and exterior walls several requirements need to be considered to meet the protection targets defined in the building codes. This involves the general construction structures and critical joining details like fixing elements of windows, doors, etc. The function of each construction structure needs to be defined, e.g. how integrity and thermal insulation criteria effects can be achieved, and how spread of fire and smoke can be limited. Three different fire scenarios can affect of exterior walls.

L. Makovicka Osvaldova et al. (Eds.): WFS 2020, *Wood & Fire Safety*, pp. 238–243, 2020.
https://doi.org/10.1007/978-3-030-41235-7_36

Flying sparks and thermal radiation due to a burning neighbouring building
Fire source outside the building (e.g. burning waste container)
Fire inside the building with flames coming out of building openings (Fig. 1).

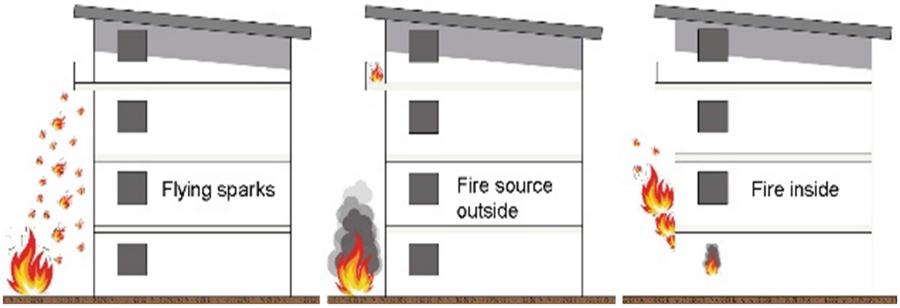

Fig. 1. Typical scenarios on exterior walls.

Fire protection requirements increase with the height and volume of the building. The function of a building element and the reaction to fire behaviour play a crucial role. In two research projects at the Department of Timber Construction, University of Innsbruck, fire protection investigations on prefabricated timber-frame façade elements are carried out. The first project focuses on the development of an ecological façade system ("E.T. prefab façade") to achieve thermal refurbishment in building classes (BC) 4 and 5 ($\leq$22 m fire escape level). In the subsequent project, the applicability of these findings for high-rise buildings is investigated. Since the use of timber in exterior walls is not permitted for high-rise buildings in Austria, the scientific question is as follows: Can a non-loadbearing prefabricated timber frame façade element be designed in such a way that it meets the required protection targets.

2 Fire Behaviour Requirements in Austria: Building Classes (BC) 1 to 5 and High-Rise Buildings

Table 1. General fire behaviour requirements according to OIB guideline 2 & 2.3 [1, 2]

Building classes (BC)	BC 1	BC 2	BC 3	BC 4	BC $5 \leq 6 \geq 6$ storeys		High-rise building
Facade systems, rear ventilated, ventilated or non-rear ventilated							
Complete system or Individual layers	E	D-d1	D-d1	B-d1	B-d1	B-d1	A2-d1
Exterior layer	E	D	D	A2-d1	A2-d1	A2-d1	A2-d1
Substructure linear and pointed	E/E	D/D	D/A2	D/A2	D/A2	C/A2	A2/A2
Thermal insulation	E	D	D	B	B	B	A2

Fire safety requirements in Austria are defined in the OIB guidelines 2 [1]. The fire protection requirements for BC 1 to 3 ($\leq$7 m fire escape level (family home, terraced house, etc.)) can usually be met with combustible materials. Concerning BC 4 ($\leq$11 m fire escape level) and BC 5 ($\leq$22 m fire escape level) the fire spread via the façade on to the second storey above the fire source must effectively be limited. The fire behaviour requirements are summarised in Table 1. Beyond BC 5 with more than 6 storeys the use of timber is becoming increasingly difficult.

3 Facade System Until BC 5 – Fire Tests and Classification

The timber frame facade element is a plastered, non-rear ventilated wall element, which is put or hanged in front of an existing wall (concrete, brick). This façade system has been developed mainly for the thermal encasement of multi-storey buildings (existing and new buildings). Comprehensive systems allow short mounting times and minimal disruption on the building site. The fire behaviour requirements of the exterior façade as a complete system are defined for BC 4 and 5 with B-d1 in Austria, as shown in Table 1. All required fire tests for classification in B-d0 according to EN 13501-1 are carried out at IBS Linz. A large-scale fire test according to ÖNORM B 3800-5 confirmed that the protection targets (fire spread, parts falling off) are achieved.

Table 2. Use of variable products for this facade system for BC 4 & 5

Layer/Element	Parameter		
Type	Fire behaviour	Dimension	Material
Plaster coating Base board	Over 40 variants of plaster and plaster base boards of different producers		
Solid timber and laminated timber	min. D-s2, d0	width $\geq$ 60 mm height $\geq$ 120 mm	Spruce, fir, pine, larch
Cavity insulation	min. B-s2, d0	120 mm $\leq$ thickness $\leq$ 360 mm	Cellulose fibre, mineral wool
Interior planking	min. D-s2, d0	9 mm $\leq$ thickness $\leq$ 15 mm	OSB, gypsum fibre, MDF board, gypsum board
Insulation in adaption layer	min. B-s2, d0	120 mm $\leq$ thickness $\leq$ 360 mm	Cellulose fibre, mineral wool

The façade system for low and mid-rise buildings is shown in Fig. 2 (left).

The exterior planking consists of a mineral plaster base board. For BC 1 to BC 3, plaster base boards can consist of renewable materials (wood fibre boards, etc.). If an interior planking is applied, it serves as an additional reinforcement during transportation and mounting procedures, it provides air tightness and a closed cavity in the

timber frame which is filled with insulation materials (e.g. cellulose). The adaption layer between the existing wall and the prefabricated timber frame element, which is made of non-retardant spruce, is filled with blow-in insulation and compensates uneven wall structures. It is filled with insulation materials during the mounting process. The façade connector SHERPA EFCON, which has been specifically developed for this façade system by our Department of Timber Construction is placed in this layer [3].

For the prefabricated plastered facade system, the development of the horizontal and vertical joint design between the elements is an essential feature, so that simple mounting is possible, and even more so, that fire protection requirements are achieved [4, 5].

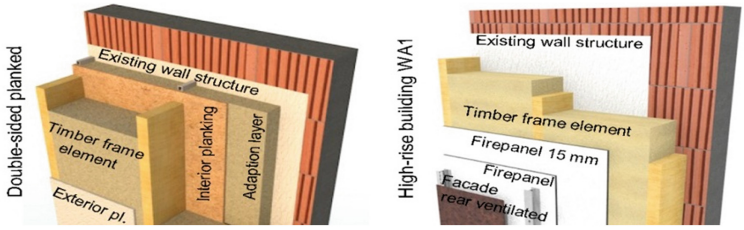

Fig. 2. Prefabricated facade elements for BC 4&5 (left) and high-rise buildings.

4 Timber Frame Elements in High-Rise Buildings

Non-loadbearing exterior walls in high-rise buildings must have a minimum fire behaviour of A2-d1, i.e. only incombustible materials must be used. But if it can be proved that the timber does not contribute to the fire within 90 min of fire exposure, the question is whether this limitation is indeed justified. In contrast to the façade structure for BC 5 the following changes for high-rise buildings are required.

The insulation material melting point must be $\geq$1000 °C, e.g. mineral wool. The façade system does not feature a plaster coating but a rear-ventilated façade system approved for high-rise buildings is used. The timer frame construction is protected by gypsum fibre boards in such a way that it does not contribute to the fire.

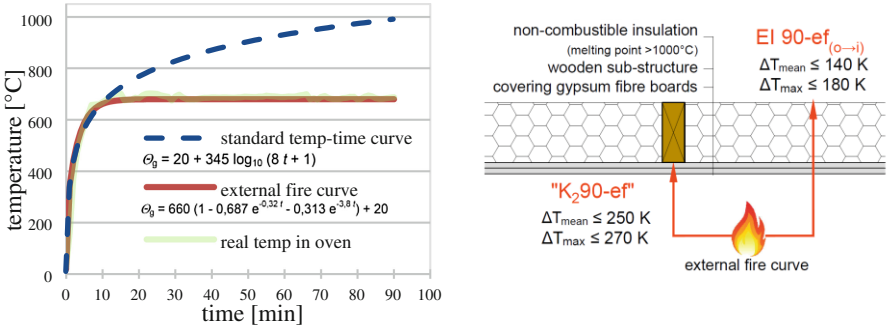

Fig. 3. Standard vs. external temp-time curve (left); performance criteria for the fire resistance and the fire protection ability (right).

Due to the fact that the façade system is the exterior part of the wall the production ability and the fire resistance of the façade is determined by using the external fire exposure curve instead of the standard temp-time curve (Fig. 3).

The test specimen (3 m high, 4 m wide) is investigated according to the fire resistance tests of non-loadbearing walls ÖNORM EN 1364-1 [6] and along the fire protection encapsulation criteria in ÖNORM EN 13501-2 [7]. Two variants of protection coverings were tested. Figure 2 (right) shows variant WA1 with complete double planking made of gypsum fibre board (Fermacell Firepanel 15 mm). The second variant WA2 has one-layer planking and additional a second layer only in front of the wooden substructure (with 40 mm overlay). The temperature increase in the wooden substructure is measured. According to the encapsulation criteria, the temperature increase must not exceed 250 K respectively 270 K throughout the entire test time. In addition the fire resistance performance criteria of this non-loadbearing exterior wall, the integrity E and thermal insulation I are evaluated. The temperature increase on the fire unexposed side of the exterior wall construction stay below the limit temperature of 140 K respectively 180 K during the test period of 90 min, according to ÖNORM EN 13501-2 [7].

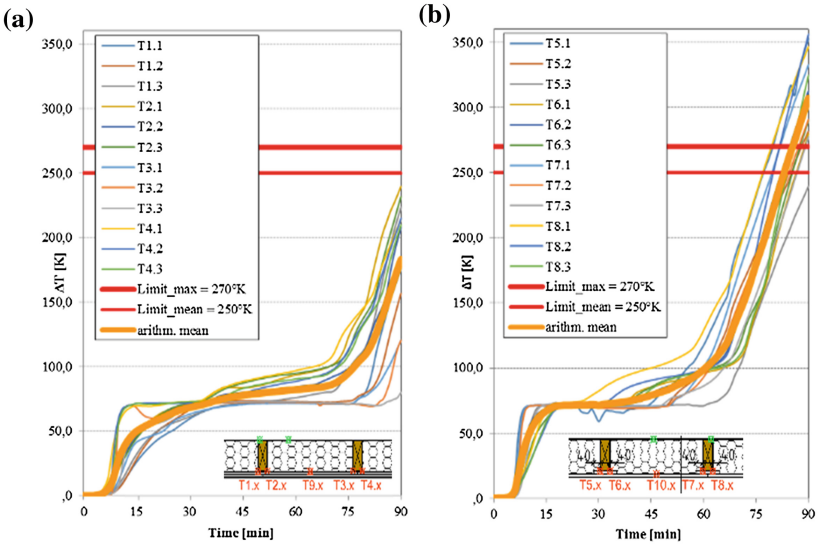

Fig. 4. a. Temperature increase in wooden substructure – WA1 double planked b. Temperature increase in wooden substructure – WA2 one-layer planking.

Figure 4a shows the measured temperature increase in the wooden substructure of WA1 with double planking. During the entire 90-min testing period the limit temperatures are not exceeded and the limit temperatures on the non-exposed side were not exceeded either. Therefore WA1 can be classified as EI 90-ef$_{(o \rightarrow i)}$ with external fire curve exposure. In WA2 the limit temperatures are exceeded after 80 and 84 min in wooden substructure (Fig. 4b) [5].

5 Conclusion

According to the current Austrian building codes the use of timber up to BC 5 is possible. In high-rise buildings, timber is generally not permitted. This paper shows in which way a combustible substructure in non-loadbearing prefabricated façade systems could be applied.

The E.T. timber frame façade system for Building Classes 4 and 5was tested as a complete system and classified as B-d0. The required protection targets are met. This façade system can be used in Austria for buildings up to BC 5 with more than 6 storeys and a fire escape level of ≤ 22 m.

For high-rise buildings the façade system was adapted and tested. WA1 meets the requested protection ability and is classified as EI 90-ef$_{(o \rightarrow i)}$ with external fire curve exposure. The investigation reveals that wooden substructures can be used without contributing to a fire within a 90-min period. This raises the question whether a general ban of combustible materials in high-rise buildings is justified. These results are based on the scientifically setup experiment according to the current codes. Clearly, in a real blaze the source of the fire may be inside the building, which can lead to higher temperatures than with the measured external fire curve in Fig. 3.

Acknowledgement. This scientific work was subsidised by Land Tirol - Wohnbauforschung, Neue Heimat Tirol Gemeinnützige WohnungsGmbH and proHolz Tirol.

References

1. Österreichisches Institut für Bautechnik (Hrsg.) (2015) OIB Guideline 2: Safety in case of fire, Vienna
2. Österreichisches Institut für Bautechnik (Hrsg.) (2015) OIB Guideline 2.3: Safety in case of fire in buildings with a fire escape level in excess of 22 m, Vienna
3. Le Levé C, Badergruber T, Kraler A, Flach M (2018) New ways in thermal façade refurbishment and a system connector for a quick and easy mounting. In: Bauingenieur, Heft 7/8-2018. Springer, Düsseldorf
4. Le Levé C, Badergruber T, Kraler A, Flach M (2016) Ökologisches Sanieren mit verputzten, vorgefertigten Fassadenelementen in der Gebäudeklasse 5 mit mehr als 6 Vollgeschossen. Final report. University of Innsbruck
5. Le Levé C, Badergruber T, Kraler A, Flach M (2018) Vorgefertigte Fassadensysteme in Holzbauweise bei Gebäuden mit einem Fluchtniveau von mehr als 22 m (Hochhausbereich). Final report. University of Innsbruck
6. ÖNORM EN 1364-1:2015 (2015) Fire resistance tests for non-loadbearing elements – Part 1: Walls. Austrian standards institute, Vienna
7. ÖNORM EN 13501-2:2016 (2016) Fire classification of construction products and building elements – Part 2: classification using data from fire resistance tests, excluding ventilation services. Austrian Standards Institute, Vienna

Experimental Study on Fire Resistance of One-Way Straight and Through Mortise-Tenon Timber Joints

Lingzhu Chen[1], Qingfeng Xu[1(✉)], Chongqing Han[2], Xi Chen[1], Xiaofeng Hu[3], and Zhengchang Wang[3]

[1] Shanghai Key Laboratory of Engineering Structure Safety, Shanghai 200032, China
20040392chen@163.com, xuqingfeng73@163.com, cx541026@hotmail.com
[2] Southeast University Architects and Engineers Co., Ltd., Nanjing 210096, China
chq_han@seu.edu.cn
[3] Southeast University, Nanjing 210096, China
702236754@qq.com, 875369688@qq.com

Abstract. Fire is one of the most frequent disasters in the world. Many traditional timber buildings were destroyed by fire, causing a large amount of culture and heritage loss. Timber joints play an important role in the stability of whole timber structures. The temperature development and fire resistance of mortise-tenon joints exposed to fire were experimentally studied in this paper. The effects of joint type and load ratio on their fire resistance were considered. Results showed that the capacity of one-way straight mortise-tenon joint was higher than through mortise-tenon joints. Temperature increased with increasing fire exposure time and decreased very slowly after the fire was stopped. The closer the thermocouples to the surface of timber beam and column were, the higher their temperature was. It was observed that for the mortise-tenon joints of the same type, the fire resistance decreased with load ratios. For the mortise-tenon joints subjected to the same load ratios, the fire resistance of one-way straight mortise-tenon joint was slightly higher than through mortise-tenon joints. The fire resistance of through mortise-tenon joints tested under the load ratio of 0.3 and 0.5 were 25 min and 20 min respectively, while the fire resistance of one-way straight mortise-tenon joints tested under the load ratio of 0.5 was 24 min.

Keywords: Qing-style timber building · One-way straight mortise-tenon joints · Through mortise-tenon joints · Fire resistance · Load ratio

1 Introduction

Fire is one of the most frequent disasters in the world. Timber joints play an important role in the stability of whole timber structures. Traditional Chinese timber structures commonly employed mortise-tenon timber joints including dovetail tenon, steamed

L. Makovicka Osvaldova et al. (Eds.): WFS 2020, *Wood & Fire Safety*, pp. 244–250, 2020.
https://doi.org/10.1007/978-3-030-41235-7_37

bun tenon, straight tenon and so on. The straight tenon joints are divided into through, one-way straight and half through mortise-tenon joints. The through mortise-tenon joints are usually used in post-and-beam structures, and manufactured into the shape of big in and small out. The penetration in part has the same height with the beam, and the height of the penetration out part is reduced by half. For one-way straight mortise-tenon joints, the penetration in and out parts have the same height with the beam. The through and one-way straight mortise-tenon joints are commonly used in the places where need connection but are not able to apply dovetail tenons. For the mortise-tenon timber joints, the cross-section of both beams and columns were reduced at the joints, which are the weakest part of beams and columns when exposed to fire. Therefore, studies on the fire mechanism of mortise-tenon timber joints are very meaningful to the protection of traditional timber buildings.

Currently, studies on mortise-tenon timber joints are mostly focus on their structural performance at room temperature. Cun et al. [1], Zhao et al. [2] and Lu et al. [3] investigated the moment bearing capacity and seismic performance of different types of mortise-tenon timber joints, and Lu et al. [3], Xie et al. [4] and Zhang et al. [5] proposed strengthening methods for different mortise-tenon timber joints. Studies on the fire performance of mortise-tenon timber joints are very limited. Zhang et al. [6] carried out fire tests on dovetail mortise-tenon joints. Results showed that the fire resistance of dovetail mortise-tenon joints decreased with increasing load ratios, and fire retardant treatment could improve their fire resistance to some degree.

In this context, this paper reports the results of fire resistance tests on one-way straight and through mortise-tenon timber joints, to provide technical reference for fire design and fire performance enhancement of traditional Chinese timber buildings.

2 Experimental Programm

2.1 Specimen Design

In total, five full-scale one-way straight and through mortise-tenon timber joints commonly used in Qing-dynasty buildings were prepared according to the construction details in *Illustration of "Engineering Practice Regulations" by the Qing Ministry of Industry* [7], among which three specimens were through mortise-tenon timber joints, and another two were one-way straight mortise-tenon timber joints. The geometry of specimens is shown in Fig. 1. Specimens TJ-1 and TJ-2 were control specimens without fire exposure and of through and one-way straight mortise-tenon timber joints respectively. TJ-3 and TJ-4 were fire exposured through mortise-tenon timber joints under load ratio of 0.3 and 0.5 respectively. TJ-5 was fire exposured one-way straight mortise-tenon timber joint under load ratio of 0.5. The load ratio was defined as the ratio between the applied load during fire and the measured ultimate load of relative control specimen.

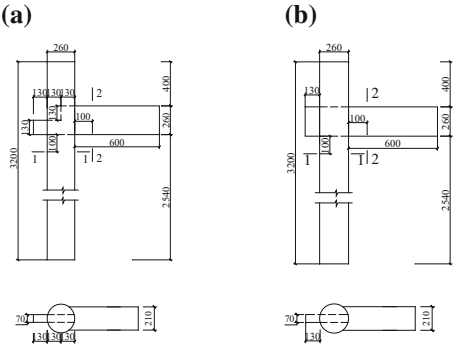

Fig. 1. Geometry of specimens: (a) through mortise-tenon timber joints; (b) one-way straight mortise-tenon timber joints

2.2 Material Properties

The timber beams and columns were made of Southern pine, which is one of the common used timber species in Qing-dynasty buildings. The measured density and moisture content of the timber beams were 596 kg/m^3 and 18.7% respectively, the measured compressive and tensile strength parallel to the grain were 26.9 MPa and 73.3 MPa, and the measured modulus of rupture and modulus of elasticity were 85.0 MPa and 7640 MPa respectively.

The measured density and moisture content of the timber columns were 641 kg/m^3 and 25.0% respectively, the measured compressive and tensile strength parallel to the grain were 20.4 MPa and 60.0 MPa, and the measured modulus of rupture and modulus of elasticity were 97.0 MPa and 8670 MPa respectively.

2.3 Instrumentation

The fire tests were conducted in the horizontal furnace. The mortise-tenon timber joints were placed vertically in the furnace, with one column end inserted into the slot reserved in the bottom of the furnace, and the other end connected to the reaction frame with anchors. The bottom 2 m height part of the columns were wrapped with fireproof wool, while the other parts of columns were exposed to fire in four sides. The beams were exposed to three-side fire. Figure 2 shows the test setup.

According to the real load of an ancient timber building, the vertical load on the column was taken as 50 kN, and kept constant. Then the load at the beam end was applied gradually through a load transfer device. The load cited later was all referred to this load. For control specimens TJ-1 and TJ-2, the load was increased until the failure of the joints. For specimen TJ-3 ~ TJ-5, the load was increased to the pre-defined load value and kept constant. Then the fire was started with the furnace temperature increased according to ISO 834 standard fire curve. During the fire, the load applied on the beams and columns were kept constant through adjusting oil pump of load jacks. The fire was stopped at the failure of the specimens.

2.4 Measurement Arrangement

LVDTs labelled as DL-1, DL-2 and DL-3 in Fig. 2 were used to record the downward movement of the beam at the distance of 20 mm, 200 mm and 500 mm from the column. Thermocouples were used to monitor temperature variations in the timber beam and column at different distance from the surface as shown in Fig. 3.

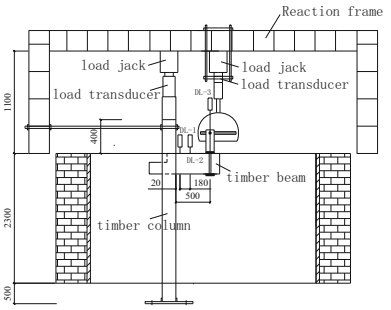

Fig. 2. Test setup

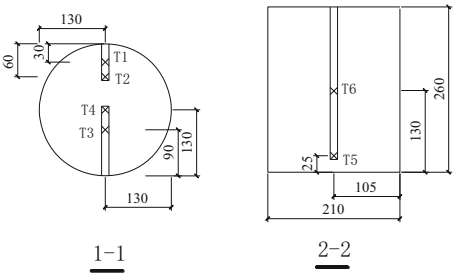

Fig. 3. Arrangement of thermocouples

3 Experimental Result and Discussion

3.1 Control Specimens TJ-1 and TJ-2

For specimen TJ-1, slight crack sound was heard at 3 kN load, and the sound was getting loud and the tenon was pulling out from the mortise when the load was increasing to 9 kN. The peak load was 9.7 kN, and pulling distance out from the mortise was increasing. Obvious extrusion deformation of mortise and tenon was observed. For specimen TJ-2, slight crack sound was heard at 17 kN load, and when the load was 21 kN, obvious rotation occurred indicating the failure of the specimen.

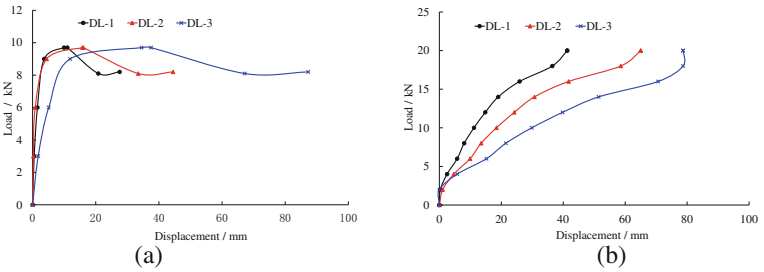

Fig. 4. Load-displacement curves of specimens: (a) TJ-1; (b) TJ-2

The load-displacement curves of specimens TJ-1 and TJ-2 were plotted in Fig. 4.

It can be observed that the through mortise-tenon timber joint TJ-1 showed a large failure displacement and good ductility, while the failure of one-way straight mortise-tenon timber joint TJ-2 occurred suddenly. The ultimate load of one-way straight mortise-tenon timber joint is relatively larger than that of through mortise-tenon timber joint. This may be mostly attributed to the larger tenon area that support the load of through mortise-tenon timber joint.

3.2 Specimens TJ-3 ~ TJ-5

White smoke was observed from the furnace at the initial of fire, and was increasing with the fire duration. The displacement was also increasing with the time. At failure, the displacement increased greatly, and the load was not able to keep due to the sudden decrease of the oil pump pressure. Specimens were taken out of the furnace after cool. The photos of specimens after fire were shown in Fig. 5. It can be seen that both beams and columns suffered serious charring, and the residual section of the tenon was very small.

(a) (b) (c)

Fig. 5. Photos of typical specimens after fire: (a) TJ-3; (b) TJ-4; (c)TJ-5

Figure 6 illustrated the measured temperature development. It can be observed that temperature increased with the fire exposure time, and decreased slowly after fire was stopped. Temperature measurement T2 increased even after the fire was stopped. This may be caused by the continuing burning of the timber. The closer the thermocouples to the surface of timber beam and column were, the higher their temperature was. There was a temperature lag at 100 °C, indicating the water evaporation of timber.

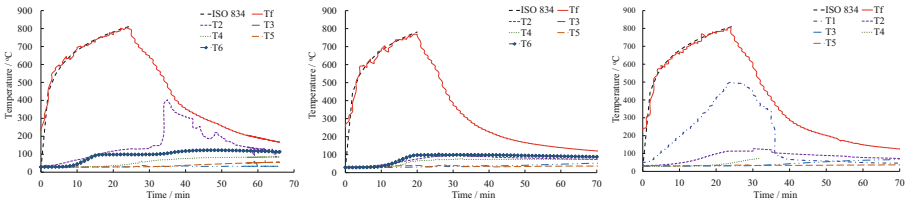

(a) (b) (c)

Fig. 6. Temperature-time curves of specimens: (a) TJ-3; (b) TJ-4; (c)TJ-5

The fire resistance was defined as the time when the variation rate of the displacement was too large to support the load. The measured fire resistance were 25 min, 20 min and 24 min for specimens TJ-3, TJ-4 and TJ-5 respectively. As expected, for the same type of mortise-tenon timber joints, their fire resistance decreased with increasing load ratios. For the mortise-tenon timber joints exposed to the same load ratio, the one-way straight mortise-tenon timber joint exhibited a slightly larger fire resistance than through mortise-tenon joint. This may be mostly attributed to the larger tenon area that support the load of through mortise-tenon timber joint during the fire. The measured fire resistance in this study was similar to the result from the study in reference [6] for dovetail mortise-tenon timber joints.

4 Conclusions

This paper presented an experimental study to investigate the thermo-structural behaviour of mortise-tenon timber joints. In total, five joints were prepared and tested exposed to fire. It can be concluded that:

(1) The capacity of one-way straight mortise-tenon joint was higher than through mortise-tenon joints.
(2) Temperature increased with increasing fire exposure time and decreased very slowly after the fire was stopped. The closer the thermocouples to the surface of timber beam and column were, the higher their temperature was.
(3) It was observed that for the mortise-tenon joints of the same type, the fire resistance decreased with load ratios. For the mortise-tenon joints subjected to the same load ratios, the fire resistance of one-way straight mortise-tenon joint was slightly higher than through mortise-tenon joints.

Acknowledgement. This work was financially supported by National Science Foundation of China (No. 51808339), Shanghai Rising-Star program (No. 17QB1403400) and Shanghai Science and Technology Commission Standard Program (No. 17DZ2202600).

References

1. Chun Q, Lu W, Wang JG, Pan JW (2015) Mechanical properties of typical mortise-tenon joints of post and lintel construction and column and tie construction of timber buildings in Jiangsu Province and Zhejiang Province. J Southeast Univ (Nat Sci Ed) 45(1):151–158
2. Zhao HT, Dong CY, Xue JY, Sui Y, Zhang HY (2010) The experimental study on the characteristics of Mortise-Tenon joint historic timber buildings. J Xian Univ Archit Technol (Nat Sci Ed) 42(3):315–318
3. Lu WD, Deng DL (2012) Experimental research on seismic performance of wooden Mortise-Tenon joints before and after reinforment. J Earthq Eng Eng Vib 32(3):109–116
4. Xie QF, Zhao HT, Xue JY, Yao K, Sui Y (2008) An experimental study on the strengthening of Mortise-Tenon joints in ancient Chinese wooden buildings. China Civil Eng J 41(1):28–34

5. Zhang FW, Xu QF, Zhang J, Liu Q, Gong CC (2016) Experimental study on seismic behavior of timber frames with Mortise-Tenon joints under different strengthening methods. J Build Struct 37(Suppl):307–313
6. Zhang J, Wang B, Hou ST, Bai YW, Zong ZL (2016) Experiment study on fire endurance of Mortise-Tenon joint on timber structures. J Hunan Univ (Nat Sci) 43(1):117–123
7. Liang SC (2006) Illustration of "engineering practice regulations" by the qing ministry of industry. Tsinghua University Press, Beijing

Fire Performance of CLT Members: A Detailed Review of Experimental Studies Across Multiple Scales

Christos Kontis, Christoforos Tsichlas, Dionysios I. Kolaitis(✉), and Maria A. Founti

Fire Engineering Unit, School of Mechanical Engineering, National Technical University of Athens, 9 Heroon Polytechniou Street, 15780 Athens, Greece
dkol@central.ntua.gr

Abstract. Cross-laminated timber (CLT) is an innovative wood product that is increasingly used in both residential and non-residential construction projects, since it offers a range of advantages, such as light carbon footprint, quick erection time, good thermal and sound insulation characteristics. CLT members have the potential to provide excellent fire resistance characteristics, often comparable to typical massive, non-combustible construction assemblies. However, the fire performance of CLT can be affected by a large variety of material and design parameters, such as physical properties (e.g. density, grain orientation), member thickness, number of plies, adhesive type, connector type, protection panels. In this context, this work presents a thorough review of recent experimental studies, aimed at determining the fire behaviour of CLT members. A large number of test results obtained in a broad range of setups, spanning multiple scales, such as cone calorimeter (50 tests), standard fire resistance furnace (90 tests) and fire compartment (20 tests), are comparatively assessed. The impact of the main material and design parameters on several important fire performance factors is investigated. Analysis of the reported experimental results allows the determination of certain global trends that are observed in the majority of cases.

Keywords: CLT · Fire performance · Experimental · Fire tests · Large scale

1 Introduction

Cross-Laminated Timber (CLT) is a relatively new timber construction technique used for the construction of mid- and high-rise buildings, which is becoming increasingly popular worldwide. The CLT system is based on prefabricated massive timber panels, consisting of 3 to 7 timber layers stacked crosswise (typically at 90°) and glued together; the thickness of each individual timber layer ranges from 10 mm to 50 mm and its width may vary from 60 mm to 240 mm. The CLT panels are used to construct load-bearing wall or floor assemblies. The CLT system offers a range of advantages, such as easy handling in construction, high level of prefabrication (that facilitates quick erections), especially for mid-rise construction (e.g. 5 to 8 storeys); good thermal

L. Makovicka Osvaldova et al. (Eds.): WFS 2020, *Wood & Fire Safety*, pp. 251–257, 2020.
https://doi.org/10.1007/978-3-030-41235-7_38

insulation, good sound insulation and a fairly good performance under fire conditions are some added benefits of CLT.

Due to the inherent nature of thick timber members to char slowly and at a predictable rate, massive timber systems can maintain significant structural resistance for an extended period of time when exposed to fire. CLT panels have the potential to provide excellent fire resistance characteristics, often comparable to typical massive assemblies of non-combustible construction. However, the CLT panels may increase the total fire load; the addition of a fire protection cladding at the exposed side increases the overall fire resistance rating of the system. In this context, several experimental studies have been performed in the past, aimed at determining the main characteristics of CLT's fire behaviour; a detailed literature review of these studies is presented here.

2 Experimental Research on the Fire Behaviour of CLT

In this work, a large number of test results obtained in a broad range of testing setups, spanning multiple scales, such as cone calorimeter (50 tests) [1–3], standard fire resistance furnace tests of wall - (40), floor - (26) and beam - (24) elements [4–19] and small-(5) and large-scale (16) fire compartment tests [1, 2, 20–26], are comparatively assessed.

2.1 Cone Calorimeter Tests

Cone calorimeter tests are essentially small-scale tests, aimed at investigating CLT self-extinction [1, 2], duration of exposure until CLT de-bonding is observed [1] and determination of the critical mass loss rate and heat flux for self-extinction [3]. Emberley et al. [1] found that debonding can occur in CLT and is accompanied by large peaks in the mass loss rate; the latter are observed when a significant portion of either the char layer or the timber plies fall off, thus reducing the thermal insulation and exposing the virgin timber to higher heat fluxes. The mass loss rate remains higher than steady-state values until the char layer increases to sufficient depth to reduce the heat flux delivered to the pyrolysis front. Crielaard et al. [2] found that a heat flux level of 5–6 kW/m^2 is the threshold where self-extinguishment is observed.

2.2 Fire Resistance Tests

Fire resistance tests employ the standard large-scale fire resistance furnaces; the CLT members are set in three main configurations: vertical walls [4–10], horizontal floors [4, 6, 7, 11–17] and beams [8, 18, 19]. In the respective fire resistance tests, either unloaded [4, 5, 11, 12, 14–16] or loaded [6–10, 13, 17–19] CLT members were tested.

Effect of Adhesive Type. The behaviour of the bonding adhesive at high temperatures can influence the falling time of the charred layers and thus play an important role in the overall fire behaviour of CLT elements [4, 5, 9, 11], since it may cause re-ignition of fresh wood, thus preventing auto-extinction and prolonging the fire duration [16].

Effect of Grain Orientation. Klippel et al. [7] and Frangi et al. [11] agree that there is no significant influence of the orientation of the layers on the charring behaviour, in both wall and floor CLT panels. Hasburgh et al. [15] compared two alternative 3-ply floor panel configurations, the traditional Long-Cross-Long (LCL) against the Long-Long-Cross (LLC) one; the average failure time for the LLC tests was found to be approximately 5% longer than the LCL tests.

Effect of Layer Thickness. An important factor that also affects the fire resistance of CLT is the thickness of each lamella. All relevant fire resistance test results agree that increasing the lamellas' thickness results in decreasing charring rates [6, 9, 11].

Effect of the Number of Layers. Frangi et al. [4] suggested that using thicker external lamellae, and a 3-ply rather than 5-ply build-up, can reduce the risk of delamination in fire and thereby reduce the effective charring rate. However, Wiesner et al. [10] observed that 3-ply wall panels failed considerably earlier than 5-ply configurations when exposed to fire, due to the critical importance of the outer layer in preventing instability failures. In addition, a comparison of a gypsum plasterboard-protected 5-ply and an unprotected 7-ply CLT floor panel [6] revealed that the latter configuration exhibits a significantly higher fire resistance index; in other words, a very thick unprotected CLT floor panel responded better than a protected thinner one.

Effect of the Panel Connectors. Both Klippel et al. [7] and Suzuki et al. [9] agree that the connectors used to join the CLT panels do not affect significantly their fire resistance. Klippel et al. [7] used two different support connectors, i.e. L-bracket and T-bracket supports; however, no significant influence on the fire behaviour of the CLT wall panels was observed.

Effect of Encapsulation. Gypsum plasterboards used to protect CLT wall elements were found to drastically improve the fire resistance of the specimens [5, 6, 8, 9, 13–15, 18]. Gypsum boards used as protective layers may delay the onset of charring by 50–75 min [5, 6]. The fire resistance of a loaded 150 mm thick panel was found to improve by approximately 10% when a 15 mm thick gypsum plasterboard was used [13]. Hasburgh et al. [14] tested 20 encapsulated floor specimens with different protection methods; they found that an air cavity between the CLT member and the protective panel increased the fire resistance (in the form of "encapsulation time") by 9%.

Comparison to EN 1995-1-2 (2004) Charring Rate Predictions. In general, the experimentally determined charring rates [4–6, 8] are found to agree well with the respective values proposed in EN 1995-1-2. However, Klippel et al. [7] and Hasburgh et al. [14] found that the measured charring rates were slightly higher (0.72 mm/min for wall elements and 0.70 to 0.79 mm/min for floor elements) than the 0.65 mm/min one-dimensional charring rate value proposed in Eurocode for the case of solid wood.

2.3 Fire Compartment Tests

In a number of experimental works, the CLT fire behaviour was investigated by using either a full-scale [1, 20–26] or a small-scale [2, 26] fire compartment. In general, the compartment temperature, opening factor and type of fire source were found to affect the CLT's rate of charring.

Heat Flux and Airflow Conditions for Self-extinguishment. Emberley et al. [1], performing full-scale fire compartment tests, observed that self-extinction of the CLT wall and ceiling occurred when the maximum incident heat flux was below 45 kW/m^2. In small-scale fire compartment tests [2], it was found that self-extinguishment of the smouldering CLT can be achieved when the incident heat flux is below 5–6 kW/m^2 and the airflow over the surface is lower than 0.5 m/s.

Char Fall-Off Condition for Self-extinguishment. Crielaard et al. [2] found that fall-off of the charred lamellae of CLT can sustain flaming combustion or revert smouldering combustion back to flaming combustion, thus preventing the CLT from self-extinguishing. Hadden et al. [22] found that self-extinction is observed in compartments with two surfaces of exposed timber; however, this is dependent on the char layer remaining attached.

Heat Release Rate and Total Energy Released. Crielaard et al. [2] found that exposed CLT increases the heat release rate (HRR) and the total energy released, thus extending the fire duration; these parameters are further increased when fall-off results in prolonged flaming. Wiesner et al. [20] found that the time to flashover was typically of the order of 5 min and the total heat release rate at flashover was up to 1709 kW. Li et al. [23] performed six full-scale room fire tests using furniture as fuel; they noticed that both the HRR and the room temperature curves followed the same trends.

Timber Depth. Wiesner et al. [20] measured the variation of in-depth temperatures in CLT panels; they noticed that self-extinction occurs at around 20 min and subsequently the depth of the char layer (i.e. the 300 °C isotherm) remains constant indicating that charring has effectively stopped. Hadden et al. [22] found that compartment temperatures are governed by the heat released in the compartment and the heat losses through the compartment boundaries. They also noticed that the higher thermal inertia of plasterboard compared to char or stone wool results in larger heat losses from the compartment and lower compartment temperatures.

Charring Rate. Wiesner et al. [20] noticed that an initial peak charring rate is observed early in all fire tests; the charring rate is subsequently reduced, due to the formation of a char layer with a quasi-steady depth. Hakkarainen [25] observed that the presence of a protective layer of gypsum plasterboard reduces the charring rate of the underlying timber, but once said protection falls off, the charring rate is then significantly increased due to the lack of an insulating layer. Kolaitis et al. [21] observed that the onset of charring is delayed when timber elements are protected by a fire protection cladding. Hadden et al. [22] observed lower charring depths on the ceiling compared to the back side of the compartment, which can probably be attributed to the lower oxygen concentration near the ceiling and the resulting lower pyrolysis rate. In contrast, Li et al. [23] observed the most extreme charring rate on the ceiling, where the most severe exposure conditions and highest temperatures were expected. The average charring rate was found to be 1.22 mm/min based on a 30 mm charring depth, which is significantly higher than the 0.65 mm/min proposed in Eurocode 5; the higher charring rate was mainly owed to the delamination of the first layer.

Fire Protection Claddings. Kolaitis et al. [21] found that gypsum plasterboards offer better fire protection than wood-based panels; in the former case, no charring was observed in the CLT elements protected by double gypsum plasterboards. Frangi et al. [24] performed a natural full-scale fire test in a 3 storey timber building; they confirmed that pure structural measures are adequate to limit the fire spread to one room, even for timber structures. In the room above the fire compartment no elevated temperatures were measured and no smoke was observed. By protecting the timber structure with gypsum plasterboards, the damage on the solid timber panels was relative small. Li et al. [23] investigated the fall-off time of gypsum boards, which is a parameter with strong uncertainty. The fall-off time is affected by several factors such as the severity of the fire, type of board, type of fastener used and also the quality of construction. They concluded that when lined with two layers of gypsum plasterboards, the CLT wall assemblies were able to withstand the fire exposure without significant damage to the gypsum boards, which remained in good shape throughout the tests except that small pieces fell-off at the back wall. In contrast, ceiling drywall was directly subjected to flame impingement, which caused earlier local damages.

3 Concluding Remarks

A large number of experimental research studies extending to multiple scales (50 cone calorimeter tests, 90 fire resistance tests and 20 fire compartment tests), aimed at determining the main characteristics affecting the overall fire behaviour of CLT members, was reviewed. Analysis of main findings, allowed the determination of the impact of several parameters, such as material properties (i.e. wood density [9], moisture content [9], grain orientation [7, 11]), the thickness and the number of plies [4, 6, 9–11], the type of adhesive used [4, 5, 9, 11, 16], the possible encapsulation method [5, 6, 8, 9, 13–15, 18, 21, 25]. It was observed that the fall-off of the charred CLT lamellae resulted in sustained combustion, preventing self-extinction [2, 22]. Since the fire behaviour of CLT members is affected by a large number of interacting physical phenomena, certain simplifying assumptions commonly used in fire engineering design methodologies may prove to be inadequate; in some cases [4–6, 8], the experimentally determined charring rates were found to agree well with the respective values proposed in EN 1995-1-2, while in other cases [7, 14] the measured charring rates were actually higher. As a result, further experimental testing, performed in a systematic manner, is necessary to improve the accuracy of the available design methods.

Acknowledgements. This work has been financially supported by the Horizon 2020 project "Build-In-Wood: Sustainable Wood Value Chains for Construction of Low-Carbon Multi-Storey Buildings from Renewable Resources" (Grant No. 862820).

References

1. Emberley R, Putynska CG, Bolanos A, Lucherini A, Solarte A, Soriguer D, Gonzalez MG, Humphreys K, Hidalgo JP, Maluk C, Law A, Torero JL (2017) Description of small and large-scale cross laminated timber fire tests. Fire Saf J 91:327–335
2. Crielaard R, van de Kuilen JW, Terwel K, Ravenshorst G, Steenbakkers P (2019) Self-extinguishment of cross-laminated timber. Fire Saf J 105:244–260
3. Emberley R, Do T, Yim J, Torero JL (2017) Critical heat flux and mass loss rate for extinction of flaming combustion of timber. Fire Saf J 91:252–258
4. Frangi A, Fontana M, Knobloch M, Bochicchio G (2008) Fire behaviour of cross-laminated solid timber panels. Fire Saf Sci 9:1279–1290
5. Craft S, Desjardins R, Mehaffey JR (2011) Investigation of the behaviour of CLT panels exposed to fire, FP Innovations Report, Canada
6. Osborne L, Dagenais C, Benichou N (2012) Preliminary CLT fire resistance testing report, NRC-CNRC Report
7. Klippel M, Leyder C, Frangi A, Fontana M, Lam F, Ceccoti A (2014) Fire tests on loaded CLT wall and floor elements. Fire Saf Sci 11:626–639
8. Schmid J, Menis A, Fragiacomo M, Clemente I, Bochicchio G (2015) Behaviour of loaded CLT wall elements in fire conditions. Fire Technol 51:1341–1370
9. Suzuki J, Mizukami T, Naruse T, Araki Y (2016) Fire resistance of timber panel structures under standard fire exposure. Fire Technol 52:1015–1034
10. Wiesner F, Randmael F, Wan W, Bisby L, Hadden RM (2017) Structural response of CLT compression elements exposed to fire. Fire Saf J 85:56–67
11. Frangi A, Fontana M, Hugi E, Jobstl R (2009) Experimental analysis of cross-laminated timber panels in fire. Fire Saf J 44(8):1078–1087
12. Leikanger Friquin K (2011) Material properties and external factors influencing the charring rate of solid wood and glue-laminated timber. Fire Mater 35:303–327
13. Menis A (2012) Fire resistance of laminated veneer lumber (LVL) and cross-laminated timber (XLAM) elements. PhD thesis, Universita degli Studi di Cagliari
14. Hasburgh L, Bourne K, Dagenais C, Ranger L, Roy-Poirier A (2016) Fire performance of mass-timber encapsulation methods and the effect of encapsulation on char rate of cross-laminated timber. In: World conference on timber engineering, Austria
15. Hasburgh L, Bourne K, Peralta P, Mitchell P, Schiff S, Pang W (2016) Effect of adhesives and ply configuration on the fire performance of southern pine cross-laminated timber. In: World conference on timber engineering, Austria
16. Johansson E, Svenningsson A (2018) Delamination of cross-laminated timber and its impact on fire development, focusing on different types of adhesives. Lund University Report 5562
17. Muszyński L, Gupta R, Hong SH, Osborn N, Pickett B (2019) Fire resistance of unprotected CLT floor assemblies produced in the USA. Fire Saf J 107:126–136
18. Wilinder P (2009) Fire resistance in cross-laminated timber, thesis (2009)
19. Lineham SA, Thomson D, Bartlett AI, Bisby LA, Hadden RM (2016) Structural response of fire-exposed CLT beams under sustained loads. Fire Saf J 85:23–34
20. Wiesner F, Bisby LA, Bartlett AI, Hidalgo JP, Santamaria S, Deeny S, Hadden RM (2019) Structural capacity in fire of laminated timber elements in compartments with exposed timber surfaces. Eng Struct 175:284–295
21. Kolaitis DI, Asimakopoulou EK, Founti MA (2014) Fire protection of light and massive timber elements using gypsum plasterboards and wood based panels: a large-scale compartment fire test. Constr Build Mater 73:163–170

22. Hadden RM, Bartlett AI, Hidalgo JP, Santamaria S, Wiesner F, Bisby LA, Deeny S, Lane B (2017) Effects of exposed CLT on compartment fire dynamics. Fire Saf J 91:480–489
23. Li X, Zhang X, Hadjisophocleous G (2015) Experimental study of combustible and non-combustible construction in a natural fire. Fire Technol 51:1447–1474
24. Frangi A, Bochicchio G, Ceccotti A, Lauriola MP (2006) Natural full-scale fire test on a 3 storey XLam timber building. In: World conference on timber engineering, Japan
25. Hakkarainen T (2002) Post-flashover fires in light and heavy timber construction compartments. J Fire Sci 20(2):133–175
26. Bartlett AI (2018) Auto-extinction of engineered timber. PhD thesis, University of Edinburgh

Building Envelope Material Solutions for the Timber Structures Intended for Housing and Accommodation in Terms of Fire Safety, Fire Progression, and Consequences of Fire

Agnes Iringová(✉)

University of Zilina, Zilina, Slovakia
agnes.iringova@fstav.uniza.sk

Abstract. The paper analyses the load-bearing construction systems in timber structures and their application in multi-storey buildings. It deals with the legislative limitations of their use in dependence on the building´s fire height, calculated fire load and the design of fire separating elements. It provides the optimized envelope material solutions in terms of thermal protection considering the sustainable construction according to Europe 2020 Strategy focusing on the use of renewable and recycled materials. Compositions of building envelopes and fire-separating structures are chosen to use in composite or flammable construction systems and apply in model solutions for buildings intended for housing and accommodation. The paper presents statistical data on the occurrence and consequences of fire in the buildings with composite and flammable construction systems compared to the buildings with non-flammable components. The paper also compares the active fire protection in buildings intended for housing and accommodation considering the requirements specified in Slovak and foreign legislation.

Keywords: Fire protection · Timber buildings · Building envelopes · Europe 2020 Strategy · Fire safety

1 Introduction

Nowadays, the low-energy buildings are often constructed using timber load-bearing systems that are preferred for the excellent static and environmental properties. The use of wood from local sources creates a significantly lower environmental footprint. The wider use of wood in building constructions is limited by its flammability and lower fire resistance of the unprotected load-bearing elements. The common-size load-bearing timber elements that meet static load capacity often do not meet the thermal protection requirements. The paper optimizes the classic as well as modern wood-based load-bearing and infill systems designed for the passive building construction in terms of the fire resistance considering the requirements for energy reduction of the designed buildings in accordance with Europe 2020 Strategy. It assesses thermal insulators and lining materials in terms of the environmental impact.

L. Makovicka Osvaldova et al. (Eds.): WFS 2020, *Wood & Fire Safety*, pp. 258–267, 2020.
https://doi.org/10.1007/978-3-030-41235-7_39

2 Theoretical Analysis of the Load-Bearing Construction Systems Currently Used in Timber Structures - Application in Multi-storey Buildings

The load-bearing construction systems can be pillar frameworks or skeletons, or solid glued-wood structures.

The static load capacity of pillar frameworks as well as glued-wood load-bearing walls is limited by the building's length. They are used in low-floor construction with two or three aboveground floors.

Timber pillar frameworks are currently the most used systems used in low-floor construction. They can be interrupted at the ceiling or continuous over the entire height. If the wall pillar load-bearing structure is interrupted at the ceiling (i.e. the wall of the next floor is mounted directly on the ceiling), it is a platform-frame construction. The second option is a balloon-frame construction, where the pillars go all the way up without interruption. This prefabricated system is similar to timber panel structures that are quick to assemble. They are produced as 1.2–1.8 mm wide small-sized ones, or 12.0–16.0 m long large-sized walls. The panel frame is made of spruce or fir wood covered with large-sized wood-based boards or thermo-insulated plasterboards.

The envelope glued-wood-based system is often used in panel buildings. CLT (cross-laminated timber) is an innovative timber product launched in Austria and Germany in the early 1990s. It is a cost-effective wood-based solution complementing the existing possibilities of skeletal combinations. It is a good substitute in the applications using concrete, masonry, or steel. CLT panels, also referred to as KLH (German abbreviation for cross-laminated timber) boards, are made of PEFC (Programme for the Endorsement of Forest Certification) certified spruce wood [1].

The panels consist of 3–7 layers of single-layer boards glued together under pressure. Practical experiences show that the construction of buildings with CLT systems can be competitive with the technologies used in buildings of medium and high fire heights above 12 m, especially in residential and multifunctional construction. The high standard of prefabrication and easy handling during the construction make it easier and faster to complete the construction. The structural system can be panel or modular. It can be used together with any other building material, such as timber, steel or concrete skeleton [1]. The panels always have an exterior thermal insulation due to the low thermal resistance. The interior side can be visible or lined with plasterboard. The surface treatment is directly dependent on the fire safety and the investor´s requirements. The solid timber structures and timber frameworks have linear load-bearing system; the load from ceilings and roofs is transmitted by load-bearing external and internal walls.

The solid glued-wood and subtle timber frameworks have the linear load-bearing system and the load from ceilings and roofs is transmitted by load-bearing external and internal walls.

The skeletal load-bearing structure is lined with panels as mentioned above. Timber frameworks are the opposite of the solid timber and pillar construction systems. Using this construction system make it possible to solve larger spans of a building and design dispositions that are more variable. The load from ceilings and roofs is transmitted into

foundations by pillars. They offer layouts that are more variable and can be used in multi-storey buildings with a fire height above 12 m. The timber elements of the load-bearing system are usually made of glued laminated timber with embedded steel joint elements. The building envelope is anchored to them. The envelope is usually self-supporting and is made of light sandwich panels, e.g. a timber framework with thermal insulation in the air gap.

The perimeter panel can be placed in front of the load-bearing construction system or recessed between the pillars. The ideal solution in terms of thermal protection and thermal bridge elimination is the installation in front of the skeletal supporting system. As for the fire protection, the perimeter panels of skeletal load-bearing systems are usually designed only as infill panels without load-bearing function. If they meet the requirements for compactness and thermal insulation on the non-radiated side of the structure at the required time, they are considered as compact structures in the calculation of the fire hazard area around the building. In the case of limited thermal insulation in the EW category, they are defined as non-compact with a partially open fire area.

Whether the envelope will be a non-compact fire-open structure depends on the thickness of thermal insulation, its flammability class, melting temperature and anchoring in the load-bearing structure without the possibility of moving (Fig. 1).

Fig. 1. The load-bearing systems currently used in timber buildings (left to right): timber skeleton; panel system - solid glued-wood structure; non-structural perimeter wall pillar framework combined with skeleton.

3 Legislative Limitations for Using Timber Load-Bearing Systems in Apartment Buildings in Terms of Fire Safety

The fire safety requirements of wood-based apartment buildings are directly dependent on their fire height and the type of construction. The definition of the construction depends on the flammability of insulating and lining materials used on the load-bearing timber elements. The fire height depends on the number of fire floors. Depending on these two parameters, the requirement for the minimum fire resistance of the load-bearing and fire-separating elements is subsequently determined for apartment buildings.

In the past, Slovak standards allowed maximally two aboveground floors in timber buildings intended for housing and accommodation. The 40-year valid fire safety requirements changed in July 2017. Revision of the Slovak standard STN 92 0201-2: Fire safety of buildings allows designing the 5-storey timber buildings intended for housing and accommodation meeting the criteria of a composite construction.

In this case, all partitions and load-bearing structures must be covered with non-combustible material. Both contact and ventilated façade lining systems must meet the fire class A1 or A2. The cavities must be completely filled with thermal insulation of the fire class A1 or A2, which must also be used in the facade insulation system. The minimal thermal degradation temperature of thermal insulation must be at least 1000 °C. Thermal insulation must be placed in such a way that it could not settle or fall out even if the envelope fails. The level of twelve meters is the limit above which the fire bands, not made of timber structural elements, have to be used in the perimeter walls. The fire resistance of load-bearing structures and partitions is 45 to 60 min for five-storey timber buildings [2]. In the case of visible wood, or if the thermal insulation in gaps or covering material does not meet the above requirements, the building has flammable structural system and its maximal allowable fire height is three floors for apartment buildings, while the fire resistance of load-bearing and fire-separating structures is 60 to 90 min (Fig. 2).

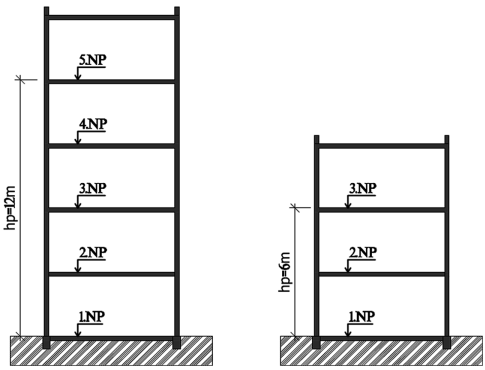

Fig. 2. Maximal allowable fire height in apartment buildings in terms of construction system (left to right): maximal fire height in apartment buildings with timber load-bearing system - composite construction unit; maximal fire height in apartment buildings - combustible construction unit.

4 Optimized Material Solutions for Building Envelopes in Terms of Thermal and Fire Protection Considering the Sustainable Construction According to Europe 2020 Strategy

The first determinant affecting the design of lightweight wood-based building envelopes is the thermal insulation efficiency and the subsequent building´s energy demand in the given climatic conditions in winter as well as in summer. Nowadays, the legislative requirements for thermal insulation of a building envelope are specified in STN 735040-2: 2012, Z1-2016 so that the structure will meet the required global indicator - primary energy in kWh/(m^2.a) within the limit of the A1 energy class. The limit values depend on the building´s category - its functional use. As of 2020, all designed buildings, including those for housing, will have to meet national energy consumption requirements in the nearly-zero energy building category within the global indicator - primary energy in kWh/(m^2.a) in the A0 energy class. Increasing requirements for reducing the heat loss passing through the perimeter structures cause increasing requirements for the thermo-insulation efficiency related to the thickness and thermal conductivity coefficient [3]. When choosing thermal insulation, it is important to take into account not only its efficiency, but also its flammability class, durability and recyclability.

The choice of thermal insulation for sandwich timber structures is conditioned by its efficiency, flammability class, durability and recyclability. The building envelope with a timber load-bearing structure should be designed so that condensation moisture would not occur on timber joints. From a hygienic point of view, the thermo-insulating layers and their physical parameters in the envelope must be designed in such a way that a minimum surface temperature above the critical surface temperature for mould growing can be kept on every point of the interior wall surface. The type, thickness and enclosure of the thermal insulation in the wall composition has a major influence on the resulting fire resistance of the timber panel as well as on the category of the structural element and unit.

The timber structures can be considered as composite systems if the all fire-separating and load-bearing constructions ensuring the building´s stability are only D2 type, while:

- load-bearing components of these construction members have TRO at least D-s2, d0,
- all gaps in these construction members are completely filled with TRO A1 or A2 components with a melting point at least 1000 °C,
- fastening of components in gaps of these construction members prevent them from moving and falling out; it is valid even if the exterior component of the construction member loses its protective function [2].

The D2 construction members do not increase the fire intensity during the required fire resistance, because building materials or elements of the flammability class other than A1 or A2 are enclosed by building materials or components of A1 or A2 flammability class so they do not ignite and do not release heat during the required fire

resistance time. The flammable materials and components inside the D2 member must not reach the flash point during the required fire resistance time; if the time is not defined, it is considered the flash point of 180 °C. The time required to reach the flash point can be demonstrated experimentally or by calculation [4].

It follows that the timber load-bearing members must be protected by linings of A1 or A2 flammability class. The thermal insulation in the air gaps as well as exterior insulation must be non-flammable with a melting point above 1000 °C and its minimum bulk density should be higher than 30 kg/m^3. Thermal insulations based on mineral wool or glass fibre meet these physical parameters.

The D3 construction members may ignite and increase the fire intensity during the required fire resistance, but cannot be considered as D1 or D2 construction members (Fig. 3).

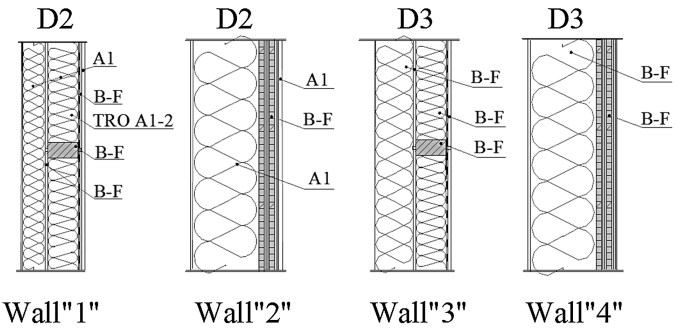

Fig. 3. Examples of building envelopes with: D2 composite construction system - see walls 1 and 2; D3 combustible construction system - see walls 3 and 4; A1 – non-combustible construction member, B-F – combustible construction member.

The further important determinant affecting the material choice for wood-based lightweight building envelopes is the environmental burden. It is defined by the consumption of built-in energy and the emissions generated throughout the entire product life cycle. The aspect of embodied energy consumption is monitored - the energy consumed throughout the product life cycle given in MJ/m^2 PEI (Primary Energy Intensity) and emissions generated by its production, use, and disposal: $CO_{2,aqu}$ - GWP (global warming potential), $SO_{2,aqu}$ - AP (acidification potential), $PO_{4,aqu}$ - EP (eutrophication potential), R - 11_{akv} - ODP (ozone depletion potential), C_2H_4 - POCP (ground - level ozone formation potential).

The equivalent to assess an environmental impact of building materials is $OI3_{KON}$ indicator referring to 1 m^2 of a structure and taking into account the third-weights of eco-indexes drawn on 1 m^2 of a structure. The further indicators to assess an environmental impact of building materials and structures include the values of CO_2 and SO_2 emission production as well as the primary energy embodied. OI3 calculates these categories important for the environmental protection on a scale of 0 to 100. Buildings have better rating if their ecological impact measured by OI3 is lower. Parametric data

of the environmental burden for the individual layers were taken from the website www.baubook.at. Proposed compositions are classified as A+ and A in terms of construction sustainability [5].

5 Material and Construction Solution for Envelopes of Buildings Intended for Housing and Accommodations - A Model Example

Requirements for the fire resistance and construction members are determined by the fire risk of the particular fire compartment and the building's fire height. The load-bearing perimeter wall ensuring the building's stability must meet the minimal REW criterion on the interior side and the REI criterion on the exterior side. The non-load-bearing perimeter wall must meet the minimal EW criterion on the interior side and the EI criterion on the exterior side [6]. The fire resistance values of wall model solutions considering the mentioned boundary conditions are given in Table 1. The part of the perimeter wall that does not meet requirements for the fire resistance or construction member is a fire-open area. Depending on the size of fire-open areas and heat flux density, a fire hazard area will arise around the building. It must not contain fire-open fire areas of neighbouring buildings or other materials that could increase the fire intensity. In wood-based structures, the surface heat flux density in fire is increased by the value of the heat flux that arises from burning of the timber structure itself, including its other combustible components.

Table 1. Physical parameters of layers in building envelope model compositions

No.	Layer type (inside to outside)	Thickness [mm]	ρ [kg/m^3]	λ W/mK	U W/m^{2}K	$\Delta OI3k_{ON}$ Pkt/m^2	CMC	CMFR [min]
W1	Gypsum plasterboard	15	900	0.25	0.14	42.4	**D2**	REI 30
	Polyethylene (PE) vapour brake	1		0.5				
	OSB boards	18	650	0.13				
	80% Glass wool MW	140	18	0.038				
	(20% Timber – frame a' = 625 mm)	(140/60)	475					
	OSB boards	18	650	0.13				
	Mineral adhesive	5		1,0				
	80% Glass wool MW	100	112	0.038				
	Silicate plaster with synthetic resin additive, reinforced	5		0,8				
W2	Gypsum plasterboard	15	900	0.25	0.14	37	**D2**	REI 30
	Cross Laminated Timber (CLT)	≥ 87	475.0	0.12				
	Mineral adhesive	5		1.0				
	80% Glass wool MW	250	140	0.038				
	Silicate plaster with synthetic resin additive, reinforced	5		0.8				

(*continued*)

Table 1. (*continued*)

No.	Layer type (inside to outside)	Thickness [mm]	ρ [kg/m^3]	λ W/mK	U W/m^{2}K	$\Delta OI3k_{ON}$ Pkt/m^2	CMC	CMFR [min]
W3	Gypsum plasterboard	15	900	0.25	0.15	46.4	**D2**	REI 30
	Polyethylene (PE) vapour brake	1		0.5				
	OSB boards	18	650	0.13				
	90% Isolena Schafwolle, Optimal,	140	18	0.043				
	(20% Timber – frame a′ = 625 mm)	(140/60)	475					
	OSB boards	18	650	0.13				
	Mineral adhesive	5		1.0				
	Wood fibre WF-W (130 kg/m^3)	150	130	0.046				
	Silicate plaster with synthetic resin additive, reinforced	5		0.8				
W4	Gypsum plasterboard	15	900	0.25	0.15	49.2	**D2**	REI 30
	Cross Laminated Timber (CLT)	≥ 87	475.0	0.12				
	Mineral adhesive	5		1.0				
	Wood fibre WF-W (130 kg/m^3)	260	130	0.046				
	Silicate plaster with synthetic resin additive, reinforced	5		0.8				

$\Delta OI3_{KON}$ - environmental index, CMC - construction member combustibility, CMFR - construction member fire resistance. Physical parameters of model compositions are taken from the producers' specifications. This table is the result of author's research.

The environmental burden is determined by the built-in energy consumption and emission production throughout the life cycle. The generally accepted equivalent for environmental impact assessment of building materials is the environmental index $OI3_{KON}$. It refers to 1 m^2 of a structure and takes into account the third-weights of eco-indexes drawn on 1 m^2 of a structure.

As of 2020, the required thermo-insulating layer of lightweight wood-based sandwich structures in energy-passive apartment buildings will have to be 260 mm thick, depending on its thermal conductivity. If it is non-flammable, it can increase the fire resistance of the building′s exterior side. If the external thermal insulation of timber sandwich envelopes is flammable and heat released by burning of 1 m^2 is higher than 100 MJ.m^{-2}, it is classified as partly fire-open area. In this case, the resulting area of the envelope fire-open area is the sum of the filling structure area and partially open area expressed by the relation:

$$S_{po} = S_{po1} + S_{po2}.k10 \quad (1)$$

where:

S_{po} - completely fire-open area (m^2),
S_{po2} - partly fire-open area (m^2),
k10 - coefficient of partly fire-open areas whose value is dependent on the heat flux areal density

6 Statistical Data on the Fire Occurrence and Consequences in Buildings Intended for Housing and Accommodation with Composite and Flammable Construction Systems

The flammability of the load-bearing system and components used is related to the fire progression and its subsequent economic consequences. The fire progression in the apartment buildings containing the composite and flammable construction systems is usually very rapid and the fire duration is long up to the complete burn down. Statistical data from 2017, gathered by the Slovak Ministry of Interior, obviously indicate that there always were human fire victims in the buildings intended for housing and accommodation containing flammable construction systems. This fact is related to the lack of fire signalisation in its first phase and consequently very rapid spread of fire.

7 Comparison of Requirements for the Installation of Active Fire Protection in Buildings Intended for Housing and Accommodation According to the Requirements of Slovak and Foreign Legislation

According to the currently valid legislation, a fire signalisation is an electric fire alarm that automatically activates a voice alarm. It primarily serves to make the evacuation faster as well as to activate the fire warning and localisation. The further aspect of an active fire protection is the installation of an automatic fire extinguisher. When the system of automatic fire extinguishing starts, the spread of fire in the building is reduced and fire is localised in the fire compartment where originated. Both types of fire-fighting equipment significantly increase the building´s fire safety and eliminate the extent of fire damage. The obligation to install fire signalisation according to Regulation No. 94/2004, as amended, is dependent on the functional use of protected areas, number of occupants, and building´s fire height. The requirement to install electric fire signalisation (EFS) in accordance with the current legislation is related only to buildings intended for accommodation with a capacity of more than 50 guests. If more than 300 guests are estimated, automatic fire extinguishers should be installed. There are no legislative requirements for the use of active fire protection in the apartment buildings in Slovakia, unlike the neighbouring EU countries where the requirement for fire automatic signalisation in residential and accommodation buildings is standard. The requirements for the sprinkler system installation in particular countries depend on the floor area and the size of residential and accommodation buildings [7–12].

8 Conclusion

As for the fire nature, its progression, and the type of the environment occupied by persons of different ages and mobility, it is necessary to give information on the fire occurrence and hazard as soon as possible.

Even small fires with a low thermal intensity can cause a lot of high toxic smoke in rooms during a short time period. Inhalation of such smoke causes unconsciousness and consequently death. This danger can be eliminated by restricting the use of flammable thermo-insulating and lining materials producing a lot of toxic gases if burning and the early fire detection.

The current Slovak legislative requirements regarding this field are insufficient. The solution is, like in neighbouring EU countries, to establish a legal obligation to install fire detectors and signalisation containing its own power supply. It is necessary to install an automatic fire signalisation so that the apartment or accommodation buildings would be safe. It would be good to make the installation of fire signalisation and its regular revision compulsory for each apartment in the building.

Acknowledgements. The paper presents the results of the project VEGA 1/0248/19.

References

1. STN EN 92 0201 – 2 Structural fire protection. Common regulations. Part 2: Building constructions
2. STN EN 73 0540 – 2 Thermal protection of buildings. Thermal performance of buildings and components. Part 2: Functional requirements
3. Makovická-Osvaldová L, Gašpercová S (2015) The evaluation of flammability properties regarding testing methods. Civ Environ Eng: Sci Tech J 11(2):142–146 ISSN 1336-5835
4. Timber structures according to Eurocode 5 - step 2, Designing details and supporting systems (in Czech), Praha 2004 ISBN 80-86 769-13-5
5. Denz P, Gmeiner H, Rohrer F, Sutter Ch (2017) Oekoindex Bauteilbewertung, Leitfaden zurökologischen Bewertung von Bauteilkonstruktionen mittels Oekoindex, Leitfaden V1.4 (Dornbirn: Energieinstitut Vorarlberg)
6. Iringová A (2017) Impact of fire protection on the design of energy-efficient and eco-friendly building envelopes in timber structures. In: Fire protection, safety and security 2017, Zvolen, 3rd–5th May 2017, Slovak Republic: conference proceedings, pp 72–78. ISBN 978-80-228-2957-1
7. Östman B, Brandon D, Frantzich H (2017) Fire safety engineering in timber buildings. Fire Saf J 91:11–20
8. The building regulation 20. Fire safety HM Government For use in England
9. Cosslam CLT technical design guide v 3.0-Canada
10. Östman B et al. (2010) Fire safety in timber buildings–technical guideline for Europe, SP Report, 19
11. CFPA (2012) Fire prevention on construction sites. Guideline no 21, Confederation of Fire Protection, Associations in Europe (CFPA E). www.cfpa-e.eu
12. FPInnovations (2013) Technical guide for the design and construction of tall wood buildings in Canada. FPInnovations, Vancouver, Canada

Fire Design Model for Timber Frame Assemblies with Rectangular and I-Shaped Members

Katrin Nele Mäger[1(✉)], Mattia Tiso[1,2], and Alar Just[1,3]

[1] Tallinn University of Technology, 19086 Tallinn, Estonia
katrin.mager@taltech.ee
[2] Saint-Gobain Isover, 68526 Ladenburg, Germany
[3] RISE Research Institutes of Sweden, 11428 Stockholm, Sweden

Abstract. Timber frame assemblies (TFA) are load-bearing or separating constructions consisting of timber members, (protective) panelling and void or insulated cavities. The primary protection for a timber member is given by the cladding on the exposed side. After the fall-off of the cladding, insulation materials protecting the sides of timber member might provide the secondary protection. This paper aims to provide an overview of the development of the charring model based on the Effective Cross-Section Method for timber frame assemblies exposed to fire depending on the type of the cavity insulation. The charring model for rectangular and I-shaped timber members is described. The model is based on an extensive fire testing program complemented by thermal simulations. The design model is aimed for the improvement of the revised Eurocode 5 part 1-2 to offer further possibilities for calculations of fire resistance.

Keywords: Fire design · Timber fame assemblies · I-joists

1 Introduction

The behaviour of timber frame assemblies in fire is influenced by the protective properties of cladding and insulation materials. The load-bearing members of timber frame assemblies may be rectangular or I-shaped cross-sections. The distances between timber members vary regionally and the dimensions depend on the availability of the raw material.

Tiso carried out an extensive experimental study of the behaviour of timber frame assemblies in fire [1]. The study, comprised of 36 model-scale furnace tests, included various cavity insulations. The test results were further analysed by thermal simulations and Protection Levels (PL) for insulation materials were defined. Werther has carried out further studies on wood and cellulose fibre insulations [2]. Additionally, I-shaped cross-sections were investigated by Mäger [3].

Members with rectangular cross-sections are normally made of sawn timber or LVL. Cross-section widths are usually from 38 to 120 mm and cross-section heights from 70 to 295 mm. Wooden I-joists, being factory-made ultra-light and highly

L. Makovicka Osvaldova et al. (Eds.): WFS 2020, *Wood & Fire Safety*, pp. 268–274, 2020.
https://doi.org/10.1007/978-3-030-41235-7_40

optimised products for load-bearing frame structures, provide an extended use for light timber frame assemblies. The joists consist of flanges (made of sawn wood, LVL or glulam) and a web (made of a wood-based board).

The design model presented in this paper is the adoption of the Effective Cross-Section Method (ECSM) to timber frame assemblies. The influence of different parameters on the charring depths for timber members of frame assemblies (TFA) is explained. Rectangular cross-sections and I-shaped cross-sections are considered.

2 Fire Experiments

The authors of this paper have performed numerous fire experiments with timber frame assemblies. The list of fire tests considered in this paper is given in Tables 1 and 2. The cavity insulation products involved in this study are high temperature extruded mineral wool (HTE), stone wool (SW), glass wool (GW), cellulose fibre insulation (CF) and wood fibre insulations (WF).

Table 1. List of fire tests of timber frame assemblies with rectangular members.

Test no.	Cavity insulation	Cross-section	Fall-off time of the cladding	Duration of the test	Test no.	Cavity insulation	Cross-section	Fall-off time of the cladding	Duration of the test
1–4	HTE	45 × 145	45	60	21	HTE2	75 × 145	30	60
5–7	SW	45 × 145	45	60	22	HTE2	75 × 145	45	60
8	GW1	45 × 145	45	52.2	23	HTE2	120 × 145	45	60
9	GW2	45 × 145	45	60	24	HTE2	120 × 145	60–68	90
10	CF	45 × 145	45	60	25	GW1	45 × 145	0	21
11	PUR	45 × 145	45	54.3	26	GW1	45 × 145	30	41
12	EPS	45 × 145	45	45	27	GW1	75 × 145	30	50
13	SW3	45 × 145	45	60	28	GW1	75 × 145	45	60
14	SW4	45 × 145	33	60	29	GW1	120 × 145	30	60
15	SW4	45 × 145	35	60	30	GW1	120 × 145	45	60
16	SW5	45 × 145	42	60	31	CF	45 × 145	0	60
17	CF1	45 × 145	45	60	32	CF	45 × 145	30	60
18	GW3	45 × 145	25.5	32.2	33	CF	75 × 145	30	56.7
19	HTE2	45 × 145	0	60	34	CF	75 × 145	45	60
20	HTE2	45 × 145	30	60	35	CF	120 × 145	30	59
					36	CF	120 × 145	45	60

The specimens subjected to standard fire exposure conditions in accordance with EN 1363-1 [4] measured roughly 1 m^2 with the tested timber member placed in the middle of the frame. The two cavities adjacent to the timber member were filled with the selected insulation. Wood battens, steel net or 5 to 10 mm overwidth were used to fix the insulation. During the tests temperatures were measured by thermocouples. After the tests residual cross-sections were measured and evaluated.

Table 2. List of fire tests of timber frame assemblies with I-joists. W for walls and F for floors.

Test no.	I-joist, height	Fall-off time of the cladding	Test duration	Test no.	I-joist, height	Fall-off time of the cladding	Test duration
W1	250	66	82.9	F1	250	44	61
W2	250	61	61	F2	200	59	65
W3	200	21	57	F3	200	22.5	33
W4	200	77	85	F4	300	15	29
W5	200	47	69	F5	220	27	31
W6	200	27	40	F6	220	25	30
				F7	220	27	30

Additionally to the fire tests an extensive program of thermal simulations was performed by Tiso [1] and by Mäger [3] to study different configurations of timber frame assemblies. Thermal material properties from EN 1995-1-2 [5] and Schleifer [6] were used. The heat transfer calculations considered 90 min of fire exposure.

3 Design Charring Model for Timber Frame Walls and Floors

Tiso [1] proposed different **protection levels** of cavity insulations against the charring (from stronger to weaker) that are determined by the relevant model scale furnace test:

- PL1 - insulation materials which guarantee that 2/3 of the lateral side of the timber cross-section is protected against charring for 60 min (e.g. stone wool, HTE).
- PL2 - insulation materials which do not guarantee the complete protection of the sides of members for up to 60 min (e.g. glass wool, cellulose fibre).
- PL3 - insulation materials which allow charring on the sides of members cross-section during the protection phase (e.g. extruded polystyrene).

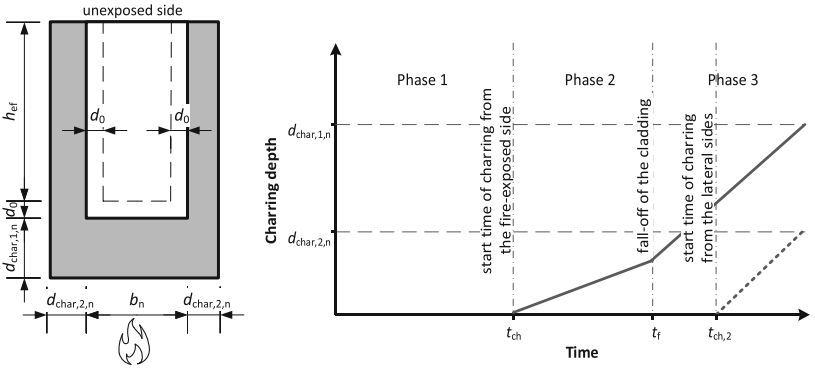

Fig. 1. Charring phases for rectangular members.

Charring Phases, Coefficients. The coefficients for the design model are determined following the principles given by König [7] and adopted to the factorized charring model. Timber members with rectangular cross-sections can have 3 different charring phases: Phase 1 (encapsulation phase) represents the phase where no charring occurs; Phase 2 represents the slow charring behind the protective panelling; Phase 3 represents the fast charring phase after the fall-off of protection. See Fig. 1.

For PL1 cavity insulation charring has to be considered only from the fire exposed side. For PL3 cavity insulation the start time of charring from the fire exposed side defines also the start time of charring on the lateral side.

For wooden I-joists there are 4 charring phases to consider (for the fire exposed side of the flange). See Fig. 2.

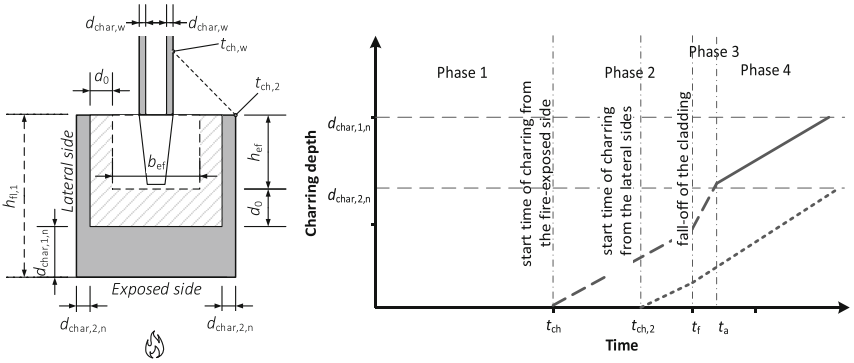

Fig. 2. Charring phases for exposed flange of an I-joist

In Phase 1 no charring occurs behind the protection until time t_{ch}. The start time of charring t_{ch} is dependent on the cladding thickness, material and the substrate. Phase 2 considers charring behind the cladding (from time t_{ch} until time t_f). The fall-off time of the cladding t_f is dependent on the cladding material, orientation and fixation. After the failure of the claddings the structural member and cavity insulation will be directly exposed to fire and the charring rate of the wooden flange will be much higher compared to the charring rate behind the cladding. Fast charring can occur for a short time and will consolidate at time t_a. After the consolidation time t_a the charring Phase 4 is considered where charring rate turns slower.

Charring Depth

Charring depth on the fire side of the cross-section is

$$d_{\text{char},1,\text{n}} = k_{\text{s,n}} k_2 \beta_0 (t_\text{f} - t_\text{ch}) + k_{\text{s,n}} k_3 \beta_0 (t - t_\text{f}). \tag{1}$$

where $k_{\text{s,n}}$ is the cross-section factor; k_2 and k_3 are the charring factors used in charring phase 2 and 3; β_0 is a basic design charring rate; t_{ch} is the start time of charring; t_f is the fall-off time of the protection system; t is the total fire exposure time.

Basic design charring rate β_0 is a physical property of a timber species. For European softwood species the basic design charring rate is 0,65 mm/min.

Cross-section coefficient $k_{s,n}$ considers the effect of cross-section width on the notional charring depth. Coefficient $k_{s,n}$ is given as a function of cross-section width.

Protection coefficients (k_2, k_3) describe the charring rates in the protected and post-protection phase. The subscript indicates the number of protection phase: k_2 is taking the influence of panelling on the charring rate into account; k_3 is taking the influence of faster charring rate after the fall-off of cladding into account. k_3 depends on the cavity insulation and can be determined using the test methodology by Tiso [1].

Charring depth on the lateral side of the cross-section is

$$d_{\mathrm{char},2,\mathrm{n}} = k_{\mathrm{s,n}} k_{3,2} \beta_0 \left(t - t_{\mathrm{ch},2}\right). \tag{2}$$

Start time of charring on the lateral side $t_{\mathrm{ch},2}$ is regarded as the beginning of charring on the three quarters of height of the cross-section:

$$t_{\mathrm{ch},2} = t_{\mathrm{f}} + 0,75h/v_{\mathrm{rec}}. \tag{3}$$

Recession speed of the insulation v_{rec} characterises a progress of charring on the lateral sides of cross-section. Recession speed is determined by model scale tests by measuring development of 300 °C isotherm between the insulation and timber member. The recession speed of traditional glass wool is 30 mm/min, 20 mm/min for cellulose fibre insulation and around 4 mm/min for stone wool.

Charring Model for I-joists

The charring model for wooden I-joists is based on the model for timber frame assemblies with rectangular cross-sections by Tiso [1]. As I-joists are more sensitive to elevated temperatures due to the small cross-section area of the flanges and a thin web, the charring calculations have been modified accordingly.

The notional charring depth on the fire-exposed side of the flange is:

$$d_{\mathrm{char},1,\mathrm{n}} = k_{\mathrm{s,n}} k_2 \beta_0 (t_{\mathrm{f}} - t_{\mathrm{ch}}) + k_{\mathrm{s,n}} k_3 \beta_0 (t_{\mathrm{a}} - t_{\mathrm{f}}) + k_{\mathrm{s,n}} k_4 \beta_0 (t - t_{\mathrm{a}}). \tag{4}$$

Where t_{a} is the consolidation time and k_4 is the consolidation factor.

The actual charring scenario may include one or more charring phases and the equation shall be modified for each case accordingly (see Fig. 2). The start time of charring on the lateral side $t_{\mathrm{ch},2}$ can occur in Phase 2, Phase 3 or Phase 4 depending on the cladding and the cavity insulation.

If the charring on the lateral sides of the flange starts before the fall-off of the fire protection system, then the charring on the lateral sides occurs in two phases:

$$d_{\mathrm{char},2,\mathrm{n}} = k_{\mathrm{s,n}} k_2 \beta_0 \left(t_{\mathrm{f}} - t_{\mathrm{ch},2}\right) + k_{\mathrm{s,n}} k_{3,2} \beta_0 (t - t_{\mathrm{f}}). \tag{5}$$

The charring depth of the web is considered from time $t_{ch,w}$ and calculated as:

$$d_{char,w} = k_2 \beta_{0,w} (t - t_{ch,w}). \quad (6)$$

$t_{ch,w}$ is the start time of charring of the web and $\beta_{0,w}$ is the charring rate of the web material.

4 Analysis and Discussion

Based on the extensive series of fire tests and simulations described above the following analysis and discussion is presented.

All the tests show that the most important fire barrier for timber frame assemblies is the cladding on the fire side. The influence of fire on reducing the size and strength of the timber member will increase extensively after the fall-off of cladding. Cavity insulations can still provide some protection.

The effect of panelling will be considered using three design parameters – start time of charring t_{ch}, fall-off time of the cladding t_f and coefficient k_2 for reduced charring behind the cladding. These parameters can be determined according to EN 13381-7 [8]. Some generic values will be given in the revised EN 1995-1-2 for gypsum boards, clay and lime plasters and stone wool boards. Claddings have to be properly fixed.

Effect of Cavity Insulation. Insulation materials can provide different contributions on the charring and heating of the timber member. The protection level (PL) of the insulation material determines the relevant charring scenario.

For timber members with rectangular cross-sections the recession of the insulation can be neglected for PL1 insulations. For exposed flanges of I-joists even a PL1 insulation can allow charring on the lateral side. Therefore, the recession speed is needed to be defined for all insulation materials.

Duration of the protective effect of insulation in the post-protection phase should be limited in the design model. Mäger [9] has proposed limits for stone wool and glass wool. When the protection by cavity insulations is considered in the design then it should be held in place during the post-protection phase (by using resilient bars of steel or wooden battens or fasteners). I-joists can hold the insulation in place more efficiently owing to their shape. Insulation can be supported by the corners of the flanges.

Simplification of Designed Cross-Sections. To keep the design model simple for engineers, the designed remaining cross-sections are counted to be rectangular. The actual charred cross-section shapes are replaced with equivalent rectangular simplifications. For initially rectangular cross-sections the equivalence is based on the section modulus and for I-joists the simplification is based on the cross-sectional area of the flange.

The flanges of I-joists are affected relatively more by corner roundings. This leads to the need to consider lateral charring in quite an early stage even if the PL1 cavity insulation is used.

Charring of the web of an I-joist can be critical for the fire resistance of the whole I-joist. Charring of the web can start early if the insulation is not properly placed or if

the insulation tends to shrink. Measurements in the fire tests have shown that the most critical zone on the web concerning the start of charring is the zone located in the line of 45° from the outer corner of the flange. Special web insulation can be applied to improve the fire resistance of an I-joist.

References

1. Tiso M (2018) The contribution of cavity insulations to the load-bearing capacity of timber frame assemblies exposed to fire. PhD thesis. TTÜ Press, Tallinn
2. Werther et al (2018) Standardisierung der brandschutztechnischen Leistungsfähigkeit von Holztafelkonstruktionen mit biogenen Dämmstoffen. TUM report. Zukunftbau
3. Mäger K, Just A (2019) Preliminary design model for wooden I-joists in fire. In: 6th Inter meeting, Tacoma
4. EN 1363-1:2012 (2012) Fire resistance tests - Part 1: General Requirements. CEN
5. EN 1995-1-2:2004 (2004) Eurocode 5 Part 1-2: Design of timber structures – Part 1-2: General – Structural fire design
6. Schleifer V (2009) Zum Verhalten von raumabschliessenden mehrschichtigen Holz-bauteilen im Brandfall. PhD thesis. ETH Zürich
7. König J, Walleij L (2000) Timber frame assemblies exposed to standard and parametric fires: part 2: a design model for standard fire exposure. Trätek report 0001001
8. EN 13381-7:2019 (2019) Test method to determine the contribution to the fire resistance of structural members - Part 7: Applied protection to timber members. CEN
9. Mäger K, Just A, Frangi A (2018) Improvements to the component additive method. In: Proceedings of the 10th international conference on structures in fire: structures in fire, Belfast

Proposal of Changes in Fire Safety Assessment for Extending the Usability of Wood in Buildings

Petr Kučera(✉), Isabela Bradáčová, Jiří Pokorný, and Tereza Češelská

VSB – Technical University of Ostrava,
Lumírova 13, Ostrava – Vyškovice, Czech Republic
petr.kucera@vsb.cz

Abstract. Structural wood and wood-based materials have gone through a major development in recent years in terms of their properties and together with the development of active elements of fire safety there is new room for adjustment of existing fire design approaches of wooden buildings. This article presents a list of technical fire safety conditions associated with designing timber structures and buildings and analyses existing barriers in utilizing timber as a construction material in terms of fire safety. The aim of this article is to propose changes in assessment of fire safety design with regards to possible risks and limitations associated with specifics of timber construction and aims towards a possible recommendation for changes and an increase of the amount of timber construction.

Keywords: Fire safety · Structural timber · Timber building · Design

1 Introduction

The share of timber construction in the total number of newly built structures is still growing, the share of timber family houses on the market was 16.1% [1], which is very low compared to other European countries, especially the Nordic countries and Austria. The reasons can be found in historical and psychological areas and subsequently in legal and technical areas [2].

A fire in buildings with wooden structures has always been a disaster with high property losses, often with fatal consequences for people's health and lives [3]. Due to experiences of big fires of towns and villages the notion that wooden buildings are less safe than, for example, brick buildings has anchored in people's subconscious, furthermore wood is susceptible to rot and wood-destroying pests [4].

The response to fires in buildings (not only wooden ones) was an effort to issue regulations that imposed obligations on citizens in the event of a fire and on the other hand volunteer and professional fire brigades prescribed their own firefighting activities. Later regulations have already dealt with fire safety requirements for the construction of at least some parts of wooden buildings and set the status and role of state fire supervision. Regulations always corresponded to the level of technology and knowledge of the period.

L. Makovicka Osvaldova et al. (Eds.): WFS 2020, *Wood & Fire Safety*, pp. 275–280, 2020.
https://doi.org/10.1007/978-3-030-41235-7_41

In Czechoslovakia in the 1960s, the rapidly expanding construction industry utilizing a new material base overtook regulations, which forced the preparation and publication of a completely new set of fire standards, which, unlike the exhaustively given requirements of older standards, was based on results of domestic and foreign testing [5, 6]. This multiply amended Standard Code is still valid in the Czech Republic.

Technical barriers are often due to not fully verified fire-technical properties of timber structures [7] and sometimes low faith in fire safety equipment (automatic fire detection, fixed firefighting system, or smoke and heat control system) [8, 9].

2 Current Conditions for the Design of Wooden Buildings

The rules of the Czech Republic concerning fire protection of buildings are binding on two levels: binding (EU regulations and laws, laws of the Czech Republic and their implementing regulations) and valid but non-binding (national fire standards specifying requirements for buildings).

The design of wooden buildings in the Czech Republic is influenced by the above-mentioned legal and technical regulations, in particular by the binding Decree no. 23/2008 Coll. [10]. The ban on the use of timber construction under specified conditions applies to: construction of a lookout tower, construction of a fuel filling station, service and repair shop, construction used for school and school facilities, agricultural construction and construction for production and storage.

Further restrictions for wooden buildings are given in the standards of the Fire Code ČSN 73 08xx. The requirements are related to the construction design, fire risk and fire height of the building.

Structural systems of buildings as a spatial structure of load-bearing and fire separating structures are divided into non-combustible, mixed and flammable systems. The classification of the structural system is determined by the types of individual vertical and horizontal structures taking into account the influence of flammable products (building materials) contained in them. Let us emphasize that in the Czech Republic, the individual building structures (as opposed to other European countries) are classified into types DP1, DP2 and DP3. Classes of reaction to fire of individual parts of the structure (sandwich structures are bearing and facing parts) are assessed and whether flammable products influence the bearing capacity and stability of the structure and whether they act as a catalyst in case of fire. Non-loadbearing flammable thermal or acoustic insulation layers shall not be evaluated if they are reliably fire protected by cladding products against fire class as A1 or A2. Timber load-bearing and fire separating structures can be of the type DP2 (fire-protected timber) or DP3 (without fireproof tiles). Wooden structures therefore influence the type of construction system of the building.

Fire risk in nonindustrial buildings, p_v, expresses the theoretical intensity of the fire and the effectiveness of fire safety measures. It is expressed in $kg.m^{-2}$, i.e. the notional amount of wood (kg) per unit area (m^2). It depends on the purpose of the building and the flammable materials and substances occurring there.

The fire height of the object h in m is given by the distance from the floor of the 1st floor (GF) to the floor of the last floor (where people permanently stay). It is thus defined differently from the construction concept of height. Typical cases of non-production buildings where the use of the wood as a structural material is restricted or completely prohibited are given in Table 1.

Table 1. Restrictions on the use of wooden buildings as non-production facilities

Type of object	Flammable structure system
Generally allowed for	$h \leq 9$ m event. $h \leq 12$ m (according to fire risk)
Exceptions:	
Outpatient facilities (with more than 3 medical facilities)	New building - banned
	Change of structure - max. GF
LZ 1 Inpatient facilities (max. 15 adults or 10 children)	New building - banned
	Change of structure - banned
LZ 2 Inpatient facilities (beds for more than 15 adults or 10 children)	New building - banned
	Change of structure - banned
Nursing homes - flats (for more than 12 persons)	New building - banned
	Change of structure - banned
Social care institutions - inpatient part (accommodation for more than 15 adults or 10 children)	New building - banned
	Change of structure - banned
Infant homes and orphanages (for more than 10 children under 3 years)	New building - banned
	Change of structure - banned
Nursery (special medical facility for children)	New building - banned
	Change of structure - banned
Kindergarten	New building - max. 2nd floor, in another building h $\leq$ 1F, bearing and fire separating structures DP1 or DP2
	Change of structure over 12 children or higher than 1st floor - prohibition
Internal assembly areas - for larger numbers of people and at a certain height level (fire risk $p_v \geq 45$ kg.m^{-2})	New building Change of structure - banned
Fire compartments below outdoor assembly areas with more than 1000 persons	Banned
OB 4 larger accommodation facility (for more than 75 people up to the 3rd floor or for more than 40 people between 1st and 8th floor)	
Wooden lookout tower Without any other purpose	Max. 4F >2F + SHZ, DHZ + EPS

Explanatory notes:
h (m) - fire height (ČSN 73 0802 [11]) - see text above
p_v (kg.m^{-2}) - fire risk in nonindustrial buildings (ČSN 73 0802 [11]) - see text above
DP1 and DP2 - type of structural part or component from the fire point of view (ČSN 73 0810 [12]) - see text above
SHZ - sprinkler fixed fire extinguishing equipment (ČSN 73 0810 [12])
DHZ - sprinkler auxiliary fire extinguishing equipment (ČSN 73 0810 [12])
EPS - automatic fire detection and alarm system (ČSN 73 0802 [11])

3 Proposal of Changes in Fire Safety Assessment of Buildings to Extend the Usability of Timber Structures

The target fire safety requirements of buildings - in accordance with European regulations - are:

- Safe evacuation of people, animals and property.
- Reduction of fire, spread of fire and its products.
- Prevention of fire spread to surrounding buildings.
- Creating conditions for effective and safe intervention of rescue teams.

The opening of opportunities for wider use of wood in construction is subject to the fulfillment of the target requirements for construction. The proposed changes are scaled from simpler changes consisting of adjusting the requirements of currently applicable regulations that can be implemented in a shorter period of time to vigorous changes that require an overall change in regulations and whose preparation and implementation is a longer process.

The simpler recommended alterations concern minor modifications to binding legislation and some requirements of the existing Code of non-binding Fire Safety Standards, while maintaining currently established rules. An example could be single-storey kindergartens, where it is forbidden to use load-bearing and fire separating structures without fire-resistant tiles (type DP3). The proposal recommends to allow these constructions in the DP3 design on condition that the buildings are equipped with an electric fire alarm. Similarly, for internal assembly areas (ČSN 73 0831 [13]), it is proposed to use wooden structures DP2 (now prohibited) under the condition that target fire safety requirements are met by an alternative procedure. For buildings OB 4, it is recommended not to take into account the fire height of the building, but only the number of floors above ground.

In wooden constructions, it is necessary to support the installation of suitable fire safety systems (electric fire alarm systems, automatic fixed fire extinguishers and smoke and heat removal systems), which react quickly to the occurrence and development of a fire without human intervention. In this way, the evacuation, localization and extinguishing of the fire can start before rescue units arrive.

All proposed amendments assume that the existing requirements for the establishment and implementation of protected escape routes remain unaffected. This means that protected escape routes must always be used for DP1 structures.

Further refinement is to affect the assessment of wood-based cladding structures in relation to their fire resistance and thus to determine the spacing and delimitation of fire-hazard areas around burning objects. Assess the cladding only according to whether or not they contribute to fire intensity.

Fire engineering, which is being gradually implemented in the design of buildings, is a set of policies and procedures designed to assess fire safety of particularly hazardous or otherwise specific buildings or technologies, with the aim of finding an effective fire protection solution while ensuring an acceptable level of risk. However, fire engineering is to be understood as a subcategory of the procedure different from both the Czech technical standard and another technical document regulating the

conditions of fire protection (Fig. 1). In the future, tools of various procedure will be refined and expanded with the assumption of a more positive evaluation of timber structures in buildings.

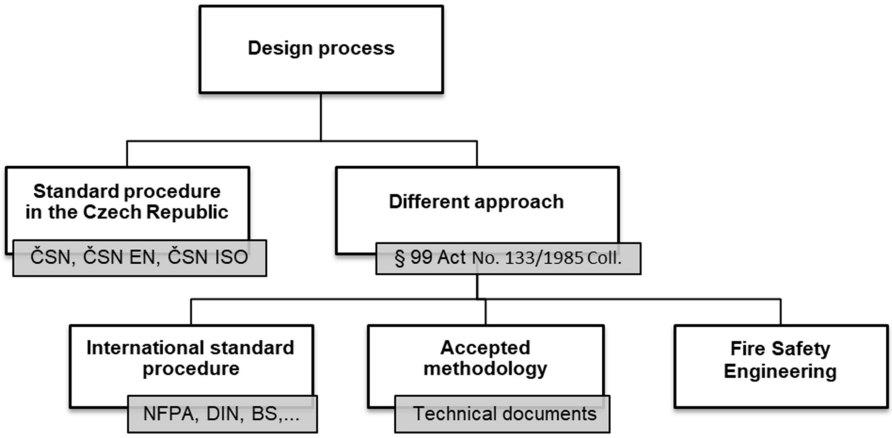

Fig. 1. The relationship between standard and different procedures [14]

However, the proposal to remove the classification of constructions of types DP1 to DP3 will require an overall change in the binding legal regulations of the Czech Republic and subsequently of the entire existing code of fire standards and a large number of other standards specifying specific requirements for fire protection. The introduction of the classification of structures on DP1 to DP3 was enforced by the original national test standard for determining the flammability of building materials, which did not allow testing of multilayered and heterogeneous products. In fact, by adopting European standards for testing and classifying construction products by reaction to fire, this obstacle has already been removed. However, such a large volume of amendments to all Czech regulations requires a longer period of time. The substitution for the classification of constructions into types DP1 to DP3 is to be the path that some European countries have already taken and others are preparing to do (e.g. Poland) - classification only for constructions that contribute to fire intensity and constructions that are not fuel.

4 Conclusion

The growing stock of wood in the Czech Republic is the cause of intensive efforts for its wider use in construction. Although timber structures and wooden buildings have many advantages, they are perceived rather negatively due to the ease of spread of fire. In the Czech Republic, the construction of wooden structures is limited and dependent on the purpose of the building, its fire height in combination with fire risk, or is not

allowed for certain types of buildings at all. Restrictions on the use of wood are mainly based on historical negative experience with fires of wooden structures.

Recently, active fire safety equipment has been increasingly used in buildings. In connection with timber constructions, these are mainly electrical fire signaling devices, which enable timely fire detection and automatic fixed fire extinguishers, which are able to limit the spread of fire or possibly to extinguish it completely. Heat and smoke evacuation devices allow evacuation and fire intervention, protect property and reduce thermal stress on building structures. Extending the requirements for the installation of active fire safety equipment is a promising way to expand the use of wood in construction sites.

Developing a different approach based on fire scenario modeling and the use of powerful computer technology can also contribute to the wider use of wood in the construction of the Czech Republic.

Many foreign countries, in particular the United States, Norway, Sweden, Denmark and others, are taking a similar approach. The Czech Republic is currently taking steps in a similar direction.

Acknowledgement. This work was supported by the project of the Ministry of the Interior of the Czech Republic No. VI 20162019034 "*Research and development of validated models of fire and evacuation and their practical application in fire safety of buildings*".

References

1. Český statistický úřad (2019) Stavebnictví se v posledních letech daří. ČSÚ, Praha
2. Heitz J (2016) Fire resistance in American heavy timber construction history and preservation. Springer, Heidelberg
3. Buchanan AH, Abu AK (2017) Structural design for fire safety, 2nd edn. Wiley, Chichester
4. Aseeva R, Serkov B, Sivenkov A (2014) Fire behavior and fire protection in timber buildings. Springer, Heidelberg
5. Reichel V (1976) Požární předpisy pro stavební objekty v praxi (Zabraňujeme škodám sv. 2). Česká státní pojišťovna, Praha
6. Reichel V (1981) Stanovení požadavků na stavební konstrukce z hlediska požární bezpečnosti (Knižnice PO sv. 57). Svaz požární ochrany ČSSR, Praha
7. Martinka J (2018) Požiarne riziko materiálov (Edícia vedeckých mohografií). Slovenská technická univerzita v Bratislave, Bratislava
8. Purkiss JA, Li L (2013) Fire safety engineering - design of structures, 3rd edn. CRC Press - Taylor & Francis Group, New York
9. Östman B, Brandon D, Frantzich H (2017) Fire safety engineering in timber buildings. Fire Saf J 91:11–20
10. Vyhláška č. 23/2008 Sb. (2008) o technických podmínkách požární ochrany staveb, ve znění pozdějších předpisů
11. ČSN 73 0802 (2009) Požární bezpečnost staveb. Nevýrobní objekty, ÚNMZ, Praha
12. ČSN 73 0810 (2016) Požární bezpečnost staveb. Společná ustanovení, ÚNMZ, Praha
13. ČSN 73 0831 (2011) Požární bezpečnost staveb. Shromažďovací prostory, ÚNMZ, Praha
14. Kučera P, Pavlík T, Pokorný J, Kaiser R (2012) Požární inženýrství v rámci plnění úkolů HZS ČR. MV Generální ředitelství Hasičského záchranného sboru ČR, Praha

Behavior of Bamboo Wall Panel at Elevated Temperature

Anu Bala, Ashish Kumar Dash, Supratic Gupta, and Vasant Matsagar(✉)

Department of Civil Engineering, Indian Institute of Technology (IIT) Delhi, Hauz Khas, New Delhi 110 016, India
matsagar@civil.iitd.ac.in

Abstract. With the development of technology, mud plaster has been replaced by cement plaster for supporting bamboo mesh in wall panels and known as ekra wall or bamcrete wall. Usually, low grade mortar is used in making the bamcrete wall, while the latest studies have used high strength mortar. Bamboo burns through pyrolysis process like wood when it is exposed to the fire condition. Fire safety is one of the major challenges for the construction industry to use the bamcrete wall panel. In the present study, performance of bamboo reinforced panels at elevated temperature is presented. Bamboo strips were inter-woven and protected by the cement mortar. The weight-loss and loss of mechanical strength of wall panel has been studied at 100 °C, 200 °C, 300 °C, and 400 °C maintained for a fixed time period.

Keywords: Bamboo · Bamcrete · Bamboo reinforced wall panel · Elevated temperature

1 Introduction

In the recent years, a lot of attention has been paid to structural sustainability, safety, durability of structures and use of new sustainable materials. Bamboo is a hemi-cellulose material (similar characteristics to timber) has high potential for sustainable structures with high economic advantages. Bamboo is used as a load-bearing material having good tensile strength (can reach up to 370 MPa), high resistance-to-weight ratio; however, applications are limited to low-rise buildings, bridges and roof systems [1, 2]. The density of the round bamboo is generally in the range of 773–993 kg/m^3 [3].

Since ancient time, bamboo has been extensively used for walling system in houses, boundary walls, etc. Houses completely made of bamboo culms are common sites in the north-eastern parts of India. Most of the old and lower economic class people have houses with mud plastered walls topped by thatch roof system. However, this practice had a drawback of termite attack on bamboo and had to be replaced frequently. An advancement to this technique gave rise to ekra wall system where mortar is used as the plastering material for bamboo and has an advantage of both protection to inhabitants from extreme weather conditions as well as enhanced lifespan for bamboo reinforcement. This system has been named as bamcrete wall panel.

L. Makovicka Osvaldova et al. (Eds.): WFS 2020, *Wood & Fire Safety*, pp. 281–287, 2020.
https://doi.org/10.1007/978-3-030-41235-7_42

A typical bamcrete house in Guwahati was dismantled after 40 years of construction [4]. Untreated bamboo was used in this construction. Bamboo inside the wall was absolutely in good condition with no deterioration, implying that bamboo inside mortar is well protected.

Popularizing this bamcrete wall panel will increase demand of bamboo, provide more diversity of agricultural production, stimulate local economy, and provide sustainable construction. Use of bamboo reinforced panel makes it economical, shock absorbing as well as environment-friendly [4].

In this study of fire resistance of bamcrete panel, it is important to understand that bamboo is expected to burn through pyrolysis process like wood when it is exposed to the fire condition. It takes longer time to achieve ignition temperature under a constant flux than plywood [5]. Globally, no standard exists to design bamboo elements under exposed fire conditions to the best of the knowledge of the authors. Due to the relatively poor understanding on the mechanical behavior of bamboo at elevated temperatures, the design guidelines are limited to low-rise structures [2]. Bamboo elements experience a significant reduction in the mechanical strength and modulus of elasticity at the elevated temperature. This reduction in strength can be delayed by using cement mortar plaster as it acts as a thermal barrier.

When concrete is subjected to elevated temperature below 300 °C, tiny cracks develop on cement mortar surface along the boundary of calcium hydroxide crystals and unhydrated cement particles. However, majority of the cracks develop in between 300 °C and 500 °C [6–8].

In view of the very little research information available on the fire safety of bamcrete wall panels, present work is focused on the determination of the behavior of single mesh bamcrete wall panel at elevated temperature. It has been reported in various studies that wood/bamboo starts charring at a temperature of about 300 °C [9, 10]; hence, in this research, to study the behavior of bamcrete panel a maximum of 400 °C temperature was considered. The weight-loss and mechanical strength of bamcrete wall panels at 100 °C, 200 °C, 300 °C, and 400 °C was analyzed for a fixed time duration.

2 Experimental Study

To fabricate the wall panels, untreated bamboo culm with three to five years old diameter of 30–40 mm was procured. The slivering (process of splitting bamboo and getting strips out of bamboo culms) was done manually to get stripes of size 20–22 mm width and 8–10 mm thickness. Metallic frame of 0.7 m × 0.7 m size was made with U-frame of 15 mm width and 30 mm depth. The bamboo strips were inter-woven inside the U-frame in vertical direction along with two rows of bamboo strip in the horizontal direction as shown in the Fig. 1.

Mortar mix (M30 grade) was prepared in mixers using plasticizers to reduce the water content and increase the strength of mix. In these mixes, *k*-factor was used to define the effectiveness of fly ash percentage, such that $w/c + kf$ is the effective w/b (water-binder ratio). The design mix chosen for the study is shown in Table 1.

Admixture of 0.35% by weight of cement and fly ash was added to give better workability. The effective w/b of 0.54 with 250 kg of water was selected for casting the panels.

Bamboo mesh were made wet before the plastering to make the matrix bind on the bamboo strips. One side of the frame is kept vertically and sprayed with mortar, finished and left to cure for one days. The other side is then cleaned off loose material and then it is plastered. The panel is then covered with jute bags and left for curing for minimum of 14 days. Simultaneously, cubes were also cast during the process and were checked for quality of mix prepared during the plastering operation. Weight of the single layer bamboo mesh panel with the frame was about 4 kg and fully cast bamcrete panel was approximately 45 kg.

Fig. 1. Inter-woven bamboo strips inside the metallic frame and fully cast panel.

Table 1. Mix Design and flexural strength results

Mix no.	w/b	Water (kg)	Cement (kg)	Fly ash (kg)	Sand (kg)	Strength 7-day (MPa)	Strength 28-day (MPa)
1	0.54	260	412	137	1361	23	39

The bamcrete panels were air-dried nearly for two months before testing its behavior under elevated temperature. The bamcrete panels were subjected to elevated temperature in a heating furnace at the temperature ranging from 100 °C to 400 °C. The heating rate of the furnace (as per ISO) was adjusted such that desired temperature of 100 °C, 200 °C, 300 °C, or 400 °C is achieved in one hour. To study the panel behavior at an elevated temperature the rate of heating of the closed chamber was maintained to achieve a particular test temperature as per the requirements [11]. After this, the sample was kept at peak temperature for a holding time of one hour. After that, heating process was switched off and samples were allowed to cool gradually within the furnace. Next day, the samples were taken out and kept for two days before testing. The weight of the panel was measured. The specimen was placed horizontally in the loading arrangement and tested as shown in Fig. 2.

Fig. 2. Experimental setup.

3 Experimental Results

Currently, no standard test methods are available to determine the fire behavior of bamcrete panels under elevated temperature to the best of the knowledge of the authors. To understand the behavior of bamcrete panels, ISO 834 [12] and ASTM 119 [13] for the fire tests of elements of building construction and materials have been used. After exposing the panels at elevated temperature, damage of the bamcrete panel can be roughly seen by visually observing the color change, texture of the surface, cracking and spalling of the panel surface [14]. In the present case, there was no such visual change except the color change of the panels. There was no change in color at 200 °C. At 300 °C, light smoke smell was experienced and there were grey patches in the periphery of the panel. At 400 °C, the smoke smell increased while dark patches were observed in the periphery of the panel.

The weight-loss reaches from 5% to 11% at an elevated temperature from 100 °C to 400 °C respectively as shown in Fig. 3. The weight-loss of the panel is related to the change of mechanical properties of the panel at an exposed condition to fire.

Transverse (vertical) load was applied to examine the flexural strength of the bamcrete panel which was exposed at elevated temperature. The flexural strength of the bamcrete panel decreases with increasing temperature as shown in Fig. 4. The flexural strength of the bamcrete panel significantly decreased after an exposure of 100 °C and there was a sharp reduction in strength beyond this point. The strength of the bamcrete panel was remaining 80% to 21% when the panel was heated at 100 °C to 400 °C, respectively. The reduction in strength of the bamcrete panel at an elevated temperature can be attributed to the dehydration of the water from the panel and charring of bamboo strips.

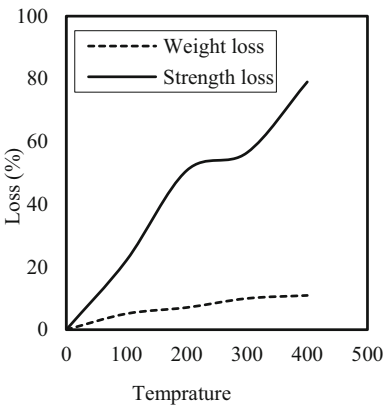

Fig. 3. Weight and strength loss with temperature.

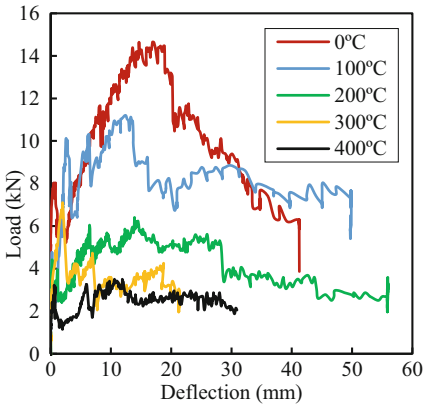

Fig. 4. Load-deflection curve with temperature.

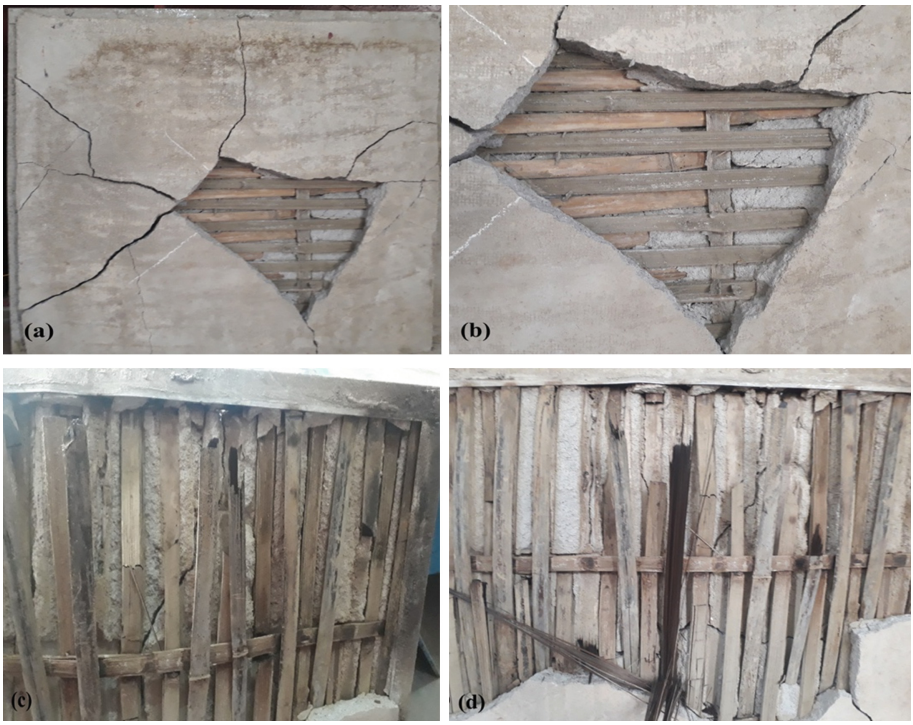

Fig. 5. Bamcrete panels after treating at elevated temperature (a) 100 °C; (b) 200 °C; (c) 300 °C; and (d) 400 °C.

After the exposure at elevated temperature for 60 min, the condition of the bamboo strips was analyzed by visually inspection of the panels. The condition of the bamboo strips at 100 °C and 200 °C was not deteriorated as it appeared same as before testing and the cement mortar was intact with both sides of the panels. This cement plaster act as a protective cover for the bamboo strips at an elevated temperature up to 200 °C.

At 300 °C temperature, the outer color of the strip was not changed, but was partially black from inside and behaved as a brittle material. At 400 °C temperature, bamboo strips were 60–70% charred and it showed grey and black color and was brittle as shown in Fig. 5.

4 Conclusions

Single mesh bamcrete panels were subjected to elevated temperature, no other visual observation was made except the color changed to yellow, grey and black with temperature change from 300 °C to 400 °C. The weight-loss of the bamcrete panels was gradually increased with increasing temperature. This reduction in weight was 5% to 11% at an elevated temperature from 100 °C to 400 °C. The flexural strength of the bamcrete panel significantly decreased after an exposure of 100 °C. The strength of the bamcrete panel were remaining 80% to 21% when the panel was heated at 100 °C to 400 °C.

References

1. Correal JF, Echeverry JS, Ramírez F, Yamín LE (2014) Experimental evaluation of physical and mechanical properties of Glued Laminated Guadua angustifolia Kunth. Constr Build Mater 73:105–112
2. Mena J, Vera S, Correal JF, Lopez M (2012) Assessment of fire reaction and fire resistance of Guadua angustifolia kunth bamboo. Constr Build Mater 27(1):60–65
3. Ghavami K (1995) Ultimate load behavior of bamboo-reinforced lightweight concrete beams. Cement Concr Compos 17(4):281–288
4. Dash AK (2018) Evaluation of bamcrete panel as an effective walling system. Doctoral dissertation, Indian Institute of Technology (IIT) Delhi, India
5. Madden J, Guiterrez M, Maluk C (2018) Structural performance of laminated bamboo columns during fire. In: Australian structural engineering conference: ASEC-2018. Engineers Australia, p 210
6. Lin WM, Lin TD, Powers-Couche LJ (1996) Microstructures of fire- damaged concrete. Mater J 93(3):199–205
7. Piasta J (1984) Heat deformations of cement paste phases and the microstructure of cement paste. Mater Struct 17(6):415–420
8. Handoo SK, Agarwal S, Agarwal SK (2002) Physicochemical, mineralogical, and morphological characteristics of concrete exposed to elevated temperatures. Cem Concr Res 32(7):1009–1018
9. Lipinskas D, Maciulaitis R (2005) Further opportunities for development of the method for fire origin prognosis. J Civ Eng Manag 1(4):299–307
10. Lingens A, Windeisen E, Wegener G (2005) Investigating the combustion behaviour of various wood species via their fire gases. Wood Sci Technol 39(1):49–60

11. Mačiulaitis R, Jefimovas A, Zdanevičius P (2012) Research of natural wood combustion and charring processes. J Civ Eng Manag 18(5):631–641
12. ISO: 834 (1999) Fire resistance tests-elements of building construction. International Organization for Standardization, Geneva, Switzerland
13. ASTM (2001) E119, standard test methods for fire tests of building construction and materials, West Conshohocken, Pennsylvania (PA), USA
14. Buchanan AH (2001) Fire engineering design guide. Centre for Advanced Engineering, University of Canterbury, New Zealand

Study of Thermal Exposure of a Seat of Fire Inside a Building with a Façade Fabricated of Timber Materials on the Construction Elements of Adjacent Facilities

Vadym Nizhnyk(✉), Serhii Pozdieiev, Yurii Feshchuk, Olexander Dotsenko, and Volodymyr Borovykov

The Ukrainian Civil Protection Research Institute, Kyiv 01011, Ukraine
nignyk@ukr.net

Abstract. Results of experimental determination of temperature changing of construction elements of adjacent buildings depending on heat exposure of a seat of fire involving façade fabricated of timber materials are submitted. We conducted processing of the experimental data derived. It follows from analysis of the experimental data that absolute deviations of experimental data for each experiment from appropriate average values do not exceed 12.6 °C that equals to 19.8% in percent expression form, and maximum root-mean-square deviation is 7.4 °C that indicates satisfactory convergence of the experimental data derived. We conducted check-up of belonging of the data derived to single general population by Fisher criterion and it confirmed that their dispersion was allowable. Dependency was drafted using numerical regression equation of the building façade surface temperature on the separation distance between such a building and seat of fire and duration of heat exposure. We showed that divergence between calculated data derived using this dependency and experimental data did not exceed 20%, and this is acceptable for further application of the results derived. Dependency of change of the temperature decrease factor on the separation distance to the heat source was determined which was of nonlinear nature.

Keywords: Fire separation distance · Temperature · Seat of fire

1 Introduction

Rational use of territories for their development causes enhancement of the building density within urban settlements and manufacturing plants. Therefore, compromise is to be reached between economic performance reflected in maximum building density at the territory and ensuring appropriate fire safety level. Ensuring of adherence to fire safety regulations can be reached using proper state-of-the-art calculation methods because tabular procedures are rather strict and obsolete.

L. Makovicka Osvaldova et al. (Eds.): WFS 2020, *Wood & Fire Safety*, pp. 288–294, 2020.
https://doi.org/10.1007/978-3-030-41235-7_43

2 Materials and Methods

Paper written by one of the authors of this one [1] written by one of the authors of this one contains analysis of methods and approaches used for the determination of fire separation distances between buildings and constructions by calculation methods. Paper written by Hrushevskiy et al. [2] contains description of a method for computational determination of fire separation distances that assumes magnitude of heat flux as significant characteristic. This criterion is evaluated by radiant heat transfer exchange laws. Drawback of such an approach is that there is no any statistical database on critical values of heat flux for various substances and materials at present. Basmanov in his paper [3] considers stochastic model of heat radiation caused by oil products burning in storage tanks. However, this paper did not gain further development as to creation of criterial and methodical bases for the determination of fire separation distances. Paper prepared by Carlsson [4] contains results of a study of fire separation distances between buildings using FDS (Fire Dynamics Simulator) software. At that, trends of changing of façade temperature depending on their separation distance from the seat of fire and duration of heat exposure were not studied.

Thus, derivation of appropriate data as to surface temperature of building façade fabricated from timber materials depending on its separation from the seat of fire is of actuality.

Purpose of this paper is the determination of the dependency of building façade surface temperature on heat exposure caused by fire involving adjacent building façade of which was fabricated of timber materials depending on its separation distance from the seat of fire and heat exposure duration.

We generated the following tasks in order to reach the purpose preset:

- To conduct experimental determination of data related to changing of the building façade surface temperature depending on heat exposure caused by fire involving adjacent building façade of which is fabricated of timber materials;
- To conduct processing of the experimental data;
- To plot building façade surface temperature versus distance between such a building and the seat of fire and duration of heat exposure.

We conducted appropriate experimental studies in order to achieve the purpose preset. Essence of this method of studying was in the simulation of fire involving adjacent building façade of which was fabricated of timber material (Fig. 1). Burning fire load is located in the room of the building fragment and constructions of its façade fabricated of timber materials. We used samples under study cut of wood simulating façade of the adjacent building subjected to exposure from the seat of fire; these samples were measuring 250 mm × 250 mm × 250 mm. Moisture content in the specimens did not exceed 12%; the tests were conducted at air temperature equal to 10 °C, atmospheric pressure of 101.0 kPa and 1.5 m/s wind speed. We installed a number of thermocouples on the surface of the samples under study facing the seat of fire which in turn were placed at a height equal to that of the lower edge of the window opening and at distances of 2 m, 4 m and 6 m, respectively, along the central axis of

the window opening and along the edges of the building fragments. We positioned the samples under study as specified by layout [5].

Fig. 1. Photo of a building fragment to simulate fire load and photo of a moment of the experimental study.

3 Results and Discussion

Using results of the experiments having been conducted we derived some data as to changing surface temperature of the samples under study versus its separation distance from the seat of fire and heat exposure duration. Figure 2 shows data on changing surface temperature of T2, T5 and T8 samples.

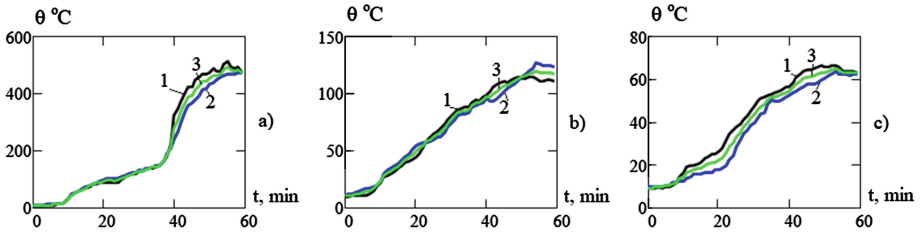

Fig. 2. Surface temperature of the samples under study versus separation distance between their location and the seat of fire and heat exposure duration: (a) data for T2 sample under study; (b) data for T5 sample under study; (c) data for T8 sample under study *(1 & 2 are results of real experiments but 3 stands for average data).*

We calculated maximum absolute, relative and root-mean-square deviations of the temperature values for the entire duration of heat exposure. We revealed that absolute deviations of the experimental values for each experiment from the average values did not exceed 12.6 °C that equals to 19.8% in percent expression form, and maximum root-mean-square deviation was 7.4 °C that indicated satisfactory convergence of the experimental data derived.

In order to check belonging of the data derived in each experiment to single general population by Fisher criterion we determined temperature dispersions (S) for the experimental data relative to average value using the following equation [6]:

$$S = \frac{1}{n-1}\sum_{i=1}^{n_i}\left(\theta_i - \overline{\theta_t}\right)^2 \quad (1)$$

Figure 3 shows temperature dispersions versus heat exposure duration for T2 sample under study.

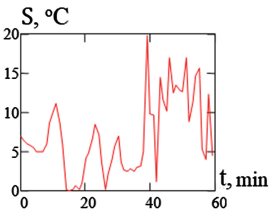

Fig. 3. Temperature dispersions versus heat exposure duration for sample No. 1 under study.

Taking into account aforementioned information, we used average temperature values for the entire duration of heat exposure as shown in Table 1 for further processing.

Table 1. Data on the surface temperature of the samples under study versus distance between their location and the seat of fire and heat exposure duration

Distance to the seat of fire L, m	Duration of heat exposure t, min.										
	1	6	12	18	24	30	36	42	48	54	60
0	9.6	332.6	617.1	659.3	710.6	755.5	821.1	831.4	854.3	664.1	552.9
2.0	10.3	12.5	47.2	85.2	96	124.75	146.05	309.75	428.05	469.9	454.55
4.0	11	13.7	29	42.7	58.2	74.1	86.6	98.05	109.55	119.25	117.7
6.8	9.55	10.4	16.5	20.5	28.9	42.3	52.1	56.4	61.8	65.45	63.25

We approximated data as to surface temperature of the samples under study (θ) shown in Table 2 using numerical regression Eq. (2) which describes relationship between surface temperature of the samples under study (θ) and heat exposure duration (t) and separation distance (L) from the seat of fire and derived five constants for this equation.

$$\theta = a_0 + \frac{a_1}{L} + a_2 t + \frac{a_3 t}{L} + \frac{a_4 t}{L^2} + \frac{a_5}{L^2} \quad (2)$$

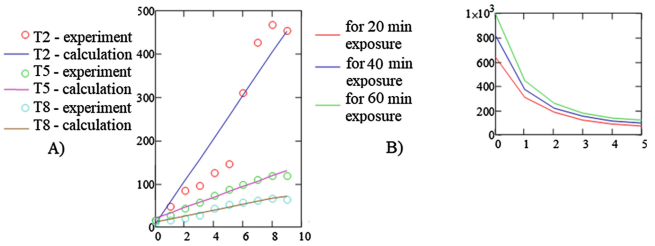

Fig. 4. Surface temperature of the timber façade of the building versus (A) Distance: 1 – L = 2 m, 2 – L = 4 m, 3 – L = 6.8 m; (B) Duration: 20 min, 40 min, 60 min.

Using Eq. (2) we derived relationships used for the computation of the dependency of temperature on heat exposure duration for the separation distance values equal to 2 m, 4 m and 6.8 m; moreover, relationships of the building façade surface temperature derived and separation distance to the seat of fire and various heat exposure duration (20 min, 40 min. and 60 min) are shown (Fig. 4). The same figure shows experimental data (Table 2) shows as circles as well. It follows from the comparison of calculated an experimental data that the largest deviation between calculated temperature values from appropriate experimental results takes place for the sample located at separation distance L equal to 2 m, but the smallest one is for the sample located at separation distance L equal to 6.8 m. Maximum deviation at that does not exceed 20.8%.

Using maximum indications of thermocouples T1 to T8 and Eq. (3) we determined values of temperature decrease factor and its changing depending on the separation distance to the seat of fire as follows:

$$k = \frac{T_{\mathrm{i}}}{\mathrm{T_H}}, \tag{3}$$

where T_{i} are values for appropriate thermocouples T1, T3, T4, T6 and T7 installed from the sides relative to axis of the window opening; and $\mathrm{T_H}$ are values for appropriate thermocouples T2, T5 and T8 installed alongside the axis of the window opening.

The results derived are shown in Table 2.

Table 2. Results of calculation of the temperature decrease factor

Distance between the heat radiation source and the samples under study	2 m		4 m		6.8 m
The spot for which k value determined	T1	T3	T4	T6	T7
k values	0.17	0.2	0.7	0.5	0.8
Average k value	0.185		0.6		0.8

Figure 5 shows plot of temperature versus separation distance at which we located samples under study relative to the seat of fire; these were installed in the longitudinal and transverse directions, respectively.

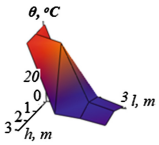

Fig. 5. Dependency of the temperature changing on the separation distance at which the samples under study are located relative to the seat of fire; these were installed in the longitudinal and transverse directions, respectively

4 Conclusions

We determined experimental data as to changing of building surface temperature on heat exposure caused by fire involving adjacent building façade of which was fabricated of timber materials and revealed that in the course of 60-min heat exposure caused by fire involving façade fabricated of timber materials on the construction elements of adjacent facilities; surface temperature of these construction elements was growing monotonously and reached maximum values of 469 °C, 19 °C and 65 °C, respectively, for separation distances to the seat of fire of 2 m, 4 m and 6.8 m.

We plotted building façade surface temperature versus separation distance of such a building from the seat of fire and heat exposure duration using numerical regression equation. Divergence of the data calculated using this relationship from the experimental values did not exceed 20%, and this is acceptable for further application of the results derived.

We revealed relationship of changing of temperature decrease factor and separation distance from the heat radiation source that is of nonlinear nature; it is expedient to take this factor into consideration when determining fire separation distances by calculation method.

References

1. Nignyk VV (2019) Approaches to the determination of fire separation distances between buildings and structures. Collection of Scientific and Technical Papers. KNUCEA, no 53, pp 215–226. [Ніжник В.В. Підходи щодо визначення протипожежних відстаней між будинками та спорудами/ Науково-технічний збірник. КНУБА. - К., 2019. - №53. – С.215–226.)]
2. Hrushevskiy BV, Yakovklev AI, Krivosheyev IA et al (1958) Fire prevention in construction. In: Kuralenkin VF (ed) HEFES 1985 4521 p. [Пожарная профилактика в строительстве/ [Грушевский Б.В., Яковлев А.И., Кривошеев И.А. и др.] под ред. В.Ф. Кураленкина.- М.: ВИПТШ, 1985. – 451 с]
3. Basmanov AE (2002) Theoretical foundations for the prevention of cascade fire spread at tank farms containing oil products and raising efficiency of its elimination. Diss. … Doctor of Technical Sciences. [Басманов А.Е. Теоретические основы предупреждения каскадного распространения пожара в резервуарных парках с нефтепродуктами и повышение эффективности его ликвидации: Дис. … доктора тех. наук:21.06.02.]

4. Carlsson E (1999) Report 5051 – External fire spread to adjoining buildings – A review of fire safety design guidance and related research – Department of Fire Safety Engineering Lund University, Sweden, 125 p
5. Nizhnyk V, Shchipets S, Tarasenko O, Kropyvnytskyi V, Medvid B (2018) A method of experimental studies of heat transfer processes between adjacent facilities. Int J Eng Technol 7 (4.3):288–292
6. Guidelines for the Conduction of Interlaboratory Tests in the Sphere of Fire Safety, UkrFSRI (2007). [Інструкція з проведення міжлабораторних порівняльних випробувань у сфері пожежної безпеки, УкрНДІПБ, 2007.]

Traditional Log Cabin – Exterior Log Wall – Fire Characteristics and Prediction Using Analysis of Thermos-Technical Properties

Stanislav Jochim[1(✉)], Linda Makovicka Osvaldova[2], and Martin Zachar[1]

[1] Technical University in Zvolen, Zvolen, Slovakia
{jochim, zachar}@tuzvo.sk
[2] Faculty of Safety Engineering, Department of Fire Engineering, University of Zilina, Žilina, Slovakia
linda.makovicka@fbi.uniza.sk

Abstract. The Article describes the fire resistance (FR) experiment of three fragments of exterior log walls with different gap adjustments between the log elements. The aim is to verify the impact of the gap adjustment for achieving the criterion of fire resistance of the insulation (I). The experiment also includes theoretical analysis of U-values of the walls and the temperatures on the unexposed side of fire at a standard temperature of 1000 °C. The aim is to verify the prediction of the I criterion for standard fire resistance tests of a construction.

Keywords: Fire resistance · Log-cabin walls · Gaps between logs · U-value

1 Introduction

Fire resistance (FR) is the ability of a fire structure to withstand a fire without losing its function over a certain period of time. Basic criteria of fire resistance are: R (load bearing capacity and stability), E (integrity) and I (insulation). According to the STN EN 1363-1 the insulation (I) criterion for fire walls is the time in minutes, during which a test sample maintains its dividing function, while the temperatures on the unexposed side cannot cause: the rise in average temperature above the initial average temperature by more than 140 °C; the increase in temperature at any spot above the initial average temperature by more than 180 °C. When assessing the fire resistance of wooden elements, the analysis is based on the fact that the cross-section of an element shrinks due to charring. The STN ENV 1995-1-2 standard stipulates the burning rate of wood to 0.8 mm/min [1–3].

The problem with the insulation criterion (I criterion) arises e.g. in the case of log structures made out of squared timber with a gap between the supporting elements (e.g. 20 mm thick, 220–340 mm wide) which can be filled with different materials having a different burning rate.

The aim of the contribution is an experimental laboratory verification of the effect of the three different structural modifications of gaps between the log elements for

L. Makovicka Osvaldova et al. (Eds.): WFS 2020, *Wood & Fire Safety*, pp. 295–302, 2020.
https://doi.org/10.1007/978-3-030-41235-7_44

meeting the I criterion and a theoretical prediction of the effect of the three different structural modifications of gaps between the log elements for meeting the I criterion at 1000 °C [4–6].

2 Material and Methodology

2.1 Test Samples - Log Fragments and the Gaps

To meet the target 1 and 2, three fragments of log walls labelled Z1/S1, Z2/S2 and Z3/S3 (Fig. 1) were used. The position of the sensors for experiment is shown in Table 1.

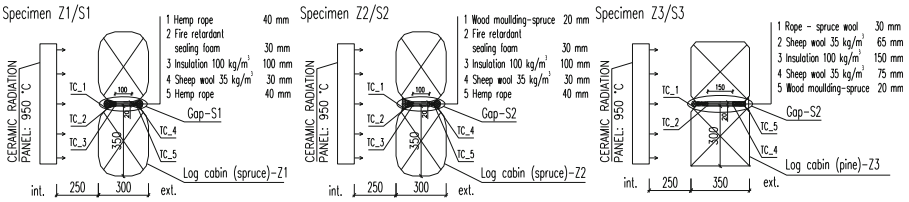

Fig. 1. Test samples - fragments of log walls: construction design, the thermocouples and the distance between the radiation panel and the sample.

Table 1. The position of thermocouples in log elements.

Thermocouple	Position of the thermocouples type K (Ni-Cr-Ni)		
	Sample Z1/S1	Sample Z2/S2	Sample Z1/S1
TS_1	Interior side	Interior side	Interior side
TS_2	Hemp rope (HR) and firefighting foam	Hemp rope (HR) and firefighting foam	Hemp rope (HR) and firefighting foam
TS_3	FF and RI	FF and RI	FF and RI
TS_4	Sheep wool and HR	Sheep wool and HR	Sheep wool and HR
TS_5	Outer Side	Outer Side	Outer Side
TS_6	Temperature in the laboratory	Temperature in the laboratory	Temperature in the laboratory

Materials listed in Table 2 were applied onto the three different construction designs and their gaps.

Table 2. The physical quantities of materials used for the construction

No	Material/reaction to fire class	The source of the physical quantities of the materials: ρ_d [kg/m^3], λ [W/(m · K)], c [J/(kg · K)], μ [1]
1.	Spruce, pine/D	STN EN ISO 10456/AC
2.	STEICO therm (SD)/E	Technical Data Sheet STEICO
3.	Insulation ISOVER N/A1	Technical Data Sheet ISOVER
4.	Sheep wool Gold isolation/E	Woolstyle SK TP-4/0117
5.	Hemp rope/E	STN 73 0540: 2012/Z12016
6.	Wood wool - F (rope moulding)	STN EN ISO 10456/AC
7.	Wood wool/E (compressed inside the gap)	
8.	Firefighting foam Wurth FP K1	STN 73 0540: 2012/Z12016

2.2 Methodology of the Experiment - Laboratory Thermal Loading of the Samples

The methodology is represented by a simulation of a fire using a radiation panel to measure the temperatures inside the gaps. Diagram of the equipment measuring the heat load of the samples to verify the insulation fire resistance criterion is shown in Fig. 2. Ceramic radiation panel was used as the radiation heat source to determine the fire spread on the surface. The distance between the radiation panel and the sample was 250 mm with the radiation intensity of 37.8 kW/m^2.

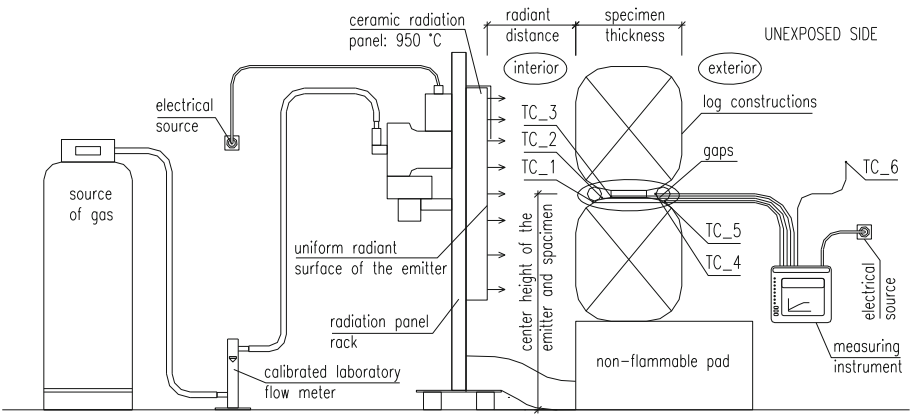

Fig. 2. Diagram of the test samples under heat load (© S. Jochim 2018)

2.3 Methodology for the Insulation Criteria Prediction - The Analysis of Temperatures and *U*-Values (A1_PTN)

The methodology lies in the analysis of the U heat transfer coefficient and surface temperatures θ_e on the unexposed side of the wall based on the standard fire temperature of 1000 °C from the indoor side (A1-PTN). The A1-PTN analysis for calculating the thermal and technical properties (TTP) of the wall fragments and their gaps (U-value, the temperature courses) in the context of the insulation criterion prediction is used along with the method of two-dimensional temperature field for stationary marginal conditions (the Therm program). Marginal conditions to determine the characteristics are shown in Table 3.

Table 3. Marginal conditions for the interior (i) and exterior side (e) of the wall

No.	Physical quantity	Symbol	Analysis thermos technical characteristics		Analysis of the fire characteristics (A1-PTN)	
			Interior (i)	Exterior (e)	Interior (i)	Exterior (e)
1.	Air/surface temperature	θ_i, θ_e [°C]	20	−15	1000	30
2.	Air humidity	w [%]	50	84	50	50
3.	Heat transfer coefficient	h_i, [W/(m^2 · K)]	8	23	8	15

2.4 Experiment Results - Thermal Loading of the Samples Based on the Insulation Criterion

Charts of the temperature curves are shown in Figs. 3, 4, 5, 6, 7 and 8, photo documentation of the time intervals of the experiment is shown in Figs. 9 and 10.

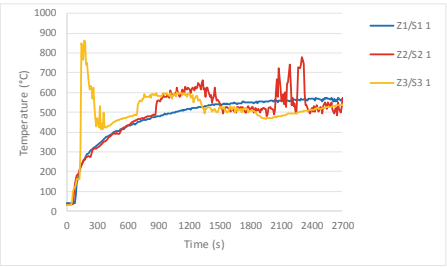

Fig. 3. Temperatures - thermocouple 1

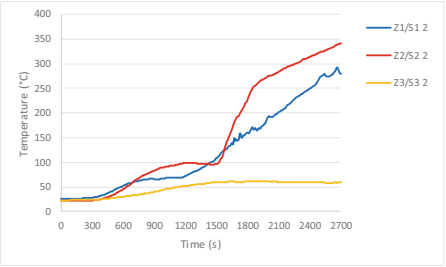

Fig. 4. Temperatures - thermocouple 2

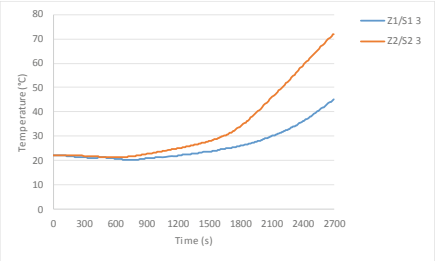

Fig. 5. Temperatures - thermocouple 3

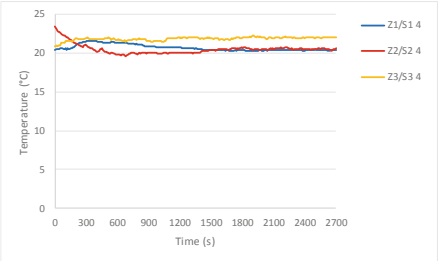

Fig. 6. Temperatures - thermocouple 4

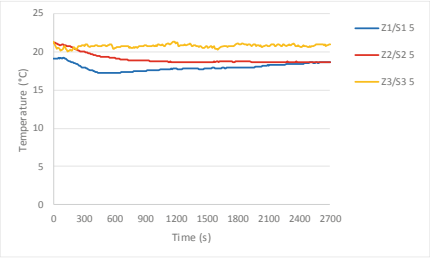

Fig. 7. Temperatures - thermocouple 5

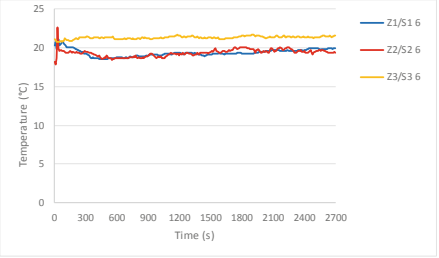

Fig. 8. Temperatures - thermocouple 6

Z1/S1 Z2/S2 Z3/S3

Fig. 9. First minute of the experiment

Fig. 10. Forty-fifth minute of the experiment

2.5 Results of the A1_PTN Analysis - Thermal and Technical Characteristics

The characteristic detail and the results determining the *U*-value and the surface temperatures of the structures are shown in Fig. 11 and Table 4.

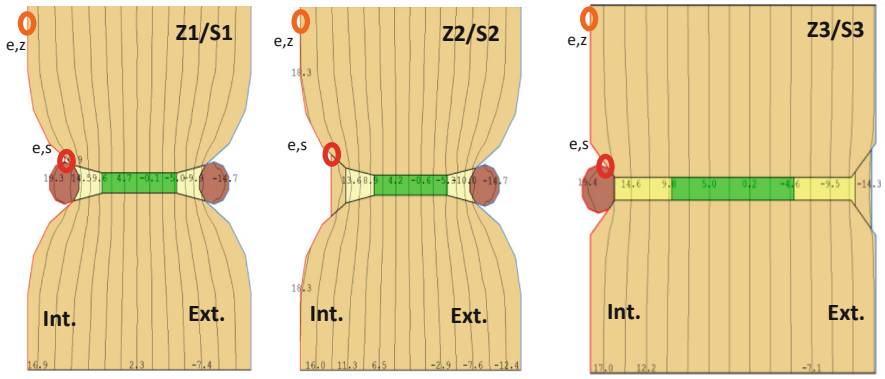

Fig. 11. Characteristic detail for the *U*-value assessment and the temperatures from the interior

Table 4. Thermal and technical properties of the constructions.

No.	Labelling construction/gap	Thickness of the element max. [mm]	Heat transfer coefficient U [W/(m^2 · K)]		Surface temperature θ_i [°C]	
			Of the log construction U_z	Of the join between the elements U_s	Log-cabin construction ($\theta_{i,z}$)	In place of contact between elements ($\theta_{i,s}$)
1.	Z1/S1	300	0.46	0.19	18.3	16.5
2.	Z2/S2	300	0.45	0.20	18.3	17.1
3.	Z3/S3	350	0.34	0.13	18.5	17.8

Symbols: Z - log construction, S - the contact zone of the log elements, the number means the type of the construction and contact zone.

2.6 The AND1-PTN Analysis and the Results for Insulation Criterion Prediction

The temperatures on the unexposed side of the structures at the standard fire temperature of 1000 °C are shown in Table 5.

Table 5. The temperatures on the unexposed side of the fire (fire temperature of 1000 °C)

No.	Labelling	Marginal conditions			Surface temperature on the unexposed side of the fire θ_e [°C]	
		$\theta_{i,PTN}$ [°C]	$\theta_{e,PTN}$ [°C]	$h_{i,PTN}$ $h_{e,PTN}$ W/(m^2 · K)	On surface construction ($\theta_{e,z,2}$)	In the place of element contact $\theta_{i,PTN}$ [°C]
1.	Z1/S1	1000	30	15	55.8	90.6
2.	Z2/S2	1000	30	15	55.2	95.8
3.	Z3/S3	1000	30	15	52.9	55.5

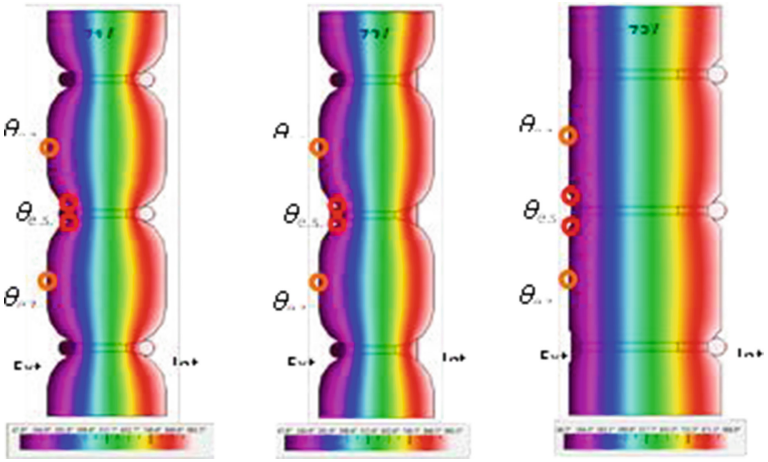

Fig. 12. Theoretical prediction of the I criterion from A1 PTN - the course of the temperatures in the cross-section of a wall fragment and the zones with peak surface temperatures $\theta_{e,z,2}$ a $\theta_{i,s,2}$ on the unexposed side (simulation of a fire from the interior with the temperature of 1000 °C).

3 Conclusion

The experiment confirmed that all three types of gaps should meet the requirement for I criterion, but under the given circumstances of a simulated fire based on the measurements of thermocouples in the position 4 and 5 (Figs. 6 and 7). The temperature on the unexposed side of wall from the radiation panel ranges between 20–25 °C (Fig. 6) and from 17 to 21 °C for the position of the thermocouple 5 (Fig. 7). Differences occur due to the ambient temperature (thermocouple 6, Fig. 8). Visual observation and photo documentation prove the fact that the insulation criterion was met - the gap did not burn through.

The A1-PTN theoretical analysis shows that the structure Z3/S3 with better thermal insulation properties i.e. lower *U*-value shows lower surface temperatures on the unexposed side of the structure during fire simulations in comparison with Z1/S1 and Z2/S2 (Fig. 12, Table 5). Higher temperature difference occurred more in S3 join in comparison with S1 and S2 i.e. temperature is lower by 28% and 39%. On the Z3 surface in comparison with Z1 and Z2, the temperature difference is insignificant i.e lower by 5%. Theoretical prediction of insulation criterion using the analysis of surface temperatures of structures on the unexposed side of the wall in a fire (by a method of two-dimensional temperature field at a stationary heat transfer) prove that it might meet the requirements in the standard tests.

Acknowledgments. The Contribution was created as part of the APVV-17-0206 project "Ultra-low-energy green buildings using wood as renewable raw material", Department of wooden structures DF TU in Zvolen in cooperation with Arborea eng. s.r.o. and YVEX s.r.o.

References

1. Dúbravská K, Mózer V, Tereňová Ľ (2017) Proposed mid-scale test for evaluation of vertical construction elements. - APVV-0057-12. WOS. In: Fire protection, Safety and security 2017: international scientific proceedings, 3rd–5th May 2017, Zvolen, Slovak Republic. ISBN 978-80-228-2957-1, pp 37–43 [CD-ROM]
2. Houdek D (1996) Building with wood for fire safety. Technická univerzita, Zvolen, 97 p
3. Schaffer EL, Marx CM, Bender DA, Woeste FE (1986) Res. Pap. FPL 467, USDA Forest Service, Forest Product Lab. Madison
4. Tereňová Ľ, Gracovský R (2017) Impact of material composition on the fire safety of wood buildings structural elements. - APVV-0057-12. - WOS. In: Fire protection safety and security 2017: international scientific proceedings, 3rd–5th May 2017, Zvolen, Slovak Republic, ISBN 978-80-228-2957-1, pp 235–242 [CD-ROM]
5. White RH (1988) Charring rates of different wood species. Ph.D. dissertation, University of Wisconsin, Madison, WI
6. STN EN 1995 – 1 – 2 Eurokód 5. Navrhovanie drevených konštrukcií. Časť 1-2: Všeobecné pravidlá. Navrhovanie konštrukcií na účinky zaťaženia požiarom (2008)

Impact of Bolt Pattern on the Fire Performance of Protected and Unprotected Concealed Timber Connections

Aba Owusu[1(✉)], Osama (Sam) Salem[2], and George Hadjisophocleous[1]

[1] Carleton University, Ottawa, ON, Canada
abaowusu@cmail.carleton.ca
[2] Lakehead University, Thunder Bay, ON, Canada

Abstract. The fire performance of concealed timber beam connections has been studied over the years, and it has been shown that such connections do not perform as well as exposed and seated connections mainly due to the reduction of the beam's cross section to accommodate the concealed steel plate. The main objective of the study presented in this paper is to investigate the performance of fully protected and unprotected concealed glued-laminated timber (glulam) beam connections when subjected to fire. For the protected connection configuration, the steel plate and bolts were fully protected from fire using wood strips and plugs, respectively. This research also studied the effect of bolt pattern on the fire performance of concealed glulam connections. Four full-size concealed glulam beam end connections: two protected and two unprotected connections were exposed to CAN/ULC-S101 standard fire, while being loaded to 100% of the ultimate design moment capacity of the weakest connection configuration. In pattern one, two rows of bolts, each of two bolts, were symmetrically positioned near the top and bottom sides of the beam cross section. While, in bolt pattern two, the bottom bolt row was shifted upward to be located at the mid height of the beam section.

Keywords: Concealed connections · Glulam beams · Fire protection · Bolt pattern · Failure time

1 Introduction

The use of wood in building construction around the world has increased considerably in the last few years due to its renewability and sustainability. In heavy timber construction, structural members are usually joined using connections involving steel plates and bolts. In case of fire, beam-to-column connections of wood structures are typically the weakest link as the presence of steel components helps in transferring heat to the interior of the wooden connection, and thus increases the charring rate and consequently decreases the connection time to failure in fire condition.

Most fire resistance studies focussed on axially loaded connections [1] under either compressive or tensile loading perpendicular to wood grain [2], or parallel to wood grain [3]. Therefore, there is urgent need to investigate the structural fire performance

L. Makovicka Osvaldova et al. (Eds.): WFS 2020, *Wood & Fire Safety*, pp. 303–310, 2020.
https://doi.org/10.1007/978-3-030-41235-7_45

of moment-resisting timber connections to fully understand the behavior of such connections that can effectively be utilized in tall wood buildings that are susceptible to lateral loads which can develop bending moments on such connections. In a few research studies, such as those conducted by Zarnani and Quenneville [4] and Xu et al. [5], numerical models were developed to determine the moment-resisting capacities and failure modes of timber-steel hybrid connections at ambient temperature. In another study [6] that was conducted to experimentally and numerically investigate the fire resistance of glulam beams of 140 × 191 × 1900 mm dimensions, it was found that steel bolts significantly influenced the charring rate and the time to failure of timber connections.

The research presented in this paper has focussed on studying the structural behaviour of concealed wood-steel-wood (WSW) glulam bolted connections at elevated temperatures of standard fire. Two connection configurations with varying bolt patterns had its steel components fire exposed, whereas the other two connection configuration replicates had its steel components protected using wood plugs and strips for steel bolt heads and nuts and plate, respectively.

2 Materials and Test Procedure

2.1 Test Specimens

Four 1600-mm long glulam beams of 184 × 362 mm cross-sectional dimensions were used in this experimental study. Each beam section was connected to a steel column by a T-stub section made of 12.7-mm (1/2″) thick steel plate and four 19.1-mm (3/4″) diameter, A325M high-strength structural bolts. The bolt end distance, edge distance and spacing were designed in accordance with CSA 086-14 [7]. The glulam material utilized in all four test specimens was black spruce–pine of 24f-EX stress grade. A slotted cut of 15-mm wide was prepared at the center of the beam cross section to accommodate the steel plate, allowing a clearance of 1 to 2 mm, as per CSA 086-14. A 30-mm diameter spade bit was used to create circular holes in the protected beam front and back faces to accommodate the bolt heads, washers, and nuts. Four steel bolts in two different patterns were arranged to form two different connection configurations that were experimentally examined. For pattern one, the bolts were symmetrically located along the beam cross section depth, near the top and bottom sides of the beam. Whereas for pattern two, the bottom row of bolts was shifted upward to be positioned at the mid height of the beam section, in order to serve within the top tensile stresses zone of the beam cross section, and ultimately further contribute to the moment-resisting capacity of the connection. Also, each connection configuration was tested with and without fire protection applied to the steel components using wood plugs and strips to protect the bolt heads and nuts and plate, respectively. Figures 1(a) and (b) show the layout of the unprotected connection configuration bolts arranged in pattern one (P1N) and pattern two (P2N), respectively. Figure 1(c) shows the layout of the protected connection configuration bolts arranged in pattern one (P1P), having the bolt heads and nuts protected using glued-in wood plugs and the steel plate top and bottom edges protected using wood strips. The wood plugs used to cover the bolt heads and nuts had thicknesses of 30 and 20 mm, respectively.

Twelve metal-shielded K-type thermocouples (TC) were installed in each test specimen at different locations of the beam connection: four TC from the beam front face (TC1 through TC4); six from the beam back face (TC5 through TC10); one from the beam top side (TC11); and one from the beam bottom side (TC12), as shown in Figs. 2(a) and (b). The figures also show the depth at which each TC was embedded inside the wood section. For instance, TC1 and TC2 were installed at 60-mm depth from the beam front face; TC3 and TC4 at 20-mm depth; TC7 and TC8 at 40-mm depth; and TC9 and TC10 at 10-mm depth. TC5 and TC6 were used to measure the steel plate temperatures and TC11 and TC12 measured the temperatures of one of the top bolts and one of the bottom bolts, respectively. For the connection configuration with fire protection, fourteen metal-shielded K-type thermocouples (TC) were used: six were installed from the beam front face and eight from the beam back face, as shown in Fig. 2(b). TC5 and TC6 measured the steel plate temperatures, TC11 and TC12 measured the temperatures of the bolt nuts underneath the 20-mm thick wood plug, whereas TC13 and TC14 measured the temperatures of the bolt heads underneath the 30-mm thick wood plug.

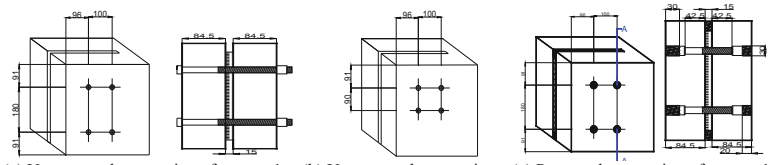

(a) Unprotected connection of pattern 1 (P1N) (b) Unprotected connection of pattern 2 (P2N) (c) Protected connection of pattern 1 (P1P)

Fig. 1. Connection configurations details

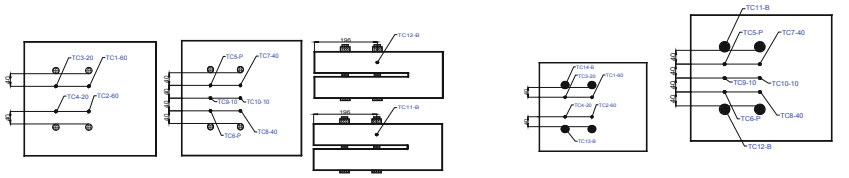

(a) configuration (P1N) thermocouples layout: beam front layout:face (left); back face (middle); and top and bottom sides (right) (right)

b) configuration (P1P) thermocouples beam front face (left); and back face

Fig. 2. Thermocouples layouts

2.2 Test Setup and Procedure

The fire resistance experiments presented in this paper were conducted at Lakehead University's Fire Testing and Research Laboratory (LUFTRL). Each glulam beam was connected at one end using T-stub steel connector and was rigidly attached to a fire-protected supporting steel column. In fire tests, all four connection configurations were exposed to CAN/ULC-S101 [8] standard fire while being loaded to 100% of the ultimate design load capacity of the weakest connection configuration. The supporting

steel column and the top side of the glulam beams were completely protected using 1.0-inch thick ceramic-fibre blanket. Figure 3 shows a fire test setup for one of the glulam beams installed inside the furnace. During fire test, the beam connection failure criterion was set to a maximum beam end deflection that corresponded to a connection rotation magnitude of 0.1 radians. One low thermal elongation ceramic rod was placed vertically through a predrilled small hole in the furnace roof and was attached to a displacement transducer installed outside the furnace to allow the measurement of the beam vertical displacements at 200-mm distance from the beam supporting column.

Fig. 3. Fire test setup

3 Experimental Results and Discussion

The experimental data measured from the fire tests were analysed to determine the connection failure loads and modes and beam-to-column rotations with respect to time.

3.1 Failure Time and Mode

3.1.1 Effect of Bolt Pattern on the Connection Time to Failure

Table 1 summarizes the results of the four fire tests. The table shows that the time to failure of the unprotected connection configuration with bolt pattern one (P1N) was 33.0 min, which was one minute more than that of the connection configuration of bolt pattern two (P2N). Whereas for the protected connections, the connection configuration with bolt arranged in pattern one (P1P) had a time to failure that was eight minutes more than that of the other connection of bolt pattern two (P2P).

Table 1. Summary of fire tests results.

Connection configuration ID	Applied moment (kN · m)	Time to failure (min)	Average charring rate (mm/min)	Failure mode
P1N	14.8	33.0	0.73	Splitting/row shear
P1P	14.8	56.0	0.90	Splitting
P2N	14.8	32.0	0.82	Splitting/row shear
P2P	14.8	48.0	1.00	Splitting
P1N	14.8	33.0	0.73	Splitting/row shear

3.1.2 Effect of Protection on the Connection Time to Failure

Table 1 shows that the time to failure of the protected connection configuration with bolt pattern one (P1P) was 56.0 min, which was 23.0 min (about 70%) more than that of the other similar connection configuration but without protection. Similarly, when considering bolts pattern two, the protected connection configuration (P2P) had a time to failure that was 16.0 min (50%) more than that of the similar connection but without protection (P2N). It was observed during the fire tests that both unprotected beam connections (P1N and P2N) began to experience slight wood split and row shear at the top bolt row which lead to failure of the connections, Fig. 4(a). However, the protected beam connections (P1P and P2P) experienced a visible split at the top row of bolts in line with the glue line plane, leading to connection failure.

(a) Unprotected connections: P1N(left); and P2N (right)

(b) Protected connections: P1P(left); and P2P (right)

Fig. 4. Connections' failure mode in fire

3.2 Connection Rotations

3.2.1 Effect of Bolt Pattern on the Connection Rotational Behavior

It was observed that the two unprotected connections (P1N and P2N) underwent similar trends of increased rotations with time in fire condition. Both beam connection configurations experienced very slight linear increase in rotation values early in the fire tests (for about 8.0 min), however, the rotation values increased exponentially after about 15.0 min from the fire test commencement, as shown in Fig. 5(a). Whereas Fig. 5(b) shows that beam configurations (P1P and P2P) experienced a linear increase

in rotation values for about 40.0 min, however, the former connection had a greater slope than the latter one. After about 40.0 min, the connection configuration with the second bolt pattern (P2P) experienced a rapid exponential increase that led to a failure time that was 8.0 min less that that of the first bolt pattern (P1P).

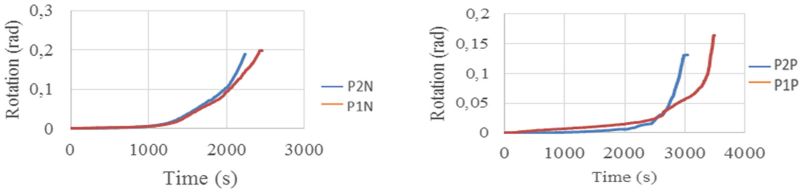

(a) Unprotected connections of bolt patterns 1 and 2 (b) Protected connections of bolt patterns 1 and 2

Fig. 5. Time-rotation relationships of all beam connections (effect of bolt pattern)

3.2.2 Effect of Fire Protection on the Connection Rotational Behavior

Figure 6(a) shows that the two tests conducted for the first bolt pattern exhibited similar linear rate of rotation increase for about 20.0 min, after which the unprotected connection (P1N) experienced an exponential increase leading to a failure time that was twenty three minutes shorter than that of the protected connections (P1P). Figure 6(b) shows the time-rotation relationships of the two beam connection configurations of the second bolts pattern during fire tests. Both connection configurations had rotations that increased linearly during the first 14.0 min of the tests followed by an exponential rise that started in the connection configuration with no protection (P2N). The time to failure of the protected connection (P2P) was about 16.0 min longer than that of the unprotected connection (P2N).

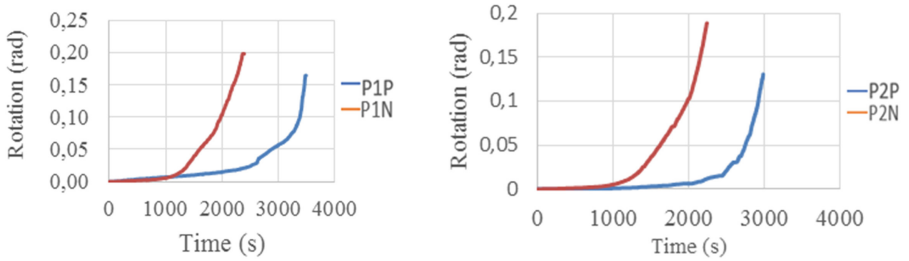

(a) Connections of bolt pattern one (b) Connections of bolt patern two

Fig. 6. Time-rotation relationships of all beam connections (effect of fire protection)

3.3 Time-Temperature Curves

Figure 7 shows the temperature values recorded during the protected connection (P1P) fire test. The figure shows that thermocouples TC-11 and TC-12 measuring the temperatures of the nuts (under 20-mm thick wood plug protection) recorded temperatures

that started to increase 20.0 min into the test; whereas the temperatures of thermo-couples TC-13 and TC-14 that recorded the temperatures of the bolt heads started to increase about 30.0 min into the test.

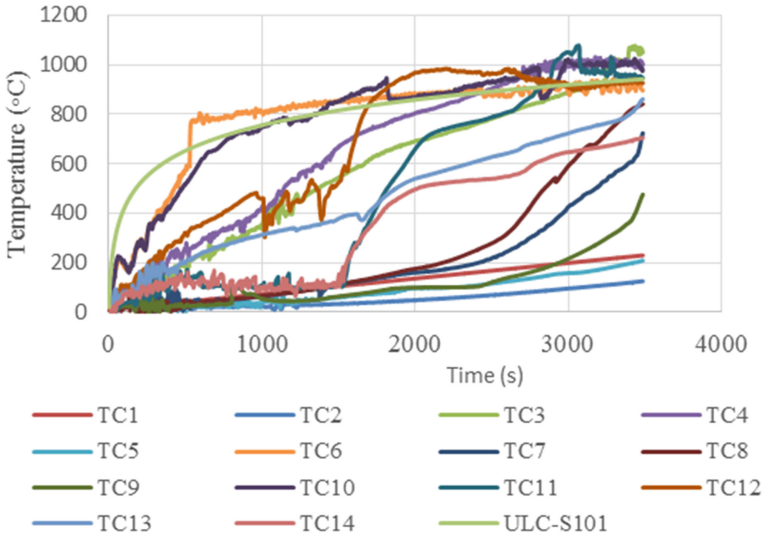

Fig. 7. Time-temperature curves for the protected connection with bolt pattern one (P1P)

4 Conclusions

In the experimental study presented in this paper, the behaviour of wood-steel-wood (WSW) concealed connections, with and without fire protection using two different bolt patterns were investigated at elevated temperatures of standard fire. The results of this study helped in drawing the following conclusions;

- The addition of wood plugs and strips to protect the steel bolt heads and nuts and plate edges, respectively, increased the connection time to failure in fire by an average of 20.0 min;
- The bolt pattern for the unprotected connections had almost negligible influence on the connection time to failure in fire; and
- the alignment of bolts with the glue line plane considerably contributed to wood splitting in the connection and led to shorter time to failure in fire condition.

References

1. Racher P, Laplanche K, Dhima D, Bouchaïr A (2010) Thermo-mechanical analysis of the fire performance of dowelled timber connection. Eng Struct 32(4):1148–1157

2. Audebert M, Dhima D, Taazount M, Bouchaïr A (2014) Experimental and numerical analysis of timber connections in tension perpendicular to grain in fire. Fire Saf J 63:125–137
3. Peng L, Hadjisophocleous G, Mehaffey J, Mohammad M (2012) Fire performance of timber connections, part 1: fire resistance tests on bolted wood-steel-wood and steel-wood-steel connections. J Struct Fire Eng 3(2):107–132
4. Zarnani P, Quenneville P (2014) Design method for coupled-splice timber moment connections. In: Proceedings of the 13th world conference on timber engineering, WCTE2014, Quebec, Canada
5. Xu BH, Bouchaïr A, Racher P (2015) Mechanical behaviour and modelling of dowelled steel-to-timber moment-resisting connections. J Struct Eng 141(6) (2015)
6. Ali S, Hadjisophocleaus G, Akotuah AO, Erochko J, Zhang X (2016) Study of the fire performance of hybrid steel-timber connections with full-scale tests and finite element modelling. In: Proceedings of the international conference on applications of structural fire engineering, Dubrovnik, 15th–16th October
7. CSA 086-14 (2014) Engineering design in wood. Canadian Standards Association, Ottawa, Ontario
8. CAN/ULC-S101-14 (2014) Standard Methods of Fire Endurance Tests of Building Construction and Materials, Fifth Edition, Canada

Effect of Thermal Loading on Various Types of Wood Beams

Stanislava Gašpercová(✉) and Miroslava Vandlíčková

Faculty of Security Engineering, University of Žilina,
ul. 1. Mája 32, 010 26 Žilina, Slovak Republic
{stanislava.gaspercova,
miroslava.vandlickova}@fbi.uniza.sk

Abstract. The paper deals with the experimental examination of flame burning on mass loss for the two types of wood beams - solid wood beam and glue laminated spruce wood timber (glulam). As for the glulam, the paper looks into the effect of the number of joints on wood burning. All samples have the same dimensions of 80 × 40 × 170 mm and moisture level of 15%. The samples are divided into three groups - glued laminated timber, glue and cross-laminated samples combined and solid wood samples. During the experiment, the samples are exposed to a flame for 10 min and the mass loss is recorded in 20 s intervals. Based on the values, the average mass loss is calculated for each set of samples. The conclusion consists of an evaluation and final findings.

Keywords: Glue laminated timber · Solid wood · Flame burning · Mass loss

1 Introduction

Wood is a building material which contains a large amount of energy accumulated during the process of photosynthesis and the subsequent endothermic reactions converting glucose to polysaccharides and lignin. This energy can be released, for example, in the process of burning [1–4].

If heat is generated by means of flame or radiant heat source, basic structural elements of wood start to break apart releasing combustible gases. With sufficient concentrations and an appropriate initiator, these gases will ignite and release enough energy for a follow-up release of combustible gases [5].

On the basis of various researches, many authors state [1, 6–10] that the temperature above 100 °C has an effect on the change in physical, structural and chemical properties of wood. The process of thermal degradation of wood is a very complex one. During combustion, each basic component of wood significantly contributes to the degradation, yet in different time intervals and at different temperatures. These findings explain thermal degradation of wood as a construction element during a fire in more detail. In addition to chemical composition, physical properties of wood also play a significant role. In addition to other important characteristics, it is mainly the density and the charring rate which have a significant impact on heat transfer and burning rate and thus on the overall development of fire.

L. Makovicka Osvaldova et al. (Eds.): WFS 2020, *Wood & Fire Safety*, pp. 311–317, 2020.
https://doi.org/10.1007/978-3-030-41235-7_46

Thermal degradation results in a change of wood color. In the end, the wood turns black indicating the presence of charred layer. Charred layer can easily absorb thermal radiation but is a poor thermal conductor due to its porous structure and chemical composition. Charred layer is considered a good thermal insulator and represents an auto-retarding layer of wood [1–3, 11, 12].

European standard STN EN 1995-1-2 Eurocode 5 (Design of timber structures - Part 1–2: General - Structural fire design) is applied to assess the effect of fire on timber constructions. When designing timber structures for fire test, it is essentially a simplification of the effect of fire on the characteristics of this structural material [13].

The second method of determining the effect of fire on wooden structures is to subject them to an experimental review. The most common ones are tests evaluating the effects of a fire on construction products such as: STN EN ISO 11925-2 Reaction to fire tests. Ignitability of products subjected to direct impingement of flame. Part 2: Single-flame source test [14].

When assessing the fire integrity of wooden elements, the analysis is based on the shrinkage of the cross section of an element as a result of burning. Some experimental researches [15–19] confirm that the burning rate of wood is constant. One of the aims of our contribution was to determine whether mass loss also remains constant in the process of wood burning. The second goal was to find out whether gluing has the effect on the thermal degradation of wood.

2 Experiment Description

Three sets of samples have been prepared for the experiment. Each set contains 8 pieces of samples of the same size - 80 × 40 × 170 mm. Each set is characterized as follows:

1. The samples have been made out of glued spruce wood with 15% moisture content with one longitudinal lap joint. Melamine-urea-formaldehyde glue was used. These are KVH beams. KVH beam is made out of several solid pieces of lamellas glued lengthwise. Weak spots in the wood such as large knots, rot, etc. are cut out [20].
2. The samples have been made out of laminated spruce wood with 15% moisture content and contained longitudinal and half lap joint. Melamine-urea-formaldehyde glue was used. These are BSH beams. BSH beam, compared with KVH beam, consists of at least 3 lamellas glued parallel to the grain with the maximum thickness of 40–45 mm. These lamellas are glued lengthwise first and the thickness is adapted accordingly. Weak spots in the wood such as large knots, rot, etc. are cut out [20].
3. The samples were made out of natural spruce wood.

Besides the samples; laboratory scales, a sample holder, a burner with propane-butane tank, a slide caliper and a timer were also needed for the experiment. The test apparatus is shown in Fig. 1.

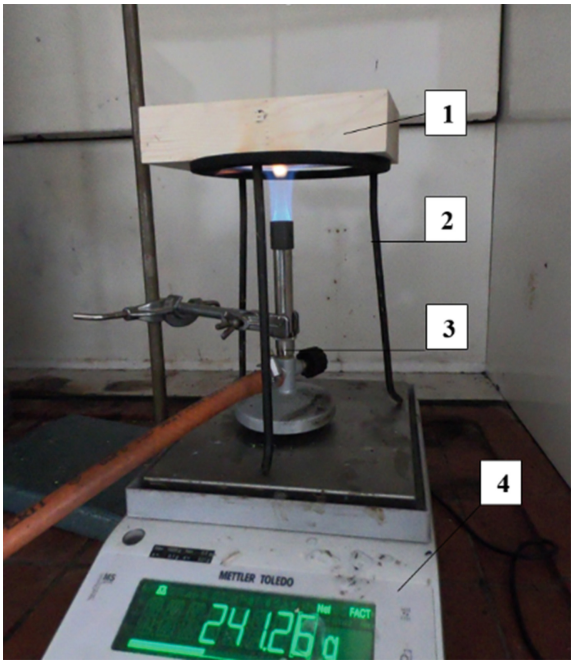

Fig. 1. Test apparatus: 1 - sample, 2 - stand, 3 - burner, 4 - laboratory scales

Testing was carried out using basic evaluation criterion of mass loss under thermal load. Samples are tested for 10 min and their weight was recorded in the interval of 20 s. The initial and final weight was needed to calculate the final mass loss of the sample according to the relation (1).

$$d_m = [(m_z - m_k)/m_z] \cdot 100. \quad (1)$$

d_m - total mass loss (%), m_z - sample weight before the experiment (g), m_k - sample weight after the experiment (g).

The test was carried out at a constant temperature and humidity in a laboratory of the Faculty of Safety Engineering. Ambient temperature was 24,5 °C at a 41% humidity. In order to ensure relevant results, the samples were heated in the lab for a period of one month and weighed every seven days. The samples were weighed before and after each experiment.

The experiment procedure was as follows: The sample was mounted onto the stand placed on the analytical scales. The propane-butane burner was lit. The flame was 100 mm high. The burner was placed between the scales and the sample. From this moment on, the time when the sample was exposed to flame was measured. Mass loss is recorded in 20 s intervals for 10 min. After 10 min, the burner was pushed away from sample and the sample was allowed to burn itself out for 20 min.

3 Experiment Results and Discussion

During the experiments, samples grew darker on the surface and a charred layer was being created. As a result of the thermal degradation of wood components, mass loss could be observed. These two criteria were important when making a final evaluation of the experiment and the results were compared with the results published by other authors.

Based on the measured data, the arithmetic mean was calculated for each set of samples and the final values have been substituted into the formula (1). The mass loss was calculated and the charred layer measured. Chart showing the percentage of mass loss is shown in Fig. 2.

Fig. 2. Mass loss percentage of wooden beams

One of the factors affecting wood burning rate as well as its mass loss is its density [6, 21]. The higher the wood density is, the slower the mass loss and the burning rate are. In the case of glulam posts, however, these hypotheses failed to be corroborated since their density ranged at an average of 380 kg · m^{-3} and the density of spruce wood was 440 kg · m^{-3} on average.

For the first four minutes of the experiment, the difference in mass loss between different sets of samples is negligible, however, from the fifth minute on we can see that glulam beams have lower mass loss compared to natural wood, check Fig. 2. This may be caused by the fact that glulam is of higher quality compared to natural wood. The lowest mass loss percentage was recorded between the ninth and tenth-minute from the beginning of the experiment. The greatest mass loss percentage was recorded around the first minute from the beginning of the experiment. This may be caused by the thickness of charred layer, which is porous and prevents direct exposure to flame for the non-degraded wood, many authors state [1, 15, 18, 22] thus it creates a thermal insulation and slows down the process of combustion. Some authors [23–25] indicate that defects in wood i.e. knots as well as thicker annual rings slow down wood charring rate and therefore the charred layer is thinner in this segment compared to a part of the wood where such defects are missing. To find out whether the hypothesis is valid for glulam samples too, the charred layer was removed and its thickness was measured in 13 different spots. The average charred layer thickness for all the experimental samples is shown in Table 1.

Table 1. Average charred layer thickness

Sample		1	2	3	4	5	6	7	8	Diameter (mm)
Thickness of the charred layer (mm)	Glulam - glued lengthwise	5.1	4.8	5.1	4.6	4.9	5.8	4.7	4.9	4.988
	Glulam - glued lengthwise and crosswise	5.2	5.1	4.9	5.3	5.3	5.4	5.1	5.2	5.188
	Natural wood	6.1	6.5	5.1	5.7	4.9	5.1	6.1	5.5	5.625

Huntier [15] looked into the problem of charred layer on a wooden beam monitoring the change in temperature in a beam's cross-section exposed to thermal loading during a fire resistance test. Charred layer is removed after the test which uncovers a layer damaged by thermal loading. This charred layer was, however, only 11–15 mm thick. Below the layer, the wood remained fully intact - this conclusion is based on the color of the wood as well as the tests which were carried out.

On the basis of the charred layer, we can conclude that gluing does not have a negative effect on the creation of a charred layer. On the contrary, the samples made from glulam had thinner charred layer than the samples of natural wood. It follows that the active cross-section, which takes part in the load shift, is protected against the effects of fire for a longer period of time. In conclusion, fire resistance is higher for glulam posts compared to solid wood beams made out of natural wood.

When comparing the samples of different tree ring density, we discovered that the side of the sample with wider annual rings has thinner charred layer than the side with thinner annual rings. The sample glulam – glued lengthwise number 8 had a wood knot and the fire operated right onto in. The sample with knot is shown in Fig. 3. The place where the wood knot had a significantly thinner charred layer than the rest of wood. However, it did not have a significant impact on the average charred layer thickness.

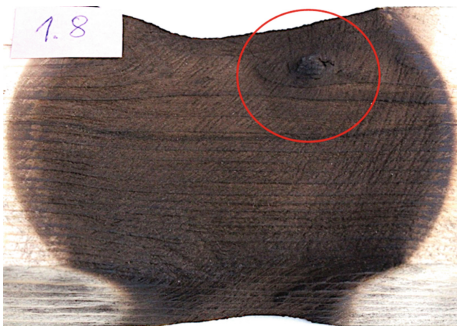

Fig. 3. Glulam sample with a knot

4 Conclusion

After carrying out the experiments and observing the mass loss of glulam and natural wood samples exposed to a flame heat source, we have now come to the conclusion that glulam is perfectly comparable with natural wood. Glulam displayed, in comparison with natural wood, even a lower mass loss. Furthermore, we have found that during the first third of the experiment, the mass loss is at its peak and represents almost half of the overall mass loss. It follows that the thickness of the charred layer is important in relation to mass loss rate. During the experiment, slight differences in mass loss as well as different thickness of the charred layer for one sample type were observed. Concerning the charred layer thickness, small differences could be caused by different tree ring density and various defects in the wood such as knots, which significantly change the nature of the flame exposure where such knot was located.

References

1. Osvald A, Štefko J (2013) Model fire of two-storey wooden building. Šmíra-print, Ostrava, p 129
2. Kadlicová P et al (2019) Effect of thermal and retarding treatment on flammability rate of tropical tree species. In: Wood research, Bratislava, pp 117–126 (2019)
3. Osvaldova LM, Gašparík M, Sotomayor Castellanos JR, Markert F, Kadlicová P, Čekovská H (2018) Effect of thermal treatment on selected fire safety features of tropical wood. In: Communications, Žilina, pp 3–7
4. Gaff M et al (2019) The effect of synthetic and natural fire-retardants on burning and chemical characteristics of thermally modified teak (Tectona grandis L.f) wood. In: Construction and building materials, pp 551–558
5. Makovická Osvaldová L, Osvald A (2015) New methods in the evaluation of flammability properties. In: Production management and engineering sciences, Tatranská Štrba, Slovakia, pp 503–508
6. Bučko J, Klaudová A, Kačík F (1994) Vacuumtrockung des Laub- und Nadelholzes. In: Theorie und praxis der Vacuum-Schnittholztrocknung. In: Internationales Wissenschatliches symposium. Zvolen: Technická univerzita vo Zvolene, pp 96–104
7. Fengel D, Wegener G (1989) Wood. Chemistry, Ultrastructure, Reactions. Walter de Gruyter, Germany, pp 26–226
8. Comben AJ (1964) The effect of low temperatures on the strength and elastic properties of timber. In: Wood science, pp 44–55
9. Kačík F, Marková I, Osvald A (1999) The changes of lignin in burning of spruce wood. In: Cellulose chemistry and technology, pp 267–275
10. Chovanec D, Osvald A (1992) Spruce wood structure changescaused by flame and radiant source. Zvolen, p 62
11. Gerhards CC (1982) Effect of moisture content and temperature on the mechanical properties of wood: an analysis of immediate effects. In: Wood and fiber, pp 4–36
12. Iringová A (2017) Lightweight building envelopes in prefabricated buildings in terms of fire resistance. In: XXVI R-S-P seminar 2017 theoretical foundation of civil engineering, Warsaw, Poland
13. STN EN 1995-1-2 Eurocode 5: Design of Timber Structures – Part 1-2: General Structural Fire Design (2004)

14. STN EN ISO 11925-2 Reaction to fire tests. Ignitability of products subjected to direct impingement of flame. Part 2: Single-flame source test (2011)
15. Huntier Z (1995) Analyse des brandverhaltens von holz und holzwerkstoffen unter berücksichtigung des einsatzes von feuerschutzmitteln. Disertation thesis, Buchverlag, Gräfelfing, p 114
16. Ladomerský J et al (2000) Energy and environment. Zvolen, Slovakia, p 184
17. Schaffer EL (1973) Elevated temperature effect on the longitudinal mechanical properties of wood. Disertation thesis, Wisconsin, USA
18. Tran HC, White RH (1992) Burning rate of solid wood measured in a heat release rate calorimeter. In: Fire and materials, pp 197–206
19. Makovická Osvaldová L, Osvald A, Mitrenga P et al (2015) Non-normalized evaluation methods of retarding effects of fire retardants for wood. In: 11th international symposium on selected processes at the wood proceedings, Dudince, Slovakia
20. BSH beams: Product information. [online]. [cite 2019-7-7]. http://www.lega.sk/images/uploads/files/BSHHranoly.pdf
21. Goring DAI (1963) Thermal softening of lignin, hemicelluloses and cellulose, p 517
22. Karlsson B, Quintiere JG (2000) Enclosure fire dynamics. CRS Press, London
23. Osvald A (1997) Fire-technical propertiers of wood and wood-based materials. Zvolen, Slovakia, pp 17–30
24. Horský D, Osvald A (1985) Methods of determination of fire-technical properties of wood and wood materials. Zvolen, Slovakia, p 169
25. Östman B (1985) Wood tensile strength of temperatures and moisture content simulating fire conditions. In: Wood science and technology, pp 103–116

A Study of the Fire Performance of Timber-Walled Compartments

Avishek Chanda(✉), Swagata Dutta, and Debes Bhattacharyya

Centre for Advanced Composite Materials,
Department of Mechanical Engineering,
University of Auckland, Auckland, New Zealand
acha553@aucklanduni.ac.nz

Abstract. The work focuses on the construction of a partial compartment with 3-ply veneer laminates and analysing the fire performance of the laminated natural composite structure. Instead of the typical L-shaped slots, the compartment was built with traditional joints that were constructed using Ados F2, a high-performance general-purpose contact adhesive composed of polychloroprene. The significant aspect of this study is the fire-performance of the sample at a larger scale with certain variabilities from the ASTM E1354 standard, to suit the current requirements. The compartment was constructed with a vertical front wall of size 300 mm × 300 mm and two parallel side walls each having size of 300 mm × 70 mm. The fire performance of the structure was evaluated by performing a modified cone calorimeter test where the cone was held in a vertical position. The tests were conducted under 35, 50 and 69 kW/m^2 heat flux values. The results show a comparatively low peak heat release rate, which can be directly attributed to the distance of the burner and the sample, along with significant temperature gradient along the surface of the main wall and an average burn time of 93 s and 84.3 s for 50 and 69 kW/m^2 heat flux values, respectively, with no burning experienced for the flux value of 35 kW/m^2. The study indicates that the fire properties of plywood, although having limiting criteria in building structures where fire is a key issue, can be used for benchmarking the future studies to introduce fire safety in plywood structures.

Keywords: Cone-calorimeter · 4-point bending · 3-ply veneer laminate · Fire performance · Thin-walled compartment

1 Introduction

Commercially available plywood of Radiata pine veneers are used in the current work. Significant value addition to these plywood laminates can be done if a technique of forming them into desired geometric structures can be introduced [1, 2]. Previous studies have shown that the only possible way of forming plywood is thermo-forming, which helps in confirming the shape of plywood [3, 4] by destroying the visco-elastic cells at high temperatures [5]. This thermo-forming is preceded by softening the plywood at a slightly elevated temperature (−70 °C), which helps in making it flexible [6]. However, the effect of spring-back is something that cannot be mitigated this way, and any thermo-forming method needs to account for spring-back that the plywood will

L. Makovicka Osvaldova et al. (Eds.): WFS 2020, *Wood & Fire Safety*, pp. 318–325, 2020.
https://doi.org/10.1007/978-3-030-41235-7_47

experience during the post-curing stage. Plywood is the most used form of wood veneers, and therefore, the ability to form plywood in desired geometric shapes has significant applications, one of which is investigated in the current study.

One significant application can be the development of light portable boxes and compartments for various purposes. Since, any box or compartment has walls which are perpendicular to each other, spring-back control is the only way to form such specific geometric shapes out of plywood. Plywood containers, if built for carrying or storing hazardous substances, should have specific and known fire-performance characteristics and thus, this paper presents a study on the fire-performance of a compartment with desired geometric dimensions. In order to generate an understanding of the fire performance, firstly the traditionally pinned or joined samples are tested against three different heat fluxes of 35 kW/m^{-2}, 50 kW/m^2 and 69 kW/m^2 in a cone-calorimeter, which has been shown to be an effective way of observing the fire-reaction properties of various elements [7–9]. Valuable insights on the various parameters, which include, but are not limited to, the heat release rate (HRR), the peak heat release value, the smoke-release rate, flame spread and amount of toxic gases (CO and CO_2), can be achieved from the cone-calorimeter test [10, 11]. However, there are certain limitations, such as the bubbling effect, in-depth absorption issue, change in the material properties and samples getting broken down or distorted due to heat, which are ignored while performing the cone tests [12–14]. However, even with these limitations, the method still offers an excellent way to study the fire-performances that can be useful for the consumer industry and for modifying building codes [15, 16].

2 Materials and Methods

2.1 Material Used

The current study is conducted on 3-ply laminates or plywood, made of Radiata pine (*Pinus radiata D. Don*). The laminates were manufactured with 0°/90°/0° ply orientations, each ply being glued to the other with the commercially used 2-pot poly (vinyl acetate) (PVA). The average amount of glue used between each layer of plywood was 250 g m^{-2}. The nominal thickness of the plywood was about 1.8 mm.

2.2 Design of the Compartment

The cone calorimeter used to perform the experiments had a few size constraints, as per the standards. The current compartment was designed to make sure the sample could get proper exposure to the heating coil and stayed within the safety limits and the outer boundary of the heating chamber. The compartment was designed to have 3 walls: the main one was 300 mm × 300 mm and the side walls were dimensioned as 70 mm 300 mm each. The design was made in a way to simulate the behaviour of a partial compartment, exposed to fire, the heat flux being directed towards the centre of the main wall. The sample was designed by gluing the side walls to the main wall with Ados F2, which is a high-performance general purpose contact adhesive composed of polychloroprene [17], as shown in Fig. 1(a). The sample holder, made of aluminium sheet-metal, Fig. 1(b), was designed to place the sample on the load cell.

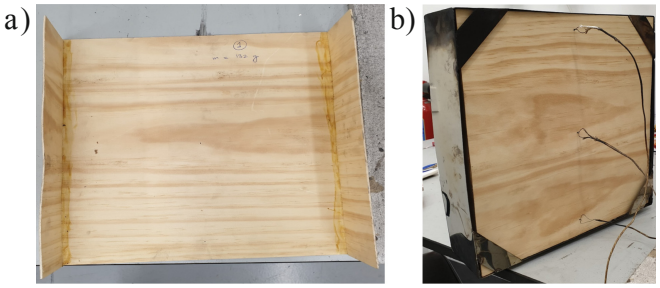

Fig. 1. Graphical illustration of (a) the constructed sample and (b) a sample inside the sample holder with the 3 k-type thermo-couples being attached to measure the temperature gradient.

2.3 Experimental Set-Up

The commercially acquired plywood sheet was cut into the required sizes of 300 mm × 300 mm and 90 mm × 300 mm, to construct the partial compartments with the help of the glue. The cone-calorimeter (FTT Limited, East Grinstead, United Kingdom) was calibrated according to the vertical testing method to measure the reaction to fire properties, namely, fire propagation, peak heat release rate and heat release rate. The basics of ASTM E1354 standard was followed to perform the tests, with variations in sample size and the standard distance between the heating coil and the sample. Three radiant heat fluxes were tested for the samples, 35, 50 and 69 kW/m^2, with the heating coil being 80 mm away from the surface of the main vertical wall. The separation was needed to make sure the spark heating can be used and could not be reduced because of the heating coils, along with the accessories, needs to sit outside the sample holder. All the samples were pre-conditioned at the room temperature of 23 °C and recommended humidity of 50%, for 24 h before starting the test [11]. The temperature profile of the heating surface at top, centre and bottom parts were measured with the help of three k-type thermo-couples, connected to a data logger, as shown in Fig. 1(b). The results concluded were averaged from 3 tests of each sample type, to minimise manual errors. The steps observed during the experiment are illustrated in Fig. 2. The stages were divided into the formation of smoke as one, the start of material degradation as two, visual degradation of the sample material from the centre as three and the fourth being the ignition stage, which is accompanied by complete degradation of the sample.

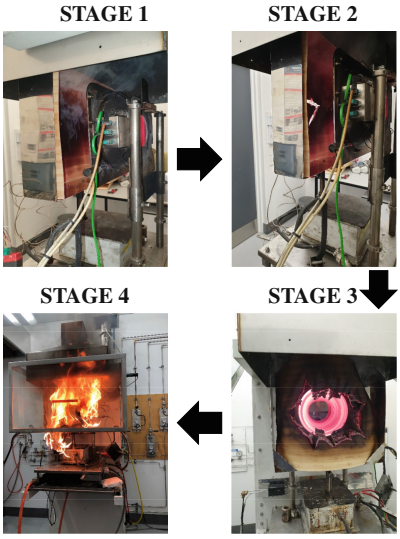

Fig. 2. Illustration of the four significant stages of the experiment carried out.

3 Results and Discussion

The ignition time (t_{ig}) for the three heating irradiances (35, 50 and 69 kW/m^2) can be observed from Fig. 3(a). The irradiance or heat flux of 35 kW/m^2 failed to give any ignition and the plywood did not experience any kind of fire, only showing gradual material degradation and smoke production. The distance and the size both might have played significant roles in the results and therefore, only the results found from the other 2 heat irradiances, where fire was experienced, are discussed in the remaining part of the section. The t_{ig} was greater for the flux of 50 kW/m^2, with an average value of 97 s, when compared to 31.7 s for 69 kW/m^2. The greater time to ignition can be directly attributed to the lesser amount of radiant heat flux, the samples being exposed to. Moreover, it can be observed from Fig. 3(b) that the temperature required for ignition (T_{ig}) was 538.6 °C for 50 kW/m^2; whereas, it was 446.5 °C for 69 kW/m^2. The decrease in T_{ig} can again be attributed to the faster ignition process fuelled by

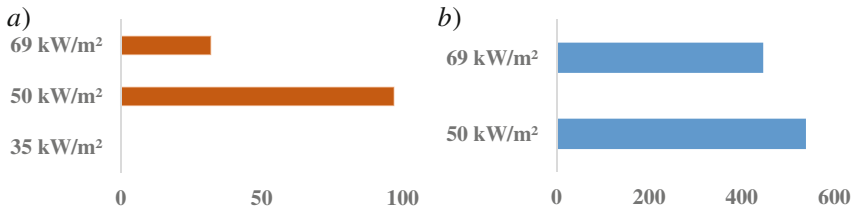

Fig. 3. Graphical representation of (a) Ignition time (t_{ig}) of plywood under 3 heating irradiances and (b) Ignition temperature (T_{ig}) of the 2 irradiances that experienced fire.

greater radiant flux and some aberrations that might be present due to the fact that manual observation was used for denoting the ignition time in each case and also, due to sample degradation, the reading of the thermocouples could vary slightly.

The heat release rates (HRRs) of the two significant irradiances are illustrated in Fig. 4. It can be observed that the HRR curves are active from the time of ignition until the flameout time, after which the amount of heat release becomes constant. The burnout time for the 50 kW/m^2 irradiance was observed to be 190.5 s and Fig. 4(a) shows that the burn-time (t_{ib}) lies in the range of 95–195 s, where the ignition time can visually be observed as 97 s, proving that the visually observed times match significantly with the results from the cone-calorimeter. Moreover, Fig. 4(b) shows a similar HRR curve which shows t_{ib} range of 30–120 s, in-line with the visually observed ignition time of 31.67 s and burnout time of 116 s for the irradiance of 69 kW/m^2. The peak heat release rate (PHRR) is observed to be 229.56 kW/m^2 for the flux of 50 kW/m^2; whereas, it is 211.85 kW/m^2 for 69 kW/m^2. The decrease in the amount of PHRR can be attributed to the aspect of the critical flammable mixture being attained at an earlier stage and the time range of burn-out being smaller.

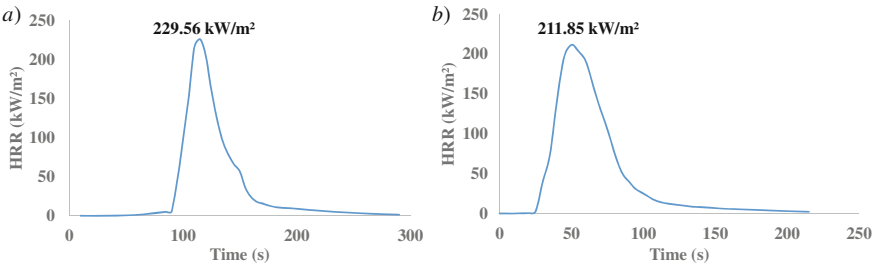

Fig. 4. Experimentally observed heat release rates (HRRs) under the heating irradiances of (a) 50 kW/m^2 and (b) 69 kW/m^2.

Figures 5(a) and (b) illustrate the mass loss for the two fluxes along with the mass loss rate (MLR), which can be represented as the derivative of the change in specimen mass with change in time. The maximum mass loss was again observed during the burning range, with the MLR being highest at 110 s for 50 kW/m^2 and at 70 s for 69 kW/m^2. For both the cases, the MLR is highest at the latter half of the burning range, close to the burnout time; whereas, the MLR is significant only during burning range. Figure 6(a) represents the total amount of heat released during both the irradiances and the maximum amount is quite similar for both the cases, being 8.9 MJ/m^2 for the flux of 50 kW/m^2 and 9.22 MJ/m^2 for 69 kW/m^2.

The higher amount of heat release in a shorter time proves that the critical flammable mixture was reached earlier, the burn-out time was lesser and the total test was completed earlier when the flux was increased. The faster burning also gave less time for smoke production as can be observed from Fig. 6(b). Another interesting finding is that the rate of smoke production for 50 kW/m^2 is almost twice that for 69 kW/m^2,

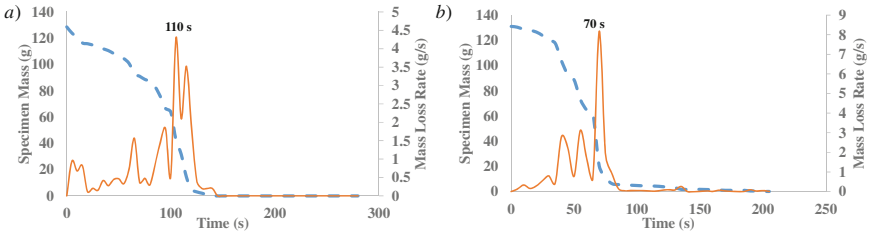

Fig. 5. Time histories of the specific mass of the sample and the mass loss rates for the two irradiances of (a) 50 kW/m^2 and (b) 69 kW/m^2.

proving longer exposure of the samples to the flux due to reduced irradiance, before complete degradation. The surface temperatures of the samples were measured with the help of the thermocouples and the average results are plotted in Fig. 7.

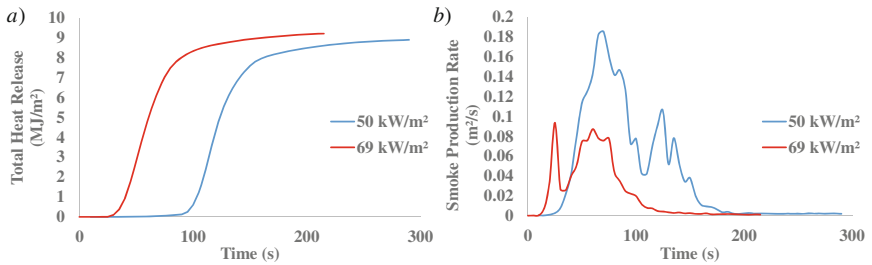

Fig. 6. Experimentally observed (a) total heat release rate (THR) of the two irradiances of 50 and 69 kW/m^2 and (b) the smoke production rate of the two irradiances.

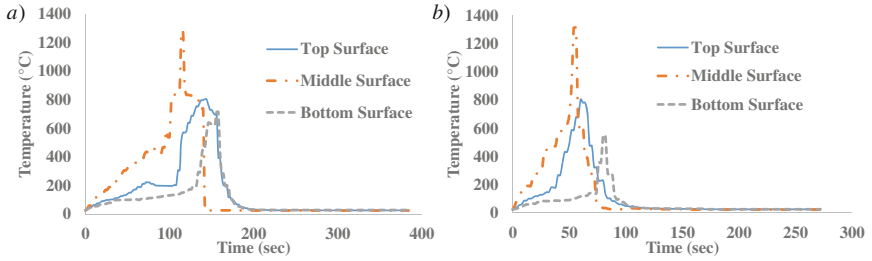

Fig. 7. The temperature profiles of the samples under vertical heating for the two irradiances of (a) 50 kW/m^2 and (b) 69 kW/m^2.

The middle surface experienced the highest temperature because the flux was directed towards the same. Furthermore, the middle surface temperatures were recorded for the shortest period of time, because the material started degrading from the middle and by the time the fire started, the thermo-couple lost all its material around the

surrounding and therefore, the readings ended abruptly. In addition, the top surface experienced higher temperatures than the bottom one, because the air-flow was from the bottom to the top, into the cone-calorimeter chamber, resulting in the upper surfaces being heated more and faster than the lower ones. Thus, for both the irradiances, the temperature of the upper surface was higher, and the highest temperature was reached earlier. Furthermore, it is also important to be noted that the effects due to an infinite or closed wall structure have been ignored due to the structural constraints of the cone-calorimeter.

4 Conclusions

The study helps in observing that for a 300 mm × 300 mm compartment, having 70 mm × 300 mm side walls on each side, with the heating coil being at a distance of 80 mm from the point of ignition; the time of ignition for 50 kW/m^2 was 97 s. Moreover, at 50 kW/m^2, the compartment had a burning range between 95–195 s with a PHRR of 229.56 kW/m^2. In addition, for 69 kW/m^2, the ignition point was observed to be 31.7 s with a burning range between 30–120 s and a PHRR of 211.85 kW/m^2. Moreover, the plywood, for the present testing conditions, failed to reach the critical flammable mixture for the irradiance of 35 kW/m^2. The entire testing process took less time for higher heat flux because the required critical flammable mixture was attained faster; whereas, the smoke production was significantly higher for a lower heat flux. Finally, the temperature variation was observed to be significant from the middle to top and bottom surfaces, with the temperature rising to its peak fastest at the centre, followed by the top due to the air-flow and then at the bottom. The study forms a stepping stone towards observing the effect on flammability due to formability, where the compartment walls will be formed using a 4-point bending rig. Positive differences can significantly aid in opening a new field for further critical investigations and possible industrial applications.

References

1. Srinivasan N (2008) Forming of woodfibre composites and veneer sheets. In: Mechanical engineering, The University of Auckland, Auckland, New Zealand, p 239
2. Srinivasan N, Bhattacharyya D, Jayaraman K (2007) Thermoforming of wood veneer composite sheets. Holzforschung 61(5):558–562
3. Chanda A, Bhattacharyya D (2018) Formability of wood veneers: a parametric approach for understanding some manufacturing issues. In: Holzforschung
4. Chanda A, Bhattacharyya D (2018) Understanding the applicability of natural fibre composites in hybrid folded structures. Adv Mater Lett 9(9):619–623
5. Penneru AP, Jayaraman K, Bhattacharyya D (2005) Strain analysis in bulk forming of wood. Holzforschung 59(4):456–458
6. Norimoto M, Gril J (1989) Wood bending using microwave heating. J Microw Power Electromagn Energy 24(4):203–212

7. Anderson M, McKeever C, Pehrson R, Barnett J (1996) An experimental study of upward flame spread on cellulosic materials. In: Proceedings of the seventh international fire safety and engineering conference INTERFLAM 1996
8. Babrauskas V, Peacock RD (1992) Heat release rate: the single most important variable in fire hazard. Fire Saf J 18(3):255–272
9. Quintiere J, Lee C-H (1998) Ignitor and thickness effects on upward flame spread. Fire Technol 34(1):18–38
10. Dutta S, Das R, Bhattacharyya D (2019) A multi-physics framework model towards coupled fire-structure interaction for Flax/PP composite beams. Compos B Eng 157:207–218
11. Dutta S, Kim NK, Das R, Bhattacharyya D (2019) Effects of sample orientation on the fire reaction properties of natural fibre composites. Compos B Eng 157:195–206
12. Hirschler MM (1999) Use of heat release rate to predict whether individual furnishings would cause self propagating fires. Fire Saf J 32(3):273–296
13. Lattimer BY, Hunt SP, Wright M, Sorathia U (2003) Modeling fire growth in a combustible corner. Fire Saf J 38(8):771–796
14. Lefebvre J, Bastin B, Le Bras M, Duquesne S, Ritter C, Paleja R, Poutch F (2004) Flame spread of flexible polyurethane foam: comprehensive study. Polym Testing 23(3):281–290
15. Board ABC (1996) Performance-based building code of Australia. Canberra, Australia
16. Hedskog B, Ryber F (1998) The classification system for surface lining materials used in buildings in Europe and Japan
17. CRC Industries NZ, ADOS F2 – High Performance General Purpose Contact Adhesive: Technical Data Sheet – 8002 (2011)

Research of Wooden Bearing Structures Behavior Under Fire Condition with Use Advanced Methods of Fire Resistance Calculation Considering Eurocode 5 Recommendation

Serhii Pozdieiev(✉), Stanislav Sidnei, Olha Nekora, and Svitlana Fedchenko

Cherkassy Institute of Fire Safety Named After Chernobyl Heroes of National University of Civil Protection of Ukraine, Onoprienko Str., 8, Cherkassy 18034, Ukraine
svp_chipbbk@ukr.net

Abstract. The article contains the research results on the behavior of a slab with a wooden frame in the conditions of exposure to fire with standard temperature regime, using the finite element method in ANSYS APDL software under nonlinear formulation. The recommendations of the second parts of Eurocode 1 and Eurocode 5 were used to set the initial data and the boundary conditions for the corresponding tasks. The calculation data were obtained regarding the temperature distributions in cross section of the slab elements and the data on its stress-strain state. The results of the calculations were compared with the experimental data and their adequacy was established. Based on the conducted researches, the calculation method for fire resistance of timber slabs was developed and tested, according to the calculated data on the stress-strain state of the slab under the influence of fire. The proposed methodology is consistent with the approach to the calculation of fire resistance of wooden building structures using the specified method and contains recommendations on basic assumptions, initial data, parameters of boundary conditions, the choice of models of materials, recommendations for building geometric and grid models, as well as the criteria for reaching the loss of fire resistance state.

Keywords: Fire resistance · Timber slabs · Advanced calculation method · Finite element method

1 Introduction

Recently, load-bearing wooden structures have been widely used to erect buildings, including multi-storey buildings for large numbers of people. Such structures, in addition to the elements of wooden frames, include also timber slabs. The wooden building structures should ensure the viability of buildings and its structures exposed to fire, in accordance with the requirements of building codes [1]. Calculation methods were applied at the design stage of the fire-resistant building structures. At present, the

L. Makovicka Osvaldova et al. (Eds.): WFS 2020, *Wood & Fire Safety*, pp. 326–332, 2020.
https://doi.org/10.1007/978-3-030-41235-7_48

theoretical and methodological basis for this approach is contained in the standard specifications [2], valid in Ukraine.

Recently, for the development of engineering calculation methods, there are applied the refined methods, based on mathematical modeling of the behavior of wooden structures under fire conditions at the macro-level with the involvement of the finite element method in its implementation in modern computing complexes such as ANSYS, Abaqus, SAFIR and SAFIR and others [3]. Considering this, the researches aimed at building reliable and accurate mathematical models of the behavior of timber structures under fire conditions are relevant.

2 Analysis of Recent Achievements and Publications

In the works [4, 5], there was proposed an approach to study the behavior of timber ceiling slabs under fire, which implies performing mathematical modeling using the finite element method (hereinafter referred to as FEM).

This approach relates to the refined calculation methods and allows an accurate description of the behavior of timber ceiling slabs under fire. The mathematical models, obtained in these works, with a large amount of calculated information, have a significant drawback – consideration of the deformation of timber ceiling slabs only at a certain level of the acting load. It should be also noted that there was little attention paid in this work to the verification of the obtained calculation data. For that matter, the purpose of the research was set.

3 Setting up a Task and Solving It

The purpose of the work is to develop a methodology for calculating the fire resistance for timber slabs, based on the defined basic parameters of stress-strain state, deformation schemes and defect distribution, applying the finite element method. The

Table 1. Basic mathematical models for calculating the slab on its fire resistance.

Physical process	Mathematical model (method) used	Source
Thermotechnical task		
Thermal conductivity	Non-stationary thermal conductivity equation approximated by FEM	[5, 6]
Boundary conditions	III kind	[5, 6]
Physical nonlinearity	The Newton-Raphson iterative method	[5, 6]
Static task		
Stress-strain state	FEM	[5, 6]
Plastic deformation with asym metrical diagrams for tension and compression	Von Mises associative theory of plastic deformation (cast iron plasticity model)	[5, 6]
Physical and geometric nonlinearity	Newton-Rafson iterative method	[5, 6]

mathematical models, with the parameters stated in Table 1, were used for the calculation.

Figure 1 shows a schematic layout of the elements of the timber slab under consideration and a layout of the thermal impact of the fire on the slab.

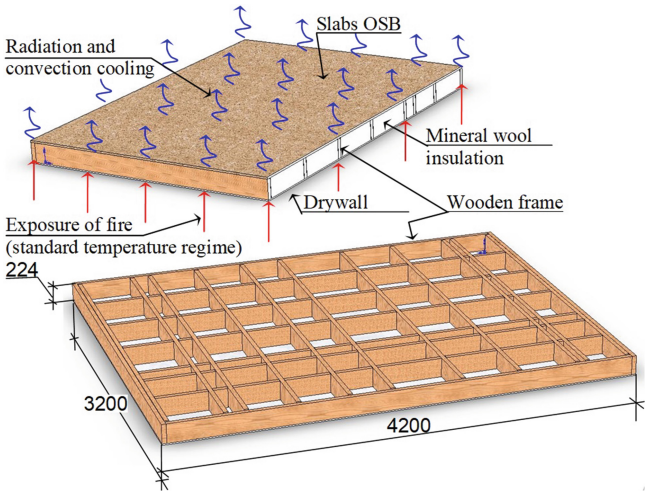

Fig. 1. The schematic layout of the timber slab and of thermal impact on it under fire.

Solving this task requires the formulation of a set of initial data, including the properties of the components of the material of the timber slab; the parameters of the boundary conditions that take into account the applied loadings, and thermal action. The Fig. 2 shows the thermophysical characteristics of the wooden frame of a slab described in the European standard [2] for the calculation of wooden structures for fire resistance. The Fig. 3 shows the mathematical models of the mechanical characteristics of the timber in beams of the slab frame.

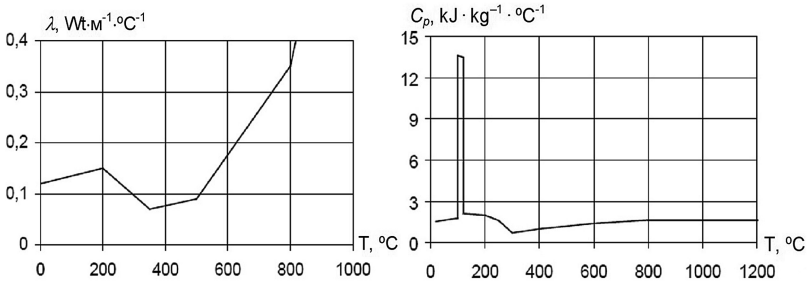

Fig. 2. Relations of wooden thermophysical characteristics from temperature: heat transfer coefficient (*left side*); specific heat (*right side*).

Figure 3 shows the thermomechanical properties of the timber, used for the calculation according to the recommendations [2].

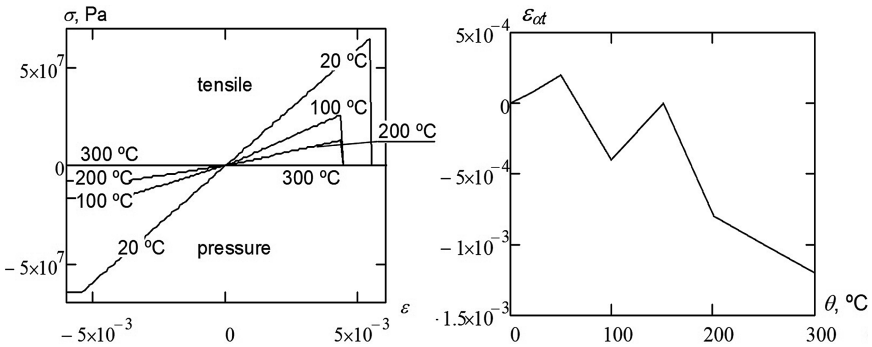

Fig. 3. Diagrams of timber deformation at different heating temperatures (left side) and temperature deformation of timber expansion (right side).

For this calculation, the grid models of timber slab have been built, with a view shown in Fig. 4, repeating the approach of the work [6].

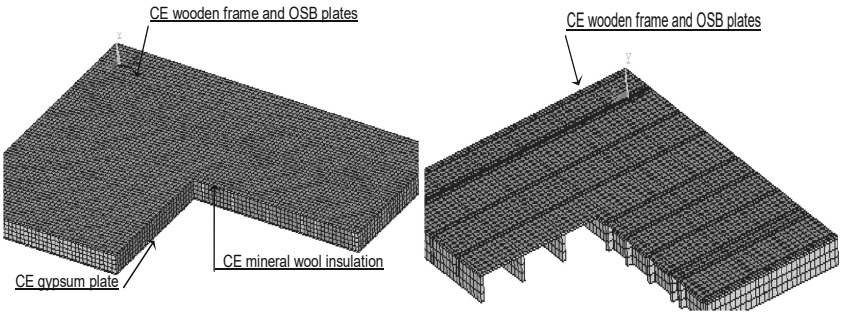

Fig. 4. Grid models: the thermal problem (*left side*); to the static task (*right side*).

4 Calculation Results

Figure 5 (left side) shows the graphs of the heating temperature dependence of the various points in cross-section of a timber ceiling slab from the time of exposure to fire with a standard temperature regime. Figure 5 (right side) shows the temperature distribution along the median longitudinal line of cross-section of the timber beams of the slab frame at different moments of exposure to fire with a standard temperature regime.

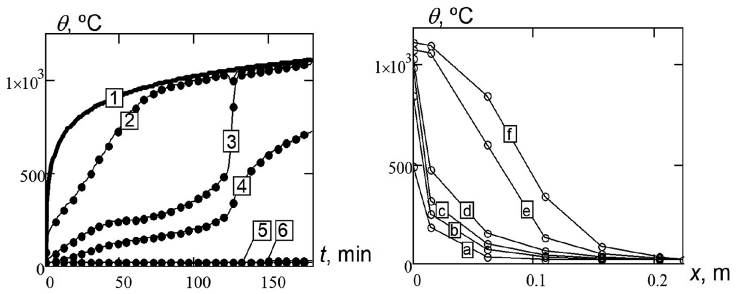

Fig. 5. Heating temperatures at various points of cross section of the timber slab from the time of exposure to fire (*left side*) (*1 - standard temperature regime of fire; 2 - surface of the slab exposed to heating; 3 - lower surface of the wooden beams; 4 - middle point of the cross section of the wooden beams; 5 - the upper surface of the wooden beams; 6 - the upper surface of the ceiling slab*) and graphs of the temperature distribution along the median longitudinal line of the cross-section of the wooden beams at different moments of exposure to fire (*right side*) (*1–30 min; 2–60 min; 3–90 min; 4–120 min; 5–150 min; 6–180 min*).

To investigate the effect of mechanical loading on a timber slab, it was researched under conditions of varying levels of the applied loading. The results are shown in Fig. 6 in the form of graphs of the maximum deflection of the slab, depending on the time of its exposure to fire with a standard temperature regime, and the graphs of changes in the rate of deflection increase.

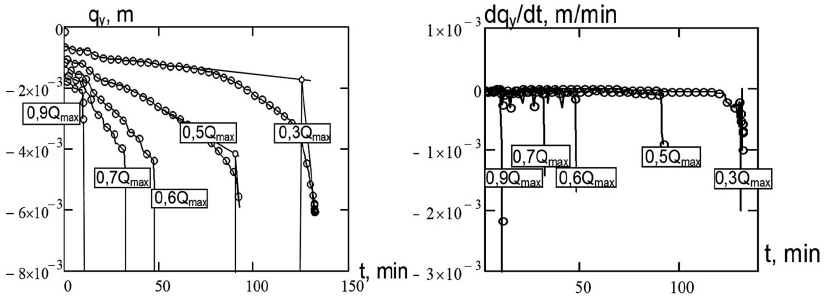

Fig. 6. Graphs of the maximum deflection of the timber ceiling slab (*left side*) and its rate of increase (*right side*), depending on the time of its exposure to fire with a standard temperature regime under varying loadings.

Curve of the maximum deflection of the timber ceiling slab on Fig. 6 let us to determine fire resistance limit of bearing capacity. Special graphical method has been offered for it. This method bases on setting tangent lines before and beyond bending of this curve. Time, corresponded of the fire resistance limit, locates on the intersection of these lines.

Figure 7 shows graphical relation fire resistance of timber slab with level of applied load. This relation has a character near to linear. The experimental researches have been

conducted for check of calculated results adequate. There were fire tests corresponded standard method with use fire furnace. The calculated and experimental figures of the maximum deflection of timber slabs exposed to fire with a standard temperature regime has been shown on Fig. 7 too.

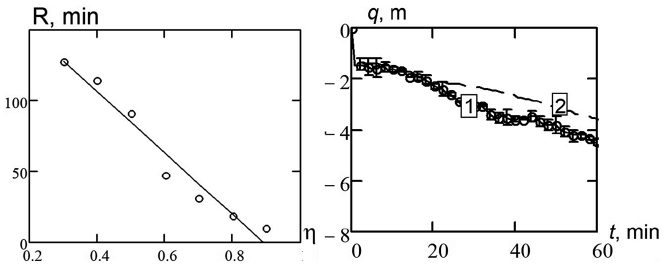

Fig. 7. Dependence of timber slab's limit fire resistance of bearing capacity with ratio of load (*left side*) and dependence of the average experimental (1) and calculated (2) values of maximum deflection of timber slabs with deviations (*right side*).

5 Conclusions

The researches of this work let us to draw the following conclusions:

- the paper substantiates a set of mathematical models for an adequate description of the wooden slab's behavior in a fire condition, including a plastic behavior model for wood using the asymmetrical diagrams of elastic-plastic strain under tension and compression, recommended by Eurocode 5;
- the relate of the fire resistance limit on the bearing capacity of a wooden slab with the applied mechanical load is investigated and it is shown that it is close to linear, which allows its use to construct simpler mathematical models for taking into account the influence of mechanical load for calculated results of the fire resistance of wooden slabs;
- the high adequacy of the calculation results was shown when comparing them with the experimental data obtained during the fire tests of the test slab.

References

1. State Building of Ukraine (2003) Fire protection. Building structures fire safety, DBN V.1.1-7-2002, p 87
2. EN 1995-1-2:2004 (2004) Eurocode 5: Design of timber structures: General-Structural fire design
3. Nekora O, Slovynsky V, Pozdieiev S (2017) The research of bearing capacity of reinforced concrete beam with use combined experimental-computational method. In: MATEC web of conferences, vol 116, p 02024. https://doi.org/10.1051/matecconf/201711602024

4. Collier PR, Buchanan AH (2002) Fire resistance of light-weight timber framed walls. Fire Technol 38:125–145
5. Demeshok V, Zalevs'ka A, Tychenko E, Zmaga Y (2017) The study of carrying capacity of timber slabs with use the finite elements method. In: MATEC web of conferences, vol 116, p 02010. https://doi.org/10.1051/matecconf/201711602010
6. ANSYS, ANSYS 9.0 Manual Set, ANSYS Inc., Southpoint, 275 Technology Drive, Canonsburg, PA 15317, USA

Forest Fires

Experimental Studies of the Localization of Combustion of Forest Fuel Material Using a Water Barrier Line

Geniy V. Kuznetsov, Ivan S. Voitkov, Roman S. Volkov, Yuliana K. Atroshenko, and Pavel A. Strizhak(✉)

National Research Tomsk Polytechnic University, 634050 Tomsk, Russia
pavelspa@tpu.ru

Abstract. The article presents the results of experimental studies of heat transfer in the layers of forest fuel (FF) at localizing the propagating fronts of its flame combustion and thermal decomposition using protective water lines. Such lines were moistened layers of forest fuel before the front of thermal decomposition. The varied parameters were the volume of poured liquid, the size of the barrier line, the conditions of material wetting, specific consumption, irrigation density, etc. The experiments were carried out with typical forest fuels: leaves, needles, and a mixture of leaves and needles. It has been experimentally established that effective conditions of combustion localization may be provided at suppressing the material burning in the vicinity of the water line boundary. The article presents the results of the analysis of the influence of the velocity of the side airflow on the values of the irrigation density required to prevent the combustion front propagation, with and without the use of an earth layer.

Keywords: Forest fuel · Combustion front · Combustion localization by water line · Experiment

1 Introduction

Forest fires are the most large-scale natural disasters [1–3] in terms of consequences: environmental, economic, social, etc. The main feature of forest fires is an extremely quick propagation of the fronts of flame burning and thermal decomposition of FF at high velocities of air flow (wind) and dry weather. This leads to multiple and significantly non-linear growth of the area of the forest burning zone in time (due to these factors, it is often difficult to predict values of the corresponding parameters).

Modern methods of localization of forest burning include the use of specialized fire-extinguishing and fire-suppressing compositions, the formation of protective lines and ditches, and the creation of counter combustion fronts [4, 5]. Each of the known methods involves time-consuming and lengthy preparatory procedures [4, 5]. Quite often, fire services specialists do not have enough time to effectively localize forest burning. In addition, it is often necessary to simultaneously supply extremely large volumes of fire-suppressing compositions, which is impossible due to the limited capacity and number of aircraft.

L. Makovicka Osvaldova et al. (Eds.): WFS 2020, *Wood & Fire Safety*, pp. 335–340, 2020.
https://doi.org/10.1007/978-3-030-41235-7_49

It is shown in [6–8] that large amounts of water supplied at a single point in time are most often used in actual practice of firefighting for suppressing the flaming combustion and pyrolysis of FF. This contributes to a significant decrease in temperature in the combustion zone, but does not always provide combustion suppression. In addition, no more than 15% of the poured water evaporates during combustion suppression. There are large reserves for saving fire extinguishing agents at their rational supply to the combustion zone or before the front.

It is advisable to optimize water consumption when localizing a forest burning site [6–8]. At the same time, it is of interest to conduct appropriate experiments with protective lines in the laboratory and then predict the characteristics of the corresponding processes for real conditions.

2 Experimental Procedure and Methods

Experimental studies were carried out to identify the dominant processes and factors that have a significant impact on the localization of flame burning and pyrolysis of typical forest fuels [8]: needles and leaves. The weight of the samples was about 50 g. The material was laid evenly in a metal pallet with dimensions: length of 310 mm, width of 195 mm, and depth of 45 mm. FF samples were pre-dried for 3–5 days at a temperature of 20 °C. Before the cycle of experiments, the humidity of the materials was determined by the method of thermal drying [8]. For this purpose, the studied FF was weighed and then placed in a drying furnace for 2–3 h at a temperature of 100 °C. After drying, the sample was cooled and re-weighed. The relative humidity of FF was determined by the formula: $\gamma f = (mfw - mfd)/mfw \cdot 100$. The established values of γf were 5–8% for birch leaves and 7–10% for fir needles.

The barrier line in this research is considered to be a moistened layer of FF before the combustion front, having fixed dimensions (width, length, and depth) and volume of accumulated water. In the course of experiments [9] it was found that the protective water line can be created through the use of several spraying schemes: before the combustion front; into the combustion front; and the combined version (before and into the combustion front). Two lines with different sizes of water droplets are used: in the line that is first along the flame burning front motion $Rd \approx 0.25$ mm (large-scale spray), and in the second $Rd \approx 0.08$ mm (fine spray). During the experiments, the spray time (and as a result, the volume of water) was varied.

3 Results and Discussion

3.1 Features of Creating the Protective Line

Figure 1 presents the results of the performed experiments. When planning experiments it was taken into account that for objective reasons, the composition of FF samples even from the same type of material (e.g., needles) in some cases is non-homogeneous. For example, one sample can contain two needles that lied on the ground for significantly different time (for example, for a month, a year, three years),

and, accordingly, differing in their condition (different degree of thermal decomposition of biomass). This factor can lead to a large spread of results of experiments on determining the characteristics of thermal decomposition and combustion of FF. Therefore, the studied processes cannot be qualified as strictly determined, and their important characteristic is the probability of suppression of the combustion process, i.e. the ratio of the number of favorable outcomes to the total number of experiments at a fixed water flow rate (Fig. 1).

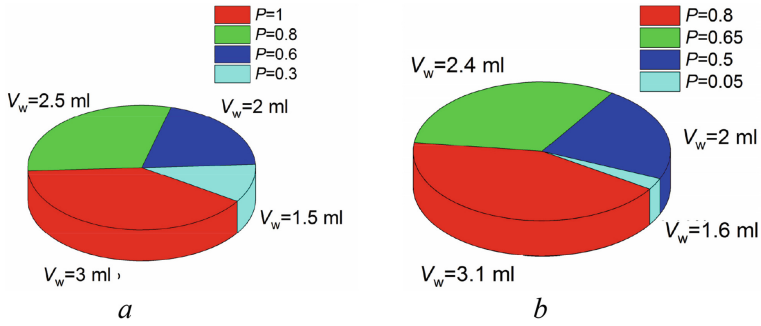

Fig. 1. Relative probability of localization of combustion of the model center of FF depending on the volume of water used: a – experiments with leaves at combined spraying of liquid; b – experiments with needles when using coarse and fine spraying.

Several conclusions can be drawn from the experiments. First, each series of experiments determines a minimum amount of water, sufficient to localize and prevent the reaction of thermal decomposition of FF (stopping of the front motion). There is no need to use an excessively large volume of water. Second, with the use of coarse (Rd $\approx$ 0.25 mm) aerosol, the minimum required volume of water is 3–4 times lower than with the use of fine (Rd $\approx$ 0.08 mm) spray. This is due to the corresponding differences in the times of localization of flame burning and pyrolysis. Third, the most effective scheme (in terms of ensuring the minimum water volume) is the creation of a barrier line by using a combined spray (the volume of water is reduced 1.5–2 times).

3.2 Features of Flame Burning and Pyrolysis of FF

The aim of the experiments was to determine the characteristics of temperature change in the FF layer at approaching fronts of flame combustion and pyrolysis, as well as to determine the characteristics of the latter. Figure 2 shows the scheme of the experiment. The technique included the following procedures: the FF layer (mass $m_f \approx 25$ g) was placed in a metal pallet (width of 230 mm and length of 300 mm); three chromel-alumel thermocouples were evenly placed over the length of the pallet (at a distance of 100, 150 and 200 mm from its left edge); the FF sample was ignited uniformly across the width on the left border of the pallet using a piezoelectric burner; the blower creating an air flow was switched on (the air flow rate varied in experiments in the range $U_a = 0.7-2$ m/s); the

experiment continued until the complete thermal decomposition of the entire FF sample (recorded based on the readings of thermocouples, as well as the results of video shooting).

After completion of the experiments, the process characteristics were recorded: L – the distance at which the flame combustion front passed, mm; L_F – the length of the flame combustion zone, mm; $L_{F\text{-}T}$ – the distance from the flame combustion front to the thermocouple junction, mm; T_f – the FF temperature in the vicinity of the thermocouple junction.

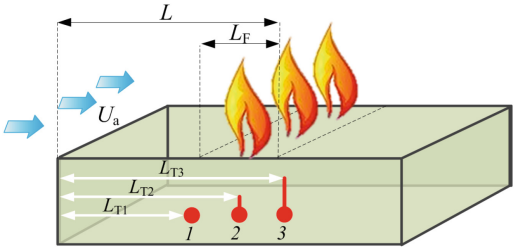

Fig. 2. Experimental scheme illustrating the main recorded characteristics of the process

Figure 3 shows temperature trends in the FF layer, changes in characteristics of the fronts of flame combustion and thermal decomposition, as well as temperature dependences on the distance to the front in the vicinity of thermocouples.

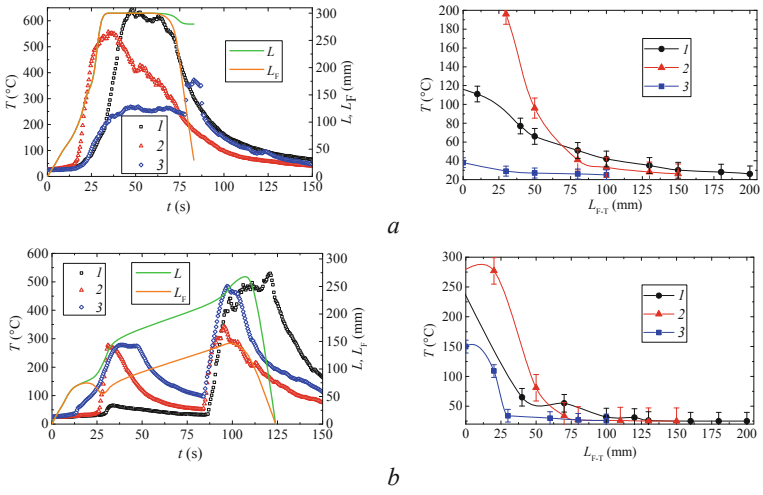

Fig. 3. Temperature change at the points of thermocouples location in the FF sample; changes in characteristics of the zone of flame combustion (left) and temperature dependence on the distance to the front (right) in the vicinity of thermocouples for the two investigated types of FF at $U_a \approx 2$ m/s; *a* – needles, *b* – leaves; *1–3* – TEP No 1–3

3.3 Determining Necessary and Sufficient Conditions for Localizing the FF Combustion

The experimental technique included the execution of sequential procedures: FF (mass $m_f \approx 25$ g) was placed in a metal tray (width of 200 mm and length of 300 mm); by analogy with para. 3.1 (using spray nozzles that generate droplets with a size $R_d = 0.1 - 0.35$ mm) the barrier line was created. In front of the line, the FF line with volume V_f remained. The following parameters were varied: the volume of dry FF, the width of the barrier line, and the density of irrigation. Figures 4, 5 present the main results of the experiments, on which several conclusions can be made.

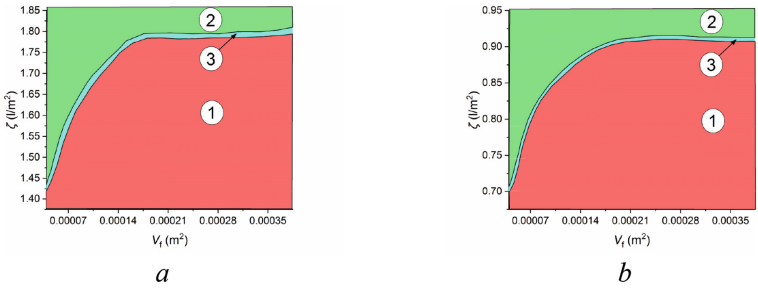

Fig. 4. Dependence of the irrigation density on the volume of FF (needles) in the presence of soil under FF and values of the air flow rate 0.5 m/s. In addition, the following areas have been identified: *1* – the passage of the barrier line by the combustion front; *2* – localization of the combustion front by the barrier line; *3* – boundary area. On the left (*a*) there are dependences for the width of the barrier line of 30 mm, and on the right (*b*) – for 60 mm

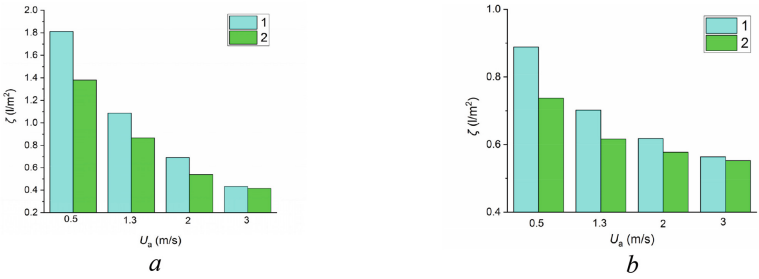

Fig. 5. Dependences of irrigation density (necessary to prevent front propagation) on air flow velocity for the studied types of FF (*a* – needles; *b* – leaves) ($\rho_f \approx 19$ kg/m^3); *1* – pallet; *2* – soil

First, with the increase in the barrier line width (in the range of 30–60 mm), the minimum irrigation density required to prevent the spread of the combustion front is reduced 1.2–1.8 times. *Second,* the increase in the width of the FF layer in front of the barrier line over 20–30 mm does not affect the outcome of the extinguishing process and the required values of irrigation density and water volume. *Third,* in the presence of a soil layer under the FF layer, the minimum irrigation density required to prevent

the spread of the combustion front increases to 30%. *Fourth,* when the lateral air flow velocity is more than 2.5–3 m/s, the irrigation density required to prevent the propagation of the combustion front is practically the same without and with the use of the soil layer.

4 Conclusion

The realized experiments allowed establishing the dependence of the localization times, the necessary and sufficient dimensions of the water barrier line, the rational volume of liquid, the specific density of irrigation and other parameters on the parameters of forest fuel, which determine the basic mechanisms, modes and processes occurring at localization of flame combustion and pyrolysis of FF. The experimental information data base has been generated to explain some well-known hypotheses regarding the choice of parameters of protective water lines, necessary and sufficient for localization of FF burning.

Acknowledgments. Research was funded by Russian Science Foundation (project 18–19–00056).

References

1. Goff HL, Sirois L (2004) Black spruce and jack pine dynamics simulated under varying fire cycles in the northern boreal forest of Quebec, Canada. Can J Forest Res 34:2399–2409
2. San-Miguel-Ayanz J, Moreno JM, Camia A (2013) Analysis of large fires in european mediterranean landscapes: lessons learned and perspectives. Forest Ecol Manag 294:11–22
3. Haas JR, Calkin DE, Thompson MP (2015) Wildfire risk transmission in the Colorado front range, USA. Risk Anal 35:226–240
4. Miyanishi K, Johnson EA, Ward PC, Tithecott AG, Wotton BM (2001) Comment - A re-examination of the effects of fire suppression in the boreal forest. Can J Forest Res 31(1462–1466):1467–1480
5. Kataeva LY, Maslennikov DA, Loschilov AA, Belyaev IV (2016) Influence of the water barrier on the dynamics of a forest fire considering the inhomogeneous terrain and two-tier structure of the forest. ARPN J Eng Appl Sci 11(5):2972–2980
6. Vysokomornaya OV, Kuznetsov GV, Strizhak PA (2014) Experimental investigation of atomized water droplet initial parameters influence on evaporation intensity in flaming combustion zone. Fire Saf J 70:61–70
7. Nakoryakov VE, Kuznetsov GV, Strizhak PA (2016) Physics of suppression of thermal decomposition of forest fuel using surface water film. J Eng Thermophys 25(4):443–448
8. Volkov RS, Kuznetsov GV, Strizhak PA (2017) Experimental study of the suppression of flaming combustion and thermal decomposition of model ground and crown forest fires. Combust Explosion Shock Waves 53(6):678–688
9. Voitkov IS, Volkov RS, Zhdanova AO, Kuznetsov GV, Nakoryakov VE (2018) Physico-chemical processes in the interaction of aerosol with the combustion front of forest fuel materials. J Appl Mech Tech Phys 29(5):891–902

Measuring the Impact of Fire Occurrence Risk on the Value of Forest Land at Growing Scots Pine (*Pinus sylvestris, L.*) and European Beech (*Fagus sylvatica, L.*) Stands in the Territory of Slovak Paradise

Ján Holécy(✉) and Michaela Korená Hillayová

Technical University in Zvolen, T. G. Masaryka 24, 962 01 Zvolen, Slovak Republic
{jan.holecy,xkorenahillayov}@tuzvo.sk

Abstract. The paper informs about the results of economic analysis concerning the projects of Scots pine (*Pinus sylvestris, L.*) and European beech (*Fagus sylvatica, L.*) growing within the territory of Slovak Paradise in the presence of the risk of fire. Risk itself is described in terms of observed probabilities of the destruction of forest stands in relation to their age. The physical inputs for both forestry projects were provided by the single-tree growth simulator SIBYLA-Triquetra calibrated for the soil and climate conditions of an observed region. As the measures of profitability for these projects, the deterministic risk-adjusted and the stochastic risk-free soil expectation values under given conditions have been calculated and compared. The risk-free soil expectation value in both cases has been estimated as the present value of future expected cash-flows in the assumed decades of an infinite forestry project given by the proposed numerical algorithm based on the theory of Markov chains. Obtained results point out the fact that the detected fire occurrence risk of growing pine in this territory is significantly higher than in the case of beech stands. This also results in a stronger unfavorable impact on the profitability of an underlying Scots pine growing project. Even though the original risk-adjusted soil expectation value at growing Scots pine is higher, the resulting risk-free soil expectation value is higher only in the case of growing European beech. Surprisingly, the risk of fire does not shorten the optimum rotation period for both of the tree-species investigated.

Keywords: Risk of forest fire · Forestry projects · Soil expectation value · Markov chains

1 Introduction

As reported by Seidl et al. [1], as well as Flannigan et al. [2] and Lindner et al. [3], forest fires belong among the most dangerous abiotic damaging agents in forestry. The ongoing global climate change considerably also increases the risk of fire in forests situated in the territory of the Slovak Paradise National Park [4]. Scots pine (*Pinus*

L. Makovicka Osvaldova et al. (Eds.): WFS 2020, *Wood & Fire Safety*, pp. 341–346, 2020.
https://doi.org/10.1007/978-3-030-41235-7_50

sylvestris, L.) and European beech (*Fagus sylvatica, L.*) represent tree-species that are growing in a profitable way in this region for centuries. However, under the conditions of increasing area of forest destroyed by fire in this territory, it becomes necessary to measure this kind of risk carefully and also to include it in the economic considerations within forest management projects.

The objective of our research was to analyze the risk of fire occurrence thoroughly and to evaluate its economic impact on both mentioned tree species growing projects.

Modelling the specific risk of fire occurrence is based on information about the probabilities of having a fire in observed pine and beech forests. These probabilities were obtained from historical data about the areas destroyed by fire within the investigated territory in the period 2008–2017. These data, provided by the forest inventory database belonging to the Institute of Forest Resources and Informatics in Zvolen (the National Forestry Center), enabled us to estimate both the vulnerabilities of forest stands in relation to their age and the corresponding fire occurrence rates (f) for selected tree-species. The estimates of probabilities $p(j)$ for the expected destruction of forest stands in particular age classes (j) were calculated on the basis of known vulnerabilities $\Delta F(j)$ as follows:

$$p(j) = k \,.\, \Delta F(j) \,.f \tag{1}$$

The symbol (k) denotes the number of assumed age classes (j) when each particular age class spans the period of 10 years. In this sense each $p(j)$ informs about the probability of a forest stand destruction for the period of 10 years. In our case (k) = 15 what means that the longest assumed rotation period (u) = 150 years at both investigated tree-species forest management projects. The point estimates of corresponding fire occurrence rates (f) at Scots pine and European beech stands were computed as the sums of population proportions of expected destroyed areas (f_j) in the particular age classes (j) of observed forest stands included in a sample. The point estimates of vulnerabilities $\Delta F(j)$ are differences between two adjacent values of the cumulative probability distribution function corresponding to the specified Weibull probability distributions W (c; γ) of the destroyed areas of forest in a sample:

$$\Delta F(j) = F(j) - F(j-1) \tag{2}$$

The mutual comparison of the detected destruction probabilities $p(j)$ of Scots pine and European beech that are related to the age of forest stands is displayed in Fig. 1.

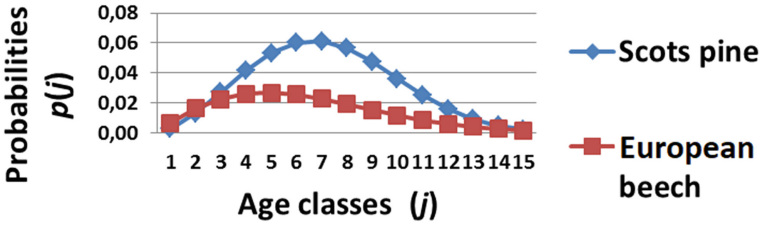

Fig. 1. Probabilities of investigated tree-species destruction by fire for 10 years

A more detailed explanation of this procedure was presented by Holecy and Hanewinkel [5]. Their applied risk description model enhances a simpler solution originally proposed by Reed [6] based on the exponentially distributed time interval between two fires. However, unlike our model, his description of risk assumes only the same probabilities of forest destruction by fire in all age classes.

Probabilities *p(j)* served as one of the essential inputs necessary to measure the impact of fire occurrence risk on the assumed forest management projects.

2 Economic Analysis of Forestry Projects in the Presence of the Risk of Fire

The economic analysis of pine (yield class 22) and beech (yield class 24) growing has been carried out by using the single-tree growth simulator SIBYLA Triquetra [7]. Based on its results, we obtained input data about the particular components of cash-flows assumed during particular decades of both projects at the explored rotation periods (u) = 10, 20, 30, … 150 years so as they are displayed in Table 1.

Table 1. Input data for the calculation of cash-flow generated in the particular decades of analyzed Scots pine and European beech forest management projects.

Age	Scots pine (mean yield class 22)			European beech (mean yield class 24)		
	Stumpage	Costs	Thinnings	Stumpage	Costs	Thinnings
(*t*)	*S*(*t*)	*C*(*t*)	*T*(*t*)	*S*(*t*)	*C*(*t*)	*T*(*t*)
(years)	(EUR/ha)	(EUR/ha)	(EUR/ha)	(EUR/ha)	(EUR/ha)	(EUR/ha)
0	0	2,963	0	0	1,623	0
10	0	857	0	0	1,559	0
20	0	804	0	0	1,443	0
30	335	487	52	0	487	0
40	1,121	487	269	1,724	487	0
50	4,539	487	308	2,977	487	86
60	7,263	487	863	6,190	487	354
70	11,258	487	1,900	11,141	487	947
80	15,269	487	1,919	17,555	487	1,245
90	16,650	487	2,716	22,006	487	1,089
100	18,474	487	1,960	26,969	487	1,017
110	19,452	487	3,010	30,686	487	1,144
120	20,118	487	3,303	35,827	487	1,697
130	19,597	487	3,182	36,630	487	1,426
140	20,180	487	1,984	35,695	487	2,197
150	21,848	487	0	35,036	487	0

The measure of soil expectation value $SEV(u)$ was selected as the criterion of feasibility for these projects. However, in order to evaluate the impact of the risk of fire on the value of this quantity, two kinds of this measure have been proposed:

1. The deterministic risk-adjusted forest soil expectation value $SEV_j(u)$ given by the familiar Faustmann formula [8] was at both projects calculated as follows:

$$SEV_j(u) = [NPV(u) \,.\, (1 + p)^u] \,/\, [(1 + p)^u - 1] \tag{3}$$

   The measure of $NPV(u)$ denotes here the net present value of the time series of cash-flows generated within an underlying forest management project lasting the assumed period of rotation (u) years. It has been computed at the selected interest rate (p) = 1.0% p. *a*. so as its level for forestry capital investments in Slovakia is recommended by Holécy [9].
2. The risk-free soil expectation value $SEV_f(u)$ is calculated by a numerical algorithm based on the theory of Markov chains as developed for forestry projects by Kouba [10]. For this purpose, an infinite forest management project was formulated by using a transition probability matrix (***P***) describing the movement of particular forest stands from lower age classes to higher ones as time goes by in the presence of fire occurrence risk, in the following way:

$$P = \begin{vmatrix} p(1) & 1-p(1) & 0 & 0 & \dots & 0 \\ p(2) & 0 & 1-p(2) & 0 & \dots & 0 \\ . & . & . & . & & \\ . & . & . & . & & \\ . & . & . & . & & \\ p(j) & 0 & 0 & 1-p(j) & \dots & 0 \\ . & . & . & . & & \\ . & . & . & . & & \\ . & . & . & . & & \\ p(k) & 0 & 0 & 0 & \dots & 1-p(k) \end{vmatrix} \tag{4}$$

The first column vector of matrix (***P***) is the vector of risk containing probabilities $p(j)$ with which forest stands growing in age class (j) will not approach higher age class ($j + 1$). Elements above the diagonal of a matrix provide additional information about the probabilities of forest survival. The element $p(k)$ is always equal to 1. The expected surviving shares (p_{ij}) of 1 ha originally planted at time (*0*) of a project and that start to grow at the beginning of the next decade ($i + 1$) are given by the vector $\boldsymbol{p}^{(i)}$:

$$p^{(i)} = p^{(0)} \cdot P^i \tag{5}$$

The initial vector $\boldsymbol{p}^{(0)}$ = [1, 0, 0,…, 0] describes the age class structure at the very beginning of a project duration. Particular elements of vectors $\boldsymbol{p}^{(i)}$ multiplied by corresponding destruction probabilities $p(j)$ and evaluated by assumed cost and revenues of a forestry project, provide information about the expected cash-flow in particular decades of the generated infinite forestry project. The algorithm was stopped

when the increment of the risk-free $NPV(nu)$ of this project for the last (n)-th assumed rotation (u) years was less than 0.001 EUR. This result was then considered as the sought value of $SEV_f(u)$.

3 Results and Discussion

The analysis described above has brought results arranged in Table 2. The decrement of land capital value due to the risk of fire is observable at the both tree-species growing projects. As the criterion of the optimum rotation (u) the maximum of the SEV (u) measure as it is recommended by Ohlin [11] has been selected.

Table 2. The measures of $SEV_j(u)$ and $SEV_f(u)$ calculated at the changing rotation period (u) years according to analyzed Scots pine and European beech forest management projects.

Rotation period	Scots pine (yield class 22)		European beech (yield class 24)	
	Soil expectation value		Soil expectation value	
(u)	$SEV_j(u)$	$SEV_f(u)$	$SEV_j(u)$	$SEV_f(u)$
(years)	(EUR/ha)	(EUR/ha)	(EUR/ha)	(EUR/ha)
10	−77,850	−39,921	−64,008	−32,928
20	−32,249	−23,512	−31,371	−19,920
30	−20,659	−17,917	−21,475	−18,656
40	−14,192	−13,192	−13,112	−12,313
50	−6,035	−6,648	−9,495	−9,487
60	−1,565	−3,187	−4,330	−5,170
70	3,726	835	1,406	−278
80	7,221	3,430	6,689	4,291
90	8,166	4,166	8,581	6,006
100	8,612	4,540	10,038	7,355
110	8,974	4,888	10,311	7,689
120	**9,211**	**5,150**	**11,274**	**8,611**
130	8,849	4,991	9,984	7,588
140	8,533	4,860	8,535	6,412
150	7,969	4,547	6,749	4,941

The economic optimum rotation periods are denoted by block letters and for all investigated projects they approach the same value $(u) = 120$ years. This means that the impact of fire occurrence risk on the capital value of land under given conditions is not so strong to result in shortening the optimum rotation by more than 10 years. Although unexpected, this fact can be reliably explained by the concept of "juvenile risk type" of forest management so as it is described and its impact on forestry projects interpreted in a textbook [12]. The fire occurrence risk specified in our case study obviously belongs

just to this category. However, the significant difference in profitability between both investigated projects appears, if due to the purposes of nature protection, the rotation period (u) lengthens intentionally up to the value of 150 years. The originally more profitable deterministic, Scots pine project, with its $SEV_f(150)$ = 7,969 EUR/ha becomes the less profitable in the presence of fire occurrence risk, when the European beech growing project with its $SEV_f(150)$ = 4,941 EUR/ha seems to be rather more profitable.

These results can help the decision-making of how to adapt forestry to the risk of fire occurrence and so to assert the strengthening of sustainable forestry principles within the territory of Slovak Paradise in practice.

Acknowledgements. The research works and the collection of data described in the present paper were carried out by using the funds of the granted research projects VEGA 1/0570/16 and VEGA 1/0500/19. The authors thank this agency for the support of their research.

References

1. Seidl R, Thom D, Kautz M, Martin-Benito D, Peltoniemi M, Vacchiano G, Wild J, Ascoli D, Petr M, Honkaniemi J, Lexer MJ, Trotsiuk V, Mairota P, Svoboda M, Fabrika M, Nagel TA, Reyer CHPO (2017) Forest disturbancies under climate change. Nat Clim Change 7:395–402
2. Flannigan MD, Stocks BJ, Wotton BM (2000) Climate change and forest fires. Sci Total Environ 262(3):221–229
3. Lindner M, Maroschek M, Netherer S, Kremer A, Barbati A, Garcia-Gonzalo J, Seidl R, Delzon S, Corona P, Kolström M, Lexer MJ, Marchetti M (2010) Climate change impacts, adaptive capacity, and vulnerability of European forest ecosystems. For Ecol Manag 259:698–709
4. Brunette M, Holecy J, Sedliak M, Tucek J, Hanewinkel M (2015) An actuarial model of forest insurance against multiple natural hazards in fir (Abies Alba Mill.) stands in Slovakia. Forest Policy Econ 55:46–57
5. Holécy J, Hanewinkel M (2006) A forest management risk insurance model and its application to coniferous stands in southwest Germany. Forest Policy Econ 8:161–174
6. Reed WJ (1984) The effects of the risk of fire on the optimal rotation of a forest. J Environ Econ Manag 11:180–190
7. Fabrika M, Vaculčiak T (2009) Modeling natural disturbances in tree growth model SIBYLA. In: Bioclimatology and natural hazards. Springer, Dordrecht, pp 155–164
8. Kilkki P (1985) Timber management planning. University of Joensuu, Joensuu, 159 p
9. Holecy J (2011) Results of the econometric model proposed for the Slovak forestry under conditions of forestland management risk (in Slovak). Financovanie Lesy – Drevo, 24th November, Zvolen, Technical University in Zvolen, pp 1–8. https://docs.google.com/file/d/1.0BxE81mUqj36TQTFEYlZJNnk3bTA/edit?pli=
10. Kouba J (2002) Das Leben des Waldes und seine Lebensunsicherheit (Forest life and ist temporal uncertainty). German J For Sci 121:211–228
11. Ohlin B (1995) Concerning the question of the rotation period in forestry. J Forest Econ 1 (1):89–114
12. Burkhardt T, Möhring B, Gerst J (2014) Modeling natural risks in forest decision models by means of survival functions. In: Kant S, Alavalapati JRR (eds) A handbook of forest resource economics, pp 322–340

Analysis of the Existence of Geospatial Data Necessary for Fire Modeling in the Republic of Serbia

Marko Marković(✉), Mirjana Laban, Jovana Maksimović, Tatjana Kuzmić, Mehmed Batilović, and Suzana Draganić

Faculty of Technical Sciences, University of Novi Sad, Dositej Obradović Square 6, Novi Sad, Republic of Serbia
marko_m@uns.ac.rs

Abstract. Wildfires have always been a threat to civil security. In some cases, they cannot be prevented. However, if fire modeling was performed in advance using the available software, it can significantly increase the level of safety in the event of their occurrence. In this paper an analysis of the existence of the geospatial data necessary for fire modeling for the selected area in the Autonomous Province of Vojvodina, Republic of Serbia, was performed. In addition to this analysis, it is recorded type of databases, in sense of coverage and data limitations, as well as date range of required data. A software that is used for this purpose, FARSITE, is described: the operating principle and the data necessary for fire modelling fire in it. Based on the research conducted in the paper, it can be concluded at which level the original geospatial data necessary for fire modeling are in the Republic of Serbia and what is necessary to do in order to improve that situation.

Keywords: Deliblato sands · Geospatial data · Fire modeling · Safety

1 Introduction

Biologically, forests are the most diverse ecosystems on Earth and are an essential factor for the survival of life on the planet. They are a natural habitat for many plant and animal species, they regulate the water regime and play a significant role in preventing floods, erosion and landslides.

According to the National Forest Inventory, Serbia is one of the medium forested countries with average forest cover. The total area under forests in Serbia is 2,254,000 hectares or 29,1%. Of this area, state forests cover 53%, while private forests cover 47% [1]. The National Reforestation Strategy seeks to raise this percentage to about 42% by 2050.

Forest fires are common causes of forest destruction, causing enormous environmental and economic damage, and loss of human lives. The greatest hazards of forest fires occur in the summer months when the air temperature is high, and the moisture content of the air is reduced. We have witnessed numerous forest fires throughout history, one of the most recent being the Amazon fires that occurred in August 2019,

L. Makovicka Osvaldova et al. (Eds.): WFS 2020, *Wood & Fire Safety*, pp. 347–353, 2020.
https://doi.org/10.1007/978-3-030-41235-7_51

which many experts call “the lungs of the planet”. This and similar events are an indisputable indication that forest fires and their modeling must be given great attention.

An official report from the European Commission on the progress of the Republic of Serbia in the EU membership negotiations for 2019 states that the Republic of Serbia is moderately prepared as regards civil protection [2]. In 2018, the Republic of Serbia adopted a Law on disaster risk reduction and emergency management [3]. The Law defines a “Risk Register” for the territory of the Republic of Serbia, which is a significant step towards the formation of a database of consistent, measurable and mutually comparable disaster data, all in line with EU recommendations.

Fire risk analysis can be performed using various software solutions such as: *Fire Area Simulator* (FARSITE) (USA) [4, 5], Fire Prediction Services (Australia) [6], Prometheus (Canada) [7], etc. Meanwhile, the software FARSITE has been integrated into the fire analysis desktop application FlamMap [5, 8].

FARSITE software has been successfully implemented in case studies in South [9] and North America [10], the Mediterranean [11], Asia [12, 13] with different scenarios due to different terrain types, meteorological parameters and spatial fuel models. FARSITE software is open source software and considering the successful implementation in various case studies around the world, the research in this paper will be based on the possibilities of its application.

The aim of this paper is to determine the possibility of using FARSITE software in a case study of Deliblato sands in the Republic of Serbia, based on an analysis of the availability of the necessary input data for fire modeling.

2 FARSITE

FARSITE is a fire growth simulation modeling system that uses spatial information on topography and fuels along with weather and wind files. It incorporates existing models for surface fire, crown fire, spotting, post-frontal combustion, and fire acceleration into a 2-dimensional fire growth model. Two-dimensional fire shapes are assumed to be generally ellipsoidal under uniform conditions. Uniform conditions occur when factors affecting fire behavior (fuels, weather, topography) are spatially and temporally constant, although these conditions rarely exist in nature [4, 5].

Several papers state that ellipsoidal shape of fire is appropriate and that it is adequate for modeling fire growth [14–16].

The FARSITE simulation model uses the Rothermel’s equation to calculate the rate of fire propagation and the Huygens principles for modeling the contour of a fire. With the Huygens principles, every point on the contour of the front of the fire becomes the source of a new fire that spreads under the influence of wind, terrain configuration and vegetation. According to this model, the rate of spread of fire is calculated based on the rate of heat transfer from the burning material to the material that has not yet burned. The model is based on the energy conservation law [4].

FARSITE requires spatial data layers for a comprehensive evaluation of surface and crown fire behavior [17]. This spatial data layers, in form of raster files, represent a georeferenced grid of pixels with specified values that describe certain characteristics of

the associated piece of ground. The first of them is a Digital Elevation Model (DEM) which refers to an elevation of the observed area. From DEM layer can be derived two other required input layers, slope and aspect. These three layers belong to topographical inputs for program FARSITE, while the rest of them are related to the vegetation. Average canopy cover, in percent, is needed as a map to compute hourly fuel moistures [17]. Data layers needed to compute crown fire initiation are average stand height and average crown base height, while a crown bulk density raster map is necessary to compute crown fire spread. An important factor in accurately predicting spatial fire behavior using FARSITE is the quality of the input spatial data layers [10]. There are no requirements for spatial resolution of input raster data in order to start simulation in FARSITE, but the most common used is 30 m. Only important request is that all raster files must be of identical resolution. All spatial data layers are integrated in the landscape file (.LCP). Weather (.WTR) file contains temporal weather stream in which daily observations on temperature, humidity and precipitation is incorporated as input layer. Wind (.WND) file, the adjustment factors (.ADJ) file and the initial fuel moistures (.FMS) file contains the data in ASCII format which is required for any FARSITE simulation. The required Input parameters used for FARSITE are listed out in the Table 1.

Table 1. Input parameters used for FARSITE software [13]

Landscape (GIS layers)	Fuel	Climatic	Ignition probability	Misc.	Ignition point
Latitude	Adjustment	Wind speed and direction	Road probability map	Burn period	Ignition point for fire point
Elevation map	**Fuel moisture**	**Relative humidity**	**Random percentage**		
Slope map		Temperature	Number of simulations		
Aspect map					
Fuel map					
Vegetation map					
Cover map					

3 Case Study – Deliblato Sands, Republic of Serbia

Serbia does not belong to countries with a high risk of wildfires, but there are areas that are classified as particularly vulnerable. According to all quantitative indicators (number of fires, area burned, total damage), the most endangered area is Deliblato sands [18]. Deliblato sands is located in the northeastern part of the Republic of Serbia and extends from southeast to northwest for a length of about 60 km. The history of wildfires in Deliblato sands dates back to the sand bonding period (1818–1918) and continues after World War I [19], as evidenced by the first fire detection watchtowers

of that time. More intensive monitoring and recording of forest fires began in 1948 and continues to this day without interruption. Since then (1948–2017), 267 forest fires have been recorded in Deliblato sands with a total area of 11,943.21 ha. The only years in which fires were not recorded were: 1980, 1992, 2004, 2006, 2008, 2010 and 2014–2017, while the years in which the most catastrophic fires occurred were: 1952, 1972, 1973, 1990, 1996. and 2007 [13]. Nearly 90% of the total number of fires is occupied by ground fires, while in the other 10% of cases, so-called high fires, occurring in the crowns of forest trees. The first high fires began to appear in the 1970s as a result of afforestation of black and white pine [20].

The critical periods for forest fires [21] are the end of winter and the beginning of spring (until the beginning of the vegetation period), and the summer months, especially the end of July and August, which is characteristic of most of central Europe (continental and temperate continental climate). The most important physical and geographical factors of the occurrence and dynamics of wildfires in the Deliblato sands are [22]: a relief, hydrographic characteristics, soil composition, climatic conditions, vegetation composition and sun activity. All these factors are subject to changes in time and space and their interdependence is more than evident. The only exception is the activity of the Sun, which affects one-way, directly or indirectly, on all other factors.

The fire protection measures applied so far in Deliblato sands are the following: fire averages, biological fire belts, care measures, propaganda measures, observation and reporting of fire, surveillance, hazard forecast, construction of water intakes, procurement of fire fighting equipment and others. All these measures are primarily preventive measures and in order to be effective they need to be improved. In order to predict better wildfires in this area, this paper presents available data sources necessary for modeling fire in the previously described FARSITE program.

4 Analysis of Availability of Data Required for FARSITE

Based on the results from Table 2, it can be concluded an obvious lack of data from the vegetation category. Only layer completely available for this region is Canopy cover from GlobeLand30 database. Some of this data types (Fuel model) is available in database “Vojvodinašume”, but not in the required raster format, which is why it is not included in the database inventory. As for topography related data, there are different sources for the Elevation layer. All of them are open source and free of charge to use, except data from national database GeoSrbija. The oldest ones date from 1999 in the NOAA GLOBE Project database, while the latest data can be found in the Global Multi-Resolution Topography (GMRT) from 2018. Aspect and Slope for the Deliblato sands area only exist in the NOAA GLOBE Project global database. Data on temperature and wind are available in two Meteoblue and Republic Hydrometeorological Service of Serbia (RHMS) databases that are updated on a daily basis. On the Meteoblue website data for the last 2 weeks are freely available and can be downloaded for desired location. Earlier data are available after paying access which lasts one year for a certain number of locations. Republic Hydrometeorological Service of Serbia (RHMS) has the same data type. Data is available by sending a formal request stating which meteorological data is required, for which place and period. According to the

Decree on Determining the Fee for Provision of Services in the Field of Meteorological and Hydrological Activity (SG RS 37/13 from 24.04.2013.) the required data are submitted on a commercial basis, i.e. they are charged. The price is set upon receipt of a formal request, the bid and the pro forma invoice are sent, and after payment and submission of proof of payment the report and invoice are sent.

Table 2. Inventory of available databases.

Database	Type of database	Contents of the database	Spatial resolution	Date of data collecting	References
GlobeLand30	Global	Canopy cover	30 m	2010[1,2]	[1]https://www.globallandcover.com/ [2][23]
Copernicus Land Monitoring Service - EU-DEM	Regional	Elevation	25 m	2011[1,2]	[1]https://www.eea.europa.eu/ [2]https://land.copernicus.eu/
DIVA-GIS Country Data	Global	Elevation	90 m	2011[1]	[1]https://www.diva-gis.org/
ALOS Global DEM	Global	Elevation	2.5–30 m	2011[1,2]	[1]https://www.eorc.jaxa.jp/ALOS/en/ [2][24]
EarthEnv-DEM90	Global	Elevation	90–1000 m	2013[1]	[1]https://www.earthenv.org/
ASTER GDEM	Global	Elevation	30 m	2013[1]	[1]https://lpdaac.usgs.gov/products/astgtmv003
The Global Multi-Resolution Topography (GMRT)	Global	Elevation	10–2000 m	2018[1]	[1]https://www.gmrt.org
NOAA GLOBE Project	Global	Elevation Slope Aspect	1000 m	1999[1]	[1]https://data.nodc.noaa.gov/
GeoSrbija	National	Elevation	2.5–1000 m	2014[1]	[1]https://geosrbija.rs
Meteoblue	Global	Temperature Wind speed Wind direction	*not a raster form of data	Daily update[1]	[1]https://www.meteoblue.com/en/
Republic Hidrometeorological Service of Serbia (RHMS)	National	Temperature Wind speed Wind direction	*not a raster form of data	Daily update[1]	[1]http://www.hidmet.gov.rs/index_eng.php

5 Conclusion

This paper analyzes the possibility of using FARSITE software, for the first time, for a one case study in the Republic of Serbia. Also, this paper gave an overview of the FARSITE software, it's significance and utilization in forest fire management. It was described types of files necessary for fire modelling in this program, as well as available databases of required data for the area of Deliblato sands, as a most endangered area in the Republic of Serbia. From obtained results can be concluded that the main limitation is the lack of vegetation data for this region. In order to collect vegetation data in risk areas in the Republic of Serbia, it would be appropriate to apply remote sensing methods such as space and airborne LiDAR (Light Detection and Ranging) missions. The data collected in this way would also be used to more accurately create a digital terrain model and therefore inputs such as: elevation, slope and aspect. Due to the lack

of required inputs for the FARSITE software, it was not possible to perform fire modeling analysis. After providing all the necessary input data, directions for future research would include the application of FARSITE software, as well as other similar open source software solutions and comparison of output data results.

Acknowledgments. The authors gratefully acknowledge the funding provided by the Faculty of Technical Sciences, Department of Civil Engineering and Geodesy under project "Theoretical and experimental research in civil engineering for the purpose of improvement of educational process and strengthening of scientific-research capacity of the department". In addition, this research has partially been supported also by the Ministry of Education, Science and Technological Development of the Republic of Serbia (Projects numbers TR37018 and III43008).

References

1. Banković S, Medarević M, Pantić D, Petrović N, Šljukić B, Obradović S (2009) Šumski fond Republike Srbije - stanje i problemi. Glas Šumar Fak 100:7–29
2. Serbia 2019 Report (2019) Directorate-General for Neighbourhood and Enlargement Negotiations (European Commission) European Commission, Brussels, Belgium, Commission Staff Working Document 52019SC0219
3. Zakon o smanjenu rizika od katastrofa i upravljanju vanrednim situacijama (2018) Službeni glasnik Republike Srbije
4. Finney MA (1998) FARSITE: Fire Area Simulator-model development and evaluation. U.S. Department of Agriculture, Forest Service, Rocky Mountain Research Station, Ft. Collins, CO, General Technical report RMRS-RP-4
5. FARSITE | Fire, Fuel, and Smoke Science Program. https://www.firelab.org/project/farsite. Accessed 22 Nov 2019
6. Fire Prediction Services: Phoenix RapidFire. https://firepredictionservices.com.au/. Accessed 22 Nov 2019
7. FireGrowthModel.ca - Home. http://www.firegrowthmodel.ca/index.php. Accessed 22 Nov 2019
8. FlamMap | Fire, Fuel, and Smoke Science Program. https://www.firelab.org/project/flammap. Accessed 22 Nov 2019
9. Osorio LYL, Bohórquez GB, Tapias EF (2019) Simulation in the farsite of a forest fire presented in the eastern hills of the town of San Cristóbal in Bogotá. Presented at the applied computer sciences in engineering, WEA 2019. Communications in computer and information science, vol 1052, pp 653–663
10. Forghani A, Cechet B, Radke J, Finney M, Butler B (2007) Applying fire spread simulation over two study sites in California lessons learned and future plans. In: 2007 IEEE international geoscience and remote sensing symposium, Barcelona, Spain, pp 3008–3013
11. Arca B, Duce P, Laconi M, Pellizzaro G, Salis M, Spano D (2007) Evaluation of FARSITE simulator in mediterranean maquis. Int J Wildland Fire 16(5):563
12. Kanga S, Singh SK (2017) Forest fire simulation modeling using remote sensing & GIS. Int J Adv Res Comput Sci 8(5):326–332
13. Kanga S, Sharma L, Pandey PC, Nathawat MS (2014) GIS modeling approach for forest fire risk assessment and management. Int J Adv Remote Sens GIS Geogr 2(1):30–44
14. Scott JH (2007) Nomographs for estimating surface fire behavior characteristics. U.S. Department of Agriculture, Forest Service, Rocky Mountain Research Station, Ft. Collins, CO, RMRS-GTR-192

15. Heinsch FA, Andrews PL (2010) BehavePlus fire modeling system, version 5.0: design and features. U.S. Department of Agriculture, Forest Service, Rocky Mountain Research Station, Ft. Collins, CO, General Technical report RMRS-GTR-249
16. Stratton RD (2009) Guidebook on LANDFIRE fuels data acquisition, critique, modification, maintenance, and model calibration. U.S. Department of Agriculture, Forest Service, Rocky Mountain Research Station, U.S. Department of Agriculture, Forest Service, Rocky Mountain Research Station, General Technical report RMRS-GTR-220
17. Keane RE, Garner JL, Schmidt KM, Long DG, Menakis JP, Finney MA (1998) Development of input data layers for the FARSITE fire growth model for the Selway-bitterroot wilderness complex, USA. U.S. Department of Agriculture, Forest Service, Rocky Mountain Research Station, Ft. Collins, CO, General Technical report RMRS-GTR-3
18. Ducić V, Milovanović B (2004) Termičke specifičnosti Deliblatske (banatske) peščare. Zb Rad Geogr Fak Univ U Beogr 52:1–12
19. Živojinović D, Sekulić D (1980) Šumski požari na Deliblatskoj peščari. Deliblatski Pesak Zb Rad IV Spec Prir Rezerv Deliblatski Pesak Šumsko Ind Komb Pančevo Druš Ekol Vojv, pp 83–100
20. Milenković M, Munćan S (2004) Ugroženost šuma Deliblatske peščare od požara. Specijalni rezervat prirode Deliblato sands, Zb Rad VII Javno Preduz Vojvodinašume Novi Sad Šumsko Gazdinstvo Banat Pančevo, pp 53–68
21. Živojinović D (1975) Šumski požari na Deliblatskom pesku posle II svetskog rata i analiza njihovih pojava. Deliblatski Pesak Zb Rad III Jugosl Poljopr-Šumar Cent Beogr Šumsko Ind Komb Pančevo, pp 165–182
22. Milenković M (2011) Fizičko-geografski faktori nastanka i dinamike šumskih požara u Deliblatskoj peščari. Doctoral dissertation, Faculty of Geography, University of Belgrade, Belgrade
23. Chen J, Cao X, Peng S, Ren H (2017) Analysis and applications of GlobeLand30: a review. ISPRS Int J Geo-Inf 6(8):230
24. Tadono T, Ishida H, Oda F, Naito S, Minakawa K, Iwamoto H (2014) Precise global DEM generation by ALOS PRISM. ISPRS Ann Photogramm Remote Sens Spat Inf Sci 4:71–76

Numerical Modeling of the Process of Thermal Impact of Wildfires on Buildings Located Near Forests

Valeriy Perminov(✉)

Tomsk Polytechnic University, 634050 Tomsk, Russia
perminov@tpu.ru

Abstract. The mathematical modeling of forest fires actions on buildings and structures have been carried out to study the effects of fire intensity and wind speed on possibility of ignition of buildings. The crown forest fire is modeled using physical two-phase model of forest fire proposed by Grishin. The hydrodynamic and thermal interactions between plume, wind flow and building are analyzed. The non-stationary three-dimensional conservation equations for turbulent flow in a multiphase reacting medium that are solved numerically under the input conditions characteristic of a large forest fire. As a result of numerical calculations, the dependences of the distances from the front of the fire to buildings at which the ignition of the latter are possible are obtained.

Keywords: Control volume · Crown fire · Fire spread · Forest fire · Mathematical model · Ignition · Building

1 Introduction

Over the past years, the cost of homes lost to wildfire in the world have increased dramatically. The protection of buildings and structures in a community from destruction by fire is a very important concern. This paper addresses the development of a mathematical model for impact of wildfires with buildings. The forest fire is a very complicated phenomenon. At present, fire services can forecast the danger rating of, or the specific weather elements relating to, forest fire. There is need to understand and predict forest fire initiation, behavior and impact of fire on the buildings and constructions. This paper's purposes are the improvement of knowledge on the fundamental physical mechanisms that control forest fire behavior. One of the first accepted method for prediction of crown fires was given by Rothermal [1] and Van Wagner [2]. The semi-empirical models [1, 2] allow to obtain a quite good data of the forest fire rate of spread as a function of fuel bulk and moisture, wind velocity and the terrain slope. But these models use data for particular cases and do not give results for general fire conditions. The discussion of the problem of modeling forest fires is provided by Grishin [3]. A mathematical model of forest fires was obtained by Grishin [3] based on an analysis of known and original experimental data, and using concepts and methods from reactive media mechanics. The physical two-phase models used in [4] may be considered as a development and extension of the formulation proposed by Grishin [3].

L. Makovicka Osvaldova et al. (Eds.): WFS 2020, *Wood & Fire Safety*, pp. 354–360, 2020.
https://doi.org/10.1007/978-3-030-41235-7_52

However, the study of crown fires initiation and spread [3, 4] has been limited mainly to cases studied of forest fires propagation without take into account the mutual interaction of crown forest fires with different obstacles (roads, glades and etc.), buildings and constructions. There are papers in the literature on the effects of combustion on wood, but mainly in laboratory conditions, the effects of a model source are considered without taking into account the spread of the combustion front of a wildland fire [5, 6]. In this paper we carry out modeling of crown forest fire initiation, spread and impact on buildings. The dangerous distances between forest and buildings are calculated in cases when the buildings will be ignited under the influence of forest fires. The calculations take into account the type of forest and its parameters, as well as wind speed, height and shape of the building in the form of a parallelepiped.

2 Physical and Mathematical Model

It is assumed that the forest can be modeled as (1) a multi-phase, multistoried, spatially heterogeneous medium; (2) in the fire zone the forest is a porous-dispersed, two-temperature, single-velocity, reactive medium; (3) the forest canopy is supposed to be non–deformed medium (trunks, large branches, small twigs and needles), which affects only the magnitude of the force of resistance in the equation of conservation of momentum in the gas phase, i.e., the medium is assumed to be quasi-solid (almost non-deformable during wind gusts); (4) let there be a so-called "ventilated" forest massif, in which the volume of fractions of condensed forest fuel phases, consisting of dry organic matter, water in liquid state, solid pyrolysis products, and ash, can be neglected compared to the volume fraction of gas phase (components of air and gaseous pyrolysis products); (5) the flow has a developed turbulent nature and molecular transfer is neglected; (6) gaseous phase density doesn't depend on the pressure because of the low velocities of the flow in comparison with the velocity of the sound; it is supposed that the optical properties of a medium are independent of radiation wavelength (the assumption that the medium is "grey"), and the so-called diffusion approximation for radiation flux density were used for a mathematical description of radiation transport during forest fires. Let the point x_1, x_2, $x_3 = 0$ is situated at the center of the surface forest fire source at the height of the roughness level, axis $0x_1$ directed parallel to the Earth's surface to the right in the direction of the unperturbed wind speed, axis $0x_2$ directed perpendicular to $0x_1$ and axis $0x_3$ directed upward (Fig. 1). The building is situated on the right part of the picture.

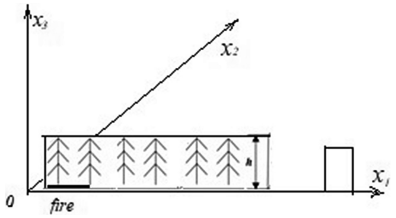

Fig. 1. The scheme of calculation domain.

Mathematically this problem is reduced to the solution of the next system of equations:

$$\frac{\partial \rho}{\partial t} + \frac{\partial}{\partial x_j}(\rho v_j) = Q, j = \overline{1,3}, i = \overline{1,3}; \tag{1}$$

$$\rho \frac{dv_i}{dt} = -\frac{\partial P}{\partial x_i} + \frac{\partial}{\partial x_j}\left(-\rho \overline{v_j' v_i'}\right) - \rho S C d v_i \boldsymbol{v} - \rho g_i - Q v_i; \tag{2}$$

$$\rho c_p \frac{dT}{dt} = \frac{\partial}{\partial x_j}(-\rho c_p v_j' \overline{T'}) + q_5 R_5 - \alpha_v (T - T_s) + k_g \left(c U_R - 4\sigma T^4\right); \tag{3}$$

$$\rho \frac{dc_\alpha}{dt} = \frac{\partial}{\partial x_j}\left(-\rho \overline{v_j' c_\alpha'}\right) + R_{5\alpha} - Q c_\alpha, \alpha = 1, 2; \tag{4}$$

$$\frac{\partial}{\partial x_j}\left(\frac{c}{3k}\frac{\partial U_R}{\partial x_j}\right) - kcU_R + 4k_S \sigma T_S^4 + 4k_g \sigma T^4 = 0, k = k_g + k_S; \tag{5}$$

$$\sum\nolimits_{i=1}^{4} \rho_i c_{pi} \phi_i \frac{\partial T_S}{\partial t} = q_3 R_3 - q_2 R_2 - k_S \left(c U_R - 4\sigma T_S^4\right) + \alpha_v (T - T_S); \tag{6}$$

$$\rho_1 \frac{\partial \phi_1}{\partial t} = -R_1, \rho_2 \frac{\partial \phi_2}{\partial t} = -R_2, \rho_3 \frac{\partial \phi_3}{\partial t} = \alpha_C R_1 - \frac{M_C}{M_1} R_3, \rho_4 \frac{\partial \phi_4}{\partial t} = 0; \tag{7}$$

$$\sum_{\alpha=1}^{3} c_\alpha = 1, P_e = \rho R T \sum_{\alpha=1}^{3} \frac{c_\alpha}{M_\alpha}, \vec{v} = (v_1, v_2, v_3), \vec{g} = (0, 0, g).$$

The system of Eqs. (1)–(7) must be solved taking into account the initial and boundary conditions:

$$t = 0 : v_1 = 0, v_2 = 0, v_3 = 0, T = T_e, c_\alpha = c_{\alpha e}, T_s = T_e, \phi_i = \phi_{ie}; \tag{8}$$

$$x_1 = 0 : v_1 = V, v_2 = 0, v_3 = 0, T = T_e, c_\alpha = c_{\alpha e}, -\frac{c}{3k}\frac{\partial U_R}{\partial x_1} + \frac{c}{2} U_R = 0; \tag{9}$$

$$x_1 = x_{1e} : \frac{\partial v_1}{\partial x_1} = 0, \frac{\partial v_2}{\partial x_1} = 0, \frac{\partial v_3}{\partial x_1} = 0, \frac{\partial T}{\partial x_1} = 0, \frac{\partial c_\alpha}{\partial x_1} = 0, \frac{c}{3k}\frac{\partial U_R}{\partial x_1} + \frac{c}{2} U_R = 0; \tag{10}$$

$$x_2 = -x_{2e} : \frac{\partial v_1}{\partial x_2} = 0, \frac{\partial v_2}{\partial x_2} = 0, \frac{\partial v_3}{\partial x_2} = 0, \frac{\partial T}{\partial x_2} = 0, \frac{\partial c_\alpha}{\partial x_2} = 0, -\frac{c}{3k}\frac{\partial U_R}{\partial x_2} + \frac{c}{2} U_R = 0; \tag{11}$$

$$x_2 = x_{2e} : \frac{\partial v_1}{\partial x_2} = 0, \frac{\partial v_2}{\partial x_2} = 0, \frac{\partial v_3}{\partial x_2} = 0, \frac{\partial T}{\partial x_2} = 0, \frac{\partial c_\alpha}{\partial x_2} = 0, \frac{c}{3k}\frac{\partial U_R}{\partial x_2} + \frac{c}{2} U_R = 0; \tag{12}$$

$$x_3 = 0 : v_1 = 0, v_2 = 0, \frac{\partial c_\alpha}{\partial x_3} = 0, -\frac{c}{3k}\frac{\partial U_R}{\partial x_3} + \frac{c}{2}U_R = 0,$$

$$\rho v_3 = \rho_0 \omega_0, T = T_0, |x_1| \le x_0, |x_2| \le x_0; \rho v_3 = 0, T = T_e, |x_1| > x_0, |x_2| > x_0; \quad (13)$$

$$x_3 = x_{3e} : \frac{\partial v_1}{\partial x_3} = 0, \frac{\partial v_2}{\partial x_3} = 0, \frac{\partial v_3}{\partial x_3} = 0, \frac{\partial T}{\partial x_3} = 0, \frac{\partial c_\alpha}{\partial x_3} = 0, \frac{c}{3k}\frac{\partial U_R}{\partial x_3} + \frac{c}{2}U_R = 0. \quad (14)$$

Here and above $\frac{\mathrm{d}}{\mathrm{d}t}$ is the symbol of the total (substantial) derivative; αv is the coefficient of phase exchange; ρ - density of gas – dispersed phase, t is time; v_i - the velocity components; T, T_S, - temperatures of gas and solid phases, U_R - density of radiation energy, k - coefficient of radiation attenuation, P - pressure; c_p – constant pressure specific heat of the gas phase, c_{pi}, ρ_i, φ_i – specific heat, density and volume of fraction of condensed phase (1 – dry organic substance, 2 – moisture, 3 – condensed pyrolysis products, 4 – mineral part of forest fuel), R_i – the mass rates of chemical reactions, q_i – thermal effects of chemical reactions; k_g, k_S - radiation absorption coefficients for gas and condensed phases; T_e - the ambient temperature; c_α - mass concentrations of α - component of gas - dispersed medium, index α = 1, 2, 3 where 1 corresponds to the density of oxygen, 2 - to carbon monoxide CO, 3 - to carbon dioxide and inert components of air; R – universal gas constant; M_α, M_C, and M molecular mass of α - components of the gas phase, carbon and air mixture; g is the gravity acceleration; c_d is an empirical coefficient of the resistance of the vegetation, s is the specific surface of the forest fuel in the given forest stratum. The source terms which characterize inflow (outflow of mass) in a volume unit of the gas-dispersed phase, the following formulae were used for the rate of formulation of the gas-dispersed mixture Q, outflow of oxygen R_{51}, changing carbon monoxide R_{52} [3]. It is supposed that the optical properties of a medium are independent of radiation wavelength (the assumption that the medium is "grey"), and the so-called diffusion approximation for radiation flux density were used for a mathematical description of radiation transport during forest fires. To close the system (1)–(7), the components of the tensor of turbulent stresses, and the turbulent heat and mass fluxes are determined using the local-equilibrium model of turbulence [3]. It should be noted that this system of equations describes processes of transfer within the entire region of the forest massif, which includes the space between the underlying surface and the base of the forest canopy, the forest canopy and the space above it, while the appropriate components of the data base are used to calculate the specific properties of the various forest strata and the near-ground layer of atmosphere. This approach substantially simplifies the technology of solving problems of predicting the state of the medium in the fire zone numerically. The thermodynamic, thermophysical and structural characteristics correspond to the forest fuels in the canopy of a different (for example pine [3]) type of forest.

3 Numerical Solution and Results

The boundary-value problem (1)–(14) is solved numerically. A discrete analog was obtained by means of the control volume method using the SIMPLE like algorithm (Patankar [7]). Fields of temperature, velocity, component mass fractions, and volume fractions of phases were obtained numerically. The first stage is related to increasing maximum temperature in the place of ignition with the result that a crown fire source appears. As a result, forest fuels in the tree crowns are heated, moisture evaporates and gaseous and dispersed pyrolysis products are generated. Ignition of gaseous pyrolysis products of the crown occurs at the next stage, and that of gaseous pyrolysis products in the forest canopy occurs at the last stage. At the moment of ignition, the gas combustible products of pyrolysis burn away, and the concentration of oxygen is rapidly reduced. The isotherms of gas phase components moved in the forest canopy by the action of wind. It is concluded that the forest fire begins to spread. Next, consider the effects of a forest fire on a nearby building. The influences of wind velocity and distance between forest and building on ignition of building are studied numerically. The results of calculations can be used to evaluate the thermal effects on the building, located near from the forest fires. The temperature fields of crown forest fire at definite moment will be interacted with the obstacle - building (Fig. 2(a) and (b)) and ignited it. Fig. 2 shows temperature fields at the different instants moments of forest fire spread for a wind speed of 15 m/s. During this process, the surface of the wall of the building heats as a result of convection and radiation heat transfer. The wood building will be ignited at definite temperature. The Fig. 3 represent the predicted distributions of temperature on the surface of the wall of the building as a function of vertical coordinate for the three selected wind speed values and different distances between forest and building. In paper [8] it is showed that the wood will be ignited when its temperature exceeds 300 °C. The results of calculations presented on Fig. 3 shows that the surface temperature reach these values at wind velocities more than 6 m/s. The height of building in these calculations was H = 3 m.

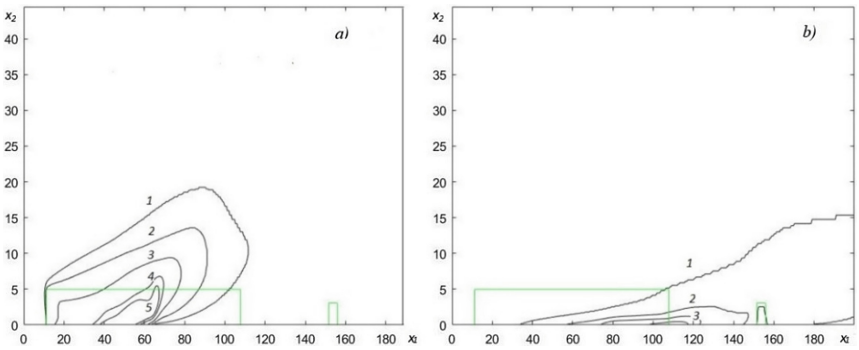

Fig. 2. Gas temperature field at *(a) t = 15* s, *(b) t = 25 s* for a wind speed of 15 m/s; 1–1.2, 2 - 1.5, 3 – 2, 4 – 3, 5 – 4; $\bar{T} = T/T_e$ T_e= 300K.

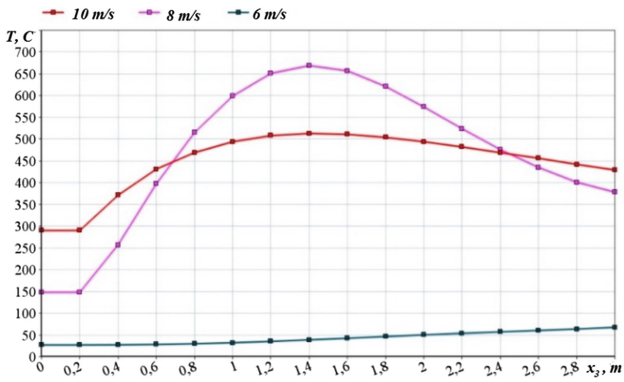

Fig. 3. The distribution of temperature on the wall of the building for three wind speed values. The distance between forest and building is 31 m.

As a result of these calculations it was defined maximum safety distances between forest and building when the building would not have been ignited by forest fire (Fig. 4). The wind speed values increase from 6 to 14 m/s. Also, it was studied the influence of the height of building on the value of safety distances. When the height of building changes from 3 to 6 m, the safety distances l also increases) for different values of wind speed. It is supposed that the optical properties of a medium are independent of radiation wavelength (the assumption that the medium is "grey"), and the so-called diffusion approximation for radiation flux density were used for a mathematical description of radiation transport during forest fires and its impact on buildings.

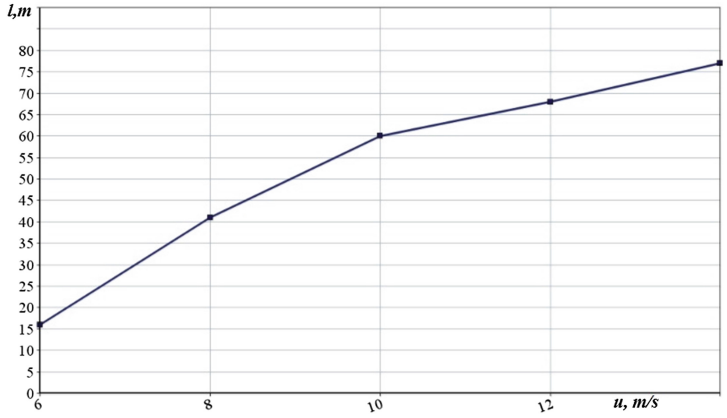

Fig. 4. The dependence of safety distances between forest and building as a function of wind speed values. H = 6 m.

4 Conclusions

A multiphase mathematical model of wind-aided crown forest fires propagating through heterogeneous fuel beds has been performed. It allows to investigate the dynamics of the impact of crown forest fires on buildings under the influence of various external conditions: (a) meteorology conditions (air temperature, wind velocity etc.), (b) type (various kinds of forest combustible materials) and their state (load, moisture etc.). The calculations let to get the maximum distance from the fire to the building in which possible ignition. It has been found that the effect of increasing the wind speed is to increase the safety distances between forest and building. The increasing of building height is observed also led to increase the safety distances between forest and building.

References

1. Rothermal RC (1972) Predicting behaviour and size of crown fires in the Northern Rocky Mountains, Res Pap INT-438. Ogden, UT: US Department of Agriculture, Forest Service, Intermountain Forest and Range Experiment Station
2. Van Wagner CE (1977) Conditions for the start and spread of crown fire. Can J For Res 7:23–34
3. Grishin AM (1997) Mathematical modeling forest fire and new methods fighting them. Publishing House of Tomsk University, Tomsk
4. Morvan D, Dupuy JL (2004) Modeling the propagation of wildfire through a mediterranean shrub using a multiphase formulation. Combust Flame 138:199–210
5. Consalvi JL, Porterie B, Nicolas S, Loraud JC, Kaiss A (2005) Modeling thermal impact of wildland fires on structures in the urban interface. Part 2: radiative impact of a fire front. Numer Heat Transf Part A 47:491–503
6. Kasymov DP, Agafontsev MV, Perminov VV, Tarakanova VA (2018) Studying the resistance to fire of wood under the different type of thermal impact while forest fires. In: Proceedings of SPIE 10833, 24th international symposium on atmospheric and ocean optics: atmospheric physics, p 1083356. https://doi.org/10.1117/12.2504454
7. Patankar SV (1981) Numerical Heat Transfer and Fluid Flow. Hemisphere Publishing Corporation, New York
8. Valendik EN, Mathveev PM, Safromov MA (1979) Large Forest Fires and Fighting with Them. Science, Moscow. (in Russian)

Method for Stand Flammability Classification

Mirosław Kwiatkowski, Ryszard Szczygieł,
and Bartłomiej Kołakowski(✉)

Forest Research Institute,
Sękocin Stary, 3 Braci Leśnej Street, 05-090 Raszyn, Poland
ibl@ibles.waw.pl

Abstract. The fire risk classification now applied in Poland to forest area allows determining fire risk category for the area of Forest District. However, it is impossible to identify the fire risk on the micro scale. The stand flammability classification according to forest habitat types was based on an analysis of fire outbreaks in the period from 2007 to 2017. In elaborating it consideration was given to the number of fires and the burnt area relative to the area occupied by particular forest habitat types and soil cover types. The classification of stands in terms of fire risk shall enable assessing it at the sub-compartment level and to create an Forest Numeric Map layer. In elaborating the final classification method, the weights of individual indices were dependent on the correlation strength of the density of fires or the burnt area and the presence of selected stand types. Taking the above into account, the formula for the cumulative flammability index was derived. The classification of stand flammability according to forest habitat types shall enable the mapping of forests in terms of their fire characteristics at the sub-compartment level. Since a sub-compartment was a basic mapping unit, this led to very detailed, but too fuzzy mapping, which could limit its practical usefulness in certain situations. Therefore, data generalization rules were developed to enable the determination of the flammability class for larger areas, a compartment and a forest range.

Keywords: Forest fire risk categories · Stand flammability classes · Forest habitat types · Soil cover types

1 Introduction

The fire risk classification now applied in Poland to forest area allows determining fire risk category for the area of Forest District, which averagely equals to 17500 ha. However, it is impossible to identify the fire risk on the micro scale. The way of determining forest fire risk in the local scale would be a complement to currently used categorization method. Moreover it would be a premise for more effective organization of the forest fire protection system, particularly in term of infrastructure and operation planning for rescue service. The results of this research enable as well to classify fuel models of forest floor as additional layer of the Forest Numeric Map. This shall meet the requirements of Directive 2007/2/EC of the European Parliament and of the Council of 14 March 2007 establishing an Infrastructure for Spatial Information in the

L. Makovicka Osvaldova et al. (Eds.): WFS 2020, *Wood & Fire Safety*, pp. 361–366, 2020.
https://doi.org/10.1007/978-3-030-41235-7_53

European Community (INSPIRE) for environment protection policy including forest fire protection.

2 Methodology

The stand flammability classification according to forest habitat types was based on an analysis of fire outbreaks in State Forests in the period from 2007 to 2017. In elaborating it, when calculating the flammability index consideration was given to the number of fires and the burnt area relative to the area occupied by particular forest habitat types and soil cover types. This index was the quotient of the proportion of fires or the burnt area and the proportion of a given stand type. In relation to the number of fires, consideration was only given to those sub-compartments where a fire had occurred, whereas in relation to the burnt area the total area affected by a fire was taken into account. These data were referred to current information about the areas of stands growing on particular sites and the soil cover types identified from detailed data on all the sub-compartments found in the Forest Data Bank. The classification of stands in terms of fire risk shall enable assessing it at the sub-compartment level and to create an LMN (Forest Numeric Map) layer with precise fire risk mapping. In elaborating the final classification method, the weights of individual indices were dependent on the correlation strength of the density of fires or the burnt area and the presence of selected stand types.

The classification of stand flammability according to forest habitat types, which has been developed as a result of the implementation of the project shall enable the mapping of forests in terms of their fire characteristics at the lower level.

At present, forest areas are mapped in terms of fire risk at two levels:

1. The national level, the classification of the Regional Directorates of State Forests (provinces, sub-regions) according to forest fire risk categories,
2. The regional level, the classification of forest districts (counties) according to forest fire risk categories.

The project involved the separation of a third forest fire risk mapping level – the local level of a forest district, considering flammability classes determined by a flammability analysis of forest habitat types and soil cover types. The fire risk mapping method provided for the use of necessary valuation data from the Information System of State Forests (SILP). Since a sub-compartment was a basic mapping unit, this led to very detailed, but too meticulous and fuzzy mapping, which could limit practical usefulness in certain situations. Therefore, data generalisation rules were developed to enable the determination of the flammability class for larger areas, a compartment and a forest district. It was decided that a generalised class should be a weighted mean of the classes of individual sub-compartments, with the qualification that where the area of the stands of any class exceeded 50% of the surface of a given area, it was assigned as a whole to that class.

3 Results

The analysis of the forest fire occurrence, which the classification of the stands is based on, distinctly shows the domination of the tree habitat types - considering both number of forest fires and burnt area. These are: fresh coniferous, fresh mixed coniferous and fresh mixed broadleaved forest. The domination of these habitat types is mostly linked to the area covered by them. More accurate information regarding stands flammability are derived from flammability indices - both for number of forest fires and burnt area (Table 1). In terms of the number of fires and burnt area dry coniferous forest should be considered as the most flammable. It is noticeable that for the wet sites flammability indices of burnt area is frequently higher than one for number of fires.

It is clearly visible that estimating the occurrence of the same group of fires in relation to soil cover around 50% occurs in stands with turf (Table 2). However, when the share of stands with turf is close to 60%, both for number of fire and burnt area, flammability indices are close to 0.8. The highest values of flammability index, in both cases, occur for stands with bare ground. Still, considering insignificant (less than 1%) share of stands with bare ground, it doesn't influence the characteristic of fires occurrence.

Another stage involved an attempt to assess the importance of particular indices for establishing the method for classifying the stand flammability where the flammability index determined for the number of fires was higher than 1. The above was conducted by determining the correlation between density of forest fires and the proportion of stands growing on the particular habitat sites (Fig. 1) and also considering the proportion of stands growing on the sites with moss, bare ground and litter. The same methodology was used for the burnt area.

Taking the above into account, the formula for the cumulative flammability index was derived:

$$\mathrm{WS} = 0.8 \cdot \mathrm{WSL} + 0.4 \cdot \mathrm{WSP} + \mathrm{if}\,(\mathrm{WPP} > \mathrm{WPL})\,0.3 \tag{1}$$

where:

WSL - the flammability index of forest habitat types for the number of fires,
WSP - the flammability index of forest habitat types for the burnt area,
WPL - the flammability index of forest soil cover types for the number of fires,
WPP - the flammability index of forest soil cover types for the burnt area.

Table 1. The occurrence of fires depending on forest habitat types and flammability indices.

Forest habitat type	Flammability index		Forest habitat type	Flammability index		Forest habitat type	Flammability index	
	W_{SL}	W_{SP}		W_{SL}	W_{SP}		W_{SL}	W_{SP}
Bb[1]	0.39	2.28						
BMb	0.62	0.80						
BMśw	1.39	1.11	BMwyżśw	1.67	1.11	BMGśw	0.60	0.29
BMw	1.59	2.15	BMwyżw	1.48	0.87	BMGw	0.10	0.39
Bs	3.40	13.17						
Bśw	1.47	1.43				BGśw	0.36	0.08
Bw	1.53	7.27						
Ł	0.65	0.80	ŁLwyż	0.00	0.00	ŁlG	0.12	0.02
LMb	0.20	0.20						
LMśw	0.76	0.62	LMwyżśw	1.44	1.21	LMGśw	0.86	0.87
LMw	0.93	1.04	LMwyżw	1.03	0.75	LMGw	1.14	0.08
Lśw	0.36	0.40	Lwyżśw	0.26	0.31	LGśw	0.11	0.16
Lw	0.32	0.38	Lwyżw	0.55	0.37	LGw	0.07	0.01
Ol	0.23	0.30						
OlJ	0.14	0.11						

W_{SL} – Flammability index according to habitat type for number of fires; W_{Sp} – Flammability index according to habitat type for burnt area; **BMśw** – *fresh mixed coniferous forest*; **BMwyżw** – *upland mixed moist coniferous forest*; **BMwyżśw** – *upland fresh mixed coniferous forest*; **BMGśw** – *montane fresh mixed coniferous forest*; **BMGw** – *montane mixed moist coniferous forest*; **BGśw** – *montane fresh coniferous forest*; **Bs** – *dry coniferous forest*; **Bśw** – *fresh coniferous forest*; **Bw** – *moist coniferous forest*; **BMw** – *moist mixed coniferous forest*; **Bb** – *bog coniferous forest*; **BMb** – *bog mixed coniferous forest*; **Ł** – *riparian forest*; **ŁLwyż** – *upland riparian forest*; **ŁlG** – *montane riparian forest*; **LMGśw** – *montane fresh mixed riparian forest*; **Ol** – *alder forest*; **OlJ** – *alder-ash forest*; **Lw** – *moist broadleaved forest*; **LMśw** – *fresh mixed broadleaved forest*; **LMwyżśw** – *upland fresh mixed broadleaved forest*; **LMwyżw** – *upland mixed moist broadleaved forest*; **Lwyżśw** – *upland fresh moist broadleaved forest*; **Lwyżw** – *upland moist broadleaved forest*; **LMw** – *moist mixed broadleaved forest*; **LMb** – *bog mixed broadleaved forest*; **Lśw** – *fresh broadleaved forest*; **LMGw** – *montane moist mixed broadleaved forest*; **LGśw** – *montane fresh broadleaved forest*; **LGw** – *montane moist broadleaved forest*

Table 2. The occurrences of fires depending on the soil cover types and forest flammability indices.

Soil cover type	Flammability index	
	W_{PL}	W_{PP}
MSZ – *moss*	1.22	0.87
MSZC – *moss/bilberry*	0.46	0.45
NAGA – *bare*	1.53	2.44
SZAD – *turf (dense)*	0.79	1.18
SZCH – *weed (dense)*	0.59	0.80
ŚCIO – *litter*	1.11	1.09
ZAD – *turf*	0.84	0.80
ZIEL – *herbaceous*	0.34	0.30

W_{SL} - Flammability index according to soil cover types for number of fires
W_{Sp} - Flammability index according to soil cover types type for burnt area

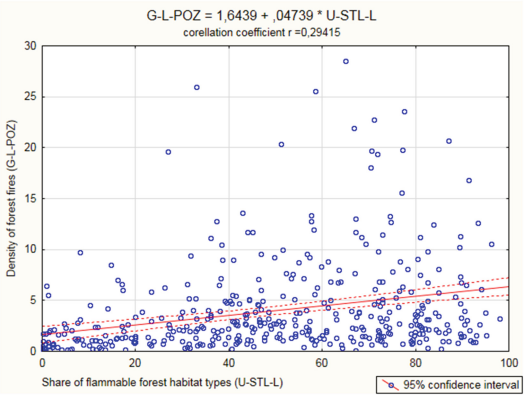

Fig. 1. The correlation between density of fires (GL - POZ) and share of forest habitat types (U-STL-L).

On this basis, it is possible to determine the stand risk class, in accordance with Table 3.

Table 3. The intervals of the cumulative flammability index for the stand flammability classes.

Value of cumulative flammability index W_S	Flammability classes
≥ 1.7	A (high)
$0.7 \div 1.7$	B (medium)
≤ 0.7	C (low)

According to the assumption above, all the stands (considering forest habitat type and soil cover) should be included in one of the below flammability classes (Table 4).

Table 4. The stand flammability classes in relation to the forest habitat type and soil cover.

Forest habitat type	Soil cover		Forest habitat type	Soil cover		Forest habitat type	Soil cover	
	SZAD, SZCH, NAGA	MSZ, MSCZ, ŚCIO, ZAD, ZIEL		SZAD, SZCH, NAGA	MSZ, MSCZ, ŚCIO, ZAD, ZIEL		SZAD, SZCH, NAGA	MSZ, MSCZ, ŚCIO, ZAD, ZIEL
Bb	B	B						
BMb	B	B						
BMśw	A	B	BMwyżśw	A	A	BMGśw	B	C
BMw	A	A	BMwyżw	A	B	BMGw	C	C
Bs	A	A						
Bśw	A	A				BGśw	C	C
Bw	A	A						
Ł	B	B	ŁŁwyż	C	C	ŁłG	C	C
ŁłG	C	C						
LMb	B	B	LMwyżśw	A	B	LMGśw	B	B
LMśw	B	B	LMwyżw	B	B	LMGw	B	B
LMw	B	C	Lwyżśw	C	C	LGśw	C	C
Lśw	B	C	Lwyżw	B	C	LGw	C	C
Lw	C	C						
Ol	C	C						

4 Summary

Comparing the flammability class determined for all sub-compartments in Poland the convergence between percentage share of sites to the area covered by particular flammability class it's clearly visible. The largest area is covered by the stands with an "B" class, which constitute 51.5% of the total forest area, followed by an "A" class stands covering 27.9% of forest land. The less numerous are the stands marked as an "C" class - cover 20.6% of forest land in Poland. This data are close to the share of the forest land according to the forest fire risk categories, which constitute (as at 31.12.2016) 34.7% for I category (highest risk), 46.79% II category (medium risk) and 18.4% for III category (low risk).

The elaborated flammability classification enables mapping forest area what can be crucial for adequate localisation of the newly formed fire protection infrastructure, increasing the efficiency of the rescue actions and correct application of prevention measures.

1. The elaborated mapping rules for forest area includes flammability and fuel types and can be used for the implementation of INSPIRE directive.
2. The classification of forest flammability according to the forest habitat type and soil cover type should be used while elaborating forest fire characteristic of the forest district and included in document "Procedures in the event of a forest fire"

Hungarian - Slovakian Cooperation Making Aerial Firefighting More Effective: Error Analysis

Agoston Restas(✉)

National University of Public Service, Budapest 1083, Hungary
Restas.Agoston@uni-nke.hu

Abstract. In many cases, suppressing forest fires are very difficult. On the one hand, the location of the fire can be so far from the fire department it takes a long time to reach by ground forces or the place of the fire front can be at such a special place the intervention is impossible to carry out by hand crew. On the other hand, the fire intensity can be so high the protection of the ground forces is not enough to carry out the suppression. In these cases, aerial firefighting can be not just an effective solution to suppress the fire front but even the only way to stop fire. That is also well known, against the effectiveness of the aerial firefighting, this method is a very expensive tool. Using mostly picture analysis, this study focuses on the tactical mistakes of the aerial firefighting to prevent wastes of the process. Summarizing the results, even if the aerial firefighting can be a very effective tool suppressing the fire, in many cases, pilots and managers make not just simply mistakes reducing the potential of the effectiveness of the method but even carry out such maneuvers which are not only ineffective but can cause even dangerous situations. This study based on a Hungarian – Slovakian cooperation during I4F project, which supported by the EU Horizon 2020 program.

Keywords: Forest fire · Aerial firefighting · Effectiveness

1 Introduction

Climate change causes extremity that can mean, on one hand, longer rainy periods or higher storm intensity with more rain in shorter periods. On the other hand, it can mean longer drought periods or heat waves with higher peak temperatures in shorter periods. Naturally, these conditions can be combinable optionally. One of the most dangerous extremities is the drought, which raises the fire risk and the intensity of the fire [1]. Higher intensity of the fires can cause more severity in the damages, lots of unintended loss in life, properties and environment [2].

There are many different tools in the hand of fire managers to suppress the forest fires, such as firefighters as hand crews, ground forces, equipped with different vehicles like special fire engines or bulldozers, and the aerial firefighting. It is generally known, aerial firefighting is a very expensive solution to suppress the fire. Because of it, recently there are many critics about the efficiency of the method [3–5]. In their studies, experts usually focus on the effectiveness of the process, how aerial firefighting can

L. Makovicka Osvaldova et al. (Eds.): WFS 2020, *Wood & Fire Safety*, pp. 367–373, 2020.
https://doi.org/10.1007/978-3-030-41235-7_54

stop the fire [6], how to reduce the rate of spread [7] or what is the risk of burning through the protected wet zone [8] but we can also find studies about wood investigation [9] and fire behavior modelling [10].

Even if the above studies demonstrate both the effectiveness and the importance of the aerial firefighting, we cannot accept tactical mistakes what are made many times generating critics against the process in the media [11].

2 Method

This research uses photos and videos to study professionally. Author had practice both as a helicopter pilot and as a fire manager, so the tactical analysis of the photos considers both professions. Author counts with tactical effectiveness as a firefighter, professional effectiveness as a pilot, and economic effectiveness – that means efficiency – as an economist. Logical conclusions as well as some mathematical formulas were also used for the results.

The picture analysis in this study is as detailed as necessary to notice or understand mistakes carried out by pilots or managers. This detail is enough at the beginning of the project to advance the effectiveness, however, later, deeper or more detailed analysis may be required.

Naturally, fire suppression takes time that depends on many factors like the scale of fire, intensity of fire front, meteorological conditions and the resources available for managers. Each picture used for this study shows only a one moment of the period of the suppression. Even if neither the circumstances of taken the photo nor the objective of the tactics are not known, photos are characterized as a moment of the activity. It means statements focus on that message of the moment that demonstrates the activity and shown on the pictures. During the analysis there were not considered any other or secondary purpose of the tactics.

3 Analysis

Aerial firefighting uses three different extinguishing materials. The most commonly used material is the water, which costs practically nothing but has a very good cooling capacity because of the evaporation heat and specific heat capacity. Against the advantages, based on practices, water has a limited suppression capacity that means about up to 3,400 kWm^{-1} fire intensity [12, 13].

Foam agent is used rarely for making classic foam structure, but more often for "wetting" water that means reducing the surface tension of the water. Long term fire retardant is a very effective suppression material, experts count that it is 6–9 times more effective than water, even if the lower value is more likely than the upper one. It is a red colored chemical, looks like slurry or clay.

Unfortunately, retardants have notable environmental impact and it is very expensive. This latest means that experts should use it with special attention. Figure 1 shows a single engine aircraft releasing retardant in front of the fire line. Picture shows low fire intensity at a stubble field, perhaps with 200–300 kWm^{-1} fire intensity but

surely less than 500 kWm^{-1}, which means that this fire could be suppressed by water but even by hand crew.

Fig. 1. Single engine aircraft releases long term fire retardant front of a low intensity fire line [14]

This release is surely effective from the tactical point of view, however surely inefficient comparing to other options such as dropping water, using hand crew or ground forces. As a basic rule, suppressing low fire intensity with retardants means that the firefighting tactic ignores economic effectiveness that is efficiency of the tactic. It is a mistake of the fire manager selecting the extinguishing material.

Fig. 2. Helicopter pilot began water release some seconds later than the optimal place requires [15]

Finding the optimal position to release extinguishing material is not easy, at it is shown in Fig. 2. Flying at low altitude results in a very small view angle on the fire front, therefore very large air tankers use many times spotter plane to help positioning the release. This method cannot be used in each case; pilots usually make the targeting alone or with some help from the ground management.

Often self-navigation results in a mistake in the positioning causing that the released water or retardant cannot help to suppress the fire. In these cases, both the extinguishing material and the resources we used for that circle can be counted as a loss value. It is a mistake of the pilot, even if it cannot avoidable in each case, however reducing this rate to minimal is highly required.

Above mentioned mistakes can be combined as it is shown by the Fig. 3. The positioning resulted in a fact, that not just the houses but also the dirt road – where burnable material cannot be seen – was covered by long term retardant. Long term retardant is good for the different vegetation to stop fires, however not ideal for protecting houses. Both the positioning and the selected suppressant were mistakes.

Fig. 3. Mistake in retardant positioning [16]

Aerial firefighting can be not just effective but even dangerous activity. Figure 4 shows a car on that retardant slurry was dropped and it was damaged seriously. The depth of the retardant is – clearly visible – more than 5 mm, that takes about 5 kgm^{-2} because the density of the mixed retardant is very close to the water density. The flying speed (v_f) during the release takes about 40 ms^{-1}, altitude (h_f) is about 20 m. During the car – retardant collision the effective surface of the car used for this test is about 10 m^2 meaning about 50 kg collide material (m_c). In ideal case, we can ignore air-drag. With the above mentioned assumptions, the collision energy is accumulated by the kinetic (E_k) and the potential (E_p) energies. Formulas of the potential (1) and the kinetic (2) energies are as follows:

$$E_p = m_c\, g\, h_f. \tag{1}$$

$$E_k = {}^1\!/_2\, m_c\, v_f^2. \tag{2}$$

Above means 50 kg × 10 ms^{-2} × 20 m = 10 kJ potential energy, and 0.5 × 50 kg × (40 ms^{-2})^2 = 40 kJ energies, together about 50 kJ energy. It is equivalent of a 100 kg metal globe impact energy after free-falling from 50 m or 1000 kg from 5 m. It is dangerous for hand crews or ground forces as example can prove it [17].

Fig. 4. Effect of retardant demonstrating aerial firefighting energy [18]

There are even other aspects of dangerous activities. In Fig. 5 we can see a CL-415 firefighter plane flying at a very low altitude during water release. The left wing is in the smoke cloud, the right one almost touches the treetop, the flame reaches the belly of the plane. Direction of the fire spread is opposite to the viewpoint, at the forefront there is no or has minimal burnable material. Without suppression, fire would go out spontaneously reaching the edge of the forest. This maneuver is not just ineffective but even very dangerous. It is a mistake of the pilot generating unnecessary risk.

Fig. 5. It is not effective but dangerous action [19]

Against all of the above presented mistakes, in critical situations, fire managers should focus on the tactical effectiveness of the method rather than efficiency even if they cannot be far apart. Sometimes there is only one professional way to suppress the fire. For example, the location of the fire may be so far away from the fire department that it takes too long time for ground forces to reach it in such a phase to be able to extinguish it with limited ground resources. Another example, when the fire front at a mountain area runs at a so special place the intervention is impossible by ground forces or hand crews. In case of high fire intensity, ground forces have no chance to suppress the fire with direct attack because the protection is not enough against the heat radiation. Hand crews can suppress fires up to 500 kWm^{-1} fire intensity using normal protection, capability of grand forces with bulldozer is about up to 2000 kWm^{-1}

intensity; however, bush fires can exceed even 3000 kWm^{-1} fire intensity. In the above given cases, aerial firefighting can be not just an effective solution to suppress the fires but even the only way to stop or reduce the spread.

4 Conclusions

Aerial firefighting can be a very effective tool suppressing the fire however in many cases pilots and managers make not just simply mistakes reducing the potential of the effectiveness of the process but even carry out such maneuvers which are not only ineffective but cause even dangerous situations. At any mistakes it should be taken into account that in many cases aerial firefighting can be not just an effective solution to suppress the fires but even the only way to stop or reduce the spread.

This study based on a Hungarian – Slovakian cooperation during the I4F project, which supported by the EU Horizon 2020 program and focused on making aerial firefighting more effective using foam instead of water or retardants.

References

1. Velas R, Majlingova A, Kacikova D (2018) Study of forest fire behavior under the meteorological conditions changed. In: Scientific conference on earth in a trap? Zvolen, Slovakia, 23 May 2018
2. Teknos L (2018) The complexity and methods of citizen emergency preparedness. Hadmernok 13(3):306–325
3. Ray K (2015) Is aerial firefighting worth it? Aerial firefighting is dangerous, expensive and environmentally damaging. So why do we do it? Report, high country news, August 03 2015. https://www.hcn.org/issues/47.13/after-a-record-setting-wildfire-a-washington-county-prepares-for-the-next-one/the-cost-benefit-analysis-of-aerial-firefighting
4. Frontline wildfire defense report: aerial firefighting: dangerous. But is it effective? (2016). https://www.frontlinewildfire.com/aerial-wildfire-fighting-how-effective-is-it/
5. Michelson M (2016) Can this $10 million firefighting machine actually stop fires? Outside Mag. https://www.outsideonline.com/2079591/can-10-million-firefighting-machine-actually-stop-fires
6. Legendre D, Becker R, Almeras E, Chassagne A (2014) Air tanker drop patterns. Int J Wildland Fire 23(2):272–280. https://doi.org/10.1071/WF13029 CSIRO Publishing
7. Plucinski MA, Pastor E (2013) Criteria and methodology for evaluating aerial wildfire suppression. Int J Wildland Fire 13(22):1144–1154. https://doi.org/10.1071/WF13040
8. Pekić Z (2017) High rate spray technique – a new way for effective aerial wildfire suppression. In: Wildfire 2007 International Wildland Fire Conference, Seville, Spain
9. Fanfarová A, Osvaldová LM, Gaspercová S (2016) Testing of fire retardants. Appl Mech Mater 861:72–79. https://doi.org/10.4028/www.scientific.net/AMM.861.72
10. Beutling A, Batista AC, Soares VR (2012) Fire behavior modeling in laboratory experiments. In: Spano DV (ed) Modelling fire behavior and risk. Universita di Sassari, Sassari
11. Serna J (2019) Firefighting aircraft 'increasingly ineffective' amid worsening wildfires. Los Angeles times, report, April 07 2019. https://www.latimes.com/local/california/la-me-aircraft-increasingly-ineffective-against-california-wildfires-20190407-story.html

12. Hardy C (1985) Chemicals for forest fire fighting. Research study. NFPA, National Fire Protection Association, Boston (1985)
13. Silva FR (2002) Investigación y Capitalización de la Experiencia en el Empleo de Medios Aéros en la Defensa Contra los Incendios Forestales, La gestión de los Medios Aéros en la defensa conzta los incendios forestales, I Simposium Internacional, Córdoba, Spain
14. Gabbert B (2012) Aerial firefighting, pictures report, fire aviation, May 11 2012. https://fireaviation.com
15. The Guardian (2018) Report about Simi Valley Fire, November 13 2018. https://www.youtube.com/watch?v=J_tgKyZy45Y
16. Gabbert B (2017) Tanker 116 sees action at Phoenix. Fire aviation. In: Fox10 news, Report: brush fire in California, June 22 2017. https://fireaviation.com/tag/t-116/
17. Thompson D (2018) Firefighter's death caused by retardant drop from 747. AP news, September 15 2018. https://apnews.com/7b72b8c13e454d46ac5489cec4cdbc3c/Firefighter's-death-caused-by-retardant-drop-from-747
18. CalFireTV (2019) Aerial firefighting drop safety video, August 23 2019. www.youtube.com/watch?v=ONdSoiI4zIA
19. Gabbert B (2014) Aerial firefighting, Pictures report, Fire aviation, August 22 2014. https://fireaviation.com

Comparison of the Effectiveness of Selected Indicators Classifying Burnt Areas on the Basis of Low Altitude Measurements

Anna Szajewska(✉)

The Main School of Fire Service, Warsaw, Poland
aszajewska@sgsp.edu.pl

Abstract. Digital image analysis has played a key role in interpreting spectral images of the ground surface for over 40 years. The physical properties of the material deposited on the surface can be estimated on the basis of reflected radiation with regard to five aspects: the spectral, polarisation, angular, time, and spatial characteristics. Tests of these properties are strongly established in satellite research, which includes remote sensing detection methods used for the classification of forest ecosystems. In terms of fire protection, the important indicators are those which determine the area of the burnt forest or soil cover. The measurements that are useful for applications in fire protection include those which are performed on the site of the event at a low altitude, as they do not impose restrictions on the time of performing the measurement, as is the case with remote sensing detection, and they have no spatial restrictions. This paper presents a comparison of the effectiveness of selected remote sensing detection indicators calculated on the basis of measurements in the visible spectrum and in near infra-red measurements. These ranges can be obtained using a single measurement detector. The example of controlled burning of the soil cover was used to carry out measurements and comparisons of the effectiveness of the indicators calculated on the basis of spectrograms made at a low altitude. The study introduces the terms of 'false acceptance' and 'false rejection'.

Keywords: Burnt area · Remote sensing indicators · Low altitude measurements

1 Introduction

Information about the burnt area of soil cover formed as a result of fire is very important for the purposes of fire safety engineering and preparing reports. Manual estimation is inaccurate and troublesome. For small fires, satellite images have spatial resolution that is too low and an area that is also characterised by time and weather limitations.

Satellite images are limited by cloudiness and the period of flight over the area of interest. The return time, depending on the type of satellite and remote sensing, may be from 5 to 26 days for satellites with a spatial resolution below 60 m.

The examination of burnt areas in this paper was based on a spectrum measurement of the image recorded from a low altitude.

L. Makovicka Osvaldova et al. (Eds.): WFS 2020, *Wood & Fire Safety*, pp. 374–378, 2020.
https://doi.org/10.1007/978-3-030-41235-7_55

The measurement method is similar to remote sensing satellite measurements, but practically, without time limits, is related to the measurement moment. On the other hand, the measurement instruments can be less complex because in practice only two spectrum ranges of the image are needed. In some cases, only one detector and two types of band-pass filters can be used to make the measurement. Such a solution radically reduces the costs of the measurement system. Table 1 lists the most important indicators that can be used to estimate the burnt area. They are determined by two spectral ranges. In addition to the indicators described, there are more advanced solutions, such as BIAS2 (Burnt Area Index for Sentinel-2) [1] operating on five spectral ranges. However, these solutions are dedicated only to a given satellite type and its detectors. For this reason, they are not applied in low altitude tests. The indicators presented in Table 1 are based on the following ranges: NIR - near infrared (wave length of 750…900 nm), RED - red band (690…750 nm), SWIR (Short Wavelength Infrared) - (0,9…2,09 μm), LSWIR (Longer Short Wave Infrared) - (2.11…2.29 μm).

Table 1. Characteristics of key indicators for estimating the burnt area.

Indicator	Tested spectral ranges	Field of test	Minimum number of detectors
NDVI	RED, NIR	Spectrum	1
SAVI	RED, NIR	Spectrum	1
BAI	RED, NIR	Spectrum	1
NBR	NIR, LSWIR	Spectrum	2
ΔNBR	NIR, LSWIR	Spectrum and time	2

Indicators NBR (Normalized Burn Ratio) [2], ΔNBR (Difference Normalized Burn Ratio) [3, 4] are based on reflected radiation in two spectral ranges: NIR and SWIR/LSWIR. The NIR and RED spectral ranges can be covered by a CMOS (complementary metal–oxide–semiconductor) photosensitive matrix. These conditions are met by NDVI (Normalized Difference Vegetation Index) [5], SAVI (Soil Adjusted Vegetation Index) [6] and BAI (Burn Area Index) indicators [7]. Regardless of the determined indicators, measurement of a burning area is subject to two types of errors. A false acceptance error occurs when an area that is not burnt is considered to be burnt. A false rejection error occurs when the indicator does not indicate burning of an area that has actually burnt. The difficulty in estimating a burnt area of soil cover using remote sensing methods is caused by the presence of at least one of these errors, which occurs in almost every measurement. The errors are opposite to each other. The proper selection of the threshold criterion for recognition of an area as burnt is a key factor affecting the reduction of the error in determining a burnt area.

2 Test Procedure

The input data used to determine the NDVI, BAI indicators came from a controlled burn of the soil cover. The measurement was performed at 1 pm, the cloud cover did not exceed 5%, air temperature 25 °C, wind speed 3–6 m/s. The experiment was carried out in spring (April 2019) when the largest numbers of small soil cover fires (less than 1 ha) are recorded in Poland. The moisture content of the combustible material was 8.5%, which was determined by means of a moisture analyzer on the basis of samples taken. During the experiment, the effect of the position of the sun on the ratio of reflected to absorbed radiation was not studied. The measuring device consisted of one monochromatic camera equipped with a CMOS matrix with an extended sensitivity range to be able to record the range outside the visible range - NIR range. A polarization filter and an automatic band filter changer (Fig. 1) were placed in front of the camera.

Fig. 1. Monochromatic camera with automatic band-pass filter changer.

The entire measuring device was placed in a basket lift in such a way to enable observation of the entire experimental burnt area from the top (Fig. 2).

The area of the experiment was mostly dry grasses. The tested area was marked with stakes in such a way as to make it possible to make a reference image on which it was possible to precisely determine the boundary between the burnt area and the area where the fire did not burn. During the controlled burn, half of the observed area was burnt. The image from altitude in NIR and RED bands was recorded.

Fig. 2. The measuring device placed in a hydraulic basket lift located above the burnt area of soil cover.

3 Measurement Result

Based on the reference image in visible light (RGB), where the burnt area occupied half of the observed area, the frame area for NIR and RED spectrograms was determined. The practical solution was to mark the area with stakes that are clearly visible on all spectrograms. This made it possible to frame the image so that the burnt area on the spectrograms was 50%. The optimum threshold value was set for individual indicators in such a way that both errors (false acceptance and false rejection) were as small as possible. Determination of the optimum threshold value is an issue of linear programming, where the function of objective F is the minimum sum of both errors (Template 1) and is simple to determine using the iterative method in the program code written for the purpose of calculations.

$$F(\delta_x, \delta_y) = \delta_x + \delta_y \rightarrow \min. \tag{1}$$

where:

δ_x: number of pixels in the image subject to a false acceptance error
δ_y: number of pixels in the image subject to false rejection error

Table 2 shows the measurement results.

Table 2. Comparison of results for NDVI, BAI and SAVI indicators for the optimum threshold value.

Indicator	NDVI	BAI
False acceptance [%]	6.8	13.2
False rejection [%]	9.8	14.4
Analysis error [%]	16.6	27.6

4 Conclusions

Determination of the optimum threshold value makes it possible to accurately estimate the burnt area of soil cover. However, a reference image is necessary to achieve that. Using only spectrograms, the threshold can be adopted a priori by agreeing to a less accurate measurement. The remote sensing method for measuring a burnt area can be used in unmanned drones. However, for this purpose, spectrograms must be supplemented with information on exact location, orientation and altitude in relation to the ground surface. Currently, colored CMOS matrixes with Bayer filter have a duplicate pixel coated with a green filter. An optimal solution would be to replace one of them with the NIR filter. Such a solution would simplify the entire structure while maintaining the possibility to observe in the visible spectrum.

References

1. Filipponi F (2018) BAIS2: burned area index for Sentinel-2. In: Proceedings of the 2nd international electronic conference on remote sensing, vol 2, p 364
2. Cocke AE, Peter AB, Fulé PZ, Joseph E, Crouse JE (2005) Comparison of burn severity assessment using Differenced Normalized Burn Ratio and ground data. Int J Wildland Fire 14:189–198
3. Escuin S, Navarro R, Fernández P (2008) Fire severity assessment by using NBR (Normalized Burn Ratio) and NDVI (Normalized Difference Vegetation Index) derived from LANDSAT TM/ETM images. Int J Remote Sens 29:1053–1073
4. Smith AMS, Drake NA, Wooster MJ, Hudak AT, Holden ZA, Gibbons CJ (2007) Production of Landsat ETM plus reference imagery of burned areas within southern African savannas: comparison of methods and application to MODIS. Int J Remote Sens 28:2753–2775
5. Rouse JW Jr, Haas RH, Schell JA, Deering DW (1973) Monitoring the vernal advancement and retrogradation (green wave effect) of natural vegetation. Prog Rep RSC 1978-1, Remote sensing center, Texas A&M University, College Station, NTIS No E73-106393
6. Huete AR (1988) A soil-adjusted vegetation index (SAVI). Remote Sens Environ 25:295–309
7. Chuvieco E, Martin MP, Palacios A (2002) Assessment of different spectral indices in the red - near-infrared spectral domain for burned land discrimination. Int J Remote Sens 23:5103–5110

Vegetation Fire Behavior Prediction in Russia

Aleksandra V. Volokitina[1(✉)], Tatiana M. Sofronova[2], and Mikhail A. Korets[1]

[1] Sukachev Institute of Forest SB RAS, Krasnoyarsk, Russia
{volokit, mik}@ksc.krasn.ru
[2] Astafiev Krasnoyarsk, State Pedagogical University, Krasnoyarsk, Russia
tmsofronova@gmail.com

Abstract. The systems for vegetation (including forest) fire behavior prediction in the USA and Canada are analyzed. The conclusion is drawn about the complexity of their use in other countries due to natural differences and historically established different approaches to the classification of vegetation. Russia has all the prerequisites to develop a system for fire behavior prediction. Developed are guidelines for improving forest fire danger rating and fire hazard assessment; classification of vegetation fuels and methods of their mapping; a registered software for automatized vegetation fuel mapping; an example of a map for the nature reserve *Stolby*. A fire spread model is selected based on the availability of the input data. A fire behavior prediction software program is developed to predict spread of tactical fire parts over the area, fire intensity, development of the fire (from the surface fire to the crown or ground one) and immediate fire effects. In addition, the program allows you to calculate the manpower and means for fire suppression. The results of a retrospective software performance test are given on the example of the nature reserve *Stolby*. The software performance test is planned to be carried out on active fires with the participation of forest fire protection experts.

Keywords: Vegetation fires · Vegetation fuel maps · Fire behavior prediction · Fire effects

1 Introduction

Fires that occur in areas covered by forest, steppe, shrub, swamp and other vegetation have long been an unresolved global problem for humanity. Especially great damage is made by forest fires during periods of massive outbreaks caused by severe droughts. It is necessary to control each occurring fire, but in conditions of a lack of manpower and means this is possible only by fire behavior prediction. The behavior of a fire that occurred in any area with vegetation, including forest one, can be characterized by the speed of the flame or flameless spread of combustion and its intensity. In addition, it is important to assess the possibility of a fire moving from one species to another, for example, transforming from the surface fire the crown or ground one, as well as to predict the possible fire effects in a particular plot. So, for example, before a fire, it is

L. Makovicka Osvaldova et al. (Eds.): WFS 2020, *Wood & Fire Safety*, pp. 379–385, 2020.
https://doi.org/10.1007/978-3-030-41235-7_56

very useful to assess the possible tree mortality (% mortality) in the tree stand by the predicted fire intensity under given meteorological conditions, tree species and its average diameter.

2 Background

The most developed systems for vegetation fire behavior prediction have been created and are being improved in the USA (BEHAVE) [1] and Canada (Fire Behavior Prediction - FBP) [2]. In the USA to date, there are already more advanced versions of the BEHAVE system: (1) BehavePlus; (2) FlamMap; (3) FARSITE; (4) FSPro. Each version of the system contains a number of models that determine the moisture content of dead and living fuel in connection with weather conditions, the effect of the terrain on the wind, the wind speed under the forest canopy at the middle flame height, the possibility of developing a surface fire into a crown one, etc. [3]. In the American national BEHAVE system, the main model is Rothermel's model [4]. The development of the system using the Rothermel's model became possible due to the formation of an information database specifically for this model based on the typical method of pyrological characterization of vegetation, namely, by dividing all the US vegetation into pyrological types - "fuel models" [5].

The Canadian Forest Fire Prediction (FBP) system has been actively developing since 1984. Its modern version includes estimates of the vegetation fuel (VF) load which is consumed in a fire, the speed and intensity of fire for typical VF complexes, as well as models for the development of fires, including crown fires [2]. In the calculations of the FBP system, two groups of factors are used: firstly, pyrological characteristic of the vegetation plots (based on their classification) and, secondly, pyrological characteristic of the weather.

Testing of models and software for predicting fire behavior in the USA and Canada imply that the systems are not highly efficient, therefore, their improvement continues there.

There is no official state system for forest fire behavior prediction in Russia yet. There are forest fire danger rating and fire hazard assessment systems that need to be improved. The forest fire monitoring system [6] has been developed quite well, which continues to be improved steadily. However, attempts to predict the behavior of forest fires remotely are also being made, but this is hardly possible without large-scale VF maps. Therefore, so far in Russia, the Guidelines for Forest Fire Detection and Suppression [7], approved by the Federal Forestry Service of Russia (order No. 100) recommended that given a complicated forest fire situation, firefighting managers make fire behavior predictions using the forest plan and tables in the appendices to the "Guidelines…" No. 4–6 and taking into account possible changes in the situation and weather. The mentioned tables contain "approximate indicators of the development and spread of forest fires" for only seven forest types in the European part of Russia and only for four forest types in the Far East of Russia, indicating the minimum, maximum and average rates of fire spread. Relevant prediction of fire behavior using such information is not possible. And the vast area of the Urals and Siberia does not have even of such approximate characteristics at the disposal of fire protection.

There were proposals to borrow a ready-made system for Russia, for example, the Canadian one due to some similarities in environmental conditions. However, with full confidence it can be argued that this will not lead to the desired results, but will only slow down the development of the Russian system, since, as practice shows, simple borrowing of existing foreign systems to predict fire behavior cannot provide a solution to the problem in other countries with different environmental conditions and with different historically established approaches to the pyrological classification of vegetation.

3 Development of the Russian Vegetation Fire Behavior Prediction System

Elements of the Russian system are currently being developed, especially actively at the Sukachev Institute of Forest, Siberian Branch of the Russian Academy of Sciences (IF SB RAS). A relatively perfect system is being created in terms of its simplicity, practicality and accuracy, taking into account the accumulated fundamental knowledge about the nature of forest fires [8].

To date, theoretical and methodological foundations of the Russian system have been developed at the IF SB RAS, including the development of a simple method for predicting the speed and intensity of a forest fire and a method for predicting post-fire tree mortality in a forest stand. However, the main attention was paid to the creation of an information database for modeling and predicting fire behavior. For this purpose, the VF classification has been developed and improved. A simple method and low-cost technology for making VF maps, which serve as the basis of the information database, have been elaborated. The maps contain a comprehensive individual and typical pyrological characterization of vegetation by forest inventory plots (while in the USA and Canada only a rough, typical characterization is used). The idea of the method is to maximize the use of available forest inventory information when developing programs for making VF maps in a computer way [9–11].

Previously, an analysis of the main existing models of fire spread abroad and in Russia was performed [12]. Most of these models, both abroad and in Russia, were developed not by forest fire scientists, but by physicists or mathematicians. The desire to describe the combustion process of the VFs as fully as possible and to take into account as many factors as possible involved in the description of the combustion processes has led to the fact that most of the developed models are currently not applicable in forest fire protection. For example, in the North America with a large number of developed models, only one semi-empirical Rothermel's model is widely used in practice [4]. The common feature of all the developed forest fire spread models is the lack of the necessary information database, including, first of all, the pyrological characteristics of VFs. Therefore, it is difficult to imagine the use of most of the proposed models in forestry practice. The only model of the surface forest fire spread in Russia for which the creation of information databases is feasible is the simple empirical model of the IF SB RAS developed by Sofronov [13, 14].

The development of the Russian system for forest fire behavior prediction has so far been very slow, since it (unlike the United States and Canada) has not been included in

the federal program, despite repeated proposals from the IF SB RAS on the need for its development. For this reason, there was no funding for conducting performance tests of the existing scientific developments of the IF SB RAS, which is an academic institution, where only fundamental research is funded. The situation changed in 2008–2010, thanks to the state contract with the Forestry Agency of the Krasnoyarsk krai and agreements with *Avialesookhrana* and the East Siberian Forest Inventory Enterprise. As a result, creation of large-scale VF maps for a number of large objects began: Chunsky forest section (Krasnoyarsk krai); nature reserves: *Stolby*, Sayano-Shushensky, Kuznetsk Alatau, Ubsunur depression.

In 2015, a software program for vegetation fire behavior prediction [15] was developed and registered. It included prediction of spread rate of tactical parts of the fire (frontal, rear, flanking), the development of fire (transition from the surface fire into the crown or ground one), and the intensity of combustion (allowing prediction of possible mortality in the stand depending on the tree species and its average diameter). In addition, the program calculates the necessary manpower and means for fire management (control or suppression).

A retrospective test of the software program on a large number of past fires in the Chunsky forestry section and in the *Stolby* nature reserve showed its good performance. Figure 1 shows an example of a VF map for the spring (fall) period of the fire season. The map depicts the primary fire carriers. Information on other VF groups, necessary for fire behavior prediction, is included in the pyrological description of the map. Figure 2 shows the result of a retrospective verification of the software program in the *Stolby* nature reserve during the spread of fire No. 4 in 2003. The table to Fig. 2 shows the characteristics of fire No. 4 calculated according to the program and the necessary manpower and means to suppress it (Table 1).

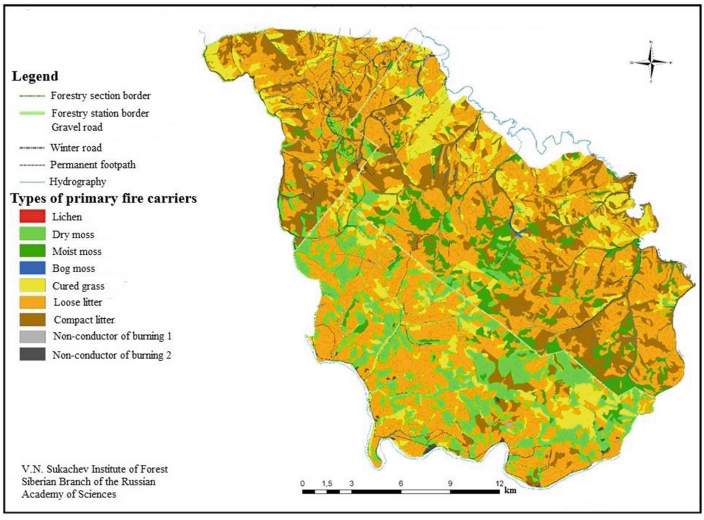

Fig. 1. Vegetation fuel map for spring (fall) period.

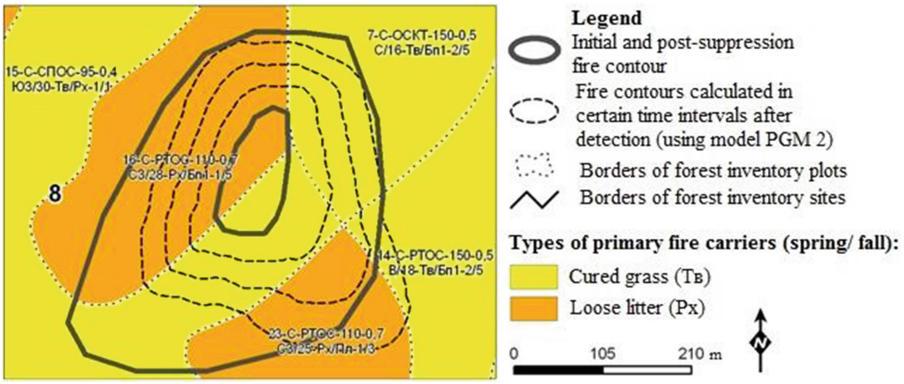

Fig. 2. Prediction of spread for forest fire No. 4 detected May 25, 2003 at 11:40 in the forest inventory unit 8 of the nature reserve *Stolby* on the area of 1 ha and suppressed May 25 at 20:30 on the area of 11 ha. Weather conditions: fire weather index – 949 units, wind – 2 m per second, relative air humidity – 31%.

Table 1. Characteristics of fire No. 4.

Fire characteristic	Time from the start of prediction		
	1	2	3
Fire area, ha	2.7	5.2	8.5
Fire perimeter, ha	620	870	1120
Perimeter spread rate, m/h	226	260	240
Area spread rate, ha/h	2	2.9	3.6
Fire front average spread rate, m/h	33	35	34
Fire edge average intensity, kW/m	112	109	107
Assessment of manpower and means for fire suppression			
Optimum suppression rate, m/h	680	780	720
Suppression duration, hour/area of burnt area after suppression, ha			
3 fire fighters	7/16	–	–
5 fire fighters	3/8	5/20	7/40
7 fire fighters	1.5/4.5	2.5/11	3.5/20
10 fire fighters	1/3.5	1.5/9	2.5/17
15 fire fighters	0.5/3	1/7	1.5/15
20 fire fighters	–	–	1/14

4 Conclusion

In Russia, there are all the prerequisites for creating a Russian system for vegetation (including forest) fire behavior prediction on the basis of long-term fundamental pyrological research, namely: VF classification and mapping methods; a practical model of fire spread, for which it is realistic to create an appropriate information database; developed and registered software programs for VF mapping and vegetation fire behavior prediction.

References

1. Burgan RE, Rothermel RG (1984) BEHAVE: fire behavior prediction and fuel modeling system – FUEL subsystem. Gen Tech rep INT-167. US Department of Agriculture, Forest Service. Intermountain Forest and Range Experiment Station, Ogden, UT, 126 p
2. Forestry Canada, Fire Danger Group (1992) Development and structure of the Canadian forest fire behavior prediction system. Science and sustainable development directorate. Inf rep ST-X-3, Ottawa, 63 p
3. Mavsar R, Cabán AG, Varela E (2013) The state of development of fire management decision support systems in America and Europe. For Policy Econ 29:45–55
4. Rothermel RC (1991) Predicting behaviour and size of crown fires in the Northern Rocky Mountains. USDA forest service, Research paper INT-438, Ogden, UT, USA, 40 p
5. Silva F, Martínez J, Machuca M, Leal JR (2013) VISUAL-SEVEIF, a tool for integrating the behavior simulation and economic evaluation of the impacts of wildfires. In: Proceedings of the fourth international symposium on fire economics, planning and policy: climate change and wildfires. General Technical report, vol 245, pp 163–178
6. Bartalyov SA, Stytsenko FV, Khvostikov SA, Lupyan EA (2017) Methodology of monitoring and prediction of fire-caused stand mortality using satellite observations data. Sovr Probl DZZ Kosm 14(6):176–193 [Current problems in remote sensing of the Earth from space]
7. Guidelines for forest fire detection and suppression [Ukazaniya po obnaruzheniyu i tusheniyu lesnykh pozharov] (1995) Federal forestry service of Russia, Moscow, 110 p
8. Volokitina AV, Korets MA, Sofronova TM (2013) Development of the Russian system of forest fire behavior prediction for fire management on GIS basis. In: International congress: forest fire fighting technologies, 11–13 November, pp 70–71. Ecology. Climate. Novosibirsk
9. Volokitina AV, Sofronova TM, Korets MA (2018) Improvement of fire danger rating in the forest [Sovershenstvovanie otsenki pozharnoy opasnosti v lesu] (Methodical guidelines). IL SO RAN, KGPU, Krasnoyarsk, 43 p
10. Volokitina AV (2014) Prediction of pyrological situations in boreal forests. Vestn KrasGAU (1), 77–83
11. Korets MA, Volokitina AV (2014) Certificate of state registration for software program: program for calculation of pyrological description of forest inventory plots no 2014660252, October 3 2014
12. Sofronov MA, Volokitina AV (2010) Analysis of forest fire spread models. Izv S-Peterb Lesotekhnicheskoy Akad (191), 78–85

13. Sofronov MA (1964) Effect of relief on forest fire in Western Sayan. In: Soviet progress in forest fire control, pp 13–21. Consultants Bureau Enterprises, New York
14. Sofronov MA, Volokitina AV, Sofronova TM (2008) Wildland fires in mountain forests [Pozhary v gornykh lesakh]. IL SO RAN, KGPU, Krasnoyarsk, 388 p
15. Korets MA, Volokitina AV (2015) Certificate of state registration for software program: program for surface fire behavior prediction no. 2015661771, November 9 2015

Use of Aviation Technology in Forest Fire Fighting in Slovakia

Kamil Matta(✉)

University of Žilina, Ul. 1. mája 32, 010 26 Žilina, Slovak Republic
Kamil.Matta@fbi.uniza.sk

Abstract. The paper deals mainly with the use of aviation technology in forest fire fighting, with a focus on the use of helicopters. Whereas most of forest fires in the past were caused by nature (e.g. lightning), the most common cause today is due to human activity. The number of forest fires nowadays is increasing worldwide due to the worsening global climate situation. Forest Fires themselves are very specific, as these are events in which special technologies need to be used. A large area of Slovakia is covered by forests and forest fires are common there. Particularly the problem is the terrain morphology, which often makes it difficult for fire-fighters to get to the fire site by surface. The use of aviation technology during extinguish a fire is thus often the most effective method. This paper therefore reflects the conditions of using aviation technology during fighting of forest fire in the territory of Slovakia. First part of the paper is focused on forest fire statistics and on the damage caused by forest fires. In the next part, regard is directed to the current conditions of use of helicopters for forest fires, along with their flight times. In the last part of the paper there is a proposal for supplement of the technique in the most endangered areas by forest fires.

Keywords: Forest fire · Extinguishing · Helicopter

1 Introduction

A forest fire is an external fire and can be understood as a fire that has arisen in a wooded environment for any reason. Despite the destructive effects on nature or human property, it must be considered as part of the ecosystem. It is also an event that is one of the longest in terms of time, because the forest fire can last several days or weeks. This represents an increased mental and physical load on firefighters, which can lead to injuries or other accidents [4]. Obviously, forest fire-fighting also incorporates other specifics, such as inaccessible terrain, lack of extinguishing agent, unstable weather conditions, which can significantly complicate intervention, and others.

A number of tactical and check-up exercises are carried out to prepare firefighters for forest fires. Nevertheless, these events are able to surprise the intervening fire brigade and commanders. This is due to the specifics of these forest fires, which have already been outlined above in the paper [1].

L. Makovicka Osvaldova et al. (Eds.): WFS 2020, *Wood & Fire Safety*, pp. 386–393, 2020.
https://doi.org/10.1007/978-3-030-41235-7_57

2 Forest Fires in Slovakia

The first records of forest fires in Slovakia date back to 1241–1242 (a period of Tartar invasions), when Tartars burned forests to expel hiding residents.

Statistics of the Fire Research Institute of the Ministry of Interior of the Slovak Republic show that for the period from 2007 to 2018 there were 3081 forest fires in Slovakia. Out of the total number of fires, forest fires account approximately for 2% of this period.

The data on the location of the fire with regard to the type of forest stand shows that the highest number of fires occurred in mixed forest and coniferous forest over ten years. According to the cause of the fire, most of the forest fires in recent years were due to the establishment of fires in nature and deliberate ignition. These causes, together with the burning of grass and dry stands in the forest protection zone, are repeated at the first rungs of the forest fire, according to the cause, also in previous years.

Statistics also show that most of these fires occurred mainly in the spring months - April and March. Temperature extremes are outmatched from year to year, and Slovakia has been plagued by high temperatures and very little precipitation (mostly storm rain) for a long time, resulting in very low soil moisture and a long-lasting dry season (Table 1).

Table 1. Fires in forest environment in Slovakia [2]

Year	Number of forest fire	Damage cost (€)
2007	482	174.729
2008	177	52.845
2009	339	701.728
2010	119	119.097
2011	259	409.505
2012	517	793.860
2013	233	270.230
2014	153	142.445
2015	242	366.870
2016	136	96.655
2017	162	410.330
2018	262	436.140
Overall	3.081	9.063.805

In Slovakia, forest areas are divided into three groups according to the threat. Areas and sub-areas with a high degree of fire risk, a medium degree of danger and a low degree of danger. This division is shown in Fig. 1 [1].

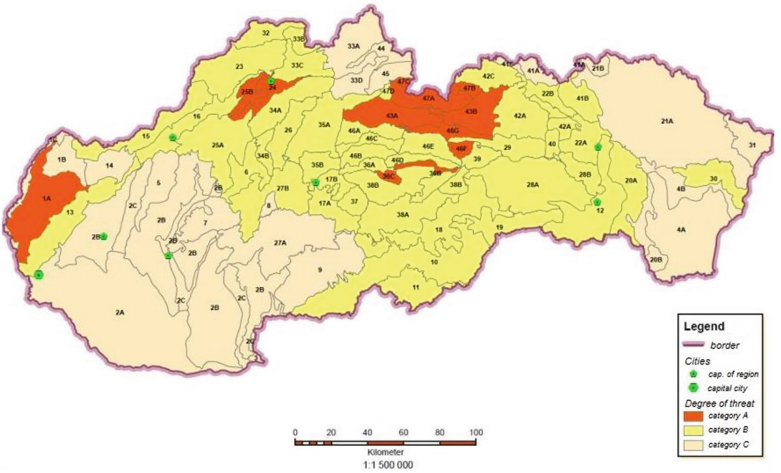

Fig. 1. Areas of Slovakia by threat degree (processor: Obrst, 2019)

3 Use of Aviation Technology in Forest Fires

Aviation technology in the form of a helicopter can be used as follow [3]:

- detection activities (localization),
- patrol activities (monitoring),
- extinguishing activities (using bags or fixed tanks).

Helicopters are a specific type of aviation technology. They have several advantages over an aircraft. The benefits of helicopter firefighting include:

- agility on a smaller area,
- possibility to stay in a hang,
- faster technology deployment option,
- possibility to transport also the firefighters and necessary equipment.

On the other side, the use of helicopter during forest fires also has disadvantages, for example:

- a smaller amount of extinguishing agent,
- shorter usage time (smaller fuel tank),
- failure or damage of the machine have always fatal consequences.

As mentioned, helicopters also perform monitoring and patrol activities, with the help of various types of cameras and instruments. The commander of the intervention who coordinates the overall firefighting activity is at the scene of the fire. Before fire fighting a briefing is carried out between the intervention commander, the helicopter crew commander (or helicopter commanders) and the coordinator who manages and coordinates the aerial part of the extinguishing. The fire extinguishing area, the meteorological conditions in the area and the methods and directions of fire arriving at

the fire shall be specified. During the flight, the helicopter is in radio communication with ground units at the fire site. The radio link provides rough helicopter guidance to the fire site to members of the ground unit of the Fire and Rescue Service in some cases. The most often used facility during forest fire fighting with the help of helicopter in Slovakia, but also in other parts of the World, is an underslung device in the form of a fire extinguishing bag or tank. The extinguishing agent is water, best with a wetting agent [5].

Helicopter Bucket
It is the most commonly used option for conveying the extinguishing agent through the air. It is a device that can transport an extinguishing agent to a fire place using a helicopter. The best known on the market are "Bambi Bucket" devices, which are manufactured by a Canadian company SEI Industries Ltd. It is the company with more than 35 years of tradition in the market with helicopter buckets. The bags can vary in volume from 0.273 m^3 to 9.842 m^3. Of course, the bag used depends on the carrying capacity of the helicopter. Besides the "Bambi Bucket", SEI Industries Ltd. also produces other buckets, which are often used in practice. These are buckets with sales name Bambi Torrentula and Bambi MAX [6].

Fixed Tank Systems
In addition to the bags, fixed tanks in the lower part of the helicopter fuselage are used, but this requires more investment and the helicopter becomes less flexible. On the other hand, it is less demanding to fly and there is no pendulum effect. However, mentioned technology is not currently used in Slovakia [7].

4 Use of Aviation Technology in Forest Fire Fighting in Slovakia

Helicopters from two ministries are used in Slovakia to fight, forest fires at this time. Specifically, the machines of the Ministry of Interior and Ministry of Defense, in the form of the army of the Slovak Republic. These helicopters are a strong support for firefighting vehicles during forest fire fighting. The most used vehicle into the terrain in Slovakia and the Czech Republic is TATRA 815 (respectively new type 815-7) [8].

4.1 Aviation Unit of the Ministry of Interior of the Slovak Republic

This unit has been operating since 1961 and has its home base is in Bratislava. In addition to several aircraft, this unit also has 3 helicopters. Two older ones type Mil Mi-171, and newer Bell 429.

Helicopters are available 24 h a day. However, working hours apply only on working days, from 7:30 a.m. to 3:30 p.m. At this time, the helicopter is immediately ready to take off. Outside this time, the capability to take off is about 90 min [5] (Fig. 2).

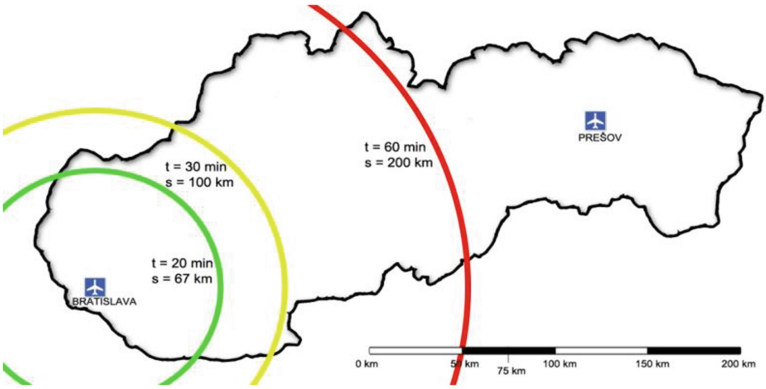

Fig. 2. Coverage by the Aviation unit of the MoI (processor: Obrst, 2019)

4.2 Slovak Air Force

In extinguishing forest fires helicopters from Helicopter Wing of General Ján Ambruš, who are based in Prešov, help out. There are 3 Mil Mi-17 helicopters, 3 Mil Mi-17LPZS type helicopters, and 6 Sikorsky UH-60 Black Hawk helicopters.

These helicopters are available on a permanent basis, as there is uninterrupted working time at the base. So helicopters can immediately take off [5] (Fig. 3).

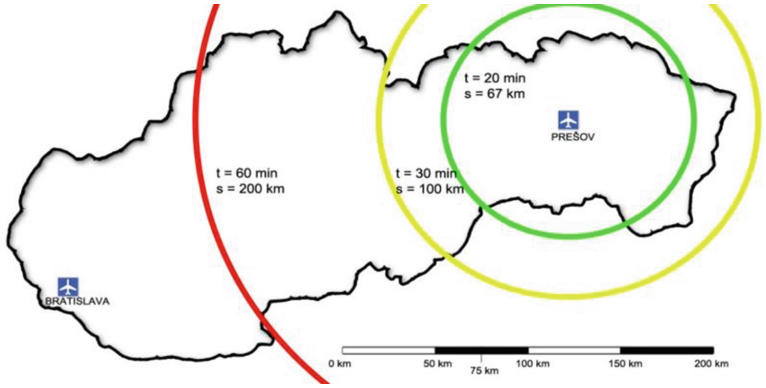

Fig. 3. Coverage by the Slovak Air Force (processor: Obrst, 2019)

4.3 Shortcomings of the Current System

Returning to the map in Fig. 1, in which areas are endangered by forest fires, we can see that the largest part of this area is located relatively far from the mentioned bases. An example could be a situation where helicopter assistance from Bratislava Airport is required outside working hours. The expected range to the fire location is 60 min.

In this case, the helicopter is only able to hit the fire site after 150 min. What's more, in this sum we missed the aerial inspection and other delays.

150 min is quite a long time. During this time, the fire may spread several tens of meters, for example due to strong winds. There are suitable several alternatives for avoiding this major disadvantage.

4.4 Recommendations to Improve the Current Situation

There are several options for improving the current situation. Of course, the main aspect will still be finances. Therefore, it would not be appropriate to build new airports or to create new special fire brigade units at the moment, which will be armed with very expensive technology.

The most acceptable solution is to use existing airports. Slovakia has a large number of smaller airports that do not serve exclusively for transport purposes.

Given the possibilities offered by airports in Slovakia and their location, three airports are considered. These are airports in Poprad, Žilina and Sliač. Out of these alternatives Žilina airport is the problematic one. There is no aviation unit under any of the ministries, nor a private company that provides aerial work by helicopter. The situation at the other two airports is different.

Airport Sliač

Airport Sliač is known as an international airport with mixed transport. Specifically, the airport provides civilian, but also military operations. Military operation is provided by the Tactical Wing of Major General Otto Smik, which belongs to the Slovak Air Force. The main tasks of the Tactical Wing are in particular to ensure the continuous protection and defense of the inviolability of the Slovak Republic's airspace within NATO's airspace (NATINAMDS - NATO Integrated Air and Missiles Defense System), and Host Nation Support Base. Civilian operations are provided by the Airport Sliač, a.s. The company is only in charge of passenger handling, refueling and commercial handling [10–13].

As an alternative to using the Sliač Airport, it would be necessary to modify the current legislation and layout of the Slovak Air Force. This would require moving at least one helicopter to Sliač Airport, along with the necessary personnel. However, it would still be a cheaper alternative. The conditions at the airport for such a variant are sufficient, as the Slovak Air Force is in charge of most of the operations, including navigation and maintenance of the airport area. The big advantage for this alternative is that the airport is owned by the state. Therefore, the necessary changes that would have to be made do not constitute such an obstacle either [12, 13].

Poprad-Tatry Airports

The airport near Poprad is categorized as an international airport. It does not include any military unit or other aviation section in the service of the state. The biggest advantage of this airport is its location. It is located near the High Tatras. It is in the High Tatras that there are frequent fires in the natural environment. Another advantage of Poprad Airport is the fact that its majority owner is Ministry of Transport and Construction of the Slovak Republic. The Ministry owns up to 97.61% [14, 15, 17]. Thanks to this fact it is possible to set up a helicopter base at this airport to help with

firefighting works. In this case, this option would be more expensive than the option in the case of Sliač Airport.

Another alternative is to use the services of a private company. Right in the city of Poprad is based TECH-MONT Helicopter company s.r.o. The company also offers forest firefighting work using the Bambi Bucket in its portfolio. Specifically, the company uses the Bambi Bucket type 5566 HD. The company uses the Mil Mi-8T helicopter for this work [18]. The company is licensed to carry out aerial work from Civil Aviation Authority of the Slovak Republic [19]. According to the civil aviation organization, TECH-MONT has a Mil Mi-8T helicopter hangar in Spišská Nová Ves, which is only 23.10 km as the crow flies from Poprad [20]. In the case of this alternative, a contract with TECH-MONT Helicopter company would have to be concluded. But in the end this alternative would not be as expensive.

5 Conclusion

Looking at Fig. 4, it is possible to see all helicopter flight times from Sliač and Poprad airports. At both airports it is necessary to modify the current regulations and establish cooperation with other ministries or a private company, in the case of covering the territory in the Poprad area.

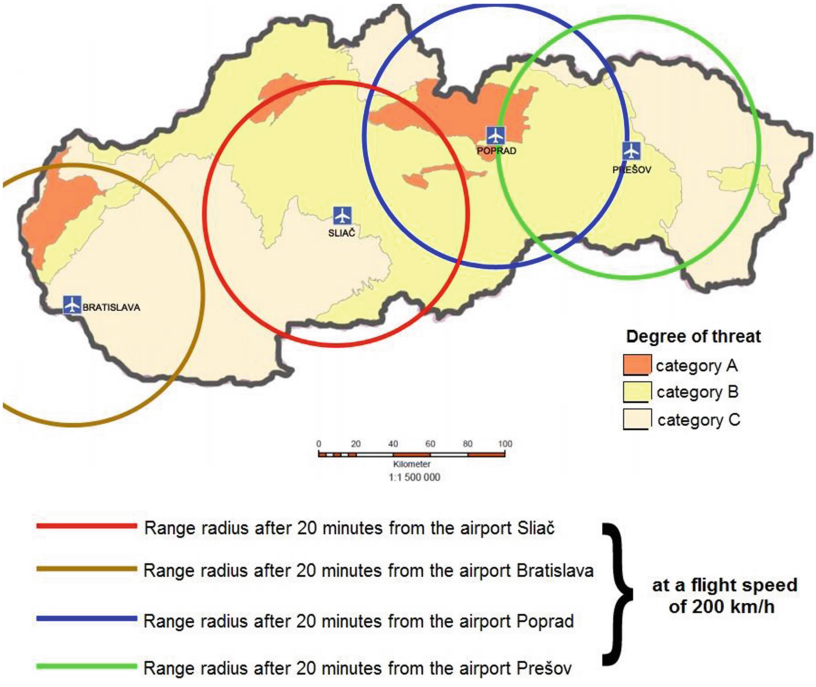

Fig. 4. Draft amendments helicopters during forest fire fighting (Obrst, 2019)

The proposed solutions do not require a lot of money. These are already functioning airports and formations. This article referred to sites that are currently not adequately covered when helicopters are needed for forest fire fighting. The paper also suggested simple solutions that could help improve this situation and better protect our forests.

References

1. Majlingová A (2015) Forest fires - current state of problem tackling in Slovak condition. In: Crisis management, vol 14, no 1, pp 47–56. EDIS, Žilina. ISSN 1336-0019
2. PTEÚ: fire analysis for 2018
3. Majlingová A et al (2018) Management and tactics of fire extinguishing in natural environment. Technical University, Zvolen
4. Osvaldova LM, Petho M (2015) Occupational safety and health during rescue activities. In: 6th International conference on applied human factors and ergonomics (AHFE), Las Vegas, NV, July 26–30, 2015. Procedia manufacturing, vol 3, pp 4287–4293
5. Holtman P (2019) Use of current techniques for forest fires. Personal communication
6. SEI Industries Ltd. (2019) Bambi bucket models for combating against wildfire. https://www.sei-ind.com/products/bambi-bucket-models/
7. Seevers M (1995) Fixed tank systems for type II and III helicopters. In: Aviation management TechTips. https://www.fs.fed.us/t-d/pubs/html/95571307/95571307.html
8. Monosi M, Janosik L (2016) An essay of firefighting vehicles' reliability. In: International conference on engineering science and production management (ESPM), Slovakia, April 16–17, 2015, pp 201–206
9. Ganteaume A, Syphard AD (2018) Ignition sources. In: Encyclopedia of wildfires and wildland-urban interface (WUI) fires. Springer, Cham. ISBN 978-3-319-51727-8
10. Blaško F et al (2004) An interpretation of results from seismic measurements on Sliač airport. Acta Montanist Slovaca 9(4):383–389
11. Airport Sliač (2019) Airport. https://airportsliac.sk/en/letisko/#content
12. Tactical Wing of Major General Otto Smik (2019) Main roles. https://lzsliac.mil.sk/23626/home.php
13. Mildeova Z (2007) Tiger squadron on exercise in Poland. In: Slovak armed forces. Media communication division, Ministry of defence, Slovak Republic (2007)
14. Csikosova A et al (2015) Segmentation of airports' customers in Slovakia. In: 2nd global conference on business, economics, management and tourism, pp 1068–1073, Prague
15. Hajduová Z et al (2010) The flights in Košice and Poprad before crisis. Acta Avionica **11**(19). Technical University of Košice
16. Frájová Z, Koščák P (2013) The use of aviation equipment in extinguishing spread fires. Acta Avionica **15**(27). Technical University of Košice
17. Airport Poprad (2019) Basic information. http://www.airport-poprad.sk/en/podstranky/letisko/informacie.php
18. Techmont (2019) Helicopters – fire fighting. http://www.techmont.sk/en/helicopters/
19. Techmont (2012) Aerial work operator certificate. http://www.techmont.sk/tech-mont-helicopter-company/certifikaty/new/sk-awoc.pdf
20. Letectvo.nsat.sk (2016) Part 145 approved maintenance organisations. http://letectvo.nsat.sk/wp-content/uploads/sites/2/2014/07/Zoznam-schvalenych-organizacii-na-udrzbu-podla-part-145-24.06.2016.pdf

Others Topics Focus on Wood & Fire Safety

Fire Protection of Steel Beams by Timber: Thermomechanical Analysis

Antoine Béreyziat[1,2(✉)], Maxime Audebert[1], Sébastien Durif[3], Abdelhamid Bouchaïr[3], Amir Si Larbi[1], and Dhionis Dhima[4]

[1] University of Lyon, ENISE, 42100 Saint-Etienne, France
{antoine.bereyziat,maxime.audebert,
amir.si-larbi}@enise.fr
[2] French Environment and Energy Management Agency (ADEME),
49004 Angers, France
[3] Université Clermont Auvergne, CNRS, SIGMA Clermont, Institut Pascal,
63000 Clermont-Ferrand, France
{sebastien.durif,abdelhamid.bouchair}@uca.fr
[4] Scientific and Technical Center for Building (CSTB),
77420 Champs-sur-Marne, France
dhionis.dhima@cstb.fr

Abstract. This study evaluates the possibility to use timber members as a complete or partial fire protection for steel beams. The hybrid elements considered are composed by I or T-shaped steel profiles partially or fully encased into timber members. The thermal behavior is analyzed by using numerical simulation and the fire resistance is calculated by using an analytical method. The thermomechanical behavior of different configurations is compared considering standard fire conditions. This study shows how the wood protection leads to non-uniform thermal conditions into steel profiles for the considered hybrid beams. Therefore, it is proposed to divide steel sections into subsets for a better analysis. This method allows evaluating the mechanical resistance of steel elements during fire, considering a non-uniform temperature distribution. The results indicate that timber protection delays considerably the failure of steel components during fire. The comparison of various configurations shows how fire resistance is improved by using timber-steel beams instead of unprotected steel profiles.

Keywords: Timber-steel hybrid beams · Fire protection · Fire resistance

1 Introduction

Timber-steel hybrid structural members can achieve great performances in multiple fields. Jurkiewiez et al. [1] observe that the reinforcement of I and T-shaped steel profiles with timber members assembled on both sides of the webs can delay the lateral buckling and the local buckling. Tavousi et al. [2] highlight the benefits that such steel-timber hybrid elements could offer for high-rise constructions in terms of cost, ease of assembly, construction time, sections dimensions, earthquake resistance and fire resistance. Sakamoto et al. [3] study the thermomechanical behavior of a steel profile

L. Makovicka Osvaldova et al. (Eds.): WFS 2020, *Wood & Fire Safety*, pp. 397–403, 2020.
https://doi.org/10.1007/978-3-030-41235-7_58

that is completely encased into timber elements and insulated from fire with a 60 mm wood thickness. The structural element is subjected to a one-hour heating phase and a three-hours cooling period while bearing mechanical load. The timber-steel beam shows a one-hour fire resistance, followed by self-extinguishing behavior during the cooling phase. The beam withstand applied load even after the fire exposure, without re-ignition, char progression or temperature rising after the test. Jang et al. [4] achieve thermal test on similar elements, steel and wood are assembled by resorcinol resin adhesive. They confirm the one-hour fire resistance of such hybrid elements by taking the critical temperature of steel as a criterion. The aim of the current study is to evaluate the thermomechanical behavior of various steel-timber hybrid configurations by using a simplified model.

2 Model

Four configurations (A to D), represented in Fig. 1, are studied. The configuration A is a control sample consisting in an I-shaped steel element without fire protection. Configurations B to D are constituted by I or T shaped-steel profiles partially or completely protected by timber elements. The way to subdivide the timber part of configuration D and to connect timber and steel will be defined in further experiments and is not taken into account in this study.

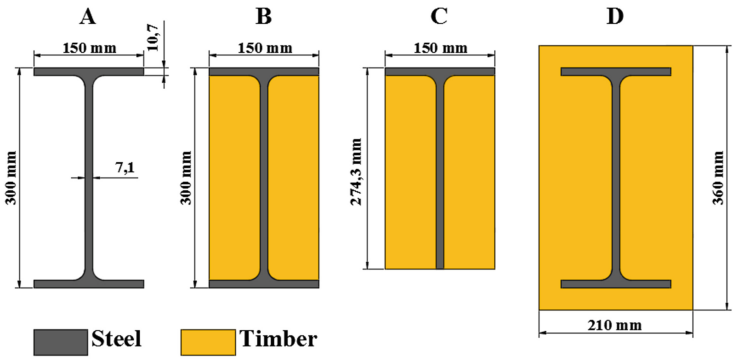

Fig. 1. Cross-sections of studied configurations.

The thermal analysis uses Finite Element Method (FEM) model to get precise temperature fields and simulate various geometries. Moreover, there is no available standard analytical method to calculate the temperature of steel members protected by timber during a fire. Thus, a 2D FEM model is created and solved using the commercial software MSC Marc-Mentat [5]. The combustion of timber is taken into account considering the evolution of its volumetric heat capacity and its thermal conductivity at high temperatures, by following the specifications of EN1995-1-2 [6]. The model does not take into account the possible fall of carbonized wood. As a result, the mesh remains unchanged over time and the boundary conditions are statically applied to the

edges of each configuration in its initial state (Fig. 1). Fillets are not modeled and thermal contact resistances between steel and timber are neglected. The mesh is continuous and made of 2D quadrilateral finite elements. Fire conditions are taken into account considering the ISO834 temperature-time curve and Eurocodes specifications [6–8]. Thus, the convection heat transfer coefficient is 25 W/m^2K, the emissivity is 0,7 for the steel surface and 0,8 for the timber surface. The initial density of timber (glulam) is taken equal to 450 kg/m^3 and its initial moisture content is 12%. The density of steel is 7850 kg/m^3 and the evolutions of its specific heat capacity and its thermal conductivity follow the specifications of EN1993-1-2 [7].

The numerical model highlights the fact that a high temperature gradient exists across the steel section of hybrid configurations as it can be seen in Fig. 2. Therefore, a simplified calculation based on the assumption of a uniform temperature in the steel cross-section does not seem to be sufficient. Figure 2 suggests that after some time of exposure, the temperature rises considerably in the steel profile's flanges while remaining significantly lower in the center part of the web. Upper and lower parts of the web constitute intermediate regions. Thus, each steel cross-section is subdivided into subsets as illustrated in Fig. 3.

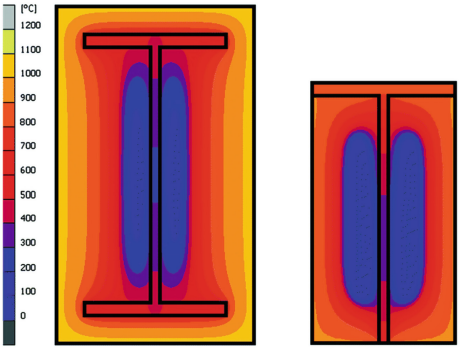

Fig. 2. Temperature field into config. D (120 min) and config. C (50 min) - 4 sides fire exposure.

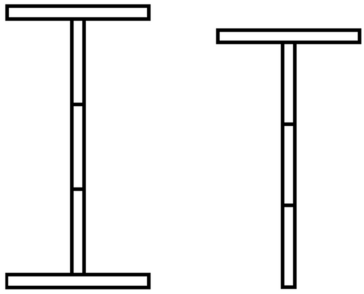

Fig. 3. Subsets of steel cross-sections.

The mechanical analysis takes into account a uniform temperature and a uniform yield strength of the steel subsets. The temperature of each subset is the mean value of the temperatures of its constitutive nodes in the FEM model. This subdivision of the steel cross-section allows approaching the non-uniformity of the temperature. At each time step, the effective yield strength of each subset is determined as a function of its temperature, by using reduction factors given by EN1993-1-2 [7] (Fig. 4). Then, the position of the plastic

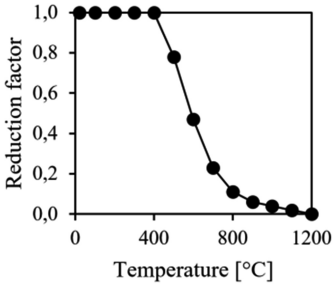

Fig. 4. Reduction factor for effective yield strength [7].

neutral axis is determined. This information allows calculating the plastic moment strength according to Eq. 1 [7] for each time step.

$$M_{Rd} = \sum_{i=1}^{n} A_i \cdot z_i \cdot f_{y(\theta),i} \tag{1}$$

M_{Rd} is the plastic moment resistance, A_i is the area of the subset i, z_i is the distance from the plastic neutral axis to the centroid of the subset i, $f_{y(\theta),i}$ is the effective yield strength of the subset i. This calculation neglects the mechanical contribution of the wood part because it is relatively weak compared to the steel part: timber performs about 10 to 25% of the total bending stiffness, depending on the hybrid beam considered. Moreover, this mechanical contribution varies as the combustion occurs. Furthermore, instability phenomena are not taken into account at the present stage of the study. In normal conditions, timber elements prevent instabilities [1], but after some time of fire exposure and combustion, this mechanical reinforcement can be questioned. In any case, the proposed calculation is valid for steel beams with class 1 or class 2 cross-section, which is the case of the profiles chosen in this study.

3 Results

Thermal model results are compared with experimental results. Configurations C with smaller elements (120 × 230 mm) is tested and modeled. The temperature of steel at mid-height of the web is observed. Model results present an average difference of 16% with test results (max 32%) (Fig. 5).

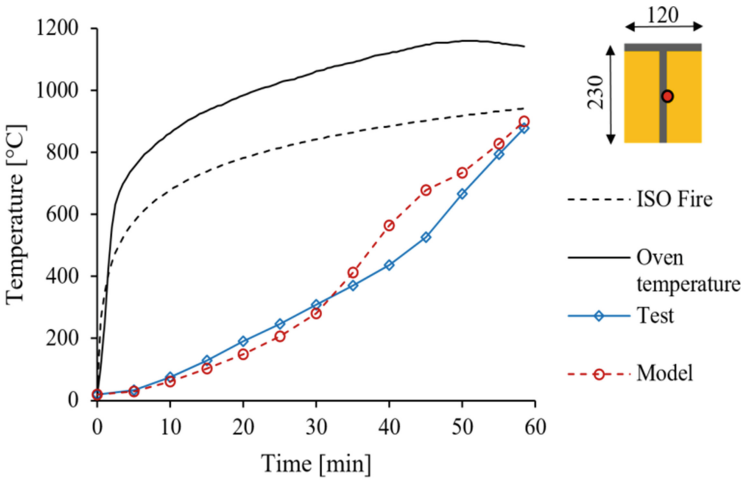

Fig. 5. Comparison of a model result with a test result.

Figure 6 shows, for each configuration, the evolution over time of the bending strength of the steel element, as the temperature increases. It is calculated considering subdivisions of the cross section to simulate the non-uniform thermal conditions in a simplified way. The presented results consider steel-timber beams exposed to fire on three faces (the bottom and the lateral ones). Configurations A, B and C are studied over a 120 min period, the configuration D is observed longer (180 min) because it needs more time to reach significant temperatures. Configuration A is taken as the reference, assuming that the fire resistance is 15 min, the corresponding degree of utilization is 32%. Table 1 provides the time needed to drop the relative resistance of steel beams to 32% for each configuration, in order to compare them.

Table 1. Fire resistance for each configuration (degree of utilization = 32%)

Config.	A	B	C	D
Time [min]	15	64	86	172

It can be observed that configurations B and C allow having a fire resistance close to 60 and 90 min compared to configuration A which normally withstand a fire exposure of 15 min. Finally, configuration D with a complete timber protection appears to have a fire resistance close to 3 h.

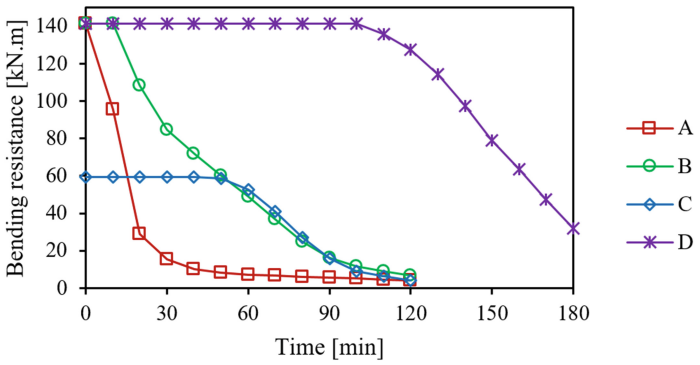

Fig. 6. Evolution of the bending moment resistance of steel profiles.

Figure 7 shows an example of the influence of the subset approach over the calculated bending resistance of hybrid beams. The subset approach leads to results similar with those of the uniform temperature approach for the configuration C. However, for configurations with I-shaped steel profile (B and D configurations), each calculation method gives different results at the beginning of the decreasing of steel mechanical properties. Therefore, subsets approach seems to be justified for high degree of utilization and for I shaped steel sections protected by timber.

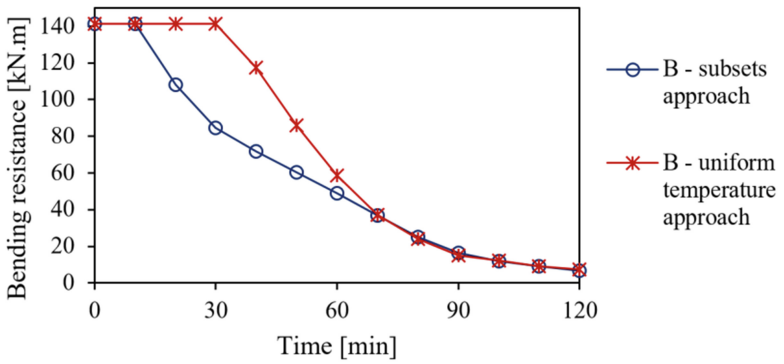

Fig. 7. Comparison of subsets approach and uniform temperature approach (config. B).

4 Conclusion

This study shows that, in fire situation, the thermomechanical behavior of steel beams is significantly improved when it is protected by timber elements. The temperature gradient into steel appears to be important, thus thermal conditions cannot be considered uniform. The subdivision of the steel cross-section into subsets allows to take into account this high temperature gradient in a simplified way. The bending moment resistance of the steel sections is calculated for each configuration, considering the various evolutions of the yield strengths of the subsets induced by their different temperature increases. The fire resistance of steel profiles is evaluated for each configuration and compared to the others. It appears that the failure of steel beams is slowed to a large extent, depending on the amount of steel surface protected by timber. Indeed, full timber protection seems to be twice as effective as partial timber protection. Even so, partial timber protection can provide significant delay to steel failure as long as the design allows considering a fire exposure on three sides only. In these conditions, wood seems to be a possible solution to protect steel against fire. Furthermore, the advantage of timber, compared to other fire protection materials, is its ability to provide mechanical support to steel against buckling effects while its lightness does not significantly increase the weight of the beam. This aspect will be evaluated in further works through mechanical modelling and testing of hybrid beams. Finally, the results presented in this study will be assessed considering thermal tests.

Acknowledgments. This work is supported by the Tremplin Carnot MECD, the French Environment and Energy Management Agency (ADEME) and the Scientific and Technical Center for Building (CSTB).

References

1. Jurkiewiez B, Durif S, Bouchaïr A (2017) Behaviour of steel-timber beam in bending. In: 8th European conference on steel and composite structures. Ernst & Sohn, Berlin, pp 2283–2291
2. Tavoussi K, Winter W, Pixner T, Kist M (2010) Steel reinforced timber structures for multi storey buildings. In: 11th world conference on timber engineering, Trentino, Italy, pp 2011–2016
3. Sakamoto I, Kawai N, Okada H, Yamaguchi N, Isoda H, Yusa S (2004) Final report of a research and development project on timber-based hybrid building structures. In: 8th world conference on timber engineering, Lahti, Finland, vol 2, pp 53–58
4. Jang S, Kim Y, Jang Y, Shin I (2010) Fire resistance of steel column glued with structural glulam covers. In: 11th world conference on timber engineering, Trentino, Italy, pp 2165–2168
5. MSC Software Corporation (2014) User's Manual Vol A: Theory and User's Information
6. European Committee for Standardization (2005) EN 1995-1-2. Part 1-2: General - Structural Fire Design. In: Eurocode 5 - Design of Timber Structures. CEN, Brussels
7. European Committee for Standardization (2003) EN 1993-1-2. Part 1-2: General - Structural Fire Design. In: Eurocode 3 - Design of Steel Structures. CEN, Brussels
8. European Committee for Standardization (2003) EN 1991-1-2. Part 1-2: General Actions - Actions on Structures Exposed to Fire. In: Eurocode 1: Actions on Structures. CEN, Brussels

Water Mist Systems in Protection of Mass Timber Buildings

Yoon Ko(✉), Max Kinateder, and Nour Elsagan

Fire Safety Unit, Construction Research Center,
National Research Council of Canada, Ottawa, Canada
yoon.ko@nrc-cnrc.gc.ca

Abstract. Water mist systems are considered for the protection of timber buildings because they use significantly less amounts of water and consequently less post-water damage. Current water mist system standards and testing protocols do not consider fire scenarios involving exposed timber elements, which pose greater fire load and hazards. Therefore, without verifications through full-scale fire tests, these existing standards and test protocols should not be incorporated in the use of water mist systems in protection of timber buildings.

Keywords: Mass timber buildings · Water mist systems · Suppression · Protection of wood

1 Introduction

With the advancements in new technologies and mass timber products, such as Cross Laminated Timber (CLT), the allowable height of wood frame buildings has increased, which raises fire safety concerns. Most of the mass timber buildings are required to be covered, encapsulated, with lining materials such as gypsum plasterboards for fire protection. However, new regulations and/or proposed changes would allow the use of exposed mass timber for tall wood buildings. Unprotected mass timber such as CLT wall and ceiling panels contribute to total fire load and fire severity [1–3].

These tall wood buildings require automatic sprinklers in order to limit the effect of fire and fire spread beyond its point of origin. Sprinkler systems are expected to achieve the objectives in application to mass timber buildings. However, a complete investigation is necessary to understand their fire suppression efficacy and post-fire water damage including potential mold problems.

Fire suppression tests conducted by the Ad Hoc Committee on Tall Wood Buildings (AHC-TWB) demonstrated that sprinkler systems designed and approved by NFPA 13 [4] would control a residential kitchen fire scenario effectively and prevent the fire spread to adjacent rooms. Full-scale apartment fire tests [5] were conducted for the International Code Council to address proposed changes to the International Building Code (IBC) 2021. The tests demonstrated that with sprinkler protection, the heavy timber member could be exposed without gypsum board protections. However, when sprinklers fail to operate, the entire unit can be engulfed in fire very quickly (i.e., without sprinkler system, the flashover occurred at 11–13 min in the kitchen/living

L. Makovicka Osvaldova et al. (Eds.): WFS 2020, *Wood & Fire Safety*, pp. 404–409, 2020.
https://doi.org/10.1007/978-3-030-41235-7_59

area, and the measured peak heat release rate was about 20 MW). The report does not provide rationales why the study selected the kitchen fire scenario, which are frequent but not as challenging scenario as living room fires involving upholstered furniture (i.e. flashover within 4–5 min).

The Swiss Federal Institute of Technology (SFIT) conducted full-scale fire suppression tests of modular wooden hotel rooms to verify the efficiency of sprinkler systems [6]. The sprinkler system with relatively fast response (with the activation temperature of about 68 °C) extinguished the fire before it could spread to the combustible surfaces of the wall and ceiling. However, water sprayed from sprinkler systems pooled on the floor.

To minimize the potential post-fire water damage in the wood frame buildings, water mist systems have been considered as an alternative solution to sprinkler systems. Water mist systems use 50% to 90% less water than the traditional sprinkler systems [7]. However, there are still many questions unanswered regarding potential benefits of water mist systems in protection of mass timber buildings and their performance in comparison to conventional sprinkler systems. The next section reviews the literature on the current regulations and standards with focus on applications of water mist systems in the protection of timber buildings.

2 Current Building Codes

The code change request (CCR) submitted by the Canadian Wood Council to the standing committee on Fire Protection for the 2020 iteration of the NBCC (National Building Code Canada) [8] included allowing encapsulated mass timber construction (EMTC) as a third category of construction type, in addition to non-combustible and combustible construction. The CCR proposes to permit EMTC in sprinklered buildings, complying with National Fire Protection Association (NFPA) 13 [4]. Further, the CCR aims at allowing up to 12 storeys (compared to 6 storeys in NBCC 2015) high for residential and business occupancies. One notable change is the permission of exposed mass timber surfaces for ceilings, walls and columns in encapsulated mass timber constructions.

NBCC allows alternative solutions provided they achieve at least the minimum level of performance required by acceptable solutions. For example, water mist systems can be considered as an alternative solution to sprinkler systems, yet the suggested water mist system should offer demonstrated levels of protection equivalent to the conventional sprinkler system. Similarly, in Section 904 of the 2015 IBC, NFPA 750 [7] is referred for standards for the design and installation of automatic water mist systems, as an alternative solution.

3 Current Standard Requirements for Water Mist Systems

In adopting water mist systems, one question that must first be answered is how water mist systems should be designed, installed and maintained in particular for the protection of timber buildings. Various available standards, such as NFPA (National Fire

Protection Association), UL (Underwriters laboratories), FM (Factory Mutual), BS (British Standards), and DIN (Deutsches Institut für Normung)/CEN (Comité Européen de Normalisation)/EN (European Norm) were reviewed in this study.

3.1 Performance Objectives and Requirements

The objectives of the sprinkler system specified by NBCC are; (1) to limit the severity and effects of fire and (2) to retard the effects of fire on areas beyond its point of origin. NBCC Section 3.2.5.12 refers to NFPA standards for sprinkler requirements, which vary depending on the occupancy type. For instance, life safety is an objective of the sprinkler system in NFPA 13 [4], NFPA 13R [9], and NFPA 13D [10]. Whereas property protection is not specified as an objective in NFPA 13R and 13D, which address sprinkler systems for residential buildings.

The objectives of water mist systems are also specific to hazard scenarios. Chapter 9 in NFPA 750; Design objectives and fire test protocols; states that water mist systems shall be designed and installed for the specific hazards and protection objectives specified in the certified listing. As a consequence, performance requirements are also specific to hazard scenarios such that only fire control and suppression rather than extinguishment are required in FM 0402 [11] and BS 8458 [12], with the focus primarily on providing life safety. Fire control means resisting fire development and holding the fire to an area. Fire suppression means reducing heat release rate of fire by lowering down the fuel burning rates, and fire extinguishment means putting out fire.

In protection of mass timber buildings; however, both life and property protection would be important so that the suppression system would provide not only fire control but also fire suppression and extinguishment. Among various applications and hazard scenarios, additional degrees of protection of life and property should be considered for residential occupancy [12]. Hence, when designing fire suppression systems, timber buildings with exposed timber elements should be considered as special cases since a greater fire load is expected than that would normally found in the conventional buildings. BS 8458 [12] also recognized that "in special circumstances with great fire loads or hazards, enhanced performance, reliability and resilience arrangement should be provided".

3.2 Design Methods and Testing Protocols

The approaches to water mist system design employed in the standards are fundamentally different from those established for conventional sprinkler systems. Conventional sprinkler systems use hazard classification systems, which categorize fire loads and degree of hazards based on occupancies. The rationale of this approach is to link levels of fire hazards to the intended use of a space [4]. The hazard classification system for the conventional sprinkler system provides design bases of the area/water density curve, which provides a required water spray rate for each of the five hazard levels in NFPA 13. Following the generic design methods in NFPA 13, sprinkler system design including water spray rates and installation requirements would be set to provide required protection for the corresponding occupancy.

Water mist standards also adopt part of the hazard classifications; however, in general water mist systems are required to be designed based on verifications through full-scale fire tests as part of listing process. This is mainly because there are many technical factors other than water spray densities affecting the efficiency of water mist systems. Although there are test protocols developed for residential and light hazards scenarios, none of these standard test protocols considered the use of water mist systems in mass timber buildings. Therefore, without verifications through full-scale fire tests, these existing standards and test protocols should not be incorporated in the use of water mist systems in protection of timber buildings.

4 Design Consideration

While hazard classification and fire loading provide design bases for sprinkler systems, water mist systems design needs to consider room conditions, in addition to fire loading in the room. This is because the effectiveness of water mist systems depends on various parameters, such as compartment variables (e.g. volume, ceiling height), ventilation conditions (e.g. door and window sizes), fuel types and water spray characteristics (e.g. droplet size, spray cone angle, spray velocity and mixing ability). This section briefly reviews why these factors are important in designing water mist systems for the protection of mass timber buildings.

Compartment Volumes and Ventilation Conditions: Building codes evolve to allow various occupancies for timber buildings, which include large spaces such as open offices and halls. In general, the volume of the compartment affects the effectiveness of water mist systems in gas phase cooling and oxygen depletion in the compartment. In addition to the volume of the compartment, large doors/windows could also challenge the fire suppression performance of water mist systems due to the difficulty in suppressing or extinguishing the fire by the oxygen depletion in the space. Thus, development of new test protocols is in need for the use of water mist system for the protection of mass timber compartments with many different compartment configurations.

Type of Fuel and Droplet Characteristics: To protect exposed mass timber ceiling or walls, spray characteristics should be carefully examined for the capability of nozzles. This will include the spray pattern of sprinkler nozzles and spray characteristics of water mist (e.g. water droplet sizes and mixing ability).

System Actuation: Quick-response thermal elements will quickly limit the fire spread and development [13]. BS 8458 requires a wet pipe system and automatic nozzles with a quick-response thermal element for residential and domestic occupancies. However, in application to timber buildings with a view to limit unnecessary water discharge, it is ideal to achieve the performance objectives without affecting sprinkler heads far away from the fire compartment.

Nozzle Spacing and Layout: The listing information should be re-assessed in application to timber buildings if the listing is particularly developed based on the tests that do not address the issues of combustible wall and ceiling lining materials around

the fire. To protect exposed walls and ceilings of mass timber structural elements, minimizing the nozzle spacing from the exposed wall and ceiling could prevent fire damages of the exposed structural elements.

Water Spray Rates and Discharge Duration: The water spray rate is the most important parameter governing the fire suppression capability of water mist systems. Discharge duration is also an important parameter for successful fire control by water mist systems, particularly to achieve fire extinguishment. BS 8458, FM 5560 [14] and NFPA 750 require the water spray rate determined through fire tests for a specific fire scenario and performance objective. NFPA 750 requires the minimum discharge duration of 30 min for light hazard occupancies, and BS 8458 requires the minimum discharge duration of 10 min and 30 min for domestic occupancies and residential occupancies, respectively. For the protection of the same occupancies built with timber structures, it is questionable whether or not these discharge duration requirements are applicable. The requirements for the discharge duration and water spray rates may need to be enhanced if a hazard assessment shows extra risks associated with exposed mass timber or special architectural design features.

Water Damage: Several sources note that water mist systems are considered to produce less water damage compared to sprinkler systems [15, 16]. However, no study has been conducted to systematically compare water damage from these two systems. In addition, probabilities of accidental discharge of sprinkler and water mist systems are not reported.

Cost Benefit Analyses of Water Mist and Sprinkler Systems: In general, installation, operation and maintenance costs are higher for water mist systems than sprinkler systems. However, amounts of water usage are much less for water mist system than sprinkler systems. Thus, this could reduce costs for water tanks and recovering water damages after a fire incident or a false activation, which might affect insurance cost in some circumstances. In fact, cost-benefit analyses should include not only initial installation costs but also long-term operation and annual inspection maintenance costs.

5 Conclusions

Current building regulations and standard requirements were reviewed for the use of water mist systems for the protection of mass timber buildings. None of the standards considers the use of water mist systems in mass timber buildings. Therefore, without verifications, these existing standards and test protocols should not be incorporated in the use of water mist systems in protection of mass timber buildings.

In addition, development of new test protocols is in need since building codes are evolving to allow various occupancies for timber buildings. Test protocols need to be developed to address important design parameters, such as the occupancy, volumes of compartments, ventilation conditions and nozzle types and layouts.

References

1. Frangi A, Fontana M, Knobloch M, Bochicchio G (2008) Fire performance of timber structures under natural fire conditions. Fire Saf Sci 1279–1290
2. Su J, Lafrance P, Hoehler M, Bundy M (2018) Fire safety challenges of tall wood buildings - Phase 2: Task 3-Cross Laminated Timber Compartment Fire tests
3. Barber D (2018) Fire safety of mass timber buildings with CLT in USA. Wood Fiber Sci 50:83–95
4. NFPA (2016) NFPA 13 Standard for the Installation of Sprinkler Systems
5. Zelinka S Hasburgh L, Bourne K, Tucholski D, Ouellette J (2018) Compartment fire testing of a two-story mass timber building (FPL-GTR-247)
6. Frangi A, Fontana M (2005) Fire performance of timber structures under natural fire conditions. Fire Saf Sci 8:279–290
7. NFPA: NFPA 750 Standard on water mist fire protection systems
8. Alam M (2018) Encapsulated Mass Timber: a new construction type for the 2020 NBC. In: The Toronto wood solutions fair, Toronto, ON, Canada
9. NFPA (2016) NFPA 13R Standard for the Installation of Sprinkler Systems in Low-Rise Residential Occupancies
10. NFPA (2019) NFPA 13D Standard for the Installation of Sprinkler Systems in One- and Two-Family Dwellings and Manufactured Homes
11. FM Global (2013) FM0402 Property loss prevention data sheets
12. BS (2015) BS 8458:2015 Fixed fire protection systems - Residential and domestic watermist systems - Code of practice for design and installation, The British Standards Institution
13. Arvidson M (2017) An evaluation of residential sprinklers and water mist nozzles in a residential area fire scenario, RISE
14. FM (2017) ANSI/FM Approvals 5560-2017 American national standard for water mist systems, FM Approvals
15. Liu Z, Kim A (1999) A review of water mist fire suppression systems – fundamental studies. J Fire Protect Eng 10:32–50
16. Mawhinney JR, Back GG (2016) Water mist fire suppression systems. In: SFPE handbook of fire protection engineering, Springer, pp 1587–1645
17. IBC (2018) Tall Mass Timber Proposals Review Guide, American Wood Council

Pyrolysis of Wood Biomass to Obtain Biochar and Its Subsequent Application

Petra Roupcova[1,2(✉)], Karel Klouda[1,2], and Simona Slivkova[1]

[1] VŠB-Technical University of Ostrava, Ostrava, Czech Republic
petra.roupcova@vsb.cz
[2] Occupational Safety Research Institute, Prague, Czech Republic

Abstract. The contribution characterizes the employed biochar (a product of low temperature pyrolysis of wooden biomass), which has demonstrated excellent sorption effects, by means of examination of its surface (SEM, BET) and by identification of its functional groups and its thermal stability (DSC, TGA). For the purposes of this contribution we modified the input materials (by using joint oxidation with various oxidizing agents and different weight ratios of biochar and graphite). On the contrary, a part of the products was reduced with the objective to obtain a material similar to a graphene molecule via reduced graphene oxide (rGO). The prepared modified samples were further tested to verify adsorption properties of biochar: the tests were performed on samples of wastewater from Slovnaft a.s. (petrochemical industry) and the results were compared with active coal for chromatography, the sorption properties of which are similar to biochar. Sulfur mustard (yperite HD) breakthrough time was also measured for the powder form. Products with a biochar layer between micro- and nano-textiles in various combinations were tested for permeation of aerosol, paraffin oil and sulfur mustard (yperite).

Keywords: Biochar · Oxidation · Application

1 Introduction

Carbonization (low temperature pyrolysis) of wooden biomass produces a multifunctional material called biochar that can be used for energy and environmental applications. It has a compact hydrophobic core surrounded by a shell with hydrophilic and other active properties. The biochar surface can be additionally activated physically [1] (with steam, CO_2, H_2) or chemically [2] (with H_2SO_4, HNO_3, H_2O_2, NaOH, $KMnO_4$). Other methods to modify properties of biochar surface include e.g. impregnation with mineral oxides, metal oxides, graphene [3] etc. or magnetic modification (Fe_2O_3) [4], while the modification also depends on a previously applied method of pyrolysis. It influences the surface character of the prepared biochar and thus also its chemical and physical properties. Parameters that affect the pyrolysis are the composition of biomass, effects of temperature - its increase rate, effects of reaction time, composition of admixtures in the biomass before the pyrolysis [3, 5–8].

In this contribution is described our work with biochar made of wooden biomass. In the first round of activities we determined its parameters, such as the surface area, type

L. Makovicka Osvaldova et al. (Eds.): WFS 2020, *Wood & Fire Safety*, pp. 410–419, 2020.
https://doi.org/10.1007/978-3-030-41235-7_60

of pores, thermal stability and functional groups on the surface. Subsequently, we modified the biochar by joint oxidation with various oxidizing agents in the environment of sulfuric acid. We also changed the weight ratios of biochar and graphite. A part of the prepared products was reduced with the objective to obtain a graphene molecule via rGO. Then we tested the prepared sorbents for various applications with a focus on removal of organic pollutants and phenols, including warfare chemical agents, mainly sulfur mustard (yperite).

What are the options to influence physico-chemical properties of biochar?

1. Before the pyrolysis it is selection of the right composition of biomass, selection and addition of composite components - graphene, oxides, magnetic oxides, clays [3, 5–7].
2. The course of the pyrolysis, its temperature, rate of temperature increase, duration of the pyrolysis [2].
3. Treatment of the product after the pyrolysis, grinding in a ball mill [9], physical modification, e.g. with steam, gases [1], chemical modification [2] e.g. acidic or alkaline, oxidation, impregnation [4] with oxides or magnetic components.

This contribution expands modifications of biochar through oxidation; it is a follow-up on previous works, specifically on preparation of hybrid compounds and their fixation into nano-textiles to form foils made of sandwich or composite materials [10–12].

2 Biochar Morphology

Physical and chemical characterization of biochar 4073: the specific surface was determined with the BET analysis as 571.6 ± 0.2 m^2/g. The volume of its monomolecular layer was 131.3 cm^3/g, which characterizes porosity of the tested material. The specific surface of micropores was 325.7 m^2/g, while the specific surface of mesopores and macropores together was 245.9 m^2/g. SEM image of the initial biochar is shown in Fig. 1. DTA and DSC are shown below along with the above-mentioned spectrums.

3 Experimental Part – Modification of Biochar

The modification of biochar by oxidation consists of placement of biochar in a strong acidic environment, addition of an oxidizing agent, cooling and subsequent heating, separation and product purification. The specific reaction conditions are provided below.

(a) Oxidation - *Biochar-OXO* (biochar, H_2SO_4, HNO_3, 35–55 °C, 10 h).
(b) Long-term joint oxidation of graphite and biochar at a laboratory temperature (biochar, graphite, H_2SO_4, HNO_3, $KClO_3$, 20 h).
c) Short-term joint oxidation of graphite and biochar at an increased temperature-*GO-Biochar* (biochar, graphite, H_2SO_4, HNO_3, $KClO_3$, 45–55 °C, 1 h).

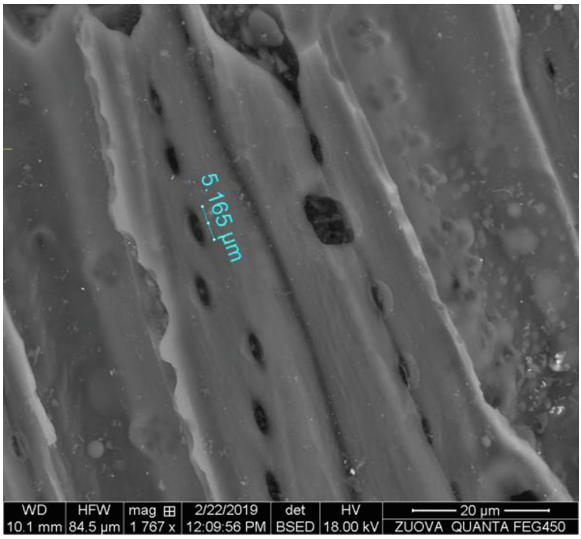

Fig. 1. SEM images of the initial biochar 4073

(d) Reaction of graphite and biochar with 30% H_2O_2- *GO-Biochar* (biochar, graphite, 30% H_2O_2, 4–5 h, sonication).
(e) Reaction of graphite and biochar with acetic anhydride -*GO-Biochar* (biochar, graphite, acetic anhydride, 2 h, sonication).
(f) Reaction of graphite and biochar with potassium permanganate in the environment of sulfuric acid only –*GO-Biochar* (biochar, graphite (2:1), H_2SO_4, $KMnO_4$).
(g) Reaction of graphite and biochar with potassium permanganate in the environment of sulfuric acid with subsequent reduction of the product – (graphite-biochar 1:1, ascorbic acid, lyophilization).

FT-IR and Raman spectrums were used for basic identification of the materials, i.e. the initial biochar, oxidized biochar prepared with the Hummers method, joint oxidation of graphite and biochar (see item 3a), chlorate, both in case of long-term contact (see item 3b) and short-term contact (see item 3c). In principle, the spectrums have the same bond vibrations of functional groups and they differ only by intensity of absorbance -OH (3400 cm^{-1}), CH (2900 cm^{-1}, C-O, C-O-C (1050 cm^{-1}) in the intervals 1300–1900 cm^{-1} (C=O, C=C, -COO-).

Based on comparison of the IR spectrums in case of oxidation with chlorate, no effects were found of the reaction time and temperature. Certain differences were found in arrangement of the products in Raman spectrums. The obtained Raman spectrums (laser 532 nm) are characterized with two distinct bands at 1596 cm^{-1} - the so-called G Peak and at 1338 cm^{-1}- pure biochar and at 1360 cm^{-1}- oxidized products, the so-called D Peak. The G and D peaks characterize sp^2 hybridization of C-C bonds; lower ratios of I_D/I_G intensities of the peaks indicate a defect or disarray in the graphite structure [13–15], e.g.

Biochar I_D/I_G = 0.904 in comparison with the oxidized biochar I_D/I_G 0,854. In case of long-term oxidation the I_D/I_G ratio was 0.827 and in case of short-term oxidation the I_D/I_G ratio was 0.068. A G-D peak appeared in the spectrum at 2970 cm^{-1} and in case of long-term oxidation also a 2D peak at 2700 cm^{-1}. It characterizes a layered structure.

4 Comparison of Thermal Stabilities of Biochar and Products Prepared by Its Modification

4.1 Initial Biochar

Exothermic decomposition of biochar up to 550 °C was at the minimum level with the weight loss of 13%. At higher temperatures up to 700 °C the weight loss was 77% with the exothermic maximum at 673 °C (see Fig. 2); before reaching the maximum the DSC curve was wavy with the overall thermal change 32.4 kJ/g.

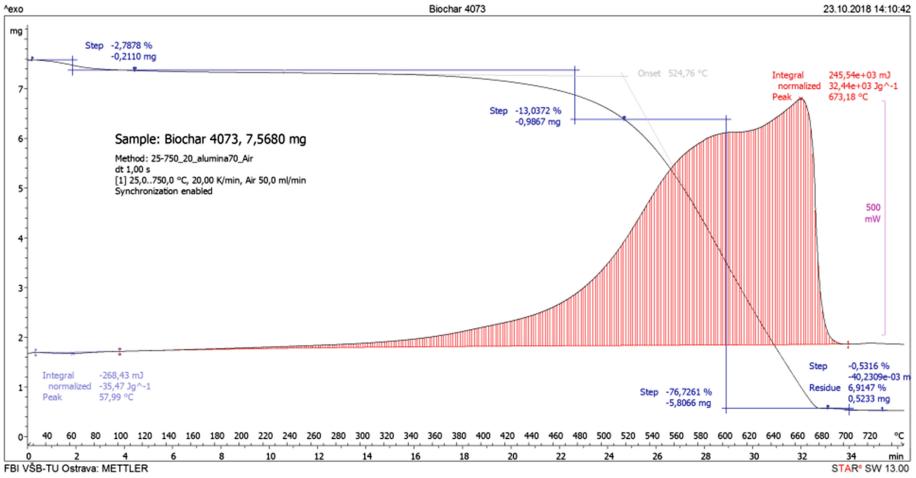

Fig. 2. TGA and DSC of biochar 4073

In the spectrum in Fig. 3, which characterizes the thermal decomposition of biochar – OXO, it is possible to identify 3 temperature intervals with significant weight losses of the sample, specifically 50–130 °C (weight loss of 17.4%), 130–300 °C (18.7%) and 300–400 °C (20.8%). This gradual cascade-like decomposition ends with an abrupt exothermic effect with the maximum at 425 °C (weight loss of 44%) with the thermal change of 13.0 kJ/g.

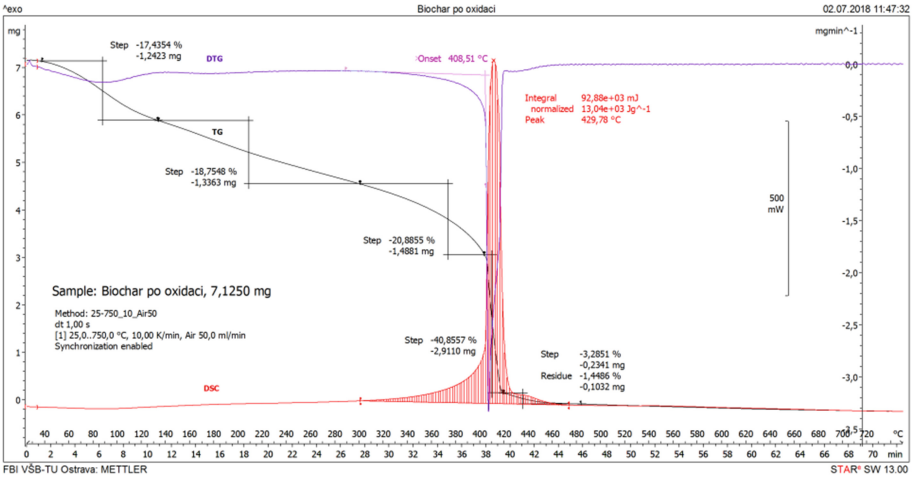

Fig. 3. TGA and DSC of biochar-OXO

4.2 Effects of Weight Ratio of Graphite and Biochar in the Process of Joint Oxidation on Thermal Decomposition

Thermal decomposition of products synthetized according to 3 f-g) demonstrated two exothermic effects (Fig. 4 GO-Bi 2:1) and (Fig. 5 GO-Bi 1:1), however, they differed in a number of other parameters. The first exothermic effects occur at the same temperature maximum of 200 °C for both the products. The second exothermic effects are different, the product with a lower content of biochar has the maximum at 534 °C and the product with a higher content of biochar (1:1) has the maximum at 486 °C with four partial maximums.

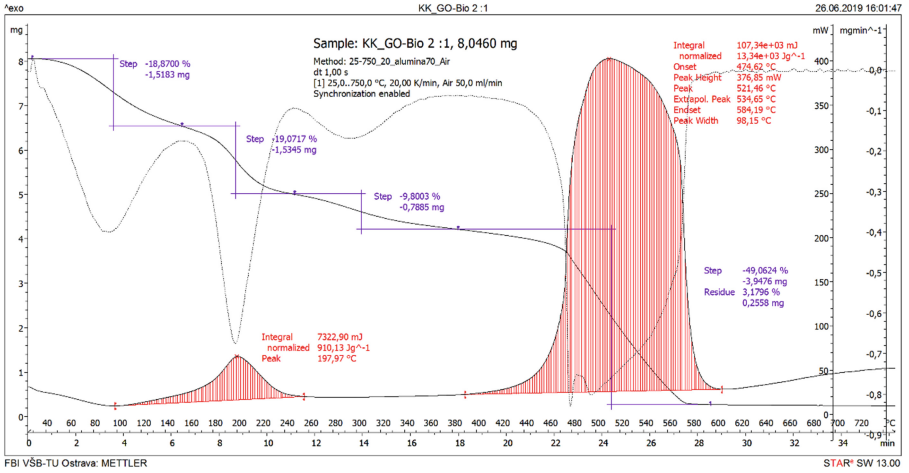

Fig. 4. TGA and DSC of GO-BIO (1:2) products

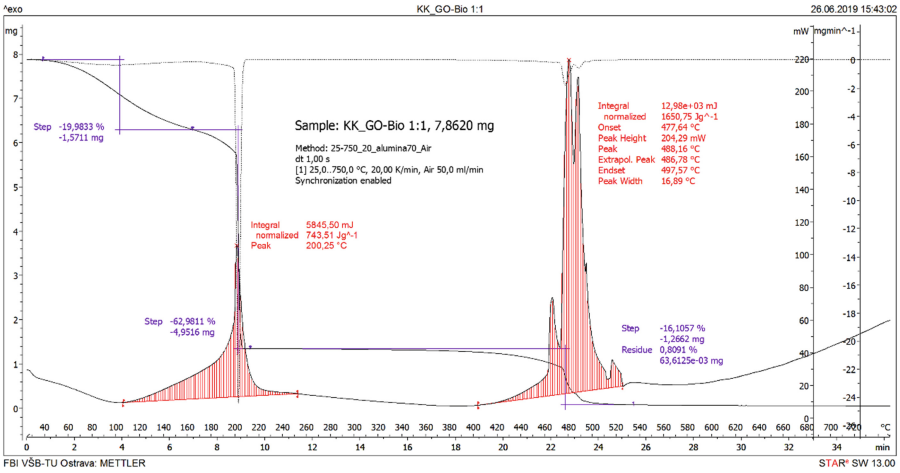

Fig. 5. TGA and DSC of GO-BIO (1:1) products

Significant differences found in the measured thermograms were the following: the weight loss at the time of the first exothermic effect for the product with a lower content of biochar was 3 times lower than for GO-BI (1:1); in case of the second exothermic effect it was the exact opposite. The product with a lower content of biochar demonstrated a broader range of temperatures of the integral second exothermic effect. Also the thermal change was higher (13.3 kJ/g compared to 1.6 kJ/g). The product with a higher content of biochar (GO-Bi 1:1) 10 g was reduced with a solution of ascorbic acid (14 g in 50 ml) at 55–65 °C for 4 h. Subsequently, it was filtered, washed with warm distilled water and ethanol and then dried for 14 h at 65 °C.

4.3 Change of Thermal Decomposition of the GO-BI (1:1) Product After Reduction

The reduced product was thermally neutral up to 380 °C (see Fig. 6). With an increasing rate of weight loss (70%) also the thermal release increased up to the maximum at 652 °C. The whole exothermic effect occurred in the temperature range 380–680 °C.

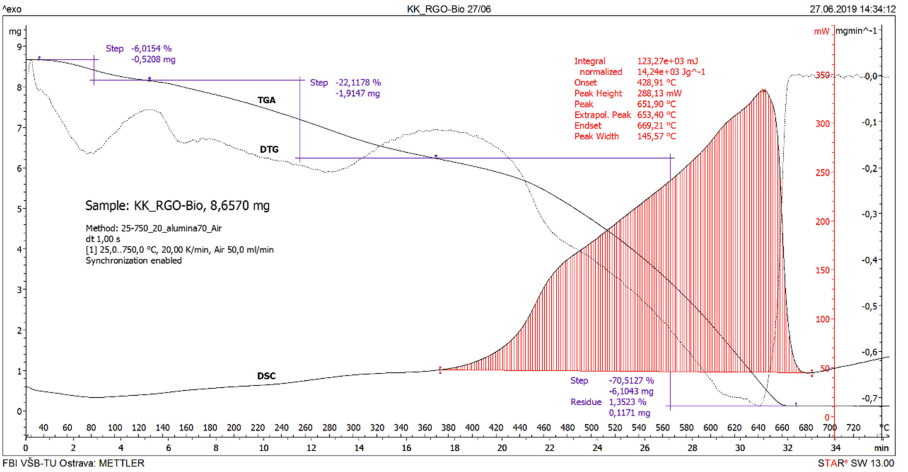

Fig. 6. TGA a DSC of reduced GO-BIO (1:1)

4.4 Thermal Analysis of Products Made by Syntheses According to Items 3(d) and 3(e)

After evaporation of moisture the thermal decomposition process was fairly similar: up to the temperature of 400 °C there were no weight losses and the reaction was thermally neutral (Figs. 7 and 8). The thermolysis occurred in two stages in the temperature ranges 400–600 °C and 660–880 °C (826 °C max) and 661–940 °C (862 °C max) for the product synthetized according to 3(d) (environment H_2O_2).

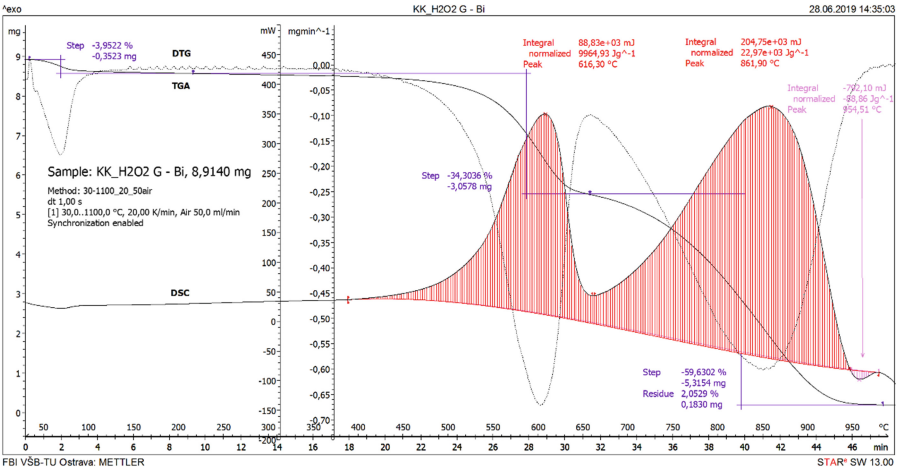

Fig. 7. TGA and DSC of the product prepared according to 3(d)

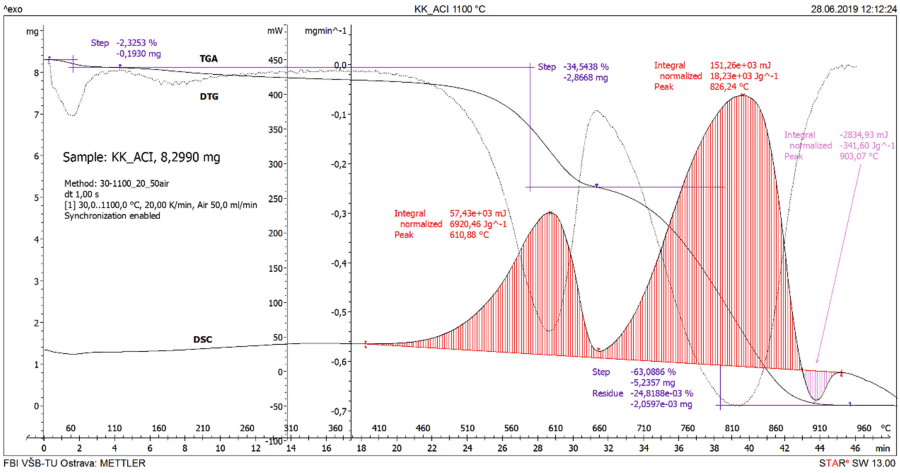

Fig. 8. TGA and DSC of the product prepared according to 3(e)

5 The Use of Biochar as an Adsorption Material

In order to verify the adsorption ability of biochar and its modifications we used samples of wastewater (crude oil) from Slovnaft, a. s (petrochemical industry). Weight and time dependences were investigated and subsequently compared with efficiency of active coal in terms of CODCr (chemical oxygen demand) and non-extractable compounds.

Results for biochar were better both for CODCr and non-extractable compounds and they are presented in a doctoral theses that describes the above-mentioned experiments in detail [16]. More tests of biochar and its modified products were performed in the National Institute for Nuclear, Chemical and Biological Protection (Státní ústav jaderné, chemické a biologické ochrany), specifically determination of breakthrough times for sulfur mustard (yperite). The dependence of breakthrough time on weight of tested samples is presented in a doctoral thesis defended at the Technical University of Ostrava [17].

Composite textile materials were prepared in cooperation with the department of non-woven textiles of the Technical University in Liberec (using a combination of technologies *spunbond*, *meltblown*, needle punched nonwovens), while biochar and some of its modifications were applied into needle-punched nonwovens and the resulting materials were investigated to determine their breathing resistance, permeation of NaCl aerosol and interception of paraffin oil [17]. The interception of paraffin oil and NaCl aerosol on those composite materials was high: over 89%. The material is breathable.

6 Conclusions

The article focuses on a description of biochar (the origin and preparation) and its characterization (SEM, BET, FT-IR, Raman). The prepared products were tested to determine dependence of their thermal decomposition on the content of input components of the synthesis. We primarily focused on effects of the weight ratio of graphite and biochar, change of reaction time or reaction substituents; the TGA and DSC analyses have confirmed dependence of temperature and weight parameters on reaction conditions. Thermal decompositions of all the tested C–compounds were exothermic. We also tested adsorption properties of the prepared products of modified biochar in contact with oil pollutants and nerve agents and also aerosol permeation. The tested applications of modified biochar have confirmed their excellent sorption properties in contact with the above-mentioned materials.

References

1. Staf M, Zalesakova K, Kyselova V, Miklova B, Skoblja S (2019) Zarizeni na pripravu a aktivaci biocharu. (Equipment for preparation and activation of biochar) Chemicke listy 113 (1):48–52. (In Czech)
2. Yakout SM (2015) Monitoring the changes of chemical properties of rice straw-derived biochars modified by different oxidizing agents and their adsorptive performance for organics. Bioremediat J 19(2):171–182
3. Ghaffar A, Younis NM (2014) Adsorption of organic chemicals on graphene coated biochars and its environmental implications. Green Proces Synth 3(6):479–487
4. Rajapakasha UA, Chen SS, Tsang DCW, Zhang M, Vithanage M, Mandal S, Gao B, Bolan NS, Ok YS (2016) Engineered/designer biochar for contaminant removal/immobilization from soil and water: potential and implication of biochar modification. Chemosphere 148:276–291
5. Zhang M, Gao B, Yao Y, Xue Y, Inyang M (2012) Synthesis, characterization, and environmental implications of graphene-coated biochar. Sci Tot Environ 435:567–572
6. Tang J, Lv H, Gong Y, Huang Y (2015) Preparation and characterization of a novel graphene/biochar composite for aqueous phenanthrene and mercury removal. Bioresour Technol 196:355–363
7. Li Y, Song N, Wang K (2019) Preparation and characterization of a novel graphene/biochar composite and its application as an adsorbent for Cd removal from aqueous solution. Korean J Chem Eng 36(5):678–687
8. Chen Z, Chen B, Zhou D, Chen W (2012) Bisolute sorption and thermodynamic behavior of organic pollutants to biomass-derived biochars at two pyrolytic temperatures. Environ Sci Technol 46(22):12476–12483
9. Zhao W, Wu F, Wu H, Chen G (2010) Preparation of colloidal dispersions of graphene sheets in organic solvents by using ball milling. J Nanomater 1–5
10. Brabencova E, Klouda K, Weisheitelova M, Placakova H (2016) Graphene-oxide and biochar interconnection. In: 1st scientific conference on CBNR protection, Kamenna, pp 239–248. (In Czech)
11. Roupcova P, Klouda K, Gembalova L, Kuzelova-Kostalova E, Chvojka J (2018) Lamineted, composite and sandwich membranes based oh graphene-oxide with nano-textiles. J Nanomed Nanotechnol 9(517):215–7439

12. Klouda K, Roupcova P, Gembalova L, Weisheitelova M, Chvojka J (2018) Laminované, kompozitní a sendvičové fólie (membrány) na bázi graphene oxidu s nanotextiliemi. (Laminated, composite and sandwich foils (membranes) based on graphene oxide and nanotextiles). In: 3rd scientific conference on CBNR protection, Kamenna, pp 97–110. (In Czech)
13. Thakur S, Karak N (2012) Green reduction of graphene oxide by aqueous phytoextracts. Carbon 50(14):5331–5339
14. Liang B, Zhan W, Qi G, Lin S, Nan Q, Liu Y, Cao B, Pan K (2015) High performance graphene oxide/polyacrylonitrile composite pervaporation membranes for desalination applications. J Mater Chem 3(9):5140–5147
15. Kuila T, Bose S, Khanra A, Mishra AK, Kim NH, Lee JH (2012) A green approach for the reduction of graphene oxide by wild carrot root. Carbon 50(3):914–921
16. Roupcova P (2018) Monitoring of ecotoxicity of carbon based nanoparticles. Dissertation, VSB-Technical University of Ostrava, Ostrava
17. Weisheitelova M (2019) Influence of decontamination agents on surfaces of selected materials during passive and active decontamination of highly toxic chemicals. Dissertation, VSB-Technical university of Ostrava, Ostrava

Wood as Fire Protection of Steel in Hybrid Structural Elements

Véronique Saulnier[1(✉)], Sébastien Durif[2], Salah Oulboukhitine[1], Abdelhamid Bouchaïr[2], and Gisèle Bihina[3]

[1] Institut Universitaire et Technologique d'Allier, Institut Pascal, 03100 Montluçon, France
veronique.saulnier@uca.fr
[2] Université Clermont Auvergne, Institut Pascal, 63000 Clermont-Ferrand, France
[3] Centre Technique Industriel de la Construction Métallique, 91190 Saint-Aubin, France

Abstract. Various solutions are used for steel-timber hybrid elements that associate two timber beams on both sides of a steel plate or a steel profile. Steel is used as mechanical reinforcement to obtain hybrid elements with high performance regarding the strength and the stiffness. Wood is a combustible material but it burns in a controlled way with low thermal conductivity. Steel is non-combustible and shows high performances in normal conditions. However, its mechanical properties decrease dramatically at elevated temperatures. Previous work on wood-steel connections highlighted the wood protection effect enhanced by the migration of water in the wood element and the absorption of some of the fire energy by vaporization of the water contained in wood. The present study focuses on the thermal performances of steel-timber cross-sections to obtain the evolution of temperature on steel element during fire exposure. The aim is to evaluate the wood material as passive fire protection for steel elements in comparison with other common solutions. Experimental program is performed using different types of wood as insulation to protect steel profiles. The thermal gradient is measured in the protected steel section using different pieces of wood in different configurations: partial or full protection with three or four exposure sides of the hybrid cross section. The tests were performed on a furnace prototype developed in the laboratory. The temperatures are measured using type K thermocouples. Results are compared with those given by a finite element model and the analytical expressions of EN1993-1-2.

Keywords: Hybrid element · Passive fire protection · Experimental tests · Steel element · Wood element

1 Introduction

The combination of wood and steel is not a new practice in building construction field. Timber structures are often assembled using rods and bolts [1]. Implementation solutions are simpler and convenient. Steel being a more resistant and stiff material than wood, brings an additional resistance to the connections between the elements of the

L. Makovicka Osvaldova et al. (Eds.): WFS 2020, *Wood & Fire Safety*, pp. 420–425, 2020.
https://doi.org/10.1007/978-3-030-41235-7_61

structure. However, the observation can be different when considering the fire resistance of these structures. Indeed, steel, under the effect of heat, will quickly lose its mechanical properties and mechanical strength calculations give a critical temperature value around 600 °C. [2]. Experimental studies performed on steel-to-timber connections using bolts and dowels have revealed a protective effect of wood on the heating of steel [3]. In fact, the migration of water contained in the wood to the metal element delays the rise of steel temperature [4].

The purpose of the study is to use wooden beams associated with I or T steel beams as a protective element. The tests attempt to establish whether the presence of wood provides thermal protection and limits the temperature rise of the steel. The initial idea being that the water contained in the wood could, by migrating towards the steel, slow down the heating of the steel during its evaporation [5]. It is also proven that the wood is an insulating material, even in its carbonized form [6–9]. However, wood is a combustible material that goes into spontaneous combustion if the heat source is about 300 °C. In order to check the validity of the hypothesis regarding the protection of steel structures by wood, thermal tests were carried out in an experimental furnace designed and manufactured in the university lab as part of this project. The tests were carried out on 200 and 140 I-steel beams and with partial or total wood protection. Experimental results are compared with numerical results in order to validate the proposed numerical model.

2 Experimental Tests

The tests were carried out in an oven with low inertia materials equipped with two oil burners. It was designed and manufactured at the university lab. The measurements were made with type K thermocouple welded to the metal profiles as recommended in the article of technical engineering [10]. The tests carried out on an unprotected metal profile with the use of a burner set for a power of 35 kW have shown that the temperature rise in the oven follows the standard fire curve. Moreover, the temperatures measured on the profile are identical to that given by the formula of the Eurocode for an unprotected metal element.

The heating of unprotected steel is given through Eq. (1) from Eurocode 3 [2]:

$$\Delta\theta = \frac{\dot{h}_{net,d}(t)}{Ca.\rho a}.A/V.\Delta t. \tag{1}$$

With: A/V the section factor for unprotected steel members [m^{-1}]; C_a specific heat of steel [J/kgK]; Δt time step[s]; ρ_a density of steel [kg/m^3]; $\dot{h}_{net,d}$ heat flow [W/m^2].

Equation (1) gives the temperature evolution in the steel during heating.

It was noticed that the temperatures recorded on the profile are very close and follow the theoretical curve (Fig. 1).

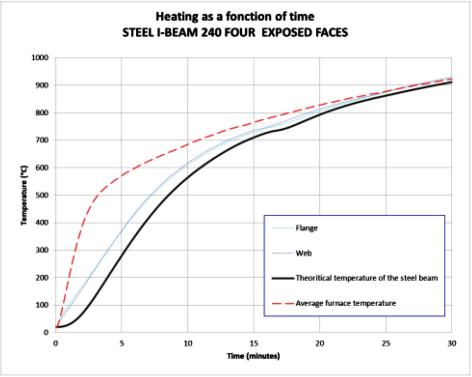

Fig. 1. Experimental and theoretical curves and a view of the beam in furnace.

The various profiles tested were exposed on three sides. They were placed in the furnace in horizontal position parallel to the flames of the burners. A single burner set at 29 kW was used when timber-steel hybrid elements are tested. The first tests were made on IPE 200 beam with a wood protection between the flanges (Fig. 2). The beam thus formed, was exposed to fire on three sides. The wood used is fir, with a measured density of 425 kg/m^3 and a moisture content of 10% (measured according to EN 13183-1). In the tested hybrid elements, 14.5 dm^3 of wood is used with a surface exposed to fire of 0.1856 m^2.

IPE 200 steel beam partly protected

Welded 140 steel beam fully protected

Fig. 2. Hybrid tested beams and furnace disposal.

The second specimen is a welded cross-section (called welded 140) with dimensions close to those of an IPE 140. The thicknesses of the flanges and the web are equal respectively to 7.2 (± 0.1) mm and 4.3 (± 0.05) mm with wood pine protection. The section factor of this profile is about 336 m^{-1} (perimeter = 534.6 mm, area = 1591.3 mm^2). The dimensions of the steel profile are chosen to obtain the chosen thickness for wood protection. Thus, the wood thickness on all sides of steel is equal to 40 mm. The timber beam has a density of 330 kg/m^3 and a moisture content of 10%. In this specimen, 12.2 dm^3 of wood is used with a surface exposed to fire of 0.2928 m^2 (Fig. 2). The burner power is identical to that of the first specimen.

3 Observations and Results

The test with IPE200 profile (Fig. 3) shows that the bottom flange exposed directly to fire heats up almost as much as the same unprotected beam. However, the upper parts of the beam remain below a temperature of 600 °C during the entire period of the performed test. After one hour, the wood was completely charred but it continues to thermally protect the beam. Weirdly a small decrease of temperature is observed on the bottom flange after 40 min despite the increase of furnace temperature.

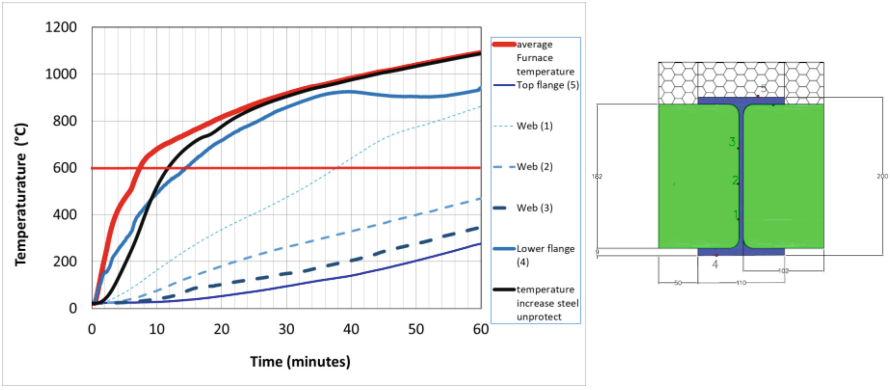

Fig. 3. Heating of IPE 200 steel beam with fir timber and theoretical curve

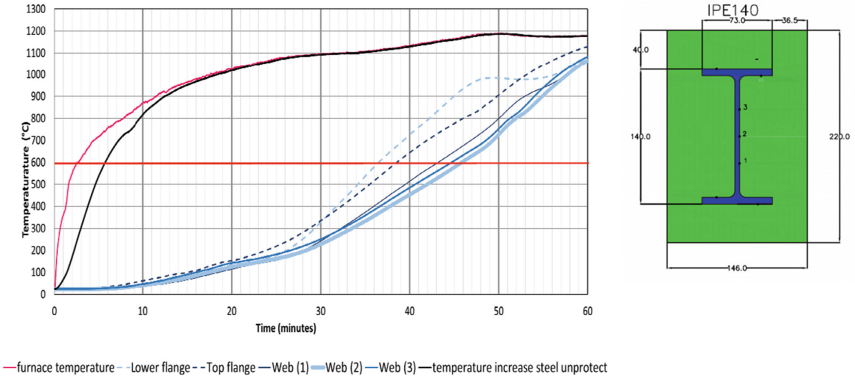

Fig. 4. Heating of welded 140 I-beam fully protected by pine wood.

The test with welded 140 profile shows a real protective effect of wood. The temperature remains below 600 °C for 35 min (Fig. 4) on all the steel cross-section. Temperature sensors located at different depths in the wood can estimate the charring

rate of wood at 1.5 mm per minute. This represents a charring rate twice that of wood exposed to a standard fire. With the energy input due to the presence of wood, the temperatures values in the furnace exceed those of iso fire by around 200 °C. For the first test, the furnace temperature deviates from the iso curve at 16 min and increases faster. For the Welded 140 I-beam, the temperature rise of the furnace is 200 °C higher than that of iso fire. The quantities of wood used are similar, 14.8 dm^3 for the IPE 200 beam and 12.2 dm^3 for the welded 140 I-beam. However, wood surfaces exposed to fire are more important in the second case. The difference in temperature rise could be explained by a higher quantity of burned wood for the second test.

4 Comparison Against Numerical Simulation

A 2D finite element heat transfer analysis is conducted to simulate the thermal behavior of the tested specimens using Ansys code [11]. The modelling is based on the thermal properties of steel and timber from [2] and [12] respectively, accounting for the density and moisture content experimental values of timber at room temperature. A comparison between the measures from thermocouples and the results from the numerical simulation is shown in (Fig. 5). The measured and calculated temperatures of the 3-side fire-exposed IPE 200 are very close, whereas the calculated heating of the 4-side fire-exposed welded140 from FEA is lower than the measured one.

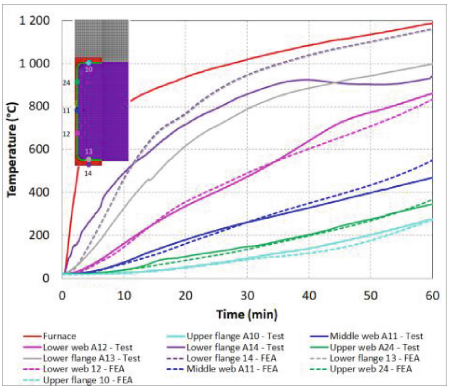

3-side fire-exposed IPE 200 with partial timber encasement

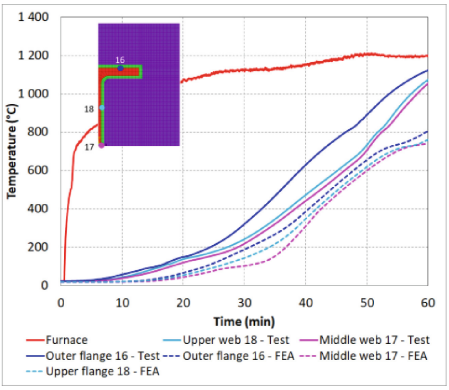

4-side fire-exposed welded 140 with full timber encasement

Fig. 5. Comparison of the measured and calculated temperatures of the steel profile.

5 Conclusion and Outlooks

The concept of a steel beam with wood protection is conceivable. For the moment, the tests carried out show a protective effect at 30 min, but we stay under an hour. There is no improvement in the heating of the steel around 100 °C like it was mentioned in the study of Audebert's [3] who conducted tests on the steel-wood assembly at the level of

connections. Despite simplifying assumptions, simulations conducted under Ansys are close to the experimental results. These first results are encouraging. The wood provides a proven thermal protection. However, its presence adds significant thermal loads. Moreover, it is not known what role the wood will play in the mechanical strength of the structure in case of fire.

This type of solution has an aesthetic interest because we will have an externally wood appearance. The most interesting tests are those carried out on partially protected beams because the quantity of wood is less important but still offers a protection of the web and the upper flange. This solution might be interesting on T-beams. Further testing is required to confirm these first results.

Aknowledgments. The authors wish to thank the Tremplin Carnot MECD and Université Clermont Auvergne for the financial support provided to the study. Gratefully acknowledgment to Myriam Moissaing, Daniel Robin, Lionel Gravillon and Manh Hung Nguyen for their help in conducting experiments.

References

1. Benoit Y (2009) Calcul des structures en bois. Editions Eyrolles, Paris
2. Eurocode 3 (2005) Design of steel structures, Part 1–2: General rules, Structural fire design, CEN
3. Audebert M, Dhima D, Taazount M, Bouchaïr A (2014) Experimental and numerical analysis of timber connections in tension perpendicular to grain in fire. Fire Saf J 63:125–137
4. Samaké A, et al (2014) Thermo-hydric transfer within timber connections under fire exposure: experimental and numerical investigations. Appl Thermal Eng 63(1): 254–265
5. Fredlund B (1993) Modelling of heat and mass transfer in wood structures during fire. Fire Saf J 20(1):39–69
6. Shafizadeh F (1982) Introduction to pyrolysis of biomass. J Anal Appl Pyrol 3(4):283–305
7. Sullivan AL, Ball R (2012) Thermal decomposition and combustion chemistry of cellulosic biomass. Atmos Environ 47:133–141
8. Mok WSL, Antal Jr MJ, Szapo P, Varhegyi G, Zelei B (1992) Formation of charcoal from biomass in a sealed reactor. Ind Eng Chem Res 31(4):1162–1166
9. Janssens ML (2004) Modeling of the thermal degradation of structural wood members exposed to fire. Fire Mater 28(2–4):199–207
10. Rogez J (1992) Mesure des températures. Ed. Techniques Ingénieur, Paris
11. ANSYS (1992) user's manual for revision 8.0, volume iv, theory. Swanson Analysis System, Inc., Houston
12. Eurocode 5 (2005) Design of timber structures, Part 1–2: General rules, Structural fire design, CEN

Electric Cables Installed in OSB Boards Surfaces and Their Temperature

Jozef Martinka(✉), Peter Rantuch, Tomáš Štefko, and Igor Wachter

Faculty of Materials Science and Technology in Trnava, Slovak University of Technology in Bratislava, Jana Bottu 2781/25, 917 24 Trnava, Slovakia
{jozef.martinka, peter.rantuch, tomas.stefko, igor.wachter}@stuba.sk

Abstract. This paper discusses the impact of low-level electrical current on the temperature of electrical cables installed in surface grooves of oriented strand board (OSB). The three-wire power electrical cable (copper conductors each with a cross-section of 1.50 mm^2) with fire reaction class $B2_{ca}$ and construction OSB intended for use in dry or humid environments were investigated. The electrical cable was powered by an alternating current (AC) power supply (230 V) and connected to incandescent light bulbs with a total power input of 200, 400 and 600 W (this power input corresponded to an electric currents of 0.87, 1.74 and 2.61 A). Incandescent light bulbs were connected in parallel to the cable. During the test, thermocouples were used to measure temperatures on the surface of the electrical cable, on the surface of the OSB at a distance of 2 cm from the centre of the cable and the ambient temperature. The data obtained show that as the electrical current increases, the temperature of the cable installed in the OSB surface grooves increases. The maximum cable temperature (30.1 °C) was recorded at an incandescent light bulb of 600 W. The recorded temperature (30.1 °C) is lower than the core temperature limit of the investigated cable under normal operation (90 °C).

Keywords: Oriented Strand Board (OSB) · Electrical cable · Electrical current · Temperature · Temperature limit

1 Introduction

Each electric conductor (excluding superconductors) releases heat because of conducting an electric current. According to Joule-Lenz law, the heat output is proportional to the electrical resistance of the conductor and square of the current. The mathematical expression of the Joule-Lenz law is (1):

$$P = I^2 \cdot R. \tag{1}$$

where P is power of heating (W), I is electrical current (A) and R is electrical resistance (Ω).

The temperature of the electric conductor or cable during operation depends on the power of heating, on the heat dissipation possibility and on the specific heat capacity. The possibility of heat dissipation from the electrical cable depends on the way of

L. Makovicka Osvaldova et al. (Eds.): WFS 2020, *Wood & Fire Safety*, pp. 426–431, 2020.
https://doi.org/10.1007/978-3-030-41235-7_62

installation (e.g., electrical cable in free air or electrical cable installed in the building structure). The possibility of heat dissipation from the electrical cable installed in the building structure depends on the method of installation in the structure (direct contact with the structure, installation in a hollow or in a protective tube).

Electrical cables are often installed in surface grooves of the Oriented Strand Board (OSB). In the case that the electrical cable is not covered by any material at the surface, heat is dissipated from the cable: by thermal conduction to the OSB in which the cable is installed and by thermal radiation and convection from the electric cable surface. The heat dissipated from the electrical cable to the OSB board is conducted by conduction inside the OSB and at the same time transferred from the board surface by thermal radiation and convection. The heat transfer from the electrical cable to the OSB and to the ambient is shown in Fig. 1.

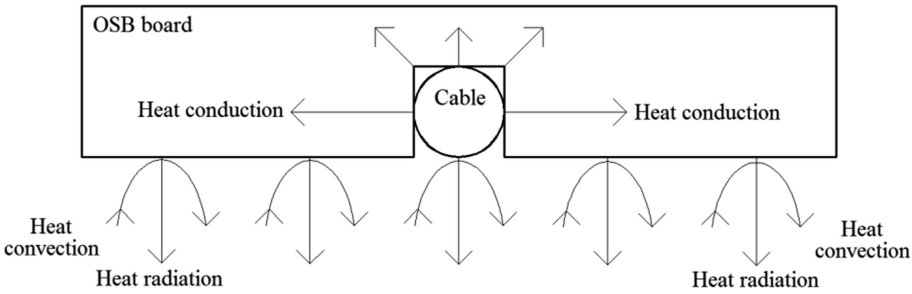

Fig. 1. Heat transfer from electrical cable into the OSB and heat transfer from electrical cable and OSB board into the ambient.

The maximum temperature of the electric cable specified by technical standards, e.g. ČSN 33 2000-5-52:2012 [1]. The maximum temperature of the electric cable according to the cited technical standard is e.g. 70 °C (isolation from polyvinyl chloride) or 90 °C (isolation from cross-linked polyethylene). Scientific papers [2–4] dealt with the issue of Joule – Lenz law in the context of heating of electric cables during operation.

Relatively few scientific papers investigate the effect of the low-level electric current on the temperature of electrical cables installed in OSB surface grooves. The aim of the present work is therefore to determine the effect of low-level electric current (up to 2.60 A) on the temperature of an electric cable (with a conductor cross-section of 1.50 mm^2) installed into a surface of OSB.

2 Materials and Methods

The temperature dependence of the electric cable (installed into the OSB surface groove) on the electric current was investigated by apparatus shown in Fig. 2

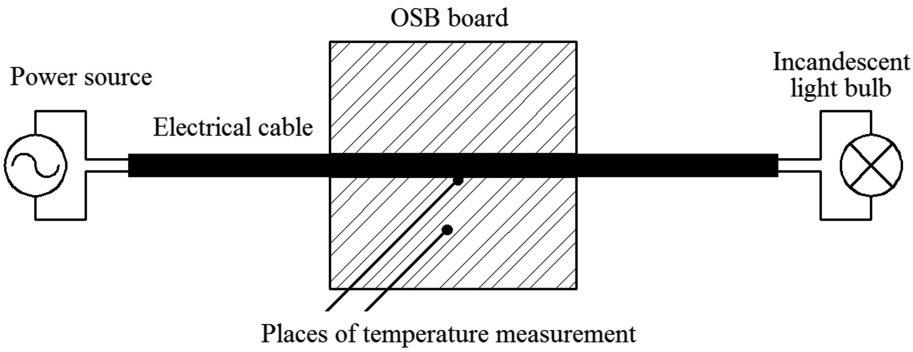

Fig. 2. Testing apparatus.

The temperature was measured on the surface of the electrical cable and on the surface of the OSB (at a distance of 2 cm from the center of the electrical cable) with K-type thermocouples (Ni-Cr-Ni). The ambient temperature by K-type thermocouple was measured too. One, two and three incandescent bulbs (parallel connection, 200 W each; i.e. 200 W, 400 W, 600 W of input power) were used as a load during measurements. The input powers corresponded (at an effective voltage value of 230 V) to a cable current load of 0.87, 1.74 and 2.61 A. The duration of one test (for one input power) was 3,600 s.

Tested OSB was OSB type 3 according to EN 300:2006 [5] (OSB for dry and wet installation) with a surface area of 150 × 500 mm and a thickness of 25.4 mm. The water content of the OSB was 5% and the corresponding density was 610 ± 15 kg/m^3. The water content was determined as follows: the water content = (water mass/dry OSB mass) * 100. Water mass was determined as the original OSB mass - the dry OSB mass. Dry OSB mass was determined as the mass of tested OBS after its dried at 103 ± 2°C temperature (to constant mass). OSB consisted of coniferous wood, polyurethane resin and paraffin. The OSB emissivity was approximately 0.90. Tested electrical cable CHKE-R was installed in the groove on the OSB surface (9 × 9 mm) located in the middle of the surface board. CHKE-R is a three-wire power cable (conductors are made from copper with a cross-section of 1.50 mm^2, insulation, bedding and sheath are made from ethylene-based polymer). Fire reaction class of tested cable is $B2_{ca}$, s1, d1, a1 with rated voltage of 600 V (AC) or 1000 V (DC) respectively. Cross-section of selected cable is shown in Fig. 3. The cable was made by VUKI, a.s., Bratislava (Slovakia).

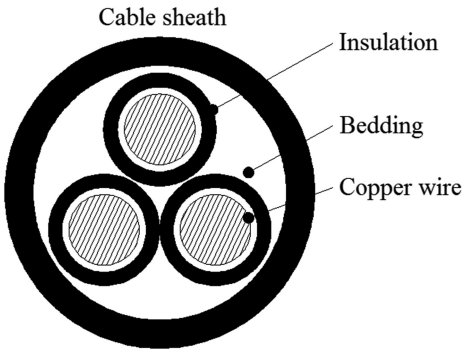

Fig. 3. Cross section of CHKE-R cable.

3 Results and Discussion

Obtained results i.e. temperature on the surface of electric cable and on OSB (2 cm from the center of the cable) together with ambient temperature for the investigated power inputs of electric bulbs (current loads of the electric cable) are shown in Fig. 4.

For comparison according to the technical standard ČSN 33 2000-5-52: 2012 [1] the temperature limit of the cross-linked polyethylene cable is 90 °C. As this limit was not exceeded (Fig. 4), it can be stated that tested configuration (for applied current load) meet the requirements of that standard.

According to [6, 7], the spontaneous ignition temperature of wood and wood-based materials is in the range of 390 to 460 °C i.e., above the achieved temperature set in this article (Fig. 4). Scientific papers [8, 9] show that wood and wood-based materials begin to thermally decompose relatively quickly (under thermal analysis conditions) at significantly lower temperatures (approximately 240 °C). However, these temperatures were not reached under the test conditions in this paper. According to [10], the thermal decomposition of the thermally least stable components of wood (especially hemicelluloses) starts from a temperature of about 160 °C. This temperature can be considered as a limit value which does not cause significant chemical composition changes when applied to the compact wood for a short time (in the order of minutes). A different way of determining the fire characteristics of wood and wood-based materials is in scientific paper [11]. According to scientific paper [12], long-term exposure to lower temperatures (60–70 °C) or to fine wood powder can cause chemical and physical properties change. These temperatures were not reached under the conditions of the experiment. Therefore, it can be stated that under conditions consistent with the experiment, the electrical cable installed in the OSB surface groove will not cause its changes in practical terms.

The obtained results will find application especially in the field of fire prevention and fire engineering. A description of the application of fire characteristics in fire engineering is stated in paper [13].

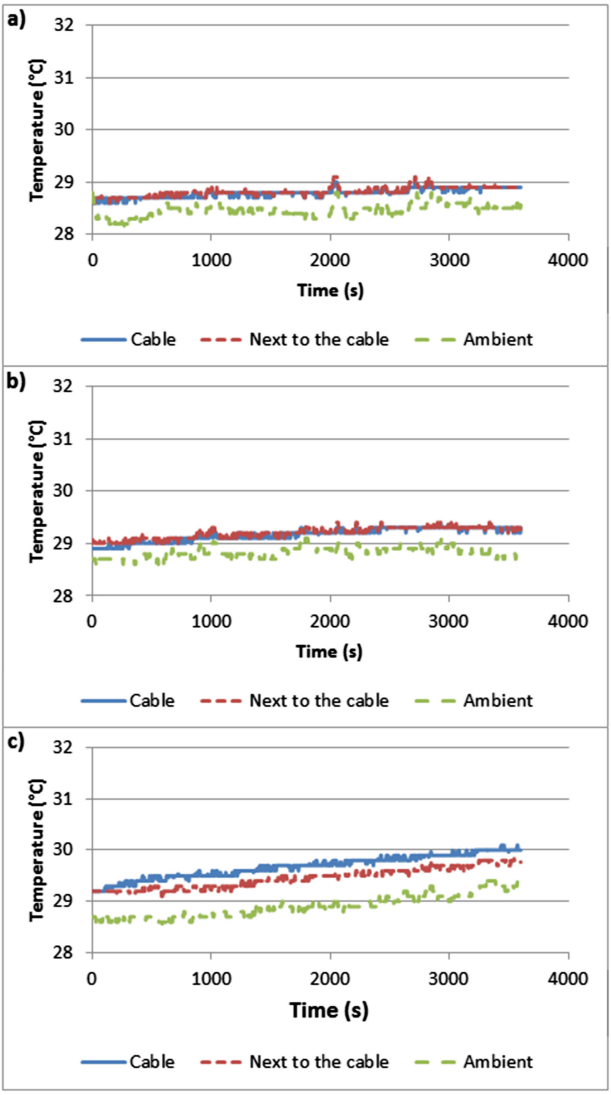

Fig. 4. Temperatures for input power of (**a**) 200 W; (**b**) 400 W; (**c**) 600 W.

4 Conclusion

In this paper, the effect of electrical current (up to 2.61 A) carried by a three-wire power cable (with a single conductor cross-section area of 1.50 mm^2) installed in the OSB surface groove on the cable temperature was assessed. Obtained results show that the maximum temperature of the electric cable (in the time interval to 3,600 s) was 30.1 °C. Therefore, under conditions consistent with the experiment (current 2.61 A and copper conductors with cross-section area 1.50 mm^2), the cable temperature limit

required by the applicable technical standards is not exceeded and there is no risk of OSB initiation or significant chemical or physical changes of OSB or cable damage due to electrical cable temperature.

Acknowledgments. This work was supported by the Slovak Research and Development Agency under the contract No. APVV-16-0223. This work was also supported by the KEGA under the contract No. 030UMB-4/2017.

References

1. ČSN 33 2000-5-52:2012 (2012) Low-Voltage Electrical Installations. Part 5-52: Selection and Erection of Electrical Equipment – Wiring Systems. Czech Office for Standards, Metrology and testing, Prague
2. Ruan J, Zhan Q, Tang L, Tang K (2018) Real-time temperature estimation of three-core medium-voltage cable joint based on support vector regression. Energies 11:1–18
3. Adi N, Vu TTN, Teyssedre G, Baudoin F, Sinisuka N (2017) DC model cable under polarity inversion and thermal gradient: build-up of design-related space charge. Technologies 5:1–16
4. Fassarela JEV, Fortes MZ, Sotelo GG (2018) Measurement, evaluation and proposed solution for power distribution arrangements with electrical cables in parallel. Measurement 119:196–204
5. EN 300:2006: Oriented Strand Boards (OSB): Definitions, Classification and Specifications. European Committee for Standardization, Brussels (2006)
6. Zachar M, Mitterova I, Xu Q, Majlingova A, Cong J, Galla S (2012) Determination of fire and burning properties of spruce wood. Drvna. Ind. 63:217–223
7. Zachar M (2010) Selected deciduous wood species flash ignition and ignition temperature determination. In: Mrackova E, Markova I (eds) Proceedings of the 3rd international scientific conference fire engineering. Technical University in Zvolen, Zvolen, pp 431–438
8. Markova I, Hroncova E, Tomaskin J, Turekova I (2018) Thermal analysis of granulometry selected wood dust particles. BioResources 13:8041–8060
9. Findorak R, Frohlichova M, Legemza J, Findorakova L (2016) Thermal degradation and kinetic study of sawdusts and walnut shells via thermal analysis. J Therm Anal Calorim 125:689–694
10. Reinprecht L, Vidholdova Z (2008) Thermowood: its preparation, properties and application. Technical University in Zvolen, Zvolen
11. Cekovska H, Gaff M, Osvaldova LM, Kacik F, Kaplan L, Kubs J (2017) Tectona grandis linn and its fire characteristics affected by the thermal modification of wood. BioResources 12:2805–2817
12. Kacik F, Velkova V, Smira P, Nasswettrova A, Kacikova D, Reinprecht L (2012) Release of terpenes from fir wood during its long-term use and in thermal treatment. Molecules 17:9990–9999
13. Mozer V (2014) An analysis of factors affecting available safe escape time. Adv Mater Res 1001:267–271

Improvement of Fire Response Efficiency by Means of Reducing the Time of Initial Fire Detection

Yuriy Klyuchka[1], Kostiantyn Afanasenko[1(✉)], and Khalid Hasanov[2]

[1] National University of Civil Defence of Ukraine, Kharkiv, Ukraine
armfree0@gmail.com
[2] Academy of the Ministry of Emergency Situations, Baku, Azerbaijan

Abstract. The paper analyzes the operation of fire emergency response units and auxiliary devices which operate in the infrared range and can be used to extinguish fires. Taking into account the Wien's displacement law, it is established that in the time interval up to 100 min the maximum emission falls on the wavelength range invisible to the human eye which confirms the practicability of using thermographic cameras in extinguishing fires.

In order to determine the fire spread time the time values of fire emergency response unit arrivals to the site of the fire were analyzed. Time values from the moment of fire break-out to the moment of arrival, control and suppression were used as initial data. 50,000 cases of fire have been processed.

An expert assessment has been carried out regarding the efficiency of using thermographic cameras during fires. There have been criteria proposed and estimates of the fire response efficiency obtained.

Keywords: Thermographic camera · Fire · Emission · Heat transfer · Fire control · Fire suppression · Efficiency

1 Introduction

One of the known approach of fire fighting effectiveness increase is optimizing tactical actions, forces and capabilities, using of modified extinguishing agents, etc.

The modern development of material has reached the point where the exploration and extinguishing of fires can be carried out not only on the basis of data in the visible to the human eye range of light waves, but also beyond it, with the help of thermal imagers [1–3]. By means of thermal imagers you can achieve:

- reduction of exploration time;
- reduction of fire localization and elimination time;
- reduction of direct and indirect material losses;
- reducing the amount of extinguishing agent used during the liquidation of the emergency;
- reducing the number of injured.

L. Makovicka Osvaldova et al. (Eds.): WFS 2020, *Wood & Fire Safety*, pp. 432–437, 2020.
https://doi.org/10.1007/978-3-030-41235-7_63

At the same time, it should be noted that the drawback is the lack of procedures for using of these devices, recommendations for tactical actions and the relevant legal framework.

It has been established that today there are no recommendations for tactical actions based on the analysis of the infrared image, both during the fire extinguishing and during the reconnaissance. For example, in the "Statute of Actions in the Emergencies for the Authorities and Units of the Rescue Service of Civil Protection" the word "thermal imager" is mentioned only once, namely, in clause 4.6.5: "Depending on the availability of forces and means, searching works are carried out on the basis and with the use: …… the readings of search devices (gas analyzers, probes, magnetometers, thermal imagers, acoustic systems); ……." [4].

The classification of the application fields of thermal imagers by fire units (Fig. 1).

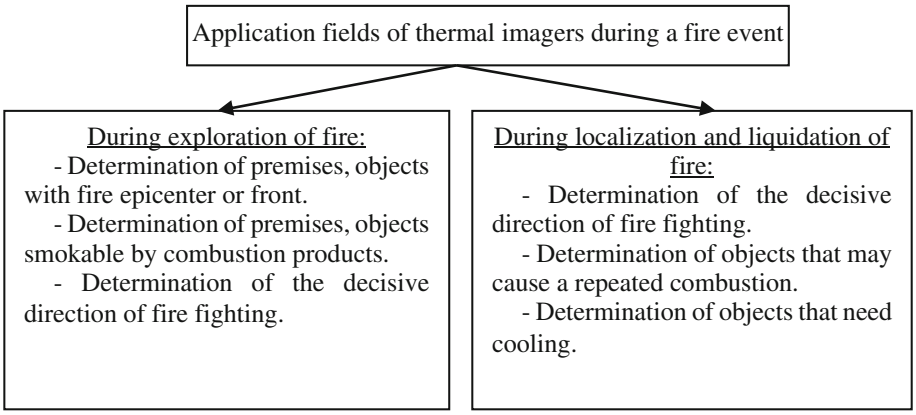

Fig. 1. Classification of application fields of thermal imagers by fire subdivisions

When determining the temperature of external enclosure structures, the time of fire development is essential, since the temperature in the premises and the heating of the building wall depends on it. In order to determine the time of fire development, the values of the arrival time of the units to the location of the fire were analyzed. The time value from the moment of the fire to the time of arrival, localization and elimination was used as the initial data. An example of the output is given in Table 1. $N = 5 \cdot 10^4$ time statistics from the time of a fire detection to the time of arrival, localization and liquidation of the fire (τ_{arr}, τ_{loc} and τ_{liq}) were processed [5].

In order to determine the laws of distribution of random variables for τ_{arr}, τ_{loc}, τ_{liq}, values were divided on n intervals ($\tau_{i(min)}$; $\tau_{i(max)}$) for histograms construction, based on the expression

$$n = 3,3 \cdot \lg(N) + 1 \approx 17. \quad (1)$$

It is found that σ_i varies in proportion to μ_i. This allows us to conclude that the random magnitude of the time of execution of a particular operation during the

Table 1. Time of fire beginning, notification, arrival of units to locations of fire, localization and liquidation

Beginning	Notification	Arrival	Localization	Liquidation
1:20	1:30	1:34	1:39	1:45
4:21	4:29	4:36	4:38	4:41
9:30	10:19	10:35	10:37	10:38
13:45	13:53	14:16	14:24	14:29
14:30	14:43	14:50	15:07	15:20
20:40	20:59	21:04	21:06	21:06
16:15	16:31	16:45	16:53	16:57
13:15	13:18	13:26	13:33	13:38
20:00	20:27	20:35	20:47	20:53
23:00	1:11	1:18	1:25	1:29

liquidation of fires has own pattern of change, which is subject to the following dependence

$$\sigma_i = 0,814\,\mu_i + 8,747, \quad \mu_i \in [28,13;\ 75,9]. \tag{2}$$

Data analysis allowed us to obtain the values of mathematical expectation and variance for the three random variables, which are presented in Table 2.

Table 2. Parameters of random variables

Arrival time (τ_{arr})		Localization time (τ_{loc})		Liquidation time (τ_{liq})	
μ_{arr}, min	σ^2_{arr}, min^2	μ_{loc}, min	σ^2_{loc}, min^2	μ_{liq}, min	σ^2_{liq}, min^2
28.13	1015.9	47.04	2183	75.9	5001

The analysis showed that the random value of time before the arrival of the units can be described by the Rayleigh distribution

$$f(x) = \begin{cases} \frac{x}{\sigma^2} \cdot \exp\left(-\frac{x^2}{2\cdot\sigma^2}\right), & x \geq 0; \\ 0, & x < 0. \end{cases} \tag{3}$$

On the basis of the obtained values of the mathematical expectation, the probability density and the distribution function (Fig. 2) for τ_{arr}, τ_{loc} and τ_{liq} according to (3) were constructed.

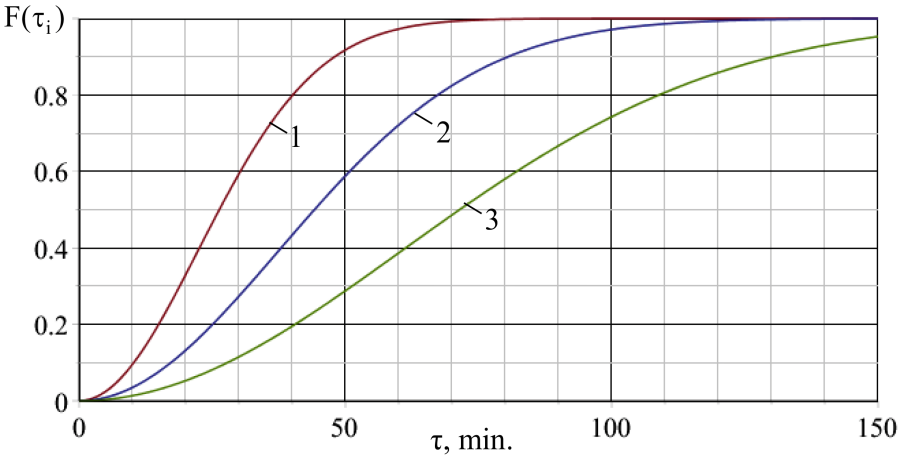

Fig. 2. Statistical distribution function: 1 – time of arrival of units to the place of fire; 2 – time to localization; 3 – time to liquidation

The analysis of the figure shows that after the beginning of the fire, within an hour, the probability of arrival of emergency and rescue units is more than 95%, localization – 70% and liquidation – 40%.

Next, an expert evaluation of the efficiency of thermal imagers using during fire-fighting was performed, the criteria of efficiency were proposed and the efficiency of the use of thermal imagers was conducted. Since thermal imagers using is not regulated at present, the efficiency of its use, therefore, depends on practical experience, understanding of the device basics and the basics of thermodynamics.

To evaluate the efficiency of the thermal imagers using, a survey of 15 experts, who have their own experience how to handle these devices and used them during fire-fighting. Each of them was asked two questions, namely:

- how many minutes the use of the thermal imager can reduce the time of fire liquidation (maximum value) z_i;
- how many percent the use of the thermal imager can reduce the time of fire liquidation (maximum value) z_i^*.

There were calculated the coefficients of variation for the values of time reduction in minutes and percentages. Figure 3 shows the contribution of each expert to the variation coefficient.

As a result, it was found that both coefficients of variation indicate average variability (up to 25%), which is quite acceptable.

Thus, it was determined that the average time reduction due to the use of the thermal imager (according to Table 2.) is 6.3 min, and the maximum – 10 min. For relative values, respectively, 12.8% and 20% are obtained.

Based on the obtained expert assessments, the efficiency of thermal imagers application was evaluated according to the criterion of relative change in the burning-surface area γ_S and the probability of localization γ_F.

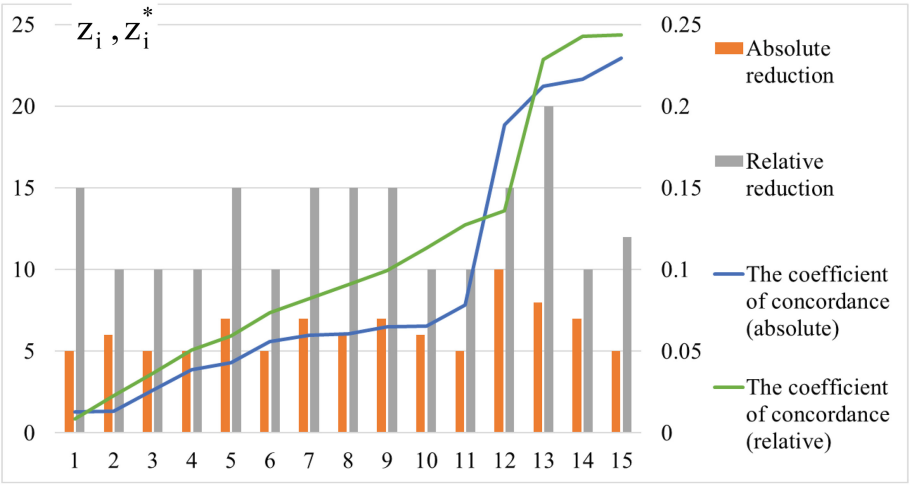

Fig. 3. Expert contribution to the variation coefficient

Then, the effect of reducing the time z of fire detection and, accordingly, the mathematical expectation μ of the area and the probability of localization can be graphically depicted in the following form (Fig. 4).

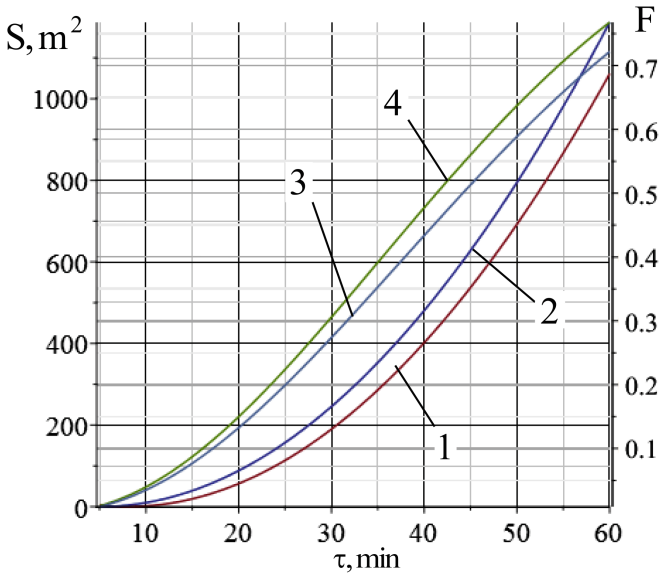

Fig. 4. Dependence of fire area (S) and probability of localization (F) on time:1 – $S|_{z=3}$; 2 – S; 3 – $F|_{\mu=47}$; 4 – $F|_{\mu=44}$

The figure points out the fact that in case of fire localization three minutes earlier, the burning-surface area decreases to 20%, and the probability increases by 0.1.

In general, it was found that using the imager and reducing the time within the expert evaluation may increase the probability of fire localization by up to 12% and reduce the burning-surface area by an average of 25%.

2 Conclusions

The statistics of the emergency units effectiveness were processed. As a result, the distribution functions of the arrival, fire localization and liquidation time were received. It is proposed to select relative changes in the burning-surface area γ_S and localization time τ_F as the performance criteria, and for the first time estimates of the effectiveness of fire liquidation are obtained.

It is established that when using the thermal imager and reducing the time within the expert evaluation, it is possible to reduce the fire localization time by up to 12% and reduce the fire area by an average of 25%.

References

1. Amon F, Hamins A, Bryner N, Rowe J (2008) Meaningful performance evaluation conditions for fire service thermal imaging cameras. Fire Safety J 43:541–550
2. Klyuchka YP, Hasanov KS, Krynska NV (2014) Analysis of applying the thermal imagers for fire extinguishing. Fire Saf Prob 36:109–116
3. The Impact of Thermal Imaging Camera Display Quality on Fire Fighter Task Performance. https://tsapps.nist.gov/publication/get_pdf.cfm?pub_id=902977
4. Statute of Actions in the Emergencies for the Authorities and Units of the Rescue Service of Civil Protection. http://search.ligazakon.ua/l_doc2.nsf/link1/RE21147.html
5. (2016) National report on the state of technogenic and natural security in Ukraine in 2015. The Ukrainian Civil Protection Research Institute, Kyiv, p 279

Assessment of Makeshift Technical Devices Used for Caving and Backfilling

Monika Šullová(✉) and Milan Konárik

Faculty of Security Engineering, University of Zilina, Žilina, Slovakia
monika.sullova@zilina.sk

Abstract. This article deals with the evaluation of makeshift technical devices used in caving and backfilling. As the HaZZ SR (Fire and Rescue Service of the Slovak Republic) does not have sufficient technical means for this kind of intervention, it is very often used makeshift sheeting from available materials that are located in the vicinity of the event. Wood as a building material plays a very important role here. Furthermore, the theoretical and practical knowledge of the intervening units is necessary to carry out stabilization of the excavations against possible further landslide and to protect the life and health of the intervening firefighters.

Provisional sheeting and, in particular, the possibility of using available materials for their construction is a maximum advantage in interventions by volunteer firefighters, who are increasingly deployed to save lives, health and property. To carry out rescue activities, volunteer firefighters are included in the nationwide deployment of forces and means of fire brigade units within the Slovak Republic, where they are often the first rescue unit at the scene of an event.

Keywords: Technical means · Stabilization · Wood · Training

1 Introduction

In today's hurried world, we very often forget the most valuable things we have. "Life and health". Our negligence can damage not only our health, but also health of others. Many times it is too late when we find that life and health are irreplaceable.

During the excavation work, the contractor is obliged to ensure the technological process by suitable technical means so as to prevent accidents and possible damage to health.

Recalled firefighters must immediately secure the space around the affected person in a very short time by means of a temporary sheeting, taking into account their own safety. Knowledge of procedures and material-technical equipment greatly influences the course of intervention.

2 Technical Means

The technical means for carrying out this kind of intervention are concentrated only on specialized units of the Fire and Rescue Corps - Rescue Brigade (HaZZ SR).

L. Makovicka Osvaldova et al. (Eds.): WFS 2020, *Wood & Fire Safety*, pp. 438–444, 2020.
https://doi.org/10.1007/978-3-030-41235-7_64

The other fire departments within the remit of the district directorates do not have such technical means and nevertheless the fire brigade is trying to provide assistance in any kind of emergency.

In most cases, it is improvised using various materials that either the fire brigade rescuers themselves make at individual fire stations or use the available means within the equipment of the HaZZ SR and sometimes also the material that is located at the site of the intervention.

Special hydraulic spreader bars and support plates to secure the excavation walls are required to perform excavation interventions. Furthermore, the safety of firefighters at the edge of the excavation and the distribution of forces of moving firefighters is allowed by boards. There are other additional means such as: wooden prisms of various sizes, ropes, field blades, pickaxes, ladders,…

2.1 Hydraulic Release Device

For the purposes of securing the walls of the excavation is used hydraulic rescue device included in the use of HaZZ SR, which is located in vehicles of the fire rescue service. These sets of hydraulic rescue devices are available at every fire station in the Slovak Republic, because they have been supplied in recent years as part of AHZS Mercedes Benz Vario (1A), Mercedes Benz Atego (1AB), Mercedes Benz Sprinter (2A) and Renault Kerax (4B).

3 Wood

Since the HaZZ SR does not have sufficient technical means, the fire brigade is forced to improvise on the scene of the intervention.

Wood plays a very important role in stabilizing excavations. It is often the only material available at the scene of the intervention. An important condition in the selection of wood is its condition and quality. We visually inspect it for visible defects.

Wood has been used for stiffeners for centuries. Especially in mining operations, but also as reinforcement in stabilization. It was easy and accessible. It also allowed good handling. As it turned out, it had one more advantage. They were said to “warn” of the disaster. Overloading began to crack “groan” and this acoustic manifestation warned of a possible collapse in the area.

Spruce was the most suitable tree of all. Spruce Picea abies belongs to the group of conifers. It is the second most widespread tree species in Slovakia, and it is the most economically important.

Wood is an extremely important raw material in terms of its physical and mechanical properties, but also in terms of its occurence in the forests of the Slovak Republic. The most important use of wood is in the form of building timber, especially for aboveground buildings. It is also used for the production of residential roof

constructions, commercial but also special buildings. It is a proven semi-finished product for the production of windows, exterior and interior doors, balconies and staircases. Spruce wood is also part of wooden buildings [1].

Wood durability is characterized as less durable and resistant to biotic pests. Spruce wood according to individual cuts is on (Fig. 1).

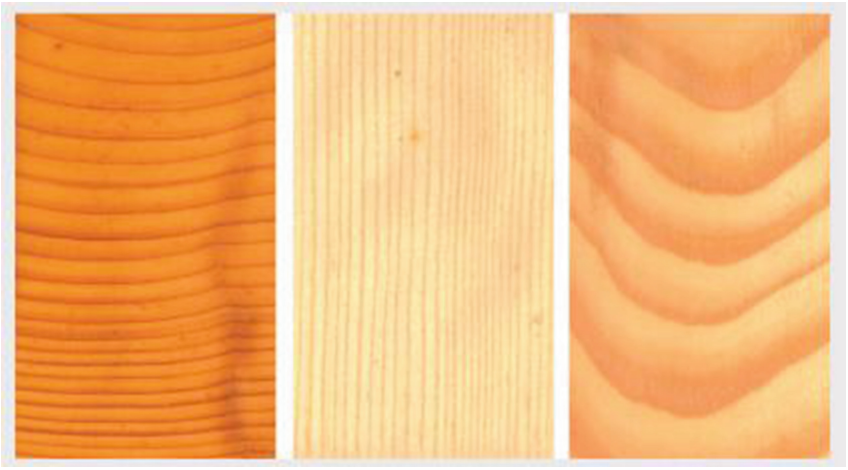

Fig. 1. Spruce wood (top to bottom (P) cross section, (R) radial section, (T) tangential section) [1]

The quality assortments of raw spruce wood represent an important raw material for the production of structural veneers for the production of plywood. Lower quality assortments are the desired raw material for the production of all types of agglomerated materials such as particle board. Thin spruce logs are used as mining and construction timber.

3.1 Wooden Stiffeners

Wooden reinforcements are an essential part of the temporary shoring. Since most fire stations do not have special equipment, the wood most commonly used around the event site such as boards, planks and prisms is used. With the help of boards, rescue firefighters can create a safe area to distribute force around the excavation. Subsequently, with the help of boards and prisms, assemble the temporary shoring in the trench for safe intervention (Fig. 2).

Fig. 2. Provisional sheeting (Author)

3.2 Support Plate (Strongback)

Plywood is a solid building material made of multiple layers of wood veneer. Its quality is indicated by the number of layers, the adhesive it is glued and the quality of the veneer. The plywood is usually made of an odd number of layers of veneer, and to increase the strength of the material, the individual layers are glued so that the fibers of the wood used are perpendicular to the previous layer. The thickness varies depending on the strength required. Some reinforced plywood may also include a metal layer that is inserted into the center of the plywood to increase strength.

They are made of deciduous and coniferous trees (spruce, pine, beech, poplar, birch) as large-area boards (Fig. 3) with dimensions of 1,250 × 2,500 mm and a thickness of 4, 5, 6, 8, 10, 12, 15, 18, 21, 27, and 30 mm. They have good dimensional stability, stable shape, and are designed as load-bearing and non-load-bearing boards for use in damp and outdoor environments [2].

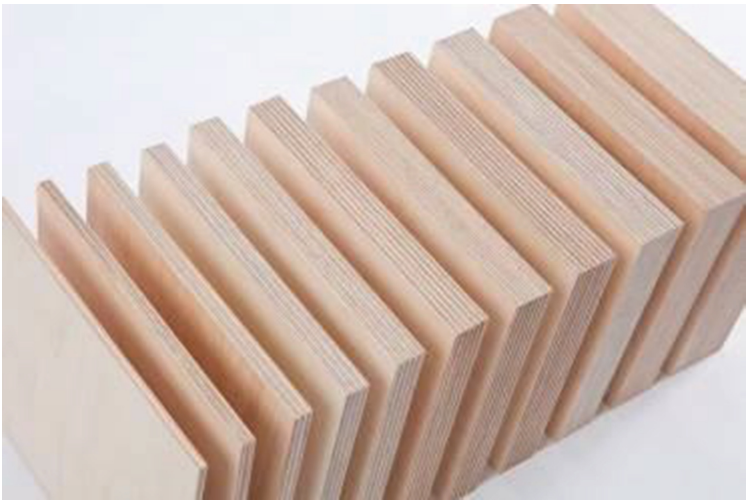

Fig. 3. Plywood waterproof Birch S/BB BFU 100 (Jafholz, 2019)

4 Methodology of Delivering from Caving and Backfilling

In order to carry out a quick and safe intervention of firefighters, material means are needed, by which every fire-fighting unit should be equipped with. For the correct use of these means, it is necessary to control the methodology of relief from caving and backfilling.

In order to ensure safe work to free the disabled, it is necessary to create a work area and a sufficiently large and safe zone around the disabled. It is important that firefighters do not move in a ditch that is not properly secured. This could result in further landslides and possible backfilling of firefighters.

In all cases, it is very important that the excavation from the excavation be treated with extreme caution. There are a number of risks that need to be considered and adhered to, as well as rescue procedures and principles of safe work [3].

In this type of intervention, firefighters proceed according to methodological sheet no. 124 - "danger of backfilling and swamping". The methodology is only a recommended procedure, according to which the intervening units should follow the actual conditions at the site of intervention.

We propose that members of DHZO (Voluntary fire brigade of the city established by the city) who are included in the nationwide deployment of forces and means within the Slovak Republic (in each municipality over 500 inhabitants), should be familiarized with this issue in cooperation with the HaZZ SR where they are destined for early intervention where every minute plays an important role.

5 Measurement Modulus of Wood Elasticity

In the meaning with health and safety at work, materials used for rescue purposes should be certified for the use. Therefore, conditions should be laid down as to what material can be used. When using wood reinforcements (prisms and slabs) it is necessary to determine the boundary conditions when determining the bending elasticity of the wood. Another possibility is to determine the global modulus of elasticity of wood according to STN EN 408.

5.1 Test Specimen

The smallest length of the sample must be 19 times the height of the cross section. If possible, must be placed into the protocol of the span of the beam. The test element is loaded to bend symmetrically in the two points with a span equal to 18 times the height, as is shown in Fig. 4. The speed of the burden must be constant. Speed shift a load of the load must not be higher than 0,003 h mm/s (Fig. 4).

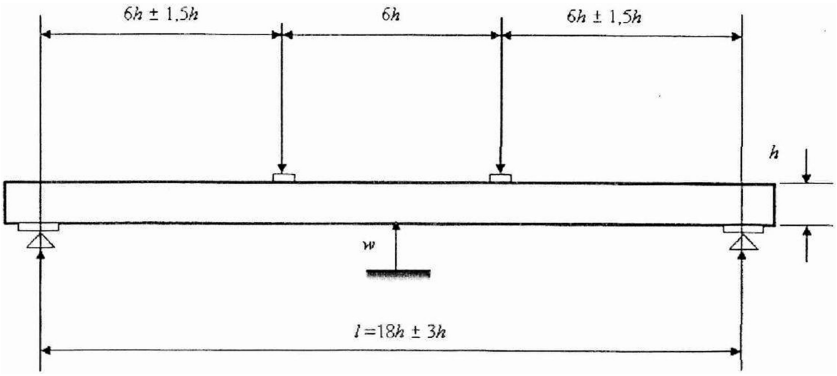

Fig. 4. Layout of test for measuring the global module of elasticity in bending (DIN EN 408)

The maximum load shall not exceed 0,4 $F_{max.est}$, or damage to the test element, if this test fails.

The anticipated maximum load $F_{max.est}$ of the tested material must be obtained either from tests on a minimum of ten space of the appropriate shape, size and quality or from a suitable known test data.

Deformation of the w must be measured in the middle of the span and in the middle of the towed or pushed to the edge. When w is measured in the neutral axis it must be the average of the measurements carried out on both sides of the test element.

Deformations shall be determined with an accuracy of 1% or deformation smaller than 2 mm with an accuracy of 0,02 mm.

5.2 Expression of the Results

Part of the graph between 0,1 $F_{max,est}$ and 0,4 $F_{max,est}$ will be used to regresívnu analysis. Finding the longest part of this section obtains a correlation coefficient of 0,99 or higher. Provided that this section covers at least the range of between 0,2 $F_{max,est}$ to 0,3 $F_{max,est}$ the global modulus of elasticity $E_{m,g}$, is calculated from the following relationship:

$$E_{m,g} = \frac{3\,al^2 - 4\,a^3}{2bh^3\left(2\frac{w_2 - w_1}{F_2 - F_1} - \frac{6a}{5Gbh}\right)} \tag{1}$$

where $F_2 - F_1$ is the increment of the load in newtons on the regressive line with the correlation coefficient of 0,99 or higher; and $w_2 - w_1$ increment of the deformation in millimeters corresponding to $F_2 - F_1$, If G is unknown it may be taken as infinity.

Modulus of elasticity is calculated with an accuracy of 1% [4].

6 Conclusion

Despite the conscious risk, every firefighter's effort is to make every effort to save human life. Key solutions in such situations tend to be non-standard. Very often it is improvised with the help of various materials that are in the vicinity of the event or that the firefighters themselves make from available means. Of course, even firefighters are trying to keep up with the times and be prepared to eliminate the various possible types of danger. Therefore, it is necessary to be prepared for less frequent, but demanding interventions of this type.

References

1. Požgaj A, Chovanec D, Kurjatko S, Babiak M (1997) Structure and Properties of Wood. Príroda, Bratislava. ISBN 80-07-00960-4
2. Preg lejka. http://cs.wikipedia.org/wiki/P%C5%99ekli%C5%BEka. Accessed 19 July 2018
3. Osvaldova LM, Osvald A (2013) Flame retardation of wood. In: Conference: 4th International Conference on Manufacturing Science and Engineering (ICMSE 2013). Advanced Materials Research, vol 690–693, pp 1331–1334
4. Morris B (2008) Holmatro rescue support and lifting technology, Praha. ISBN 978-90-812796-1-1
5. Svetlik J, Vel'as A (2016) The safety training in the municipality. In: 8th International Conference on Education and New Learning Technologies (EDULEARN), 2016 EDULEARN16. EDULEARN Proceedings, Barcelona, Spain, 04–06 July 2016, pp 1350–1355
6. Osvaldova LM, Gaspercova S (2015) The evaluation of flammability properties regarding testing methods. Civil Environ Eng 11(2):142–146
7. Monosi M, Janosik L (2016) An essay of firefighting vehicles' reliability. In: Conference: International Conference on Engineering Science and Production Management (ESPM), Slovakia, 16–17 April 2015, pp 201–206
8. Osvaldova, LM, Petho M (2015) Occupational safety and health during rescue activities. In: Conference: 6th International Conference on Applied Human Factors and Ergonomics (AHFE). Procedia Manufacturing, Las Vegas, NV, 26–30 July 2015, vol 3, pp 4287–4293

Experimental Evaluation of the Effectiveness of the Use of Thermal Imagers in Fires Extinguishing with the Presence of Wooden Combustible Substances

Yuriy Klyuchka[1], Kostiantyn Afanasenko[1(✉)], and Khalid Hasanov[2]

[1] National University of Civil Defence of Ukraine, Kharkiv, Ukraine
armfree0@gmail.com
[2] Academy of the Ministry of Emergency Situations, Baku, Azerbaijan

Abstract. In the paper have been further development a mathematical model, that used the equation of non-stationary thermal conductivity. This model describes the thermal effect of the fire on the readings of the imager. The measurements of temperatures of external structures during fires showed the adequacy of the mathematical model with an error of up to 35%, which indicates the possibility of its use in temperature estimation. It has been experimentally shown that the identification of flames by means of a thermal imager through the double-glazed window at the initial stage of the fire is impossible due to the absorption of infrared radiation. It is only possible to identify a fire while the window is warming. The temperature of glass pack during fires was investigated experimentally. The error on the temperature difference, i.e. the change from the initial temperature, is estimated. As a result, it is found that the error does not exceed 35%.

Keywords: Fire · Thermal imager · Effectiveness · Thermogram · Wood · Fire extinguishing

1 Introduction

Any stage of the fire is accompanied by the process of electromagnetic radiation in and out of the optical range. So, it can be stated that the analysis and extinguishing of fires can be performed not only on the basis of data in the visible to the human eye range of light waves, but also beyond, using pyrometers or thermal imagers.

Radiation of flames or heated structures has different spectral composition, depending on the combustion temperature, the type of chemical reaction. At the same time, the main elements that can be observed with the help of a thermal imager are walls, windows, doorways and, directly, flames and smoke.

Obviously, the research of the temperature of enclosing structures (walls) is more inertial than the study through the window, doorways, which are affected by the thermophysical characteristics of these elements.

Modeling the temperature of the structures exterior surfaces, which depends on the ability to determine the fire using a thermal imager, will depend on the amount of

L. Makovicka Osvaldova et al. (Eds.): WFS 2020, *Wood & Fire Safety*, pp. 445–450, 2020.
https://doi.org/10.1007/978-3-030-41235-7_65

temperature in the room, the nature of its change, the properties of the wall material and other parameters.

Taking into account that the geometric dimensions of buildings (premises), often one or two orders of magnitude greater than thickness, the problem of heat transfer as one-dimensional can be consider. Then, in the event of a fire, there is a change in temperature inside the premise, which leads to a change in the parameters of the wall according to the expression [1, 2].

$$\frac{\partial}{\partial \tau} T(x,\ \tau) = a_{st} \cdot \frac{\partial^2}{\partial x^2} T(x,\ \tau), \tag{1}$$

where a_{st} – the coefficient of thermal conductivity of the wall; $T(x,\ \tau)$ – the temperature value at a distance x from the inner surface of the wall at time τ.

Heat transfer coefficients play an important role in the calculation of thermal fields. The results of theoretical and experimental researches of a number of authors relative to the coefficient of heat transfer indoors during fires have shown that their value can be in the range from 114 to 260 W/(m^2•K) [3].

Then the mathematical model of the description of the dangerous fire factors and the type of wall material (enclosing structures) influence on the thermal imager readings can be written in the form

$$\begin{cases} \frac{\partial}{\partial \tau} T(x,\ \tau) = a_{st} \cdot \frac{\partial^2}{\partial X^2} T(x,\ \tau); \\ \lambda_{st\,1} \frac{\partial}{\partial X} T(x,\ \tau)|_{x=x_1} = 1.66 \cdot (1 + 10^{-3}(T_{1s} - 20)) \cdot \Delta T^{1/3}\left(T_1 - T_{pom}\right); \\ \lambda_{st\,2} \frac{\partial}{\partial X} T(x,\ \tau)|_{x=x_2} = \left(5.07v^{0.656} + 3.25e^{-1.91v}\right)(T_{vs} - T_2); \\ T(x,\ 0) = T_0; T_{pom} = 345 \cdot \lg(8 \cdot \tau + 1) + T_0; \\ \lambda = \frac{0.002899}{T_{vs}}; r(\lambda, T) = \frac{2\pi hc^2}{\lambda^5} \cdot \frac{1}{e^{\frac{hc}{\lambda k T_{vs}}} - 1}; \\ \frac{\Delta T}{T_2} = \frac{1}{4}\frac{\Delta \varepsilon}{\varepsilon}, \end{cases}$$

where v – the wind speed, m/s; T_{1s} – temperature of the inner surface of the wall, °C; ΔT – the difference in ambient temperatures inside the premise T_{pom} and T_{1s}, °C; ε, $\Delta\varepsilon$ – the radiation coefficient and its change when the temperature changes; h – Planck's constant (h = 6.62 • 10^{-34}, J · s); c – speed of light (c = 3 • 10^8, m/s); λ – wavelength, m; $r(\lambda, T)$ – spectral density of energy luminosity; T_{vs}, T_2 – ambient temperature outside the premise and outside wall temperature, °C.

In Figs. 1 and 2, according to (4), the dependences of the temperature in the section of the wall on time are given.

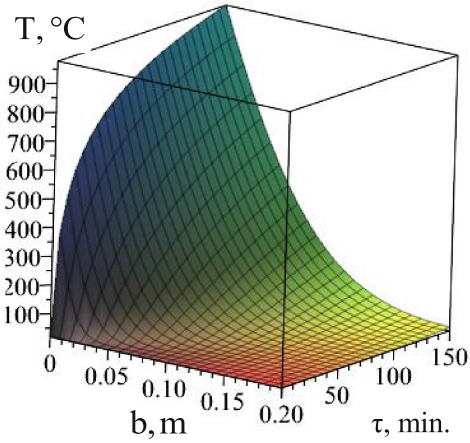

Fig. 1. Dependence of temperature in section of wall (b) on time (τ)

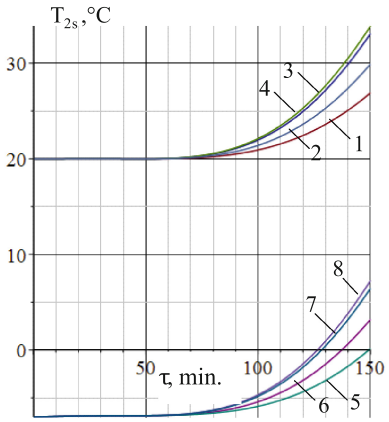

Fig. 2. Dependence of the temperature of the wall outer surface on time: 1, 5 for α_1 = 25 W/(m^{2}K); 2, 6 for α_1 = 50 W/(m^{2}K); 3, 7 for α_1 = 115 W/(m^{2}K); 4, 8 for α_1 = 150 W/(m^{2}K); 1, 2, 3, 4 for T_2 = 20°C; 5, 6, 7, 8 for T_2 = −20°C

It is established that up to an one hour of time, with high thermal resistance of the wall, there is almost no difference in the level of temperature on the outer surface of the wall. At the same time, the change of the mode of heat exchange in the premise, namely the coefficient of heat exchange by 100 ÷ 200% leads to an increase in the outside temperature by 12 ÷ 14%.

In Fig. 3 shows the dependence of the building walls surface temperature on the wind speed at different values of T_1 and the characteristics of the wall. Curves 2, 3, 4 are based on premise temperatures of 150 °C and 400 °C, which are reached within first minutes of fire.

The analysis of the figure shows that the temperature of the wall outer surface changes significantly at wind speeds less than 5 m/s. In addition, at high wind speeds (above 10 m/s), the difference in the wall temperature when changing T_1 and the wall thermal characteristics almost disappears. Thus, the application of local changes in the characteristics of the buildings enclosure structures does not make it possible to reliably determine the presence of fire in the premise.

A question how the wall thickness influences on the rate of its heating has been investigated and was answered that the temperature can change by almost 50% when the thickness of the wall changes by only 20 ÷ 25%.

Investigation of heat transfer through the double-glazed windows showed that at the moment of fire unit arrival, regardless the conditions of heat transfer, increasing temperature of windows would be sufficient to identify the fire according to the results of thermograms (the experiment was carried out using argon filled double glazing). This, in turn, will reduce the time to detect a fire.

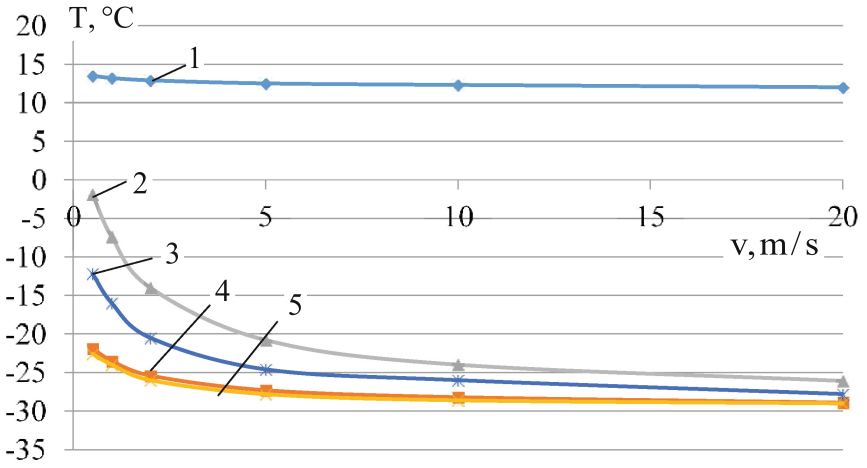

Fig. 3. Dependence of the building walls surface temperature on the wind speed at different values of T_1 and the characteristics of the wall: 1 – T_{1s}; 2 – T_{2s} (T_1 = 150 °C); 3 – T_{2s} (T_1 = 400 °C + 0,1 m ins.); 4 – T_{2s} (T_1 = 150 °C + 0, 1 m ins.); 5 – T_{2s}

There are the results of experimental studies on the temperature of building external structures in stationary conditions and in the conditions of fire, namely:

- experimental evaluation of the wall surface temperature during a fire;
- experimental evaluation of the wall surface temperature depending on the characteristics of the wall and wind speed;
- experimental evaluation of the temperature of the double-glazed windows under fire conditions.

The dependence of the theoretical and experimental values of the surface temperature and the relative errors depending on the wind speed under stationary conditions are shown in Fig. 4 ($\alpha_2 = 25$ W/(m^{2}K)). Photo of thermograms are shown in Fig. 5. During the experiment, the wind speed had a deviation of not more than 2 m/s, which is due to natural fluctuations in speed.

The analysis of Fig. 4 shows that the difference between theoretical values and experimental values does not generally exceed 20%, which is quite acceptable for this type of research.

At Fig. 6a the results of the experimental studies, namely the photo of the flame in the infrared spectrum, and Fig. 6b – view of this flame through the double glazing in the same spectrum. The figure shows that it is impossible to identify the flames through the glass. At the same time at Fig. 6c shows a photo of the glass from the inner surface from the effects of flames in the infrared spectrum.

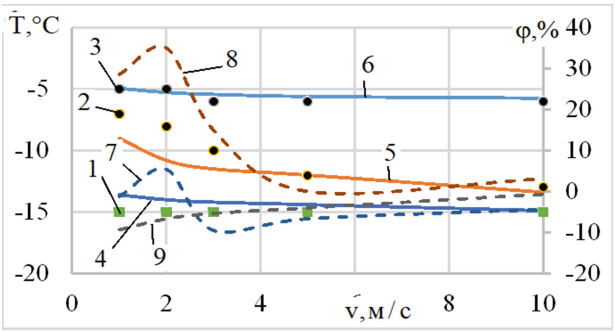

Fig. 4. Dependence of theoretical and experimental values of surface temperature and relative errors (φ) depending on wind speed: 1–3 – experimental data; 4–6 – theoretical; 7–9 – relative errors; 1, 4, 7 – ($T_2 = -15$ °C; 10 cm warming); 2, 5, 8 – ($T_2 = -15$ °C); 3, 6, 9 – ($T_2 = -6$ °C; 10 cm warming)

Fig. 5. Thermogram of the building surface

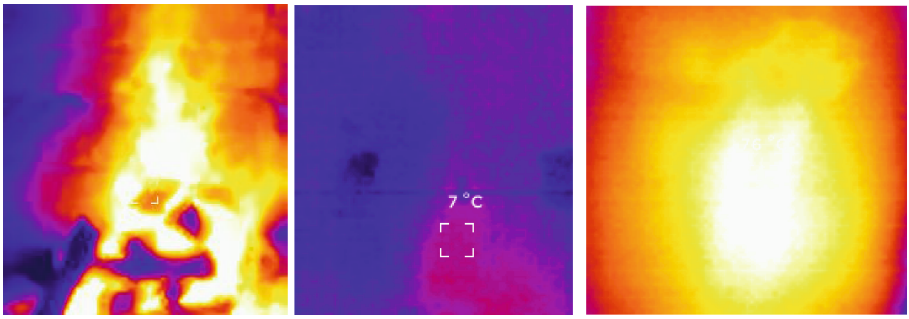

Fig. 6. Thermograms from the thermal imager: a – flame; b – thermogram of flame through glass; c – the heated side of the glass (after 2 min)

In this way, it was experimentally confirmed that it was impossible to detect a fire by passing the flame radiation through the double-glazed window at the initial stage of the fire. It is only possible to identify a fire while the window is warming.

The following was an experimental research of the glass unit temperature during a fire. At Fig. 7 shows the experimental values of the temperature and the range of theoretical temperature values that could have been at that time.

Areas 1 ($T_{2s0} = 20$ °C; $\alpha_2 \in [25; 50]$ W/(m^{2}K)) and 2 ($T_{2s0} = -20$ °C; $\alpha_2 \in [25; 50]$ W/(m^{2}K)) correspond to the possible theoretical temperature ranges, subject to fluctuations in wind speed and indoor temperature during a fire.

The temperature difference error, i.e. the change from the initial one, was estimated. As a result, it was found that the error does not exceed 35%.

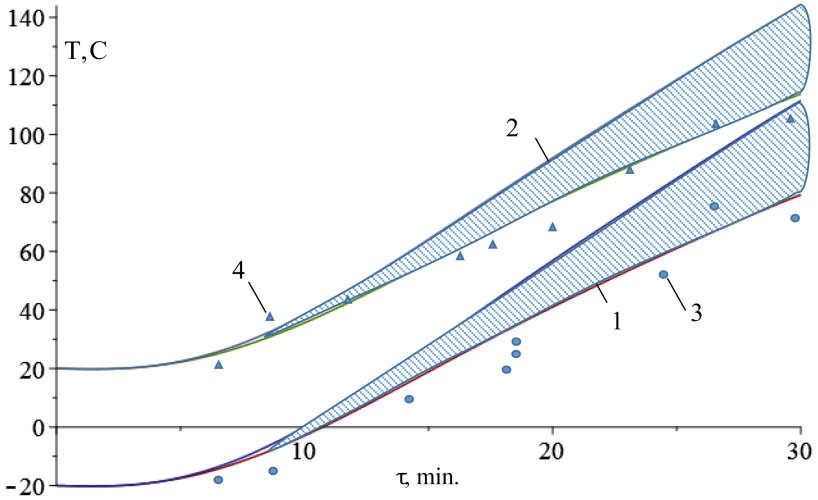

Fig. 7. Comparison of experimental and theoretical results of the double-glazed window temperature during a fire: 1, 2 – theoretical double-glazed window temperature ranges; 3, 4 – respectively experimental data on the glass unit temperature

2 Conclusions

As a result of work is further development a mathematical model using the equation of non-stationary thermal conductivity to describe the fire thermal effect on the readings of the thermal imager. The measurements of external structures temperatures during fires showed the adequacy of the mathematical model with an error of up to 35%, which indicates the possibility of its use in temperature estimation.

Experimentally it is shown that the flame identification with the help of the thermal imager through a double-glazed window at the initial stage of a fire is impossible due to the absorption of infrared radiation by the latter. It is possible to identify the fire only in the process of heating the double-glazed window.

Experimentally it has been studied the temperature of the double-glazed windows during the fires. It is estimated the error within the temperature difference, that is, the change from the initial temperature. As a result, it was found that the error does not exceed 35%.

References

1. Koshmarov YuA, Astapenko VM, Molchadskiy IS, Shevlyakov AN (1988) Termogazodinamika pozharov v pomeshcheniyakh (Thermo- and gasdynamics of Indoor Fires). Stroyizdat Publ., Moscow, 418 p
2. Drysdale D (1990) An Introduction to Fire Dynamics. Stroyizdat, 421 p
3. Molchadsky IS (2005) Fire in Structure. Fire prevention, Moscow, 456 p

Poster Abstracts

The Impact of Material Solutions on Fire Safety of Timber Frame Structures

Paweł Sulik(✉) and Bartłomiej Sędłak

Instytut Techniki Budowlanej, Zakład Badań Ogniowych, Ksawerów 21, 00611 Warsaw, Poland
p.sulik@itb.pl

Abstract. Due to its flammability, timber elements require solutions that increase the level of fire safety. Usually, this does not apply to the fire resistance range (load-bearing capacity R), where the cross-section of the element plays a decisive role, and properly designed, allows obtaining the appropriate fire resistance class. The situation is different in the range of reaction to fire and fire spread. Timber elements usually get a reaction to fire class D, however, in various material configurations, timber construction elements get a much higher class of reaction to fire, even B.

The article presents the results of the reaction to fire and fire spread tests of timber structures with different material solutions in the form of thermal insulation and claddings, and their impact on the fire safety of such solutions was given (Fig. 1).

Keywords: Fire safety · Fire spread · Reaction to fire · Timber elements

Fig. 1. Samples of 1800 × 2300 mm wood components during fire testing (fire spread).

L. Makovicka Osvaldova et al. (Eds.): WFS 2020, *Wood & Fire Safety*, p. 453, 2020.
https://doi.org/10.1007/978-3-030-41235-7

Properties of Flammable Materials in Passenger Cars Describing Their Fire Behavior

Petra Bursíková(✉), Romana Friedrichová, Libor Ševčík, Milan Růžička, and Jan Karl

Ministry of Interior of the Czech Republic General Directorate – Fire Rescue Service of the Czech Republic, Technical Institute of Fire Protection, S. Písková 42, 14301 Prague, Czech Republic
petra.bursikova@tupo.izscr.cz

Abstract. In passenger cars, there are a number of components that are made of flammable materials. For these materials, information on their material composition and fire technical characteristics is not available. The most represented brands of passenger cars in the Czech Republic were selected from which flammable materials were taken. First, material composition was described using infra-red spectroscopy. The heat resistance data on the cone calorimeter were measured. The heat release rate indicates the size of the fire hazard, expresses the rate of flammability of the materials, and can also serve as an important tool in modelling fire. Another determined fire characteristics was the flammability of materials. Flash-ignition temperature and spontaneous-ignition temperature give the possibility to predict at which ambient temperature the material will burn. It allows to back describe the likely behavior of the material under the given conditions. The differential scanning calorimetry method was used to describe the behavior of materials during heating. The DSC curve provides information on whether the material melts or decomposition, at what temperature and how much energy we need to supply. Knowledge of fire technical characteristics of flammable parts of the vehicle is therefore an important during investigating the causes of fires and the performance of state fire supervision. These data are also useful for mathematical modelling of fires.

Keywords: Passenger car · Fire technical characteristics · FTIR

L. Makovicka Osvaldova et al. (Eds.): WFS 2020, *Wood & Fire Safety*, p. 454, 2020.
https://doi.org/10.1007/978-3-030-41235-7

Experimental Study of the Combustion of a Single Biomass Particle

Acevedo Pahola, Angel Martinez, Lacour Corine, and Coppalle Alexis(✉)

Normandie University, INSA Rouen, UNIROUEN, CNRS, CORIA, 76000 Rouen, France
coppalle@coria.fr

Abstract. Biomass valorisation for energy production is considered as one of the best ways to overcome the petroleum's depletion, move forward in the environmental protection concerns, but also to provide the energetic request. The combustion of biomass is an efficient valorization pathway but it still requires fundamental knowledge. To go deeper, some authors use simulation analysis combined with experimental results where a good agreement is appreciated. In the same sense, the present study explores experimentally the combustion of a single biomass particle as woody pellets and wood. An experimental free-ventilated system is built with a cone calorimeter as radiative heat source in order to heat the particles. A weighing scale is used to measure mass degradation during combustion process, and a type-k thermocouple allows measuring the temperature evolution in the center of the particle. As a result, curves of temporal evolution of mass degradation and central temperature are acquired for each kind of particle. This allows to observe the three main phases of combustion process (particle drying, volatiles combustion, and char's combustion), besides a superposition of homogeneous and heterogeneous combustions phases. Considering that the elemental composition of woody pellet and wood particles are close, similar combustion phases are identified with different time steps (Fig. 1).

Keywords: Biomass · Combustion · Wood

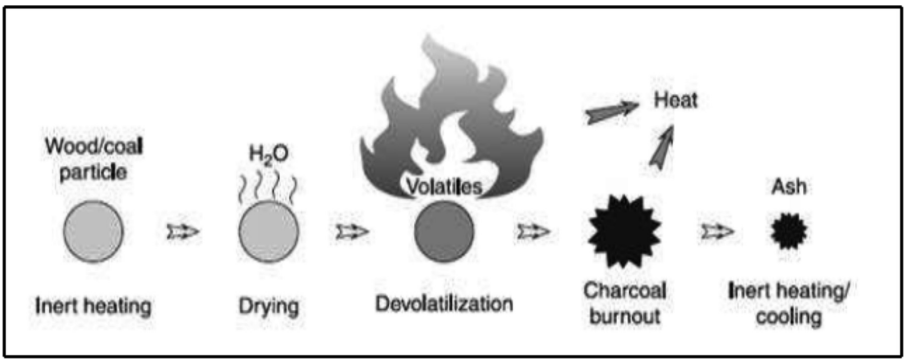

Fig. 1. Combustion stages of a single biomass particle (Rosendal et al. 2013).

L. Makovicka Osvaldova et al. (Eds.): WFS 2020, *Wood & Fire Safety*, p. 455, 2020.
https://doi.org/10.1007/978-3-030-41235-7

Research on Electrical Fault Beads Ignition Ability-a Potential Source of Wildland Fires

Huifei Lü, Jun Deng(✉), Lei Bai, Weifeng Wang, and Jingyu Zhao

School of Safety Science and Engineering, Xi'an University of Science and Technology (XUST), Xi'an, Shaanxi Province, People's Republic of China
dengj518@xust.edu.cn

Abstract. Wildland fire is a serious problem in numerous areas of the world. The problem [1] is an increasing concern, especially electrical fault arc beads ignite the forest aspect, because of the damage it causes to the buildings, environment, social development, and human health. An arc is a high-temperature luminous electric discharge that forms across a gap between two bodies. Temperatures within the arc are in the range of several thousand degrees. For a fire, the arc beads have a stronger ignition ability and the process is more complicated, which ignition divides three process [2]: The generation of the beads and their thermochemical state; their flight by plume lofting and wind drag and the particle thermo-chemical change during the flight; finally, the particle lands ignite the fuel, and the sustained ignition and burning of the combustible material. This work examines how fuel dryness effect the ability of the fuel to be ignited by an arc bead. A fault arc bead was generated by using self developed, which has different energy. Fuels were prepared out of alpha cellulose materials (same composition as wood), which has various moisture content. The relationship among the arc energy, the bead diameter, the ignition phenomenon is indicated that trend of approximate quadratic function in ignition area. Moreover, before 175 J, as the trigger energy increased, the size of the ignitable bead gradually decreased. But, after 175 J, the results in contrast. The non-combustible region is approximately a cubic function. The diameter of the bead decreases first, then increases, and then stabilizes. In addition, the beads with diameter more than 3 mm are more prone to fire. Therefore, proper energy and diameter are key parameters for evaluating wildland fires.

Keywords: Forest · Temperature · Particle · Fuel

References

1. National Fire Protection Association (2017) NFPA 921: Guide for fire and explosion investigations. National fire protection association, pp 921–929
2. Fernandez-Pello C (2017) Wildland fire spot ignition by sparks and firebrands. Fire Saf J 91:2–10

L. Makovicka Osvaldova et al. (Eds.): WFS 2020, *Wood & Fire Safety*, p. 456, 2020.
https://doi.org/10.1007/978-3-030-41235-7

Heat Flux from Wood Filled Transport Package Impact Limiter Under Fire Conditions

Martin Feldkamp(✉), Marina Erenberg, Marko Nehrig, Claus Bletzer, André Musolff, and Frank Wille

Bundesanstalt Für Materialforschung Und - Prüfung (BAM), Safety of Transport Containers, Berlin, Germany
martin.feldkamp@bam.de

Abstract. Packages for the transport of high-level radioactive material must withstand severe hypothetical accidents. Regulatory test conditions shall cover these severe accident conditions and consist of mechanical tests and a following thermal test. To withstand the mechanical tests heavy weight packages are often designed with impact limiters consisting of wood encapsulated in steel sheets. The thermal test is defined precisely in the IAEA-regulations [1] as a 30 min fully engulfing 800°C fire. After the fire phase a pre-damaged impact limiter might continue burning or smouldering and influence the cask thermal behaviour with its energy release. The energy transferred from the impact limiter to the cask is of importance for the safety of transport packages. A full-scale fire test with an impact limiter of 2.3 m in diameter and filled with spruce wood was designed and performed [2, 3]. The impact limiter continued burning for 3 days. Energy transfer and temperature measurements were performed (Fig. 1).

Keywords: Fire testing · Large scale testing · Spruce wood

Fig. 1. 30 min propane gas fire engulfment of wood filled impact limiter in the BAM TTS fire test facility.

L. Makovicka Osvaldova et al. (Eds.): WFS 2020, *Wood & Fire Safety*, pp. 457–458, 2020.
https://doi.org/10.1007/978-3-030-41235-7

References

1. International Atomic Energy Agency (IAEA); Regulations for the Safe Transport of Radioactive Material, 2018 Edition. Specific Safety Requirements No. SSR-6 (Rev. 1), Vienna (2018)
2. Feldkamp, M et al: Behavior of wood filled impact limiters during the IAEA thermal test. In: Proceedings-CD, ASME 2017 Pressure Vessels & Piping Conference (PVP 2017), Waikoloa, Hawaii, USA
3. Erenberg, M et al: Experimental investigations of the burning behaviour of transport package impact limiters and of fire spread impact onto the cask. In: Proceedings of the ASME 2018 Pressure Vessels and Piping Conference, Prague, Czech Republic

Gaseous and Particulate Emissions of a Feed-Pellet Domestic Boiler

Angel Martinez(✉), Corine Lacour, Jérôme Yon, and Alexis Coppalle

INSA Rouen, CORIA Laboratory, Normandie University, 76000 Rouen, France
alexis.coppalle@coria.fr

Abstract. The goal of this study is to investigate the influence of the feeding mode on the particulates and gaz emissions from a domestic boiler. Different feeding operating conditions are considered (pulsed and continuous alimentations) in a drop-feed-pellet boiler (20 kW). Gaseous and particulate emissions were sampled at the vicinity of the boiler outlet. Mass concentrations were measured with a PPS and particle sizes thanks to a Scanning Mobility Particle Sizer (SMPS and ELPI). Finally, a gas analyzer (TESTO) is used. Results show an increase of the carbon monoxide emissions for pulsed feeding mode between 400–800 ppm, whereas the maximum pics observed for the continuous feeding were 100–200 ppm. The typical size for particles appears to be in the range 50–60 nm, i.e ultrafine soot particles, for all the operating conditions (Fig. 1).

Keywords: Biomass · Combustion · Pollutant emissions

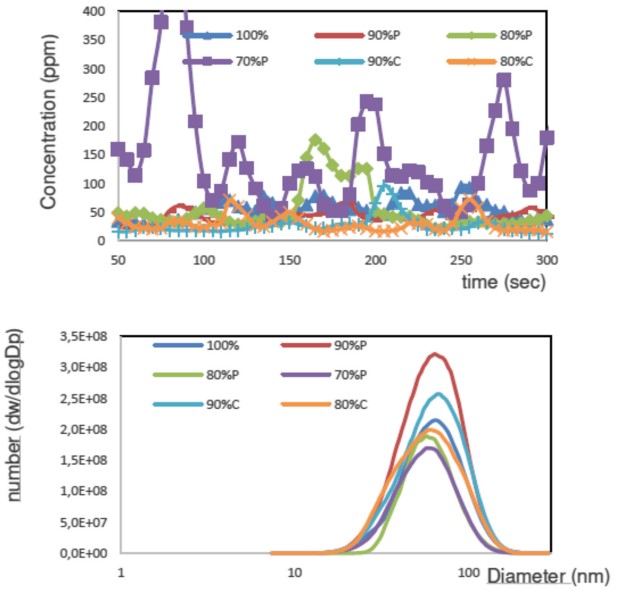

Fig. 1. For different pellet feeding (C continuous, P pulsed), Upper part: CO concentrations, lower part: particle sizes

L. Makovicka Osvaldova et al. (Eds.): WFS 2020, *Wood & Fire Safety*, p. 459, 2020.
https://doi.org/10.1007/978-3-030-41235-7

Study on Design Fire Protection Elements in Wooden Facades

María Pilar Giraldo[2(✉)], Ana María Lacasta[1], and Andreu Segura[1]

[1] Barcelona School of Building Construction (EPSEB), Universitat Politècnica de Catalunya, Av. Dr. Marañón, 44-50, 08028 Barcelona, Spain
[2] Forest Science and Technology Centre of Catalonia (CTFC), Catalan Institute of Wood (INCAFUST), Ctra. Sant Llorenç de Morunys, Km 2, Solsona, 25280 Lleida, Spain
Pilar.giraldo@incafust.cat

Abstract. During the last years, fire propagation on facades has been awakening a growing interest. Fires such as it did in the Grenfell tower in London (2017) have highlighted the risk involved, among other aspects, because the use of combustible facade claddings [1, 2].

Wood is a material highly resistant to fire when used in structural elements with enough cross section. However, it is a combustible and flammable material with classification D-s2, d0 according to the Euroclasses of reaction to fire. For this reason, in several European countries, building regulations restrict the use of wood as a facade cladding material. The Spanish technical code of buildings (CTE) is not excessively restrictive with combustible coatings, allowing its use in buildings up to 18 m. However, the use of wood claddings is significantly low compared to other European countries, mainly due to the distrust generated by its combustibility.

The application of passive protection measures, through elements linked to the facade design, can minimize the risk of fire propagation [3]. In this study, fire dynamics simulation techniques (FDS) are used to evaluate the influence of the size and location of elements such as eaves and protection bands in fire propagation through the window openings by "leapfrog" effect.

Keywords: Combustible cladding · Fire dynamics simulation · Fire performance on façade · Flame spreading control · Wooden façades · Configuration of the façades

References

1. Martin Y, Eeckhout, S, Lassoie L, Winnepenninckx E, Deschoolmeester B (2017) Fire safety of multi-storey building facades. Belgian Building Research Institute (BBRI). D/2017/0611/12
2. Sans J, et al (2019) Estudio sobre la Problemática Generada por la Propagación de Incendios en Fachadas de Edificios. Col·legi/Associació d'Enginyers Industrials de Catalunya
3. Oleszkiewicz. I (1991) Vertical separation of windows using spandrel walls and horizontal projections. Fire Technol 27:334–340

L. Makovicka Osvaldova et al. (Eds.): WFS 2020, *Wood & Fire Safety*, p. 460, 2020.
https://doi.org/10.1007/978-3-030-41235-7

Evaluation of the Link Between Pre-fire Fuel Estimates and Fire Radiative Energy for Large Fires in Portugal

Célia M. Gouveia[1,2(✉)], Catarina Alonso[2], and Patrícia Páscoa[1,2]

[1] Instituto Dom Luiz, Faculdade de Ciencias da Universidade de Lisboa, Campo Grande, Edifício C8, Piso 3, 1749-016 Lisbon, Portugal
cmgouveia@fc.iul.pt
[2] Instituto Portugues do Mar e da Atmosfera, Lisbon, Portugal

Abstract. Climate conditions and land use change or a combination of both conditions are linked with the recent history of recurrent fires over Mediterranean regions in general and in particular in Portugal. Wet and mild winters, together with dry and warm summers, favour the growth of vegetation and its subsequent low moisture content, increasing fuel availability. The assessment and management of fuel loads are essential to understand and minimize fire risk. The structural risk depends on the type of available fuel and on the age of vegetation. Therefore, reducing fuel loads is often required to mitigate fire severity. Active fire observations of fire radiative power (FRP) and derived Fire Radiative energy (FRE) have been shown to be correlated to rates of biomass combustion. The Meteosat FRP-PIXEL product is delivered in near real-time by the EUMETSAT Land Surface Analysis Satellite Applications Facility (LSA SAF), since 2004 with 15- min temporal resolution. We propose to do the first assessment, for Portugal, of the relationship between Fire Radiative Energy (FRE) per fire and pre-fire fuel load estimates, as obtained from Dry Matter Productivity (DMP), disseminated by Copernicus Global Land Service (CGLS) at 1 km spatial resolution since 1999. The analysis is performed for the main land cover types in Portugal that show high sensitivity to wildfires. The severest wildfire events in Portugal, namely the fires of 2005, 2012 and 2017 will be analysed in detail and the obtained results related with soil moisture, fuel type and fire size.

Keywords: Fire radiative power · Fire Radiative Energy · Pre-fire fuel · Wildfire

L. Makovicka Osvaldova et al. (Eds.): WFS 2020, *Wood & Fire Safety*, p. 461, 2020.
https://doi.org/10.1007/978-3-030-41235-7

Reduction of Flammability of Synthetic and Natural Composite Materials Based on Formaldehyde-Containing Bonding Agents

Anatolii Chernov[1(✉)], Andrey Shmakov[1], Oleg Korobeinichev[1], Munko Gonchikzhapov[1], and Valeriy Tatarenko[2]

[1] Voevodsky Institute of Chemical Kinetics and Combustion, Siberian Branch, Russian Academy of Sciences, Novosibirsk, Russia
[2] Siberian State University of Geosystems and Technologies, Novosibirsk, Russia
chernov@kinetics.nsc.ru

Abstract. A study has been held to compare flammability of chipboard samples with carbamide formaldehyde or amino formaldehyde resin as binder and with additives of inorganic (ammonium polyphosphate) and organic flame retardants and modifiers (oxidized polysaccharides). To determine the flammability of the chipboard samples under study, the limiting oxygen index method (LOI) was applied. Dependence of the LOI of the chipboard samples produced under laboratory conditions on the concentration of the additives of flame retardants and modifiers has been investigated. The results obtained have shown that introducing into the composition of chipboards raises the LOI to more than 40%, which should significantly improve the FST (Fire, Smoke, Thermal) parameters of the materials of this type.

Keywords: Limiting oxygen index · Flammability · Composite materials · Chipboard materials · Fire safety · Flame retardant · Modified polysaccharides · Ammonium polyphosphate

L. Makovicka Osvaldova et al. (Eds.): WFS 2020, *Wood & Fire Safety*, p. 462, 2020.
https://doi.org/10.1007/978-3-030-41235-7

Components Decisive for the Failure of Chosen Fireproof Separating Elements

Daniel Izydorczyk(✉), Bartłomiej Sędłak, and Paweł Sulik

Fire Research Department, Building Research Institute, Warsaw, Poland
d.izydorczyk@itb.pl

Abstract. Technical assessment of timber fire doors, in terms of functional and operational properties, once they are installed in the building, does not differ from the assessment of the normal door. It is not a complicated operation, and indeed we do it daily by opening and closing of these elements. However, we can not assess the most important parameter of these products, from the safety point of view, which is a non-invasive confirmation of the declared fire resistance class. Appearing in the last period problems with this kind of products are confirmed by the control tests of the doors dismantled from the building or purchased on the market. Number of negative test results indicates that the problem is not individual, but rather related to a substantial part of the market, which would mean that in the number of buildings in Poland, there could be a problem with the installed fire doors, which has an emergency condition. The paper presents the useful from a practical point of view elements and procedures for investors and persons receiving the object, enabling more accurate verification of the declaration of fire doors in relation to the reality. Key elements that can be verified, check or estimate was discussed. The most common irregularities, defects and the way how to detect them and eliminate was presented (Fig. 1).

Keywords: Fireproof separating elements · Fire doors · Fire integrity · Thermal insulation

Fig. 1. Example of improper hardware (on the left) and lack of suitable intumescent seals (on the right).

L. Makovicka Osvaldova et al. (Eds.): WFS 2020, *Wood & Fire Safety*, p. 463, 2020.
https://doi.org/10.1007/978-3-030-41235-7

Flame-Retardant and Smoke-Suppressed Silicone Foams with La/Mg/Zn/al Layered Double Hydroxide and Zinc Borate

Furu Kang[1,2(✉)], Jun Deng[1,2], and Jingyu Zhao[1,2]

[1] School of Safety Science and Engineering, Xi'an University of Science and Technology (XUST), Xi'an 710054, People's Republic of China
[2] Shaanxi Key Laboratory of Prevention and Control of Coal Fire, XUST, Xi'an 710054, People's Republic of China
kangfuru@stu.xust.edu.cn

Abstract. Silicone foams (SiFs) are high-performance materials but can combust and release choking smoke in a fire. A flame-retardant system for SiFs was successfully obtained through a synergistic combination of La/Mg/Zn/Al layered double hydroxide (La/Mg/Zn/Al -LDH) and zinc borate (ZB). The structure and performance of La/Mg/Zn/Al-LDH and ZB were characterized by Fourier transform infrared spectroscopy (FTIR), X-ray diffraction (XRD), scanning electron microscopy (SEM), and energy dispersive spectrometer (EDS). The smoke suppression, flame retardance, and thermal stability of SiFs with La/Mg/Zn/Al-LDH and ZB were tested using the limiting oxygen index (LOI), UL-94 test, smoke density test, cone calorimeter, and thermogravimetry. The peak heat release rate reduction of SiFs containing 18 wt% La/Mg/Zn/Al-LDH reached 26%. After incorporating 2 wt% ZB in the SiFs/La/Mg/Zn/Al-LDH system, the flame retardant property was further improved. Specifically, it could achieve the UL-94-V0 rating (3 mm thick), the LOI increase to 32.4%, and maximum smoke density decrease by 40%. Furthermore, thermogravimetric analyzer results indicated that the addition of La/Mg/Zn/Al-LDH and ZB could improve the weight loss and the char formation of the materials significantly.

Keywords: Silicone foams · Flame retardancy · Smoke suppression · Thermal stability · La/Mg/Zn/Al layered double hydroxide · Zinc borate

L. Makovicka Osvaldova et al. (Eds.): WFS 2020, *Wood & Fire Safety*, p. 464, 2020.
https://doi.org/10.1007/978-3-030-41235-7

New Method for Mineralization of Wood for Improved Fire Properties

Andreja Pondelak(✉), Rožle Repič, Tomaž Pazlar, Nataša Knez, Friderik Knez, and Andrijana Sever-Škapin

Slovenian National Building and Civil Engineering Institute, Dimičeva 12, 1000 Ljubljana, Slovenia
andreja.pondelak@zag.si

Abstract. Wood is an important engineering material due to its remarkable properties. Flammability is one of its main drawbacks, which can be improved by different approaches, like use of fire-retardants. Since some of the fire-retardants are at least partially toxic and subject to stringent restrictions, the future lies in use of nontoxic and "eco-friendly" fire-retardants. One of the most promising methods is incorporation of calcium carbonate into the wood's structure (i.e. mineralized wood). Carbonates have been considered as "green" fire-retardants because they release non-flammable gases such as CO_2 and H_2O upon endothermic decomposition. The research group from Slovenian National Building and Civil Engineering Institute has proposed a new method for mineralization of wood to improve its resistance to fire which has been recently patented [1]. New method enables us fully effective mineralization of wood, through impregnation with solution of metal acetoacetates which transforms into $CaCO_3$. Incorporation of $CaCO_3$ in the spruce is presented in Fig. 1. Improvement in fire resistance was shown and is presented in the abstract entitled *Fire properties of beech wood mineralized by a novel mineralization technique* by R. Repič et al.

Keywords: Acetoacetate · Calcium carbonate · Fire retardant · Mineralization

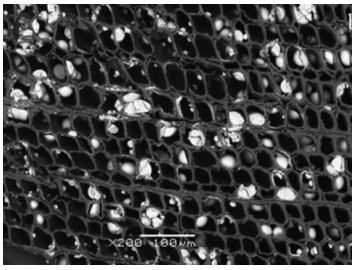

Fig. 1. SEM image of spruce $CaCO_3$ mineralized with a new method.

L. Makovicka Osvaldova et al. (Eds.): WFS 2020, *Wood & Fire Safety*, pp. 465–466, 2020.
https://doi.org/10.1007/978-3-030-41235-7

Reference

1. Pondelak, A, Sever Škapin, A, Knez, N, Škrlep, L, Knez, F, Pazlar, T, Legat, A: Postopek mineralizacije lesa z uporabo raztopin acetoacetatov za izboljšanje bistvenih lastnosti lesa : patentna prijava št, p, 201900260. Urad Republike Slovenije za intelektualno lastnino, Ljubljana (2019)

Fire Properties of Beech Wood Mineralized by a Novel Mineralization Technique

Rožle Repič(✉), Andreja Pondelak, Nataša Knez, Friderik Knez, and Andrijana Sever-Škapin

Slovenian National Building and Civil Engineering Institute, Dimičeva 12, 1000 Ljubljana, Slovenia
rozle.repic@zag.si

Abstract. Wood is one of the most important materials, used in construction. As a material, wood is simple to work with and has good mechanical properties in relation to its mass. However wood is prone to burning, which is its weakness.

In this work we present improved fire-resistance of mineralized wood by a new method - impregnation with solution of metal acetoacetate (see abstract entitled *New method for mineralization of wood for improved fire properties* by Pondelak et al.).

We mineralized beech (*Fagus sylvatica*) wood, the most common Slovenian deciduous tree species. Samples were prepared 100 mm × 100 mm × 10 mm in size, without visual defects. Samples were vacuum/pressure impregnated with the uptake of dry $CaCO_3$ of 8,8% ± 0,5%. For testing improvement of reaction to fire cone calorimetry (Fire Testing Technology) with 50 kW/m^2 of incident heat flux was used.

Mineralised wood ignites later in regard to untreated wood and less heat is produced during fire. Smoke emissions are reduced also. Heat release profiles (Fig. 1) shows, that mineralized wood ignites later than untreated. That is due to better thermal conductivity of mineralised wood. Fire growth rate index (FIGRA) is reduced substantially. When burning, $CaCO_3$ releases carbon dioxide (CO_2), which cools combustible gases and dilutes them, some water (H_2O) is also released, which cools the fuel and combustible gases even more.

Keywords: Fire · Mineralization · Wood · Wood protection

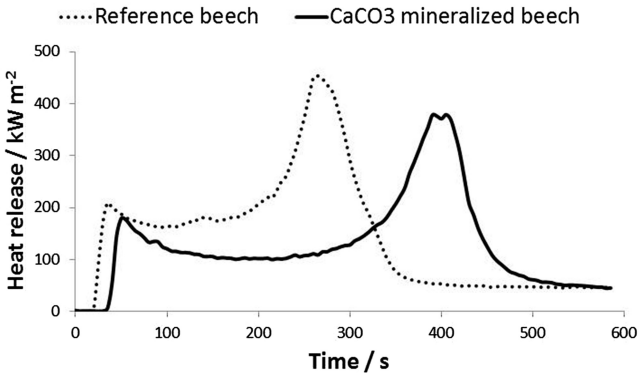

Fig. 1. Heat release rate of $CaCO_3$ mineralized beech wood.

L. Makovicka Osvaldova et al. (Eds.): WFS 2020, *Wood & Fire Safety*, p. 467, 2020.
https://doi.org/10.1007/978-3-030-41235-7

Flammable Load as a Trigger of Fire After a Road Accident Resulting in Death from Burning

Martin Skripko(✉)

University of Zilina/Tapír s.r.o, ÚZVV, Zilina, Slovakia
martinskripko@gmail.com

Abstract. On 23.8.2017 during the night hours, a traffic accident occurred in which one person burned. The cause of the traffic accident was a bad driving technique. During the expertise of the traffic accident, uncertainty was found. It was the beginning of a fire in the rear part of a diesel vehicle and it was not clear why a diesel car had ignited without a clear cause. The finding of the traffic accident showed that there was a presence of a flammable substance. It was determined by using a specially trained police dog. The dog was used to detect flammable liquids at the right rear axle. The handler said that the dog would not identify diesel. Further, the investigation found the presence of colour sprays. The leakage of the colour in the trunk of the car had caused the fire.

Keywords: Traffic accident · Diesel · Burning

L. Makovicka Osvaldova et al. (Eds.): WFS 2020, *Wood & Fire Safety*, p. 468, 2020.
https://doi.org/10.1007/978-3-030-41235-7

Influence of the Convection Coefficient for the Modelisation of a Fire Test on a Nuclear Transport Package

Norma Verbrugghe(✉), Gaël Desroches, Marianne Moutarde, and Florence Gauthier

Institut de Radioprotection et de Sûreté Nucléaire (IRSN), PSN-EXP/SSTC, Fontenay-aux-Roses, Île-de-France, France
norma.verbrugghe@irsn.fr

Abstract. Nuclear transport packages are used for the protection and transportation of nuclear material by road, train or boat. Therefore, the packages containing the most dangerous materials have to go through many reglementary tests, including a fire test of 30 min at 800 °C.

To demonstrate the safety of the package, such a test may be performed on a model of the package, or numerically, with boundary conditions representative of the fire (surface emissivity, environment temperature, convection coefficient…).

The guidelines of the regulation give a value of the convection coefficient during the fire, 10 $W/m^2/K$. Recent research [1] suggests that this value may not be representative of such a fire, and may have to be scaled up. But does a higher convection coefficient necessarily have an impact on the temperatures of the package? In order to answer that question, IRSN has performed calculations on a dummy transport package. This package, 7 m high and a 3 m diameter, is used for the transportation of nuclear materials with a high thermal power.

To attest (or contest) the influence of the convection coefficient, this coefficient will take its value within a range from 0 (no convection) to 80 $W/m^2/K$. The temperature in the package during the fire phase, as well as during the cooling phase which follows the fire, will be observed and the influence of the convection coefficient will be analysed.

Keywords: Convection · Fire · Nuclear safety · Package

Reference

1. Feldkamp M, Quercetti T, Wille F (2019) Fire reference test for IAEA package thermal testing in a propane gas fire test facility PATRAM 2019, New Orleans, LA, USA

L. Makovicka Osvaldova et al. (Eds.): WFS 2020, *Wood & Fire Safety*, p. 469, 2020.
https://doi.org/10.1007/978-3-030-41235-7

Establishment of Local-Scale Weather Forcing Conditions to Iberia's Largest Fires

Inęs Vieira[1(✉)], Ana Russo[1], Ricardo M. Trigo[1,2], and Célia M. Gouveia

[1] Instituto Dom Luiz, Faculdade de Ciencias da Universidade de Lisboa, Campo Grande, Edifício C8, Piso 3, 1749-016 Lisbon, Portugal
[2] Instituto Portuguęs do Mar e da Atmosfera, Lisbon, Portugal
inesv7l4@gmail.com

Abstract. The Mediterranean region is characterized by frequent summer wildfires which represent an environmental and socioeconomic burden. Some Mediterranean countries are particularly prone to Large Fires (LF), namely Portugal, Galicia (Spain), Greece, and southern France. In this study, we identify summer LF (June-September) for fifty-four provinces of the Iberian Peninsula (IP) according to their local-scale weather conditions and to drought conditions as measured by two fire weather indices (Duff Moisture Code and Drought Code).

A cluster analysis method was enforced to establish a limited set of Fire Weather Types (FWT), each characterized by a combination of meteorological conditions leading to a better understanding of the relationship between meteorological drivers and fire occurrence. For each province, two significant FWT were identified. One dominated by high positive temperature anomalies and negative humidity anomalies (FWT1), and the other by intense zonal wind anomalies (FWT2) with two distinct subtypes in Iberia (FWT2_E and FWT2_W). Consequently, three distinct regions in the IP are identified: (1) dominated by FWT1, which is responsible for the largest amount of area burned in most of central-West provinces of Iberia; (2) the regions where the FWT2_E, associated with east winds is predominant, which are concentrated in the Northwest regions of the IP and the (3) regions where second subtype dominates, related with west winds (FWT2_W) in the easternmost provinces of the peninsula. Furthermore, it was possible to verify that for each of the three regions the influence of the variables under study varies at different timescales.

This study reinforces the importance of studying the problem associated with LF for regions where similar conditions were verified regardless the national borders. Acknowledgements: This work was supported by national funds through FCT (Fundação para a Ciência e a Tecnologia, Portugal) under project IMPECAF (PTDC/CTA-CLI/28902/2017). The authors also thank Miguel M. Pinto for extracting data.

Keywords: Large fire · Fire weather types · Duff moisture code · Drought code

L. Makovicka Osvaldova et al. (Eds.): WFS 2020, *Wood & Fire Safety*, p. 470, 2020.
https://doi.org/10.1007/978-3-030-41235-7

Preparation and Property of Microcapsules for Fire Prevention

Kai Wang(✉), Yunzhong He, Jun Deng, and Furu Kang

Xi'an University of Science and Technology,
College of Safety Science and Engineering, Xi'an, Shaanxi, China
wangk912@xust.edu.cn

Abstract. Ammonium phosphate is one of excellent flame-retardant and halogen-free materials, but easy to absorb moisture and turn unstable. Microcapsule, a new fire preventing and controlling material, was prepared by the situ polymerization method, in which ammonium phosphate was core material and melamine and formaldehyde were wall materials. In this paper, microcapsules were tested to identify characterization of the appearance and thermal stability by SEM, FTIR and TG methods. The experiment results showed that characteristic absorption peak of ammonium phosphate and melamine formaldehyde resin could be found from microcapsule. The thermal decomposition process of microcapsule in the air atmosphere was different from that of ammonium phosphate. By contrast of ammonium phosphate, the mass loss ratio of microcapsule is lower before 300°C, because of the stability of wall material. After 300°C, wall and core materials all participated in reactions and pyrolyzed, the mass loss ratio of microcapsule is higher. The results showed that the thermal stability of the microcapsule is better at low temperature which could be used in fire prevention materials (Fig. 1).

Keywords: Ammonium polyphosphate · Microcapsule · Fire prevention

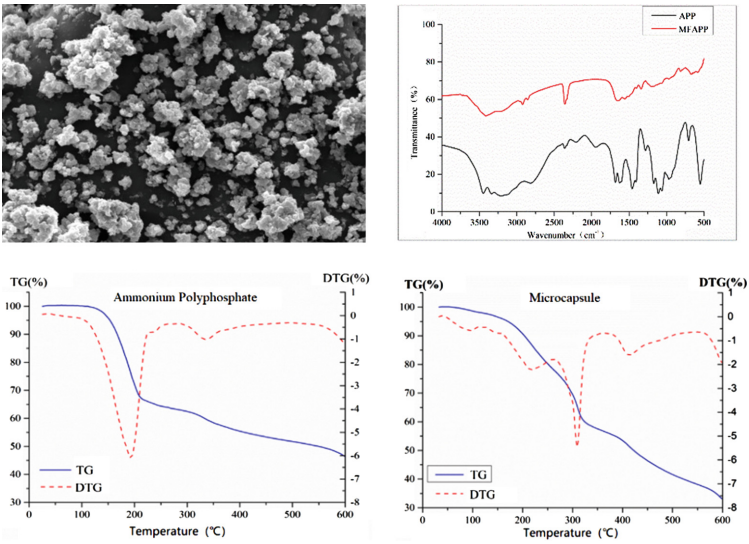

Fig. 1. SEM, FTIR and TG analysis results

L. Makovicka Osvaldova et al. (Eds.): WFS 2020, *Wood & Fire Safety*, p. 471, 2020.
https://doi.org/10.1007/978-3-030-41235-7

Experimental Study of Flame Height of Double Oil Tank Fires Under Different Lip Heights and Distances

Ruowen Zong(✉)

State Key Laboratory of Fire Science,
University of Science and Technology of China, Hefei, Anhui 230026, China
zongrw@ustc.edu.cn

Abstract. The combustion behavior of double oil tank fires will be influenced by its interaction of flames. This paper presents the experiments to investigate the evolution of the visible flame height of double oil tank fires under different diameters, lip heights and distances. The experimental results show that the visible flame height decreases with the increase of the lip height. The visible flame height increases with the increase of the tank distance without merging while the merging flame height increases significantly. The model of the visible flame height of double oil tanks fire has been proposed, which considered the tank diameter, lip height, and tank spacing.

Keywords: Double oil tank fires · Flame height · Tank spacing

L. Makovicka Osvaldova et al. (Eds.): WFS 2020, *Wood & Fire Safety*, p. 472, 2020.
https://doi.org/10.1007/978-3-030-41235-7

Fire Safety Evaluation on Cultural Relics in Shaanxi, China

Jiajia Song, Jingyu Zhao(✉), Kai Wang, and Jun Deng

College of Safety Science and Engineering,
Shaanxi Key Laboratory of Prevention and Control of Coal Fire,
Xi'an University of Science and Technology, Xi'an 710054, Shaanxi, China
songjiajia07@sina.com

Abstract. Hierarchical management and control of fire prevention on buildings of cultural relics had an extraordinary necessity. For the importance on fire safety of buildings of cultural relics, this paper analyses the potential dangers and fire characteristics of the buildings. Combined with the existing building fire prevention code, a qualitative evaluation method based on the nature of use, preventive ability, control conditions and hazard degree were established. The cultural relics were selected in Yan'an, Shaanxi, China, in which carried out the fire safety assessment. The degree of use nature was determined by building type and personnel factor. The degree of preventive ability was captured by analyse the combustion performance, fire prevention zone, and building height.

Moreover, the control condition degree was achieved by calculate the fire prevention spacing, firefighting lane and potential danger, and the hazard degree was divided by the importance of the relic's buildings.

Keywords: Fire prevention · Potential dangers · Fire safety · Preventive ability · Control condition · Hazard degree

L. Makovicka Osvaldova et al. (Eds.): WFS 2020, *Wood & Fire Safety*, p. 473, 2020.
https://doi.org/10.1007/978-3-030-41235-7

Fire Tests of CLT Specimen Protected by Intumescent Paint

Lars Sørensen(✉) and Frank Markert

Department of Civil Engineering, Technical University of Denmark (DTU), Kgs. Lyngby, Denmark
Lsso@byg.dtu.dk

Abstract. Fire tests of CLT specimen protected by water based intumescent paint designed for wood are conducted at DTU FireLab. The tested CLT was 40 mm thick of dimension 250 · 250 mm. The intumescent paint is applied in one to four layers given different layer thicknesses on the specimen. Additionally, a protecting topcoat layer is added for half of the tests as it is recommended by the manufacturer to protect the coating from water and weather conditions. The treated specimen are exposed to different heat radiations in a H-TRIS experimental setup, which originally was build to mimic furnace tests, but also has been applied to coating systems [1, 2]. The time to ignition and the charring rate inside the CLT was determined by thermocouples using the 300°C temperature criterion for the on-set of wood charring. The results were compared to literature values. It was found that the observed average charring rate was about 1 mm/min comparable to similar literature values for CLT, but larger than the recommended charring rate of 0.63 mm/min indicated in the Eurocodes.

It is found that intumescent paint coatings applied on wood provides passive fire protection to CLT, and the coatings ability to decrease the pyrolysis rate substantially. Furthermore, the time to ignition of the wood is increased. It is found that the protecting topcoat has some influence on the performance of the intumescent coatings.

The experiments described here have been conducted by J. A. Wolters as part of his Master thesis on Experimental Analysis of Fire Properties using H-TRIS and PTHFM, January 2020, Technical University of Denmark. His work is greatly acknowledged.

Keywords: CLT · Fire test · Intumescent paint on wood

References

1. Elliott A, Temple A, Maluk C, Bisby L (2014) Novel testing to study the performance of intumescent coatings under non-standard heating regimes. Fire Saf Sci 11:652–665
2. Lucherini A, Abusamha N, Segall-Brown J, Maluk C (2018) Experimental study on the onset of swelling for thin intumescent coatings. J Phys: Conf Ser 1107:032017

L. Makovicka Osvaldova et al. (Eds.): WFS 2020, *Wood & Fire Safety*, p. 474, 2020.
https://doi.org/10.1007/978-3-030-41235-7

Fire Resistance of Wooden Panels with Retarded Clay Plaster

Radovan Gracovský, L'udmila Tereňová(✉), and Anna Danihelová

Department of Fire Protection, Technical University in Zvolen, Zvolen, Slovakia
terenova@tuzvo.sk

Abstract. The fire resistance test of three wooden structures was carried out in a certified testing room. The constructions consisted of a wooden frame of external wooden cladding, ecological-based thermal insulation (cork, hemp insulation and wood-fibre board). OSB board with 4–5 mm clay plaster was applied from the inside. The plaster was modified with other inorganic materials to increase the fire resistance. In addition to classical fire resistance measurements, thermocouples were also applied in the area of construction sample. All three samples withstood under test conditions according to a standard fire resistance curve of time of 120 min. According to temperatures, best results came for cork followed by wood-fibre board and worst for cannabis insulation.

Keywords: Fire testing · Fire resistance · Wooden structure

L. Makovicka Osvaldova et al. (Eds.): WFS 2020, *Wood & Fire Safety*, p. 475, 2020.
https://doi.org/10.1007/978-3-030-41235-7

New Type Fire-Retardant for Various Wood Products

Jussi Ruponen[1,2(✉)] and Jari Kukkonen[1,2]

[1] Palonot Oy, Espoo, Finland
[2] Department of Bioproducts and Systems, Aalto University, Espoo, Finland
jussi.ruponen@palonot.com

Abstract. A novel fire retardant Palonot F1, launched by Palonot Oy, approaches fire retardation with chemistry different from the conventional solutions. The patented technology of Palonot F1 bases on ionic liquid (ILs), and it provides substantial fire safety, the most powerful within the market, and on a remarkably low price compared to established fire-retardant technologies. One key feature of the product is that it neither solidifies nor reaches a crystalline structure. The product itself is sustainable, safe and non-corrosive fire-retardant solution and contains no substances of very high concern.

Palonot F1 can be applied for various wood products. One of the most simple application technology of Palonot F1 is the post-manufacture surface treatment of plywood. The recommendation is to apply spraying or roller spreader technology for freshly sanded plywood maximum 16 h from hot pressing. Both sides of the panel can be surface treated simoultaneously, and the panels should be stacked directly in order to avoid any drying before stacking. The penetration of the chemical continues within the stack. This way, the highest Euroclass B-s1, d0 fire retardancy is reached and the end products will fulfil the criteria of EN 16755, class DRF INT2.

For particleboard production, Palonot F1 should be mixed to surface layer chips either before or after drying of the chips. The core layer chips should be ordinary, non-treated chips for a cost efficient B-s1, d0 process. For MDF process, the pipeline should have an injection possibility for a thorough spreading before the fibre flow has dried too much.

Regarding structural products, especially LVL or CLT the recommendation is to complete either immersion or pressure treatment for the veneers or boards. If the treatment is completed in green condition, the spreading of the chemical will be more controlled and more evenly distributed. The even distribution of the ionic-liquid based solution guarantees the powerful performance in the case of fire, leading to extremely low retention levels compared to that of the industry is used to.

Finally, according to the our studies for load-bearing structures, the results indicate that Palonot F1 significantly reduces the charring rate of LVL in comparison to the non-treated LVL reference material – by ca. 39%. Therefore, our technology would enable reaching possibly REI 100 with the dimensions that currently are classified to REI 60.

Keywords: B-s1 · d0 · Cost efficiency · Reduced charring rate

L. Makovicka Osvaldova et al. (Eds.): WFS 2020, *Wood & Fire Safety*, p. 476, 2020.
https://doi.org/10.1007/978-3-030-41235-7

Author Index

L. Makovicka Osvaldova et al. (Eds.): WFS 2020, *Wood & Fire Safety*, pp. 477–480, 2020.
https://doi.org/10.1007/978-3-030-41235-7